

IL NUOVO CIMENTO

ORGANO DELLA SOCIETÀ ITALIANA DI FISICA

SOTTO GLI AUSPICI DEL CONSIGLIO NAZIONALE DELLE RICERCHE

VOL. V, N. 5

Serie decima

1° Maggio 1957

Interference Effects between Members of Parity Doublets in the Lee-Yang Theory (*).

R. GATTO

Istituto di Fisica dell'Università - Roma
Istituto Nazionale di Fisica Nucleare - Sezione di Roma

(ricevuto l'11 Settembre 1956).

Summary. — LEE and YANG have shown that from the assumption that the approximate equality of masses of the τ - and θ -mesons follows from a symmetry principle it follows that particles of odd strangeness exist in parity doublets. It could be possible to observe in some cases interferences between amplitudes relative to the two components of doublets. It can be shown, for example, that the angular correlation in the cascade $\Xi^- \rightarrow \Lambda^0 + \pi^-$, $\Lambda^0 \rightarrow p + \pi^-$ is given by

$$F(\cos \theta) = \exp[-\lambda_+ t] F_+(\cos \theta) + \exp[-\lambda_- t] F_-(\cos \theta) + \\ + \exp[-\frac{1}{2}(\lambda_+ + \lambda_-)t] \cos(\nu_+ - \nu_-)t F'(\cos \theta)$$

where λ_+ , λ_- , and ν_+ , ν_- are the inverse lifetimes and masses of Λ_+^0 , Λ_-^0 respectively, $F_+(\cos \theta)$ and $F_-(\cos \theta)$ are symmetric for $\theta \rightarrow \pi - \theta$, while $F'(\cos \theta)$ is antisymmetric; t is the time the Λ^0 has lived. The oscillatory interference term will be observable only if the mass difference is $\sim 10^{-5}$ eV or smaller. If the electromagnetic interaction is minimal only the weak interactions can contribute to the mass differences which could result in this case $\sim 10^{-5}$ eV or smaller. Quite similar considerations can be developed for the correlation in the cascade $(K^- + p)_{\text{bound}} \rightarrow Y + \pi$, $Y \rightarrow N + \pi$.

This is a brief communication on what I call the « coherence effects » in the Lee-Yang parity doublets theory of strange particles. I shall only report some main conclusions. I may remark that a parallel investigation has been carried

(*) Presentato al Congresso di Torino, 11-16 Settembre 1956.

out by MORPURGO and similar results have recently also been obtained by Lee and Yang.

It is assumed in the Lee-Yang theory that the approximate equality of mass of τ and θ follows from a symmetry principle. A necessary consequence is that particles of odd strangeness exist in parity doublets. Let us consider a cascade process such as $\Xi^- \rightarrow \Lambda^0 + \pi^-$, $\Lambda^0 \rightarrow p + \pi^-$, or similarly, $(K^- + p)_{\text{bound}} \rightarrow Y + \pi$, $Y \rightarrow N + \pi$. The intermediate hyperon can have even or odd intrinsic parity. We discuss the distribution of the angle θ between the line of flight of the hyperon and the direction of emission of its decay pion in the hyperon center of mass system. Let us fix our attention to the case of the Ξ^- cascade. Similar conclusions also hold for the $(K^- + p)_{\text{bound}}$ cascade but in the Ξ^- case we can assume that perturbation theory is valid and so obtain more compact expressions. If we assume that the interaction hamiltonian is invariant under time reversal we obtain for the distribution of $\cos \theta$

$$(1) \quad F(\cos \theta) = \exp[-\lambda_+ t] F_+(\cos \theta) + \exp[-\lambda_- t] F_-(\cos \theta) + \\ + \exp[-\frac{1}{2}(\lambda_+ + \lambda_-)t] \cos(\nu_+ - \nu_-) t F'(\cos \theta),$$

where: λ_+ , λ_- are the inverse lifetimes of Λ_+^0 , Λ_-^0 respectively; ν_+ , ν_- the masses; t the time the hyperon has lived before decaying; F_+ , F_- the distributions in the case that only Λ_+^0 , Λ_-^0 respectively existed, and F' the interference term between the two members of the parity doublet. F_+ and F_- only contain even powers of $\cos \theta$ and therefore they are symmetric about 90° . F' only contains odd powers of $\cos \theta$ and therefore it is antisymmetric about 90° . I would like to note that if the alternate possibility is assumed of parity non-conservation in weak interactions, then one obtains a symmetric distribution in the $K^- + p$ case (a strong and a weak interaction) and a distribution in general *not symmetric* in the Ξ^- case (two weak interactions). The oscillating interference term in (1) can be observed only if the mass difference $\nu_+ - \nu_-$ is very small, say $\sim 10^{-5}$ eV, otherwise the very rapid oscillations will average to zero. Such very small mass differences are expected in the case the electromagnetic interaction is invariant under parity conjugation so that only the weak interactions can contribute to the mass differences. If photons only interact with charges and currents — this is the postulate of minimal electromagnetic interaction — then the electromagnetic interaction is invariant under parity conjugation and the mass differences are only due to weak interactions.

In conclusion we would like to stress the two peculiar consequences of the Lee-Yang parity doublet theory: (i) certain terms occur in the angular correlations which are not symmetric about 90° ; (ii) the angular correlations have

a rather peculiar dependence on time. The observation of the interference term would constitute a rather strong evidence in favor of the Lee-Yang theory and in favor of the postulate of minimal electromagnetic interaction. On the other hand failure of observing two different lifetimes for the Σ^\pm emerging from K^- capture would be a strong argument against the theory.

RIASSUNTO (*)

LEE e YANG hanno dimostrato che dall'ipotesi dell'eguaglianza approssimativa delle masse dei mesoni τ e θ , per un principio di simmetria segue che le particelle di stranezza dispari esistono in doppietti di parità. Sarebbe possibile osservare in alcuni casi interferenze tra le ampiezze relative ai due componenti dei doppietti. Si può dimostrare, ad esempio, che la correlazione angolare nella cascata $\Xi^- \rightarrow \Lambda^0 + \pi^-$, $\Lambda^0 \rightarrow p + \pi^-$ è data da

$$F(\cos \theta) = \exp[-\lambda_+ t] F_+(\cos \theta) + \exp[-\lambda_- t] F_-(\cos \theta) + \\ + \exp[-\frac{1}{2}(\lambda_+ + \lambda_-)t] \cos(v_+ - v_-)t F'(\cos \theta),$$

dove λ_+ , λ_- , e v_+ , v_- sono gli inversi delle vite medie e delle masse di Λ_+^0 , Λ_-^0 , rispettivamente $F_+(\cos \theta)$ e $F_-(\cos \theta)$ sono simmetriche per $\theta \rightarrow \pi - \theta$, mentre $F'(\cos \theta)$ è antisimmetrico; t è il tempo che il Λ^0 ha vissuto. Il termine d'interferenza oscillatorio sarà osservabile solo se la differenza di massa è $\sim 10^{-5}$ eV o minore. Se l'interazione elettromagnetica è minima, solo le interazioni deboli possono dare un contributo alle differenze di massa che potrebbero risultare in questo caso $\sim 10^{-5}$ eV o minori. Si possono fare considerazioni del tutto simili per la correlazione nella cascata $(K^- + p)_{\text{lim}} \rightarrow Y + \pi$, $Y \rightarrow N + \pi$.

(*) Traduzione a cura della Redazione.

The Annihilation of a Nucleon-Antinucleon System into a K-Anti K Pair (*).

R. GATTO

Istituto di Fisica dell'Università - Roma
Istituto Nazionale di Fisica Nucleare - Sezione di Roma

(ricevuto l'11 Settembre 1956)

Summary. — The selection rules are derived for the annihilation of a nucleon-antinucleon system into a K-anti K pair. The selection rules follow from conservation of angular momentum, of parity, of the charge conjugation quantum number, and from charge symmetry. Moreover it is shown that, if the Lee-Yang parity doublets theory holds, other selection rules can be derived from the conservation of two new quantum numbers, E and F .

You have learned from the contribution of Professor AMALDI that there is a definite evidence in favor of the emission of K-mesons in the annihilation of antinucleons. For the reaction nucleon + antinucleon \rightarrow K + antiK one finds the following selection rules:

Initial state of \bar{p} -p	Final state	Final state
singlets $J = L - 1$	P	P
triplets $J = L$ $J = L + 1$	$C \quad P$	$P \quad E$ P
Initial state of \bar{p} -n	Final state	Final state
singlets $J = L - 1$	P	P
triplets $J = L$ $J = L + 1$	$P \quad G$	$P \quad F$ P

(*) Presentato al Congresso di Torino, 11-16 Settembre 1956.

These rules follow from conservation of the charge conjugation quantum number (C), of parity (P), and of the quantum number G ($G = C \exp[i\pi I_2]$). Moreover other selection rules are indicated which follow from conservation of the new quantum numbers E and F , which we shall now discuss. DALITZ has shown that, if parity is conserved in the decays $K_{3\pi}^+ \rightarrow \pi^+ + \pi^+ + \pi^-$ and $K_{2\pi}^+ \rightarrow \pi^+ + \pi^0$, these two modes of decay cannot be due to the same particle. On the other hand the masses, the lifetimes, the cross sections of all K-mesons are coincident within experimental errors. Two different possibilities have been discussed. A first possibility is that parity is not conserved in weak interactions. A second possibility is to assume that at least two different K-mesons exist: the τ and the θ . In this case the approximate equality of masses suggests the existence of a symmetry principle responsible for the degeneration. This symmetry principle, discussed by Lee and Yang, is equivalent to assuming that the strong hamiltonian commutes with a parity conjugation operator C_P : This symmetry principle leads here to the existence of the quantum numbers E and F . E and F are defined by: $E = CC_P$ and $F = C \exp[i\pi I_2]C_P$.

RIASSUNTO (*)

Si derivano le regole di selezione per l'annichilazione di un sistema nucleone-anti-nucleone in una coppia K-anti K. Le regole di selezione conseguono dalla conservazione del momento angolare, della parità, del numero quantico della coniugazione delle cariche e dalla simmetria delle cariche. Si dimostra inoltre che, se è valida la teoria di Lee-Yang dei doppietti di parità, si possono derivare altre regole di selezione dalla conservazione di due nuovi numeri quantici, E ed F .

(*) Traduzione a cura della Redazione.

K⁻ Interactions in Hydrogen.

L. W. ALVAREZ, H. BRADNER, P. FALK-VAIRANT (*), J. D. GOW,
A. H. ROSENFELD, F. T. SOLMITZ and R. D. TRIPP

Radiation Laboratory, University of California - Berkeley, California

(ricevuto l'11 Dicembre 1956)

Summary. — K⁻-meson from the Bevatron have been stopped in a 10 in. hydrogen bubble chamber. This is a preliminary report on the first 137 interactions. There are photographs confirming the existence of the $\bar{\theta}^0$ and the Σ^0 , which must be lighter than the Σ^- by at least several MeV. Σ 's are produced more profusely than Λ 's in the absorption of K⁻ by protons: we observe the production ratios $\Sigma^- : \Sigma^+ : \Sigma^0 : \Lambda \simeq 4 : 2 : 2 : 1$. The large observed absorption cross-section of slow K⁻ by protons suggests that the interaction takes place in p states as well as in s states. There is evidence that the spin of the Σ is greater than $\frac{1}{2}$. There is no evidence for parity doublets. Our data rule out the proposed selection rule $\Delta I = \pm \frac{1}{2}$. The accepted value for the mean life τ_Λ is checked, and we find $\tau_{\Sigma^-} = (1.83 \pm 0.26) \cdot 10^{-10}$ s and $\tau_{\Sigma^+} = (0.86 \pm 0.17) \cdot 10^{-10}$ s.

1. - Introduction.

From examination of the interaction of slow K-mesons with hydrogen and deuterium a great deal can be learned about the properties of not only the K-mesons, but also the Σ and Λ hyperons and the $\bar{\theta}^0$ -mesons that are produced. Many authors have pointed out the experimental importance of stopping K⁻ in hydrogen^(1,4) but this experiment became feasible only this year when hydrogen bubble chambers were operated successfully at the Bevatron.

(*) On leave from C.E.A., Saclay, France.

(1) K. M. CASE, R. KARPLUS and C. N. YANG: *Phys. Rev.*, **101**, 358 (1956).

(2) R. GATTO: *Nuovo Cimento*, **3**, 5 (1956).

(3) T. D. LEE: *Phys. Rev.*, **99**, 337 (1955).

(4) S. GASIOROWICZ: *Isotopic Spin Conservation in K⁻ Interaction with Nuclear Matter*, UCRL-3074, July 1955.

This is a preliminary report on the first 137 interactions seen in the Berkeley 10 inch hydrogen chamber. Because of the limited statistics most of the quantitative analysis is still uncertain; however, there are enough data to permit the following conclusions:

a) $\Sigma^0, \bar{\theta}^0$. - The experiment furnishes excellent evidence for the existence of a neutral Σ hyperon and of a neutral K-meson ($\bar{\theta}^0$) with the strangeness of the K⁻ and decaying into two charged pions. The Σ^0 must be lighter than the Σ^- by at least several MeV.

b) *Strong interactions involving strange particles.* - No violation of the Gell-Mann-Nishijima scheme was observed in the absorption of the K⁻-mesons by protons. Σ 's are produced somewhat more profusely than Λ 's in these absorptions. We observe the production ratios $\Sigma^- : \Sigma^+ : \Sigma^0 : \Lambda \cong 4 : 2 : 2 : 1$.

The large observed cross-section of slow K⁻ by protons suggests that the interaction takes place in *p*-states as well as in *s*-states.

The absorption of Σ^- 's by protons leads to comparable numbers of Σ^0 's and Λ 's.

c) *Hyperon spins.* - The angular distribution of the decay products of the charged Σ 's suggests that the Σ has a spin greater than $\frac{1}{2}$; this suggestion is strengthened by similar evidence from emulsion experiments. The corresponding evidence for Λ 's is still quite inconclusive.

d) *Parity doublet question.* - If the Σ 's and Λ 's exist in parity doublets, one would expect to observe two lifetimes (for Σ^+ , Σ^- , and Λ) and forward-backward asymmetries in the decay distributions. No evidence for either one of these effects was found.

e) *Hyperon decay mechanism.* - The observed lifetime ratio $(\tau_{\Sigma^-}/\tau_{\Sigma^+}) = 2.2 \pm 0.5$ and the branching ratio $(\Sigma^+ \rightarrow p + \pi^0)/(\Sigma^+ \rightarrow n + \pi^+) = 1.0 \pm 0.2$ are in conflict with the predictions based on the *I*-spin selection rule $\Delta I = \pm \frac{1}{2}$.

f) *Hyperons lifetimes.* - The accepted value of the Λ^0 lifetime is checked, and our knowledge of the Σ^+ and Σ^- lifetimes is considerably improved by this experiment. We find:

$$\tau_{\Lambda} = (3.25 \pm 0.6) \cdot 10^{-10} \text{ s},$$

$$\tau_{\Sigma^+} = (0.86 \pm 0.17) \cdot 10^{-10} \text{ s},$$

$$\tau_{\Sigma^-} = (1.83 \pm 0.26) \cdot 10^{-10} \text{ s}.$$

The experiment is still in progress. There are plans to observe K⁻ absorption in deuterium.

2. - Experimental.

The experimental arrangement is shown in Fig. 1. The « K^- beam» consists mainly of μ -mesons and electrons with a slight contamination of K^- .

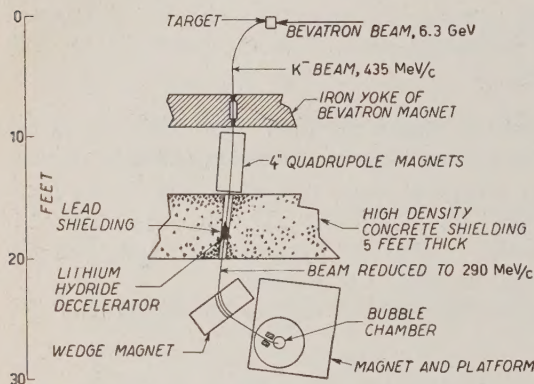


Fig. 1. - K^- meson beam.

We believe that careful scanning of our photographs can detect with nearly 100% efficiency K^- interactions leading to charged secondaries. However some of the data in this preliminary report are based on a quick scan ($\sim 80\%$ efficient) which was done while the run was in progress.

3. - Distribution of events.

Seventeen of the K 's decayed in flight; the rest interacted with protons, either in flight (11 cases) or after the K had come to rest and formed a K -mesic atom (126 cases).

Table I-A lists the eight possible reactions compatible with the energy available and with conservation of strangeness^(6,7) and involving previously identified or postulated particles. We have not yet considered the relatively rare electromagnetic decays or interactions involving charged particles. We have observed all the reactions listed in Table I (except VII and VIII) and no others.

⁽⁵⁾ L. W. ALVAREZ: *Berkeley Bubble Chamber*, 1956, CERN Symposium.

⁽⁶⁾ M. GELL-MANN: *Phys. Rev.*, **92**, 833 (1953); M. GELL-MANN and A. PAIS: *Proceedings of the Glasgow Conference* (London and New York, 1955).

⁽⁷⁾ K. NISHIJIMA: *Prog. Theor. Phys.*, **12**, 107 (1954).

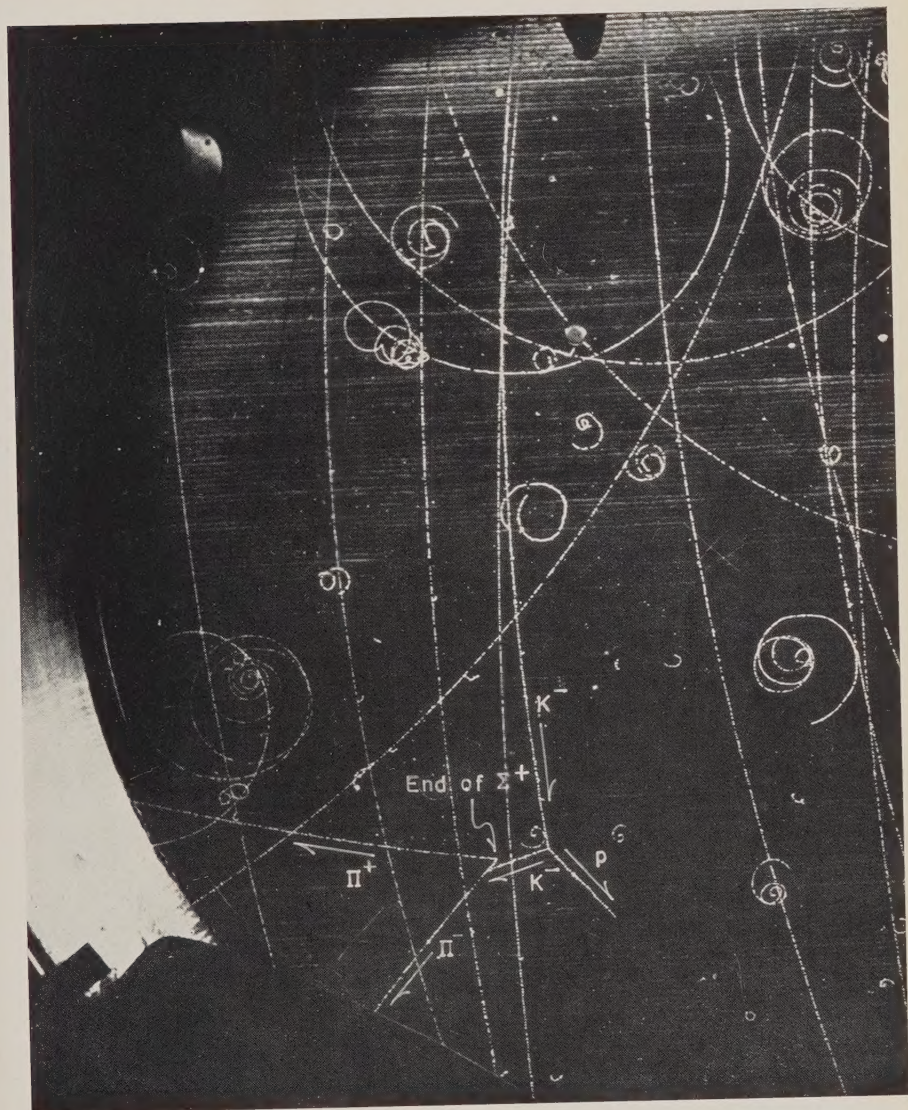


Fig. 2. - A K^- scatters elastically on a proton before coming to rest and forming a K-mesic atom. Then $K^- + p \rightarrow \pi^- + \Sigma^+$; $\Sigma^+ \rightarrow \pi^+ + n$. The horizontal lines spaced about 1 mm apart in the chamber are caused by light scattered in passing through a «Vetnetian blind» used in the dark-field illumination system.

L. W. ALVAREZ, H. BRADNER, P. FALK-VAIRANT, J. D. GOW,
A. H. ROSENFELD, F. T. SOLMITZ and R. D. TRIPP

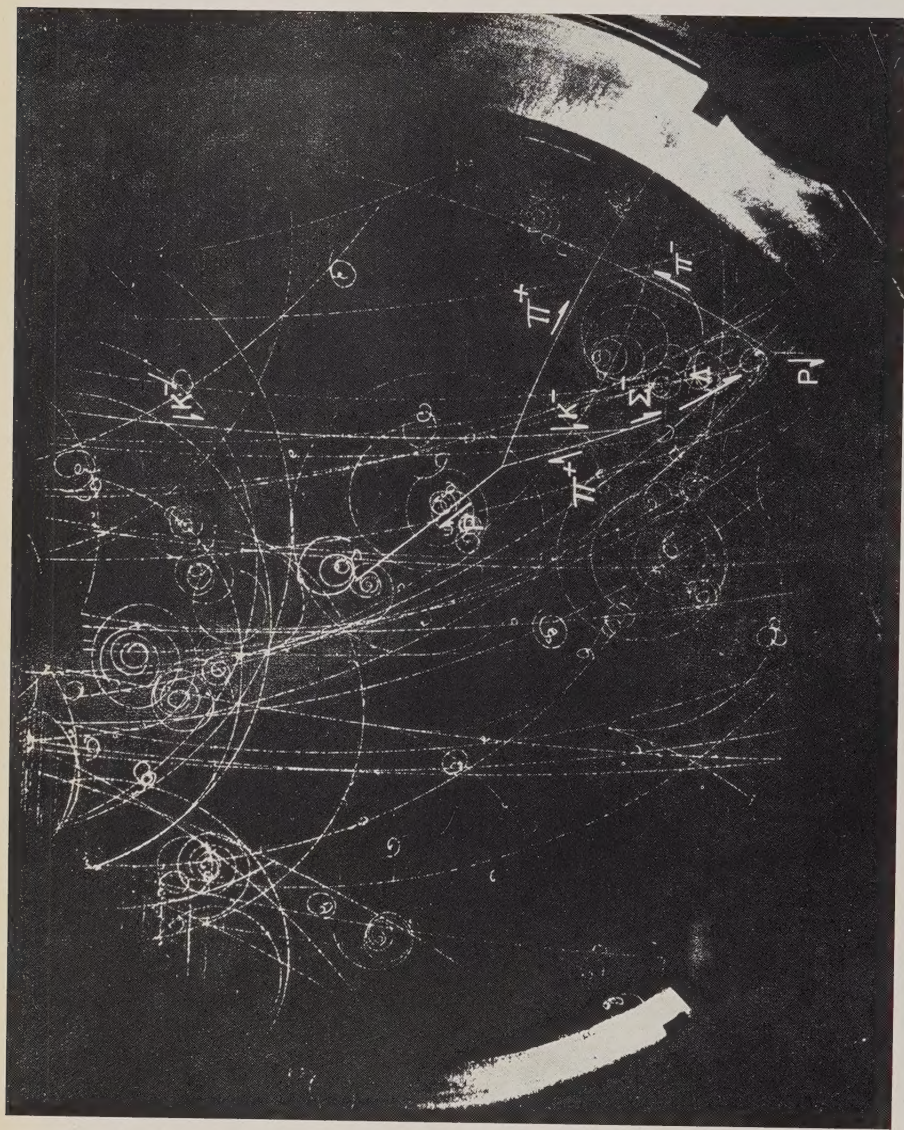


Fig. 3. - A K-mesic atom disintegrates into $\Sigma^- + \pi^+$. The Σ^- goes its full range, comes to rest, and is captured by a proton, whereupon it produces $\Sigma^0 \rightarrow \Lambda + \gamma$. The π^+ is scattered by a proton.

L. W. ALVAREZ, H. BRADNER, P. FALK-VAIRANT, J. D. GOW,
A. H. ROSENFELD, F. T. SOLMITZ and R. D. TRIPP



Fig. 4. Production of a $\bar{\theta}^0$.

TABLE I.— *Distribution of Events (*)*.A) K⁻ interactions.

K ⁻ + p →	Circumstances of K ⁻ interactions			
	In flight		At rest	Total
I. K ⁻ + p (elastic scatter)	3		—	3
II. K ⁻ + n $\left\{ \begin{array}{l} \theta_1 \longrightarrow \left\{ \begin{array}{l} \pi^+ + \pi^- \\ \pi^0 + \pi^0 \end{array} \right. \\ \theta_2 \text{ or } \tau^0 \text{ decay} \end{array} \right.$	(1) ^(a)	K _Q ^(b)	(2) ^(a)	3
		None observed		
III. $\Sigma^+ + \pi^-; \Sigma^+ \longrightarrow \left\{ \begin{array}{l} n + \pi^+ \\ p + \pi^0 \end{array} \right.$	0 1		14 13	28
IV. $\Sigma^- + \pi^+ \left\{ \begin{array}{l} \Sigma^- \longrightarrow n + \pi^- \\ \Sigma^- \text{ interacts} \end{array} \right.$	4 0		44 7	55
V. $\Sigma^0 + \pi^0; \Sigma^0 \rightarrow \gamma + \Lambda, \Lambda \rightarrow \left\{ \begin{array}{l} p + \pi^- \\ n + \pi^0 \end{array} \right.$	0	K _Q ^(b)	14	14
VI. $\Lambda + \pi^0; \Lambda \rightarrow \left\{ \begin{array}{l} p + \pi^- \\ n + \pi^0 \end{array} \right.$	1	K _Q ^(b)	7	8
VII. $\Lambda + \pi^0 + \pi^0$		None observed		
VIII. $\Lambda + \pi^+ + \pi^-$	0		0	0
Total excluding K _Q	10		101	111
K _Q ^(b)				26 ^(b)
Total Interactions				137

B) Σ^- Interactions.

$\Sigma^- + p \rightarrow$	Circumstances of Σ^- interactions			
	In flight		At rest	Total
IX. $\Sigma^- + p$ (elastic scatter)	0		—	0
X. $\Sigma^0 + n; \Sigma^0 \rightarrow \gamma + \Lambda; \Lambda \rightarrow \left\{ \begin{array}{l} p + \pi^- \\ n + \pi^0 \end{array} \right.$	0	Σ_Q ^(b)	2	2
XI. $\Lambda + n; \Lambda \rightarrow \left\{ \begin{array}{l} p + \pi^- \\ n + \pi^0 \end{array} \right.$	0	Σ_Q ^(b)	2	2
Σ_Q^- events ^(b)	1		2	3
Total	1		6	7

(^a) Indicates identification uncertain.

(^b) Between 20 and 40 K's disappear in the chamber, yielding no visible interaction or decay products. We call these "K_Q" endings, and assume that there are 26 of them. Σ_Q are defined analogously.

(*) *Note added in proof.* — In the continuation of the experiment, the number of analyzed hyperons has been doubled. All the qualitative conclusions suggested by the earlier events are now strengthened, with the following important exception. Preliminary analysis of the present angular distribution, which now includes 155 Σ -decays, shows that it has become consistent with isotropy.

The K^- -mesons produced 83 charged Σ hyperons. All the Σ^+ and 48 Σ^- decayed; 7 Σ^- interacted with protons—one in flight, and six after they had come to rest and formed an atom with hydrogen.

In analogy with Table I-A), Table I-B) lists the possible reactions for $\Sigma^- + P$.

Some of the bubble chamber pictures are reproduced in Figs. 2, 3 and 4.

4. — The charged Σ hyperons.

The Σ^- coming from stopped K 's (Reaction III) have a kinetic energy T_{Σ^-} of 13.8 MeV (181.2 MeV/c) ⁽⁸⁾. We have 27 such Σ^+ , all of which decay in flight. The distribution of the times in flight is given in Fig. 5. The mean life is

$$t_{\Sigma^+} = (0.86 \pm 0.17) \cdot 10^{-10} \text{ s}.$$

There are no accurate measurements with which this result may be compared; there are several estimates by nuclear emulsion workers ⁽⁹⁾.

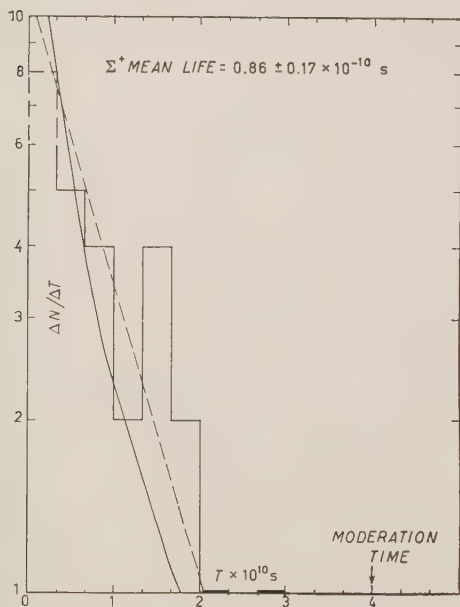


Fig. 5. — Distribution in time of the Σ^+ decays. Four short Σ 's were found whose charge could not be determined. Two of these were arbitrarily called Σ^+ and are represented by a dashed area. Straight line is best fit for a unique mean life of $0.86 \cdot 10^{-10}$ s. The solid curve represents a mixture of two mean lives (see Sect. 5).

⁽⁸⁾ W. W. CHUPP, S. GOLDBABER and F. H. WEBB (*The Mass of the Negative K Meson and Negative Σ Hyperon*, UCRL-3584, Nov. 1956) have used their own events plus some found by other emulsion groups (W. F. FRY, J. SCHNEPS, G. A. SNOW and M. S. SWAMI: *Phys. Rev.*, **103**, 226 (1956)) to compute the following masses (in MeV):

$$\begin{aligned} m_{K^-} &= 493.7 \pm 0.7, & m_{\Sigma^+} &= 1189.3 \pm 0.5, \\ m_{\Sigma^-} &= 1196.5 \pm 0.9, & m_{\Sigma^-} - m_{\Sigma^+} &= 7.3 \pm 0.8. \end{aligned}$$

⁽⁹⁾ See, for example, W. F. FRY, J. SCHNEPS, G. A. SNOW and M. S. SWAMI: *Phys. Rev.*, **100**, 950 (1955).

We have taken the density of liquid hydrogen at the time of bubble formation to be 0.060 g/cm³ (see Appendix); this leads to a Σ^+ range of 1.29 cm and a moderation time of $3.98 \cdot 10^{-10}$ s, or 5.7 mean lives.

The Σ^- is (7.3 ± 0.9) MeV heavier than the Σ^+ ⁽⁹⁾. The Σ^- coming from stopped K's (Reaction IV) should have $T_{\Sigma^-} = 12.6$ MeV (173.8 MeV/c), a range $R_{\Sigma^-} = 1.09$ cm ⁽¹⁰⁾, and a moderation time of $3.45 \cdot 10^{-10}$ s.

As shown in Table I, 44 such Σ^- 's decay and seven interact. We can use these events to calculate a mean life

$$t_{\Sigma^-} = (1.83 \pm 0.26) \cdot 10^{-10} \text{ s.}$$

This agrees with the mean life reported by BRUDE *et al.* ⁽¹¹⁾, who observed the reaction $\pi^- + \text{P} \rightarrow \Sigma^- + \text{K}^+$, using a propane bubble chamber. They found $t_{\Sigma^-} = 1.4^{+1.6}_{-0.5} \cdot 10^{-10}$ s.

The mean life was calculated on the assumption that all 4 decays occurred in flight. Actually the uncertainty in range measurements is such that we cannot rule out the possibility that as many as six of the Σ^- could have come to rest before decaying. If all six come to rest, our mean life should be increased by a factor 44/38, i.e., by $\sim 15\%$.

The total path traversed by the 55 Σ^- was 27 cm. In our liquid hydrogen, a cross-section of 1 barn corresponds to a mean free path of 30 cm. These facts give some idea of the cross-section associated with the one Σ^- that interacted in flight.

5. - Can there be two Σ lifetimes?

There have been many attempts to explain how two particles with apparently different parity (the τ and the θ) can have the same mass.

LEE and YANG and GELL-MANN ⁽¹²⁾ have suggested the idea of parity doublets. If the K-mesons are doublets, then Σ and Λ hyperons must also be doublets—specifically there should be two Σ^+ (and two Σ^-) of opposite parity and presumably with different lifetimes ⁽¹³⁾.

⁽¹⁰⁾ The observed range of the 6 Σ^- is (1.07 ± 0.03) cm; we thus confirm the Σ^- mass value obtained from nuclear emulsion technique.

⁽¹¹⁾ R. BRUDE, M. CHRÉTIEN, J. LEITNER, N. P. SAMIOS, M. SCHWARTZ and J. STEINBERGER: *Phys. Rev.*, **103**, 1827 (1956).

⁽¹²⁾ T. D. LEE and C. N. YANG: *Phys. Rev.*, **102**, 290 (1956); J. J. MURRAY and M. GELL-MANN (private communication).

⁽¹³⁾ Moreover, according to this theory there should be equal numbers of the two sorts of K's produced at the target. There is good evidence that the mean lives of the charged K's of both parities are indeed very similar, so that the two parities of K should come to rest in our chamber in about equal numbers and make comparable numbers of even- and odd-parity Σ 's.

We have tried to fit our observed distribution of Σ^+ lifetimes by assuming that we have equal numbers of Σ^+ of each parity, and that the mean lives for the two cases are τ and $B\tau$. We find a best fit for $B = 1$ (i.e. for the assumption that the Σ has a unique mean life), and the fit becomes increasingly poor with increasing B . The distribution of decay times to be expected for the case $B = 4$ is given in Fig. 5; it can be seen that for values of B this great or greater the fit becomes noticeably bad ⁽¹⁴⁾.

The Σ^- can be treated the same way as the Σ^+ , and the conclusions are qualitatively the same. The Σ^- lifetime distribution does not extend over so many mean lives as that for the Σ^+ , therefore our 55 Σ^- 's are no more valuable for this analysis than our 28 Σ^+ 's.

A different test for the existence of parity doublets is considered below.

6. - Angular distribution of Σ decay products.

The angular distribution of hyperon decay products with respect to the hyperon direction of flight is of interest both because it may yield some information on the spin of the Σ and because a fore-aft asymmetry would confirm the existence of parity doublets ⁽¹⁵⁾. The two aspects of the problem may conveniently be separated for the following reason. If the Σ has a well-defined parity, the angular distribution of its decay products can contain only terms which are even in $\cos \theta$. If the Σ is a parity doublet, then additional odd terms are allowable. If the angular distribution is folded about 90° , these odd terms must cancel, and one is left with a folded angular distribution that is independent of the existence or non-existence of parity doublets.

6.1. Spin of the Σ . - The folded angular distribution for the Σ^+ decay products is independent of the decay mode of the Σ^+ ($\rightarrow N + \pi^+$ or $P + \pi^0$)

⁽¹⁴⁾ The problem can be discussed more quantitatively as follows. For a mixture of Σ 's assume a probability of decay at a time t

$$P(t, \tau, B) = \frac{1}{2} \left(\frac{1}{\tau} \exp \left[-\frac{t}{\tau} \right] + \frac{1}{B\tau} \exp \left[-\frac{t}{B\tau} \right] \right), \quad (1 < B < \infty).$$

A likelihood function $L(B)$ is then defined as follows: let $L(\tau, B) = \prod_{i=1}^{28} P(t_i, \tau, B)$; then the value of τ that will maximize L is roughly that which makes the mean life of the particle mixture equal to the observed mean life $0.86 \cdot 10^{-10}$ s. However this guess can be slightly improved upon, and for each assumed value of B a value of τ called τ_B has been calculated such that $L(\tau_B, B) \equiv L(B)$ is a maximum. We then find that $L(B)$ is very nearly of the form $L(B)/L(1) = 10^{-B/3.7}$. This confirms the qualitative observation that a value of B greater than 4 is improbable.

⁽¹⁵⁾ T. D. LEE and C. N. YANG: *Phys. Rev.* **104**, 882 (1956).

but it is not in general the same as the angular distribution of the Σ^- decay products. If, however, the K⁻ has spin zero and is captured from an s -state or a $p_{\frac{1}{2}}$ state of the K-mesic atom, then both Σ^+ and Σ^- must be produced in the same angular momentum and spin states, leading to the same angular distribution of their decay products.

6'1.1. $S_{\Sigma} = \frac{1}{2}$. — The folded distribution for the decay of a spin $\frac{1}{2}$ particle must be isotropic. If we can show that our (folded) data are inconsistent with isotropy, then S_{Σ} must be $> \frac{1}{2}$. In order to make this test quantitatively it is convenient to analyze the events (total number = N) into n_p polar events ($|\cos \theta| > \frac{1}{2}$) and n_e equatorial events, with $n_p + n_e = N$. The data are given in Table II. For the Σ^- we find $n_p^-/N^- = 25/41 = 0.61 \pm 0.08$, and for the Σ^+ , $n_p^+/N^+ = 15/24 = 0.625 \pm 0.10$.

These values are to be compared with the expected value $n_p/N = \frac{1}{2}$ for an isotropic distribution. The result for either the Σ^- or the Σ^+ taken separately is almost consistent with isotropy; however, the argument against isotropy becomes stronger if both results are considered together. Let us therefore

TABLE II. — *Angular distribution (centre of mass) of the pions from Σ decay* ^(a).

$x = \cos \theta_{\Sigma\pi}$	Forward				Backward				Total	Probability
	1 ↓	$\frac{3}{4}$ ↓	$\frac{1}{2}$ ↓	$\frac{1}{4}$ ↓	0 ↓	$\frac{1}{4}$ ↓	$\frac{1}{2}$ ↓	$\frac{3}{4}$ ↓	1 ↓	
<i>Experimental distribution:</i>										
$\Sigma^- \rightarrow \pi^- + n$	9	3	7	3	4	2	7	6	41	—
$\Sigma^+ \rightarrow \pi^+ + n$	1	3	1	1	2	0	2	1	11	—
$\Sigma^- \rightarrow \pi^0 + p$	3	2	3	2	0	0	1	2	13	—
Total	13	8	11	6	6	2	10	9	65	—
Folded through 90°	—	—	—	—	12	13	18	22	65	—
<i>Theoretical distribution:</i>										
$S_{\Sigma} = \frac{1}{2}$	$f(\theta) = \text{constant}$				16.25	16.25	16.25	16.25	65	8.2%
$S_{\Sigma} = \frac{3}{2}$	$f(\theta) = 1 + 3x^2$				8.6	11.7	17.8	26.9	65	21%
$S_{\Sigma} = \frac{5}{2}$	$f(\theta) = 1 - 2x^2 + 5x^4$				11.7	10.1	12.6	30.6	65	18%

^(a) We have included only the Σ 's from K's that came to rest. The theoretical distributions for $S_{\Sigma} = \frac{1}{2}, \frac{3}{2}$, are calculated on the assumption that the Σ originates from a K-mesic atom with angular momentum $\frac{1}{2}$ (for example, capture of a spinless K from an s -state). The calculation of the probability that our data are consistent with isotropy is discussed in the text and in footnote ⁽¹⁶⁾. The probability associated with the angular distributions assumed for $S_{\Sigma} = \frac{3}{2}$ is calculated in similar fashion. For $S_{\Sigma} = \frac{5}{2}$ we applied the χ^2 test for the separate units of solid angle given in the table, instead of further grouping the data into two intervals as done for $S_{\Sigma} = \frac{1}{2}, \frac{3}{2}$. This was done because any lumping would tend to wash out the sharp forward peaking of the theoretical distribution.

assume that the true distributions of the decay products of Σ^+ and of Σ^- are both isotropic (for example because $S_\Sigma = \frac{1}{2}$), and calculate the probability that the data should fit this assumption as badly as they do, or worse. Since both

Σ^+ and Σ^- are here assumed to have identical (isotropic) distributions, we can combine the data, and we then find $n_p/N = 0.615 \pm \pm 0.06$, and the probability of finding a deviation from 0.50 this large or larger is 8.2%⁽¹⁶⁾. The combined distribution is plotted in Fig. 6.

Since receipt of a private communication from Professor W. F. FRY (university of Wisconsin), we attach added significance to the evidence against isotropy for Σ decay. The Madison emulsion group find the same ratio n_p/N , based on 84 hyperon decays, as we do from our 65 cases.

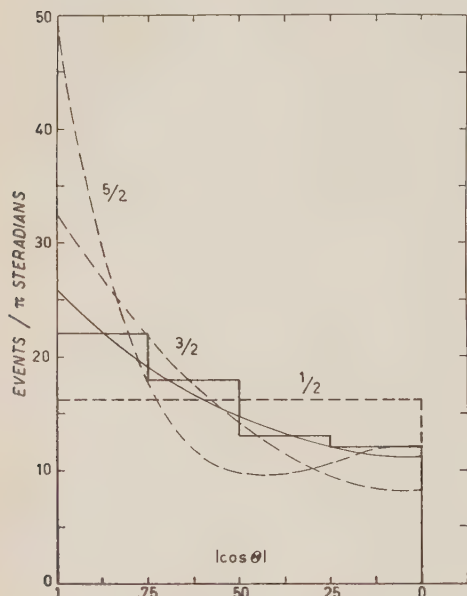


Fig. 6. — Angular distribution of the pion produced in Σ decay. The histogram represents the sum of Σ^+ and Σ^- events, folded through 90° . The three dashed curves represent the theoretical distribution for Σ 's of spin $\frac{1}{2}$, $\frac{3}{2}$, and $\frac{5}{2}$ (the latter two are valid only for K^- captured in a state of angular momentum $\frac{1}{2}$). The thin solid line is the best fit to our data on the assumption that the distribution is of the form $(1 + A \cos^2 \theta)$.

leads to $A = 1.3 \pm_{0.8}^{1.3}$. This angular distribution is plotted as a thin solid line in Fig. 6, and it can be seen that it fits the data well within our statistical errors.

6.1.2. $S_\Sigma = \frac{3}{2}$. — It can be shown in general that in the angular distribution of decay products of a particle of spin S no term in $\cos \theta$ raised to a power greater than the $(2S - 1)$ -th can appear. If we take $S_\Sigma = \frac{3}{2}$, the angular distribution must be of the form $(1 + A \cos^2 \theta)$. For the combined Σ^+ and Σ^- decays our experimental result $n_p/N = 0.615 \pm 0.06$

⁽¹⁶⁾ For the binomial distribution $P(n_p, N) = C_N^{n_p} (\frac{1}{2})^N$, the probability $P(n > 40, N = 65)$ is 4.1% (see *Tables of the Cumulative Binomial Probability Distribution*, Cambridge, Mass., 1955). The distribution is of course symmetric in n_p and $n_{\bar{p}}$, and we must take into account the additional 4.1% probability that $n_{\bar{p}} > 40$, i.e., that $n_{\bar{p}} \leq 25$. Therefore the total probability of finding a fit this bad or worse is 8.2%. It may be noted that the above formulation reduces to the usual χ^2 test in the limit of large statistics.

Let us, therefore, consider this case $S_{\Sigma} = \frac{3}{2}$ in more detail. The angular distribution is governed by the total angular momentum J of the K-mesic atom from which the Σ originates⁽¹⁷⁾. GATTO has pointed out that K's are quite possibly absorbed from p -states as well as from s -states⁽²⁾. We shall assume that the spin of the K is zero; then we need discuss only the two cases $J = \frac{1}{2}$ and $J = \frac{3}{2}$.

a) $J = \frac{1}{2}$. — (If the K is captured from an s -state, this is the only case we need consider). For this simple case, the folded angular distribution is unique⁽¹⁷⁾, namely, it is proportional to $1 + 3 \cos^2 \theta$. It can be seen from Fig. 6 and from Table II that the fit is only moderately good.

b) $J = \frac{3}{2}$. — The angular distribution is no longer unique, but depends upon the amplitudes of various angular momentum states in which the Σ is produced (and A_{+} —for the Σ^{-} decays—and A_{-} could be different). Although A is not unique, it must lie in the range -1 to $+3$ (as must A_{+} and A_{-}).

Since $J = \frac{1}{2}$ forces A to be 3, we conclude that if the K absorption takes place partly from s -state and partly from p -states A must lie in the range -1 to $+3$. Our best value of $A = 1.3$ evidently falls within this range. Our individual values of A_{+} and A_{-} are almost equal to A , and individually pass this test.

6.1.3. $S > \frac{3}{2}$. — On the basis of our data we certainly cannot rule out $S > \frac{3}{2}$. However, it may be of some interest to note that if S_{Σ} is large and J small the angular distribution becomes sharply peaked towards 0° to 180° . Our data show no sharp peaking. This peaking is already apparent for the case $J = \frac{1}{2}$, $S_{\Sigma} = \frac{5}{2}$, which is included in Table II and in Fig. 6.

6.2. *Fore-aft asymmetry*. — LEE and YANG⁽¹⁵⁾ have shown that if the Σ has mixed parity (see Section 5) its decay products could show a fore-aft asymmetry. This asymmetry need not be the same for each of the three possible modes of decay: $\Sigma^{-} \rightarrow N + \pi^{-}$, $\Sigma^{+} \rightarrow N + \pi^{+}$, and $\Sigma^{+} \rightarrow P + \pi^{0}$ should be considered separately. The data are displayed in Table III.

There is some preference for forward over backward, but only one of the three modes is peaked forward by more than one standard deviation. Any conclusion drawn from this single mode is weakened by data from the Wisconsin emulsion group, who inform us that they have 38 examples of this mode of decay, divided equally between forward and backward.

⁽¹⁷⁾ S. B. TREIMAN: *Phys. Rev.*, **101**, 1216 (1956).

TABLE III. — Evidence for possible asymmetries in Σ decay. Forward and backward refers to the pion direction in the centre of mass system relative to the Σ direction.

	No. in forward hemisphere	No. in backward hemisphere	Total	
	n_f	n_b	N	n_f/N
$\Sigma^- \rightarrow \pi^- + N$	22	19	41	0.536 ± 0.08
$\Sigma^+ \rightarrow \pi^+ + N$	6	5	11	0.545 ± 0.15
$\Sigma^- \rightarrow \pi^0 + P$	10	3	13	0.769 ± 0.12

7. — Σ^0 and Λ hyperons.

$\Lambda \Sigma^0$ is expected to decay rapidly ($\sim 10^{-20}$ s) into $\Lambda + \gamma$; thus the Σ^0 should be detectable via its secondary γ or Λ originating essentially from the point of production of the Σ^0 . We have as yet no γ -ray converter inside the bubble chamber, but if the Λ decays through its charged mode, then we can detect it with high efficiency (the bubble chamber is large compared with the mean decay distance of a slow Λ).

Both Σ^0 and Λ can be made by the interactions of K^- with protons (Reactions V through VIII) or of Σ^- with protons (Reactions X and XI), but the primary Λ 's can be distinguished from those which are the daughters of Σ 's by measurements of the Λ energy.

7.1. Hyperons from K^- . — For neutral hyperons coming from a K^- mesic atom, $T_{\Sigma^0} = 13.5$ MeV (179.8 MeV/c)⁽¹⁸⁾, $T_{\Lambda} = 28.7$ MeV (253.0 MeV/c), for the two-body Reaction VI. For the three-body Reactions VII and VIII, $0 < T_{\Lambda} < 8$ MeV.

The energy spectrum of the Λ 's coming from K^- mesic atoms is given in Fig. 7. The various contributing spectra are drawn schematically in the upper part of the figure and the experimental distribution is given below. Our best estimate is that of the 21 events 14 ± 2 are Σ^0 's and 7 ∓ 2 are primary Λ 's.

We shall now discuss the experimental spectrum in more detail: with our present technique, we can measure the kinetic energy of a Λ to about 2 MeV if the secondary proton stops in the chamber—if it does not stop the uncertainty is greater. With this coarseness of measurement, we cannot resolve the line from the continuum. Not only do the two merge, but also the mixing makes the peak in the experimental spectrum appear at a slightly lower energy than that of the line. We attribute the one at 47 MeV to a K^-p interaction

⁽¹⁸⁾ We have taken $m_{\Sigma^0} = 1193$ MeV; this guess is based on the evidence presented in Sect. 7.2.

in flight. It is not surprising that we should observe one such interaction: for the 78 Σ^\pm from K's that have come to rest, we see five made by K's still in flight; therefore for 21 (primary and secondary) Λ 's coming from K's at rest, there should be about one made by a K still in flight.

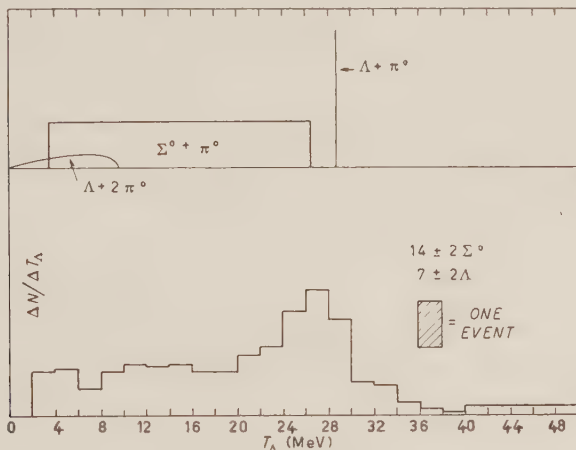


Fig. 7. — Energy spectrum of Λ 's from K^- captured by protons. The spectrum of secondary Λ 's from Σ^0 's will be a rectangle (as drawn) if the Σ^0 has spin $\frac{1}{2}$; in any case this spectrum must be symmetric about its average energy. The histogram is constructed by assigning to each event a rectangle of unit area (indicated in black); the width of the rectangle shows the energy uncertainty of that Λ .

We feel that the contribution of Reaction VII to the spectrum is quite small because the phase space is an order of magnitude less than that available to Reactions V and VI. Moreover there is the experimental evidence that we do not see the easily detectable Reaction VIII, which should show up more strongly because (a) we can detect it even if $\Lambda \rightarrow N + \pi^0$, (b) it can proceed through states in which the two pions have either I -spin 1 or 0, whereas Reaction VII is limited to $I = 0$.

7'2. Hyperons from Σ^- interactions; mass of the Σ^0 . — When a Σ^- comes to rest and is captured by a proton, it can yield primary Λ 's (Reaction XI) with a kinetic energy $T_\Lambda = 36.9$ MeV. If $m_{\Sigma^-} - m_{\Sigma^0} > m_\Sigma - m_p = 1.3$ MeV, the Σ^- can also give Σ^0 's by Reaction X. These Σ^0 's will give rise to a spectrum of secondary Λ 's, and the limits of this spectrum depend sensitively on $m_{\Sigma^-} - m_{\Sigma^0}$.

We have observed four Λ 's from stopped Σ^- ; two of them had T_Λ consistent with 36.9 MeV and were evidently primaries; for the other two, T_Λ

was (2.8 ± 0.5) and (4.5 ± 0.5) MeV, and these we interpret as secondaries. These two events show that $1.7 \text{ MeV} < (m_{\Sigma^-} - m_{\Sigma^0}) < 22.7 \text{ MeV}$. Fig. 8 shows the likelihood function for $m_{\Sigma^-} - m_{\Sigma^0}$ based on these two events under the assumption that the Σ^0 decays isotropically. It can be seen that the most probable value of m_{Σ^0} is somewhere between m_{Σ^-} and m_{Σ^+} .

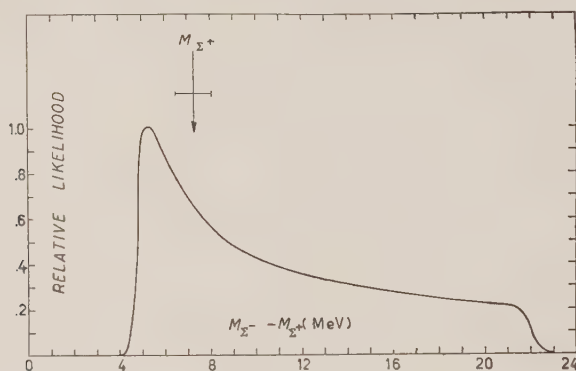


Fig. 8. — Relative likelihood for Σ^0 mass values based on the kinetic energies of three Σ^0 's coming from Σ^- absorptions. One additional event, found after the text for this paper was completed, has been included in computing the likelihood function.

7.3. *Mean life of the Λ .* — On the assumption that the Λ has a unique mean life, we calculate from our 25 Λ 's

$$\tau_{\Lambda} = 3.25 \pm 0.6 \cdot 10^{-10} \text{ s.}$$

This is in a good agreement with the values $3.7^{+0.6}_{-0.5}$ given by PAGE⁽¹⁹⁾, and $2.0^{+1.3}_{-0.7}$ by BUDDE *et al.*⁽¹¹⁾. The distribution of these 25 events in flight time is consistent with a unique mean life. The average K stops about 10 cm from the wall of the chamber, and the flight time for a typical Λ (20 MeV) to reach the walls (if it does not first decay) is a little more than 10^{-9} s. We could therefore miss extremely long-lived Λ 's. If short- and long-lived Λ 's are assumed to be produced in equal numbers, then we can put a lower limit of $\sim 5 \cdot 10^{-9}$ s on the lifetime of the long-lived component.

8. — Angular distribution of Λ decay products.

The angular distribution of Λ decay products gives information on the Λ spin. The considerations are analogous to those in the preceding section.

⁽¹⁹⁾ D. I. PAGE: *Phil. Mag.*, **45**, 863 (1954).

Experimentally, the analysis is more difficult because of our inability to distinguish (except on a statistical basis) many of the primary Λ 's and those coming from Σ 's. About all that can be done at this time is to add the angular distribution from all our Λ 's (primary and secondary) coming from stopped K's and to see whether the distribution is consistent with isotropy.

We find $n_p/N = 15/24 = 0.62 \pm 0.10$.

There have been a number of experiments on the production and subsequent decay of Λ 's (^{11,20,21}) that should shed some light on the spin on the Λ : however the evidence still seems inconclusive. Considerations of the ratio of mesonic to non-mesonic decay of light hyperfragments do suggest that $S_\Lambda = \frac{1}{2}$ (^{22,23}). Our value of n_p/N is not inconsistent with this conclusion.

9. - The θ^0 meson.

Three events have been observed in which a neutral particle is produced in a K⁻-p interaction and decays into two charged light particles (one of these is shown in Fig. 4). The kinematics suggest the θ_1 decay: $\theta_1 \rightarrow \pi^+ + \pi^-$. In order to conserve strangeness the neutral heavy meson that was produced must have been a $\bar{\theta}^0$, which then decayed as a θ_1 (^{24,25}).

The kinetic energies of the 3 θ^0 's are (10 ± 2), (9 ± 2), and (1.5 ± 1) MeV (²⁶). Since they are not of unique energy, at least one of them, and possibly all, must have been produced by a K⁻ in flight. We cannot rule out interactions in flight because Coulomb scattering of a stopping particle produces fluctuations of track curvature such that occasionally a K could disappear 10 cm before the end of its range (when it still has ~ 30 MeV kinetic energy) and still look as if it had come to rest. Bubble counting leads to a comparable uncertainty.

It must be remarked that the low-energy θ^0 was found in one of our most

(²⁰) M. W. FOWLER, R. P. SHUTT, A. M. THORNDIKE and W. L. WHITTEMORE: *Phys. Rev.*, **98**, 121 (1954).

(²¹) W. WALKER and W. SHEPARD: *Phys. Rev.*, **101**, 1810 (1954).

(²²) M. A. RUDERMAN and R. KARLUS: *Phys. Rev.*, **102**, 247 (1956).

(²³) H. PRIMAKOFF, *Nuovo Cimento*, **3**, 1394 (1956).

(²⁴) M. GELL-MANN and A. PAIS: *Phys. Rev.*, **97**, 1387 (1955).

(²⁵) A reaction has been reported by FOWLER, MAENCHEN, POWELL, SAPHIR and WRIGHT (*Phys. Rev.*, **103**, 208 (1956)) in which the production of a θ^0 was required for kinematical reasons and in order to preserve strangeness. However the postulated $\bar{\theta}^0$ was not observed to decay. Also R. G. GLASSER and N. SEEMAN (abstract submitted for APS meeting, Chicago, Nov. 1956) report evidence for neutral particles which may be $\bar{\theta}^0$'s and which are capable of producing hyperons in an interaction.

(²⁶) The mass of the $\bar{\theta}^0$ enters into the calculation of the kinetic energies, but in a very insensitive way. For this calculation we assume $m_{\bar{\theta}^0} = m_{K^-}$.

unsatisfactory photographs, where the beam was many times as intense as it should have been. This event could possibly be just a small-angle pion-proton scattering.

If our two high-energy θ^0 's come from stopped K 's, then the mass of the θ^0 must be smaller than that of the K^- by about 15 MeV. This is in disagreement with Thompson's finding that the mass of the θ^0 and the K^+ are equal within ± 5 MeV (²⁷). Our two high-energy θ 's both come forward from the place where the K^- disappears, so we can get agreement with Thompson's mass by postulating that the K^- charge-exchanged when it still had a kinetic energy of about 10 MeV ($R \sim 1.5$ cm).

On the assumption that there are no parity doublets, half the \bar{K}^0 's produced should decay in the chamber as θ_1 's, and about 90% of the other half should escape from the chamber before decaying as θ_2 's. We may not observe all the θ_1 's however, since there may be a decay mode $\theta_1 \rightarrow \pi^0 + \pi^0$ (although there is some evidence that this is absent). In summary, if the K is not a parity doublet we can expect to detect one-half or less of the $\bar{\theta}^0$'s. (If K 's are a parity doublet, half of them will be long lived τ 's, and we can then expect to detect $\leq \frac{1}{4}$ of the total number produced). BUDDE *et al.* (¹¹) find experimentally that a fraction $\alpha \sim \frac{1}{3} \pm \frac{1}{6}$ of the θ^0 's produced in high-energy $\pi + p$ collisions decay in their bubble chamber. We have identified three θ_1 events; dividing three by α we suggest that there are probably (9 ± 3) $\bar{\theta}^0$'s made altogether, 6 of them showing up as $K\theta$'s.

10. - Matrix elements and phenomenology.

10'1. *Production of Σ 's.* - We assume conservation of isotopic spin I during the production of Σ^+ , Σ^- , and Σ^0 via Reaction III, IV, and V. We shall also make the much less justified assumption that only one atomic state (i.e. only one total angular momentum and orbital angular momentum) is dominant in the K^- capture. Both the states $I = 1$ and $I = 0$ are involved; our data permit us to estimate the relative strength and phase of the matrix elements J_1 and J_0 (⁴). We shall show that $|J_1| \lesssim |J_0|$, and $\varphi \approx 70^\circ$

Let

$$\frac{J_1}{J_0} = r \exp[i\varphi],$$

and let $\Sigma^{+ \rightarrow 0}$ stand for the number of hyperons produced. Then we have

$$(1) \quad \frac{\Sigma^-}{\Sigma^+} = \left| \frac{r \exp[i\varphi] + \sqrt{2/3}}{-r \exp[i\varphi] + \sqrt{2/3}} \right|^2$$

(²⁷) R. W. THOMPSON, J. R. BURWELL, H. O. COHN, R. W. HUGGET and C. J. KARZMARK: *Phys. Rev.*, **95**, 661 (1954).

and

$$(2) \quad \frac{\Sigma^- + \Sigma^+}{2\Sigma^0} = \frac{3}{2}r^2 + 1 \geq 1.$$

From the experimental numbers $\Sigma^{+,0}$ let us now calculate r and φ .

From Eq. (1) and the value $\Sigma^-/\Sigma^+ = 2$ (see Table II), we obtain the lower limit $r \geq 0.14$.

There is considerable uncertainty about the total numbers of Σ^0 's produced because the secondary Λ 's may decay by the neutral mode or there could also be a long-lived type of Λ . If α is the fraction of Λ 's decaying by the charged mode, then $\alpha\Sigma^0$ is the number of observed Σ^0 (14 according to Table I).

The value α is subject to the following considerations:

- 1) Inserting the lower limit $r \geq 0.14$ into Eq. (2), we find

$$(\Sigma^- + \Sigma^+) = 83 \geq 1.03 \cdot 2 \Sigma^0 = 1.03 \cdot 2 \cdot 14/\alpha,$$

hence $\alpha \geq 0.35$.

- 2) From the number of K_0 endings we estimate $0.4 < \alpha < 0.6$.

- 3) BUDDE *et al.* ⁽¹¹⁾ have examined the associated production of Λ 's in high-energy $\pi + p$ collisions and find $0.18 < \alpha < 0.45$.

- 4) The proposed I -spin selection rule for strange-particle decays, $\Delta I = \pm \frac{1}{2}$ ⁽⁶⁾, requires $\alpha = \frac{2}{3}$.

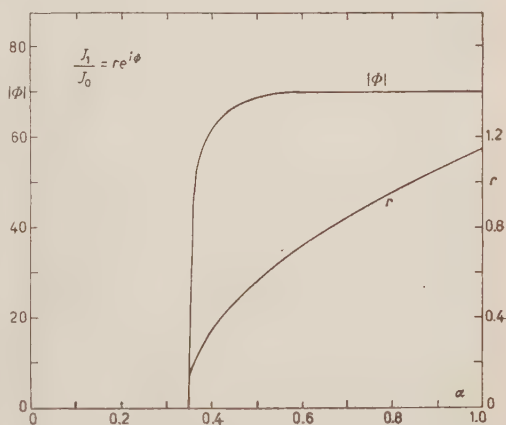


Fig. - 9. Ratio of the I spin 1 and I spin 0 matrix elements (J_1 and J_0) for the reaction $K^- + p \rightarrow \Sigma + \pi$ as a function of α , the fraction of Λ 's decaying into $\pi^- + p$ in the chamber.

Fig. 9 gives r and φ as functions of α . J_1/J_0 can be used to calculate the relative abundance of Σ 's produced by K^- interactions with neutrons.

10'2. Relative production of Λ 's and Σ 's. - Since Λ 's are assumed to have I -spin 0, Reaction VI can proceed only in an $I = 1$ state; we shall call the

matrix element for this process G_1 . We wish to compare G_1 with the matrix element J_1 responsible for Σ production, which has already been discussed in Sect. 10'1. Again assuming conservation of isotopic spin, we find

$$\left| \frac{G_1}{J_1} \right|^2 = \frac{\Lambda}{\Sigma^+ + \Sigma^- - 2\Sigma^0} = \frac{\Lambda_{\text{observed}}}{\alpha(\Sigma^- + \Sigma^+) - 2\Sigma_{\text{observed}}^0};$$

here α is, as before, the fraction of Λ 's observed to decay into charged particles. Our data suggest that $\alpha = 0.5 \pm 0.1$; inserting this into Eq. (3), we find

$$\left| \frac{G_1}{J_1} \right|^2 = \frac{7 \pm 3}{11 \pm 11} \sim \frac{2}{3}.$$

Observations of K^- stars in nuclear emulsion have already led to the suggestion that the production of Σ 's may be more intense than that of Λ 's⁽²⁸⁾.

11. - Decay of the Σ hyperon.

The decay products of the Σ^+ represent mixtures of $I=\frac{1}{2}$ and $I=\frac{3}{2}$ states, whereas for Σ^- the final state is entirely $I=\frac{3}{2}$. If we define the ratio of the $I=\frac{1}{2}$ to the $I=\frac{3}{2}$ matrix elements for the Σ^+ as

$$R_{\frac{1}{2}}/R_{\frac{3}{2}} = x \exp[i\psi],$$

we have the branching ratio

$$(4) \quad f \equiv \frac{\Sigma^+ \rightarrow P + \pi^0}{\Sigma^+ \rightarrow N + \pi^+} = \frac{2 + x^2 - 2\sqrt{2}x \cos \psi}{1 + 2x^2 + 2\sqrt{2}x \cos \psi};$$

experimentally we find $f = 1.0 \pm 0.2$. Solving for x , we get

$$(5) \quad x = \frac{-\sqrt{2}(f+1) \cos \psi \pm [2(1+f)^2 \cos^2 \psi - (2f-1)(f-2)]^{\frac{1}{2}}}{2f-1}.$$

A number of authors have pointed out that the symmetry and unitarity of the S -matrix implies that $\psi = (\delta_{\frac{3}{2}} - \delta_{\frac{1}{2}})$ ⁽²⁹⁻³¹⁾; here $\delta_{\frac{3}{2}}$, $\delta_{\frac{1}{2}}$ are the $I=\frac{3}{2}$, $\frac{1}{2}$ π - p phase shifts appropriate to the parity and angular momentum of the final

⁽²⁸⁾ S. GOLDHABER: *Proceedings of the Sixth Annual Rochester Conference*, April 1956.

⁽²⁹⁾ G. TAKEDA: *Phys. Rev.*, **101**, 1547 (1956).

⁽³⁰⁾ M. KAWAGUCHI and K. NISHIJIMA: *Prog. Theor. Phys.*, **15**, 182 (1956).

⁽³¹⁾ B. D'ESPAGNAT and J. PRENTKI: *Nuovo Cimento*, **3**, 1045 (1956).

state: these are determined uniquely by the spin and parity of the Σ^+ . Table IV lists the values of $|x|$ we find by using Eq. (5) and our experimental branching ratio $f = 1$ for various spin and parity assignments.

TABLE IV. - Σ Decay.

Type of Σ π -p system		$\cos(\delta_{\frac{3}{2}} - \delta_{\frac{1}{2}})^{(a)}$	$ x = (R_{\frac{1}{2}})/(R_{\frac{3}{2}}) ^{(b)}$	$\frac{1+x^2}{3} \left(\frac{\tau_{\Sigma^-}}{\tau_{\Sigma}} \text{ if } \Delta I = \frac{1}{2} \right)$
$\frac{1}{2}^+$ $\frac{3}{2}^+$ $\frac{3}{2}^-$ $\frac{1}{2}^-$	$S_{\frac{1}{2}}$	0.95	0.18 or 5.5	0.34 or 11
	$P_{\frac{1}{2}}$	1.00	0.17 or 5.8	0.34 or 12
	$P_{\frac{3}{2}}$	0.76	0.22 or 4.5	0.35 or 7
	$d_{\frac{3}{2}}$	1.00	0.17 or 5.8	0.34 or 12
higher spins	d and higher	1.00	0.18 or 5.8	0.34 or 12

^(a) Phase shifts from *Proceedings of the Sixth Annual Rochester Conference*, April 1956.

^(b) $R_{\frac{1}{2}}$ and $R_{\frac{3}{2}}$ are the matrix elements for decay into $I = \frac{1}{2}$ and $I = \frac{3}{2}$ states.

Several authors have discussed the decay of hyperons (^{29,31-33}). One suggestion is to demand that the interaction responsible for the decay be a spinor in I space (implying $\Delta I = \pm \frac{1}{2}$ in the decays) (³⁰⁻³²).

This assumption leads to the relationship

$$(6) \quad \frac{\tau_{\Sigma^-}}{\tau_{\Sigma}} = \frac{1}{3} (1 + x^2).$$

From the last column of Table IV we see that our observed lifetime ratio ($\tau_{\Sigma^-}/\tau_{\Sigma^+} = 2.2 \pm 0.5$) conflicts with Eq. (6) for all possible spin and parity assignments (³⁴) (*).

(³²) M. KAWAGUCHI and K. NISHIJIMA: *Prog. Theor. Phys.*, **15**, 180 (1956).

(³³) C. ISO and M. KAWAGUCHI: *Prog. Theor. Phys.*, **16**, 177 (1956).

(³⁴) The conflict is smallest for the $(3/2)^+$ assignment, and in that case would be removed if the branching ratio were as large as 1.4 and $\tau_{\Sigma^-}/\tau_{\Sigma^+}$ as large as 3.2. However, these values are both two standard deviations away from our best values; this can be seen with the help of the plot of f versus $\frac{1}{3}(1+x^2)$ given by ISO and KAWAGUCHI (³³).

(*) Note added in proof. - Recent evidence against parity conservation in weak interactions involving neutrinos suggests that parity conservation may also be violated in other weak interactions such as hyperon decays which do not involve neutrinos. R. GATTO has investigated the relationship between f and $\tau_{\Sigma^-}/\tau_{\Sigma^+}$ using only the assumption of invariance under time reversal and finds that if parity is not conserved in the Σ -decay, then, regardless of the spin of the Σ , our data are consistent with the selection rule $\Delta I = \pm \frac{1}{2}$.

12. - K^- interactions in flight.

Nine K^- interactions in flight have been definitely identified, three of these as elastic scatterings. The number of interactions in flight should probably be increased by about six for the \bar{K}^0 contribution⁽³⁵⁾. In order to calculate a cross-section based on the observed track length of stopping K^- 's, one must count only those interactions (about $\frac{3}{4}$ of the total) in which the K would have stopped in the chamber if it had not interacted. We obtain an absorption cross-section of (210 ± 100) mb and a scattering cross-section of (45 ± 30) mb; the average K^- enters the chamber with about 30 MeV. The uncertainties are evidently too large to permit any clear-cut conclusions, but it is interesting to note that complete S -wave absorption ($\pi\lambda^2$ averaged over the K^- path) is about 200 mb; complete S -wave absorption implies an equal elastic cross-section. Our large absorption cross-section suggests that P waves as well as S waves contribute to the interaction.

13. - Decays in flight.

Seventeen K^- mesons decay in the chamber before coming to rest. This number is consistent with the number of expected decays from the known K lifetime. At present our momentum measurements are not sufficiently precise to distinguish between most of the K decay modes; however, 4 τ^- decays were observed (Fig. 10). They have been analyzed by BERNARD WALDMAN, who finds $m_{\tau^-} = 492 \pm 5$ MeV ($963 \pm 10 m_e$)⁽³⁶⁾. As early as 1953 VAN LINT and TRILLING observed a τ^- whose mass they calculated as (493 ± 3) MeV⁽³⁷⁾. Our mass value corroborates theirs but is of little help in reducing the uncertainty. These masses for the τ^- agree with the better-known mass $((494 \pm 0.5)$ MeV) of the positively charged K ⁽³⁸⁾.

* * *

It would have been impossible to carry out the work described in this paper without the co-operation of many individuals and groups, some members of the Radiation Laboratory and some not. Often this experiment required

⁽³⁵⁾ We assume that two observable and four unobservable \bar{b}^0 's are produced in flight (see Sect. 9).

⁽³⁶⁾ B. WALDMAN: *A Mass Determination of a τ^- Meson*, UCRL-3507, Aug. 1956.

⁽³⁷⁾ V. A. J. VAN LINT and G. H. TRILLING: *Phys. Rev.*, **92**, 1089 A (1953).

⁽³⁸⁾ H. H. HECKMAN, F. M. SMITH and W. H. BARKAS: *Nuovo Cimento*, **4**, 51 (1956).

L. W. ALVAREZ, H. BRADNER, P. FALK-VAIRANT, J. D. GOW,
A. H. ROSENFELD, F. T. SOLMITZ and R. D. TRIPP



Fig. 10. — K decay in flight: $\tau^+ \rightarrow \pi^+ + \pi^- + \pi^0$.

extraordinary effort by supporting personnel. Space does not permit us to acknowledge the help of each person by name. Among those who contributed in large measure, however, we wish to acknowledge the work of the bubble chamber operating crews, under the direction of RICHARD L. BLUMBERG, ROBERT WATT, and GLEN ECKMAN. The personnel of the University of California Chemistry Department Liquified Gases Plant, under the direction of Dr. DAVID LYON, provided large quantities of liquid hydrogen and nitrogen, operating for long hours, often at plant capacity.

We wish also to thank the Bevatron operating staff, as directed by Dr. EDWARD J. LOFGREN and Mr. HARRY HEARD; the scanners; and also Prof. BERNARD WALDMAN, who worked with us during the summer. Professors ROBERT KARPLUS, T. KOTANI, MALVIN RUDERMAN, and many others provided very helpful discussions on the theoretical aspects of this experiment.

This work was done under the auspices of the U.S. Atomic Energy Commission.

APPENDIX

Experimental details.

We are convinced that a careful, experienced scanner detects K-mesons stopping in the chamber with very nearly 100% efficiency (providing beam and bubble chamber conditions are reasonably good). Sometimes a fast scan is done during a run to check on conditions; this is only about 80% efficient.

The identification of most of the events is very simple and can be done by inspection. Thus when a K⁻ stops, leading to a Σ , one observes the characteristic collinear Σ and π tracks, with a secondary π track originating from the end of the Σ ; the stopping K⁻ and the Σ are heavily ionizing, the two π 's minimum ionizing; one can get additional kinematic checks by making rough curvature (and hence momentum) measurements with the help of templates. For K endings leading to Λ 's the identification is just as easy. Only in the case of K₀'s (i.e., K endings giving no visible products) is there some difficulty in identification: A short, fairly straight, heavily ionizing track going through the entrance window can be either a K⁻ or a proton going in the opposite direction; a π^- charge-exchange scattering may also look like a K⁻ ending if the chamber is oversensitive (since in that case minimum and heavily ionizing tracks tend to have similar appearance).

Lengths, angles, and curvatures were measured with ruler, protractor, and templates on projections of the two stereophotographs; then the corresponding spatial quantities were obtained by desk calculation (a faster and more accurate method of analysis is being developed). These measurements

are adequate for obtaining the lifetimes of the hyperons and the angular distribution of their decay products.

The Q -values of the various reactions and decays observed could in principle be determined from the range and curvature measurements. For instance, the Q -value of the reaction $K^- + p \rightarrow \Sigma^- + \pi^+$ could be determined either from the curvature of the π^+ track or from the range of the Σ^- in case it stops. If the measurement accuracy were limited by multiple scattering or by Bohr straggling, we could determine the Q -value to about 1 MeV from a single event. However, at present we have some difficulty in getting accurate momentum measurements from either curvature or range. We suspect that curvature is not reliable to better than about 10% because of turbulence; the range-energy relation is also still uncertain because we have not yet measured the density of the superheated hydrogen. Preliminary measurements of the ranges of μ 's in π - μ -decays, and extrapolation from the most recent thermodynamic data on liquid hydrogen both indicate that the appropriate density is $(0.060 \pm 0.002) \text{ g/cm}^3$.

RIASSUNTO

Si presenta una relazione preliminare su 137 interazioni a riposo di mesoni K prodotti dal Bevatrone con i protoni dell'idrogeno liquido di una camera a bolle di 25 cm di diametro. Si sono ottenute fotografie confermant l'esistenza della Λ^0 e della Σ^0 ; la massa di quest'ultima risulta minore di quella della Σ^- di almeno qualche MeV. L'assorbimento dei K^- da parte dei protoni dà luogo più frequentemente alla produzione di Σ che di Λ ; le abbondanze da noi osservate stanno nei rapporti: $\Sigma^- : \Sigma^+ : \Sigma^0 : \Lambda \sim 4 : 2 : 2 : 1$. Il fatto che la sezione d'urto osservata per assorbimento dei K^- di bassa energia è alta, suggerisce che l'interazione ha luogo sia in stati p che in stati s . I dati indicano anche che lo spin della Σ è maggiore di $\frac{1}{2}$, mentre non danno alcuna indicazione dell'esistenza dei doppietti di parità ed escludono la validità della regola di selezione proposta $\Delta I = \pm \frac{1}{2}$. Si dà una verifica del valore accettato per la vita media τ_Λ e si trova $\tau_{\Sigma^-} = (1.83 \pm 0.26) \cdot 10^{-10} \text{ s}$ e $\tau_{\Sigma^+} = (0.86 \pm 0.17) \cdot 10^{-10} \text{ s}$.

Caratteristiche delle disintegrazioni nucleari prodotte da protoni di 140 ± 6 MeV.

III. — Nuclei leggeri.

S. JANNELLI e F. MEZZANARES

Istituto di Fisica dell'Università - Messina

(ricevuto il 14 Dicembre 1956)

Riassunto. — Si studiano le disintegrazioni prodotte da protoni di 140 MeV negli elementi leggeri (C, N, O) delle emulsioni Ilford G5 da 600 μ m. Sono state prese in considerazione 220 stelle (delle quali 108 cercate sistematicamente « per area »). Sono riportati i valori più attendibili di alcune grandezze caratteristiche del processo di disintegrazione preso in esame, ricavati dai dati del presente lavoro e da quelli di altri AA. Vengono riconosciute singolarmente le disintegrazioni prodotte nei diversi elementi: queste si accordano all'ipotesi di una struttura a particelle α dei nuclei leggeri ed agli schemi proposti. Tali schemi rendono conto del 45% circa delle disintegrazioni avvenute, nei rimanenti casi si ha l'emissione di alcune particelle (per processi di evaporazione locale, ad es.) e di un frammento ($Z > 2$). La frequenza delle disintegrazioni nei diversi elementi sembra dipendere essenzialmente dalla loro abbondanza nell'emulsione.

Lo studio delle disintegrazioni prodotte da nucleoni di alta energia negli elementi leggeri (C, N, O) dell'emulsione si presenta con caratteri diversi da quello relativo agli elementi pesanti.

Infatti, se è applicabile ^(1,2) alla prima fase della disintegrazione il modello della cascata nucleonica col metodo di Montecarlo, non può applicarsi la teoria dell'evaporazione alla fase che la segue per la quale d'altronde non è disponibile alcuna teoria statistica che serva ad interpretarla.

(¹) H. MUIRHEAD e W. G. V. ROSSER: *Phil. Mag.*, **46**, 652 (1955).

(²) J. COMBE: *Journ. Phys. et Rad.*, **46**, 445 (1955); *Suppl. Nuovo Cimento*, **3** 182 (1956).

Tali disintegrazioni, sono state studiate dapprima da un punto di vista statistico ^(3,4) nel campo di energia (~ 140 MeV) da noi considerato, ed in campi di energia diversi dal nostro oltre che dai predetti A.A. da LOCK e coll. ⁽⁵⁾.

Particolare menzione deve farsi dei lavori di MUIRHEAD e coll. ⁽¹⁾ e di COMBE ⁽²⁾ i quali (nel nostro campo di energia i primi) hanno approfondito lo studio delle disintegrazioni prodotte in elementi leggeri tentandone, come si è detto, una interpretazione della prima fase in termini di cascata nucleonica e cercando di riconoscere le singole reazioni che prendevano origine negli atomi di C, N, O.

Abbiamo ritenuto opportuno occuparci dell'argomento allo scopo di dare risultati statisticamente più validi usando un campione più vasto e più omogeneo (in quanto relativo ad un solo valore dell'energia dei primari) di quelli usati finora ed allo scopo di riconoscere, in quanto possibile, le singole reazioni che prendono origine dalla disintegrazione dei nuclei degli elementi leggeri dell'emulsione.

1. - Procedimento sperimentale e definizioni.

La ricerca è stata condotta su emulsioni (*) Ilford G5 da $600\text{ }\mu\text{m}$ esposte al fascio di protoni del ciclotrone di Harwell (140 ± 6 MeV).

Sono state prese in considerazione 220 stelle prodotte in elementi leggeri, delle quali 108 cercate sistematicamente « per area » e il resto a caso per accrescere il numero di eventi presi in considerazione.

Per quanto riguarda il modo con cui sono state cercate le stelle, i criteri di separazione tra le stelle prodotte in elementi pesanti e leggeri e la legittimità dell'aggiunta delle stelle cercate a caso, rimandiamo alle nostre precedenti comunicazioni ⁽⁶⁾.

Nelle stelle prodotte in elementi leggeri le tracce corte ($\leq 5\text{ }\mu\text{m}$) non sono state considerate « rinculi » nel senso che ad essi comunemente si attribuisce nella disintegrazione dei nuclei pesanti, ma « rami », attribuibili a particelle con $Z \geq 2$ (vedi parte I).

Fra tali tracce è opportuno però distinguere le particelle α da quelle a numero atomico maggiore ($Z \geq 3$) che chiameremo « frammenti », f ; tale distinzione è

⁽³⁾ P. E. HODGSON: *Phil. Mag.*, **44**, 1113 (1953); **45**, 190 (1954).

⁽⁴⁾ M. GRILLI, P. E. HODGSON, M. LADU e B. VITALE: *Nuovo Cimento*, **1**, 314 (1955).

⁽⁵⁾ W. O. LOCK e P. V. MARCH: *Proc. Roy Soc.*, A **230**, 222 (1955).

(*) Ringraziamo i Ch.mi Proff. A. ROSTAGNI ed N. DALLAPORTA, dell'Università di Padova, che ci hanno cortesemente concesso le lastre sulle quali è stata condotta la presente ricerca ed il Dr. M. GRILLI per l'aiuto gentilmente prestato.

⁽⁶⁾ S. JANNELLI e F. MEZZANARES: parte I: *Suppl. Nuovo Cimento*, **4**, 939 (1956); parte II: *Nuovo Cimento*, **5**, 380 (1957).

ovviamente solo approssimativa in alcuni casi e può farsi in base alla compatibilità della disintegrazione osservata (numero delle cariche totalmente presenti nella stella) col numero delle cariche in gioco (7, 8, 9, rispettivamente per C, N, O).

In base a tale criterio nelle stelle a piccolo numero di rami (≤ 3) le tracce corte vengono comunemente interpretate come frammenti, mentre nelle altre, per lo più, possono interpretarsi come particelle α .

La presenza di « tracce a martello » nelle stelle osservate in elementi leggeri ^(7,8) avvalorava l'ipotesi che non tutte le tracce corte ($\leq 5 \mu\text{m}$) possono attribuirsi a particelle α .

Anche nel corso della presente ricerca è stata trovata una stella, Fig. 1, nella quale è riconoscibile nella traccia *a* un ${}^8_3\text{Li}$ che decade, a fine percorso, dando origine a due α (*b* e *b'*).

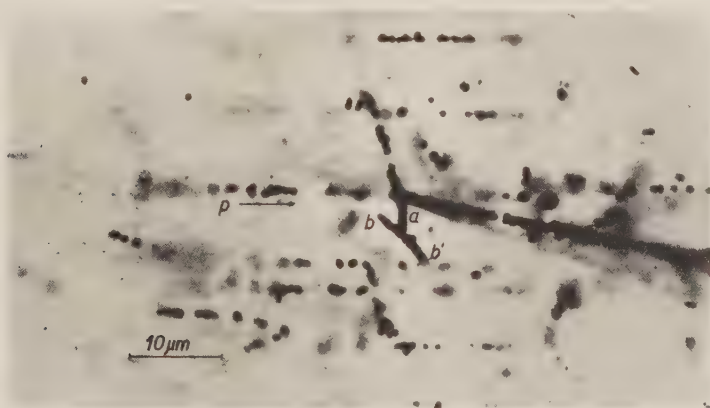


Fig. 1. — Microfotografia di una stella 4r in nucleo leggero; *p*: protone incidente; *a*: ${}^8_3\text{Li}$; *b*, *b'*: particelle α .

Per le notazioni adoperate nel presente lavoro facciamo riferimento ai nostri precedenti ⁽⁶⁾ notando soltanto che in questo gli angoli e le grandezze che da essi dipendono sono riferite al sistema del baricentro poichè, a differenza che per gli elementi pesanti, la correzione relativa è spesso di una certa entità ($\sim 5^\circ$).

⁽⁷⁾ E. W. TITTERTON: *Phil. Mag.*, **42**, 113 (1951).

⁽⁸⁾ M. DEMEUR, A. HULEUX e G. VANDERHAEGHE: *Nuovo Cimento*, **4**, 509 (1956).

2. - Distribuzione angolare dei rami.

Le Figg. 2 e 3 danno, rispettivamente, le distribuzioni angolari dei rami grigi (142), $T > 30$ MeV, e neri (795), $T \leq 30$ MeV, nella Fig. 3 è riportata per confronto la distribuzione isotropa (istogramma a contorno tratteggiato).

La Tab. I dà i valori di F_G e F_N e dell'angolo medio $\bar{\xi}$, confrontati con i dati di altri autori: non è chiaro se gli autori citati (qui e nel seguito) si riferiscono al sistema del baricentro o a quello del laboratorio, in tale ultima ipotesi (che ci sembra più probabile) l'accordo con i nostri dati sarebbe ancora migliore.

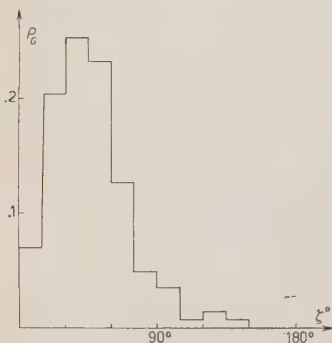


Fig. 2. - Distribuzione angolare dei rami grigi.

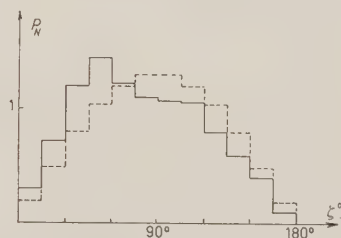


Fig. 3. - Distribuzione angolare dei rami neri.
[-----] Distribuzione angolare isotropa.

TABELLA I. - *Frazione in avanti F ed angolo medio $\bar{\xi}$ per le tracce grige e nere.*

	F_G	F_N	ξ_G	$\bar{\xi}_N$
MUIRHEAD	0.96 ± 0.04	—	$41.7^\circ \pm 4.1^\circ$	—
NOSTRI	0.94 ± 0.02	0.6 ± 0.01	$46.5^\circ \pm 2.2^\circ$	$80.2^\circ \pm 1.4^\circ$

Dai valori surriferiti risulta evidente che le tracce G appartengono alla cascata nucleonica la quale si svolge prevalentemente in avanti, mentre le N possono pure in parte attribuirsi alla cascata.

3. - Distribuzione angolare dei protoni e delle particelle α (≤ 30 MeV)

Effettuata, fra le tracce che terminano in emulsione, la distinzione fra i protoni e le particelle α dalla conta delle lacune ed entro un angolo di dip di 25° , si sono ottenute le distribuzioni angolari che, corrette per le perdite geometriche, vengono riportate nelle Figg. 4 e 5, mentre la Tabella II dà i valori corretti di F_p e F_α confrontati con quelli degli altri autori.

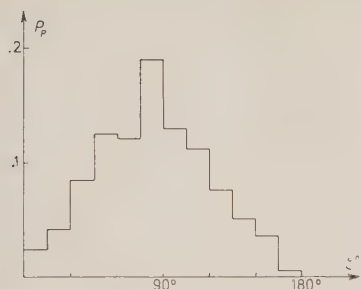
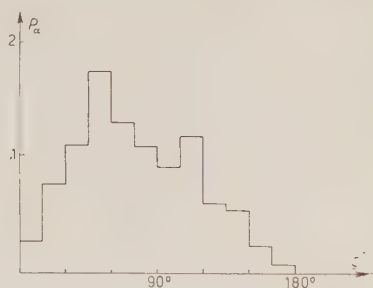


Fig. 4. - Distribuzione angolare dei protoni.

Fig. 5. - Distribuzione angolare delle particelle α .TABELLA II. - *Frazione in avanti F per i protoni e le particelle α (≤ 30 MeV).*

	F_p	F_α
GRILLI	0.58 ± 0.2	0.66 ± 0.17
HODGSON	0.68 ± 0.05	0.71 ± 0.03
MUIRHEAD	0.70 ± 0.03	0.71 ± 0.03
NOSTRI	0.59 ± 0.04	0.64 ± 0.03

Il valore

$$F = 0.53 \pm 0.08$$

della frazione in avanti per i frammenti, prossimo a quello della distribuzione isotropa, conferma la nostra interpretazione di questi come risultato della frammentazione del nucleo piuttosto che come rinculi nucleari (che dovrebbero essere fortemente collimati in avanti) e la notevole diversità dall'analogo valore per le particelle α conferma la legittimità dei criteri adottati per distinguere queste dai frammenti (che, evidentemente, avranno una distribuzione isotropa poichè nessuno di essi è attribuibile alla cascata nucleonica).

La Tabella III dà i valori del rapporto Π_α delle particelle α a tutte quelle cariche emesse (entro 30 MeV).

TABELLA III. - *Rapporto Π_α delle particelle α a tutte le particelle cariche emesse (≤ 30 MeV).*

	Avanti	Indietro	Totale
GRILLI	0.61 ± 0.15	0.50 ± 0.15	0.55 ± 0.1
MUIRHEAD	—	—	0.48 ± 0.03
NOSTRI	0.56 ± 0.03	0.48 ± 0.03	0.53 ± 0.02

L'elevato valore di Π_α è facilmente interpretabile con l'ipotesi, generalmente accettata, di una struttura a particelle α dei nuclei leggeri.

La collimazione in avanti dei protoni e delle particelle α non è attribuibile al moto del baricentro (poichè in tale sistema sono misurati gli angoli) e può quindi affermarsi la presenza di protoni e particelle α di bassa energia ($T \leq 30$ MeV) fra le particelle della cascata nucleonica.

La differenza fra il nostro valore di Π_α e quello di MUIRHEAD, piuttosto elevata, anche se entro i limiti degli errori, potrebbe attribuirsi alla circostanza che gli autori citati ⁽¹⁾ forse hanno calcolato Π_α , considerando fra i protoni anche le particelle di energia > 30 MeV (tracce grige). In tal caso il nostro valore risulta

$$\Pi_\alpha = 0.45 \pm 0.02,$$

in migliore accordo con i dati di MUIRHEAD e coll. Non siamo in grado però di precisarlo poichè essi ⁽¹⁾ non distinguono Π_α secondo che le particelle siano state emesse in avanti o indietro: infatti, se si considerano le tracce grige, $(\Pi_\alpha)_{\text{avanti}}$ deve essere evidentemente più piccolo di $(\Pi_\alpha)_{\text{indietro}}$ (per i nostri dati rispettivamente: $0.44 \pm 0.02 \div 0.47 \pm 0.03$).

I dati di Grilli ⁽⁴⁾ si riferiscono come i nostri (Tabella III) a tracce nere. Per analogia a quanto fatto per gli elementi pesanti ci sembra più opportuno calcolare Π_α solo relativamente alle tracce nere.

Con i medesimi criteri ⁽⁶⁾ esposti nella nostra precedente nota, poichè le particelle vengono emesse isotropicamente nel processo di frammentazione che segue la cascata (anche se non interpretabile in termini evaporativi), è possibile dedurre, rispettivamente fra i protoni e le α , le frazioni P_{cp} , $P_{c\alpha}$ di particelle della cascata:

$$P_{cp} = 0.20 \pm 0.02, \quad P_{c\alpha} = 0.32 \pm 0.03.$$

Nella Tabella IV sono riportati i valori delle grandezze caratteristiche quali possono ricavarsi mediando sui nostri dati e su quelli degli autori citati ^(1,3,4).

TABELLA IV. — Parametri caratteristici delle stelle prodotte in nuclei leggeri da protoni di 140 MeV.

		Presente lavoro	Media ponderale
Π_α	F_G	0.94 ± 0.02	0.94 ± 0.02
	F_P	0.59 ± 0.04	0.66 ± 0.02
	F_α	0.64 ± 0.03	0.66 ± 0.02
	{ Avanti	0.56 ± 0.03	0.56 ± 0.02
	{ Indietro	0.48 ± 0.03	0.48 ± 0.02
	{ Totale	0.53 ± 0.02	0.51 ± 0.01

4. - Distribuzione energetica dei protoni e delle particelle α (\dots 30 MeV)

Fra le tracce a morte, già distinte in protoni e particelle α , si è risalito dalla misura del range all'energia, e le distribuzioni energetiche ottenute, corrette per le perdite geometriche, sono riportate nelle Figg. 6, 7: il fatto che



Fig. 6. - Distribuzione energetica dei protoni.

Fig. 7. - Distribuzione energetica delle particelle α .

parte delle tracce corte sono state da noi considerate frammenti e quindi escluse dalla distribuzione angolare delle particelle α porta a notevoli differenze con i dati di Hodgson ⁽³⁾ mentre il confronto con Muirhead e coll. ⁽¹⁾ è soddisfacente.

Nella tabella V sono riportate i valori dell'energia media \bar{T} confrontati con quelli degli altri autori.

TABELLA V. - Energia media $\bar{T}(30)$ dei protoni e delle particelle α .

		Avanti	Indietro	Totale
GRILLI	{ protoni	9.6	8.7	9.2
	{ particelle α	8.5	7	8
NOSTRI	{ protoni	11.2 ± 0.8	8.6 ± 0.7	10.2 ± 0.6
	{ particelle α	7.6 ± 0.5	6.3 ± 0.5	7.2 ± 0.4

Può osservarsi che per le particelle emesse nell'emisfero anteriore, l'energia media è maggiore e ciò è da attribuire alla presenza, prevalentemente tra esse, di particelle della cascata che sono le più energiche.

Le differenze fra i nostri dati e quelli riportati per confronto possono attribuirsi al fatto che i nostri sono riferiti a particelle con energia fino a 30 MeV,

mentre gli autori citati prendono come limite superiore rispettivamente 20 MeV per i protoni e 40 MeV per le particelle α .

5. - Conclusioni.

La prima fase del processo di disintegrazione dei nuclei leggeri colpiti da particelle di alta energia può interpretarsi col modello della cascata nucleonica: MUIRHEAD e coll. ⁽¹⁾ e COMBE ⁽²⁾ hanno ad essa applicato il metodo di Montecarlo.

Una prima distinzione può farsi fra le stelle a seconda del numero dei rami grigi della cascata; tale distinzione, eseguita solo fra le prime 108 stelle ricercate sistematicamente, è riportata nella Tabella VI.

TABELLA VI. - *Classificazione delle stelle secondo il numero dei rami grigi.*

0 r_G		45.4 ± 5	
1 r_G		51.8 ± 4.7	
2 r_G		2.8 ± 1.6	

Il confronto con Combe ⁽²⁾ e Bernardini e coll. ⁽⁹⁾ non è molto significativo a causa della diversità dei valori dell'energia dei protoni incidenti. Nella cascata nucleonica però vengono anche emessi protoni e particelle α di bassa energia: in base ai nostri dati si può concludere che, per ogni stella, vengono emessi, oltre gli eventuali neutroni, 0.9 protoni e 0.7 particelle α .

Se le particelle della cascata sono protoni ⁽¹⁾ l'energia media di eccitazione del nucleo residuo è di 23 MeV: nell'ipotesi, generalmente ammessa, della costituzione a particelle α dei nuclei di C ed O (rispettivamente: 3α e 4α) e pensando il nucleo di N costituito da 2α ed un deutone diremo *frammentazione completa* del nucleo il suo spezzarsi nei costituenti.

La *frammentazione completa* del nucleo eccitato potrà aver luogo solo se l'energia di eccitazione del nucleo residuo è almeno uguale alla soglia per le reazioni $^{12}_6\text{C}(p; 3\alpha, p)$; $^{14}_7\text{N}(p; 3\alpha, d, p)$ oppure $^{14}_7\text{N}(p; 3\alpha, 2p, n)$; $^{16}_8\text{O}(p; 4\alpha, p)$ cioè rispettivamente 7.3; 17.5 oppure 19.8; 14.5 MeV.

Se l'eccitazione del nucleo non raggiunge la soglia per le suddette reazioni si avrà, nei processi seguenti la cascata nucleonica, solo l'emissione di alcune particelle e di un frammento ($3 \leq Z \leq 8$): questo è il caso delle stelle ad 1, 2, 3 rami, di parte delle 4r e di alcune 5r.

Sè invece l'eccitazione supera la soglia di tanto quanto basta (28.2 MeV

⁽⁹⁾ G. BERNARDINI, E. T. BOTH e S. G. LINDENBAUM: *Phys. Rev.*, **88**, 1017 (1952).

per z) per spezzare una o più particelle z nei loro componenti ($2p$, $2n$) si avranno delle reazioni più complesse e stelle quindi a maggior numero di rami: almeno 5 rami e comunque non più di 8 per l'energia dei nostri primari.

Le disintegrazioni che possono aver luogo sono rappresentabili secondo i seguenti schemi:

$$\begin{aligned} {}^{4k}_{2k}X + p &= (k-i)\alpha + (2i+1)p + 2in + Q & k=3; i=0, 1, \dots 3 \text{ per } C, \\ & & k=4; i=0, 1, \dots 4 \text{ per } O, \end{aligned}$$

$${}^{4k+2}_{2k-1}Y + p = (k-i)\alpha + (2i+2)p + 2in + Q \quad k=3; i=0, 1, \dots 3 \text{ per } N.$$

Per quanto si è detto uno o più protoni emessi nella frammentazione completa del nucleo possono essere sostituiti da un deutone o da un tritone e risulterà diminuito, di 1 o 2 il numero dei neutroni emessi (per ogni d o t).

Se nel processo della cascata viene emessa una particella α invece che un protone le espressioni precedenti non vengono alterate anche se, ovviamente, saranno diverse, ma di poco, le soglie per le reazioni di *frammentazione completa* poichè il nucleo residuo che la subisce non è più quello di partenza (${}^{12}_6C$, ${}^{14}_7N$, ${}^{16}_8O$) ma, rispettivamente 9_5B , ${}^{11}_6C$, ${}^{13}_7N$.

Con le ipotesi fatte circa la costituzione dei nuclei di C , N , O dovrebbe escludersi l'emissione di neutroni nel processo della cascata e le stelle $0r_i$ della Tabella VI andrebbero interpretate piuttosto come se nella cascata fossero state emesse particelle α o protoni *neri* (≤ 30 MeV).

Tenuto conto dei criteri adottati per la distinzione fra p ed α e della compatibilità delle reazioni con le cariche totalmente in gioco, si è cercato di riconoscere singolarmente le reazioni osservate.

A tale scopo si è preso in considerazione un campione di 181 stelle comprendente le 108 cercate sistematicamente e, delle altre, solo una parte scelta a *caso* e proporzionalmente alle sezioni d'urto per i diversi tipi di stelle (cfr. parte I).

È così possibile giungere alla conclusione che nel 56% dei casi non si ha la *frammentazione completa* del nucleo e che le restanti stelle, escluso un 14% di attribuzione incerta, possono suddividersi secondo come indicato nella Tabella VII.

Le disintegrazioni ${}^{12}_6C(p; 3z, p)$; ${}^{14}_7N(p; 3z, d, p)$ e ${}^{16}_8O(p; 4z, p)$ sono individuabili con buona precisione poichè, essendo emesse solo particelle cariche, è possibile controllarle mediante la conservazione dell'impulso e dell'energia.

Le stelle $5r$ in N possono attribuirsi ai due schemi indicati nella Tabella VII (a causa della relativa povertà dei dati sperimentali non vengono distinte): dalle nostre osservazioni sembra che circa la metà di esse sono attribuibili al primo schema per il quale è possibile il controllo di cui si è detto.

Il controllo da noi eseguito è anche conferma dell'esattezza dei criteri adot-

TABELLA VII. — *Percentuali dei modi di disintegrazione dei nuclei leggeri.*

$^{12}_6\text{C}$	4r	(p; 3 α ,)	$^{11}_2$ } 2.2	13.2 ± 2.6
	5r	(p; 2 α , 3p, 2n)		
$^{14}_7\text{N}$	5r	{ (p; 3 α , d, p) (p; 3 α , 2p, n)	2.8 } 1.1	3.9 ± 1.4
	6r	(p; 2 α , 4p, 3n)		
$^{16}_8\text{O}$	5r	(p; 4 α , p)	4.4 } 6.6 } 0.6 } 0.6 }	12.2 ± 2.5
	6r	(p; 3 α , 3p, 2n)		
	7r	(p; 2 α , 5p, 4n)		
	8r	(p; α , 7p, 6n)		

tati per separare le stelle secondo la loro origine (in elementi pesanti o leggeri) e per distinguere i protoni dalle particelle α .

Ci si deve attendere che la frequenza delle disintegrazioni nei diversi elementi della emulsione dipenda essenzialmente dalla loro abbondanza relativa: ciò è valido per il totale delle disintegrazioni osservate mentre il confronto può farsi solo per le stelle in cui non viene emesso un frammento e per le quali è stata possibile l'attribuzione ai diversi elementi: esse costituiscono circa il 30% di tutte le disintegrazioni prese in considerazione.

Poichè tutte le stelle di attribuzione incerta sono fra le 4r e le 5r, viene sottovalutata la prima delle disintegrazioni in C e le 5r in O rispetto alle 6r.

Entro tali limiti si può affermare che mentre le quantità di C, N, O stanno come 4.7 : 1 : 3.5 le stelle attribuite ai diversi elementi stanno come 3.4 : 1 : 3.1. Nei limiti degli errori sperimentali il confronto è soddisfacente.

* * *

Ci è gradito ringraziare i Ch.mi Proff. V. POLARA e G. CORTINI per l'interesse prestato al presente lavoro e le utili discussioni sull'argomento.

SUMMARY

The nuclear disintegrations produced in the light elements (C, N, O) of Ilford G5 600 μm emulsions by 140 MeV protons have been studied. 220 stars (of which 108 found by systematic scanning) have been examined. The most reliable values of some characteristic parameters, in the examined process of disintegration, resulting from the data of the present work and from those of others, are here given. The disintegrations produced in the various elements are recognized: these are in accordance with the α -particle model of the light nuclei and with the proposed schemes. Such schemes give an explanation for about 45% of the occurred disintegrations, in the remaining cases there is the emission of some particles (by local evaporation, e.g.) and of a fragment ($Z \geq 3$). It seems that the frequency of the disintegrations in the various elements depends essentially on their abundance in the emulsion.

Statistical Approach to the Domain of Action of Collective Co-ordinates in the Many Body Problem (*) (1).

J. K. PERCUS and G. J. YEVICK

Walter Kilde Laboratory of Physics, Stevens Institute of Technology - Hoboken, New Jersey

(ricevuto il 15 Dicembre 1956)

Summary. — The collective co-ordinates have a mathematical boundary whose nature is investigated in this paper. This is accomplished by comparing expressions for the partition function in collective co-ordinate space and configuration co-ordinate space. The resulting decomposition of the collective space into two-dimensional subspaces, whose extent is independent of wave-number, permits approximation to many body correlations. It also implies a new simple approximation to the many body partition function, some consequences of which are examined.

Introduction.

In preceding papers (2), the role of the collective co-ordinate $q_k = \sum_i \exp[ik \cdot r_i]$ for analyzing the classical many body problem was indicated. We have also touched upon the peculiar mathematical properties of the q_k — in particular, the boundedness of q_k . Preliminary calculations (3) based on random walk considerations show that each q_k , while mathematically limited in magnitude to the value N (the number of particles), spends most of its time around zero, with a standard deviation of the order of \sqrt{N} . In any approximation method

(*) Supported by Office of Naval Research, Contract NONR 26311, NR 017617.

(1) Portions of this paper were first presented at the Washington Meeting of the American Physical Society, April, 1954. See *Phys. Rev.*, **95**, 624 A (1954).

(2) G. J. YEVICK and J. K. PERCUS: *Phys. Rev.*, **101**, 1186 (1956), Paper I; J. K. PERCUS and G. J. YEVICK: *Phys. Rev.*, **101**, 1192 (1956), Paper II.

(3) J. K. PERCUS and G. J. YEVICK: *Dynamical Lagrangian for the Many Body Problem* (Paper III), recently submitted to *Nuovo Cimento*.

for treating the many body problem, using the q_k , the precise domain of action is clearly a matter of great importance. This is especially true in quantum mechanics.

The basic idea in this paper is to express the partition function both in q -space and in configuration space, and then to compare the two, each suggesting approximations to be made in the other. In this way, for example, we obtain the moments of the q_k , which if exact are sufficient to map out the boundary in q -space. The approximate decomposition into two dimensional subspaces carried out here presumably washes out fine details of the boundary, but its justification can only come by the fruit it yields.

An immediate result of the above decomposition is an approximate evaluation of the partition function. This evaluation depends upon the self-consistent computation of a number of parameters, an analysis of which will be deferred to a succeeding paper. However, application is made to the case of low density fluids, and to the general problem of many body correlations, in order to indicate qualitative bounds on the validity of the present treatment.

1. - Summary of previous results.

We review, with slight modification, the formulation developed in Paper III ⁽³⁾. The many body problem to be considered is represented by the Lagrangian

$$(1) \quad L_x = \frac{1}{2} \sum_i m \dot{x}_i^2 - \frac{1}{2} \sum_i \sum_{j \neq i} V(x_i - x_j),$$

where x_i is the co-ordinate of the i -th particle located in a one-dimensional periodic box of length L ; L_x is now replaced by a « dynamical » Lagrangian given by

$$(2) \quad L_q = \frac{1}{2} \sum_{\{k\}} \left\{ \frac{\mu_k}{Nk^2} |\dot{q}_k|^2 - \nu_k |q_k|^2 \right\} + \frac{N}{2} \sum_{\{k\}} \nu_k + \frac{1}{2} N \mu_0 \dot{X}^2,$$

where X is the center of mass and q_k is the collective co-ordinate defined by

$$(3) \quad q_k \equiv \sum_i \exp[ikx_i].$$

Moreover, the μ_k and ν_k are specified by

$$(4) \quad \mu_k = (mN \sum_{\{l\}} \sigma_{kl}^{-1}) / (\sum_{\{l\}} \sigma_{ll}^{-1})$$

and

$$(5) \quad \nu_k = \sum_{\{l\}} \sigma_{kl}^{-1} (V\sigma)_l,$$

where $(V\sigma)_l$ is the l -th Fourier component of $V(x)\sigma(x)$. If N is the number of particles in the box, then the set $\{k\}$ consists of any N integral multiples of $k_0 = 2\pi/L$ with the restriction that the presence of k in the set implies that of $-k$; further we assume $k = 0$ to be included in $\{k\}$. The function $\sigma(x)$ denotes the two particle distribution function defined for near equilibrium conditions by

$$(6) \quad \lim_{T \rightarrow \infty} \frac{1}{T} \int_0^T g(x_i, x_j) dt = \frac{1}{L^2} \iint g(x_i, x_j) \sigma(x_i - x_j) dx_i dx_j,$$

for an arbitrary function g . The matrix $\sigma = (\sigma_{kl})$ is defined as that of the Fourier components of $\sigma(x)$:

$$(7) \quad \sigma_{kl} = \sigma_{k-l} = \frac{1}{L} \int_{-L/2}^{L/2} \sigma(x) \exp[i(k-l)x] dx.$$

2. - Partition function in x and q space.

We shall find it convenient to employ the real variables

$$(8) \quad c_k = \frac{q_k + q_k^*}{2}, \quad s_k = \frac{q_k - q_k^*}{2i};$$

the Lagrangian of (2) now becomes

$$(9) \quad L(\{c_k, s_k\}, \dot{X}) = \sum_{\{k>0\}} \left(\frac{\mu_k}{Nk^2} \dot{c}_k^2 - \nu_k c_k^2 \right) + \sum_{\{k>0\}} \left(\frac{\mu_k}{Nk^2} \dot{s}_k^2 - \nu_k s_k^2 \right) + N \sum_{\{k>0\}} \nu_k - \frac{1}{2} N(N-1) \nu_0 + \frac{1}{2} N \mu_0 \dot{X}^2.$$

The Hamiltonian for (9) is as follows:

$$(10) \quad H_q = \sum_{\{k>0\}} \left(\frac{Nk^2}{4\mu_k} \dot{\chi}_k^2 + \nu_k c_k^2 \right) + \sum_{\{k>0\}} \left(\frac{Nk^2}{4\mu_k} \dot{\Xi}_k^2 + \nu_k s_k^2 \right) - N \sum_{\{k>0\}} \nu_k + \frac{1}{2} N(N-1) \nu_0 + \frac{1}{2} \frac{P^2}{N\mu_0}.$$

where

$$(11) \quad \chi_k = \partial L / \partial \dot{c}_k, \quad \Xi_k = \partial L / \partial \dot{s}_k \quad \text{and} \quad P = \partial L / \partial \dot{X}.$$

The partition function in q -space may now be written as

$$(12) \quad Z_q = \frac{1}{h^N} \left\{ \exp \left[-\theta \left(\frac{1}{2} N(N-1) v_0 - N \sum_{\{k>0\}} \nu_k \right) \right] \cdot \right. \\ \cdot \int \dots \int \exp [-\theta P^2 / 2N\mu_0] dX dP \prod_{\{k>0\}} \exp \left[-\frac{N\theta k^2 \chi_k^2}{4\mu_k} \right] d\chi_k \cdot \\ \cdot \prod_{\{k>0\}} \exp \left[-\frac{N\theta k^3 \Xi_k^2}{4\mu_k} \right] d\Xi_k \prod_{\{k>0\}} \exp [-\theta \nu_k (c_k^2 + s_k^2)] dc_k ds_k \left. \right\}.$$

The integrals over P , χ_k , and Ξ_k are easy to evaluate. Eq. (12) is transformed into

$$(13) \quad Z_q(\theta, L) = \frac{1}{h^N} \left(\frac{2\pi N\mu_0}{\theta} \right)^{\frac{1}{2}} \left\{ \prod_{\{k>0\}} \frac{4\pi\mu_k}{N\theta k^2} \right\} \cdot \\ \cdot \left\{ \exp \left[-\theta \left(\frac{1}{2} N(N-1) v_0 - N \sum_{\{k>0\}} \nu_k \right) \right] \right\} \cdot \\ \cdot \int \dots \int \prod_{\{k>0\}} \exp [-\theta \nu_k (c_k^2 + s_k^2)] dc_k ds_k \cdot dX.$$

We shall also require the partition function in absolute space, which is given by

$$(14) \quad Z_r(\theta, L) = \frac{1}{N!} \left(\frac{2m\pi}{\theta h^2} \right)^{N/2} \int \dots \int \exp \left[-\frac{\theta}{2} \sum_{i \neq j} V(x_i - x_j) \right] dx^N,$$

where the momentum dependence has been integrated out. In (13) and (14), θ denotes $1/KT$.

3. - Comparison of partition functions.

According to the Lagrangian of Eq. (2), the q_k behave, locally, as independent harmonic oscillators. However, as we have discussed in Papers I and III, the volume in q_k -space is not just the direct product of intervals along the q_k -axes; thus the boundary which a given q_k will see depends upon the location of the other q_k 's. If one takes a long time exposure, appropriate for an equilibrium state, of the space available for the pair q_k, q_{-k} , a function $g_k(q_k, q_{-k})$ results which according to the analysis of Paper III, extends to

about $|q_k|^2 = N$. Thus, in the picture in which the pairs (q_k, q_{-k}) , and the single co-ordinate X , are regarded as independent entities, the decomposition of the integral in Eq. (13) is to be written as

$$(15) \quad \int \dots \int \prod_{\{k>0\}} \exp[-\theta \nu_k (c_k^2 + s_k^2)] dc_k ds_k \cdot dX = \\ = \int 1 \cdot dX \prod_{\{k>0\}} \int \int \exp[-\theta \nu_k (c_k^2 + s_k^2)] g_k(c_k, s_k) dc_k ds_k \cdot$$

It was noted in Paper III that the μ_k of Eq. (4) may be taken as close to m . Since $\sum_{\{k\}} \mu_k = Nm$, we then have

$$\left(\prod_{\{k\}} \mu_k \right)^{1/N} = m \prod_{\{k\}} \exp \left[\frac{1}{N} \ln \left(1 + \frac{\mu_k - m}{m} \right) \right] = \\ = m \exp \left[\frac{1}{N} \sum_{\{k\}} \frac{\mu_k - m}{m} + \frac{1}{2N} \sum_{\{k\}} \left(\frac{\mu_k - m}{m} \right)^2 + \dots \right] = m \exp \left[\frac{1}{2N} \sum_{\{k\}} \left(\frac{\mu_k - m}{m} \right)^2 + \dots \right] -$$

and so through first order terms,

$$(16) \quad \left(\prod_{\{k\}} \mu_k \right)^{1/N} = m ;$$

it develops that the precise value of this product is not crucial to the ensuing discussion. Finally, then, we may rewrite Eq. (13) as

$$(17) \quad Z_o(\theta, L) = N^{\frac{1}{2}} \prod_{\{k>0\}} \left(\frac{2}{Nk^2} \right) \left(\frac{2m\pi}{\theta h^2} \right)^{N/2} \exp \left[-\frac{1}{2} \theta N(N-1) \nu_0 \right] \cdot \\ \cdot \int 1 \cdot dX \prod_{\{k>0\}} \int \int \exp[-\theta \nu_k (c_k^2 + s_k^2) + N\theta \nu_k] g_k(c_k, s_k) dc_k ds_k \cdot$$

Let us now focus our attention on $Z_r(\theta, L)$ in Eq. (14), which we wish to write in a form in which comparison may be made with Eq. (17). This end is achieved first by noting again the fact implicit in the transition from Eq. (1) to Eq. (2): for equilibrium processes, we may replace $V(x)$ by $V^*(x)$ defined by

$$(18) \quad V^*(x) = \sum_{\{k\}} \nu_k \exp[ikx] .$$

Next, the transformation law for the volume element from x -space to q -space

may be written as

$$(19) \quad dx^N = N! J \left(\frac{x}{c, s, X} \right) \prod_{\{k>0\}} dc_k ds_k \cdot dX,$$

where $J(x/c, s, X)$ is the Jacobian for the transformation, and where we have used the fact that a single traversal of x -space spans q -space $N!$ times. Employing Eqs. (18) and (19), one readily finds that Eq. (14) may be written as

$$(20) \quad Z_x(\theta, L) = \left(\frac{2m\pi}{\theta\hbar^2} \right)^{N/2} \exp \left[-\frac{1}{2} \theta N(N-1)v_0 \right] \cdot \\ \cdot \int \dots \int \prod_{\{k>0\}} \exp [-\theta v_k(c_k^2 + s_k^2 - N)] J(x/c, s, X) \prod_{\{k>0\}} dc_k ds_k \cdot dX.$$

Assuming the identity of Eqs. (17) and (20) establishes the relation between $g_k(c_k, s_k)$ and $J(x/c, s, X)$: except for normalization, $g_k(c_k, s_k)$ may be regarded as the dynamical projection of $J(x/c, s, X)$ onto the c_k, s_k plane, and indeed in the present approximation, J is the product of its projections. This is, of course, consistent with our original picture of $g_k(c_k, s_k)$.

We proceed next to examine more closely the decomposability implied by Eqs. (17) and (20), thereby setting the stage for the evaluation of both g_k and $Z(\theta)$.

4. - Decomposition of the partition function.

In this section we shall analyze the factor in Eq. (20) given by

$$(21) \quad \int \dots \int \prod_{\{k>0\}} \exp [-\theta v_k(c_k^2 + s_k^2)] J(x/c, s, X) \prod_{\{k>0\}} dc_k ds_k \cdot dX = \\ = N! \int \dots \int \prod_{\{k>0\}} \exp [-\theta v_k Q_k^2] dx^N,$$

where

$$(22) \quad Q_k^2 \equiv q_k l_k^* = \sum_{i,j} \exp [ik(x_i - x_j)].$$

To the extent that the decomposition of the Jacobian into the g_k is kinematic, the g_k will be independent of the v_k ; the form of Eq. (17) then implies that each factor $\exp [-\theta v_k Q_k^2]$ in Eq. (21) should contribute separately to the value of the integral. Let us now examine the nature of the argument which is required to produce such a decomposition of the x -space integral (21).

For the purpose at hand, it is sufficient to evaluate integrals of the form

$$(23) \quad L^{-N} \int \dots \int \prod_{\alpha=1}^n (q_{k_{\alpha}}) dX^N;$$

here the k_{α} need not be distinct. We may expand the product in the integrand of Eq. (23) in the following manner. Let $\{R_1, R_2 \dots R_N\}$ be a decomposition into ordered subsets, some of which may be empty, of the set of $\{k_{\alpha}\}$; we assume for convenience that no k_{α} is zero. Then from the definition (3) of q_k , it is clear that Eq. (23) may be written as the sum over decompositions:

$$(24) \quad \sum_{\text{decomp.}} L^{-N} \int \dots \int \exp \left[i \sum_{j=1}^N \left(\sum_{k_{\alpha_j} \in R_j} k_{\alpha_j} \right) x_j \right] dx^N.$$

In order to analyze Eq. (24), we shall assume explicitly that the wave-number spectrum is of a «random» type, containing numerous gaps, as in Paper II; the extent to which one is justified in making this assumption must be found in the results of the theory. Now the separate terms in Eq. (24) integrate to either unity or zero, with unity occurring only if the coefficient of each x_i vanishes. But since the set of all $\{k\}$ in the spectrum is of random type, except for the enforced pairing of k and $-k$, the only vanishing linear combinations of k_{α} which are present in profusion are those which vanish strictly by virtue of being composed of vanishing pairs $k, -k$. Thus, we may assume that each R_i consists of a set S_i together with its set of reversed sign wave numbers \bar{S}_i ; two consequences stem from this fact.

First, the complete set of $\{k_{\alpha}\}$ must likewise decompose into reversed-sign pairs, which means that the only integrals of type (23) which are significantly different from zero can be written as

$$(25) \quad L^{-N} \int \dots \int \prod_{k>0} (Q_k^2)^{n_k} dX^N.$$

Next, since each k multiplying an x_i must be associated with a $-k$, a given decomposition may be indicated diagrammatically by a set of directed «momentum» loops, an entering or exiting arrow corresponding to k or $-k$; a typical example is shown in Fig. 1. Now, the distinct k 's at a given vertex x_i are totally unrelated; this means that the total number of diagrams is the product of the number containing only k_1 loops, the number containing only k_2 loops, etc. In other words,

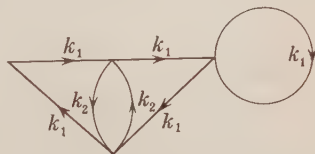


Fig. 1. — A typical term for the integration of $(Q_{k_1}^2)^5 (Q_{k_2}^2)^2$.

we conclude that

$$(26) \quad L^{-N} \int \dots \int \prod_{k \neq 0} (Q_k^2)^{n_k} dx^N = \prod_{k > 0} \left[L^{-N} \int \dots \int (Q_k^2)^{n_k} dx^N \right],$$

so that as far as x -space integration is concerned, the Q_k^2 may be regarded as independent variables.

Finally, we apply Eq. (26), through Eq. (21), to the evaluation of Z_x in Eq. (20), and obtain at once

$$(27) \quad Z_x(\theta, L) = \frac{L^N}{N!} \left(\frac{2m\pi}{\theta k^2} \right)^{N/2} \exp \left[-\frac{1}{2} \theta N(N-1) \nu_0 \right] \cdot \prod_{\{k > 0\}} \frac{1}{L^N} \int \dots \int \exp [-\theta \nu_k (Q_k^2 - N)] dx^N.$$

5. - Extent of q -space.

Having now shown that as a result of the gap spectrum of wave numbers, the q -space decomposition is ν_k -independent and thus essentially kinematical, we are prepared to evaluate the function g_k of Eq. (15) which determines the space available to a pair q_k, q_{-k} . A comparison of Eqs. (17) and (27), an identity in θ and the ν_k , tells us at once that, except perhaps for normalization,

$$(28) \quad \iint \exp [-\theta \nu_k Q_k^2] g_k(c_k, s_k) dc_k ds_k = (e/2N)(\langle k \rangle L)^2 L^{-N} \int \dots \int \exp [-\theta \nu_k Q_k^2] dx^N;$$

the $e/2N$ factor in Eq. (28) arises from using the Stirling approximation for $(N!)^{2/(N-1)}$, and $\langle k \rangle$ denotes the geometric mean of the set $\{k \neq 0\}$. Since Eq. (28) is an identity in θ , the exponential may be replaced by an arbitrary function of Q_k^2 . Let us further observe that a shift of origin of x -space, serving to rotate the pair c_k, s_k , can have no physical effect in a translation invariant system; thus g_k can be a function only of the magnitude Q_k , and not of the « angle » $\varphi_k = \text{tg}^{-1}(s_k/c_k)$. Hence Eq. (28) takes the form

$$(29) \quad \int_0^\infty f(Q_k^2) g_k(Q_k) Q_k dQ_k = (e/4\pi N)(\langle k \rangle L)^2 L^{-N} \int \dots \int f(Q_k^2) dx^N.$$

There remains only the problem of extracting g_k from Eq. (29).

A simple combinatorial argument is utilized in Appendix I to prove that

$$(30) \quad L^{-N} \int \dots \int Q_k^{2n} dx^N = (-)^n (n!)^2 \text{ coef. } y^n \text{ in } (J_0(2\sqrt{y}))^N;$$

since Eq. (30) is independent of k , $g_k(Q)$ should likewise be independent of k , and this validates the normalization used in Eq. (29). We then have, employing Eqs. (29) and (30),

$$(31) \quad \int_0^\infty J_0(2\sqrt{Q^2 y}) g(Q) Q dQ = (e/4\pi N) (\langle k \rangle L)^2 L^{-N} \int \dots \int J_0(2\sqrt{Q^2 y}) dJ^N \\ = (e/4\pi N) (\langle k \rangle L)^2 L^{-N} \sum_{n=0}^\infty (-)^n y^n / (n!)^2 \int \dots \int Q^{2n} dx^N = \\ = (e/4\pi N) (\langle k \rangle L)^2 (J_0(2\sqrt{y}))^N.$$

Applying a Bessel transform (4) to Eq. (31), there results

$$(32) \quad g(Q) = (e/2\pi N) (\langle k \rangle L)^2 \int_0^\infty J_0(2\sqrt{Q^2 y}) (J_0(2\sqrt{y}))^N dy;$$

an asymptotic evaluation of the integral on the right hand side of Eq. (32) presented in Appendix II, finally yields

$$(33) \quad g(Q) = (e^3 2\pi N^2) (\langle k \rangle L)^2 \exp[-Q^2/N] \left(1 - \frac{1}{2N} h(Q^2/N)\right),$$

where h has leading term unity. Eq. (33) is the basic result of this section.

One observes that the domain of action represented by $g(Q)$ is independent of k , and for all practical purposes, extends only to $Q \sim \sqrt{N}$; these results coincide with those obtained in Paper III. In fact, the characteristic dependence of $\exp[-Q^2/N]$ is precisely that which was given by the random walk interpretation. Regarding $g(Q)$ as a projection of the Jacobian, its form coincides with that obtained by other investigators (5,6), in a somewhat different context.

(4) W. MAGNUS and F. OBERHETTINGER: *Special Functions of Mathematical Physics* (Chelsea, 1949), p. 136.

(5) D. PINES and D. BOHM: *Phys. Rev.*, **85**, 352 (1952).

(6) A. A. BROYLES: *Phys. Rev.*, **100**, 1184 (1955).

6. - Effect of decomposability on many-body correlations.

The decomposability of q -space into two-dimensional subspaces and the rewriting of the kernel of the partition function integral in terms of the q_k , while of clear computational aid, have thus far been given only limited physical significance. Although our formalism has been centered on the two-body correlation function and should not be required to predict more than this, it does make definite statements as to higher correlations, which should yield further information as to the approximations actually involved and the limitations of the present simplified approach.

The instantaneous s -body distribution function is clearly given by

$$(34) \quad \varrho(y_1, y_2, \dots, y_s) = \frac{(N-s)!}{N!} \sum_{i_1 \neq i_2 \neq \dots \neq i_s} \delta(y_1 - x_{i_1}) \dots \delta(y_s - x_{i_s});$$

taking Fourier components, we readily find that for $s = 1, 2, 3, 4, \dots$

$$(35) \quad \left\{ \begin{aligned} L\rho_k &= \frac{1}{N} q_k, \\ L^2\rho_{kl} &= \frac{1}{N(N-1)} [q_k q_l - q_{k+l}], \\ L^3\rho_{klm} &= \frac{1}{N(N-1)(N-2)} [q_k q_l q_m - \sum q_k q_{l+m} + 2q_{k+l+m}], \\ L^4\rho_{klmn} &= \frac{1}{N(N-1)(N-2)(N-3)} [q_k q_l q_m q_n - \sum q_k q_l q_{m+n} + \\ &\quad + \sum q_{k+l} q_{m+n} + 2 \sum q_{k+l+m} q_n - 6q_{k+l+m+n}], \end{aligned} \right.$$

and so forth. In computing the mean distributions over time or phase space, we recognize that for a translation invariant state, $\varrho_{k_1 \dots k_s} = 0$ unless $\sum k_j = 0$; hence

$$(36) \quad \left\{ \begin{aligned} L\langle \varrho_k \rangle &= \delta_{k,0}, \\ L^2\langle \varrho_{kl} \rangle &= \frac{1}{N(N-1)} [\langle q_k q_k^* \rangle - N] \delta_{k+l,0}, \\ L^3\langle \varrho_{klm} \rangle &= \frac{1}{N(N-1)(N-2)} [\langle q_k q_l q_m \rangle - \sum \langle q_k q_k^* \rangle + 2N] \delta_{k+l+m,0}, \\ L^4\langle \varrho_{klmn} \rangle &= \frac{1}{N(N-1)(N-2)(N-3)} [\langle q_k q_l q_m q_n \rangle - \sum \langle q_k q_l q_{k+l}^* \rangle + \\ &\quad + \sum \langle q_{k+l} q_{k+l}^* \rangle + 2 \sum \langle q_k q_k^* \rangle - 6N] \delta_{k+l+m+n,0}, \text{ etc.} \end{aligned} \right.$$

Thus far, all is exact. Now, since the kernel $\exp[-\theta \sum_{i>j} V(x_i - x_j)]$ of the partition function, which represents the canonical many body distribution, has been written (Eq. (17)) as a product of separate functions of $q_k q_k^*$, the argument of Sect. 4 tells us that in the present approximation, an average of the form $\langle q_{k_1} q_{k_2} \dots q_{k_n} \rangle$ is non-zero only if its factors separate into q_0 's and pairs $q_k q_k^* - q_l q_{-l}$. Indicating the quantities obtained in this way by bars, we now have

$$(37) \quad \langle \bar{q}_k \rangle = \langle q_k \rangle$$

$$\bar{q}_{kl} = q_{kl} \quad ,$$

but

$$L^3 \langle \bar{q}_{klm} \rangle = 1/N(N-1)(N-2) \cdot$$

$$\cdot [\sum N \delta_{k0} \langle q_l q_l^* \rangle - 2N^3 \delta_{k0} \delta_{l0} - \sum \langle q_k q_l^* \rangle + 2N] \delta_{k+l+m,0} \quad ,$$

with higher order distributions following in a similar manner. One notes that (37) does correspond to a sequence of many body distributions in the sense that integration over one particle yields the next lower distribution, as verified by

$$\langle \bar{q}_{k0} \rangle = \langle \bar{q}_k \rangle, \quad \langle \bar{q}_{kl0} \rangle = \langle \bar{q}_{kl} \rangle, \quad \text{etc.} \quad .$$

According to (37), the 3-body distribution is completely determined by the 2-body distribution, so that there is in a certain sense no «intrinsic» 3-body correlation. Such a concept is somewhat nebulous⁽⁷⁾ and so to fix our ideas, we reverse the Fourier transform⁽⁸⁾, and easily obtain

$$(38) \quad \langle \varrho(x, y, z) \rangle - \langle \bar{\varrho}(x, y, z) \rangle =$$

$$= N^2/(N-1)(N-2) \langle (\varrho(x) - 1/L)(\varrho(y) - 1/L)(\varrho(z) - 1/L) \quad .$$

One may argue that the relative deviation in Eq. (38) is generally small; it certainly is if space consists largely of regions in which one of the factors in Eq. (38) is uncorrelated with the product of the other two. As one goes to higher distributions, the mixed two body terms still predominate, many body correlations being crudely chains of two body correlations, and one approaches computation of quantities involving such higher order terms with increasing

⁽⁷⁾ For another form in which 2-body distributions determine 3-body distributions, see J. G. KIRKWOOD and E. M. BOGGS: *Journ. Chem. Phys.*, **10**, 394 (1942).

⁽⁸⁾ We imagine the wave number spectrum arranged e.g. to contain k, l, m when we are examining q_{klm} in detail; thus q_{klm} is «continuous» in k, l, m , etc.

trepidation. Nonetheless, specific many body terms, such as $\langle q_k q_k q_{-k} q_{-k} \rangle$, do make their appearance in our approximate formulation, so that « intrinsic » terms are not entirely neglected. One may conclude that a configuration space interpretation of the basic fact that « phonons » $q_{\pm k}$ of wave number $\pm k$ are regarded as interacting only with themselves is not wholly appropriate.

7. - Evaluation of the partition function.

Inserting the principal term in the asymptotic expression (33) for $g(\theta)$ into (17), we have

$$(39) \quad Z(\theta, L) = N^2 L^N / \sqrt{2} \left(\frac{4m\pi}{\theta \hbar^2 N^3} \right)^{N/2} \exp \left[-\frac{1}{2} \theta N(N-1) v_0 \right] \cdot \prod_{\{k>0\}} \int_0^\infty \exp \left[-\left(\theta v_k + \frac{1}{N} \right) (Q_k^2 - N) \right] Q_k dQ_k.$$

Before proceeding further, an interesting consequence of Eq. (39) should be pointed out. We have noted that the restricted domain of action for Q_k prevented a direct integration over c_k and s_k in the harmonic oscillator partition function (13); however, we now observe from (39) that the boundary effect may be completely simulated by replacing the force constant v_k in the integration by an effective force constant

$$(40) \quad v_k \rightarrow v'_k = v_k + 1/N\theta.$$

A similar result has been obtained by PINES and BOHM⁽⁹⁾.

The integration of (39) is readily accomplished⁽¹⁰⁾; taking logarithms, we then have

$$(41) \quad \ln Z(\theta, L) = \text{const} + N \ln (L\theta^{-\frac{1}{2}}) - \frac{1}{2} N(N-1) v_0 \theta + \sum_{\{k>0\}} (N\theta v_k - \ln (1 + N\theta v_k)),$$

from which the various thermodynamic parameters follow at once, as e.g.

$$(42) \quad C_v = k\theta^2 \partial^2 \ln Z / \partial \theta^2, \quad pL\theta = L \partial \ln Z / \partial L.$$

⁽⁹⁾ D. PINES and D. BOHM: op. cit., p. 353.

⁽¹⁰⁾ The integral appears to diverge when $v_k + 1/N\theta < 0$; a more careful treatment of $g(Q)$ shows it to be finite but large. However, the self-consistent formulation given below operates to minimize the occurrence of this situation.

Actual computation, however, awaits evaluation of the v_k which enter into Eq. (4.1), Eq. (5) then shifts the problem to the determination of the σ_k . But since the statistical state of the system is now known, σ_k is readily obtained. From the definition (6), it readily follows that $\sigma_k = L^2 \langle Q_{k, -k}^2 \rangle$, in the notation of Sect. 6. Hence

$$(43) \quad \sigma_k = 1/N(N-1)[\langle Q_k^2 \rangle - N];$$

since the only portion of the q -space partition function kernel which affects $\langle Q_k^2 \rangle$ is $\exp[-(\theta v_k + 1/N)(Q_k^2 - N)]$, we have for $k \neq 0$,

$$(44) \quad \sigma_k = \frac{\int_{-N}^{\infty} \exp[-(\theta v_k + 1/N)(Q_k^2 - N)](Q_k^2 - N) d(Q_k^2 - N)}{N(N-1) \int_{-N}^{\infty} \exp[-(\theta v_k + 1/N)(Q_k^2 - N)] d(Q_k^2 - N)}.$$

Integrating Eq. (44) and rewriting Eq. (5) in juxtaposition, the v_k and σ_k are thus determined by the « self-consistent » set

$$(45) \quad \begin{aligned} \sigma_k &= -(1/N - 1)N\theta v_k / (1 + N\theta v_k), & k \neq 0, \\ \sigma_0 &= 1, \\ \sum_{\{l\}} \sigma_{k-l} v_l &= (V\sigma)_k. \end{aligned}$$

At this point, it is convenient to consider the sound velocity at wave-number k . If q_k oscillates nearly harmonically in time at angular frequency ω_k , then clearly

$$(46) \quad \omega_k^2 = \langle \dot{q}_k \dot{q}_k^* \rangle / \langle q_k q_k^* \rangle.$$

But from $\dot{q}_k = ik \sum_i \dot{x}_i \exp[ikx_i]$, we have $\langle \dot{q}_k \dot{q}_k^* \rangle = Nk^2 \langle \dot{x}^2 \rangle = Nk^2/m\theta$; together with Eq. (43), this yields

$$(47) \quad \omega_k^2 = (1/m\theta)k^2 / (1 + (N-1)\sigma_k),$$

from which the velocity $v(k) = d\omega_k/dk$, or

$$(48) \quad v(k) = (m\theta)^{-\frac{1}{2}} (d/dk) k (1 + (N-1)\sigma_k)^{-\frac{1}{2}}.$$

It is of interest to note that, using Eq. (45), Eq. (47) becomes

$$(49) \quad \omega_k^2 = (Nk^2/m)(v_k + 1/N\theta);$$

referring to Eq. (2), this is the oscillation frequency which would be expected for $\mu_k = m$ as in Eq. (16), and the modified force term given by Eq. (40).

We return to the evaluation of the partition function. This requires solution of the set (45), which for a given $V(x)$ is trivial in principle but scarcely so in practice; relevant techniques will be treated in detail in a following paper. For the present, it will suffice to examine a special case, that of the low density limit. For low density, as is well known⁽¹¹⁾, the (nearly normalized) 2-body distribution function is given by the Boltzmann factor:

$$(50) \quad \sigma(x) = \exp[-\theta V(x)] .$$

We shall require σ_k as $k \rightarrow 0$, which for a potential which is asymptotically zero, becomes

$$(51) \quad \lim (k \rightarrow 0) \sigma_k = \beta_1(\theta)/L ,$$

where

$$\beta_1(\theta) = \int (\exp[-\theta V(x)] - 1) dx ;$$

β_1 is the 2-body cluster integral of the Ursell cluster expansion⁽¹²⁾. It follows from Eq. (45) that (assuming continuous v_k)

$$(52) \quad v_0 = -(\beta_1/L\theta)/(1 + N\beta_1/L) .$$

But for low density, Eq. (41) reduces to

$$(53) \quad \ln Z(\theta, L) = \text{const} + N \ln (L\theta^{-\frac{1}{2}}) - \frac{1}{2}N^2\theta v_0 ;$$

comparing with the standard cluster expansion⁽¹²⁾

$$(54) \quad \ln Z(\theta, L) = \text{const} + N \ln (L\theta^{-\frac{1}{2}}) + \left[\frac{\beta_1 N^2}{2L} + \frac{\beta_2 N^3}{3L^2} + \dots \right] ,$$

we observe that the v_0 term includes all 2-body cluster effects and introduces some 3-body terms as well. Finally, we compare the hydrodynamic sound velocity at constant temperature

$$(55) \quad c = (\partial p / \partial \rho)^{\frac{1}{2}} = (mN\theta)^{-\frac{1}{2}} (-L^2 \partial^2 \ln Z / \partial L^2)^{\frac{1}{2}} ,$$

⁽¹¹⁾ H. S. GREEN: *Molecular Theory of Fluids* (New York, 1952), p. 75.

⁽¹²⁾ J. E. MAYER and M. G. MAYER: *Statistical Mechanics* (New York, 1940), p. 291.

with $c = c(0)$ from Eq. (48). Both yield precisely the same expression

$$(56) \quad c = (m\theta)^{-\frac{1}{2}}(1 + N\beta_1/L)^{-\frac{1}{2}},$$

to the order indicated, a useful check on internal consistency.

APPENDIX I

Evaluation of an integral.

In order (a) to evaluate the extent of q -space and (b) to obtain an approximate expression for the partition function, we must explicitly determine the following integral occurring in Eq. (26) of the body:

$$(1) \quad \left\{ \begin{aligned} D_n^N &= L^{-N} \int \dots \int Q_k^{2N} dx^N, \\ &= L^{-N} \int \dots \int \sum_{i,j} \exp[ik(x_i - x_j)]^n dx^N, \\ &= L^{-N} \int \dots \int \sum_{\{i_\alpha\}\{j_\alpha\}} \exp\left[ik \sum_{\alpha=1}^n (x_{i_\alpha} - x_{j_\alpha})\right] dx^N. \end{aligned} \right.$$

We observe immediately that, since $k \neq 0$, any x_{i_α} which is present in Eq. (1) must be matched by an identical x_{j_β} , for the integration over an unmatched x_i yields zero. Thus the $\{j_\alpha\}$ must be a permutation of $\{i_\alpha\}$. For each such permutation, the value of the integral will be one. Thus, we are left with the problem of determining the number of ways, D_n^N , that n integers, with repetitions allowed, may be chosen from 1 to N and then permuted. We shall show that D_n^N is given by

$$(2) \quad D_n^N = \sum_{\sum_{j=1}^N m_j = n} \left(\frac{n!}{m_1! \dots m_N!} \right)^2$$

To prove this, let m_j be the number of times that the integer j between 1 and N appears in the sequence $\{i_\alpha\}$ of n integers. Clearly this set $\{i_\alpha\}$ is one of $n!/m_1! \dots m_N!$ possible sequences for a given choince of $m_1 \dots m_N$. Likewise, the same is true for the $\{j_\alpha\}$. Therefore, for a particular choice of m 's with $\sum_{j=1}^N m_j = n$, the total number of possible pairs of sequences $\{i_\alpha\}$ and $\{j_\beta\}$ is $(n!)^2/(m_1! \dots m_N!)^2$. We conclude from this that D_n^N is given by (2).

We next note that D_n^N is also equal to $(n!)^2$ times the coefficient of y^n in $(\sum_{m=0}^{\infty} y^m/(m!)^2)^N$, or

$$(3) \quad D_n^N = (-)^n (n!)^2 \text{ coef. } y^n \text{ in } \left(\sum_{m=0}^{\infty} (-y)^m/(m!)^2 \right)^N \\ = (-)^n (n!)^2 \text{ coef. } y^n \text{ in } (J_0(2\sqrt{y}))^N.$$

Summing up, we have

$$(4) \quad L^{-N} \int \dots \int Q_k^{2N} dx^N = (-)^n (n!)^2 \text{ coef. } y^n \text{ in } (J_0(2\sqrt{y}))^N.$$

APPENDIX II

Evaluation of distribution function.

In order to obtain the distribution for the extent of q -space we have to evaluate the integral

$$(1) \quad K_N(Q) \equiv \int_0^{\infty} J_0(2\sqrt{Q^2 y} (J_0(2\sqrt{y}))^N dy.$$

We note that

$$(2) \quad J_0(2\sqrt{y}) = 1 - y + y^2/4 - y^3/36 + \dots$$

and

$$(3) \quad J_0(2\sqrt{y}) \exp[y] = 1 - y^2/4 - y^3/9 + \dots,$$

whence

$$(4) \quad J_0^N(2\sqrt{y}) = \exp[-Ny] (1 - Ny^2/4 - Ny^3/9 + \dots).$$

Thus

$$(5) \quad K_N(Q) = \int_0^{\infty} \exp[-Ny] (1 - Ny^2/4 - Ny^3/9 \dots) J_0(2\sqrt{Q^2 y}) dy.$$

Let us define

$$(6) \quad I(N) = \int_0^{\infty} \exp[-Ny] J_0(2\sqrt{xy}) dy;$$

therefore Eq. (5) becomes

$$(7) \quad K_N(Q) = I(N) - (N/4)I''(N) + (N/9)I'''(N) + \dots$$

But $I(N)$ is a well-known integral ⁽¹³⁾

$$(8) \quad I(N) = (1/N) \exp[-x/N];$$

we conclude then that

$$K_N(Q) = (1/N) \exp\left[\frac{-Q^2}{N}\right] \left(1 - \frac{1}{2N} \left(1 - \frac{2Q^2}{N} + \frac{1}{2} \left(\frac{Q^2}{N}\right)^2 + \dots\right)\right).$$

⁽¹³⁾ W. MAGNUS and F. OBERHETTINGER: *Special Functions of Mathematical Physics* (Chelsea, 1949), p. 131.

RIASSUNTO (*)

Le coordinate collettive hanno un contorno matematico la cui natura si esamina nel presente lavoro. A tal fine si confrontano le espressioni della funzione di partizione nello spazio delle coordinate collettive ed in quello delle coordinate di configurazione. La risultante decomposizione dello spazio collettivo in due sottospazi bidimensionali, la cui estensione è indipendente dal numero d'onde, consente di approssimare la funzione di partizione di più corpi. Ciò implica anche una nuova semplice approssimazione della funzione di partizione di più corpi, alcune conseguenze della quale si discutono.

(*) Traduzione a cura della Redazione.

Multiple Meson Production in the Cosmic Radiation.

E. LOHRMANN

*Hochspannungslaboratorium Hechingen - Germany
Physikalisches Institut der Universität - Bern*

(ricevuto il 20 Dicembre 1956)

Summary. — 6 jets were selected from about 250 found in cosmic ray plates with the aim to get events representing nucleon-nucleon collisions as closely as possible. Scattering measurements on the shower particles showed that the mean total energy of the mesons in the center of mass system was 0.35 GeV for about 100 GeV primary energy and 0.4 to 1 GeV for primary energies of 1000 GeV and more. A large fraction of the particles has small energies in the c.m.-system, thus favouring the Heisenberg theory of multiple meson production. No relation between the anisotropy of the angular distribution in the c.m.-system and the inelasticity was found. The inelasticity seems to vary within wide limits. An analysis of the angular distribution of 6 further jets presumably produced by mesons was carried out. The mean energy of these jets was 200 GeV. The angular distribution in the c.m.-system is isotropic within the limits of error.

1. - Introduction.

During the last years a considerable amount of work has been published on multiple meson production by high energy particles of the cosmic radiation in nuclear emulsions (^{1-29,37}). The analysis of these high energy stars (jets)

(1) A. ENGLER, U. HABER-SCHAIM and W. WINKLER: *Nuovo Cimento*, **12**, 930 (1954).

(2) R. G. GLASSER, D. M. HASKIN, M. SCHEIN and J. J. LORD: *Phys. Rev.*, **99**, 1555 (1955).

(3) K. GOTTSTEIN and M. TEUCHER: *Zeits. f. Naturforsch.*, **8a**, 120 (1953).

(4) C. C. DILWORTH, S. J. GOLDSACK, T. F. HOANG and L. SCARSI: *Nuovo Cimento*, **12**, 1261 (1953).

(5) T. F. HOANG: *Journ. Phys. et Rad.*, **15**, 337 (1954).

(6) D. LAL, YASH PAL, B. PETERS and M. S. SWAMY: *Phys. Rev.*, **87**, 545 (1952).

is complicated by the fact that most collisions occur between a nucleon of the cosmic radiation and some heavier nucleus of the emulsion. It is then generally assumed that at very high energies part of the mesons are produced in a collision between the primary and one of the nucleons of the nucleus. The picture of a pure nucleon-nucleon (N-N) collision is then falsified by subsequent collisions inside the nucleus of the mesons produced in the primary act, which will lead to scattering and production of more mesons. In most of the work published it was attempted to minimize this influence of secondary interactions by selecting stars with not more than 4 grey or black prongs. This would indicate that the excitation transferred to the nucleus and hence the influence of secondary collisions are small. This assumption can furthermore be controlled by measuring the energy of the shower particles, which will also give additional information on the mechanism of the multiple production. Little is known in the high-energy region up to now so we have analyzed 3 jets of about 100 GeV primary energy and 3 jets with energies $\gtrsim 1000$ GeV by

-
- (7) T. F. HOANG: *Journ. Phys. et Rad.*, **14**, 395 (1953).
 (8) D. LAL, YASH PAL and RAMA: *Suppl. Nuovo Cimento*, **12**, 347 (1954).
 (9) C. C. DILWORTH, S. J. GOLDSACK, T. F. HOANG and L. SCARSI: *Nuovo Cimento*, **11**, 424 (1954).
 (10) C. C. DILWORTH, S. J. GOLDSACK, T. F. HOANG and L. SCARSI: *Compt. Rend.*, **236**, 1551 (1953).
 (11) D. HOPPER, S. BISWAS and J. F. DARBY: *Phys. Rev.*, **84**, 457 (1951).
 (12) M. DEMEUR, C. C. DILWORTH and M. SCHÖNBERG: *Nuovo Cimento*, **9**, 92 (1952).
 (13) R. R. DANIEL, J. DAVIES, J. H. MULVEY and D. H. PERKINS: *Phil. Mag.*, **43**, 753 (1952).
 (14) E. PICKUP and L. VOYVODIC: *Phys. Rev.*, **84**, 1190 (1951).
 (15) J. J. LORD, J. FAINBERG and M. SCHEIN: *Phys. Rev.*, **80**, 970 (1950).
 (16) D. LAL, YASH PAL, B. PETERS and M. S. SWAMY: *Proc. Ind. Acad. Sci.*, **36**, 75 (1952).
 (17) J. H. MULVEY: *Proc. Roy. Soc., A* **221**, 367 (1954).
 (18) J. E. NAUGLE and P. S. FREIER: *Phys. Rev.*, **92**, 1086 (1953).
 (19) H. L. BRADT, M. F. KAPLON and B. PETERS: *Helv. Phys. Acta*, **23**, 24 (1950).
 (20) C. CASTAGNOLI, G. CORTINI, C. FRANZINETTI, A. MANFREDINI and D. MORENO: *Nuovo Cimento*, **10**, 1539 (1953).
 (21) G. BERTOLINO and D. PESCIETTI: *Nuovo Cimento*, **12**, 630 (1954).
 (22) M. SCHEIN, R. G. GLASSER and D. M. HASKIN: *Nuovo Cimento*, **2**, 647 (1955).
 (23) G. BERTOLINO: *Nuovo Cimento*, **2**, 1130 (1955).
 (24) G. BERTOLINO: *Nuovo Cimento*, **3**, 141 (1956).
 (25) A. WATAGHIN: *Nuovo Cimento*, **4**, 154 (1956).
 (26) F. A. BRISBOUT, C. DAHANAYAKE, A. ENGLER, Y. FUJIMOTO and D. H. PERKINS: *Phil. Mag.*, **1**, 605 (1956).
 (27) L. V. LINDERN: *Zeits. f. Naturforsch.*, **11a**, 340 (1956).
 (28) E. LOHRMANN: *Zeits. f. Naturforsch.*, **11a**, 561 (1956).
 (29) A. DEBENEDETTI, C. M. GARELLI, L. TALLONE and M. VIGONE: *Nuovo Cimento*, **4**, 1142 (1956).

measuring the angular distribution and the energy of the shower particles. Measurements in the low energy region should be useful to check the assumptions made above by comparison with jets produced by artificially accelerated particles as soon as they become available. The aim of this investigation was to find out the fraction of the primary energy which is transferred to the mesons, and the angular and energy distributions in the center of mass (c.m.) system, assuming a primary N-N interaction.

2. - Selection of events.

All the jets selected had 3 or less grey or black prongs. The primary particles were all singly charged. The length of the shower in one plate had to be so large as to allow reasonable scattering measurements. All measurements (including multiple scattering) had to be consistent with the assumption of a N-N-collision (symmetry in the c.m. system, see also ref. ^(5,2,7,27)). The number of shower particles had to be > 10 to allow a statistically significant treatment for the individual events. 6 jets from a total of 250 events with energies > 40 GeV found in 3 stacks of stripped emulsions complied with these conditions. No conclusions whatsoever can be drawn on the prong number distribution or the distribution of the inelasticity, as one must expect a severe scanning bias in this kind of work. This bias should also be energy dependent, as a highly collimated jet is not so easily overlooked as one of lower energy.

3. - Measuring procedure.

Particles having relatively great angles in the laboratory-(L)-system were expected to have low energies. Their scattering was measured directly. Elimination of spurious scattering was made after the proposal of ref. ⁽³⁰⁾ and ⁽²⁸⁾ by determining the spurious scattering from tracks of very high energy in the same region of the plate, having about the same direction and the same dip. A signal to noise ratio of 2 was demanded, else the measurement was assumed to give a lower limit only. The particles with small angles in the L-system should have high energies. They were determined by relative scattering measurements. It was confirmed that spurious scattering could be neglected in these cases as long as the separation between the tracks did not exceed 40μ ⁽³¹⁾. This was the maximum separation of all tracks measured in the horizontal

⁽³⁰⁾ F. A. BRISBOUT, C. DAHANAYAKE, A. ENGLER, P. H. FOWLER and P. B. JONES: *Nuovo Cimento*, **3**, 1400 (1956).

⁽³¹⁾ S. BISWAS, B. PETERS and RAMA: *Proc. Ind. Acad. Sci.*, **A 41**, 154 (1955).

as well as in the vertical direction. No correlation between the distance between the tracks and their scattering could be found in this case. In order to get the necessary signal to noise ratio, very long cells had to be used. Thus the statistical error of the measurement of an individual track was as a rule rather large, so that in many cases only the mean energy of a group of particles could be stated in a meaningful way.

4. - Angular distribution and primary energy.

The primary energy was deduced from the angular distribution of the shower particles. As a first approximation the method of CASTAGNOLI *et al.* ⁽²⁰⁾ was used giving:

$$\ln \gamma_s = -\frac{1}{n_s} \sum_i \ln \operatorname{tg} \vartheta_{Li},$$

γ_s : total energy of the nucleon in the c.m.-system in units of its rest energy:

ϑ_{Li} : angle of the i -th shower particle in the L-system.

The results were in all cases in accord with the « half angle formula »

$$\gamma_s = 1/\operatorname{tg} \vartheta_{L\frac{1}{2}};$$

$\vartheta_{L\frac{1}{2}}$ is the angle enclosing half of the shower particles. The transformation of the angles into the c.m.-system was carried out taking regard of the meson energy. According to WINKLER ⁽³²⁾ all mesons were assumed to have equal energies in the c.m.-system, which was determined from the scattering measurements. The meson energy does not enter in a critical way except for very large angles in the c.m.-system. Thus a slight adjustment of γ_s ($< 10^0$) was sufficient to reach symmetry in the c.m.-system in all cases. A peak at 180° due to a few tracks was assumed to arise from secondary interactions. These tracks were left off (see Table I).

5. - Energy of the mesons in the c.m.-system.

The scattering measurements gave for some of the tracks only a lower limit for the energy in the c.m.-system. This is partly caused by the fact that most measurements were carried out by relative scattering in the forward cone to minimize the influence of secondary interactions. It is well known

⁽³²⁾ W. WINKLER: *Helv. Phys. Acta*, **29**, 267 (1956).

that by measurements of this kind the scattering of a single track having a much higher energy than the rest of the particles cannot be determined. We have in Table I stated the fraction of particles having total energies $< 2m_{\pi}c^2$ in the c.m.-system, to show that a great part of them has rather low energies and that the lower limit of the mean energy values given should not be too low. In some cases the scattering measurements on the fast particles could be checked by energy measurements on the decay- β -rays from the π^0 -mesons. An upper limit for the mean energy in the c.m.-system could in some cases be given by the method of the maximum angle. The energy determination from the maximum angle of the shower particles in the L-system was found to give too high values for the mean meson energy in a number of events which could be well measured; thus it was taken as an upper limit in some other cases.

The particles were assumed to be π -mesons. This assumption can be safely made in the low energy interactions. On the high energy events, most measurements were made in the forward cone, so the results are practically not altered if a small fraction of the particles were K-mesons, as can be seen from the transformation law. (See remarks of jet 7 for an exception).

6. - Results.

The results are summarized in Table I.

TABLE I.

jet no.	n_H	n_s	E_0 GeV	γ_s	E_m GeV	E_{\max} GeV	K %	Q %	A %	tracks left off
1	1	11	1700	30	> 0.41	1.1 (*)	> 11	30	55	0
2	1	29	2200	34	≥ 0.42	1.5 (*)	≥ 27	43	32	1
3	0	12	130	8.6	0.39	0.55 (+)	40	33	42	0
4	4	16	100	7.5	0.35	—	50	—	37	5
5	0	19	37	4.5	0.32	—	100	38	38	3
6	3	36	700	19 ± 4	0.60	—	75	—	24	5
7	1	23	3800	45	~ 0.40	1.3 (+)	18	70	36	1

(*) See remarks.

(+) From the maximum angle (see above).

n_H number of black and grey tracks.

n_s number of shower particles.

E_0 primary energy.

E_m mean total energy of mesons in the c.m.-system.

E_{\max} an upper limit for E_m .

K fraction of the energy available in the c.m.-system which goes into the meson field (inelasticity).

Q fraction of particles having a total energy $< 2m_{\pi}c^2$ in the c.m.-system.

A it is defined by $A = n_s(|\cos \theta_c| < 0.5)/n_s$, θ_c is the angle in the c.m.-system. $A = 0.5$ means an isotropic angular distribution, $A < 0.5$ means a distribution peaked at 180° and 0° .

The following comments on the individual events should be made:

Jet 1: If one assumes that this event is due to a proton-proton collision and interprets the black track as due to the recoiling proton (energy 97 MeV), one gets $E_m = 1.1$ GeV and $K = 31\%$. This would be consistent with all other measurements, but cannot of course be proved. It shows however, that some stars with low K and one black track could be thus explained. It should be noted that the angular distribution is isotropic, which would contradict the Fermi theory because of the small inelasticity.

Jet 2: E_m was determined by measurements in the forward cone as in jet 1. The upper limit E_{\max} comes from the total energy available, it corresponds to $K = 100\%$.

Jet 3: It could be due to a proton-proton collision, as the number of shower particles is even.

Jet 4: The analysis showed that the event cannot be well interpreted as a N-N-collision. It was included only to show that a large fraction of the particles may have low energies.

Jet 5: This event cannot be a pure p-p-collision, as the number of shower particles is odd. This fact was also noticed in the kinematic analysis, where 3 tracks had to be left off to get symmetry.

Jet 6: Scattering measurements could be made in the forward and backward cone. The upper limit of γ_s results from the visible energy, the lower limit from demanding equal mean energies of the particles in the forward and backward cones in the c.m.-system.

Jet 7: On account of the very high energy of this jet some of the shower particles could be K-mesons. If one assumes all particles to be π -mesons, $E_m = 0.33$ GeV. Because of this low value the result is altered if one assumes that 30% of the particles are K-mesons as is suggested by recent experiments⁽²⁶⁾. In this case one gets $E_m = 0.4$ GeV. K is calculated with this value and a ratio of charged to neutral K-mesons equal to 1.

7. - Conclusions.

The mean energy of the mesons in the c.m.-system is in accord with other measurements made up to now^(2,3,27-29,33,34). It seems to exhibit little fluctuations as compared to the inelasticity K . The mean energy rises very slowly with primary energy. It is about 0.35 GeV at about 100 GeV (jet 3, 4, 5)

⁽³³⁾ F. D. HÄNNI, C. LANG, M. TEUCHER, H. WINZELER and E. LOHRMANN: *Nuovo Cimento*, **4**, 1473 (1956).

⁽³⁴⁾ S. KANEKO, O. KUSUMOTO and S. MATSUMOTO: private communication (preprint 1957).

and between 0.4 and 1 GeV at about 1000 GeV and higher (jet 1, 2, 6, 7). This is also in accord with the Heisenberg theory^(35,36) of multiple meson production, which predicts a logarithmic increase of E_m with γ_s . But the data are up to now also in agreement with E_m rising like $E_0^{\frac{1}{2}}$ after proper normalization. This is predicted by the theories of Fermi⁽³⁷⁾ and Landau⁽³⁸⁾. There is however a rather large fraction Q of particles with low energies in the c.m.-system. This would favour the Heisenberg theory which predicts the most probable energy value to lie at very low energies. In the case of jet 5 the energy distribution could be determined (Fig. 1). It also shows, that the

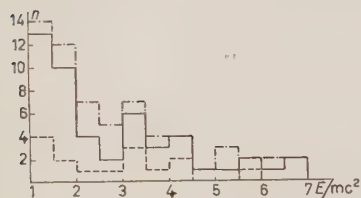


Fig. 1. — Energy distribution of the shower particles in the c.m.-system. E : total energy; m pion mass; n number of particles. - - - jet 5 this work. — ref. (3) and (27) included. - · - ref. (28) included.

emission of particles with low energies is favoured. This agrees also with results obtained previously. Measurements of the energy of the shower particles and energy distribution in the c.m.-system have been given by ref. (2,3,27-29). They all show that particles in the lowest energy intervals are the most frequent. All measurements are thus compatible with an energy spectrum of the form dE/E^2 as proposed by HEISENBERG.

There seems to be no connection between the inelasticity K and the anisotropy A , although this is suggested by some theories.

This can be seen by comparing our 6 jets and others (see ref. (2,3,27-29,33,34)) with one another. Every combination of K and A seems to occur. Further data are necessary, however, as not all of the events can probably be interpreted as N-N-collisions (although they look like such) the analysis could thus be in error in some cases described up to now.

8. — Jets produced by mesons.

In an event of type 20+56 p and primary energy about 10^{13} eV found in this laboratory⁽²³⁾ 6 jets have been found in the forward cone, two of which were produced by neutral particles and 4 by shower particles from the primary interaction. Most of these 6 jets should therefore be produced by a meson. Table II shows the results of an angular analysis of the jets (no

(35) W. HEISENBERG: *Zeits. f. Phys.*, **126**, 569 (1949).

(36) W. HEISENBERG: *Zeits. f. Phys.*, **133**, 65 (1952).

(37) E. FERMI: *Progr. Theor. Phys.*, **5**, 570 (1950); *Phys. Rev.*, **81**, 683 (1951).

(38) L. D. LANDAU: *Akad. Nauk S.S.S.R.*, **17**, 51 (1953); S. Z. BELENKIJ and L. D. LANDAU: *Suppl. Nuovo Cimento*, **3**, 15 (1956).

scattering measurements could be made). In all but one of the cases good symmetry of the angular distribution in the c.m.-system could be reached by choosing the proper value for γ_s and by leaving off at most 2 of the tracks with angles $> 60^\circ$ in the L-system. For the transformation of the angular distribution the mean energy of the mesons was taken from the Heisenberg theory; as was mentioned earlier the angular distribution depends only for very large angles in the c.m.-system on the meson energy. For $\cos \vartheta_c < -0.8$ it was taken into account, that

mesons emitted with small angles in the forward and backward directions appear to have higher energies in the c.m.-system, ^(2,27,28). In any case not too much weight ought to be attached to these particles, as the influence of secondary collisions must also be regarded

to be greatest for the largest angles in the L-system. The angular distribution of all jets (excluding no. 11) is shown in Fig. 2. There seems to be a slight asymmetry in the c.m.-system, but it is not statistically significant (on a 5% level of significance). A slight anisotropy which is indicated, is also not significant, the anisotropy coefficient A being $A = 0.39 \pm_{0.07}^{0.10}$. A χ^2 -test showed, that the angular distribution is compatible with an isotropic distribution on a 5% level of significance.

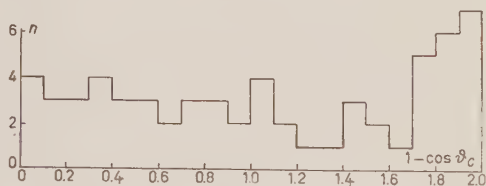


Fig. 2. - Angular distribution of 5 jets produced by mesons in the c.m.-system.

TABLE II.

jet no.	n_H	n_s	γ_s	E_0	A	tracks left off	primary
8	3	9	12	270	0.50	2	charged
9	0	17	12	270	0.29	0	charged
10	20	22	4	30	0.40	2	charged
11	23	37	10	190	0.32	9	neutral
12	1	8	11	230	0.38	1	neutral
13	3	11	7	90	0.27	0	charged

The meaning of n_H , n_s , γ_s , E_0 , A is the same as in Table I.

* * *

The author wishes to express his sincere thanks to Prof. Dr. E. SCHOPPER and Prof. Dr. F. G. HOUTERMANS for their interest and for giving him the possibility to work in Berne and to Prof. Dr. C. PEYROT for many stimulating

discussions. The financial help from the Deutsche Forschungsgemeinschaft is gratefully acknowledged. He is also indebted to the Schweizer Nationalfonds and the Office of Naval Research which provided for the stacks, and to the scanning staffs of Berne and Hechingen.

RIASSUNTO (*)

Tra circa 250 jets trovati in lastre nucleari ne furono scelti 6 nell'intento di trovare degli eventi rappresentanti con la massima possibile fedeltà collisioni nucleone-nucleone. Misure di scattering effettuate sulle particelle degli sciami dimostrarono che l'energia media totale dei mesoni nel sistema del centro di massa era di 0.35 GeV per circa 100 GeV di energia primaria e da 0.4 a 1 GeV per energie primarie di 1000 GeV ed oltre. Una gran parte delle particelle ha debole energia nel sistema del centro di massa, appoggiando pertanto la teoria di Heisenberg della produzione multipla dei mesoni. Non si è trovata alcuna relazione fra l'anisotropia della distribuzione angolare nel sistema del centro di massa e l'anelasticità. L'anelasticità sembra variare entro vasti limiti. Abbiamo eseguito un'analisi della distribuzione angolare di 6 ulteriori jets presumibilmente prodotti da mesoni. L'energia media di questi jets risultò di 200 GeV. La distribuzione angolare è isotropica entro i limiti di errore.

(*) Traduzione a cura della Redazione.

Reciprocal Static Solutions of Field Equations Involving an Asymmetrical Fundamental Tensor.

H. A. BUCHDAHL

Hobart - Tasmania

(ricevuto il 28 Dicembre 1956)

Summary. — It is shown that from any given static solution of the field equations of Einstein's unitary field theory another static solution may be inferred by inspection. Some special cases are considered.

I. — Introduction.

1. — Let Y_n denote an n -dimensional space provided with a linear connection $\Gamma_{\sigma\alpha}^\tau$ which depends only upon an asymmetrical fundamental tensor $g_{\alpha\kappa}$. Then in particular the Y_4 forms the basis of the unitary field theory of Einstein (¹). His definitions of the various kinds of covariant derivatives, of transposition invariance of hermiticity, of curvature tensors, and of the notation relating to all these will be taken over into the present context, on the understanding that all greek indices shall run from 1 to n , instead of from 1 to 4. On the other hand, contrary to the usual practice of establishing a relation between $g_{\alpha\kappa}$ and $\Gamma_{\sigma\alpha}^\tau$ by applying Palatini's device to some action integral, the hermitean relation

$$(1.1) \quad g_{\lambda\kappa\lambda} = g_{\alpha\kappa\lambda} - \Gamma_{\alpha\lambda}^\sigma g_{\sigma\kappa} - \Gamma_{\lambda\kappa}^\sigma g_{\alpha\sigma} = 0,$$

will here be postulated from the outset. (This has the advantage that one may study for instance the effect of conformal transformations on the Einstein

(¹) A. EINSTEIN: *The Meaning of Relativity*, 5-th edition (London, 1951). Appendix II.

tensor (cf. §§ 5, 6) irrespectively of the subsequent choice of the action integral and subsidiary conditions which generate the field equations.) In view of the identity

$$(1.2) \quad g_{\nu\kappa}^{\mu} = g_{\nu}^{\mu} \Gamma_{\kappa}^{\nu},$$

which easily follows from (1.1), the equation

$$(1.3) \quad \Gamma_{\nu}^{\nu} = 0$$

is equivalent to

$$(1.4) \quad g_{\nu}^{\mu} = \varepsilon^{\mu\sigma_1\sigma_2\cdots\sigma_{n-3}\tau} \varphi_{\sigma_1\sigma_2\cdots\sigma_{n-3}\tau},$$

where $\varepsilon^{\mu\sigma_1\sigma_2\cdots\sigma_{n-3}\tau}$ is the numerical contravariant tensor-density of Levi-Civita, and $\varphi_{\sigma_1\sigma_2\cdots\sigma_{n-3}}$ is a completely skew-symmetric tensor. If $R_{\mu\kappa}$ is the hermitean Einstein tensor

$$(1.5) \quad R_{\mu\kappa} = \Gamma_{\mu\kappa,\sigma}^{\sigma} - \frac{1}{2}(\Gamma_{\mu\sigma,\kappa}^{\sigma} + \Gamma_{\sigma\kappa,\mu}^{\sigma}) - \Gamma_{\mu\tau}^{\sigma} \Gamma_{\sigma\kappa}^{\tau} + \Gamma_{\mu\kappa}^{\sigma} \Gamma_{\sigma\tau}^{\tau},$$

and if the equation (1.3) is required to be identically satisfied, then the vanishing of the hamiltonian derivatives of the Lagrangian

$$(1.6) \quad \mathfrak{R} = g^{\mu\kappa} R_{\mu\kappa},$$

with respect to the essential field variables $g_{\mu\kappa}^{\mu}, \varphi_{\sigma_1\cdots\sigma_{n-3}}$ implies the equations (cf. § 9a)

$$(1.7) \quad R_{\mu\kappa} = 0, \quad R_{[\mu\kappa,\lambda]} = 0.$$

When $n = 4$, eqs. (1.1), (1.3) and (1.7) constitute Einstein's set I-b (loc. cit. p. 144). (Schouten's general notation ⁽²⁾ for the symmetric and skew-symmetric parts of quantities will be used here side by side with Einstein's more specialised notation.)

I now define the fundamental tensor $g_{\mu\kappa}$ to be *static* with respect to the co-ordinate x_a if the relations

$$(1.8) \quad g_{\mu\kappa,a} = 0, \quad g_{ai} = g_{ia} = 0$$

are satisfied. Roman indices everywhere take the values $1, 2, \dots, a-1, a+1, \dots, n$, the index a being fixed throughout. When (1.8) is satisfied it is often convenient to indicate the (in general) non-vanishing components of

⁽²⁾ J. A. SCHOUTEN: *Ricci-Calculus*, 2-nd edition (Berlin, 1954), Chap. I, 14.

the fundamental tensor by (g_{ik}, g_{aa}) ; and any other tensor which depends only on the g_{ix} and their derivatives may then also be called static. The theorem to be proved can now be stated as follows:

If the equations

$$(1.9) \quad g_{i\kappa;\lambda} = 0, \quad \Gamma_i = 0, \quad R_{ix} = 0, \quad R_{[ix\lambda]} = 0$$

are satisfied by the static fundamental tensor (g_{ik}, g_{aa}) then they are also satisfied by the fundamental tensor $((g_{aa})^{2/(n-2)}g_{ik}, (g_{aa})^{-1})$.

Two solutions so related will be called *reciprocal* to each other; and the process of passing from a solution to its reciprocal may be called a «reciprocal transformation». The theorem above is an extension of the corresponding result previously obtained ⁽³⁾ for the case of a symmetrical fundamental tensor, though the method of proof is somewhat different. With $n = a = 4$ the known general static spherically symmetric solution of Einstein's field equations of course transforms into itself under a reciprocal transformation (§ 10); and in § 11 a static solution of these equations is obtained without «solving» them in the ordinary sense of the term.

II. - The static Lagrangian.

2. - With $n \geq 4$ throughout, let $g_{ix} = (g_{ik}, e^{2\gamma})$ be a static fundamental tensor in Y_n , with which the linear connection $\Gamma_{\sigma\sigma}^i$ is associated through (1.1). The components of this connection may then be referred to the Y_{n-1} whose fundamental tensor is g_{ik} , and in which the scalar field γ is given, in the following manner. One has

$$g_{aa,a} = 0 = 2\Gamma_{aa}^a g_{aa} = 2\Gamma_{aa}^a g_{aa},$$

whence

$$(2.1) \quad \Gamma_{aa}^a = 0.$$

Next

$$\frac{1}{2}(g_{as,a} + g_{ia,a} - g_{aa,i}) = -e^{2\gamma}\gamma_{,i} = \Gamma_{aa}^s g_{s,i},$$

in view of (1.1). Hence if a^{ik} is the tensor reciprocal to g_{ik}

$$(2.2) \quad \Gamma_{aa}^s = -a^{is}e^{2\gamma}\gamma_{,i}.$$

⁽³⁾ H. A. BUCHDAHL: *Quart. Journ. Math.*, 5 (18), 1161 (1954) (Oxford).

Continuing in this way one obtains without difficulty the remaining equations

$$(2.3) \quad \underset{\circ}{\Gamma}_{ai}^a = g_{si} a^{st} \gamma_{,t}, \quad \underset{\circ}{\Gamma}_{ia}^a = g_{is} a^{st} \gamma_{,t};$$

$$(2.4) \quad \underset{\circ}{\Gamma}_{ik}^a = 0; \quad \underset{\circ}{\Gamma}_{ia}^k = \underset{\circ}{\Gamma}_{ai}^k = 0;$$

$$(2.5) \quad \underset{\circ}{\Gamma}_{ik}^{rs} = \underset{\circ}{\Gamma}_{ik}^{rs}.$$

3. - From (2.3) it follows that

$$(3.1) \quad \underset{\circ}{\Gamma}_i = \Gamma_i + g_{is} a^{st} \gamma_{,t}.$$

From (1.2) on the other hand one infers that

$$(3.2) \quad \underset{\circ}{\Gamma}_i = \Gamma_i + h_{is} g_{\vee}^{st} \gamma_{,t},$$

where h_{ik} is the tensor reciprocal to g_{ik} . The important identity implied by this result, viz.

$$(3.3) \quad g_{is} a^{st} = h_{is} g_{\vee}^{st},$$

may also be confirmed directly. From it certain other useful identities follow easily, e.g.

$$(3.4) \quad p^{ik} = g_{ik} - a^{ik} = g_{is} g_{\vee}^{tk} h_{st},$$

$$(3.5) \quad h_{ik} = g_{si} g_{tk} a^{st},$$

and so on.

4. - From the results of Sec. 2 it follows that $\underset{\circ}{R}_{ai} = \underset{\circ}{R}_{ia} = 0$, so that

$$(4.1) \quad \underset{\circ}{R} = g^{\alpha\alpha} \underset{\circ}{R}_{\alpha\alpha} = g^{ik} \underset{\circ}{R}_{ik} + g^{aa} \underset{\circ}{R}_{aa}.$$

Now the non-vanishing terms of $\underset{\circ}{R}_{aa}$ are

$$(4.2) \quad \begin{aligned} \underset{\circ}{R}_{aa} &= \underset{\circ}{\Gamma}_{aa,s}^s + \underset{\circ}{\Gamma}_{st}^t \underset{\circ}{\Gamma}_{aa}^s - \underset{\circ}{\Gamma}_{aa}^s \underset{\circ}{\Gamma}_{sa}^a \\ &= -e^{-2\nu} [(a^{st} \gamma_{,s})_{,t} + a^{st} \gamma_{,s} \gamma_{,t}], \end{aligned}$$

where subscripts following a colon denote covariant differentiation in Y_{n-1} . Note that the following convention is being used throughout. An index is called a positive, a negative, or a null-index according as it has, in the usual notation, a + sign, a - sign, or a zero placed under it to indicate its character during covariant differentiation. Any index whose character is not so indicated explicitly shall be understood to be a null-index.

Next one has

$$\begin{aligned}
 (4.3) \quad R_{ik} &= R_{ik} - \frac{1}{2} (F_{ia,k}^a + F_{ak,i}^a) + F_{ik}^s F_{sa}^a - F_{ia}^a F_{ak}^a \\
 &= R_{ik} - \gamma_{ik} - g_{is} g_{tk} a^{st} a^{tm} \gamma_{:l} \gamma_{:m},
 \end{aligned}$$

where R_{ik} refers to Y_{n-1} . (4.1) therefore becomes

$$(4.4) \quad R_{\circ} = R - [g^{st} \gamma_{:st} + (a^{st} \gamma_{:st}) + 2a^{st} \gamma_{:s} \gamma_{:t}].$$

III. - Conformal transformations.

5. - In any Y_n the fundamental tensor \bar{g}_{ik} will be called *conformal* to the fundamental tensor g_{ik} if there exists a scalar function $e^{2\sigma}$ such that

$$(5.1) \quad \bar{g}_{ik} = e^{2\sigma} g_{ik}.$$

If the linear connections $\Gamma_{\rho\sigma}^{\tau}$, $\bar{\Gamma}_{\rho\sigma}^{\tau}$ are associated with \bar{g}_{ik} , g_{ik} respectively, one has

$$\bar{g}_{ik;\lambda} = e^{2\sigma} (g_{ik;\lambda} + g_{ik} \sigma_{,\lambda}) = e^{2\sigma} (\bar{\Gamma}_{ik\lambda}^{\tau} g_{\tau\lambda} + \bar{\Gamma}_{\lambda\sigma}^{\tau} g_{ik}).$$

Writing

$$(5.2) \quad \bar{\Gamma}_{\rho\sigma}^{\tau} = \Gamma_{\rho\sigma}^{\tau} + \gamma_{\rho\sigma}^{\tau},$$

this gives

$$(5.3) \quad \gamma_{i\lambda}^{\tau} g_{\tau\kappa} + \gamma_{\lambda\kappa}^{\tau} g_{i\tau} = 2g_{i\kappa} \sigma_{,\lambda}$$

as the equation determining $\gamma_{\rho\sigma}^{\tau}$. From it certain results required later may be derived as follows. Transvecting (5.3) with $g^{i\kappa}$ one has

$$(5.4) \quad \gamma_{i\tau}^{\tau} = n\sigma_{,i}.$$

Alternatively transvecting with $g^{i\lambda}$

$$(5.5) \quad \omega^i \equiv g^{\alpha\beta} \gamma_{\alpha\beta}^i = g^{i\alpha} (2\sigma_{,\alpha} - \gamma_{\beta\alpha}^{\beta}).$$

On the other hand, from (1.2), writing $\gamma_{\alpha\beta}^{\beta} = \gamma_{\alpha}$,

$$\begin{aligned}
 (e^{(n-2)\sigma} g_{\vee}^{i\alpha})_{,\alpha} &= e^{(n-2)\sigma} g_{\vee}^{i\alpha} (\Gamma_{\alpha}^{\alpha} + \gamma_{\alpha}) \\
 &= e^{(n-2)\sigma} [g_{\vee,\alpha}^{i\alpha} + (n-2)g_{\vee,\alpha}^{i\alpha} \sigma_{,\alpha}],
 \end{aligned}$$

whence it follows that

$$(5.6) \quad \gamma_i = (n-2)h_{i\alpha}g^{\alpha\beta}_V\sigma_{,\beta}.$$

Therefore, using (5.4-6) and (3.3)

$$(5.7) \quad \omega^i = -(n-2)g^{\alpha\kappa}(\delta^{\beta}_{\kappa} + g^{\alpha\beta}_{\alpha\kappa})\sigma_{,\beta} = -(n-2)a^{\alpha\kappa}\sigma_{,\alpha}.$$

Finally, transvect (5.3) with $g^{\alpha\kappa}g^{\iota\beta}\gamma^{\lambda}_{\lambda\beta}$. After changing dummy indices one obtains at once

$$(5.8) \quad \pi \equiv g^{\alpha\kappa}\gamma^{\sigma}_{\iota\kappa}\gamma^{\tau}_{\sigma\kappa} = \omega^{\alpha}\sigma_{,\alpha}.$$

6. - If \bar{R} , R are associated with $\bar{g}_{\alpha\kappa}$ and $g_{\alpha\kappa}$ respectively one obtains directly on inserting (5.1-2) in (1.5) and using (5.4)

$$\begin{aligned} \bar{R} &= e^{-2\sigma}[R + g^{\alpha\kappa}(\gamma^{\sigma}_{\iota\kappa\sigma} - n\sigma_{,\iota\kappa} - \gamma^{\sigma}_{\iota\kappa}\gamma^{\tau}_{\sigma\kappa} + \gamma^{\sigma}_{\alpha\kappa}\gamma^{\tau}_{\sigma\tau})] \\ &= e^{-2\sigma}[R + \omega^{\sigma}_{,\sigma} - n g^{\sigma\tau}\sigma_{,\sigma\tau} - \pi + n\omega^{\sigma}\sigma_{,\sigma}]. \end{aligned}$$

(Covariant differentiation here refers to $g_{\alpha\kappa}$).

In view of (5.7-8) this finally becomes

$$(6.1) \quad \bar{R} = e^{-2\sigma}[R - n g^{\sigma\tau}\sigma_{,\sigma\tau} - (n-2)(a^{\sigma\tau}\sigma_{,\sigma})_{,\tau} - (n-1)(n-2)a^{\sigma\tau}\sigma_{,\sigma}\sigma_{,\tau}].$$

IV. - Reduction of the Lagrangian.

7. - Consider in Y_n the static fundamental tensor $g_{\alpha\kappa} = (\bar{g}_{ik}, \epsilon^{2\gamma})$. Then in view of (4.4)

$$(7.1) \quad R_{\circ} = \bar{R} - [\bar{g}^{st}\gamma_{:,st} + (\bar{a}^{st}\gamma_{:,s})_{:,t} + 2\bar{a}^{st}\gamma_{:,s}\gamma_{:,t}],$$

where covariant differentiation here refers to \bar{g}_{ik} . Now write

$$(7.2) \quad \bar{g}_{ik} = \epsilon^{2\sigma}g_{ik}, \quad \text{so that} \quad g_{\alpha\kappa} = (\epsilon^{2\sigma}g_{ik}, \epsilon^{2\gamma}).$$

Then from (6.1), keeping in mind that g_{ik} is the fundamental tensor of a Y_{n-1} , not a Y_n ,

$$(7.3) \quad \bar{R} = e^{-2\sigma}[R - (n-1)g^{st}\sigma_{:,st} - (n-3)(a^{st}\sigma_{:,s})_{:,t} - (n-2)(n-3)a^{st}\sigma_{:,s}\sigma_{:,t}].$$

The semicolon now refers to covariant differentiation with respect to g_{ik} . Now

$$(7.4) \quad \gamma_{:,s} = \gamma_{,s} = \gamma_{;s},$$

and

$$\begin{aligned}
 (7.5) \quad \bar{a}^{st} \gamma_{;s};_t &= (e^{-2\sigma} a^{st} \gamma_{;s})_{;t} + \bar{F}_{tt}^t e^{-2\sigma} a^{st} \gamma_{;s} \\
 &= (e^{-2\sigma} a^{st} \gamma_{;s};_t + \gamma_{tt}^t e^{-2\sigma} a^{st} \gamma_{;s} \\
 &= e^{-2\sigma} [(a^{st} \gamma_{;s})_{;t} + (n-3) a^{st} \sigma_{;s} \gamma_{;t}], \quad \text{by (5.4).}
 \end{aligned}$$

In a similar way, using (5.7),

$$(7.6) \quad \bar{g}^{st} \gamma_{;st}^+ = e^{-2\sigma} [g^{st} \gamma_{;st}^+ + (n-3) a^{st} \sigma_{;s} \gamma_{;t}].$$

The density \mathfrak{H} is obtained from R by multiplying by w , where

$$(7.7) \quad w = (\det g_{ik})^{\frac{1}{2}} = e^{(n-1)\sigma + \gamma} (\det g_{ik})^{\frac{1}{2}} = e^{(n-1)\sigma + \gamma} w.$$

Inserting (7.3-6) into (7.1), and keeping in mind that $w_{;s} = 0$ one has finally

$$\begin{aligned}
 (7.8) \quad \mathfrak{H} &= e^{(n-3)\sigma + \gamma} \{ \mathfrak{H} - g^{st} [(n-1) \sigma_{;st} + \gamma_{;st}] - [a^{st} ((n-3) \sigma_{;s} + \gamma_{;s})]_{;t} - \\
 &\quad - a^{st} [(n-2)(n-3) \sigma_{;s} \sigma_{;t} + 2(n-3) \sigma_{;s} \gamma_{;t} + 2\gamma_{;s} \gamma_{;t}] \}.
 \end{aligned}$$

8. - (a) If S is any scalar

$$(8.1) \quad g^{st} S_{;st}^+ = (g^{st} S_{;s})_{;t} - g^{st} S_{;s} \Gamma_t^s = (g^{st} S_{;s})_{;t} + g_V^{st} \Gamma_s^s S_{;t}.$$

Eq. (7.8) may then be rewritten so that only ordinary instead of covariant derivatives appear in it. Thus

$$\begin{aligned}
 (8.2) \quad \mathfrak{H} &= e^{(n-3)\sigma + \gamma} \{ \mathfrak{H} - [g^{st} ((n-1) \sigma_{;s} + \gamma_{;s})]_{;t} - [a^{st} ((n-3) \sigma_{;s} + \gamma_{;s})]_{;t} - \\
 &\quad - a^{st} [(n-2)(n-3) \sigma_{;s} \sigma_{;t} + 2(n-3) \sigma_{;s} \gamma_{;t} + 2\gamma_{;s} \gamma_{;t}] - g_V^{st} \Gamma_s^s [(n-1) \sigma_{;t} + \gamma_{;t}] \}.
 \end{aligned}$$

Whenever \mathfrak{H} serves as the Lagrangian of an action integral which is to be varied subject to the condition that all variations vanish on the boundary of the region of integration contemplated, any terms of \mathfrak{H} which are in the form of an *ordinary* divergence are redundant. Accordingly I shall use the symbol \doteq to indicate equality if terms constituting an ordinary divergence be rejected. For instance, rejecting a term $-[(e^{(n-3)\sigma + \gamma})_{;s} a^{st}]_{;t}$ on the right hand side of (8.2) one gets

$$\begin{aligned}
 (8.3) \quad \mathfrak{H} &\doteq e^{(n-3)\sigma + \gamma} \{ \mathfrak{H} - [g^{st} ((n-1) \sigma_{;s} + \gamma_{;s})]_{;t} - a^{st} [(n-3) \sigma_{;s} \sigma_{;t} + \gamma_{;s} \gamma_{;t}] - \\
 &\quad - g_V^{st} \Gamma_s^s [(n-1) \sigma_{;t} + \gamma_{;t}] \}.
 \end{aligned}$$

(b) Two cases need now to be considered, viz.

$$(8.4) \quad \left\{ \begin{array}{ll} \text{(i)} & \sigma = 0, \quad \gamma = \varphi, \\ \text{(ii)} & \sigma = \frac{2}{n-3}\varphi, \quad \gamma = -\varphi, \end{array} \right.$$

where φ is a scalar function. Let λ be a numerical factor which has the alternative values $\lambda = 1$ and $\lambda = (n+1)/(n-3)$ in cases (i) and (ii) of (8.4) respectively. Then the corresponding alternative forms of (8.3) are both contained in the equation

$$(8.5) \quad \mathfrak{H} \doteq e^{\varphi} \{ \mathfrak{H} - \lambda [(g^{st}\varphi_{,s})_{,t} + a^{st}\varphi_{,s}\varphi_{,t} + g_{\nu}^{st}F_{s,t}] \}.$$

To this the ordinary divergence $\lambda(g^{st}\varphi_{,s}e^{\varphi})_{,t}$ may be added, so that

$$(8.6) \quad \mathfrak{H} \doteq e^{\varphi} [\mathfrak{H} + \lambda (p^{st}\varphi_{,s} - g_{\nu}^{st}F_{s,t})].$$

V. - Proof of the theorem.

9. - (a) If, in the general case, one adds to the variation $\delta\mathfrak{H}$ of \mathfrak{H} the ordinary divergence $(-g^{\nu\kappa}\delta\Gamma_{\nu\kappa}^{\sigma} + \frac{1}{2}g^{\nu\sigma}\delta\Gamma_{\nu\kappa}^{\kappa} + \frac{1}{2}g^{\sigma\kappa}\delta\Gamma_{\nu\kappa}^{\nu})_{,\sigma}$ and rewrites the derivatives of the $g^{\alpha\beta}$ everywhere by means of (1.1) (which, it will be remembered, was postulated at the outset), then one obtains at once

$$(9.1) \quad \delta\mathfrak{H} \doteq R_{\nu\kappa}\delta g^{\nu\kappa} + \frac{1}{2}g^{\nu\kappa}(F_{\nu}\delta\Gamma_{\kappa}^{\sigma} - F_{\kappa}\delta\Gamma_{\nu}^{\sigma}),$$

numerous other terms cancelling out. If one lays down that (1.3) shall be identically satisfied one is simply left with

$$(9.2) \quad \delta\mathfrak{H} \doteq R_{\nu\kappa}\delta g^{\nu\kappa} + R_{\nu\kappa}^{\nu}\delta g^{\nu\kappa},$$

subject to the condition (1.4). If $\delta\mathfrak{H}$ is to vanish for arbitrary $\delta g^{\nu\kappa}$, $\delta q_{\sigma_1 \dots \sigma_n}$, eqs. (1.7) must be satisfied.

(b) Returning to the notation of Sect. IV, the field equations may be taken to arise (by variation of g^{ik} and q) from the Lagrangean given by (8.6) in the special case in which only static fundamental tensors are contemplated; and provided the variations are carried out subject to the condition (1.3) the equations which result must be just (1.7), purely formal differences aside. Now, because of (3.2) and (5.6),

$$(9.3) \quad F_s = F_s + h_{st}g_{\nu}^{tk}[(n-3)\sigma_{,k} + \gamma_{,k}] = F_s + h_{st}g_{\nu}^{tk}\varphi_{,k},$$

in view of (8.4); so that

$$(9.4) \quad g_{\sqrt{0}}^{\mu\nu} \Gamma_s = g_{\sqrt{0}}^{\mu\nu} \Gamma_s - p^{kt} \varphi_{,k}, \quad \text{by (3.4).}$$

Hence, keeping in mind that Γ_n vanishes identically in the static case, comparison of (9.4) with (8.6) shows that in the presence of the condition $\Gamma_t = 0$ one has simply

$$(9.5) \quad \mathfrak{R} \doteq e^{\varphi} \mathfrak{R},$$

in both of the cases (8.4). Accordingly, if the static fundamental tensor (g_{ik}, g_{nn}) satisfies the equation (1.9) one need only choose $q = \frac{1}{2} \log g_{nn}$ and the theorem stated in Sect. I follows at once.

VI. - Ancillary results.

10. - It is of interest to confirm explicitly the invariance under a reciprocal transformation of the general static spherically symmetric solution of Einstein's field equations ($n = a = 4$), as obtained by WYMAN⁽⁴⁾ and BONNOR⁽⁵⁾. It suffices to consider the result of WYMAN who assumed g_{23} to be real. It should be noted that to conform with the definition of static tensors one must take g_{14} to be zero. Write, as usual,

$$(10.1) \quad \begin{cases} g_{11} = -\alpha, & g_{22} = (\operatorname{cosec}^2 \theta) g_{33} = -\beta, & g_{44} = \gamma, & g_{23} = f \sin \theta, \\ & g_{i\kappa} = 0 \quad (i \neq \kappa), & g_{i4} = 0, & g_{12} = g_{13} = 0, \end{cases}$$

where α, β, γ, f are functions of r only, the co-ordinates used being $r, \theta, q, t = x_1, x_2, x_3, x_4$. The solution in question is then

$$(10.2) \quad \begin{cases} f + i\beta = 16m^2 b^2 \gamma^{-1} (c + i)^{-1} (e^a \gamma^b + e^{-a} \gamma^{-b})^{-2} \\ \alpha = \gamma'^2 (f^2 + \beta^2) (4m^2 \gamma)^{-1}. \end{cases}$$

Here γ is an arbitrary function of r ; m and c are real arbitrary constants; b is of the form $\frac{1}{2}(1 + ih)^{\frac{1}{2}}$, where h is another real arbitrary constant; whilst a is a complex arbitrary constant. If quantities with a subscript 1 refer to the solution obtained by the reciprocal transformation of (10.2) one has at

⁽⁴⁾ M. WYMAN: *Can. Journ. Math.*, **2**, 427 (1950).

⁽⁵⁾ W. B. BONNOR: *Proc. Roy. Soc.*, A **209**, 353 (1951).

once

$$(10.3) \quad \begin{cases} f_1 + i\beta_1 = \gamma^2(f + i\beta) = 16m^2b^2\gamma(c + i)^{-1}(e^a\gamma^b + e^{-a}\gamma^{-b})^{-2} \\ \alpha_1 = \gamma^2\alpha = \gamma\gamma'^2(f^2 + \beta^2)(4m^2)^{-1} = \gamma^{-2}\gamma'^2(f_1 + i\beta_1)^2(4m^2)^{-1} \\ \gamma_1 = \gamma^{-1}. \end{cases}$$

If one now replaces γ by γ_1^{-1} in the extreme right hand members of the first two of eqs. (10.3), $f_1 + i\beta_1$ and α_1 become the same functions of γ_1 as $f + i\beta$ and α are of γ except that $-a$ now appears in place of a . Since a and γ are arbitrary it follows that (10.3) is only trivially distinct from (10.2), as it must be.

It should be noted that m has been supposed not to be zero. If $m = 0$ another form of the solution applies in which, however, $\gamma = 1$; so that this is of no interest in the present context.

11. — An example of the generation of solutions of the field equations ($n=4$) by means of reciprocal transformations is the following. The fundamental tensor

$$(11.1) \quad \begin{cases} g_{11} = g_{22} = g_{33} = -1, & g_{44} = 1, & g_{23} = c = \text{const}, \\ g_{i\underline{x}} = 0 \quad (i \neq \underline{x}), & g_{i4} = 0, & g_{12} = g_{13} = 0, \end{cases}$$

which is static with respect to x_4 , trivially satisfies the field equations, since all the $I_{\sigma\sigma}^{\tau}$ are zero. The co-ordinate transformation

$$(11.2) \quad x_1 = x'_1 \cosh x'_4, \quad x_4 = x'_1 \sinh x'_4,$$

followed by suppression of all primes, leads to the (again static) fundamental tensor

$$(11.3) \quad g_{11} = g_{22} = g_{33} = -1, \quad g_{44} = x_1^2, \quad g_{23} = c,$$

and all other components zero. A reciprocal transformation then yields the following non-trivial solution of the field equations:

$$(11.4) \quad \begin{cases} g_{11} = g_{22} = g_{33} = -x_1^4, & g_{44} = x_1^{-2}, & g_{23} = cx_1^4, \\ g_{i\underline{x}} = 0 \quad (i \neq \underline{x}), & g_{i4} = 0, & g_{12} = g_{13} = 0. \end{cases}$$

(b) It may be noticed that Papapetrou's⁽⁶⁾ spherically symmetric so-

⁽⁶⁾ A. PAPAPETROU: *Proc. Roy. Irish Acad.*, **52**, 69 (1948).

lution

$$(11.5) \quad \begin{cases} g_{11} = -(1 - 2m/r)^{-1}, & g_{22} = g_{33} \operatorname{cosec}^2 \theta = -r^2, \\ g_{44} = (1 - 2m/r)(1 + l^4/r^4), & g_{14} = l^2/r^2, \\ g_{\iota\kappa} = 0 \quad (\iota \neq \kappa), & g_{2\kappa} = 0, \quad g_{12} = g_{24} = 0, \end{cases}$$

where m and l^4 are real constants of integration, is not static with respect to t , unlike the solution which occurs in § 10 above. It is however static with respect to φ . The appropriate reciprocal transformation will therefore generate a new solution of the field equations: this multiplies all the non-vanishing $g_{\iota\kappa}$ of (11.5) except g_{33} by $r^4 \sin^4 \theta$, whilst the new g_{33} itself becomes $r^{-2} \operatorname{cosec}^2 \theta$. This solution, unlike (11.5), is not spherically symmetric. However, it is not likely to possess any physical interest.

RIASSUNTO (*)

Si dimostra che a partire da una qualsiasi data soluzione statica delle equazioni di campo della teoria del campo unificato di Einstein, si può, per ispezione, desumere un'altra soluzione statica. Si considerano alcuni casi particolari.

(*) *Traduzione a cura della Redazione.*

A Kinematical Test for the Relation between the Coupling Constants in Meson Theory.

K. HIDA

Department of Physics, University of Hiroshima - Hiroshima, Japan

(ricevuto il 9 Gennaio 1957)

Summary. — Using the approach to a solution of the quantum field theory presented by LANDAU and co-workers, the relation between the renormalized and unrenormalized coupling constants, in S(S) and PS(PS) meson theories, will be re-examined. Then a kinematical method to test this relation, without calculating directly divergent integrals, will be presented, using the properties of the isotopic spin operator. With this method, it will be shown, in S(S) and PS(PS) meson theories, that the relation between the coupling constants obtained by the use of their method can not give correct informations about the quantum field theory.

1. — Introduction.

Since an interesting model of non-relativistic field theory has been presented by LEE^(1,2), it has become one of the most important question to ask whether in more realistic field theories such a disaster as in the case of the Lee model, which is nicknamed the ghost, also appears or not. This question has been answered by many authors⁽³⁻⁶⁾. According to them the renormalized

(¹) T. D. LEE: *Phys. Rev.*, **95**, 1329 (1954).

(²) G. KÄLLÉN and W. PAULI: *Dan. Mat. Fys. Medd.*, **30**, No. 7 (1955).

(³) L. D. LANDAU, A. A. ABRIKOSOV and I. M. HALATNIKOV: *Dokl. Acad. Nauk USSR*, **95**, 497, 773, 1177 (1954); **96**, 261 (1954).

(⁴) A. A. ABRIKOSOV, A. D. GALANIN and I. M. HALATNIKOV: *Dokl. Acad. Nauk USSR*, **97**, 793 (1954).

(⁵) I. YA. POMERANČUK, V. V. SUDAKOV and K. A. TER-MARTIROSYAN: *Phys. Rev.*, **103**, 784 (1956).

(⁶) S. KAMEFUCHI and H. UMEZAWA: *Prog. Theor. Phys.*, **15**, 298 (1956).

coupling constant g_c^2 and the renormalization constants Z_i are expressed in terms of the unrenormalized coupling constant g_0^2 , the renormalized mass m and cut-off momentum λ as follows:

$$(1.1) \quad g_c^2 = g_0^2 Q^{-1}, \quad Z_i = Q^{b_i} \quad \text{and} \quad Q = 1 + \alpha g_0^2 \log \frac{\lambda^2}{m^2},$$

where $\infty > \alpha > 0$, $0 > (b_2, b_3) > -\infty$ and $-2b_1 + 2b_2 + b_3 = -1$.

In this equation the terms

$$(1.2) \quad g_0^{2m} \left(g_0^2 \log \frac{\lambda^2}{m^2} \right)^n, \quad (m, n \geq 1),$$

have been neglected.

At a glance it can be seen that Eq. (1.1) has a similar relation between g_c^2 and g_0^2 as that of the Lee model, and this fact means that the renormalization philosophy suffers from the ghost disaster in realistic cases as well as in the Lee model. In order to study the self consistency of the renormalization philosophy in realistic cases, therefore, it would be important to examine if the properties of Eq. (1.1) give us a correct information about the relation between g_c^2 and g_0^2 or Z_i and g_0^2 in the realistic quantum field theories.

One of the most direct methods to examine this would be to compare Eq. (1.1) with the results obtained by usual perturbation calculations. Unfortunately it is very hard to calculate uniquely the diverging parts of renormalization constants up to higher order than the g_0^2 . One way to calculate diverging parts uniquely is to introduce a single cut-off in the Hamiltonian in the very beginning but this is a very difficult problem (⁷).

For this reason we shall present in this paper, in S(S) and PS(PS) meson theories, a kinematical method to study Eq. (1.1) using the properties of the isotopic spin operator. With this method, it is not necessary to calculate directly the diverging parts of renormalization constants. Sect. 2 will be devoted to reexamine some properties of Eq. (1.1) in S(S) and PS(PS) meson theories. In Sect. 3 we shall present the kinematical method mentioned above. In Sect. 4 this method will be applied to Z_1 and Z_2 up to the g_0^4 order, and to Z_3 up to the g_0^6 order. Then it will be shown, in S(S) and PS(PS) meson theories, that Eq. (1.1) can not give correct informations about the quantum field theory.

2. - Some identities for the renormalization constants.

As a preparation to investigate whether the properties of Eq. (1.1) give us correct informations about the quantum field theory or not, we shall re-

(⁷) G. KÄLLÉN: *Proceedings of the Sixth Rochester Conference on High Energy Nuclear Physics*, 1956.

examine in this section some properties of Z_i given by Eq. (1.1) in S(S) and PS(PS) meson theories. This equation, in principle, can be obtained with the aid of the Dyson-Schwinger integral equations. For simplicity's sake, however, the Pomeraňuk, Sudakov and Ter-Martirosyan's method⁽⁵⁾ will be used in this paper. According to their method, Eq. (1.1) can be obtained directly without solving the integral equations, using the renormalizability conditions⁽⁸⁾, the propagators and the vertex part for large momenta up to the g_0^2 order.

First, let us consider the simplest case where the essential part of the interaction Hamiltonian H_i , in pure neutral S(S) and PS(PS) meson theories, is given by

$$(2.1) \quad \begin{cases} H_i = g_0 \bar{\psi} \psi \varphi, \\ H_i = i g_0 \bar{\psi} \gamma_5 \psi \varphi, \end{cases}$$

respectively, and denote the vertex part and the proper self energy parts of nucleon and meson in S(S) case by Γ^S , Σ^S and Π^S and those in PS(PS) case by Γ^{PS} , Σ^{PS} and Π^{PS} respectively, then the following equations are obtained up to the g_0^2 order for large momentum — $p^2 \gg m^2$ (*):

$$(2.2) \quad \begin{cases} \Delta V(p_1, p_2) = \frac{1}{g_0} \Gamma^S(p_1, p_2) - \frac{1}{i g_0 \gamma_5} \Gamma^{PS}(p_1, p_2) \sim 0, \\ \Delta \Sigma(p) = \Sigma^S(p) - \Sigma^{PS}(p) \simeq -i m \frac{g_0^2}{4\pi} \log \frac{\lambda^2}{m^2}, \\ \Delta \Pi(p^2) = \Pi^S(p^2) - \Pi^{PS}(p^2) \simeq -i m^2 \frac{g_0^2}{\pi} \log \frac{\lambda^2}{m^2}. \end{cases}$$

As will be seen from Eq. (2.2), the large parts of $\Delta \Sigma$ and $\Delta \Pi$ contribute only to the nucleon and meson self energies respectively, and in both S(S) and PS(PS) cases the vertex part or the propagators are expressed approximately by the same functions. In fact we get, in both S(S) and PS(PS) cases, up to the g_0^2 order for the case — $p^2 \gg m^2$:

$$(2.3) \quad (+) \quad \begin{cases} \Gamma^{PS}(p_1, p_2) / \gamma_5 \simeq \Gamma^S(p_1, p_2) \simeq 1 + \frac{g_0^2}{8\pi} \log \frac{\lambda^2}{p^2}, \\ S'_F(p) / S_F(p) \simeq 1 - \frac{g_0^2}{8\pi} \log \frac{\lambda^2}{p^2}, \\ A'_F(p) / A_F(p) \simeq 1 - \frac{g_0^2}{2\pi} \log \frac{\lambda^2}{p^2}. \end{cases}$$

(8) M. GELL-MANN and F. E. LOW: *Phys. Rev.*, **95**, 1300 (1954).

(*) At large momenta, the vertex part $\Gamma(p_1, p_2)$ depends approximately on the largest of the momenta p_1 , p_2 and $(p_1 - p_2)$. Hereafter we shall denote this by p .

(+) This equation differs from that in reference (5) by a constant factor.

Making use of the renormalizability conditions and Eq. (2.3), simple calculations yield:

$$(2.4) \quad \alpha = \frac{1}{2\pi}, \quad b_1 = b_2 = -\frac{1}{4} \quad \text{and} \quad b_3 = -1,$$

for the pure neutral S(S) and PS(PS) cases, which shows that the renormalization constants in pure neutral S(S) theory are equal to those in pure neutral PS(PS) theory, and in both theories Ward's identity for renormalization constants holds⁽⁹⁾, as in the case of the quantum electrodynamics⁽¹⁰⁾.

Next, we shall consider the most general case where the interaction Hamiltonian is given by

$$(2.5) \quad \begin{cases} H_i = \sum_{j=1}^4 g_{0j} \bar{\psi} \tau_j \psi \varphi_j, & \text{for the S(S) case,} \\ H_i = i \sum_{j=1}^4 g_{0j} \bar{\psi} \gamma_5 \tau_j \psi \varphi_j, & \text{for the PS(PS) case,} \end{cases}$$

where

$$(2.6) \quad g_{0j} = a_j g_0, \quad \tau_4 = 1 \text{ (c-number)} \quad \text{and} \quad a_1 = a_2.$$

Due to invariance under the charge conjugation, a_1 must be equal to a_2 , and any two of three factors a_1 , a_3 and a_4 can take values independent from each other. In this general case the vertex part and the proper self energy parts differ from the corresponding ones in the pure neutral case only by isotopic spin parts, as shown by Figs. 1 and 2 in the g_0^2 order.

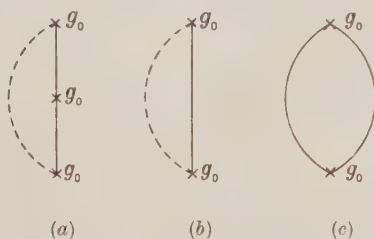


Fig. 1. - Pure neutral case.

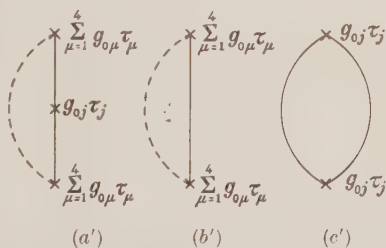


Fig. 2. - General case.

⁽⁹⁾ K. HIDA and S. MACHIDA: *Prog. Theor. Phys.*, **13**, 219 (1955).

⁽¹⁰⁾ For example, R. T. MATTHEWS and A. SALAM: *Rev. Mod. Phys.*, **23**, 311 (1951).

For these parts we get,

$$(2.7) \quad \left\{ \begin{array}{l} \sum_{\mu=1}^4 a_{\mu}^2 \tau_{\mu} \tau_j \tau_{\mu} = \begin{cases} -a_j \tau_j (2a_1^2 + a_3^2 - 2a_j^2 - a_4^2), & \text{for } j = 1, 2 \text{ or } 3, \\ a_4 (2a_1^2 + a_3^2 + a_4^2), & \text{for } j = 4, \end{cases} \\ \sum_{\mu=1}^4 a_{\mu}^2 \tau_{\mu}^2 = (2a_1^2 + a_3^2 + a_4^2), \\ \text{Sp}(a_j^2 \tau_j^2) = \begin{cases} 2a_j^2, & \text{for } j = 1, 2 \text{ or } 3, \\ a_4^2, & \text{for } j = 4, \end{cases} \end{array} \right.$$

where suffix j specifies the type of the external mesons.

As was shown by Eq. (2.7), the isotopic spin parts depend on suffix j . This fact means that nine renormalization constants generally may appear in this case, which are denoted by $Z_{i,j}$ ($j = 1$ or $2, 3$ and 4). Using the same method as in the pure neutral case, we get

$$(2.8) \quad (g_{c,j})^2 = g_0^2 Q_j^{-1} \quad \text{and} \quad Z_{i,j} = Q_j^{b_{i,j}},$$

where $Q_j > 0$, $0 > (b_{2,j}, b_{3,j}) > -\infty$ and $-2b_{1,j} + 2b_{2,j} + b_{3,j} = -1$. Q_j and $b_{i,j}$ are listed in Table I.

TABLE I. - Q_j and $b_{i,j}$ for both S(S) and PS(PS) theories.

The type of external mesons	Q_j	$b_{1,j}$	$b_{2,j}$	$b_{3,j}$	Restriction for a_j^2
$j=1$ or 2	$1 + (3a_1^2 + a_3^2) \cdot \frac{g_0^2}{2\pi} \log \frac{\lambda^2}{m^2}$	$\frac{(a_3^2 - a_4^2)}{4(3a_1^2 + a_3^2)}$	$-\frac{(2a_1^2 + a_3^2 + a_4^2)}{4(3a_1^2 + a_3^2)}$	$\frac{2a_1^2}{(3a_1^2 + a_3^2)}$	$a_1^2 \neq 0$
$j=3$	$1 + (a_1^2 + a_3^2) \cdot \frac{g_0^2}{\pi} \log \frac{\lambda^2}{m^2}$	$\frac{(2a_1^2 - a_3^2 - a_4^2)}{8(a_1^2 + a_3^2)}$	$-\frac{(2a_1^2 + a_3^2 + a_4^2)}{8(a_1^2 + a_3^2)}$	$-\frac{a_3^2}{(a_1^2 + a_3^2)}$	$a_3^2 \neq 0$
$j=4$	$1 + a_4^2 \frac{g_0^2}{2\pi} \log \frac{\lambda^2}{m^2}$	$-\frac{(2a_1^2 + a_3^2 + a_4^2)}{4a_4^2}$	$-\frac{(2a_1^2 + a_3^2 + a_4^2)}{4a_4^2}$	-1	$a_4^2 \neq 0$

Eq. (2.8) and Table I give us the following two identities for the renormalization constants in S(S) and PS(PS) meson theories:

- i) The renormalization constants in the S(S) case $Z_{i,j}^s$ are equal to those

in the PS(PS) case $Z_{i,j}^{\text{PS}}$:

$$(2.9) \quad Z_{i,j}^{\text{S}} = Z_{i,j}^{\text{PS}}.$$

ii) Especially in both neutral ($j = 3$ and $a_1 = 0$) and pure neutral ($j = 4$) cases, there hold Ward's identities for the renormalization constants:

$$(2.10) \quad \left\{ \begin{array}{l} Z_{1,3}^{\text{S}}|_{a_1=0} = Z_{2,3}^{\text{S}}|_{a_1=0}, \quad Z_{1,3}^{\text{PS}}|_{a_1=0} = Z_{2,3}^{\text{PS}}|_{a_1=0}, \\ Z_{1,4}^{\text{S}} = Z_{2,4}^{\text{S}} \quad \text{and} \quad Z_{1,4}^{\text{PS}} = Z_{2,4}^{\text{PS}}. \end{array} \right.$$

3. - A kinematical method to test eq. (2.8).

As was shown in Sect. 2, Eq. (2.8) has been obtained with use of the renormalizability conditions, the vertex part and the propagators only up to the g_0^2 order. From this fact a question arises: When Eq. (2.8) is expanded in a power series of g_0^2 , is this expression for Eq. (2.8) equal to the results obtained by perturbation calculations in every order of g_0^2 ? Though in the g_0^2 order both expressions coincide exactly, we can say nothing of what may happen until we shall calculate the higher order divergent integrals. In order to calculate these divergent integrals uniquely, on the other hand, a single cut off must be introduced in the Hamiltonian in the very beginning, and at the end of all calculations this cut off must be made to tend to infinity, but this problem is very hard to solve. For this reasons, we shall present in this paper a kinematical method to test Eq. (2.8) without use of the direct calculations, using the properties of the isotopic spin operator.

If the interaction Hamiltonian is given by Eqs. (2.5) and (2.6), the vertex part and the proper self energy parts of nucleon and meson are expanded as

$$(3.1) \quad \left\{ \begin{array}{l} \Gamma_j(p, p) = \gamma_j[A_j + (i\gamma p + m)A'_j(p)], \\ \Sigma(p) = -(\gamma p - im)B_j + (\gamma p - im)^2 B'(p), \\ \Pi_j(p^2) = -i(p^2 + \mu^2)C_j + (p^2 + \mu^2)^2 C'_j(p^2), \end{array} \right. \quad (j = 1 \text{ or } 2, 3 \text{ and } 4),$$

then it can be shown by a method similar to that given by DYSON⁽¹¹⁾ that

$$(3.2) \quad \left\{ \begin{array}{l} Z_{i,j} = [1 + A_j]^{-1}, \\ Z_{2,j} = [1 + B_j]^{-1}, \\ Z_{3,j} = [1 + C_j]^{-1}, \end{array} \right. \quad (j = 1 \text{ or } 2, 3 \text{ and } 4),$$

(11) F. J. DYSON: *Phys. Rev.*, **75**, 1736 (1949).

where Σ , B_j , B' and $Z_{2,j}$ are independent of the suffix j , and A_j , B_j and C_j are functions of the unrenormalized coupling constant and the renormalized masses.

First, let us consider the simplest case where the interaction Hamiltonian is given by Eq. (2.1). If we define A , B and C as

$$(3.3) \quad A = A_4 \Big|_{\substack{a_1=a_3=0 \\ a_4=1}}, \quad B = B_j \Big|_{\substack{a_1=a_3=0 \\ a_4=1}} \quad \text{and} \quad C = C_4 \Big|_{\substack{a_1=a_3=0 \\ a_4=1}},$$

and denote the contribution to A (B or C) from each Feynman's diagram in a g_0^{2n} order, of which the vertex part (the proper self energy part of nucleon or meson) consists, by A_i^n (E_i^n or C_i^n), then A (B or C) can be expressed as

$$(3.4) \quad A = \sum_{n=1}^{\infty} \sum_i g_0^{2n} A_i^n, \quad (B = \sum_{n=1}^{\infty} \sum_i g_0^{2n} B_i^n \quad \text{or} \quad C = \sum_{n=1}^{\infty} \sum_i g_0^{2n} C_i^n),$$

where the suffix i runs from 1 to the total number of the graphs in a g_0^{2n} order. In the next place, we shall return to the most general case. In this case the vertex part and the proper self energy parts differ from the corresponding ones in the pure neutral case only by the isotopic spin parts, and the isotopic spin space is orthogonal to the Lorentz space. The following equations, therefore, are obtained instead of Eq. (3.4)

$$(3.5) \quad \left\{ \begin{array}{l} A_j = \sum_{n=1}^{\infty} \sum_i g_0^{2n} D_{i,j}^n (a_1^2, a_3^2, a_4^2) A_i^n, \\ B_j = \sum_{n=1}^{\infty} \sum_i g_0^{2n} E_i^n (a_1^2, a_3^2, a_4^2) B_i^n, \\ C_j = \sum_{n=1}^{\infty} \sum_i g_0^{2n} F_{i,j}^n (a_1^2, a_3^2, a_4^2) C_i^n, \end{array} \right. \quad (j = 1 \text{ or } 2, 3 \text{ and } 4),$$

where $D_{i,j}^n$, E_i^n and $F_{i,j}^n$ depend only on the isotopic spin parts.

Inserting this expression for A_j into the first of Eq. (3.2), and expanding $Z_{1,j}$ in powers of g_0^2 , we get

$$(3.6) \quad Z_{1,j} = [1 + A_j]^{-1} = 1 - D_{1,j}^1 A_1^1 g_0^2 + \{ (D_{1,j}^1 A_1^1)^2 - D_{1,j}^2 A_1^2 - D_{2,j}^2 A_2^2 - \dots \} g_0^4 + \dots \\ (j = 1 \text{ or } 2, 3 \text{ and } 4).$$

On the other hand, from Eq. (2.8) the following equation is obtained

$$(3.7) \quad Z_{1,j} = \left[1 + g_0^2 \alpha_j \log \frac{\lambda^2}{m^2} \right]^{b_{1,j}} = \\ = 1 + b_{1,j} \alpha_j \log \frac{\lambda^2}{m^2} g_0^2 + \frac{b_{1,j}(b_{1,j}-1)}{2} \left(\alpha_j \log \frac{\lambda^2}{m^2} \right)^2 g_0^4 + \dots \\ (j = 1 \text{ or } 2, 3 \text{ and } 4).$$

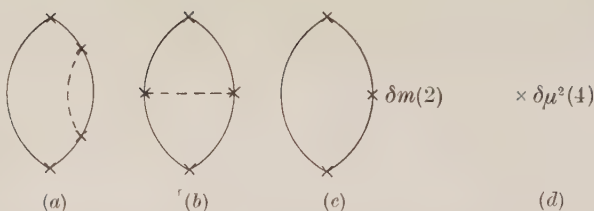


Fig. 3. — Proper self energy graphs of meson in the g_0^4 order, where $\delta m(2)$ and $\delta\mu^2(4)$ denote the self energy of the nucleon in the g_0^2 and of the meson in g_0^4 order respectively.

As will be seen from Fig. 1 (c'), 3 (a) and 3 (b), we have to calculate the following isotopic spin parts:

$$(4.2) \quad \left\{ \begin{aligned} F_{1,j}^1(a_1^2, a_3^2, a_4^2) &= \begin{cases} 2a_j^2, & \text{for } j = 1, 2 \text{ or } 3, \\ a_4^2, & \text{for } j = 4, \end{cases} \\ F_{1,j}^2(a_1^2, a_3^2, a_4^2) &= \text{Sp} \left(\sum_{\mu=1}^4 a_j^2 a_\mu^2 \tau_j \tau_\mu \tau_\mu \tau_j \right) = \\ &= \begin{cases} 2a_j^2(2a_1^2 + a_3^2 + a_4^2), & \text{for } j = 1, 2 \text{ or } 3, \\ a_4^2(4a_1^2 + 2a_3^2 + a_4^2), & \text{for } j = 4, \end{cases} \\ F_{2,j}^2(a_1^2, a_3^2, a_4^2) &= \text{Sp} \left(\sum_{\mu=1}^4 a_j^2 a_\mu^2 \tau_j \tau_\mu \tau_j \tau_\mu \right) = \\ &= \begin{cases} -2a_j^2(2a_1^2 + a_3^2 - 2a_j^2 - a_4^2), & \text{for } j = 1, 2 \text{ or } 3, \\ a_4^2(4a_1^2 + 2a_3^2 + a_4^2), & \text{for } j = 4. \end{cases} \end{aligned} \right.$$

Using Eqs. (3.5) and (4.2), we get

$$(4.3) \quad C_j = \begin{cases} 2a_j^2 c_1^2 g_0^4 + 2a_j^2 \{ (2a_1^2 + a_3^2 + a_4^2) c_1^2 - (2a_1^2 + a_3^2 - 2a_j^2 - a_4^2) c_2^2 \} g_0^4 + \dots & \text{for } j = 1, 2 \text{ or } 3, \\ a_4^2 c_1^2 g_0^4 + a_4^2 \{ 4a_1^2 + 2a_3^2 + a_4^2 \} (c_1^2 + c_2^2) g_0^4 + \dots & \text{for } j = 4. \end{cases}$$

Inserting these equations into Eq. (3.2),

$$(4.4) \quad Z_{3,j} = \begin{cases} 1 - 2a_j^2 c_1^2 g_0^2 + 2a_j^2 \{ 2a_j^2 (c_1^2)^2 - (2a_1^2 + a_3^2 + a_4^2) c_1^2 + (2a_1^2 + a_3^2 - 2a_j^2 - a_4^2) c_2^2 \} g_0^4 \dots & \text{for } j = 1, 2 \text{ or } 3, \\ 1 - a_4^2 c_1^2 g_0^2 + a_4^2 \{ a_4^2 (c_1^2)^2 - (4a_1^2 + 2a_3^2 + a_4^2) (c_1^2 + c_2^2) \} g_0^4 + \dots & \text{for } j = 4 \end{cases}$$

are obtained.

(Case A) $j = 1$ or 2 ($a_1 \neq 0$).

From Eq. (2.8) and Table I, on the other hand, the following equation is obtained:

$$(4.5) \quad Z_{3,j} = \left[1 + (3a_1^2 + a_3^2) \frac{g_0^2}{2\pi} x \right]^{-2a_1^2/(3a_1^2 + a_3^2)} = \\ = 1 - a_1^2 \frac{g_0^2}{\pi} x + a_1^2(5a_1^2 + a_3^2) \frac{g_0^4}{4\pi^2} x^2 + \dots, \quad \text{for } j = 1 \text{ or } 2,$$

where $x = \log \lambda^2/m^2$. Comparing Eq. (4.4) with Eq. (4.5), we get

$$(4.6) \quad C_1^1 = \frac{x}{2\pi},$$

$$(4.7) \quad (2a_1^2 + a_3^2 + a_4^2)C_1^2 - (a_3^2 - a_4^2)C_2^2 = - (a_1^2 + a_3^2) \frac{x^2}{8\pi^2}.$$

As was shown by Eq. (4.6), C_1^1 is independent of a_i^2 factors. The structure of Eq. (4.7) is such that, though in this equation any two of three a_i^2 factors may take values independent from each other, the total number of the independent equations for c_1^2 and c_2^2 is two. Solving these equations, in fact, we get a unique solution:

$$(4.8) \quad C_1^2 = C_2^2 = - \frac{x^2}{16\pi^2},$$

which is independent of a_i^2 factors.

(Case B) $j = 3$ ($a_3 \neq 0$).

From Eq. (2.8) and Table I, we get

$$(4.9) \quad Z_{3,3} = \left[1 + (a_1^2 + a_2^2) \frac{g_0^2}{\pi} x \right]^{-a_3^2/(a_1^2 + a_2^2)} = \\ = 1 - a_3^2 \frac{g_0^2}{\pi} x + a_3^2(a_1^2 + 2a_2^2) \frac{g_0^4}{2\pi^2} x^2 + \dots$$

Comparing Eq. (4.4) with Eq. (4.9), one obtains Eq. (4.6) and

$$(4.10) \quad (2a_1^2 + a_2^2 + a_4^2)C_1^2 - (2a_1^2 - a_2^2 - a_4^2)C_2^2 = - \frac{a_1^2 x^2}{4\pi^2}.$$

(Case C) $j = 4$ ($a_4 \neq 0$).

From Eq. (2.8) and Table I, we get

$$(4.11) \quad Z_{3,4} = \left[1 + a_4^2 \frac{g_0^2}{2\pi} x \right]^{-1} = 1 - a_4^2 \frac{g_0^2}{2\pi} x + a_4^4 \frac{g_0^4}{4\pi^2} x^2 + \dots$$

Comparing Eq. (4.4) with Eq. (4.11), one obtains Eq. (4.6) and

$$(4.12) \quad c_1^2 + c_2^2 = 0.$$

Eq. (4.10) has also the same structure and the same solution as Eq. (4.7). Eq. (4.12) is independent of a_i^2 factors. Further calculations show that $C_i^{3,3}$ depend on a_i^2 factors explicitly.

In the next place, we shall test $Z_{1,j}$ up to the g_0^4 order. Now we shall denote the contributions to A from Feynman's diagrams which are shown by Fig. 1 (a), 4 (a), 4 (b), and 4 (c), by A_1^1 , A_1^2 , A_2^2 and A_3^2 respectively. If $Z_{1,j}$ given by Eq. (2.8) is equal to that to be obtained by perturbation calculations, then the contributions to A from Fig. 4 (d), 4 (e), and 4 (f) may be neglected.

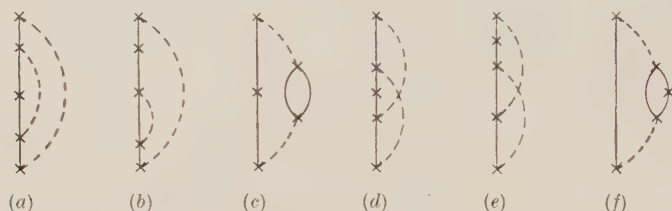


Fig. 4. - Feynman's diagrams for the vertex part in the g_0^4 order.

Making use of the same method as that in the case of $Z_{3,j}$, we get the following results:

(Case A) $j = 1$ or 2 ($a \neq 0$).

$$(4.13) \quad \left\{ \begin{aligned} A_1^1 &= \frac{x}{8\pi}, \\ (a_3^2 - a_4^2)^2 A_1^2 - (a_3^2 - a_4^2)(2a_1^2 + a_3^2 + a_4^2) A_2^2 - (2a_3^4 - a_4^4) A_3^2 &= \\ &= \frac{x^2}{128\pi^2} (a_3^2 - a_4^2)(12a_1^2 + 5a_3^2 - a_4^2). \end{aligned} \right.$$

(Case B) $j = 3$ ($a_3 \neq 0$).

$$(4.14) \quad \left\{ \begin{aligned} A_1^1 &= \frac{x}{8\pi}, \\ (2a_1^2 - a_3^2 - a_4^2)^2 A_1^2 - (2a_1^2 - a_3^2 - a_4^2)(2a_1^2 + a_3^2 + a_4^2) A_2^2 - \\ &\quad - (4a_1^4 - 2a_3^4 - a_4^4) A_3^2 = \frac{x^2}{128\pi^2} (2a_1^2 - a_3^2 - a_4^2) (10a_1^2 + 7a_3^2 - a_4^2). \end{aligned} \right.$$

(Case C) $j = 4$ ($a_4 \neq 0$).

$$(4.15) \quad \left\{ \begin{aligned} A_1^1 &= \frac{x}{8\pi}, \\ (2a_1^2 + a_3^2 + a_4^2)^2 (A_1^2 + A_2^2) + (4a_1^4 + 2a_3^4 + a_4^4) A_3^2 = \\ &= \frac{x^2}{128\pi^2} (2a_1^2 + a_3^2 + a_4^2) (2a_1^2 + a_3^2 - 3a_4^2). \end{aligned} \right.$$

As will be seen from Eqs. (4.13), (4.14) and (4.15), A_1^1 is independent of a_i^2 factors but A_1^2 , A_2^2 and A_3^2 do depend on a_i^2 factors explicitly. Further calculations for $Z_{2,j}$ show that B_1^1 is independent of a_i^2 factors but B_i^2 's do depend on a_i^2 factors, as in the case of A_1^1 and A_i^2 's. Summing these results, we get Table II. Therefore we may conclude, in the S(S) and PS(PS) meson theories, that the relation between the renormalized coupling constant and the unrenormalized one, or the renormalization constants and the unrenormalized coupling constant obtained by the method of the reference ⁽³⁾, can not coincide with that to be obtained by perturbation calculations.

TABLE II. - Test for $Z_{i,j}$ given by Eq. (2.8).

	g_0^2	g_0^4	g_0^6
$Z_{1,j}$	Yes	No	
$Z_{2,j}$	Yes	No	
$Z_{3,j}$	Yes	Yes	No

* * *

The author would like to thank for Prof. K. SAKUMA for his continuous encouragement.

RIASSUNTO (*)

Si riesamina la relazione tra le costanti d'accoppiamento nelle teorie mesoniche $S(S)$ e $PS(PS)$ utilizzando il tentativo di soluzione della teoria quantica dei campi proposto da LANDAU e coll. Si presenta poi un metodo cinematico per saggiare questa relazione senza il calcolo diretto di integrali divergenti, servendosi delle proprietà dell'Operatore di spin isotopico. Si dimostra poi con questo metodo che nelle teorie mesoniche $S(S)$ e $PS(PS)$ le relazioni tra le costanti d'accoppiamento ottenute coi rispettivi metodi non possono fornire informazioni corrette sulla teoria quantica dei campi.

(*) *Traduzione a cura della Redazione.*

A Triggered Spark Counter.

T. E. CRANSHAW and J. F. DE BEER

A.E.R.E. - Harwell

(ricevuto l'11 Gennaio 1957)

Summary. — The behaviour of a triggered parallel plate spark counter has been investigated as a possible means of determining the trajectories of ionizing particles. Efficiencies, in an air-spaced counter, were 99%, with a rate of random breakdowns less than 1%.

1. — Introduction.

Various authors ⁽¹⁻³⁾ have reported on the construction and characteristics of spark counters. In its simplest form a spark counter consists of two parallel plates to which a high voltage is applied. When a charged particle traverses the counter, leaving some ions in the gap, a spark discharge occurs. A serious difficulty in this type of detector is the prevention of «spurious» discharges, unconnected with the ionizing events which it is desired to detect.

Recently CONVERSI *et al.* ^(4,5) described the construction and characteristics of what they called a hodoscope chamber. Glass tubes are filled with ~ 350 mm neon and then placed between parallel conducting plates. When an ionizing particle goes through the apparatus, a high voltage pulse is applied to the plates. A glow discharge is produced in those tubes which the particle has traversed and not in the others.

(*) On leave from the University of Potchefstroom, South Africa.

(1) J. W. KEUFFEL: *Rev. Sci. Instr.*, **20**, 202 (1949).

(2) R. W. PIDD and L. MADANSKY: *Phys. Rev.*, **75**, 1175 (1949).

(3) E. ROBINSON: *Proc. Phys. Soc.*, A **66**, 73 (1953).

(4) M. CONVERSI and A. GOZZINI: *Nuovo Cimento*, **2**, 189 (1955).

(5) M. CONVERSI, S. FOCARDI, C. FRANZINETTI, A. GOZZINI and P. MURTAS: *Suppl. Nuovo Cimento*, **4**, 234 (1956).

In the present experiments, we have combined these techniques in the following way. High voltage pulses are applied to the plates of a parallel plate condenser when an ionizing particle traverses the condenser. A spark discharge is established near the track of the particle. We have investigated the dependence of the efficiency on various parameters, using an experimental counter with 1 mm spacing between the plates, and also report on counters specially designed for high efficiency. The accuracy with which particle trajectories can be determined was investigated photographically.

2. - Arrangements for the experimental counter.

The experimental arrangements are represented schematically by Fig. 1. G is a Geiger telescope which gives a coincidence pulse when an ionizing particle goes through the detector.

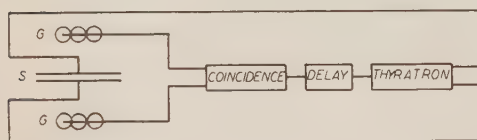


Fig. 1.

This pulse, after going through a delay network, triggers a hydrogen thyatron which switches a high voltage pulse onto the detector. The thyatron circuit is shown in Fig. 2. The thyatron is non-conducting when its grid is at earth potential so that the condenser C charges up to the supply voltage through the high resistance R_1 . When a positive trigger of ~ 300 V is applied to the grid, the thyatron fires and discharges C through R . At A a pulse appears with maximum amplitude equal to the supply voltage, its time of decay being given by the time constant RC . This high voltage pulse is applied to the detector S through the resistance R_2 which limits the

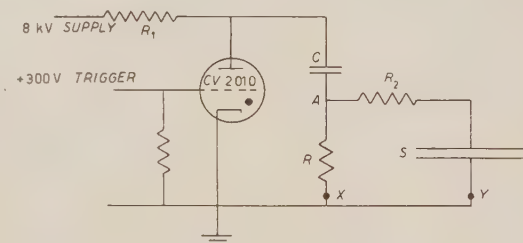


Fig. 2.

current to a value below the maximum permissible thyatron current, (20 A for the CV2110). To clear «old» ions from the gap, a clearing field is applied between the plates by inserting a battery in position X or Y . The 300 V trigger pulse is obtained via a pulse transformer from a smaller thyatron which discharges a $3 \mu s$ delay line. Supply voltages up to 8 kV were used. The voltage supply is a voltage multiplier circuit (Cockcroft-Walton-type) using metal rectifiers.

The detector consisted of a simple parallel plate condenser of $10 \times 10 \text{ cm}^2$ area with 1 mm separation between the plates. The edges were carefully rounded off in order to weaken the field along them.

3. - Theoretical considerations.

We make the initial assumption that the presence of an ion in the gap at the instant the applied pulse reaches a critical value is a necessary and sufficient condition for the initiation of a spark discharge. Let the distance between the plates be d and n the specific ionization in air of a minimum ionizing particle traversing the plates perpendicularly. Due to the strong electron affinity of oxygen all electrons are captured as soon as they are formed. The process of ionization therefore causes the formation of positive ions (mainly nitrogen) and an equal number of negative oxygen ions. If we assume the mobility of the ions to be constant over the range of variation in clearing field under consideration, and the same for both positive and negative ions which is true enough for our present purpose, then the velocity is given by

$$(1) \quad v = KV,$$



Fig. 3.

where V is the clearing voltage.

The space x (Fig. 3) is such that no ion which was formed in it, is still in the gap after time t . We distinguish between two cases: (i) ions of either sign can initiate a discharge, (ii) ions of one sign only can initiate a discharge.

In case (i) it is evident that

$$(2) \quad x = 2vt - d$$

and the sensitive space

$$(3) \quad \begin{cases} s = d - x \\ = 2(d - vt); & vt > d/2 \\ = d & vt \leq d/2. \end{cases}$$

In case (ii)

$$s = d - vt.$$

The theoretical efficiency of the counter is the probability than an ion which can initiate a discharge exists in the gap when the pulse is applied, i.e.

In case (i)

$$(5) \quad \left\{ \begin{array}{ll} \varepsilon = 1 - \exp[-2n(\bar{d} - vt)] ; & vt > d/2 \\ \varepsilon = 1 - \exp[-nd] ; & vt \leq d/2 . \end{array} \right.$$

In case (ii)

$$(6) \quad \varepsilon = 1 - \exp[-n(d - vt)] .$$

If n is taken equal to ~ 22 ion pairs per cm, both equations (5) and (6) give $\sim 90\%$ as the maximum efficiency obtainable with a 1 mm gap.

4. - Performance of experimental counter.

The experimental efficiency of the detector is defined as the number of spark discharges divided by the number of coincidences registered by the counter telescope. Various factors have an influence on the efficiency e.g. pulse size, rise time of pulse, delay between passage of particle and application of pulse, magnitude of clearing field, separation between plates, and atmospheric pressure. The quantitative influence of some of these factors governing the efficiency has been investigated and will now be discussed in succession.

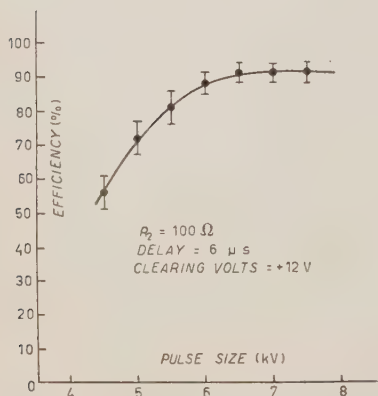


Fig. 4.

(a) *Pulse size.* - Pulses of various sizes were applied to the detector while the other factors were kept constant. The dependence of efficiency on pulse size is shown in Fig. 4, from which it is evident that there is a useful plateau almost 2000 V wide, the upper limit being set by the occurrence of spurious

discharges. A spurious discharge is one which occurs when a pulse is applied to the detector in the absence of any triggering particle. By cleaning and drying the surfaces carefully and excluding light, it was possible to reduce the fraction of spurious breakdowns to less than 1%.

(b) *Decay time of pulse.* — In the range 10^{-7} s to 10^{-4} s, no effect of the decay time on the efficiency was found. This is to be expected, as the spark discharge is established in a time of the order of 10^{-8} s. When the decay time, however, is increased beyond say $50 \mu\text{s}$, the rate of random breakdowns increases as a result of the increase in the sensitive time of the detector.

(c) *Clearing field and delay.* — The variation of the efficiency with clearing field for several delay times has been determined. Equations (5) and (6) suggest that we plot $\ln(1 - \epsilon)$ against v . We call $(1 - \epsilon)$ the inefficiency and

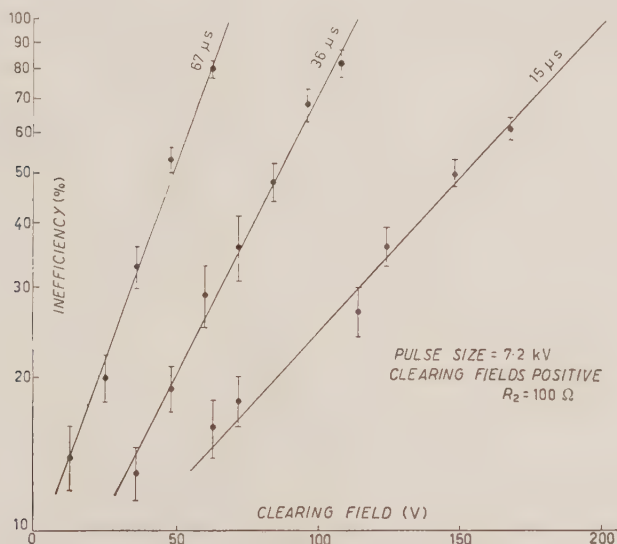


Fig. 5.

in Fig. 5 this has been plotted on a logarithmic scale against clearing voltage. The experimental points lie on straight lines which all extrapolate back to approximately the same value of the inefficiency at zero clearing voltage. The relation between efficiency and clearing voltage as predicted by equations (5) and (6) is represented by the straight lines (a) and (b) respectively in Fig. 6 where the inefficiency is plotted on a logarithmic scale against vt/d . An average value of 93% for the efficiency at zero clearing voltage has been taken from the experimental results of Figs. 4 and 5. This value is slightly higher than one would expect with a 1 mm air-spaced gap under atmospheric pressure and a value of 22 ion pairs/cm for the specific ionization. It seems likely that δ -rays may contribute towards this higher efficiency (see later). The experimental points of Fig. 5 have been transferred to Fig. 6 and nor-

malized at $vt/d = 1$, assuming constant mobility. The mobility can readily be calculated, since, when $KVt = d$, the efficiency is zero. Thus we get from Fig. 5:

$$K = 22 \pm 1 \text{ cm/s/V at } 650 \text{ V/cm, delay } 67 \mu\text{s},$$

$$K = 24.4 \pm 1 \text{ cm/s/V at } 1150 \text{ V/cm, delay } 36 \mu\text{s},$$

$$K = 33 \pm 1 \text{ cm/s/V at } 2000 \text{ V/cm, delay } 15 \mu\text{s}.$$

These values may be compared with the value $K = 33 \text{ cm/s/V}$ given by WILKINSON⁽⁶⁾, who also remarks that the mobility decreases with age of the ions.

It is clear that the experimental points lie on line (b) rather than on (a) showing that equation (6) gives the correct relation between the efficiency and the clearing voltage. This suggests that spark discharges are initiated by ions of one sign only. The question now arises as to whether the discharges are being initiated by the positive or by the negative ions. It seems likely that the negative ions are responsible since according to LOEB⁽⁷⁾ the binding energy of the electron to the oxygen molecule is only $\sim 0.34 \text{ V}$ and at a value of $X/p \approx 90$ (X = field strength in V/cm; p = pressure in mm Hg) it becomes detached and gains sufficient energy to initiate an electron-photon avalanche. In these experiments the value of X/p lies between 80 and 100. On the other hand the positive ions, being much more massive, do not obtain sufficient energy between successive collisions to produce further ionization.

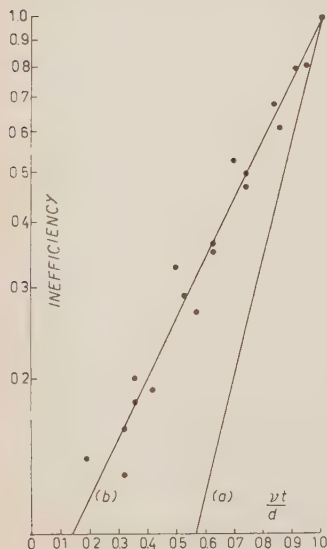


Fig. 6.

(d) *Rise time of pulse and polarity of clearing field.* — A decrease in efficiency was observed when the resistor R_2 was increased gradually. Fig. 7 shows how the efficiency depends on the value of R_2 . If, instead of increasing R_2 , the capacity of the detector was increased, the behaviour was similar. It has also been observed that the efficiency had a different value when the polarity of the clearing voltage was reversed. Fig. 8 shows the dependence of the inefficiency on the clearing field for different

(⁶) D. H. WILKINSON: *Ionization Chambers and Counters* (Cambridge, 1950).

(⁷) L. B. LOEB: *Phys. Rev.*, **48**, 684 (1935).

polarities of the clearing field. These two effects have been investigated more carefully and we found that both can be explained by the clearing done by the applied pulse before it reaches the critical value for a discharge. For a certain finite rise time this clearing action is independent of the clearing voltage and may be represented by the constant c . If the clearing field has the same polarity as the pulse, c adds to vt and the equation for the efficiency is

$$(7) \quad \varepsilon = 1 - \exp[-n(d - vt - c)].$$

If on the other hand the polarity of the clearing voltage is opposite to that of the pulse, the actual amount of clearing done stays equal to c as long as $vt < c$ and is equal to vt if $vt \geq c$. In this case therefore

$$(8) \quad \begin{cases} \varepsilon = 1 - \exp[-n(d - c)]; & vt < c, \\ \varepsilon = 1 - \exp[-n(d - vt)]; & vt \geq c. \end{cases}$$

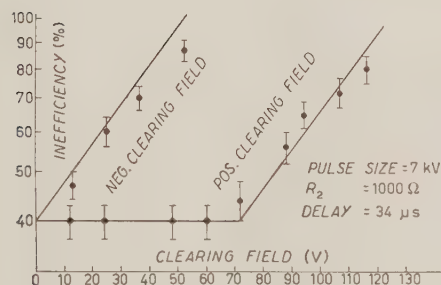


Fig. 8.

respectively. The agreement with the experimental points may be considered as very satisfactory.

A theoretical evaluation of c from the parameters of the experiment, requires a knowledge of the mechanism of spark discharges and accurate values of ion mobilities for fields up to 80 kV per cm.

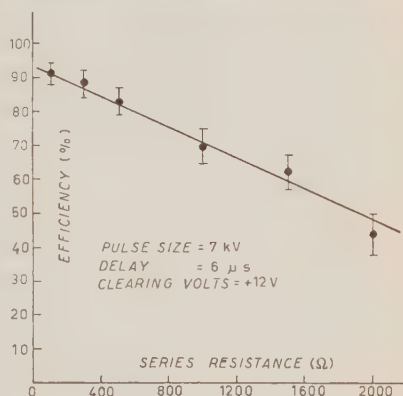


Fig. 7.

When $v = 0$, equations (7) and (8) give the same value for the maximum efficiency

$$(9) \quad \varepsilon_{\max} = 1 - \exp[-n(d - c)].$$

From Fig. 8 we get $\varepsilon_{\max} \approx 0.6$ which means $c \approx 0.058$ cm. Equations (7) and (8) with this value of c and $K = 24$ cm/s/V, are represented in Fig. 8 by the curves (a) and (b)

5. - Further developments.

(a) The efficiency is seen to increase with decreasing rise time and therefore with decreasing R_2 . In order, therefore, to obtain the maximum efficiency, R_2 must be made as small as possible. It cannot, however, be decreased indefinitely because the maximum permissible instantaneous current through the thyatron will be exceeded. Alternatively the area of the detector, and therefore its capacitance may be made small. This places a serious restriction on the utility of the detector.

(b) As can be seen in Fig. 4, the maximum obtainable efficiency with a 1 mm gap (and air under atmospheric pressure) is $\sim 92\%$. Although this may be adequate in certain applications, it is desirable to increase this figure. This can be done by increasing the separation. With a 3 mm gap for instance, an efficiency of 99% is obtainable. This increase, however, requires a high pulse voltage (~ 20 kV). As a hydrogen thyatron usually cannot be operated beyond 10-12 kV, the most obvious means of achieving this pulse would be to use a pulse transformer. This transformer has to meet both the requirements of excellent high frequency response and high power handling capacity. A transformer of this description has been made and quite satisfactory performance was obtained with it. One serious disadvantage is that the impedance is stepped up by the square of the turns ratio, which in turn requires that C (Fig. 2) has to be increased. Another disadvantage is the high magnetising energy required by the core for good transient response.

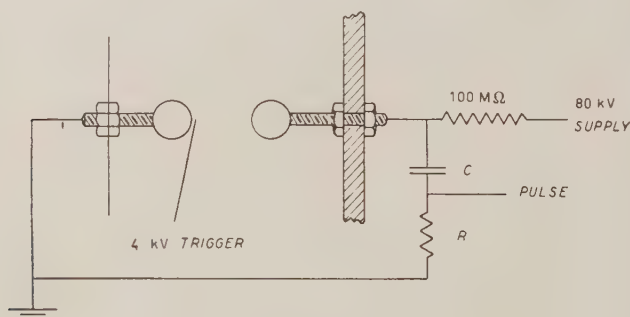


Fig. 9.

Most of the above mentioned difficulties have been overcome by using a single air-spaced spark gap to trigger the detector. The original thyatron is now only used to trigger the spark gap (Fig. 9).



Fig. 10.

A detector with 2.5 mm separation has been operated in this way and a similar performance as before was obtained except for the higher maximum efficiency ($\sim 99\%$).

6. - Photographic recording of trajectories.

Three identical units, each consisting of two detectors were lined up in the solid angle of the counter telescope. Six high voltage condensers were used with one spark gap to apply the pulses. Photographs of a large number of events were taken, of which some typical ones are displayed in Fig. 10. Photographs (a) and (b) show the ideal behaviour as the sparks apparently lie exactly on the trajectory of the particle. In photographs (c) one of the sparks is slightly displaced from the real trajectory as indicated by the others. The cause of these displacements (1-2 mm) has not been investigated thoroughly but it seems likely that knock-on electrons are responsible for this effect as they will be heavily ionizing. This view is supported by a number of photographs like the one in Fig. 10(d) in which two sparks occurred in the same gap, one of which is slightly displaced from the trajectory.

7. - Conclusions.

(i) We have shown that spark discharges can be produced with high efficiency in an air-spaced gap between parallel plates which is pulsed after the passage of an ionizing particle.

(ii) The pulse may be applied many microseconds after the passage of the particle, with a probability of a discharge which depends on a static clearing field.

(iii) The number of « spurious » discharges can be kept below 1%.

(iv) The spark occurs where a particle has traversed the detector except in a few cases ($\sim 10\%$) where knock-on electrons probably are responsible for slight displacements.

* * *

The authors wish to express their thanks to the U.K.A.E.A. for permission to publish these results and to Dr. E. BRETSCHER for his kind interest during these investigations.

RIASSUNTO (*)

Si è esaminato il comportamento di un contatore a scintille a placche parallele comandato, per studiare la possibilità di utilizzarlo nella determinazione delle traiettorie di particelle ionizzanti. I rendimenti di un contatore con aria fra le placche risultarono il 99% con meno dell'1% di scariche casuali.

(*) *Traduzione a cura della Redazione.*

Thermodynamical Theory of Thermal Conduction of Dielectrics under Electric Fields.

S. MASCARENHAS

Escola de Engenharia de São Carlos, Dep. de Física - Universidade de São Paulo, Brasil

(ricevuto il 16 Gennaio 1957)

Summary. — The abnormal heat transmission of a fluid dielectric under electrical fields can be conveniently described as a cross-effect between thermal and electrical forces. The author studies the case of low fields for a plane cell when convection effects are absent. He is also led to the converse effect, i.e., the variation of the electrical conductivity with the thermal force.

1. — The author has observed and described elsewhere ⁽¹⁾ a strong variation of the thermal conductivity of insulating liquids under the action of electrical fields.

The action of the field is such as to always increase the heat transmission independently of the direction of the field. We have also observed the effect with alternating fields.

It can be shown experimentally that there are two distinct effects as the field value is increased: one in which there are no hydrodynamical effects of the field upon the fluid (for low fields) and another in which turbulence sets in and the heat transmission is strongly dependent upon forced-field-convection ⁽²⁾.

The first behavior displays a quadratic dependence of the thermal conductivity with tensions applied across the cell ⁽³⁾. The other one shows a

⁽¹⁾ S. MASCARENHAS: *An. Acad. Brasil. Ci.*, **27**, 11 (1955); **28**, 1, 99 (1956).

⁽²⁾ See R. KRONIG and G. ASHMAN: *Appl. Sci. Res.*, **1** (1949) and G. A. OSTROUMOV: *Žu. Eksper. Teor. Fiz.*, **30**, 2 (1956).

⁽³⁾ S. MASCARENHAS: *Thesis* (Univ. S. Paulo, 1956).

rather complicated behavior which (when «break-down» does not occur) shows a saturation of the heat transmission for very high values of the tension. We have also observed and described ⁽³⁾ elsewhere that the hydrodynamical effect begins at a very characteristic field for each dielectric (about 1 kV/cm for oleic acid, 0.2 kV/cm for naphtalene).

2. — Focusing our attention on the behavior under low fields we can obtain from the principles of the thermodynamics of irreversible processes the observed interaction between the thermal and electrical forces as regards the heat conductivity as follows:

Let us consider a plane parallel condenser filled with a homogeneous fluid dielectric, and let there be applied across the plates both an electric and a thermal potential difference.

The equations of motion can be written ⁽⁴⁾ as

$$(1) \quad J_q = -L_{11} \text{grad } \theta/\theta + L_{12} E$$

$$(2) \quad j = -L_{21} \text{grad } \theta/\theta + L_{22} E$$

where J_q and j are the thermal and electrical fluxes, $-\text{grad } \theta/\theta$ and E the corresponding forces and L_{11} , L_{12} , L_{21} and L_{22} the phenomenological coefficients.

From the Onsager relation:

$$(3) \quad L_{12} = L_{21} .$$

And with this result one can write:

$$(4) \quad J_q + L_{11} \text{grad } \theta/\theta = (jE - L_{22} E^2)/-\text{grad } \theta/\theta .$$

The left member of this equation can be identified with the excess thermal flux ΔJ_q , which is evidently null when there is no applied electrical field. This excess flux can be written as

$$(5) \quad \Delta J_q = -k \text{grad } \theta + k_0 \text{grad } \theta .$$

In this equation we have written k and k_0 for the thermal conductivities with and without the application of the electrical field. Taking account of the fact that $j = \sigma E$ and $j_0 = \sigma_0 E$ (σ and σ_0 electrical conductivities with and

⁽⁴⁾ See for instance S. R. DE GROOT: *Thermodynamics of Irreversible Processes* (Amsterdam 1951).

without the application of a temperature gradient), one obtains

$$(6) \quad k = k_0 + (\sigma - \sigma_0)\theta \frac{E^2}{\text{grad}^2 \theta}.$$

And as $-\text{grad } \theta = (\theta_s - \theta)/\lambda$ (θ_s and θ the equilibrium temperatures of the plates, λ the distance between them), eq. (6) transforms to

$$k = k_0 + \frac{(\sigma - \sigma_0)\theta}{(\theta_s - \theta)^2} \lambda^2 E^2.$$

But $\lambda E = V$, thus:

$$(7) \quad k = k_0 + \frac{(\sigma - \sigma_0)\theta}{(\theta_s - \theta)^2} V^2.$$

This is our central result.

3. — Our formula (7) seems to be well supported by experimental results since:

- a) the variation of k does not depend on the sign of the field;
- b) the observed quadratic dependence of k upon V .

Attention must be called to the fact that this theory points also to the converse effect of the one treated here: the variation of σ with $-\text{grad } \theta/\theta$.

It is also to be noted from (7) that if $\sigma < \sigma_0$ (i.e. the electrical conductivity diminishes with the thermal force), $k < k_0$ and the thermal conductivity will also decrease with the applied field.

We think that our thermodynamical treatment can be extended to encompass the hydrodynamical effects by assuming a third term and a corresponding third equation of motion to take care of convection currents within the fluid. Finally our results provide a possible explanation for the recently observed phenomenon⁽⁵⁾ of field-induced melting of dielectrics.

* * *

We are indebted to T. A. SOUTA, A. TAVARES, E. RODRIGUES and L. P. MAIA for helpful discussions.

⁽⁵⁾ J. COSTA RIBEIRO: *An. Acad. Brasil. Ci.*, **26**, 2, 349 (1954).

RIASSUNTO (*)

L'anormale trasmissione di calore di un dielettrico fluido sotto l'azione di campi elettrici può essere opportunamente descritta come un effetto combinato di forze termiche ed elettriche. L'autore studia il caso di campi deboli per una cella piana in assenza di effetti di convezione. Considera anche il caso inverso, cioè la variazione della conduttività elettrica con la forza termica.

(*) *Traduzione a cura della Redazione.*

Bounds on Phase Shifts (*).

J. B. KELLER

Institute of Mathematical Sciences, New York University - New York, N. Y.

(ricevuto il 18 Gennaio 1957)

Summary. — It is shown that for certain potentials, the WKB method yields a lower bound for the exact phase shift, and for some other potentials it yields an upper bound. Another method for obtaining bounds is also described.

1. — Introduction.

The phase shift δ for a potential V at energy E is defined in terms of a solution $u(r)$ of the following problem:

$$(1) \quad u'' + [k^2 - U(r)]u(r) = 0,$$

$$(2) \quad u(0) = 0.$$

In (1), $U(r) = 2m\hbar^{-2}V(r)$ and $k = \hbar^{-1}(2mE)^{\frac{1}{2}}$. If $U(r)$ tends to zero fast enough as $r \rightarrow \infty$, then $u(r)$ is of the form

$$(3) \quad u(r) \sim A \sin(kr + \delta) \text{ as } r \rightarrow \infty.$$

The constant δ in (3) is the phase shift and the constant A is an amplitude factor. Since (3) determines δ only within an integral multiple of π , we also require that δ depend continuously on $U(r)$ and vanish when $U(r) \equiv 0$.

(*) The research reported in this article was done at the Institute of Mathematical Sciences, New York University, and has been made possible through support and sponsorship extended by the Geophysics Research Directorate, Air Force Cambridge Research Center, under Contract No. AF19(122)-463.

Then δ is uniquely determined and satisfies the well known

Monotonicity Theorem: If $V_1 \leq V_2$ for all $r \geq 0$ then $\delta_1 \geq \delta_2$.

In the following sections we will use this theorem to obtain bounds on δ . As an example, since $\delta = 0$ when $V = 0$ we see that $\delta \geq 0$ if $V \leq 0$ and $\delta \leq 0$ if $V \geq 0$.

2. - The case $E > V$.

Assume that $E > V$ for all r , and let $v(r)$ be the WKB solution of (1) and (2), i.e.,

$$(4) \quad v(r) = k^{\frac{1}{2}}(k^2 - U)^{-\frac{1}{2}} \sin \left[\int_0^r (k^2 - U)^{\frac{1}{2}} dr \right].$$

The phase shift of $v(r)$, which we will call δ_{WKB} , is

$$(5) \quad \delta_{\text{WKB}} = \int_0^{\infty} [(k^2 - U)^{\frac{1}{2}} - k] dr.$$

Now the function $v(r)$ is not only the WKB solution of (1) and (2) but it is also an exact solution of the following problem:

$$(6) \quad v'' + \left[k^2 - U - \frac{1}{4(k^2 - U)} \left\{ U'' + \frac{5(U')^2}{4(k^2 - U)} \right\} \right] v = 0$$

$$(7) \quad v(0) = 0.$$

Since this problem is of the same type as (1) and (2) with a different potential (*), the monotonicity theorem is applicable and yields

Theorem I: If $E > V$ and $V'' + 5(V')^2/4(E - V) \geq 0$ (≤ 0) for all $r \geq 0$ then

$$\delta \geq \delta_{\text{WKB}} \quad (< \delta_{\text{WKB}}).$$

From this theorem, since $5(V')^2/4(E - V) \geq 0$, we obtain

Corollary I: If $E > V$ and $V'' \geq 0$ for all $r \geq 0$ then $\delta \geq \delta_{\text{WKB}}$.

(*) The potential in (6) is precisely V if and only if $V = E - (a + br)^{-4}$ where a and b are constants. In this case the WKB solution is also the exact solution of (1) for a single value of E . However, this potential vanishes at infinity only if $E = 0$, and only then is a phase shift defined.

3. - The general case.

Let us now treat the case in which $E = V$ at $r = a$ and $E > V$ for $r > a$, while for $0 \leq r < a$ no restriction is placed upon V . We will consider $w(r)$, the modified WKB solution of (1) and (2) defined by

$$(8) \quad w(r) = \begin{cases} 0 & 0 \leq r \leq a \\ k^{\frac{1}{2}}(k^2 - U)^{-\frac{1}{2}} \sin \left[\int_a^r (k^2 - U)^{\frac{1}{2}} dr \right] & a \leq r. \end{cases}$$

This function and its first derivative are zero at $r = a$. It satisfies (6) for $r \geq a$ and has the phase shift

$$(9) \quad \bar{\delta}_{\text{WKB}} = \int_a^\infty [\sqrt{k^2 - U} - k] dr - ka.$$

For $0 \leq r \leq a$, $w(r)$ is identically zero, which corresponds to an infinite repulsive potential in this range. Thus the monotonicity theorem is applicable to w and u . In the range $0 \leq x \leq a$ the potential to which w corresponds is positive infinite and therefore $> V$. Thus if the potential in (6) exceeds V in the range $x > a$, the phase shift of w will be less than that of u . Therefore we have

Theorem II: If $E = V(a)$ while $E > V$ and $V'' + 5(V')^2/4(E - V) \geq 0$ for all $r > a$, then $\delta \geq \bar{\delta}_{\text{WKB}}$.

As before we have

Corollary II: If $E = V(a)$ while $E > V$ and $V'' \geq 0$ for all $r > a$, then $\delta \geq \bar{\delta}_{\text{WKB}}$.

Theorem II can also be proved without reference to an infinite potential. We merely note that for $r \geq a$ Sturm's theorem shows that the zeroes of u separate those of w . Then the definition of the phase shift in terms of zeroes of the wave function yields the result.

4. - An example.

As an example of the last result, let us consider the equation

$$(10) \quad u'' + \left[k^2 - \frac{\nu(\nu + 1)}{r} \right] u = 0.$$

This equation has the following solution which vanishes at $x = 0$:

$$(11) \quad u = \sqrt{2\pi kr} J_{v+\frac{1}{2}}(kr) \sim \sin \left[kr - v \frac{\pi}{2} \right].$$

The phase shift is thus

$$(12) \quad \delta = -v \frac{\pi}{2}.$$

Now the potential $v(v+1)/r^2$ equals k^2 for $r = k^{-1}[v(v+1)]^{\frac{1}{2}}$ and is less than k^2 for larger values of r . Furthermore the second derivative of the potential is positive provided that $v > 0$. Therefore, Corollary II applies and yields

$$(13) \quad \delta = -v \frac{\pi}{2} > \delta_{\text{WKB}} = - \int_{k^{-1}[v(v+1)]^{\frac{1}{2}}}^{\infty} \left\{ \left[k^2 - \frac{v(v+1)}{r^2} \right]^{\frac{1}{2}} - k \right\} dr = \sqrt{v(v+1)} - v \frac{\pi}{2}.$$

In addition, since the potential in (10) is positive, we know that $\delta \leq 0$. The graph shows δ and $\bar{\delta}_{\text{WKB}}$ as functions of v for $v > 0$. At $v = 0$ both phase shifts are zero since then the potential is zero. As v increases $\bar{\delta}_{\text{WKB}}$ rapidly approaches $\delta - \pi/4$.

The phase shift of the usual WKB method approaches δ as v increases, in contrast to the phase shift of $w(r)$, the modified WKB solution, which approaches $\delta - \pi/4$. The extra $\pi/4$ in the usual WKB result comes from using a different solution in the range $0 \leq r \leq a$.

5. - Exponential and Yukawa potentials.

The repulsive exponential potential $V_0 \exp[-r/b]$ satisfies the conditions of Corollary I provided that $0 \leq V_0 \leq E$. For $V_0 \geq E$ it satisfies the conditions of Corollary II. Thus we obtain a lower bound on the phase shift for any repulsive exponential potential. We also have the upper bound zero because the potential is positive. The attractive exponential satisfies the conditions of Theorem I [$V'' + 5(V')^2/4(E - V) \leq 0$] when $-4E \leq V \leq 0$. In this case we obtain an upper bound on the phase shift. Since the potential is negative, we also have zero as a lower bound.

The bounds just considered may be computed explicitly (*). Thus we have from (5), when $V_0 E^{-1} \leq 1$, letting $y = r/b$,

$$(14) \quad \delta_{\text{WKB}} = kb \int_0^{\infty} [(1 - V_0 E^{-1} e^{-y})^{\frac{1}{2}} - 1] dy = \\ = 2kb \left[(1 - V_0 E^{-1})^{\frac{1}{2}} - 1 - \log \frac{(1 - V_0 E^{-1})^{\frac{1}{2}} + 1}{2} \right].$$

In Fig. 2, δ_{WKB} is shown in the range $-4 \leq V_0 E^{-1} \leq 0$ where it is an upper bound, and in the range $0 \leq V_0 E^{-1} \leq 1$ where it is a lower bound. For $V_0 E^{-1} \geq 1$ we have from (9)

$$(15) \quad \bar{\delta}_{\text{WKB}} = kb \int_{\log V_0 E^{-1}}^{\infty} [(1 - V_0 E^{-1} e^{-y})^{\frac{1}{2}} - 1] dy - kb \log V_0 E^{-1} = \\ = kb[2(\log 2 - 1) - \log V_0 E^{-1}].$$

In Fig. 2, $\bar{\delta}_{\text{WKB}}$ is shown in the range $V_0 E^{-1} > 1$ where it is a lower bound.

The repulsive Yukawa potential $V_0 b \exp[-r/b]/r$, $V_0 \geq 0$, also satisfies the

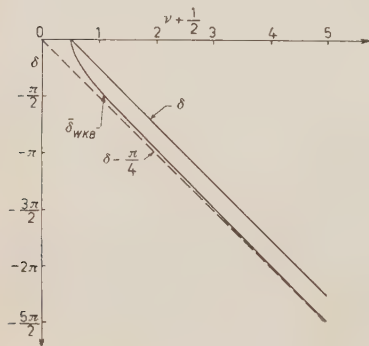


Fig. 1. — Comparison of the lower bound $\bar{\delta}_{\text{WKB}}$ given by (13), and the exact phase shift δ [equation (12)] for the Bessel function $\sqrt{kr} J_{\nu+1}(kr)$. Both phase shifts are shown as functions of ν for $\nu \geq 0$. The lower bound approaches $\delta - \pi/4$ as ν becomes large.

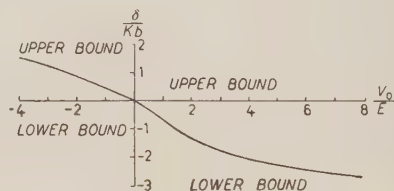


Fig. 2. — Bounds on the phase shift for the exponential potential $V_0 \exp[-r/b]$. For an attractive potential the upper bound δ_{WKB} , given by (14), is shown in the range $-4 \leq V_0/E \leq 0$. Zero is a lower bound. For a repulsive potential, δ_{WKB} is a lower bound in the range $0 \leq V_0/E \leq 1$ and $\bar{\delta}_{\text{WKB}}$ [equation (15)] is a lower bound when $V_0/E \geq 1$, while zero is an upper bound.

(*) The integral in (14) was evaluated by introducing the new variable

$$z = (1 - V_0 E^{-1} e^{-y})^{\frac{1}{2}}.$$

That in (15) was reduced to (14) by introducing the new variable

$$z = y - \log V_0 E^{-1}.$$

conditions of Corollary II and thus (9) yields a lower bound on the phase shift for this potential. The upper bound zero follows from the positiveness of the potential. In the case of the attractive Yukawa potential Theorem I applies provided that $0 \geq V_0 E^{-1} \geq -84$ since then $V'' + 5(V')^2/4(E - V) \leq 0$, and an upper bound is obtained. The lower limit -84 is nearly the smallest value of $V_0 E^{-1}$ for which the above inequality is satisfied for all r , and was obtained by simple computations.

6. - Conclusion.

The procedure here used to obtain bounds on phase shifts is a special case of the following method: Let $v(r)$ be any twice differentiable function with the properties $v(0) = 0$ and $v \sim \sin(kr + \delta_1)$. Define $k^2 - U_1$ as the quotient $v''(r)/v(r)$. Then $v(r)$ satisfies the equation $v'' + (k^2 - U_1)v = 0$. Now compare U_1 with U of equation (1). If $U_1 \geq U$ ($U_1 \leq U$) for all r then the Monotonicity theorem applies and $\delta_1 \geq \delta$ ($\delta_1 \leq \delta$). Of course the success of the method depends upon the skill (or luck) with which $v(r)$ is chosen.

RIASSUNTO (*)

Si dimostra che per determinati potenziali il metodo di WKB fornisce un limite inferiore per lo spostamento di fase esatto e per alcuni potenziali fornisce un limite superiore. Si descrive anche un altro metodo per ottenere limiti.

(*) Traduzione a cura della Redazione.

Determination of Distortion Vectors in Nuclear Emulsions.

TSAI-CHÜ

Faculté des Sciences, Sorbonne - Paris

(ricevuto il 23 Gennaio 1957)

Summary. — We try to determine distortion vectors by multiple scattering measurements made on inclined tracks both in projection and in depth. Distortion vectors of different orders can be deduced from formulas expressed in terms of ordinate differences of multiple scattering. The magnitudes of distortion vectors determined are in good agreement with those obtained by other methods.

1. - Introduction.

Numerous studies have been made in recent years on measurements of ionization and multiple scattering of trajectories produced by ionizing particles in nuclear emulsions. However, the precision of these measurements is limited by their statistical fluctuations. The energy value deduced from them is by far inferior to that derived from the residual range of a particle coming to rest in the emulsion. So the actual range of a particle in emulsion is the most important quantity for precise measurements. But we must bear in mind that the dilatation or contraction of the range of a particle caused by distortion may not be negligible, particularly in the case of steep tracks. Up to the present, only a few studies^(1,2) have been made on the measurement of distortions in nuclear emulsions.

Distortions of nuclear emulsions are introduced mainly during the manufacturing and processing stages. The emulsion is then in the state of a viscous liquid and has only shearing stresses parallel to the supporting glass plate. Hence the distortion is composed only of vectors parallel to the emulsion

⁽¹⁾ M. COSYNS and G. VANDERHAEGHE: *Bull. Cen. Phys. Nucl.*, No. 15 (1950).

⁽²⁾ G-STACK COLLABORATION: *Nuovo Cimento*, **2**, 1063 (1955).

surface. It has been developed ⁽¹⁾ in the following form:

$$K_0 + K_1 \left(\frac{z}{t} \right) + K_2 \left(\frac{z}{t} \right)^2 + K_3 \left(\frac{z}{t} \right)^3 + \dots,$$

where t represents the thickness of the emulsion, z the height measured from the glass plate; K_0, K_1, K_2, \dots are zero, first second, ... order vectors of distortion. At the emulsion surface ($z = t$), the total distortion is reduced to the sum of all the vectors. The convergence of this series requires either that all the vectors decrease quickly as their order increases or that they decrease slowly and have alternative signs. It is very likely that the distortion series are in most cases alternative.

Vector K_0 is a displacement of the whole emulsion block without changing the shape or length of the track. Vector K_1 does not produce any curvature on a straight track but it changes the length and direction of the track. In the case of the second and higher order vectors, both the length and shape of the track are affected. Observed through a microscope, the components perpendicular to the projected trajectory produce the C- or S-shaped distortions; the components parallel to it produce similar distortions in the vertical projection. The first order vector has been determined (i) by measuring the steep tracks passing through successive emulsions and (ii) by measuring the anisotropic distributions of radioactive α -particles caused by distortion. The higher order vectors have been determined (i) by geometrical methods and (ii) by multiple scattering.

2. - Second and higher order distortion vectors.

Supposing the X - and Y -axes lie in a plane parallel to the emulsion surface, we choose the X -axis approximately parallel to the projected trajectory, the Y -axis perpendicular to it and the Z -axis perpendicular to the emulsion surface, pointing from the glass support toward the air. Let (x_0, y_0, z_0) be the co-ordinates of a point situated on the trajectory at the time of exposition, and the co-ordinates of this point after development will be (x, y, z) ; they are connected by the following equations

$$(1) \quad x = x_0 + K_1 \cos \alpha_1 \left(\frac{z}{t} \right) + K_2 \cos \alpha_2 \left(\frac{z}{t} \right)^2 + \dots,$$

$$(2) \quad y = y_0 + K_1 \sin \alpha_1 \left(\frac{z}{t} \right) + K_2 \sin \alpha_2 \left(\frac{z}{t} \right)^2 + \dots,$$

$$(3) \quad z = z_0,$$

where $\alpha_1, \alpha_2, \dots$ are angles made by the distortion vectors with the X -axis. We have dropped out the zero order vector and assumed that the distortion is uniform throughout the emulsion. Components $K_1 \cos \alpha_1, K_2 \cos \alpha_2, \dots$ are parallel to the trajectory and components $K_1 \sin \alpha_1, K_2 \sin \alpha_2, \dots$ are perpendicular to it; they have a positive sign for dilatation and a negative sign for contraction.

Neglecting the small multiple scattering, the equations of a straight track before distortion are

$$(4) \quad y_0 = a_0 + a_1 x_0$$

$$(5) \quad x_0 = b_1 z_0 = b_1 z$$

and after distortion

$$(6) \quad y = a'_0 + a'_1 x + a'_2 x^2 + a'_3 x^3 + \dots$$

$$(7) \quad x = b'_1 z + b'_2 z^2 + \dots$$

The coefficients in equations (6) and (7) can be expressed in terms of those in (4), (5) and the components of distortion vectors; they decrease quickly with i . The ratio a'_i/a'_{i-1} or b'_i/b'_{i-1} is smaller than $1/1000$ for $t = 600 \mu\text{m}$. The variables x, x_0 depend directly on z and the variables y, y_0 on z indirectly. Therefore in equations (1) and (2) we may consider z as the only independent variable. Differentiating (1) and (2) twice with respect to z and summing up over the whole trajectory, we obtain

$$\sum \frac{d^2 x}{dz^2} = \sum \frac{2K_2 \cos \alpha_2}{t^2}, \quad \sum \frac{d^2 y}{dz^2} = \sum \frac{2K_2 \sin \alpha_2}{t^2}.$$

We have neglected the higher order components and on account of (4) and (5), we have assumed $\sum d^2 x_0/dz^2 = \sum d^2 y_0/dz^2 = 0$. The second order distortion vector can be calculated from multiple scattering measurements in y and z by the following formulas:

$$(8) \quad K_2 \cos \alpha_2 = \frac{t^2}{2(n-1)} \sum \frac{d^2 x}{dz^2} = \\ = -\frac{t^2}{2(n-1)} \sum \frac{d^2 z}{dx^2} \left(\frac{dx}{dz} \right)^3 = -\frac{n^2 dx}{2(n-1)} \sum \frac{d^2 z}{dz'^2},$$

$$(9) \quad K_2 \sin \alpha_2 = \frac{t^2}{2(n-1)} \sum \frac{d^2 y}{dz^2} = \frac{t^2}{2(n-1)} \sum \left\{ \frac{d^2 y}{dx^2} \left(\frac{dx}{dz} \right)^2 + \left(\frac{dy}{dx} \right) \left(\frac{d^2 x}{dz^2} \right) \right\} = \\ = \frac{n^2}{2(n-1)} \sum d^2 y + \frac{K_2 \cos \alpha_2}{(n-1)} \sum \frac{dy}{dx} + \dots$$

$n = t/dz$ is the number of sections contained in the emulsion. In order to adapt the formula to scattering measurements, the dependent (x) and the independent variable (z) in (8) are interchanged. The second term in formula (9) is already much smaller than the first; all the other terms can be dropped out.

In a similar way, we can derive the components of the higher order vectors. However, the second derivatives in (8) and (9) as shown below do contain their components, but in different proportions. For example:

$$(10) \quad \left\{ \begin{array}{l} \sum \frac{d^2 x}{dz^2} = \sum \frac{2K_2 \cos \alpha_2}{t^2} + \sum \frac{6K_3 \cos \alpha_3 z}{t^3} + \sum \frac{12K_4 \cos \alpha_4 z^2}{t^4} + \dots, \\ \text{or} \\ \frac{t^2}{2n} \sum \frac{d^2 x}{dz^2} = K_2 \cos \alpha_2 + \frac{3}{2} K_3 \cos \alpha_3 + \frac{4}{2} K_4 \cos \alpha_4 + \frac{5}{2} K_5 \cos \alpha_5 + \dots \end{array} \right.$$

The second order components derived in (8) and (9) contain the sum of all the higher order components, and, in addition, half the third components, 2/2 times the fourth, 3/2 times the fifth, etc.

3. - First order distortion vector.

It is impossible to calculate the first order vector without knowing the initial direction of a track before distortion. Although the change of direction caused by the first order vector is constant, it cannot be separated from the initial direction. The formulas given below enable us to calculate the first order components for tracks with known initial directions. Differentiating again equation (1) and (2) and summing up, we have

$$\begin{aligned} \sum \frac{dx}{dz} &= \sum \frac{dx_0}{dz} + \sum \frac{K_1 \cos \alpha_1}{t} + \sum \frac{2K_2 \cos \alpha_2 z}{t^2}, \\ \sum \frac{dy}{dz} &= \sum \frac{dy_0}{dz} + \sum \frac{K_1 \sin \alpha_1}{t} + \sum \frac{2K_2 \sin \alpha_2 z}{t^2}, \end{aligned}$$

where $dx_0/dz = b_1$ and $dy_0/dz = a_1 b_1$ have constant values and represent the direction of the undistorted track. They are combined linearly with terms containing the first order vector. Simplifying the above equations, we have, for the first order components

$$(11) \quad K_1 \cos \alpha_1 = -K_2 \cos \alpha_2 + \sum \Delta x - \sum \Delta x_0,$$

$$(12) \quad K_1 \sin \alpha_1 = -K_2 \sin \alpha_2 + \sum \Delta y - \sum \Delta y_0.$$

It is necessary in the above formulas that the values of $\sum \Delta x_0$, $\sum \Delta y_0$ must be known. (i) For tracks perpendicular to the plane of emulsion $\Delta x_0 = \Delta y_0 = 0$, we can calculate $K_1 \cos \alpha_1$ and $K_1 \sin \alpha_1$ directly from (11) and (12). (ii) For steep tracks traversing successive emulsions, $\sum \Delta x_0$ and $\sum \Delta y_0$ can be estimated from the distance between the two points of entry at the glass plates, if vector K_0 is neglected. (iii) For tracks measured along the x -axis parallel to the x_0 -axis, we have $y_0 = a_0$ and $\Delta y_0 = 0$, $K_1 \sin \alpha_1$ can be calculated from (12). (iv) For general cases, $K_1 \sin \alpha_1$, calculated without the term $\sum \Delta y_0$, will have a larger positive value for a positive $\sum \Delta y_0$, and a smaller value for a negative $\sum \Delta y_0$, and vice versa for a negative $K_1 \sin \alpha_1$.

It may be interesting to try to calculate the first order components from the third differences of multiple scattering, because it is known in scattering measurements that the third differences are nearly free from distortion and approach the value of true scattering. Differentiating (1) and (2) three times with respect to the projected trajectory (s), as it is done in scattering measurements made in depth, we have

$$(13) \quad \sum \frac{d^3 x}{ds^3} - \sum \frac{d^3 x_0}{ds^3} = \frac{K_1 \cos \alpha_1}{t} \sum \frac{d^3 z}{ds^3} + \frac{2K_2 \cos \alpha_2}{t^2} \left\{ \sum 3 \left(\frac{dz}{ds} \right) \left(\frac{d^2 z}{ds^2} \right) + \sum z \frac{d^3 z}{ds^3} \right\},$$

$$(14) \quad \sum \frac{d^3 y}{ds^3} - \sum \frac{d^3 y_0}{ds^3} = \frac{K_1 \sin \alpha_1}{t} \sum \frac{d^3 z}{ds^3} + \frac{2K_2 \sin \alpha_2}{t^2} \left\{ \sum 3 \left(\frac{dz}{ds} \right) \left(\frac{d^2 z}{ds^2} \right) + \sum z \frac{d^3 z}{ds^3} \right\}.$$

In case the higher order vectors K_3, K_4, \dots can be neglected, we have

$$\frac{d^3 x}{dz^3} - \frac{d^3 x_0}{dz^3} = \frac{d^3 y}{dz^3} - \frac{d^3 y_0}{dz^3} = 0.$$

Similar differences of other third derivatives taken with respect to undistorted co-ordinates (x_0, y_0 and s_0) are also zero. Since the lengths of s and s_0 are nearly equal (within 10%) and s varies slowly with z , we have tried to calculate $K_1 \cos \alpha_1$ from (13) by making the left member equal to zero.

4. - Application and results.

We have applied the above formulas to obtain the actual length of a hyperon track in emulsion. This track is produced by a short prong from a

nuclear interaction ⁽³⁾. It traverses 24 plates before leaving the stack and has dip angles varying from 15 to 30° and a total length of 3.75 cm in emulsion. The mass of this particle ⁽⁴⁾ has been measured by change of ionization and range. It results in a value of (1.35 ± 0.10) times that of a proton. As the ratio of masses between a hyperon and a proton depends directly on the ratio of ranges, which is not very far from 1 and as the range of a particle is usually dilated by distortion, so proton tracks in badly distorted plates can easily be mistaken for hyperon tracks. Therefore, it is important to eliminate the dilatation caused by distortion. The distortion vectors are deduced only from scattering measurements made on the same track. This method permits us to obtain quickly the average distortion vectors of all the plates measured throughout the same region where the track passes.

The track is found in the stack S36 of $10 \times 15 \text{ cm}^2 \times 600 \mu\text{m}$ plates, developed at Bristol to a low minimum of ionization. Each plate is cut into two along the middle line perpendicular to the long edges. The track is nearly parallel to the long edge (within 20°) and lies at a distance of 2 cm from the edge. Scattering measurements in projection are made in basic cells of 50 μm and are repeated several times; measurements in depth are made in cells of 25 μm ; distortion vectors are calculated from cells of 50 and 100 μm with all overlapping combinations possible. Table I gives the results obtained for the 24 plates. There is only a slight predominance of contraction for the second order component ($K_2 \sin \alpha_2$) parallel to the short edge; contraction is found in 14 plates and dilatation in 10. The average numerical value for this component is $\pm 16 \mu\text{m}$; the algebraic mean is $-4 \mu\text{m}$, i.e. a net contraction of 4 μm per plate. On the contrary, the component parallel to the long edge ($K_2 \cos \alpha_2$) shows a great predominance of contraction; 17 plates of contraction against 7 plates of dilatation; the average numerical value for the 24 plates is $\pm 52 \mu\text{m}$ and the algebraic mean is $-44 \mu\text{m}$. $K_2 \cos \alpha_2$ shows a large contraction of 44 μm per plate. The second order distortion vector for the 24 plates has an average contraction of 45 μm , and it has a direction nearly parallel to the long edge. For the latter component, the ordinate z is measured by the usual methods. An elaborate and special arrangement for scattering measurements in depth ⁽⁵⁾ will be quite interesting for distortion studies.

We have estimated one component of the third order vector from the following formula

$$K_3 \sin \alpha_3 = \frac{n^2 \sum d^2 y}{6}.$$

⁽³⁾ TSAI-CHÜ: *Nuovo Cimento*, **3**, 921 (1956).

⁽⁴⁾ TSAI-CHÜ and M. MORAND: *Phys. Rev.*, **104**, 1493 (1956).

⁽⁵⁾ C. MABBOUX-STROMBERG: *Ann. Phys.*, **9**, 441 (1954).

TABLE I.

Plate No.	$K_2 \sin \alpha_2$	$K_2 \cos \alpha_2$	$K_1 \sin \alpha_1 / K_2 \sin \alpha_2$	$K_1 \cos \alpha_1 / K_2 \cos \alpha_2$
24	- 8	+ 6	- 1.9	- 0.4
23	- 11	+ 17	- 3.5	- 4.3
22	- 21	+ 5	- 2.4	+ 4.3
21	- 22	- 30	- 1.4	- 2.2
20	- 11	- 5	- 1.8	- 36.1
19	- 37	- 90	- 0.7	- 0.9
18	+ 25	- 162	- 1.7	- 1.5
17	+ 14	- 39	- 2.4	- 0.9
16	- 47	- 34	- 0.7	- 0.4
15	+ 2	- 73	+ 14.1	- 3.4
14	- 11	- 108	- 2.6	- 2.4
13	- 15	- 69	- 0.2	- 3.7
12	- 5	- 7	- 7.4	- 0.9
11	- 19	- 200	- 0.9	- 4.2
10	- 30	+ 6	- 1.8	+ 9.5
9	+ 2	+ 3	- 4.8	- 0.1
8	+ 32	+ 37	- 1.0	- 2.3
7	+ 23	- 73	- 1.6	- 0.4
6	- 3	- 22	- 3.7	- 2.2
5	+ 14	- 61	- 0.9	- 4.2
4	+ 3	- 39	+ 1.3	+ 0.6
3	+ 22	+ 16	- 2.0	- 1.5
2	+ 15	- 37	- 1.1	- 5.9
1	- 3	- 107	- 18.0	- 2.5

This component should be small but it is derived from the product of n^2 and $\sum d^3y$. Any unbalanced spurious and true scatterings in the sum d^3y are enlarged by the factor n^2 . Thus the product will give an apparent large distortion. Spurious scattering does not depend on the cell length (L) for the Koritska microscope; true scattering depends on L^3 and the product with unbalanced scatterings will decrease quickly with n . So the apparent distortion due to them becomes less important for larger cells. Therefore, it is necessary to measure a number of tracks by using cells equal to or greater than $100 \mu\text{m}$. The average magnitude of this component is of the order $\pm 7.5 \mu\text{m}$ per plate.

The two components $K_1 \sin \alpha_1$ and $K_1 \cos \alpha_1$ of the first order vector are calculated from the ratio between each component of the first and second order vectors by (12) and (13) respectively. The ratios found in the 24 plates are generally negative excepting two or three cases. $K_1 \sin \alpha_1$ is calculated from (12) by neglecting $\sum \Delta y_0$. Since $K_2 \sin \alpha_2$ shows no preferential direction in the plates, the negligence of this term is presumed not to introduce any systematic error on the average value of $K_1 \sin \alpha_1$. The average ratio

$K_1 \sin \alpha_1 / K_2 \sin \alpha_2$ for the 24 plates is -2.0 and $K_1 \sin \alpha_1$ is $+9 \mu\text{m}$ per plate. $K_1 \cos \alpha_1$ is calculated from (13) by neglecting the left member. Since the value $\sum d^2$ may sometimes be very small, $K_1 \cos \alpha_1$ is deduced from the average $K_2 \cos \alpha_2 / K_1 \cos \alpha_1$ of 50 and $100 \mu\text{m}$. The average ratio $K_1 \cos \alpha_1 / K_2 \cos \alpha_2$ is -2.8 and $K_1 \cos \alpha_1$ has a mean value of $+121 \mu\text{m}$ per plate. Therefore the first order vector for the 24 plates has an average dilatation of $121 \mu\text{m}$ per plate and it has a direction nearly parallel to the long edge; the ratio between the magnitudes of the first and second order vectors is -2.7 . The average magnitudes and directions of the distortion vectors are found to be in excellent agreement with the results obtained by detailed measurements ⁽²⁾ of individual plates, but the large dispersion of some values in Table I must be due to fluctuations.

As shown above, distortion increases the length of a track in emulsion whilst processing decreases it. The grain density of a track after processing is slightly decreased on the emulsion surfaces. A small part of the trajectory on the surface near the air is even etched off during processing and some grains on the surface near the glass may not be developed at all. Consequently, the height of the emulsion, when deduced from that of the hyperon track, is found to be of an average 2.5% smaller than the thickness of the emulsion. The track is dilated $24(121 - 44)/375 = 4.9\%$ by distortion, shortened 2.5% by processing and it remains a net dilatation of 2.4% . In other words the, mass of the hyperon will be decreased only by a few percent. Hence our conclusion that the particle is a hyperon is still valid.

RIASSUNTO (*)

Per mezzo di misure di scattering multiplo eseguite su tracce inclinate sia nella proiezione verticale che nell'orizzontale, cerchiamo di determinare i vettori di distorsione. Vettori di distorsione di ordini differenti possono dedursi da formule espresse in termini di differenze di ordinate dello scattering multiplo. I moduli dei vettori di distorsione così determinati sono in buon accordo con quelli ottenuti con altri metodi.

(*) Traduzione a cura della Redazione.

New Experimental Evidence for the Tunnel Theory of Cosmic Ray «Jets».

C. B. A. McCUSKER

Dublin Institute for Advanced Studies

F. C. ROESLER

Imperial Chemical Industries Limited, Billingham Division

(ricevuto il 4 Febbraio 1957)

Summary. — The predictions of the tunnel theory of cosmic ray jets are compared with recent experimental evidence, particularly with the detailed data of the jet found by DEBENEDETTI *et al.* Excellent agreement is found between the new experimental data and the earlier theoretical predictions. A list of 74 jets with $\gamma_p > 500$ is given in an appendix.

1. — Introduction.

The term «jet» was coined by the Bristol Group to describe those very high energy stars in photographic emulsions in which the minimum ionization tracks are concentrated in a narrow cone in the forward direction. A peculiarity of many such stars is the absence or near absence of black or grey prongs.

Here, and in our earlier papers, the term jet is restricted to events with primary energy above about 500 GeV. It is perhaps worth noting that some other authors have used the word jet for any event with few or no heavy prongs, whatever the primary energy. It is obvious that not all high energy events in photographic emulsions can be nucleon-nucleon encounters. In fact, since hydrogen forms only a small part of emulsion, the great majority of encounters must be with complex nuclei. For these, the frequency ratio of glancing to other collisions is easily computed and is always small. Since

interaction cross-sections at these high energies are approximately geometric, a non-glancing collision will lead to a cascade process within the nucleus. This cascade will be rather peculiar, since the interaction mean free path in nuclear matter is very short and the scattering angles are very small at these high energies. A detailed treatment ⁽¹⁾ of this cascade leads to the conclusion that, for a central collision and for primary energies greater than 16A GeV, an approximately cylindrical tunnel will be punched through the nucleus. A denotes the Atomic Weight. For this cylindrical tunnel the theoretical treatment of the inter-nuclear cascade is quite simple.

It is worth stressing that any model of meson production, with respect to the individual nucleon-nucleon collisions, can be fitted into this cascade theory. On the other hand, given the manner in which n_s (the number of observed shower particles) (*) varies with γ_p , the cascade theory can be used to estimate the multiplicity of meson production in nucleon-nucleon collisions at a given primary energy. Further, the way in which the multiplicity varies with energy can be determined; and also, more roughly, the impact parameter, the probable target nucleus, and the primary energy for any particular event. One can also predict the way in which, at a particular energy, n_s will vary with A. Using the results available up to September 1952, the expression

$$(1) \quad f_{\text{emp}} = (1.0 \pm 0.2) \left(\frac{E'}{Mc} \right)^{0.25 \pm 0.5},$$

was deduced in our first paper for the number of charged shower particles produced on average in a nucleon-nucleon collision at a primary energy E' . Later ⁽²⁾, the results of KAPLON and RITSON for collisions at 5000 GeV with emulsion, copper, and lead, were compared with the predictions of the theory. This additional evidence for the variation of n_s with A confirmed relation (1) and agreed with the earlier theoretical predictions.

In the mean time, a good many more jets have been found. A summary (possibly incomplete) of the total evidence is given in Appendix I. One particularly beautiful example of a jet has been found by the Turin Group of DEBENEDETTI, GARELLI, TALLONE, and VIGONE ⁽³⁾. These workers give not only the angles of all particles in the laboratory system, but have in addition been able to determine the momenta of all secondaries which have minimum ionization and also the energy carried by the neutral component.

⁽¹⁾ F. C. ROESLER and C. B. A. McCUSKER: *Nuovo Cimento*, **10**, 127 (1953).

(*) The Bristol notation is used here. $\gamma_p = 2/\overline{\varphi^2}$, where φ are the angles of the secondaries to the primary direction in the laboratory system.

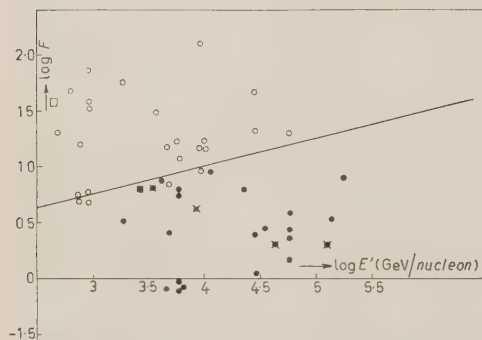
⁽²⁾ C. B. A. McCUSKER and F. C. ROESLER: *Phys. Rev.*, **91**, 769 (1953).

⁽³⁾ A. DEBENEDETTI, C. M. GARELLI, L. TALLONE and M. VIGONE: *Nuovo Cimento*, **4**, 1142 (1951).

We wish to point out in this note that practically all the newly available evidence is again in good agreement with the predictions of our theory. For the Turin jet, in particular, the experimentally determined primary energy agrees remarkably well with our theoretical value. Anticipating, it may be stated that this jet is most probably due to a near central penetration of a silver nucleus.

2. - The general evidence.

A jet in a photographic emulsion is the result of an event which may vary in type from a genuine nucleon-nucleon collision to a central collision with silver. Under either of these two extreme assumptions, one can obtain from the tunnel theory fictitious values for the multiplicity of charged particles in the individual nucleon-nucleon collision and for the total primary energy of the event. Thus for every jet for which these calculations are carried out, using the observed values of n_s and γ_p , two pairs of values f , E' will be obtained. These can be plotted on a graph of $\log f$ against $\log E'$ (Fig. 2 in ref. (1)). If in reality the fluctuations of the true multiplicities are not too big, then the two groups of points derived from the two extreme assumptions about the impact parameter should occupy two different domains. The lower boundary of the upper group of points will define the conditions for true nucleon-nucleon collisions, and a curve or line drawn along this lower boundary will give the true variation of multiplicity with energy in nucleon-nucleon collisions. Similarly, the upper boundary of the lower group of points will define true central collisions with silver. (Intermediate impact parameters can be determined analogously). It was, in fact, found in our first paper that this separation into two domains occurs, and the law (1) was determined in this way.



In Fig. 1 of the present paper the evidence from jets published since 1953 is treated in the same way. Once again, it is seen that

Fig. 1. - The multiplicity function f and the estimated primary energy for jets obtained since 1953 assuming a) that the event was a nucleon-nucleon collision (open circles) and b) that it was a central collision with silver (solid circles). The event of Debenedetti *et al.* is shown by squares. A superimposed cross implies an α -particle primary. The line represents the law given by equation (1):

of Debenedetti *et al.* is shown by squares. A superimposed cross implies an α -particle primary. The line represents the law given by equation (1):

the groups fall into separate domains, and again the law given by (1) is a good fit for the lower boundary of the upper group. It also fits the upper boundary of the lower group. The coincidence of the two boundaries suggests that our assumption in (1), namely that the multiplicity function f is constant along the tunnel, is true at least to a first approximation. Only one event would have been a poor fit. This was the $5+4p$ star reported by the Bristol Group. In our first paper it was noted that a $0+4p$ star was likewise a poor fit. It seems likely that these discrepancies are due to the difficulty of determining γ_p accurately with only 4 shower particles. Accordingly, only events with $n_s \geq 6$ have actually been used in the present plot.

3. - The Turin jet.

For the Turin jet $\gamma_p = 456$, $n_s = 39$. This gives on the assumption of a nucleon-nucleon collision the fictitious values

$$f(s_1) = n_s - 1 = 38,$$

$$E'_{\text{GeV}}(s_1) = 0.93 \gamma_p = 424 \text{ GeV}.$$

Alternatively, the assumption of a central collision with silver gives

$$f(2R, \text{Ag}) = 0.77 A^{-\frac{1}{3}}(n_s - 1) = 6.31$$

$$E(2R, \text{Ag}) = 1.21 A^{\frac{1}{3}} \gamma_p = 2626 \text{ GeV}.$$

It is interesting to consider if either of these two hypotheses is correct. From the position of the points on the diagram, the event would seem to be a near central collision with silver. If this is so, the theoretically predicted primary energy is 2626 GeV. This is in good agreement with the experimentally determined values $E' > 2100$ GeV. The value of f is 6.3, which agrees well with the values derived from the Kaplon-Ritson result in particular and from all jet events so far observed. As to the number of heavy prongs, one can proceed in this fashion. The limiting energy above which the tunnel is cylindrical is $16A$, i.e. for silver 1728 GeV. The primary energy of the Turin jet is known to be greater than this, both from the evidence of the secondaries and from the fit in our diagram. Thus according to the theory a cylindrical tunnel is punched through the nucleus. This process communicates energy to the residual nucleus in two ways ⁽⁴⁾: firstly by friction due to the breaking of the nucleonic bonds, which contribution is likely to be

(4) W. HEITLER and CH. TERREAUX: *Proc. Phys. Soc.*, A **66**, 929 (1953).

small, and secondly by the creation of an additional surface (the tunnel walls), which increases the surface energy of the nucleus. HEITLER and TERREAUX have calculated that for a diametrical passage through a silver nucleus the total energy communicated to the remaining nucleus is

$$U \sim 80 \div 150 \text{ MeV.}$$

One can then use the theory of LECOUTEUR ^(5,6), to find the expected number of heavy prongs, which is, in fact, 3. This is the number found experimentally. Thus this jet is in excellent agreement with the tunnel theory, provided one assumes it is produced by a near central collision with silver.

If then one briefly considers the alternative hypothesis, that this is a nucleon-nucleon collision, one sees that the estimated primary energy is much lower than the experimental values. The multiplicity of charged particles (> 37) is much too high to agree with the experimental results of KAPLON and RITSON, and the presence of three heavy prongs is difficult to explain.

4. - Conclusion.

On examination of all the evidence available to us it appears that the tunnel theory of jets can:

- a) explain the variation of n_s with γ_p in high energy events;
- b) explain the variation of n_s with A at a particular energy;
- c) lead, in many cases, to a reasonable estimate of the nature of the collision, e.g. whether it is a nucleon-nucleon collision or a central collision with silver;
- d) give a good estimate of the true energy of the primary;
- e) establish the connection between the multiplicity of the charged secondaries and the energy for nucleon-nucleon collisions;
- f) lead to a reasonable estimate of the number of heavy prongs;
- g) explain in terms of a widening, trumpet-shaped tunnel the stars of very large n_s and N_h which are sometimes observed at lower energies.

* * *

We wish to thank all those who have sent us details of jets before publication.

⁽⁵⁾ K. J. LE COUTEUR: *Proc. Phys. Soc.*, A **63**, 259 (1950).

⁽⁶⁾ K. J. LE COUTEUR: *Proc. Phys. Soc.*, A **65**, 718 (1952).

APPENDIX

List of Jets.

Jet No.	Primary	N_h	n_s	γ_D	References
1	p	0	4	2000	DANIEL <i>et al.</i> : <i>Phil. Mag.</i> , 43 , 753 (1952)
2	p	0	7	2200	»
3	p	0	28	2000	»
4	p	1	9	1300	»
5	p	2	24	400	»
6	p	3	7	2300	»
7	α	3	36	500/ n	»
8	p	4	20	800	»
9	α	4	50	800/ n	»
10	p	5	26	650	»
11	p	14	47	400	»
12	p	7	18	10000 (*)	GEROSA and LEVI SETTI: <i>Nuovo Cimento</i> , 8 , 601 (1951).
13	p	0	7	1000 (*)	BISWAS and HOPPER: <i>Phys. Rev.</i> , 86 , 209 (1952).
14	p	2	15	30000 (*)	LORD, FAINBERG and SCHEIN: <i>Nuovo Cimento</i> , 7 , 774 (1950).
15	Mg	not known	207	7100/ n (*)	LAT <i>et al.</i> : <i>Proc. Ind. Acad.</i> , 36 , 75 (1948).
16	α	»	84	3000	KAPLON and RITSON: <i>Phys. Rev.</i> , 88 , 386. (1952)
17	α	»	92	6000	»

(*) Author's estimate.

TABLE I: *continued.*

Jet No.	Primary	N_h	n_s	γ_p	References
18	α	»	56	480	»
19	p	»	24	4 000	»
20	p	»	20	1 300	»
21	p or n	»	9	4 500	»
22	p or n	»	26	19 500	»
23	p or n	»	16	1 300	»
24	p or n	»	24	1 800	»
25	p or n	»	19	6 100	KAPLON and RITSON: <i>Phys. Rev.</i> , 88, 386. (1952)
26	p or n	»	18	1 300	»
27	p	»	24	5 100	»
28	p or n	»	17	500	»
29	p or n	»	24	8 900	»
30	p or n	»	16	1 000	»
31	p or n	»	11	640	»
32	p or n	»	36	19 400	»
33	p or n	»	15	30 000	»
34	p or n	»	24	800	»
35	p or n	»	15	800	»
36	p or n	»	15	50 000	»
37	p or n	»	10	5 000	»
38	p or n	»	14	7 200	»
39	p	»	15	32 000	»

TABLE I: *continued.*

Jet No.	Primary	N_h	n_s	\mathcal{V}_D	Reference
40	p	»	18	23 000	»
41	p	0	10	10 000 (+)	KAPLON, RITSON and WALKER: <i>Phys. Rev.</i> , 90 , 716. (1953)
42	p	0	16	10 000 (+)	»
43	p	2	19	10 000 (+)	»
44	p	4	12	10 000 (+)	»
45	p	6	15	10 000 (+)	»
46	p	15	16	10 000 (+)	»
47	p	27	36	1 000	BRISBOUT <i>et al.</i> : <i>Phil. Mag.</i> 48 , 605 (1956)
48	p	0	22	30 000	»
49	p	13	17	800	»
50	p	18	58	2 000	»
51	p	0	32	4 000	»
52	p	7	49	700	»
53	p	23	126	10 000	»
54	p	0	18	6 000	»
55	p	0	16	5 000	»
56	p	0	8	5 000	»
57	p	13	38	1 000	»
58	p	5	4	3 000	»
59	α	5	40	30 000/ n	»
60	α	17	123	800/ n	»

(+) Median energy for the group; individual values not quoted.

TABLE I: *continued.*

Jet No.	Primary	N_h	n_s	γ_p	Reference
61	α	1	41	$10\,000/n$	»
62	α	20	80	$2\,000/n$	»
63	α	0	10	$2\,000/n$	»
64	p	12	50	30 000	MULVEY: private communication
65	p	22	76	1 000	»
66	n	0	6	1 000	»
67	p	1	5	10 000	»
68	p	0	4	730	GOLDSACK: private communication
69	p	1	4	2 200	»
70	p	1	6	830	»
71	not given	2	21	530	»
72	p	3	6	1 000	»
73	p	3	5	730	»
74	p	3	39	500	DEBENEDETTI <i>et al.</i> : <i>Nuovo Cimento</i> , 4 , 1142 (1956)

RIASSUNTO (*)

Si confrontano con recenti dati sperimentali, specialmente con i dati dettagliati del jet trovato da DEBENEDETTI *et al.*, le predizioni della teoria del tunnel per i jet dei raggi cosmici. Si trova un eccellente accordo tra i nuovi dati sperimentali e le precedenti predizioni teoriche. Nell'appendice si dà un elenco di 74 jet con $\gamma_p \geq 500$.

(*) Traduzione a cura della Redazione.

On the Atomic Displacements Produced by α -Particles in Germanium.

A. ASCOLI, M. ASDENTE and E. GERMAGNOLI

Laboratori CISE - Milano

(ricevuto il 7 Febbraio 1957)

Summary. — The number of negative carriers which are removed from the conduction band by irradiation of germanium single crystals with ^{210}Po α -particles is measured from the initial rate of decrease of conductivity in n -type germanium. It has been found that (79 ± 5) electrons are removed by a 5.30 MeV α -particle. The possibility of comparing this result with the theory of atomic displacements by high energy charged particles is discussed.

1. - Introduction.

Heavy charged particles are known to be effective in producing noticeable changes in physical properties of semiconducting materials even if the irradiation doses are rather small. This is related to lattice disordering due to Coulomb scattering phenomena, as previously discussed by SEITZ ⁽¹⁾.

The theory developed by the above mentioned author and its subsequent elaboration ⁽²⁾ make it possible to calculate the number of lattice defects introduced by every kind of charged particles of known energy.

The dependence of electric conductivity of Ge n upon the integrated dose of charged particles has been described by several authors and has been qualitatively explained by LARK-HOROVITZ and coworkers ^(3,4), at least for irradiation at temperatures not too far from room temperature.

⁽¹⁾ F. SEITZ: *Disc. Faraday Soc.*, **5**, 271 (1949).

⁽²⁾ F. SEITZ and J. S. KOEHLER: *Solid State Physics*, **2** (New York, 1955), p. 305.

⁽³⁾ H. M. JAMES and K. LARK-HOROVITZ: *Zeits. Phys. Chem.*, **198**, 107 (1951).

() See for instance: H. Y. FAN and K. LARK-HOROVITZ: *Defects in Crystalline Solids* (London, 1955), p. 232.

It is assumed that atomic interstitials and vacancies produced by irradiation introduce respectively donor and acceptor levels. Experimental evidence for both kinds of levels is given by the decrease in conductivity of irradiated n and strongly p -germanium. In particular, acceptor levels are effective in removing electrons which lie in the conduction band and, when some hypotheses are made concerning the position in the gap of donor and acceptor levels introduced during the irradiation, the initial decrease in conductivity of Ge n , its conversion to p -type and the subsequent increase in p conductivity are consistent with the theoretical predictions.

Changes of Hall coefficient and of optical properties of Ge single crystals also agree with such a scheme.

2. - On the comparison between theoretical and experimental results.

For ^{210}Po α particles (5.30 MeV) the calculated number of atomic displacements is ≈ 130 (2). What can be directly deduced from conductivity measurements with irradiated n -type germanium is however the number of negative carriers which are removed from the conduction band by an impinging α particle.

Difficulties may arise in deducing the number of atomic displacements per α particle from the experimental datum, because the rate of removal of carriers at a fixed flux of α particles depends upon the Fermi level in the semiconductor and the energy distribution within the gap of the electronic levels which are introduced by disordering centers.

The Fermi level can be calculated and therefore in order to compare experimental data with theoretical predictions some information concerning the spectrum of introduced levels is necessary.

This fact has been pointed out to explain the different rates of removal of carriers found by some authors; BRATTAIN and PEARSON (5) concluded that 78 electrons are removed from the conduction band per α particle; LARK-HOROVITZ and coworkers (6,7) found values of 95 and 180 for Ge samples of differential initial conductivities. All these measurements were performed at room temperature or thereabout, where healing of defects may be important: this effect was plausibly taken into account by considering only the rates of

(5) W. H. BRATTAIN and G. L. PEARSON: *Phys. Rev.*, **80**, 846 (1950); measured with a $0.125 \Omega^{-1} \text{cm}^{-1}$ Ge sample at room temperature.

() Unpublished work; measured at room temperature.

(7) H. Y. FAN and K. LARK-HOROVITZ: *Reports of International Kolloquium über Halbleiter und Phosphore* (Garmisch-Partenkirchen, August 1956); measured at 0°C .

change in the conductivity of the semiconducting crystals for very small integrated doses, because in these conditions neither annealing nor changes of carrier mobility due to lattice disordering are expected to be important; anyway measurements at different temperatures were considered advisable for the purpose of further check of the results.

3. - Experimental method.

The number n^* of negative carriers which are removed from the conduction band by an α particle is given by

$$n^* = \frac{l^2}{e\mu\Phi'_\alpha} \left| \frac{d\Sigma}{dt} \right|_0$$

where l is the length of the irradiated Ge sample,
 e is the elementary charge,
 μ is the mobility of negative carriers,
 Φ'_α is the total flux of α particles on the sample,
 $\left| \frac{d\Sigma}{dt} \right|_0$ is the initial rate of change of the conductance of the sample

As previously pointed out, the number N of atomic displacements per α -particle can be deduced from n^* only if the spectrum of electronic levels which are introduced from irradiation is known.

Information about the level distribution within the gap can be obtained for instance from the behaviour of $(-\Delta n - \Delta p)/\Phi_{\alpha \text{ int}}$ as a function of the position E_F of the Fermi level. Here Δn and Δp are respectively the changes of negative and positive carrier concentrations due to the integrated flux $\Phi_{\alpha \text{ int}}$. This function is expected to be constant as long as E_F does not cross anyone of the introduced levels, to undergo a sharp drop when this happens.

This kind of analysis has been made in the case of electron irradiation by FAN and LARK-HOROVITZ⁽¹⁾ who found that an electron level actually exists in the gap at about 0.2 eV from the conduction band and probably another level exists at 0.1 eV.

The interpretation of such results may be complicated by possible differences in the disordering action of each kind of particles, which determine a difference in the spectrum of introduced levels.

The results which will be discussed in the next section confirm this fact and are consistent with what has been recently obtained by FAN and LARK-HOROVITZ⁽²⁾ with ^{210}Po α -particle irradiation.

4. - Measuring technique.

Single crystals of *n*-type germanium have been used; their conductivity was about $0.3 \Omega^{-1} \text{ cm}^{-1}$ and their typical sizes were 0.5 cm wide, 2 cm long $\leq 2 \cdot 10^{-2}$ cm thick.

These thicknesses of the samples were obtained with the help of CP4 chemical etching⁽⁸⁾: we did not think it necessary to work with very thin samples because we were mainly interested in changes of conductance. Besides readily detectable effects of about 10% or more were obtained under irradiation.

The electrical contacts on germanium were provided by silver-electroplating the ends of the samples: only the unplated region of the Ge single crystals (about 1 cm long) was irradiated. The ends of the Ge samples were tightened between thin gold foils by means of brass springs. Contact resistance which were steady and less than $10^{-1} \Omega$ were obtained in this way and current lines were strictly longitudinal and parallel all along the sample.

The symmetry of experimental arrangement was effective to keep thermoelectric emf very small in the investigated interval of temperature (from -78°C to $+65^\circ \text{C}$); barrier effects resulted to be of an order of magnitude comparable to the sensitiveness of our apparatus and they were taken into account by averaging the experimental curves obtained letting the current circulate successively in both directions.

The conductance of Ge samples was measured by means of a d.c. decimal potentiometer and then comparing the terminal voltage of the samples with the terminal voltage of a standard resistor which was in series with it.

An accuracy better than 1% was obtained in all cases. The currents within the samples were about 10^{-4} A, so that no appreciable over-temperatures occurred. The accuracy of the voltage setting at the potentiometer was 10^{-6} V and the measuring apparatus was able to detect voltage differences as small as 10^{-6} V.

For the present measurements a thin source of α particles, whose activity was approximately 4 mC, has been used. It has been supplied by the Radiochemical Centre of Amersham (England). ^{210}Po is electroplated onto Pt and covered with a thin mica sheet (1 mg cm^{-2}); the diameter of the source is 5.5 mm.

The α source was located at 1 cm from the Ge sample and irradiations were carried out in vacuo: a brass shield was interposed between source and Ge crystal and was removable from outside so that irradiation could be started when the whole set-up had reached thermal equilibrium at the chosen temperature.

(8) J. P. MCKELVEY and R. L. LONGINI: *Journ. Appl. Phys.*, **25**, 634 (1954).

5. - Results.

5.1. Calibration of the flux of α particles. - The ^{210}Po source was calibrated with a previously described method ⁽⁹⁾. The flux of α particles onto the Ge samples was measured by comparing the counting rates which were obtained with a thin ^{210}Po source, equal in size to the calibrated source but about 10^{-3} times as intense, in two different conditions: once with a 2π geometry and once with the source at 1 cm from the detector whose surface was so shielded that only a small region (about 0.5 cm^2) was irradiated. In this way a geometry was obtained which was identical to the one which had been used in the measurements with Ge, and the effective solid angle viewed by Ge samples was calibrated. Calibrations were performed in vacuo and a ZnS(Ag) scintillator was used to detect α particles. According to the obtained results we assumed that the number of α particles impinging onto Ge was

$$\Phi_{\alpha} = (4.48 \pm 0.29) \cdot 10^{-2} I_{\alpha} \text{ cm}^{-2} \text{ min}^{-1},$$

where I_{α} is the absolute intensity of the intense ^{210}Po source. Taking $I_{\alpha} = (7.98 \pm 0.42) \cdot 10^3 \text{ min}^{-1}$ at a reference day, correcting for the decay of ^{210}Po and taking into account the actual sizes of the Ge surfaces in each irradiation, Φ_{α} became known.

5.2. Number of negative carriers removed per α particle. - Table I summarizes the experimental results.

TABLE I.

temperature $^{\circ}\text{C}$	$\mu^{(+)} (\text{cm}^{-2} \text{ V}^{-1} \text{ s}^{-1})$	$n^* = (l^2/e\mu\Phi_{\alpha}) d\Sigma/dt _0$	corrected n^* (for 5.3 MeV)
-78	$6.98 \cdot 10^3$	62	67
0	$4.21 \cdot 10^3$	75	81
+22	$3.75 \cdot 10^3$	80	86
+65	$3.06 \cdot 10^3$	75	81

(⁺) Calculated from $\mu = 19 \cdot 10^{16} T^{-3/2}$ ⁽¹⁰⁾.

The probable accuracy of the given values of n^* is 10%; the main causes of uncertainty are related to the absolute calibration of ^{210}Po source and to the difficulty of correctly extrapolating to zero irradiation time the curves

⁽⁹⁾ A. ASCOLI, M. ASDENTE and E. GERMAGNOLI: *Nuovo Cimento*, **4**, 946 (1956).

⁽¹⁰⁾ W. SHOCKLEY: *Electrons and Holes in Semiconductors* (New York, 1955), p. 287.

giving the rate of change in conductance. Two typical irradiation curves are given in Fig. 1 and Fig. 2. The experimental data refer to α particles of the

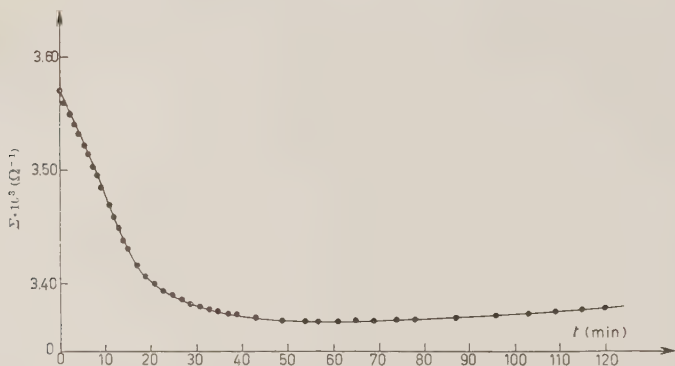


Fig. 1. — Changes in conductance of Ge *n* under irradiation with α -particles. Temperature 0 °C.

energy of 4.55 MeV, which is the residual energy with which they emerge from the mica sheet; energy losses within the emitting layer are negligible. The spread in the energy of α particles, due to absorption within the mica sheet and to deviation from ideal collimation, was examined and resulted

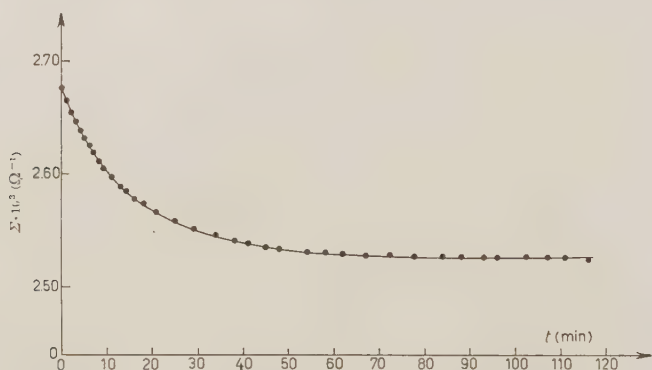


Fig. 2. — Change in conductance of Ge *n* under irradiation with α -particles. Temperature - 78 °C.

to be only few percent. In order to make our results comparable with those quoted in references ^(5,7), experimental data were also referred to 5.3 MeV

α particles; formulae given by SEITZ and KOEHLER ⁽²⁾ were used to this purpose.

5.3. *Tentative search of level distribution within the gap.* — A plot of $(-\Delta n + \Delta p)/\Phi_{\alpha \text{ int}}$ as a function of $E_c - E_F$ is given in Fig. 3.

It may be deduced from it that a distribution of levels in the investigated energy range rather than a well localized electron level is introduced.

6. — Conclusion.

The average value of n^* is 79 ± 5 which represents the number of negative carriers which are removed from the conduction band by a 5.30 MeV α particle in germanium. No significant dependance of n^* on the temperature was found; this fact seems to point out that within the limits of accuracy of the measurement and in the investigated interval of temperature, the initial rate with which electrons are removed from the conduction band does not depend on the temperature. Therefore possible changes in the mechanism of production of both donor and acceptor levels during irradiation at different temperatures do not affect the present results.

Concerning the distribution of electron levels, which are introduced into the gap by disordering centers, the results which are shown in Fig. 3 suggest that in the investigated range the levels are smeared out rather than well defined in energy.

Actually the above mentioned curve is somewhat questionable because it had to be constructed under the hypothesis that the mobility of carriers is unchanged under irradiation. It is however worthwhile to point out that a gradual decrease in carrier mobility is not likely to change the qualitative trend of the curve nor the present conclusions.

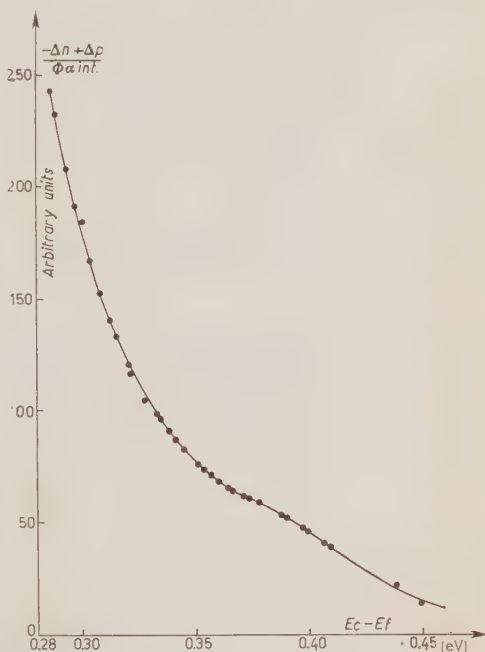


Fig. 3. — Experimental curve describing the behaviour of $(-\Delta n + \Delta p)/\Phi_{\alpha \text{ int}}$ as a function of $E_c - E_F$.

The initial section of the curve given in Fig. 3 fits reasonably well with the curve obtained by FAN and LARK-HOROVITZ ⁽⁴⁾ by means of electron irradiation, so that it is reasonable to assume that the defects which are responsible for the steep decrease of the $(-\Delta n + \Delta p)/\Phi_{\alpha \text{ int}}$ function near $E_c - E_f \cong 0.20$ eV in the curve obtained by FAN and LARK-HOROVITZ are of the same kind as those induced by α particles. The scattered distribution of levels which is suggested by our curve seems however to point out that α particle irradiation introduces some other and not easily definable kind of defects, namely clusters of vacancies and interstitials.

Therefore a quantitative analysis of effects is not easy for α particles and the calculated number of displacements cannot be immediately compared with experimental results; measurements with long range particles, like high energy electrons which mainly produce single interstitial-vacancy pairs, are likely to be more reliable for the purpose of such a comparison.

* * *

We wish to thank the Firm Siemens-Schuckert (Erlangen) for having supplied us the single crystals of germanium.

Thanks are also due to Prof. G. BOLLA, to Prof. F. FUMI and to Prof. E. GATTI for their interest in the present work.

We are grateful to Prof. F. SEITZ for his comments about this research.

RIASSUNTO

Il numero degli elettroni che sono rimossi dalla banda di conduzione per irraggiamento di monocristalli di germanio con particelle α del ^{210}Po è stato valutato misurando la decrescita iniziale di conducibilità elettrica di campioni di germanio di tipo n . Si è trovato che 79 ± 5 elettroni sono rimossi da ogni particella di 5.30 MeV. La possibilità di confrontare questo risultato con la teoria del disordinamento atomico da parte di particelle pesanti cariche viene discussa.

Evidence for a Heavy Neutral K-Particle and its Cascade Decay.

M. S. SINHA and S. N. SENGUPTA

Bose Institute - Calcutta

(ricevuto l'8 Febbraio 1957)

Summary. — Two cases of V^0 -decays have been obtained in both of which one of the secondaries is found to be heavier than a pion and is found to decay into a thinly ionizing particle at the end of its range. Approximate momenta and ionization estimates lead to a low Q -value of about 10 MeV if the secondaries are taken to be a K and a π -meson. These events therefore give evidence for the existence and cascade decay of a neutral heavy meson of mass near about $1270 m_\pi$. This particle is believed to be a bound excited state of an ordinary K-meson with a pion.

Anomalous V^0 -events have been from time to time recorded along with the normal ones. The recent analysis by ARNOLD *et al.* ⁽¹⁾ of five events confirms the existence of such anomalous cases. The main criterion for regarding these cases as anomalous is that the Q -value of all such events falls far outside the known Q -values of either Λ^0 or θ^0 decays. The normal decay modes of Λ^0 and θ^0 have a common negative secondary and the positive secondary is either a proton (Λ^0) or a pion (θ^0). A number of V^0 events can be explained in terms of the decay scheme $V_3^0 \rightarrow K^\pm + L^\pm$ (BARKER ⁽²⁾, LEIGHTON *et al.* ⁽³⁾), but the further decay of the heavy secondary (K^\pm) has not so far been observed even though quite a good number of cascade hyperon decays have been observed.

⁽¹⁾ W. H. ARNOLD jr., W. MARTIN and H. W. WYLD: *Phys. Rev.*, **100**, 1545 (1955).

⁽²⁾ K. H. BARKER: *Proc. Roy. Soc., A* **221**, 328 (1954).

⁽³⁾ R. B. LEIGHTON, S. D. WANLASS and C. D. ANDERSON: *Phys. Rev.*, **89**, 148 (1953).

We reproduce in the Figs. 1 and 2, two V^0 events in which one of the secondaries from the V^0 event decays inside the cloud chamber, giving rise to a minimum ionizing particle, which at least in Fig. 1, is not an electron and has a momentum of more than 180 MeV/c. These pictures were obtained at the high altitude research station of the Bose Institute, Darjeeling (2300 m.)

In Fig. 1, the V^0 decays at O into two minimum ionizing particles OS and OAB . The left branch OA of the V^0 suffers a nuclear inelastic scattering at A and emerges with an ionization of more than twice minimum. The small blob just below the plate A also supports the view that this is a nuclear scattering. The particle AB then gradually increases in ionization to more than four times minimum before entering the bottom plate of the cloud chamber and then decays into the thinly ionizing particle BC , which passes through seven radiation lengths and 46 g of Pb equivalent and still remains at minimum ionization. Hence BC cannot be an electron and if it is a π -meson it has a momentum greater than 180 MeV/c, which agrees well with the observed momenta of secondaries from S-particles. The intersection of AB and BC inside the bottom brass plate of the cloud chamber is established within ± 2 mm in stereo-projection. The eleven plates in this picture are alternatively lead (10.8 g) and copper (5.6 g) beginning and ending with copper.

Apart from losing an unknown amount of energy by the nuclear collision at A , the particle OAB has passed through 90 g of Pb equivalent before decaying. The secondary OS passes right through 80 g of lead equivalent and shows an increase in ionization before entering the last copper plate. Taking this particle to be a pion its momentum at the point of emission is obtained to be 235 ± 21 MeV/c, if the increase in ionization in the last portion of the track is taken to be real. The range of 40 ± 5 g of Pb equivalent of AB after it shows more than twice minimum ionization, easily identifies it with a K-meson. A proton, a K-meson ($963 m_e$), and a pion with twice minimum ionization would have a range of 72, 38 and 10 g of Pb respectively. The angle between the two secondaries of the V^0 is remarkably low and is found to be $6^\circ \pm .5$.

The second picture (Fig. 2) resembles the first picture in many respects. The V^0 decays at O and the left branch OS of almost minimum ionization penetrates 35 g of Pb equivalent and then goes out of illumination through the rear of the chamber. The right branch OAB exhibits more than minimum ionization after passing through the first plate (11.2 g of Cu), suffers an elastic scattering of 20° at A , becomes more than three times minimum before entering the last plate (11.2 g of Cu) where it decays into a thinly ionizing particle BC . Although the decay of the right branch of the V^0 is definitely established in this picture, the nature of the particle BC can not be ascertained, since the secondary did not have the opportunity to pass through any more plates inside the chamber. The plates in this picture are alternately copper (11.2 g) and

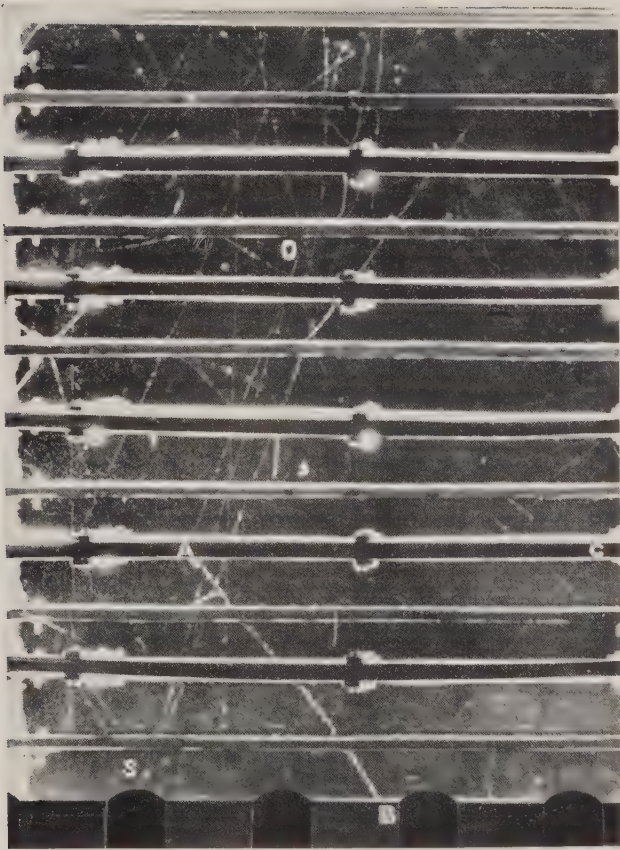


Fig. 1. - Photograph of a V^0 -event in which the left branch OAB suffers an inelastic scattering at A and decays at B into the thinly ionizing particle BC .

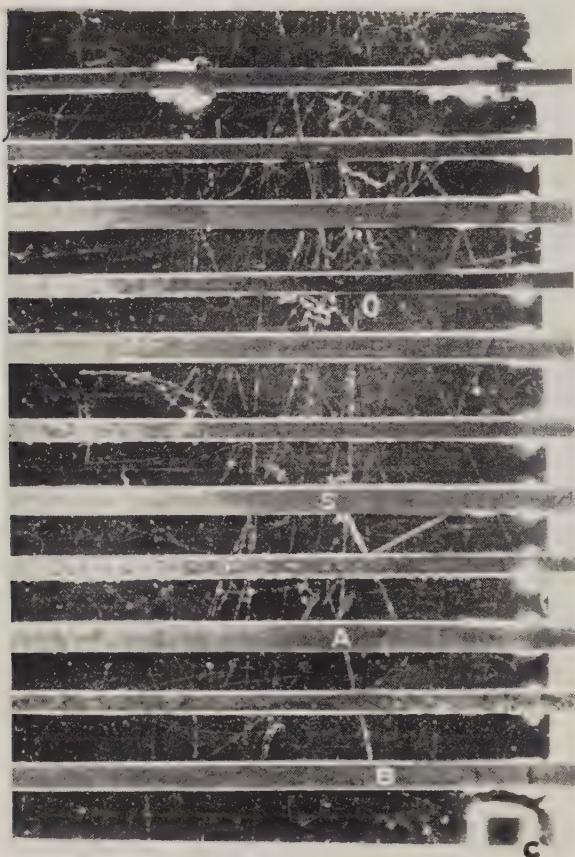


Fig. 2. — Photograph of a V^0 -event in which the right branch OAB suffers an elastic scattering at A and decays at B into the thinly ionizing particle BC .

Al (2.6 g), the last one being copper and the top plate only is lead (10.8) g. It will thus be seen that the particle OAB has a total range of (66 ± 8) g and a range of (51 ± 8) g of lead equivalent, after showing more than minimum ionization and hence can neither be a proton nor a pion. This particle is therefore reasonably identified as a K-meson. As the particle OS leaves the chamber within a short distance it is difficult to measure the angle between the V^0 secondaries in this case. It is found to be $8^\circ \pm 2$.

1. - Estimation of Momenta.

It is unfortunate that we do not observe any nuclear event, in both the pictures, to which we can ascribe the production of the V^0 's and thus evaluate p_T and Q -values accurately. Nevertheless the momentum of the secondary OS in Fig. 1 and that of OAB in Fig. 2 can be determined within small limits from the data presented above. The range of AB in Fig. 1 is known but the loss in momentum of OA at A due to the inelastic scattering is unknown. It is definitely larger than 150 MeV/c as is evident from the change in ionization from minimum to more than twice minimum. The loss in energy can also be not more than .5 GeV, for then it would have resulted in the boiling off of some nuclear particles from the lead nucleus with which it has made an inelastic collision. Hence the momentum of the K-meson, OAB in Fig. 1, is fixed between $0.525 \div 1.5$ GeV/c. Similarly, the momentum of the light secondary OS in Fig. 2, can be stated to be higher than 200 MeV/c (min. ionization after passing through 35 g of Pb equivalent) taking it to be a pion. Its upper limit is expected not to exceed half the momentum of the particle OAB , which is 3.5 times heavier. On this basis the momentum of the lighter secondary in Fig. 2 has been taken to be $200 \div 250$ MeV/c. All these data are collected in Table I.

TABLE I. - Momenta, energies and Q -values for the two V^0 -events.

	K-meson				L-meson			
	Momentum in GeV/c	Energy in GeV	I/I_m	θ	Momentum in GeV/c	Energy in GeV	I/I_m	Q in MeV
Case I (Fig. 1)	$0.525 \div 1.0$	$0.72 \div 1.12$	1 and > 2 after the scattering	6°	$0.5[0.235 \pm 0.021]$	0.274 ± 0.028	1	$5 \div 10$
Case II (Fig. 2)	0.445 ± 0.032	0.663 ± 0.042	1.5 after passing through 11.2 g of Cu	$8^\circ \pm 2$	$0.2 \div 0.25$	$0.244 \div 0.287$	1	$8 \div 17$

It is noteworthy that in both cases the angle between the secondaries is low. Assuming a two-body decay this fact points to low p_T and Q -values. We now make use of the following equations from PODOLANSKY and ARMENTEROS ⁽⁴⁾ to find the Q -values:

$$E_1 E_2 - p_1 p_2 \cos \theta = \frac{1}{2}(M^2 - m_1^2 - m_2^2)$$

and

$$M = m_1 + m_2 + Q,$$

where θ is the angle between the secondaries and the energy, momentum and Q -value are all expressed in energy units. Subscript 1 refers to the K-meson and 2 to the L-meson. Eliminating M and substituting $m_1 = 0.493$ and $m_2 = 0.139$ GeV for the K and pion mass, we get

$$Q = (E_1 E_2 - p_1 p_2 \cos \theta - .0686)/.632 \text{ GeV},$$

where the energy and momenta are now expressed in GeV and GeV/c, and we neglect $Q^2/2$ in comparison with $(m_1 + m_2)Q$. The Q -values calculated from this equation for the two cases are given in the last column of Table I. It is surprising that the Q -values ($5 \div 10$ MeV, $8 \div 17$ MeV) agree so closely for the two events and also with the Q -value of 11 MeV obtained by COWAN ⁽⁵⁾ from his remarkable V^0 -event of a negative secondary of protonic mass and a positive pion. If we take the negative secondary in COWAN's picture to be a K-meson the Q -value comes out as 18 MeV.

2. - Interpretation.

It is not possible in the present cases to determine which of the secondaries is positive. But it is likely that the heavy secondary is positive in view of the large excess of positives amongst slow K-particles observed by the Manchester, École Polytechnique and CIT groups. We therefore interpret these two events as the decay of a neutral particle of mass close to $1270 m_e$ to a K and an L-meson (π) with a low Q -value (~ 10 MeV). The neutral hyperon Λ^0 , with a low Q -value has often been regarded (POWELL ⁽⁶⁾) as the bound excited state of a proton with a pion. Similarly we may regard

⁽⁴⁾ J. PODOLANSKY and R. ARMENTEROS: *Phil. Mag.*, **45**, 13 (1954).

⁽⁵⁾ E. W. COWAN: *Phys. Rev.*, **94**, 161 (1954).

⁽⁶⁾ C. F. POWELL: *Nature*, **173**, 469 (1954).

this neutral particle to be an excited state of the ordinary K-meson ($964 m_c$) bound with a pion such that

$$(1) \quad \Lambda^0 \rightarrow K^+ + \pi^- + 10 \text{ MeV}.$$

Since the right branch of the V^0 -event in Fig. 2 shows more than minimum ionization from the start, has a range quite inconsistent with a pion or a proton and decays in the last plate, the question of identifying this event with a Λ^0 or a θ^0 does not arise, and this event has to be interpreted according to scheme (1). The V^0 event of Fig. 1, however, can be interpreted as a θ^0 -event in which the left branch is a pion which has disappeared and produced a K-meson at A. We have calculated the energy of the left branch taking it to be a pion and found it to be 2.8 GeV. The disappearance of such a large amount of energy producing only one charged particle of 0.7 GeV, is, in our opinion, quite unlikely. Furthermore there is evidence in emulsion work that a K-meson keeps its identity after an inelastic scattering (ROSSI⁽⁷⁾). Event 1, Fig. 6, described by MENON⁽⁸⁾ is very similar to the inelastic scattering at A in the event shown in Fig. 1. We also find that the heavy secondary has made a large angle scattering in both the events which shows that this secondary has high nuclear interaction cross-section.

GELL-MANN and PAIS⁽⁹⁾ have predicted the existence of a second θ^0 -particle, the θ_2^0 , with a lifetime considerably longer than that of the normal θ^0 ($\rightarrow \pi^+ + \pi^- + 215 \text{ MeV}$) and with a decay mode different from the latter. It has also been suggested by PAIS and PICCIONI⁽¹⁰⁾ that some of the anomalous θ^0 events may be θ_2^0 -decays. The present anomalous V^0 -events may therefore represent the decay of the θ_2^0 . The absence of any nuclear interaction close to the decay points indicates that the V^0 's were produced outside the chamber and hence point to a long life-time ($> 10^{-9} \text{ s}$). The mass of these neutral particles, however, differs considerably from that of θ_1^0 , if the lighter secondary is assumed to be a pion, and this is not in accord with the prediction of the Gell-Mann-Pais scheme.

The mass value $1270 m_c$ obtained from these two V^0 events, however, agrees remarkably well with the mass of the neutral K-particle (K^0) produced along with Λ^0 by the 1.37 GeV pion beam of the Brookhaven cosmotron (FOWLER *et al.*⁽¹¹⁾). The masses of the K^0 in the cases A and B of these

(7) B. ROSSI: *Proc. Fifth Annual Rochester Conference*, 129 (1955).

(8) M. G. K. MENON: *Proc. Fifth Annual Rochester Conference*, 80 (1955).

(9) M. GELL-MANN and A. PAIS: *Phys. Rev.*, **97**, 1387 (1955).

(10) A. PAIS and O. PICCIONI: *Phys. Rev.*, **100**, 1487 (1955).

(11) W. B. FOWLER, R. P. SHUTT, A. M. THORNDIKE and W. L. WHITEMORE: *Phys. Rev.*, **91**, 1287 (1953).

workers have been re-estimated by THOMSON ⁽¹²⁾ and are $(1280 \pm 70) m_e$ and $(1190 \pm 80) m_e$. In both these cases the decay of the K^0 was not observed, but its mass was determined indirectly by comparing momentum and energy of the observed Λ^0 with the known energy of the incident pion and assuming that only one more neutral particle was produced along with the Λ^0 .

* * *

The work was performed with financial support from the AEC., Government of India. We are grateful to Dr. D. M. BOSE, Director, of the Bose Institute, for his kind interest and for offering facilities to work at the high altitude station of the Bose Institute at Darjeeling.

(¹²) R. W. THOMSON: *Report of Progress in Cosmic Ray Physics*, vol. 3, p. 325.

RIASSUNTO (*)

Si sono osservati due casi di decadimento di V^0 nei quali uno dei secondari si trova essere più pesante di un pione e decadere in una particella debolmente ionizzante alla fine del suo range. Momenti approssimati e stime della ionizzazione portano ad un basso valore di Q di circa 10 MeV se i secondari si assumono essere un mesone K ed uno π . Questi eventi testimoniano pertanto in favore dell'esistenza e il decadimento in cascata di un mesone pesante neutro di massa prossima a circa $1270 m_e$. Si ritiene che questa particella sia uno stato eccitato legato di un ordinario mesone K con un pione.

(*) Traduzione a cura della Redazione.

Possible Explanations of the Decay Processes of the Pion in the Frame of the « Universal » Fermi Interaction.

G. MORPURGO

Istituto di Fisica dell'Università - Roma

Scuola di Perfezionamento in Fisica Nucleare dell'Università - Roma

(ricevuto l'11 Febbraio 1956)

Summary. — Two possible independent ways of reconciling the observed rates of the pion decay processes with the predicted values which one obtains if the processes take place through the « Universal » Fermi Interaction are suggested; one depends on the freedom which we have in establishing the correspondence between $P\bar{N}e\nu$ and $P\bar{N}\mu\nu$, the other on the modifications which the value of the ratio $|g_A|^2/|g_T|^2$ of the axial to the tensor coupling constant may suffer on account of the possible non invariance under time reversal of the β interaction. The predicted values for the ratios between the rates of the processes $\pi \rightarrow e + \nu$, $\pi \rightarrow e + \nu + \gamma$ and $\pi \rightarrow \mu + \nu$ are compatible with the present evidence.

1. — As well known ⁽¹⁾, one may look at the decay processes of the pion

- | | |
|-----|------------------------------------|
| (1) | $\pi \rightarrow e + \nu$ |
| (2) | $\pi \rightarrow e + \nu + \gamma$ |
| (3) | $\pi \rightarrow \mu + \nu$ |

as two step processes induced on the one hand by the Yukawa interaction which couples the pion to the nucleon antinucleon field and on the other by the « Universal » ⁽²⁾ interactions which couple the nucleon antinucleon field respectively to the $e\nu$ and $\mu\nu$ fields.

⁽¹⁾ Compare the review article by L. MICHEL in *Progr. in Cosmic Rays Physics* (New York, 1952).

⁽²⁾ We shall write the « Universal » interaction between four fermion fields a, b, c, d ,

However the results of the quantitative analysis which have been made ^(3,4) of the processes (1), (2), (3) appear to be rather discouraging and have led ⁽⁴⁾ to the conclusion that it appears difficult to reconcile the processes in question with the description through the intermediary of the Universal Fermi Interaction. In fact:

1) the predicted ratio between the rates of (1) and of (3) is in the best conditions:

$$(1) \quad r_{e/\mu} = \frac{\text{Rate (1)}}{\text{Rate (3)}} \sim 10^{-4} ;$$

2) the predicted ratio between the rates of (2) and of (3) is:

$$(5) \quad r_{e\gamma/\mu} = \frac{\text{Rate (2)}}{\text{Rate (3)}} > 0.025 \text{ } ^{(5)} .$$

The experimental value of $r_{e/\mu}$ appears already smaller than 10^{-1} (LOKANATHAN and STEINBERGER ⁽⁶⁾ give $r_{e/\mu} = 0.3 \pm 0.9 \cdot 10^{-1}$).

But, even worse, the experimental value of $r_{e\gamma/\mu}$ is surely smaller than 0.001 (ANDERSON ⁽⁷⁾).

in the form:

$$(*) \quad H_{abcd} = g_S S_{abcd} + g_V V_{abcd} + g_T T_{abcd} + g_A A_{abcd} + g_P P_{abcd} ,$$

where the sign conventions of MICHEL are used and where S, V, T, A, P , are the usual five invariants. It is in the spirit of the « Universality » of the Fermi interaction that the three processes: A) $N \rightarrow P + e + \nu$; B) $\mu \rightarrow e + \nu + \nu$ (or $\bar{\nu}$); C) $\mu^- + P \rightarrow N + \nu$ have to be accounted for by the same values of the constants g_S, g_V, g_T, g_A, g_P . There is however no general rule, at the moment, to prescribe the order in which the quadruples of fermions have to be inserted in (*). As well known the order is essential and in Sect. 3 we shall exploit just such freedom.

The new features arising in this problem from mixing in (*) couplings and pseudo-couplings will be discussed in Sect. 4.

⁽³⁾ The processes (1) and (3) have been first discussed by M. RUDERMANN and H. FINKELSTEIN [*Phys. Rev.*, **76**, 1458 (1949)] and by J. STEINBERGER [*Phys. Rev.*, **76**, 1180 (1949)].

⁽⁴⁾ The process (2) as well as the other two have been very recently reconsidered by IWATA, OGAWA, OGONOKY, SAKITA, ONEDA [*Progr. Theor. Phys.*, **13**, 19 (1955)] and by S. B. TREIMAN and H. M. WYLD [*Phys. Rev.*, **101**, 1553 (1956)]. Use is made frequently in this note of the results of this papers.

⁽⁵⁾ This is the result of TREIMAN and WYLD ⁽⁴⁾. It has to be mentioned that, as usual in this kind of calculations, a divergent integral appears in the evaluation of this figure; it is made finite by a cut off about M (nucleon mass).

⁽⁶⁾ S. LOKANATHAN and J. STEINBERGER: CU-81-55-ONR-110-1.

⁽⁷⁾ I thank prof. H. ANDERSON for having communicated this to me (result from ANDERSON-LATTES experiment).

The purpose of this note is to provide two independent arguments which may modify the figures in (4) and (5) so as to get agreement with the experimental values and solve, consequently, this difficulty. The two arguments are of a different nature and the question which of the two is the correct explanation of the facts is left open.

To present such arguments it is necessary first to recall briefly the derivation of the figures given in (4) (5); this will be done in the next section.

2. — In deriving ⁽⁴⁾ the values given in (4) and (5), the quadrilinear Fermi interaction between $\text{PN}\mu\nu$ was obtained from that responsible for the β -decay (where the operators are supposed to be inserted in the conventional order $(\psi_p^+ \Gamma \psi_N)(\psi_e^+ \Gamma \psi_\nu)$) by the substitution:

$$(6) \quad \begin{pmatrix} \text{PNev} \\ \text{PN}\mu\nu \end{pmatrix}$$

of the muon to the electron (Symmetrical Correspondence).

This entails that the rates of the $\pi \rightarrow \mu + \nu$ and $\pi \rightarrow e + \nu$ processes are obtained the one from the other by the simple substitution of the muon to the electron mass. Excluding from the start the P interaction from the Universal Interaction ⁽⁸⁾, since it would lead to a ratio $r_{e\mu} \sim 5$, the only remaining part of the interaction which may be responsible for the processes (1) and (3) is the A one; it is this part which gives rise to the ratio $\sim 10^{-4}$ reported in (4); the other interactions (S , V , T) give a vanishing matrix element for the pion decay into a lepton and a neutrino (since the pion is ps coupled to the nucleon field).

We know however that the A part of the interaction, if present at all, is small in the Universal Fermi interaction ⁽⁹⁾:

$$(7) \quad |g_A|^2 \leq \left(\frac{1}{50}\right)^2 |g_T|^2.$$

Therefore the process (2) prefers to take place through the T part of the interaction — with the emission of the γ the selection rule (Furry theorem) which prevents the neutrino-lepton decay through T is no more effective. So the radiative process (2) turns out to be much faster than the non radiative one and the figure in (5) is obtained.

⁽⁸⁾ The present data on the β phenomena do not require its presence.

⁽⁹⁾ The value given in (7) is the one used by TREIMAN and WYLD; but even if $|g_A|^2/|g_T|^2$ should be $< 1/(10)^2$ no one of the arguments would be changed. Compare however the Sect. 4 for the new situation arising from the possible non reality of the constants.

At this point we may illustrate the two possibilities which we see for solving this situation. We illustrate in the next section the first one.

3. — We begin by remarking that, after all, there is no need for postulating the correspondence (6). On account of the intricacies of the nuclear dynamics, the process $\mu^- + P \rightarrow N + \nu$ tells us nothing about the correspondence to be chosen between the particles P, N, e, ν and P, N, μ, ν . We may therefore, without renouncing to describe the processes (1), (2), (3) through the intermediary of an Universal Fermi Interaction, renounce simply to the symmetrical correspondence (6).

Suppose we choose instead the correspondence:

$$(8) \quad \begin{pmatrix} PNe\nu \\ P\nu\mu N \end{pmatrix}.$$

This amounts simply to assume that, in the Universal interaction (*) ⁽¹⁾ the four fields P, N, μ, ν have to be inserted, as indicated by (8), in the order $a \equiv P, b \equiv \nu, c \equiv \mu, d \equiv N$, the constants g_i remaining of course the same.

This new interaction $H_{P\nu\mu N}$ is however equivalent to an interaction written in the old order $H_{PN\mu\nu}$ (the order on which the discussion of the past section was based) but with different coupling constants; such new constants may be obtained ⁽¹⁰⁾ considering that each of the invariants (S, T, V, A, P) with the fields P, N, μ, ν inserted in the old order is equal to a combination of the same invariant with the fields P, N, μ, ν inserted in the new order:

$$(9) \quad \left\{ \begin{array}{l} S_o = \frac{1}{4}S_n - \frac{1}{4}V_n + \frac{1}{4}T_n + \frac{1}{4}A_n - \frac{1}{4}P_n \\ V_o = -S_n - \frac{1}{2}V_n \quad -\frac{1}{2}A_n - P_n \\ T_o = \frac{3}{2}S_n \quad -\frac{1}{2}T_n \quad -\frac{3}{2}P_n \\ A_o = S_n - \frac{1}{2}V_n \quad -\frac{1}{2}A_n + P_n \\ P_o = -\frac{1}{4}S_n - \frac{1}{4}V_n - \frac{1}{4}T_n + \frac{1}{4}A_n + \frac{1}{4}P_n \end{array} \right.$$

where n and o mean respectively new and old order.

On the basis of the above formulas (9) we may now discuss the following case. Suppose that the β interaction contains only an S and T part; as well known, such a prescription, namely:

$$(10) \quad g_s = -g_t (\neq 0), \quad g_v = g_a = g_p = 0$$

⁽¹⁰⁾ M. FIERZ: *Zeits. f. Phys.*, **104**, 553 (1937); E. R. CAIANIELLO: *Nuovo Cimento*, **8**, 479 (1951); L. MICHEL: *Thèse* (Paris, 1953).

is able to explain all the β phenomena and also the μ decay phenomena ⁽¹¹⁾, provided only that in the μ decay the two neutrinos are assumed to be different. The addition of a V part would not however change any one of the arguments below.

Then the $\pi \rightarrow e + \nu$ decay is forbidden:

$$\text{Rate } (\pi \rightarrow e + \nu) = 0.$$

The rate of the $\pi \rightarrow e + \nu + \gamma$ decay will be the same as before, since it is determined by the T interaction, the amount of which is supposed to be the same as before.

The rate of the $\pi \rightarrow \mu + \nu$ decay is however considerably increased with respect to the previous treatment, in which the correspondence (6) was assumed. In fact the coupling constant of the A term which appears in the $\text{PN}_{\mu\nu}$ interaction is zero, by construction, when such interaction is written in the new order, but becomes, when it is rewritten in the old order:

$$g_{A(o)} = g_{S(n)}$$

as appears from the formulas (9).

Therefore the rate of the $\pi \rightarrow \mu + \nu$ decay is increased by a factor 2500 with respect to the situation discussed in the past section. Correspondingly $r_{e\nu/\mu}$ is decreased in the same ratio and may be now as low as:

$$r_{e\nu/\mu} = \frac{0.025}{2500} = 10^{-5}.$$

We thus obtain a completely reasonable situation, in which one has no $\pi \rightarrow e + \nu$ decay at all, and a ratio of $\pi \rightarrow e + \nu + \gamma$ to $\pi \rightarrow \mu + \nu$ decay not in contradiction with the present facts. The situation is not worsened if we include in the β interaction an axial part of the same order of magnitude of that considered in the past section; the only effect of such term would be that of making the $\pi \rightarrow e + \nu$ decay not absolutely forbidden; still on account of the increase of the $\pi \rightarrow \mu + \nu$ rate the ratio $r_{e/\mu}$ would be decreased by a factor 2500 with respect to the ratio given in the past section thus becoming $\sim 10^{-7}$. Only the inclusion of a P part in the β interaction might create difficulties to the scheme presented here.

It has also to be mentioned that the increase of the rate of the $\pi \rightarrow \mu + \nu$ decay with respect to that obtained using the conventional correspondence

⁽¹¹⁾ L. MICHEL and A. S. WIGHTMAN: *Phys. Rev.*, **93**, 354 (1954). The correspondence between $\text{PN}_{\text{e}\nu}$ and $\mu_{\text{e}\nu}$ to be associated with (10) is $(\frac{\text{PN}_{\text{e}\nu}}{\mu_{\text{e}\nu}})$.

of the past section is welcome; in fact, as pointed out in ref. (1), it was difficult to see how a coupling term as small as that given in (7) might reproduce the observed rate of the $\pi \rightarrow \mu + \nu$ decay ($\sim 10^{-8}$ s).

We may therefore say that, even if the «symmetrical» correspondence (6) cannot agree with the facts, still there is no need to renounce to the description of the decay processes through the Universal Fermi Interaction, but one may simply choose another correspondence namely the one given by (8). This conclusion is unaffected by any mixture of couplings and pseudocouplings (non conservation of parity) (12) which appears to be needed on the basis of recent evidence (13), except for one point which will be discussed in the next section.

4. — The possibility of the mixtures, which we have just mentioned, even without affecting directly the above arguments, may however change possibly the value of the ratio $|g_A|^2/|g_T|^2$ given in (7) on which the whole discussion is based. We have so a second possibility for getting agreement between the pion decay and the Universal Fermi Interaction: a possibility which is completely independent from the one discussed in the past section; this will be discussed here.

If the reality condition on the constants of the β decay interaction is abandoned, which is the case if the interaction, besides not conserving the parity and the charge conjugation, is not invariant with respect to time reversal, the absence of the Fierz interferences in the β spectra, is no more a proof that the relative percentages of T and A interaction are very different. Infact the Fierz interferences are determined by the combination:

$$\text{Re}(g_T g_A^* + g_T' g_A'^*)$$

and their absence shows that either the relative percentages of the A and T interactions are very different, or that the phase differences between A and T , A' and T' are near 90° .

In order to conclude that (7) still holds one has to measure independently the imaginary part of $g_T g_A^* + g_T' g_A'^*$. As pointed out by LEE, OEHME and YANG (14), such measurement may be performed by studying the *momentum dependence* of the $\cos \theta$ asymmetry in the β emission from an oriented nucleus like ^{60}Co . Up to now there is no information on this point. If it should turn out that $|g_A|^2 + |g_A'|^2$ has the same order of magnitude as $|g_T|^2 + |g_T'|^2$ then, there should be possibly no need of the change of correspondence suggested in the

(12) T. D. LEE and C. N. YANG: *Phys. Rev.*, **104**, 254 (1956).

(13) C. S. WU *et al.*: to be published.

(14) T. D. LEE, R. OEHME and C. N. YANG: to be published.

Sect. 3. One would then get an $r_{e/\mu}$ value as the one given in (4) and $r_{e\gamma/\mu}$ value most probably not in contraddiction with the experiment (around 10^{-5}); the value of $r_{e\gamma/\mu}$ is difficult to state exactly also because it may depend on interferences between the contributions of the A and T terms, in the β interaction, which would be now comparable. Our conclusion is therefore that there are presently at least two independent ways to reconcile the π decay processes with the « Universal » Fermi Interaction. Of course further experiments, aiming to establish the values of the constants in the β interaction, will be most useful *also* in this connection ⁽¹⁵⁾.

(¹⁵) The spectrum and the rate of the $\pi \rightarrow \mu + \nu + \gamma$ process may provide an independent check of the ideas presented here. It is planned to study such problem in the future.

RIASSUNTO

Vengono suggeriti due diversi modi possibili di conciliare le probabilità osservate dei processi di decadimento del mesone π con i valori prevedibili che si ottengono se tali processi avvengono tramite l'Interazione « Universale ». Un modo dipende dalla libertà che esiste nello stabilire la corrispondenza fra $P_{N\bar{e}\nu}$ e $P_{N\bar{\mu}\nu}$; l'altro si basa sui cambiamenti che il valore del rapporto $|g_A|^2/|g_T|^2$ può avere a causa della possibile non invarianza rispetto a inversione di tempo della interazione β . I valori che si prevedono per i rapporti tra le probabilità dei processi $\pi \rightarrow e + \nu$, $\pi \rightarrow e + \nu + \gamma$ e $\pi \rightarrow \mu + \nu$ sono compatibili coi dati sperimentali attuali.

On Neutron-Proton Scattering (*).

E. CLEMENTEL and C. VILLI (+)

Istituti di Fisica dell'Università di Padova e di Trieste (+)

Istituto Nazionale di Fisica Nucleare - Sezione di Padova

(+) Istituto Nazionale di Fisica Nucleare - Gruppo di Trieste

(ricevuto il 13 Febbraio 1957)

Summary. — General expressions for the nucleon-nucleon elastic scattering cross-section and polarization are derived from the transition matrix up to the orbital angular momentum $L = 3$. A detailed investigation on the reliability of the approximation restricted to partial waves corresponding to $L \leq 2$ has been carried out. The charge independence of nuclear forces and the continuity of the phaseshifts versus neutron energy has been taken into account. It is shown that because of the change of sign of the singlet S phaseshift at about 220 MeV, following from the analysis of proton-proton data, the n-p differential cross-section at 260 MeV cannot be fitted in the lowest approximation without destroying either the continuity of the phaseshift solutions in the energy interval ranging from 27 to 260 MeV or the charge independence of nuclear forces, or both. It is also shown that the high energy n-p solutions cannot be continuously linked to the low energy ones if the S phaseshift for the singlet state is assumed positive throughout the considered energy interval. The effect of the 3S_1 - 3D_1 coupling is discussed in detail at 95 MeV.

Introduction.

In recent years several efforts have been made to obtain information on the neutron-proton interaction at high energies from the analysis of the differential cross-sections of neutrons elastically scattered by protons. Some of these attempts, based on a low order ($L \leq 2$) partial wave approximation and on the assumption of charge independence of nuclear forces, have ap-

(*) The results of this investigation have been reported at the International Conference on Nuclear Reactions, Amsterdam, July 1956 (*Physica*, **22**, 1173 (1956)).

parently succeeded in fitting the neutron-proton angular distribution at 260 MeV in terms of two different sets of phase shifts, suggesting physical features of the high energy n-p interaction, which are mutually contradictory. From one of these two analyses ⁽¹⁾ it appears that the n-p interaction is attractive both in singlet odd and triplet even states, whereas from the other analysis ⁽²⁾ it turns out that the attraction is restricted only to the singlet odd states and the triplet ones give a repulsive interaction. It will be seen that this paradoxical situation arose because the analyses were limited either to a single scattering energy or to a narrow energy interval.

In the present analysis all phase shift solutions fitting the data equally well will be considered and discussed. It has been found rather illuminating, either physically or mathematically, to examine the phase shift evolution versus energy in a very wide energy interval. If one assumes that the phase shifts must be well behaved and satisfy the continuity requirement versus neutron energy, then, as it will be seen, the continuity provides a necessary but not sufficient criterion for discriminating, at a given scattering energy, among the manifold of mathematical solutions, the physical ones. If this criterion is ignored, it may happen that the results of the analysis are completely misleading and physically inconsistent, although the phase shifts may well fit the data. As it will be shown later, this is just what happens at 260 MeV in the $L = 2$ partial wave approximation with no coupling between the triplet S and D states. This approximation will be examined in great detail from 27 to 260 MeV, not obviously because it is believed particularly reliable, but because it is the starting point of higher order approximations. To fit the data the criterion of minimum for the least squares sum N will be used. Aesthetical fits based on a mere graphical reproduction of the measured cross-section in terms of phase shifts are dangerously misleading in this kind of analyses.

The general expressions for the neutron-proton scattering cross-section and polarization are derived in Sect. 1 from the transition matrix for a two-nucleon system. An analytical approach to the $L = 2$ partial wave approximation with no $^3S_1 - ^3D_1$ coupling is outlined in Sect. 2. The phase-shift solutions from 27 to 260 MeV are discussed in Sect. 3, 4 and 5. In Sect. 6 the scattering data at 95 MeV are analyzed taking into account the n-p polarization. The effect of the $^3S_1 - ^3D_1$ coupling is also discussed.

⁽¹⁾ R. M. THALER and J. BENGSTON: *Phys. Rev.*, **94**, 679 (1954); R. M. THALER, J. BENGSTON and G. BREIT: *Phys. Rev.*, **94**, 683 (1954).

⁽²⁾ C. A. KLEIN: *Nuovo Cimento*, **2**, 38 (1955).

Symbols and notation.

K_L	singlet phase shift for the orbital angular momentum L ;
δ_{JL}	triplet phase shift for the total angular momentum J and orbital momentum L ;
$\sigma(\vartheta)$	neutron-proton differential cross-section;
$\varrho = \sigma(180^\circ)/\sigma(0^\circ)$	n-p asymmetry ratio;
A_n, B_n	coefficients of the n-p angular distribution and polarization calculated in terms of phase shifts;
$\cos 2K_L = c_L, \quad \sin 2K_L = s_L$	
$\cos 2\delta_{JL} = c_{JL}, \quad \sin 2\delta_{JL} = s_{JL}$	
$(\alpha \beta) = \sin \alpha \sin \beta \sin (\alpha - \beta)$	
$(\alpha, \beta) = \sin \alpha \sin \beta \cos (\alpha - \beta)$	
$z_0 = \sin^2 (K_0)$	
$z_1 = \sum_{J=0}^2 (2J+1) \sin^2 (\delta_{JL})$	
$z_2 = \sum_{J=0}^2 (2J+1) \sin \delta_{JL} \cos \delta_{JL}$	
$z_3 = (3/2) \sin^2 (\delta_{11}) + (7/2) \sin^2 (\delta_{21}) + 4(\delta_{01}, \delta_{21}) + 9(\delta_{11}, \delta_{21})$	
$N = \sum_{\vartheta} \left[\frac{\sigma_{\text{theor}}(\vartheta) \cdot \sigma_{\text{exp}}(\vartheta)}{\Delta \sigma} \right]^2$	

1. - Transition matrix for the neutron-proton system.

For a two-nucleon system S^2 is a constant of motion, provided the interaction Hamiltonian is symmetric in the spin vectors of the two nucleons ⁽³⁾. The scattering amplitude can then be written as

$$(1) \quad f(\vartheta, \varphi) = \sum_{S=0,1} \sum_{M' M} \mathcal{M}_{M' M}^S(\vartheta, \varphi) \chi_{M'}^S a_M^S,$$

where the matrix element $\mathcal{M}_{M' M}^S$, which physically represents the scattering

⁽³⁾ For the experimental evidence of this fact see D. FELDMAN: *Proceedings of the Rochester Conference* (1956), p. II-1.

amplitude of the wave outgoing in the state $L'SJM'$ ($M_s = M$, $M_L = M - M'$) and due to the wave incoming in the state $LSJM$ ($M_s = M$ because $M_L = 0$), is given by (4.5)

$$(2) \quad \mathcal{M}_{M'M}^S(\vartheta, \varphi) = (1/2ik) \sum_{J=0}^{\infty} \sum_{L=|J-S|}^{J+S} \sum_{L'=|J-S|}^{J+S} i^{L-L'} [4\pi(2L+1)]^{\frac{1}{2}} \cdot (LSOM|JM)(L'S, M-M', M'|JM)(\mathcal{S}_{J,L'L} - \delta_{L'L}) Y_{L',M'-M}(\vartheta, \varphi).$$

For an unpolarized beam, the amplitudes a_M^S have to be normalized according to $|a_M^S|^2 = \frac{1}{4}$. For singlet states ($S = 0$, $L = L' = J$, $M = M' = 0$) the scattering matrix $\mathcal{S}_{J,L'L}$ is simply given by $\mathcal{S}_{J,J} = \exp[2iK_J]$. Therefore, introducing the notation

$$(3) \quad Q_J = (1/2i)(\mathcal{S}_{J,J} - 1) = \exp[iK_J] \sin K_J,$$

and using the orthogonality relations of the vector addition coefficients, we obtain

$$(4) \quad k\mathcal{M}_0(\vartheta) = \sum_{J=0}^{\infty} [4\pi(2J+1)]^{\frac{1}{2}} Q_J Y_{J0}(\vartheta).$$

In order to avoid bulk symbols we shall use \mathcal{M}_0 and $\mathcal{M}_{M'M}$ to denote the singlet respectively the triplet matrix; the matrix

$$(5) \quad \mathcal{M} = \left(\begin{array}{c|c} \mathcal{M}_0 & 0 \\ \hline 0 & \mathcal{M}_{M'M} \end{array} \right)$$

will be called (6) the transition matrix.

For triplet states the scattering matrix has to take into account the coupling between the states having the same parity $(-1)^{J \pm 1}$. The general expression of the matrix $\mathcal{S}_{J,L'L}$ in terms of the coupling ϵ_J , which measures the amount of admixture of the state $L = J+1$ to the state $L = J-1$, has been given by BLATT and BIEDENHARN (5). Introducing a new matrix R with elements

$$(6) \quad R_{J,L'L} = (1/2)i^{L-L'-1}(\mathcal{S}_{J,L'L} - \delta_{L'L}),$$

(4) J. ASHKIN and TA-YOU WU: *Phys. Rev.*, **73**, 973 (1948).

(5) J. M. BLATT and L. C. BIEDENHARN: *Rev. Mod. Phys.*, **24**, 258 (1952); *Phys. Rev.*, **86**, 399 (1952).

(6) R. OEHME: *Phys. Rev.*, **98**, 147 (1955).

the transition matrix for $S = 1$, following from Eq. (2), reads

$$(7) \quad k\mathcal{M}_{M'M}(\vartheta, \varphi) = \sum_{J=0}^{\infty} \sum_{L=|J-S|}^{J+S} \sum_{L'=|J-S|}^{J+S} [4\pi(2L+1)]^{\frac{1}{2}} \cdot (L10M | JM)(L'1, M-M', M' | JM) R_{J,L'L} Y_{L',M-M'}(\vartheta, \varphi).$$

The elements of the R -matrix are given in Table I, where, according to (3), $Q_{JL} = \exp[i\delta_{JL}] \sin \delta_{JL}$.

TABLE I. — Elements $R_{J,L'L}$ of the matrix R .

$L' \backslash L$	$J-1$	J	$J+1$
$J-1$	$Q_{J,J-1} \cos^2 \varepsilon_J + Q_{J,J+1} \sin^2 \varepsilon_J$	0	$\frac{1}{2}(Q_{J,J+1} - Q_{J,J-1}) \sin 2\varepsilon_J$
J	0	Q_{JJ}	0
$J+1$	$\frac{1}{2}(Q_{J,J+1} - Q_{J,J-1}) \sin 2\varepsilon_J$	0	$Q_{J,J+1} \cos^2 \varepsilon_J + Q_{J,J-1} \sin^2 \varepsilon_J$

Denoting simply with R_{JL} the diagonal and with R_J the non diagonal elements of the R -matrix, we have derived from Eq. (7) explicit expressions for the elements of the transition matrix \mathcal{M} for triplet states up to $L = 3$, including the coupling of the two states $J = 1$ ($^3S_1 - ^3D_1$) and $J = 2$ ($^3P_2 - ^3F_2$). As it has been shown by WOLFENSTEIN and ASHKIN (7), the invariance of the matrix $\mathcal{M}_{M'M}$ under space reflections requires that

$$(8) \quad \begin{cases} \mathcal{M}_{-1-1} = \mathcal{M}_{11}, & \mathcal{M}_{0-1} = -\mathcal{M}_{01} \exp[-2i\varphi], \\ \mathcal{M}_{1-1} = \mathcal{M}_{-11} \exp[-4i\varphi], & \mathcal{M}_{-10} = -\mathcal{M}_{10} \exp[2i\varphi], \end{cases}$$

and therefore the triplet transition matrix $\mathcal{M}_{M'M}$ is completely defined by the following five elements

$$(9a) \quad k\mathcal{M}_{11} = [R_{10} + (\sqrt{2}/2)R_1](4\pi)^{\frac{1}{2}}Y_{00} + \\ + [(3/2)Q_{11} + (3/2)R_{21} + (\sqrt{6}/2)R_2](4\pi/3)^{\frac{1}{2}}Y_{10} + \\ + [(1/2)R_{12} + (\sqrt{2}/2)R_1 + (5/2)Q_{22} + 2Q_{32}](4\pi/5)^{\frac{1}{2}}Y_{20} + \\ + [R_{23} + (\sqrt{6}/2)R_2 + (7/2)Q_{33} + (5/2)Q_{43}](4\pi/7)^{\frac{1}{2}}Y_{30},$$

$$(9b) \quad k\mathcal{M}_{01} = [- (3/2)Q_{11} + (3/2)R_{21} + (\sqrt{6}/2)R_2](4\pi/3)^{\frac{1}{2}}Y_{11} + \\ + [- (\sqrt{3}/2)R_{12} - (\sqrt{6}/2)R_1 - (5\sqrt{3}/6)Q_{22} + (4\sqrt{3}/3)Q_{32}](4\pi/5)^{\frac{1}{2}}Y_{21} + \\ + [- (2\sqrt{6}/3)R_{23} - 2R_2 - (7\sqrt{6}/12)Q_{33} + (5\sqrt{6}/4)Q_{43}](4\pi/7)^{\frac{1}{2}}Y_{31}.$$

() L. WOLFENSTEIN and J. ASHKIN: *Phys. Rev.*, **85**, 947 (1952).

$$(9c) \quad k\mathcal{M}_{-11} = [(\sqrt{6}/2)R_{12} + \sqrt{3}R_1 - (5\sqrt{6}/6)Q_{22} + (\sqrt{6}/3)Q_{32}](4\pi/5)^{\frac{1}{2}}Y_{22} + \\ + [(\sqrt{30}/3)R_{23} + \sqrt{5}R_2 - (7\sqrt{30}/12)Q_{33} + (\sqrt{30}/4)Q_{43}](4\pi/7)^{\frac{1}{2}}Y_{32},$$

$$(9d) \quad k\mathcal{M}_{10} = [-Q_{01} + R_{21} - (\sqrt{6}/2)R_2](4\pi/3)^{\frac{1}{2}}Y_{1,-1} + \\ + [-\sqrt{3}R_{12} + (\sqrt{6}/2)R_1 + \sqrt{3}Q_{32}](4\pi/5)^{\frac{1}{2}}Y_{2,-1} + \\ + [-\sqrt{6}R_{23} + 2R_2 + \sqrt{6}Q_{43}](4\pi/7)^{\frac{1}{2}}Y_{3,-1},$$

$$(9e) \quad k\mathcal{M}_{00} = [R_{10} - \sqrt{2}R_1](4\pi)^{\frac{1}{2}}Y_{00} + \\ + [Q_{01} + 2R_{21} - \sqrt{6}R_2](4\pi/3)^{\frac{1}{2}}Y_{10} + \\ + [2R_{12} - \sqrt{2}R_1 + 3Q_{32}](4\pi/5)^{\frac{1}{2}}Y_{20} + \\ + [3R_{23} - \sqrt{6}R_2 + 4Q_{43}](4\pi/7)^{\frac{1}{2}}Y_{30}.$$

If Coulomb effects are neglected, the matrix elements given by Eqs. (4) and (9) are valid also for the proton-proton system, provided the odd singlet and even triplet terms are dropped (Pauli principle) and each matrix element is multiplied by a factor 2. This factor is obviously required by the symmetrization respectively antisymmetrization of the remaining even singlet and odd triplet terms. If the coupling for $J=2$ is ignored (for $\varepsilon_J \rightarrow 0$, $R_{JL} \rightarrow Q_{JL}$ and $R_J \rightarrow 0$), the Coulomb effects can be taken into account simply by substituting in Eqs. (4) and (9) $Y_{\lambda\mu}$ with $Y_{\lambda\mu} \exp[2i\sigma_\lambda]$, where σ_λ is the Coulomb phase shift. When the mixing between the 3P_2 and 3F_2 states is not neglected, the final formulas are much more complicated, and alternative expressions have already been given⁽⁸⁻¹⁰⁾.

This formalism will now be used to derive the expressions for the neutron-proton differential cross-section and polarization.

1.1. *Scattering cross-section.* — The scattering cross-section is given by (7)

$$(10) \quad \sigma(\vartheta) = (1/4) \text{Tr} \langle \mathcal{M}^\dagger \mathcal{M} \rangle = (1/4) \{ |\mathcal{M}_{20}|^2 + |\mathcal{M}_{00}|^2 \} + \\ + (1/2) \{ |\mathcal{M}_{11}|^2 + |\mathcal{M}_{10}|^2 + |\mathcal{M}_{01}|^2 + |\mathcal{M}_{-11}|^2 \}.$$

Eq. (10) can also be put in the form

$$(11) \quad k^2\sigma(\vartheta) = \sum_{n=0}^{2L_{\max}} A_n P_n(\cos \vartheta).$$

(⁸) G. BREIT, G. B. HERMAN and M. H. HULL jr.: *Phys. Rev.*, **97**, 1051 (1955).

(⁹) E. CLEMENTEL and C. VILLI: *Nuovo Cimento*, **2**, 1165 (1955).

(¹⁰) H. P. STAPP: *University of California Thesis*, UCRL-3098 (1955).

The general expressions for the angular distribution coefficients A_n will not be given here, because they appeared in a recent paper of FESHBACH and LOMON⁽¹¹⁾ just in the approximation we have been working in deriving the transition matrix \mathcal{M} . Explicit expressions of the A_n 's will be given in Sect. 2 for $L_{\max} = 2$. According to the previous considerations, for identical (uncharged) particles one has to multiply the given $\sigma(\theta)$ by 4 and drop the terms forbidden by the Pauli principle⁽¹²⁾.

1'2. Polarization. — The polarization in a nucleon-nucleon collision, to be detected with a double scattering experiment, is defined as (7)

$$(12) \quad \sigma(\vartheta) \mathbf{P}(\vartheta) = (1/4) \text{Tr} (\mathcal{M} \mathcal{M}^\dagger \boldsymbol{\sigma}),$$

where $\mathbf{P}(\vartheta) = P(\vartheta) \mathbf{n}$, being \mathbf{n} a unit vector normal to the plane of scattering. If one expresses $\boldsymbol{\sigma}$ in the same representation as the transition matrix \mathcal{M} , from Eqs. (10) and (12) it follows

$$(13) \quad k^2 \sigma(\vartheta) P(\vartheta) = (1/2\sqrt{2}) \text{Im} [\mathcal{M}_{10} \exp[i\varphi] - \mathcal{M}_{01} \exp[-i\varphi]]^* \cdot [\mathcal{M}_{11} - \mathcal{M}_{-11} \exp[-2i\varphi] + \mathcal{M}_{00}].$$

The products of the spherical harmonics which appear in Eq. (13) are all of the type (9)

$$(14) \quad [4\pi/(2l+1)]^{1/2} [4\pi/(2l'+1)]^{1/2} Y_{lm}(\vartheta, \varphi) Y_{l'm'}^*(\vartheta, \varphi) \exp[-iM\varphi] = (-1)^{1/2(m+m'-|M|)} \sum_{L=|l-l'|}^{l+l'} \frac{[(L-|M|)!]^{1/2}}{[(L+|M|)!]^{1/2}} \cdot (l'00|L0)(l'l', m, -m'|LM) \sin^{|M|} \vartheta \left(\frac{d}{d \cos \vartheta} \right)^{|M|} P_L(\cos \vartheta),$$

(11) H. FESHBACH and E. LOMON: *Phys. Rev.*, **102**, 891 (1956). The results of these Authors follow from the concise expression of $\sigma(\vartheta)$ given by BLATT and BIEDENHARN, who, using the powerful Racah technique, do not need the explicit knowledge of the transition matrix. This matrix is nevertheless extremely useful in discussing several problems connected with nucleon-nucleus scattering. See for instance: W. B. RIESENFELD and K. M. WATSON: *Phys. Rev.*, **102**, 1157 (1956).

(12) For the proton-proton system, if we denote by $\mathcal{M}^{(a)}$ the antisymmetrized matrix with Coulomb factor (see above) but without couplings, the scattering amplitude corresponding to Eq. (1) reads

$$f^{(a)}(\vartheta, \varphi) = \sum_{S=0,1} \sum_{M} \{ \mathcal{M}_{M'M}^{(a)S}(\vartheta, \varphi) + f_{\mathcal{C}}^{(a)S}(\vartheta) \delta_{M'M} \} \chi_M^S a_M^S,$$

where $f_{\mathcal{C}}^{(a)S}(\vartheta) = f_{\mathcal{C}}(\vartheta) + (-1)^S f_{\mathcal{C}}(\pi - \vartheta)$ is the antisymmetrized Coulomb scattering amplitude [see ref. (9), Sect. 1]. Therefore $(1/4) \text{Tr} \mathcal{M}^{(a)\dagger} \mathcal{M}^{(a)}$ gives only the so called nuclear part of the differential cross-section. Most of the formalism required to evaluate the right hand side of Eq. (10) for identical particles can be found in the Appendix of ref. (9).

where $|M| = |m - m'| = 1$. Therefore, using the recursion relation $P'_{L-1}(x) = P'_{L-1}(x) + (2L+1)P_L(x)$, Eq. (13) can be written in the following form

$$(15) \quad k^2 \sigma(\vartheta) P(\vartheta) = \sin \vartheta \sum_{n=0}^{2L_{\max}-1} B_n P_n(\cos \vartheta).$$

For identical particles, only the odd B_n 's, multiplied by 4, have to be retained, once all the even triplet terms have been dropped.

The expansion coefficients B_n for the neutron-proton polarization, following from the transition matrix elements given in Eqs. (9), are

$$(16a) \quad 4B_0 = \text{Im} \{ 2Q_{01}[R_{10} - R_{12} - (\sqrt{2}/2)R_1 + Q_{32}]^* + \\ + 3Q_{11}[R_{10} - R_{12} - (3\sqrt{2}/2)R_1 + 3Q_{32}]^* + \\ + 5Q_{22}[R_{21} - R_{23} - (\sqrt{6}/6)R_2 + Q_{43}]^* - \\ - 9Q_{32}[R_{21} + (2/3)R_{23} - (14/27)R_2 + (7/9)Q_{33} - (13/9)Q_{43}]^* + \\ - (7/6)Q_{33}[R_{10} - R_{12} - (\sqrt{2}/2)R_1]^* - \\ - (9/2)Q_{43}[R_{10} + R_{12} - (\sqrt{2}/2)R_1]^* + 5R_{10}[R_{21} - (2/3)R_{23}]^* + \\ + R_{12}[4R_{21} - (17/3)R_{23} - (3\sqrt{6}/2)R_2]^* + \\ + (5\sqrt{2}/2)[R_{21} - (2/3)R_{23}]R_1^* \},$$

$$(16b) \quad 4B_1 = \text{Im} \{ (6Q_{01} + 9Q_{11})[R_{21} - R_{23} - (\sqrt{6}/6)R_2 + Q_{43}]^* + \\ + 5Q_{22}[R_{10} - R_{12} - (\sqrt{2}/2)R_1 + 3Q_{32}]^* - \\ - 7Q_{32}[2R_{10} + (13/7)R_{12} - \sqrt{2}R_1]^* + \\ + (21/2)Q_{33}[R_{21} - R_{23} - (\sqrt{6}/6)R_2 + 2Q_{43}]^* - \\ - (3/2)Q_{43}[17R_{21} + 13R_{23} - (9\sqrt{6}/2)R_2]^* - 9R_{10}R_{12}^* - \\ - (9\sqrt{2}/2)R_{12}R_1^* - 5R_{21}[3R_{23} - (\sqrt{6}/2)R_2]^* - 5\sqrt{6}R_{23}R_2^* \},$$

$$(16c) \quad 4B_2 = \text{Im} \{ (10Q_{01} + 15Q_{11})Q_{32}^* + \\ + 10Q_{22}[R_{21} - R_{23} - (\sqrt{6}/6)R_2 + (5/2)Q_{43}]^* - \\ - 3Q_{32}[R_{21} + (68/7)R_{23} - (14\sqrt{6}/9)R_2 + (20/3)Q_{33} - (50/21)Q_{43}]^* + \\ + (35/6)Q_{33}[R_{10} - R_{12} - (\sqrt{2}/2)R_1]^* - \\ - (45/2)Q_{43}[R_{10} + R_{12} - (\sqrt{2}/2)R_1]^* - (50/3)R_{10}R_{23}^* + \\ + R_{12}[18R_{21} - (4/3)R_{23} - 3\sqrt{6}R_2]^* - (25\sqrt{2}/3)R_{23}R_1^* \},$$

$$(16d) \quad 4B_3 = \text{Im} \{ (14Q_{01} + 21Q_{11})Q_{43}^* + 15Q_{22}Q_{32}^* - 27Q_{32}R_{12}^* + \\ + 7Q_{33}[(3/2)(R_{21} - R_{23}) - (\sqrt{6}/4)R_2 + (38/9)Q_{41}]^* - \\ - Q_{43}[(11/2)R_{21} + (791/18)R_{23} - (27\sqrt{6}/4)R_2]^* - \\ - (30R_{21} + 5\sqrt{6}R_2)R_{23}^* \},$$

$$(16e) \quad 4B_4 = \text{Im} \{ 20Q_{22}Q_{43}^* - Q_{32}[(300/7)R_{23} + 15Q_{33} - (13/7)Q_{41}]^* - 36Q_{43}R_{12}^* \},$$

$$(16f) \quad 4B_5 = \text{Im} \{ (25/9)(7Q_{33} + 20R_{23})Q_{43}^* \}.$$

The expansion coefficients B_n , given by Eqs. (16), can be easily expressed in terms of phase shifts and couplings. In fact, because of Eq. (13) and the matrix elements listed in Table I, one has

$$(17) \quad \begin{cases} \text{Im} (Q_{JL}Q_{J'L'}^*) &= \sin \delta_{JL} \sin \delta_{J'L'} \sin (\delta_{JL} - \delta_{J'L'}) \equiv (\delta_{JL} | \delta_{J'L'}), \\ \text{Im} (Q_{JL}R_{J',J'+1}^*) &= (\delta_{JL} | \delta_{J',J'+1}) \cos^2 \varepsilon_{J'} + (\delta_{JL} | \delta_{J',J'-1}) \sin^2 \varepsilon_{J'}, \\ \text{Im} (R_{J,J-1}R_J^*) &= \text{Im} (R_{J,J-1}R_J^*) - (1/2)(\delta_{J,J-1} | \delta_{J,J+1}) \sin 2\varepsilon_J, \\ \text{Im} (R_{J,J-1}R_{J,J+1}^*) &= (\delta_{J,J-1} | \delta_{J,J+1}) \cos 2\varepsilon_J. \end{cases}$$

For completeness sake we list in Table II for $m' = -1$ the coefficients of $\sin \theta$ which appear in the expansion (14).

TABLE II. — Coefficients of the expansion in Legendre polynomials of the product $\langle \sin \theta \rangle^{-1} [4\pi/(2l+1)]^{1/2} [4\pi/(2l'+1)]^{1/2} Y_{lm} Y_{l'm'}^* \exp [-iM\varphi]$ for $m' = -1$ ($M = m - m'$). For $m' = 1$ all the terms change sign.

lm	$l'm'$	$l'=1, m'=-1$	$l'=2, m'=-1$	$l'=3, m'=-1$
$l=0, m=0$	$(\sqrt{2}/2) P_0$	$(\sqrt{6}/2) P_1$	$(\sqrt{3}/6) (P_0+5P_2)$	
$l=1, m=0$	$(\sqrt{2}/2) P_1$	$(\sqrt{6}/6) (P_0+2P_2)$	$(\sqrt{3}/2) (P_1+P_3)$	
$l=2, m=0$	$(\sqrt{2}/2) P_2$	$(\sqrt{6}/10)(2P_1+3P_3)$	$(\sqrt{3}/42) (7P_0+17P_2+18P_4)$	
$l=3, m=0$	$(\sqrt{2}/2) P_3$	$(\sqrt{6}/14)(3P_2+4P_4)$	$(\sqrt{3}/126) (27P_1+49P_3+50P_5)$	
$l=2, m=2$	$(\sqrt{3}/6) (P_0-P_2)$	$(3/10) (P_1-P_3)$	$(3\sqrt{2}/14) (P_2-P_4)$	
$l=3, m=2$	$(\sqrt{15}/10)(P_1-P_3)$	$(\sqrt{5}/70)(7P_0+5P_2-12P_4)$	$(\sqrt{10}/210)(18P_1+7P_3-25P_5)$	

Our results have been checked for the proton-proton system in the limit of no mixing and without Coulomb effects against those derived by HULL and SALPERSTEIN⁽¹³⁾, and with the result of STAPP by including the coupling of the $J=2$ state⁽¹⁴⁾.

⁽¹³⁾ M. H. HULL jr. and A. M. SALPERSTEIN: *Phys. Rev.*, **96**, 806 (1954). See Eqs. (3), (4) and (5).

⁽¹⁴⁾ The $\cos \theta$ -term of Feshbach and Lomon [Eq. (49) of ref. (11)] has not been

2. Analytical approach to the $L_{\max} = 2$ partial wave approximation.

Limiting the expansion (11) to $L_{\max} = 2$ and considering only the coupling between the states 3S_1 and 3D_1 , the neutron-proton differential cross-section can be written in the following form,

$$(18) \quad k^2\sigma(\theta) = (1/4)k^2\sigma^{(1)}(\theta) + \sum_{n=0}^4 A_n^{(0)} P_n(\cos \theta),$$

where $\sigma^{(1)}(\theta)$ is the scattering cross-section for isotopic spin $T=1$ and the $A_n^{(0)}$'s are the expansion coefficients for the isotopic spin $T=0$ cross-section ($A_n = A_n^{(0)} + A_n^{(1)}$). The cross-section $\sigma^{(1)}(\theta)$ is nothing but the nuclear part of the proton-proton angular distribution⁽⁹⁾ with Coulomb phase shifts zero. In our approximation $\sigma^{(1)}(\theta)$ depends only on the singlet S and D and triplet P phase shifts. The $A_n^{(0)}$'s ($L_{\max} = 2$) are given by the following expressions

$$(19a) \quad 4A_0^{(0)} = 3 \sin^2(\delta_{10}) + 3 \sin^2(\delta_{12}) + 3 \sin^2(K_1) + 5 \sin^2(\delta_{22}) + 7 \sin^2(\delta_{32}),$$

$$(19b) \quad 4A_1^{(0)} = 6(K_0, K_1) + 12(K_1, K_2) + 9(\delta_{11}, \delta_{22}) + \\ + (\sqrt{2} \cos \varepsilon_1 - \sin \varepsilon_1)^2 [2(\delta_{12}, \delta_{10}) + 3(\delta_{10}, \delta_{11})] + \\ + (\cos \varepsilon_1 + \sqrt{2} \sin \varepsilon_1)^2 [2(\delta_{10}, \delta_{01}) + 3(\delta_{12}, \delta_{11})] + \\ + 10(\cos \varepsilon_1 + \sin \varepsilon_1/\sqrt{50})^2 (\delta_{10}, \delta_{21}) + \\ + 10(-\sin \varepsilon_1 + \cos \varepsilon_1/\sqrt{50})^2 (\delta_{12}, \delta_{21}) + \\ + 3(\delta_{21}, \delta_{22}) + (84/5)(\delta_{21}, \delta_{32}),$$

$$(19c) \quad 4A_2^{(0)} = 6 \sin^2(K_1) + (25/4) \sin^2(\delta_{22}) + (40/7)(\delta_{32}, \delta_{22}) + (48/7) \sin^2(\delta_{32}) + \\ + 3(\sin 2\varepsilon_1 + \sin^2 \varepsilon_1/\sqrt{2})^2 \sin^2(\delta_{10}) + \\ + 3(-\sin 2\varepsilon_1 + \cos^2 \varepsilon_1/\sqrt{2})^2 \sin^2(\delta_{12}) + \\ + 10(\sin \varepsilon_1 + \cos \varepsilon_1/\sqrt{2})(\delta_{22}, \delta_{12}) + \\ + 10(\cos \varepsilon_1 - \sin \varepsilon_1/\sqrt{2})(\delta_{22}, \delta_{20}) + \\ + 6(\cos 2\varepsilon_1 - \sin \varepsilon_1 \cos \varepsilon_1/\sqrt{2})^2 (\delta_{12}, \delta_{10}) + \\ + 14(\cos \varepsilon_1 + \sqrt{2} \sin \varepsilon_1/7)^2 (\delta_{32}, \delta_{10}) + \\ + 14(\sin \varepsilon_1 - \sqrt{2} \cos \varepsilon_1/7)^2 (\delta_{32}, \delta_{12}),$$

found to agree with our one, which follows from the combination $B_1 = (3/2)B_3 + (15/8)B_2$, reduced according to their approximation (S and P waves with 3P_2 - 3F_2 coupling). On the other hand, in the limit of zero coupling the expression of Feshbach and Lomon does not reproduce the result given by several Authors.

$$(19d) \quad 4A_3^{(0)} = 6(\delta_{01}, \delta_{32}) + 12(\delta_{11}, \delta_{32}) + 18(K_1, K_2) + 12(\delta_{21}, \delta_{22}) + \\ + (36/5)(\delta_{21}, \delta_{32}) + (54/5)(\delta_{10}, \delta_{21}) \sin^2 \varepsilon_1 + \\ + (54/5)(\delta_{12}, \delta_{21}) \cos^2 \varepsilon_1,$$

$$(19e) \quad 4A_4^{(0)} = (40/7) \sin^2 (\delta_{22}) + (100/7)(\delta_{32}, \delta_{22}) + (22/7) \sin^2 (\delta_{32}) + \\ + (108/7)(\delta_{10}, \delta_{32}) \sin^2 \varepsilon_1 + (108/7)(\delta_{12}, \delta_{32}) \cos^2 \varepsilon_1.$$

Also if we assume, in the spirit of the charge independence hypothesis, the singlet S and D and triplet P phase shifts as known from the proton-proton scattering, no definite answer can be obtained from the equations $A_n = \mathcal{A}_n$, where the \mathcal{A}_n 's are the least squares expansion coefficients directly obtained from the experimental data, since the number of unknowns (six) is larger than the number of the experimental coefficients (five). It is therefore necessary to simplify the relations (19) by neglecting the interaction in some states. As a first step we shall neglect both the singlet D state and the ${}^3S_1 - {}^3D_1$ coupling, assuming the three triplet D phase shifts all equal ($\delta_{21} = \delta_{22} = \delta_{23} = {}^3K_2$). In this approximation, which will be called as alternative L of the $L \leq 2$ partial wave analysis, the A_n 's, obtained by adding the distribution coefficients for the two isotopic spin states, are given by the following relations ⁽¹⁵⁾

$$(20a) \quad 4A_0 = (21/2) + z_0 + z_1 - (3/2)(c_{10} + c_1 + 5C_2),$$

$$(20b) \quad 4A_1 = (3/2)(1 + 2z_1) - z_1(c_{10} + 2C_2) + z_2(s_0 + 2S_2) - \\ - (3/2)(c_1 + c_0) + (3/2)(s_0s_1 + c_0c_1),$$

$$(20c) \quad 4A_2 = (297/14) + z_3 - (3/2)(5c_{10} + 2c_1) - (105/14)C_2 + \\ + (15/2)(s_{10}S_2 + c_{10}C_2),$$

$$(20d) \quad 4A_3 = 3z_1(1 - C_2) + 3z_2S_2,$$

$$(20e) \quad 4A_4 = (135/7)(1 - C_2),$$

where $S_2 = \sin 2({}^3K_2)$ and $C_2 = \cos 2({}^3K_2)$. From Eqs. (20) it is found

$$(21a) \quad \cos 2\delta_{10}^\pm = p(K_0) \pm [p^2(K_0) - q(K_0)]^{\frac{1}{2}},$$

⁽¹⁵⁾ The coefficients $A_n^{(1)}$ are given in ref. ⁽⁹⁾ and they are: $A_0^{(1)} = z_0 + z_1 + 5 \sin^2 (K_2)$, $A_2^{(1)} = z_3 + (50/7) \sin^2 (K_2) + 10(K_0, K_2)$, $A_4^{(1)} = (90/7) \sin^2 (K_2)$.

$$(21b) \quad \cos 2K_1^\pm = r(K_0) - \cos 2\delta_{10}^\pm,$$

$$(21c) \quad \cos 2(^3K_2) = 1 - (28/135)A_4,$$

where

$$(22a) \quad p(K_0) = urt(K_0), \quad q(K_0) = u[t^2(K_0) - v^2],$$

$$(22b) \quad r(K_0) = 2 + (28/27)A_4 + (2/3)(z_0 + z_1 - 4A_0),$$

$$(22c) \quad u = (v^2 + w^2)^{-1}, \quad v = (14/9)A_4 - 3, \quad w = (15/2) \sin 2(^3K_2),$$

$$(22d) \quad t(K_0) = (2/3)(12A_0 - 6A_2 + A_4) - [3 + 2(z_0 + z_1) - z_3].$$

The peculiar feature of the problem exhibited by this procedure is that c_{10} and c_1 depend only on the even experimental coefficients of the n-p angular distribution. Furthermore, since the proton-proton isotropy at high energies implies z_3 negligible, c_{10} and c_1 practically depend on the p-p phase shifts through the combination $z_0 + z_1$ only. It follows that the odd angular distribution coefficients, given by Eqs. (19 *b, d*), responsible for the asymmetry of the n-p cross-section around 90°, are entirely determined by the n-p phase shifts, calculated in terms of the even \mathcal{A}_n 's. Because of the combination $z_0 + z_1$, the dependence of the triplet even (δ_{10} and 3K_2) and the singlet odd (K_1) phase shifts on the p-p singlet S and triplet P ones, implied by the charge independence hypothesis, is ambiguous. This happens mainly because the odd angular coefficients A_1 and A_3 are not very sensitive functions of z_1 and z_2 . Since 3K_2 is small throughout the energy interval ranging from 27 to 260 MeV, A_3 does not contribute strongly to the n-p asymmetry at high energies. The contribution to A_1 of the terms in z_1 and z_2 is smaller than the one of the third term. It follows that the hypothesis of the charge independence is not very critical in this approximation. This circumstance, which will be exemplified in Sect. 4, justifies, at least partially, the contradictory results of previous analyses.

Since, according to Eqs. (21) and (22) only the equations $A_n = \mathcal{A}_n$ with even n can be satisfied, the value of the least squares sum N , calculated in terms of the phase shifts, will be in general larger than the value \mathcal{N} , given by the least squares fit parameters. The simplest refinement of the considered alternative I is to include the interference between the singlet S and D waves, in order to reduce the deviation $\Delta = N - \mathcal{N}$, at the expenses of the odd coefficients only (alternative II). In fact, according to Eqs. (19), this amounts to add the contribution $3(K_1, K_2)$ to A_1 and $(9/2)(K_1, K_2)$ to A_3 , where $4(K_1, K_2) = s_1 s_2 + (1 - c_1)(1 - c_2)$. This alternative II implies that the in-

fluence of the singlet D state is negligibly small on the proton-proton cross-section, which is probably true because of the observed isotropy of the experimental p-p angular distribution for ϑ larger than about 30° .

3. - Discussion on the n-p phaseshift solutions in the $L \leq 2$ partial wave approximation with no coupling.

The mathematical consequence of the physical assumption that the nuclear forces are charge independent, is clearly exhibited by Eqs. (21) and (22): the phase shifts δ_{10} and K_1 can be considered as functions of the singlet S phase shift both through z_0 and the triplet P phase shift combinations z_n ($n = 1, 2, 3$), parametrized as function of K_0 according to the procedure described in ref. (9,16).

Apart from the fourfold ambiguity on the P triplet set, which has been already discussed in ref. (16), the a priori number of 16 sets ($\delta_{10}, K_1, {}^3K_2$), consistent with Eqs. (20), are reduced to four taking into account that \mathcal{A}_2 can be reproduced, using Eq. (20c), provided s_{10} and S_2 have the same sign below about 18 MeV and opposite sign at higher energies. Since the deuteron bound state requires that at zero energy $\delta_{10} = \pi$ and from the effective range theory it follows that $\delta_{10} \simeq \pi/2$ at about $E = 18$ MeV, the only possible choice is δ_{10} positive throughout the energy interval and therefore the condition $s_{10} > 0$ implies $S_2 < 0$ at energies higher than about 18 MeV. It follows that

in the considered approximation 3K_2 must be negative throughout the energy interval, as it is also in principle required by the n-p asymmetry around 90° at high energies. This conclusion would be not valid if the triplet P phase-shift combination z_2

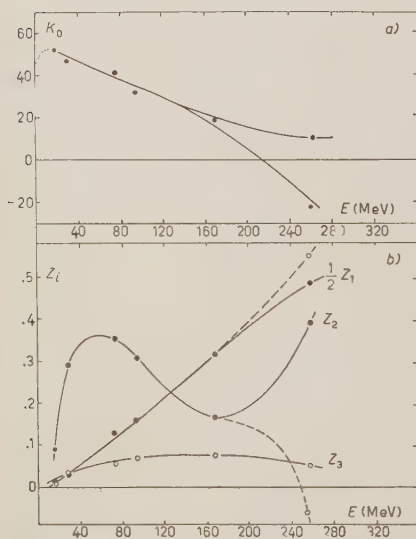


Fig. 1. - (a) Behavior of the singlet S phase shift K_0 versus energy obtained from the analysis of proton-proton scattering cross-sections (16). The two different energy dependences of K_0 above ~ 160 MeV are consistent with the p-p polarization at 170 and 260 MeV. (b) Triplet P phase-shift combinations z_n ($n = 1, 2, 3$) versus energy obtained from p-p scattering data (16). The dotted curves correspond to $K_0 > 0$ up to 260 MeV.

(16) E. CLEMENTEL, C. VILLI and L. JESS: *Nuovo Cimento*, **5**, 907 (1957).

were negative. As far as the proton-proton experimental data are trustworthy, the possibility for z_2 to be negative at low energies is excluded (Fig. 1).

The remaining four solutions are finally reduced to two by neglecting those labelled with (-) in Eqs. (21). According to the available experimental data, these solutions do not exist at energies lower than about 170 MeV. They suddenly appear above this energy, are well behaved up to 260 MeV and then seem to disappear again. If one restricts the analysis to the energy interval 170–260 MeV, these solutions will appear acceptable, but nevertheless they must be rejected on continuity grounds. The two distinct sets of n-p phase shifts (δ_{10} , K_1 , 3K_2), which are left, are characterized by (a) $s_1 > 0$, (b) $s_1 < 0$. Let us first consider the energy dependence of K_0 shown by the lower curve in Fig. 1a. Then, in the energy interval between 27 and 260 MeV, the solution (a) gives an asymmetry ratio varying between 0.43 and 1.22, whereas the solution (b) gives $1.23 > \rho > 0.80$. It is clear therefore that solution (a) is in principle acceptable at 260 MeV, but it must be rejected at lower energies because predicting a predominant forward scattering, which has never been observed. The solution (b) is satisfactory at low energies, but is unacceptable at 260 MeV, because conflicting with the observed backwards scattering. Since, at least up to 260 MeV, the phaseshift $|K_1|$ turns out to be a monotonically increasing function of the energy, it has to be chosen either always positive or always negative. It follows that in the alternative I it is impossible to fit the n-p scattering data at 260 MeV preserving both the charge independence and the continuity of the phase shifts versus energy. This conclusion is not altered if we consider the energy behavior of K_0 above ~ 160 MeV shown by the upper curve in Fig. 1a. In this case the odd coefficient A_3 is responsible for the wrong asymmetry shown by the calculated cross-section. The choice ${}^3K_2 > 0$ at 260 MeV would sensibly improve the fit, but the continuity would be destroyed. In the former case the failure of the considered approximation is due essentially to the negative value of K_0 at 260 MeV, which implies $A_1 > 0$ if the singlet P state is repulsive. The elimination of the calculated predominant forward scattering at 260 MeV would require attraction in the singlet P state. Again, this is conflicting with the continuity at lower energies.

4. – Discussion on the neutron-proton scattering at 260 MeV.

We shall now give quantitative support to the conclusions of Sect. 3. The solutions obtained by THALER and BENGSTON (1) at 260 MeV belong to those which we have labelled with (—); as we have already seen, they must be rejected. The condition $z_2 < 0$ (which is not required to reproduce the dip of the p-p differential cross-section when $K_0 < 0$), leads to a fit of the n-p dif-

ferential cross-section at 260 MeV at the expenses of the continuity towards lower energies. Starting from the solutions quoted in ref. (1), i.e. $K_0 = 30.9^\circ$, $K_1 = 13.3^\circ$, $\delta_{10} = 50.8^\circ$ and ${}^3K_2 = 9.9^\circ$, we have determined z_2 from the condition $N(z_2) = \text{minimum}$. It is found $z_2 = -1.2$ and $N = 29.1$, whereas $\mathcal{N} = 27.7$. Since $\Delta = 1.4$, this solution with the adjusted negative value for z_2 fits well the cross-section, but it is not supported by the p-p scattering data (Fig. 1).

TABLE III. - Triplet P phase shifts (in degrees) at 260 MeV ($K_0 = -22^\circ$; $p_{\text{exp}}(45^\circ) = 0.337$).

Set	δ_{01}	δ_{11}	δ_{12}	p (45°)
A	17.5	-25.0	15.5	0.338
B	-11.0	31.5	-8.5	-0.235
C	81.0	0.5	3.0	0.152
D	-74.0	6.5	3.5	0.179

From the measured differential cross-section at 260 MeV (17) it is found $\mathcal{A}_0 = 0.915$, $\mathcal{A}_1 = -0.148$, $\mathcal{A}_2 = 0.929$, $\mathcal{A}_3 = -0.082$ and $\mathcal{A}_4 = 0.343$. Using Eqs. (21) one has $|K_1| = 53.3^\circ$, $\delta_{10} = 6.9^\circ$, ${}^3K_2 = -10.9^\circ$. These solutions are not altered if we assume $K_0 = -22.0^\circ$ or $K_0 = 11.0^\circ$ (Fig. 1), since the phase shifts depend only on the combination $z_0 + z_1$, which in both cases is equal to 1.122. Practically the same value ($z_0 = 0.281$, $z_1 = 0.865$) is also given by Thaler and Bengtson's analysis. It is therefore clear that in the considered approximation the n-p phase shifts do not depend strongly on the n-p ones because of the existence of the plateau on the p-p differential cross-section. This circumstance has been already pointed out in Sect. 2.

TABLE IV. - Triplet P phaseshifts (in degrees) at 260 MeV ($K_0 = 11^\circ$; $p_{\text{exp}}(45^\circ) = 0.337$).

Set	δ_{01}	δ_{11}	δ_{21}	p (45°)
A	16.5	-32.0	11.5	0.339
B	-19.0	30.0	-14.0	-0.388
C	78.0	-14.5	4.0	0.210
D	-79.5	12.0	-6.0	-0.320

The solutions found at 260 MeV by KLEIN (2) are $K_0 = -43^\circ$, $K_1 = 49^\circ$, $\delta_{10} = -22^\circ$, ${}^3K_2 = -2^\circ$, $\delta_{01} = -50^\circ$, $\delta_{11} = 5^\circ$ and $\delta_{21} = 8.6^\circ$. The values of the triplet P phase shifts are close to those of the set D associated to $K_0 = -43^\circ$

(17) E. KELLY, G. LEITH, E. SEGRÈ and C. WIEGAND: *Phys. Rev.*, **79**, 96 (1950).

(Table V). The different values of K_0 found by Klein compared with those following from our analysis ($K_0 = -22.0^\circ$ or $K_0 = 11.0^\circ$) is of no importance as far as the fit of the n-p differential cross-section is concerned, since again the combination $z_0 + z_1$ has in both cases approximately the same value. The strong negative value of δ_{10} , given by Klein, in no way is found as a solution of the n-p phase shift equations at 260 MeV. Since the zero energy value of δ_{10} is π , a negative value for this phase shift obviously implies that there exists a scattering energy at which the triplet S phase shift is zero. According to the available experimental data it is excluded in our approximation (identical to the one used by Klein) that this can possibly occur. Therefore, if we want to preserve the continuity of δ_{10} throughout the energy interval, we must reject Klein's solution. Apart from this, Klein's solution has also to be rejected because it gives a very poor fit to the data. In fact, it is found $N = 69.9$ and the deviation from the least squares fit has the unacceptable value $1 = 39.9$.

TABLE V. — Triplet P phaseshifts (in degrees) at 260 MeV ($K_0 = -43^\circ$).

Set	δ_{01}	δ_{11}	δ_{21}
<i>A</i>	18.5	-17.5	13.2
<i>B</i>	-10.0	26.0	-5.2
<i>C</i>	52.7	-2.2	2.5
<i>D</i>	-44.2	10.7	6.5

The possibility for the phase shift δ_{10} to be negative at 260 MeV has been investigated in detail. The singlet S and triplet P phase shifts have been kept fixed, and we have searched for a solution at 260 MeV corresponding to $s_1 < 0$, continuously linked to lower energy solutions having δ_{10} positive. The negative value of K_0 at 260 MeV has been considered. The new solution was found to be $K_0 = -22.0^\circ$, $K_1 = 22.0^\circ$, $\delta_{10} = -16.6^\circ$ and ${}^3K_2 = -10.1^\circ$. According to this solution the phase shift δ_{10} should become zero at about 220 MeV, i.e. at about the same energy at which K_0 changes sign. The continuity is thus preserved but the new solution is still unacceptable because it gives $N = 74.2$ and the deviation from the least squares fit is even larger than that implied by Klein's solution.

The discouraging features of the phase shift fitting mechanism implied by the alternative I at 260 MeV are not overcome by the introduction of the singlet D wave. To understand how the phase shift K_2 works in fitting the n-p data, we assume still valid all the arguments which have allowed us to confine the discussion on the two sets (a) $s_1 > 0$ and (b) $s_1 < 0$, each of which is consistent with the four sets of P triplet phase shifts. When $K_2 = 0$, the n-p cross-section calculated at high energies shows an insufficient asymmetry

around 90° , because the odd coefficients are slowly varying functions of the neutron energy. Since the experimental data seem to require negative odd coefficients, the function (K_1, K_2) , defined in Sect. 2, must be negative and therefore s_1 and s_2 must have opposite sign. We recall that, according to previous considerations, the attraction in the singlet P state is incompatible with the n-p data at low energies, where the singlet D state interaction is certainly absent or negligibly small. We are led therefore to assume $K_1 < 0$ and $K_2 > 0$ throughout the energy interval. This conclusion is also in agreement with the analysis of p-p data at 170 MeV ⁽¹⁶⁾. Since the effect of the attraction in the singlet D state is to increase the odd angular coefficients of the n-p differential cross-section, we must conclude that K_2 is small up to scattering energies at which the n-p measured cross-section is nearly symmetric around 90° , i.e. up to about 90 MeV.

An attempt to fit the 260 MeV data assuming $K_1 = -54.0^\circ$ and adjusting the odd coefficients by varying K_2 has proved unsuccessful. The criterion adopted was to vary $N(K_2)$ and to determine K_2 from the condition $N = \text{minimum}$. The value of K_2 found in this way is too large (20°) and the fit very poor ($N = 85.2$). This negative result can be easily understood since at the limit of $K_2 = 0$ the odd coefficients are $A_1 = 0.377$ and $A_3 = -0.058$, and the elimination of the predominant forward scattering requires a strong attractive interaction in the singlet D state. Being $A_1 > |A_3|$ when $K_2 = 0$, it follows that when A_1 approaches \mathcal{A}_1 , the other odd coefficient is distorted and the n-p cross-section is not even approximately reproduced. The choice $K_0 = 11^\circ$ does not improve sensibly this situation.

5. - Analysis of the neutron-proton scattering from 27 to 215 MeV.

The discussion of Sects. 3 and 4 is valid in the limit of zero coupling between the triplet S and D states. For low energies the very effect of the coupling is to modify the strength of the interaction in the triplet S state but not its attractive nature. For higher energies the predictions on the triplet D state, following from the preceding discussion, are expected to be substantially altered by the coupling. It is, however, believed that a general picture of the phase

shift behavior from zero energy up to 215 MeV in the alternative II of the $L \leq 2$ approximation may help for a better understanding of the results obtained including the coupling and higher order waves.

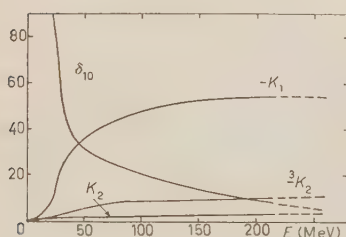


Fig. 2. - Behavior of the phase shifts K_1 , K_2 , 3K_2 , δ_{10} versus neutron energy. The phase shifts are given in degrees.

The results of the analysis are given in Table VI and in Fig. 2. The calculated cross-sections are compared with the experimental data ⁽¹⁸⁾ in Fig. 3.

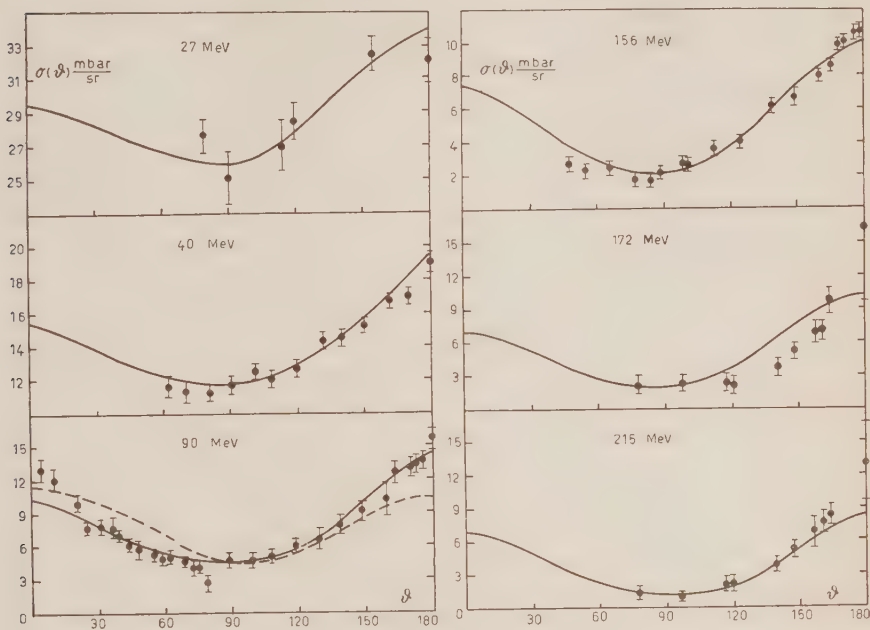


Fig. 3. — Theoretical n-p differential cross-sections (solid lines), calculated with the phaseshifts listed in Table VI, compared with the experimental data at: 27 MeV [J. E. BROLLEY jr., J. H. COON and J. L. FOWLER: *Phys. Rev.*, **82**, 190 (1951)], 40 and 90 MeV [J. HADLY, E. L. KELLY, C. E. LEITH, E. SEGRÈ, C. WIEGAND and H. F. YORK: *Phys. Rev.*, **75**, 351 (1949); R. WALLACE: *Phys. Rev.*, **81**, 139 (1951); O. CHAMBERLAIN and J. W. EASLY: *Phys. Rev.*, **94**, 208 (1954)], 156 MeV [T. C. RANDLE, A. E. TAYLOR and E. WOOD: *Proc. Roy. Soc.*, **213**, 392 (1952)], 172 and 215 MeV [G. R. MOTT, G. L. GUERSNEY and K. B. NELSON: *Phys. Rev.*, **88**, 15 (1952)]. The dotted curve at 90 MeV has been calculated with the phase shifts given in Table VII.

The differential cross-section at 27, 156 and 172 MeV is not well defined around 90° and the least squares coefficients are not continuously linked with those at 40 and 90 MeV. At 27 MeV the coefficient \mathcal{A}_4 is negative and therefore incompatible with Eq. (21d). At 156 and 172 MeV the least squares fit of the differential cross-section turns out to be nearly symmetric around 90°: \mathcal{A}_4 and

⁽¹⁸⁾ For reader's convenience we refer to: L. BERETTA, C. VILLI and F. FERRARI: *Suppl. Nuovo Cimento*, **12**, 499 (1954), where all the experimental data used in our analysis can be found collected. The original papers are listed in the caption of Fig. 3.

TABLE VI. - Phase shifts (in degrees) K_0 , K_1 , K_2 , 3K_2 , δ_{10} , δ_{01} , δ_{11} and δ_{21} at 27, 40, 90, 156, 172 and 215 MeV. The four sets on the right follow from fourfold ambiguity on the triplet P state. Only the sets A and D fit the proton-proton polarization at 170 MeV (16).

$E(\text{MeV})$	K_0	K_1	K_2	3K_2	δ_{10}	set	δ_{01}	δ_{11}	δ_{21}
27	49.0	-15.0	0	-0.9	78	A	10.0	-4.5	4.0
						B	-7.0	7.5	-1.0
						C	13.5	-2.0	2.0
						D	-9.5	6.0	2.0
40	45.5	-32.8	1.3	-5.1	35.0	A	14.0	-6.0	6.0
						B	-8.0	11.5	-1.5
						C	21.5	-3.0	2.5
						D	-16.0	8.0	2.5
90	34.0	-44.1	2.2	-8.2	21.7	A	20.0	-12.0	7.0
						B	-17.0	16.0	-2.5
						C	31.0	-6.5	2.5
						D	-24.0	12.0	2.5
155	21.0	-50.0	3.1	-9.2	14.0	A	21.5	-19.0	9.0
						B	-18.0	22.5	-6.5
						C	45.5	-9.0	2.5
						D	-42.0	13.0	2.5
172	13.0	-51.2	3.3	-9.5	13.0	A	22.0	-20.5	9.5
						B	-18.5	23.0	-7.0
						C	50.5	-9.5	2.5
						D	-46.0	15.0	3.0
215	14.0	-53.0	4.2	-10.1	9.5	A	23.0	-26.0	11.0
						B	-21.5	27.5	-9.0
						C	59.5	-12.5	3.5
						D	-58.5	13.5	-2.5
	0	-53.0	4.2	-10.1	9.5	A	21.0	-24.0	12.5
						B	-16.5	28.5	-9.5
						C	62.5	-7.5	2.5
						D	-58.0	12.0	3.0

\mathcal{A}_3 are too large at 156 MeV and too small at 172 MeV. Although the analytical procedure, outlined in Sect. 2, is free from the uncertainties due to the erratic behavior of the experimental odd angular coefficients, the analysis at 27, 156 and 172 MeV has been carried out by varying the least squares sum $N(K_1, \delta_{10}, {}^3K_2)$ in the (c_1, c_{10}, C_2) -space. According to the discussion in Sects. 3 and 4, the

restrictive conditions $s_1 < 0$ and $s_2 < 0$ have been taken into account. At 90 MeV, where the cross-section has been measured at 28 angles, no minimum of N exists for $K_2 < 0$. This is also true at 40, 156 and 172 MeV.

6. - Effect of the 3S_1 - 3D_1 coupling. Analysis of the 95 MeV polarization data.

The recent measurements ⁽¹⁹⁾ of the neutron-proton polarization at 95 MeV provide the best criterion to decide upon the reliability of the approximations we have used in analysing the scattering data.

Including all the waves up to $L_{\max} = 2$, the coefficients B_n , given by Eqs. (16), become explicitly

$$(23a) \quad 4B_0 = [2(\delta_{01}|\delta_{10}) + 3(\delta_{11}|\delta_{10}) - 2(\delta_{01}|\delta_{12}) - \\ - 3(\delta_{11}|\delta_{12})][\cos 2\varepsilon_1 + (\sqrt{2}/4) \sin 2\varepsilon_1] - \\ - 5(\delta_{21}|\delta_{10})[\cos^2 \varepsilon_1 + (4/5) \sin^2 \varepsilon_1 + (\sqrt{2}/4) \sin 2\varepsilon_1] - \\ - 5(\delta_{21}|\delta_{12})[\sin^2 \varepsilon_1 + (4/5) \cos^2 \varepsilon_1 - (\sqrt{2}/4) \sin 2\varepsilon_1] + \\ + 2(\delta_{01}|\delta_{32}) + 3(\delta_{11}|\delta_{32}) - 5(\delta_{21}|\delta_{22}) + 9(\delta_{21}|\delta_{32}),$$

$$(23b) \quad 4B_1 = 6(\delta_{01}|\delta_{21}) + 9(\delta_{11}|\delta_{21}) - 9(\delta_{10}|\delta_{12})[\cos 2\varepsilon_1 + (\sqrt{2}/4) \sin 2\varepsilon_1] - \\ - 5(\delta_{10}|\delta_{22})[\cos^2 \varepsilon_1 + (\sqrt{2}/4) \sin 2\varepsilon_1 - \sin^2 \varepsilon_1] - \\ - 5(\delta_{12}|\delta_{22})[\sin^2 \varepsilon_1 - (\sqrt{2}/4) \sin 2\varepsilon_1 - \cos^2 \varepsilon_1] + \\ + (\delta_{10}|\delta_{32})[14 \cos^2 \varepsilon_1 + (7\sqrt{2}/2) \sin 2\varepsilon_1 + 13 \sin^2 \varepsilon_1] + \\ + (\delta_{12}|\delta_{32})[14 \sin^2 \varepsilon_1 - (7\sqrt{2}/2) \sin 2\varepsilon_1 + 13 \cos^2 \varepsilon_1] + 15(\delta_{22}|\delta_{32}),$$

$$(23c) \quad 4B_2 = 18[(\delta_{10}|\delta_{21}) \sin^2 \varepsilon_1 + (\delta_{12}|\delta_{21}) \cos^2 \varepsilon_1] + 10(\delta_{01}|\delta_{32}) + \\ + 15(\delta_{11}|\delta_{32}) - 10(\delta_{21}|\delta_{22}) + 3(\delta_{21}|\delta_{32}),$$

$$(23d) \quad 4B_3 = 27[(\delta_{10}|\delta_{32}) \sin^2 \varepsilon_1 + (\delta_{12}|\delta_{32}) \cos^2 \varepsilon_1] + 15(\delta_{22}|\delta_{32}),$$

while B_4 and B_5 are zero.

The least squares fit of the experimental results expanded according to Eq. (15) gives $\mathcal{B}_0 = 0.164 \pm 0.017$, $\mathcal{B}_1 = 0.333 \pm 0.031$ and $\mathcal{B}_2 = 0.055 \pm 0.038$. The theoretical values for B_n have been calculated using the P triplet phase

⁽¹⁹⁾ G. H. STAFFORD, C. WHITHEAD and P. HILLMAN: unpublished. We thank the Authors for having informed us of their results prior to publication.

shifts given in Table III of ref. (16) and interpolating at 95 MeV the solutions listed in Table VI. The results turned out to be unsatisfactory for any one of the four P triplet sets. This failure of the alternative I to reproduce the polarization data at 95 MeV means simply that the effect of the ${}^3S_1 - {}^3D_1$ coupling is here much more critical than in fitting the angular distribution.

The possibility to fit the polarization data at 95 MeV with $\mathcal{B}_3 = 0$ suggests that the two uncoupled D waves are negligibly small. We have used therefore Eqs. (23) with $\delta_{22} = \delta_{32} = 0$. In this approximation, for a given value of ϵ_1 the coefficient \mathcal{B}_1 fixes a correlation between the two phase shifts δ_{10} and δ_{12} , being the triplet P phase shifts known from the analysis of p-p scattering data. In this way one of the two phase shifts, let us say δ_{12} is parametrized as a function of ϵ_1 and δ_{10} . By fitting the other two parameters \mathcal{B}_0 and \mathcal{B}_2 the correct pair $(\epsilon_1, \delta_{10})$, and consequently δ_{12} , can be fixed. We have applied this procedure for the set A of the triplet P solutions at 95 MeV, and the results are summarized in Table VII.

TABLE VII. — Phase-shift solutions for n-p scattering at 93 ± 3 MeV, derived from scattering and polarization data.

K_0	K_1	K_2	δ_{01}	δ_{11}	δ_{21}	δ_{10}	δ_{12}	ϵ_1
32	-25	2	20	-12	7	50	-10	19

The singlet phase shifts K_1 and K_2 have been evaluated by fitting the scattering data at 90 MeV. The theoretical values of the expansion coefficients, following from the phase shifts listed in Table VII, are $B_0 = 0.158$, $B_1 = 0.333$ and $B_2 = 0.055$ for the polarization, while for the differential cross-section we obtain $A_0 = 0.741$, $A_2 = 0.152$, $A_2 = 0.470$, $A_3 = -0.078$ and $A_4 = 0.004$. The theoretical differential cross-section is given in Fig. 3. The same procedure applied to the set D ($K_0 = 32$, $\delta_{01} = -26$, $\delta_{11} = 12$, $\delta_{21} = 2.5$) gave the best, but nevertheless poor, fit to the polarization data with the choice $\delta_{10} = 19$, $\delta_{12} = -29.7$ and $\epsilon_1 = 15$ ($B_0 = 0.123$, $B_1 = 0.333$ and $B_2 = 0.067$). The better agreement ($B_0 = 0.191$, $B_1 = 0.372$, $B_2 = 0.059$) obtained with a similar P set by PHILLIPS (20), who found the other phase shifts very close to those given in Table VI, is due to the higher value of δ_{21} .

It is clear from this analysis that polarization and scattering data at (93 ± 3) MeV are incompatible. In fact, while the polarization results seem to require $\delta_{22} = \delta_{32} = 0$ ($\mathcal{B}_3 = 0$), a better fit of the differential cross-section

(20) R. J. N. PHILLIPS: *Proceedings of the Rochester Conference* (1956), p. II-22.

needs at least these two waves to be taken into account, otherwise the paradoxical situation arises, that a «lower» approximation (alternative I) gives a better fit than a «higher» one, as it is shown in Fig. 3. In any case, the only conclusion we can draw from this circumstance is that, as far as the fit of the differential cross-section is concerned, the effect of all three D phase shifts, although assumed equal, is more important than the combined effect of the coupled one and of the coupling. This probably justifies the success obtained using the alternative I from the very beginning of this kind of investigations.

* * *

We are pleased to thank Prof. V. PAVIČIĆ, Director of the Nuclear Science Institute of Belgrade, for several facilities in using the Electronic Computer of the Institute, and Dr. L. BERETTA and Dr. L. JESS for computational assistance and for very valuable help in check calculations.

RIASSUNTO

Espressioni generali per la sezione d'urto differenziale elastica nucleone-nucleone e per la polarizzazione sono ricavate dalla matrice di transizione, valutata sino al momento angolare $L = 3$. La validità dell'approssimazione $L \leq 2$ è studiata in dettaglio, tenendo conto sia della indipendenza dalla carica delle forze nucleari sia della continuità delle soluzioni in funzione dell'energia del neutrone. Si dimostra che, a causa del cambiamento di segno della fase del singoletto S , la sezione d'urto differenziale $n-p$ non può essere riprodotta nell'approssimazione più bassa senza distruggere l'indipendenza dalla carica o la continuità delle soluzioni nell'intervallo $27 \div 260$ MeV, o entrambe. Si dimostra anche che le soluzioni $n-p$ alle alte energie non possono essere raccordate con continuità con quelle alle basse energie se si assume la fase del singoletto S positiva in tutto l'intervallo. L'effetto dell'accoppiamento 3S_1 - 3D_1 è discusso in dettaglio a 95 MeV.

The Production of Heavy Mesons and Hyperons by π^- -Mesons of 4.5 GeV/c.

B. P. EDWARDS, A. ENGLER (*), M. W. FRIEDLANDER (+) and A. A. KAMAL

H. H. Wills Physical Laboratory - University of Bristol

(ricevuto il 13 Febbraio 1957)

Summary. — A systematic investigation has been carried out, using nuclear photographic emulsions, into the production of heavy unstable particles by π^- -mesons of 4.5 GeV/c. From 2854 stars, 4 hyperons and 4 heavy mesons were found which had velocities of less than $0.7c$, and which satisfied certain geometrical selection criteria. One hyperon produces a secondary π -meson which comes to rest in the emulsion stack. The mass of this hyperon, shown to be negatively charged by the nuclear capture of its secondary particle, is $(2352 \pm 5) m_e$.

1. — Introduction.

In high energy collisions between π -mesons and nuclei or nucleons, heavy mesons and hyperons may be produced. The study of the fundamental meson-nucleon interaction is best performed with expansion, diffusion or bubble chambers; in photographic emulsion, most of the interactions occur in complex nuclei and the observed phenomena depend strongly on secondary interactions and scattering of the particles on their way out of the nuclei in which they were produced. A systematic investigation into the nature and frequency of production of the strange particles in emulsion is still of use, since the results may be correlated with those obtained from single nucleon collisions, and may further be used in connection with other experiments for which the present research is almost entirely confined to the emulsion method. It was in this latter connection that the present investigation was started. An

(*) Now at The University of Rochester, N. Y.

(+) Now at Washington University, St. Louis, Mo.

examination of the nuclear disintegrations produced by cosmic-ray particles having energies in the range $10^{12} \div 10^{13}$ eV indicated that as large a fraction as one quarter of the shower particles could be heavy mesons, hyperons or anti-nucleons. (BRISBOUT *et al.* (1)). If this should be correct, then one might expect secondary nuclear disintegrations produced by these shower particles to show an anomalously high number of heavy mesons and hyperons emerging from them, since it is expected that these particles will most probably emerge or convert, the one into the other, in collisions. The shower particles most amenable to an investigation of this type are those in the outer cores of the jets, where the average energy of the particles is $5 \div 10$ GeV; particles of these energies may be sufficiently slowed down by interacting that they will come to rest within the emulsion stack and will then be well identified.

The yield of heavy mesons and hyperons from these secondary stars must be compared with that from stars produced by π -mesons; any difference in the frequency of emerging heavy mesons and hyperons may then be attributed to the presence of strange particles amongst the jets' secondaries.

Accordingly, suitable tracks were selected from stars produced in emulsions exposed to the 4.5 GeV/c π^- -meson beam at Berkeley. These tracks were then followed and the particles which had produced them were identified. From 2854 stars, 950 tracks were followed, and 4 hyperons and 4 positive heavy mesons found. In addition, 2 hyperfragments were found during the scanning for stars, one heavy meson was found in the more detailed examination of parent stars of particles found in the systematic search, and one hyperon was found in following out tracks, but these cannot be included in some of the calculations, as they did not lie within the strict selection criteria. Since all the hyperons were found in a manner unbiased as regards their lifetime or appearance at decay, an estimate of their mean life was made.

Other experiments with which the present results may be compared, are those of DAHANAYAKE *et al.* (2) who performed an experiment substantially the same as this but using a random selection of cosmic-ray produced stars,

(1) F. BRISBOUT, C. DAHANAYAKE, A. ENGLER, Y. FUJIMOTO and D. H. PERKINS: *Phil. Mag.*, **1**, 605 (1956).

(2) C. DAHANAYAKE, P. FRANCOIS, Y. FUJIMOTO, P. IREDALE, C. J. WADDINGTON and M. YASIN: *Nuovo Cimento*, **1**, 888 (1955).

(3) M. SCHEIN, D. M. HASKIN and R. G. GLASSER: *Nuovo Cimento*, **3**, 131 (1956).

(4) W. B. FOWLER, R. P. SHUTT, A. M. THORNDIKE and W. L. WHITEMORE: *Phys. Rev.*, **90**, 1126 (1953); **91**, 1287 (1953); **94**, 861 (1954).

(5) W. WALKER and W. SHEPARD: *Phys. Rev.*, **101**, 1810 (1954).

(6) H. BLUMENFELD, E. T. BOOTH, L. M. LEDERMAN and W. CHINOWSKY: *Phys. Rev.*, **102**, 1184 (1956).

(7) R. BUDDE, M. CHRETIEN, J. LEITNER, N. P. SAMIOS, M. SCHWARTZ and J. STEINBERGER: *Phys. Rev.*, **103**, 1827 (1956).

(8) W. B. FOWLER: *Proceedings of the 6-th Rochester Conference* (1956), p. VI-27.

and SCHEIN, HASKIN and GLASSER⁽³⁾ who also exposed their emulsion to the Berkeley beams. Experiments in hydrogen have been performed at Brookhaven by FOWLER *et al.*⁽⁴⁾, WALKER and SHEPARD⁽⁵⁾, BLUMENFELD *et al.*⁽⁶⁾, BUDDLE *et al.*⁽⁷⁾, and at Berkeley by FOWLER *et al.*⁽⁸⁾.

The production of the strange particles is discussed, and the production cross section estimated. In one event, a hyperon secondary stops within the stack and an accurate mass value may be calculated; this value is $2352 \pm 5 m_e$.

2. - Experimental procedure.

The stack used consisted of 80 emulsion sheets, each $30 \text{ cm} \times 20 \text{ cm} \times 600 \mu\text{m}$, where the π -meson beam traversed the stack along the longer axis. An unbiased selection of stars was made by scanning along the π -meson tracks, and 203 stars were found in this way. Because this method of finding stars is slow, area scanning was then employed and 2651 more stars found.

Tracks were selected only if they satisfied two criteria: (i) the normalized grain density g^* (as determined from the mean gap length) was ≥ 1.5 , and (ii) the angle of emission from the parent star corresponded to a projected length of at least 5 mm per plate and the range was at least 5 mm. These selection rules and the choice of areas for scanning, ensured that K-mesons of the maximum acceptable energy would be brought to rest within the stack. The solid angle containing all acceptable tracks was 12% of the total solid angle, but since the π -meson beam was very nearly parallel to the plane of the emulsion there is a bias towards accepting tracks at small angles to the direction of the incoming π -mesons.

Having selected the tracks, all those with $g^* \geq 2.5$ were followed to their ends; on those with $1.5 \leq g^* < 2.5$, multiple scattering measurements together with the value of g^* were used to obtain an approximate mass value; the standard deviation in each g^* measurement was about 5%, and in $\bar{\alpha}$ about 15%. If the mass appeared to be significantly less than that of the proton, the track was followed to its end; if the mass appeared to be protonic or greater, the track was followed for at least 5 cm, in which distance a hyperon having a mean life of $1.4 \cdot 10^{-10}$ s would have at least 70% probability for decay.

Scattering measurements in this stack may be considered generally reliable, since it has been well calibrated during an extensive investigation into the effects of spurious scattering, which was shown to be small in this stack (BRISBOUT *et al.*⁽⁹⁾). Ionization measurements have been normalized against tracks of the beam π -mesons.

⁽⁹⁾ F. BRISBOUT, C. DAHANAYAKE, A. ENGLER, P. H. FOWLER and P. B. JONES: *Nuovo Cimento*, **3**, 1400 (1956).

3. - Experimental results.

From 2851 stars examined, 950 tracks which satisfied the selection criteria were followed, and 4 hyperons and 4 heavy mesons found. One of the 4 hyperons and one of the 4 heavy mesons were from the same star and both produced flat tracks; our 8 particles therefore represent 7 events in which at least one charged unstable particle emerged from the disintegration. In addition, one hyperon and one heavy meson were found, but these had tracks of less than 5 mm per plate; two hyperfragments were also found.

Tables I, II and III contain the data relating to these particles. No attempt was made to obtain very accurate mass values from direct measurements on the tracks of the primary particles further than their original identification. Where possible, the K-meson decay modes were identified, and the hyperon decay Q -values calculated.

TABLE I. - *Heavy Mesons.*

Number	Parent Star	Range (mm)	Energy (MeV)	Decay mode	Angle of emission from parent star
1	9 + 1	53.84	105	K_L	48
2	14 + 3	40.80	89	K_L	16
3	21 + 1	14.13	48	$K_{\mu 2}$	170
4	5 + 1	25.52	68	—	7°
5	10 + 2	16.00	52	$K_{\mu 2}$	172

TABLE II. - *Hyperons.*

Number	Parent star	Length (mm)	t 10^{-10}	T 10^{-10} s	Angle of emission (°)	Energy at emission (MeV)	SECONDARY		
							Decay angle (laboratory system)	Length observed (mm)	Q -value (MeV)
1	7 + 1	16.64	1.35	3.55	22.5	115 ± 2	119 ± 1.5	50.45	123 ± 2.5
2	5 + 1	19.50	1.06	7.44	28.7	217 ± 15	36	(steep)	
3	14 + 3	25.30	1.24	6.15	47	253 ± 17	5.5 ± 0.2	65.90	114 ± 8
4	16 + 5	1.91	0.20	1.65	63	63 ± 6	128 ± 2	5.20	107 ± 11
5	15 + 5	2.09	0.17	2.77	87.7	95 ± 6	54 ± 1	28.90	—

K_2 and Y_3 from same star; angle between them 16°.

K_4 and Y_5 from same star; angle between them 30°.

t = observed time of flight.

T = available time of flight.

TABLE III. - *Hyperfragments.*

Number	Parent star	Range (μm)	SECONDARIES		
			Identity	Range (μm)	Total charge
1	10 + 1	31	D, T	1250	} 5 or 6
			P ?	6.3	
			P ?	5.8	
			D, T	34	
			P	732	
2	16 + 1	23	P, D	24	} 3
			P, D, T	534	
			P, D	689	

The proportions of stars and tracks for different star sizes, (counting only the non-shower particles) are shown in Table IV. The distributions for the line and area scans are both shown, and have been normalized, assuming that both methods record *all* stars with $N_h \geq 11$. It is clear that most of the smaller stars were missed in the rapid scanning, but that the number of *tracks*

TABLE IV. - *Star-size distribution.*

N_h	Line Scan 426 stars (%)	Area Scan 2651 stars (%)	Percentage of tracks	
			line	area
0	13.4	0	0	0
1	15.3	0.3	2.5	0
2	6.1	1.3	2.0	0.4
3	9.9	2.4	4.9	1.2
4	6.3	3.2	4.2	2.1
5	5.9	3.7	4.9	3.1
6	5.4	3.2	5.4	3.2
7	5.2	3.3	6.0	3.8
8	4.5	2.9	6.0	3.8
9	3.5	2.7	5.2	4.0
10	2.8	2.4	4.6	4.0
≥ 11	21.9 (*)	21.9 (*)	54.4 (*)	54.4 (*)
		47.3		80.0
		Star efficiency		Track efficiency

(*) Line and area scans normalized on number of stars with $N_h \geq 11$.

missed is small. The figures for the line-scan stars include 223 stars found by CLARKE and MAJOR (private communication) in a stack exposed under similar conditions.

4. - Discussion.

4.1. *Production of charged heavy mesons and hyperons.* - In the systematic search, seven stars contained at least one charged heavy meson or hyperon lying within the geometrical and grain density acceptance limits. These stars come from a sample of 2651 area-scan stars and 203 line-scan stars. Had the scanning been 100% efficient, then 5813 ($= 2651/.473 \pm 203$) stars should have been found in the same area (cf. Table IV); our 8 particles should similarly be increased to (10 ± 3) particles, to allow for flat tracks from the smaller stars, missed in the scanning. The cross-section for star production by 4.5 GeV/c π^- -mesons is ~ 30 mb and therefore a lower limit for the production of «slow» charged K and Y-particles ($\beta < 0.7$) in emulsion nuclei may be estimated as $(10/5813) \cdot 30 \sim 0.05$ mb. An upper limit for the production of «slow» K and Y-particles of about ~ 0.4 mb is obtained by integrating over the whole solid angle (assuming an isotropic distribution in the laboratory system). These estimates assume that the loss of K^\pm -mesons by charge exchange scattering is approximately balanced by the reverse effect and also that the loss of charged hyperons by interaction with nucleons within the target nucleus is small.

Recent results (FOWLER *et al.* (6)), indicate that at these incident energies, the process $\pi + N \rightarrow Y + K + n\pi$ becomes increasingly important as compared to the reaction $\pi + N \rightarrow Y + K$. An analysis of our results in terms of the elementary π -nucleon interaction is therefore almost impossible at present especially as our knowledge of the interaction of K-mesons and hyperons with nuclear matter is still very limited. However our limits for the production cross-section of charged unstable particles do not seem unreasonable, if compared with the results of the Brookhaven groups at lower incident energies.

It might be interesting to compare the production of heavy unstable particles in disintegrations produced by π^- -mesons with those produced by nucleons. In the experiment of DAHANAYAKE *et al.*, most of the incident particles were cosmic ray protons with a mean energy of ~ 10 GeV. The energy available in the center of mass in this case is approximately equal to that in a π -nucleon collision, if the π had an energy of ~ 4.6 GeV. After correcting for geometrical factors, we find that the production of slow strange particles in our experiment is of the same order of magnitude as in the cosmic ray experiment. Exper-

iments of WRIGHT *et al.* ⁽¹⁰⁾ also show that the cross-section for production of heavy unstable particles is of the same order of magnitude for p-p and π^- -p interactions, in contrast with Brookhaven measurements (BERLEY and COLLINS ⁽¹¹⁾) at about half the available center of mass energy, which indicated a large difference between the p-nucleon and π^- -p cross-sections for the production of heavy unstable particles.

In all of the discussion on the production of strange particles we have not mentioned the possibility of the reaction



SCHEIN, HASKIN and GLASSER reported a ratio of $K^+/K^- \sim 1$ from observations on *stopping particles* in an emulsion-stack exposed to the π^- -beam of the Berkeley Machine, but it is not stated what the energies of these particles were, nor how many were found. The area scanning which was used is certainly biased against finding heavy meson decays, as compared to interactions at rest.

No negative K-meson was observed in our experiment. This may be due to the lower probability of the above reaction as compared with that producing a Y-K pair (and at the Bevatron, the positive K-meson beam is many more times as intense as the negative) or to a strong dependence of negative K-meson production upon angle, so that, for example, almost all of them were emitted forwards and would therefore be too fast to fall within the acceptance criteria of this experiment. Moreover, since most of the observed interactions occurred in heavy nuclei (a bias due to the selection of large stars) some of the created negative K-mesons might not have emerged since their interaction cross-section with nuclear matter is almost geometrical.

Summing up, we may say that no satisfactory answer, as regards the production of heavy unstable particles in the elementary π -nucleon interaction may be obtained with production occurring in heavy nuclei and with the available statistics. For comparison with strange particle emission from proton-induced or from jet's secondary stars in emulsion, an additional experiment should be performed with π^+ -mesons. In such an experiment, and in the present one the observed yields are effectively averaged over all the complications a large nucleus can produce and the results are strictly comparable with the jets' secondary stars.

4.2. Lifetime of charged hyperons. — The five hyperons were found by systematically following tracks from stars, without knowing their identities a priori. In each case, the charged secondary was lightly ionizing, and in three cases

⁽¹⁰⁾ R. W. WRIGHT, W. M. POWELL, G. MAENSCHEN and W. B. FOWLER: *Bull. Am. Phys. Soc.*, **1**, 386 (1956).

⁽¹¹⁾ D. BERLEY and G. B. COLLINS: *Bull. Am. Phys. Soc.*, **1**, 320 (1956).

could be identified as a π -meson. A hyperon which decayed in flight to produce a proton and a π^0 -meson as secondaries would only have been detected if the decay was clearly indicated by a sharp deviation in the track accompanied by a significant decrease in grain density. Sharp single scatters were not analyzed as $\Sigma^+ \rightarrow p + \pi^0$ decays; previous attempts (DAHANAYAKE *et al.* ⁽²⁾) have not proved fruitful. The lifetime for the decay $\Sigma^\pm \rightarrow \pi^\pm$ has been calculated for the five events observed. In only one case (Y 1) do we know the sign of charge of the hyperon - the secondary came to rest and produced a capture star, identifying itself as a π^- -meson, and therefore the hyperon as negatively charged. Since all our hyperons came from stars which also contained shower particles, Σ^+ as well as Σ^- could have been produced, charge being conserved by pions.

Using a maximum likelihood calculation for the mean lifetime of the five hyperons, we find

$$\langle \theta \rangle = (8^{+8}_{-4}) \cdot 10^{-11} \text{ s},$$

where the limits refer to $1/e$ values in the likelihood function in $1/\theta$.

BUDDE *et al.* ⁽⁷⁾, using a propane bubble chamber and selecting only the hydrogen events, will observe a pure sample of Σ^- -hyperons, provided that the strangeness selection rules are obeyed. They found a lifetime of $(1.4^{+1.6}_{-0.6}) \cdot 10^{-10}$ s, which agrees with the value of $(1.86 \pm 0.26) \cdot 10^{-10}$ s, found by ALVAREZ *et al.* ⁽¹²⁾. These latter workers, examining the capture of negative K-meson in liquid hydrogen, also reported a value of $(0.86 \pm 0.17) \cdot 10^{-10}$ s for the lifetime of the Σ^- -particle. With only five events in our experiment, the precision of the lifetime estimate is such that we cannot exclude the possibility that our sample contains hyperons of positive and negative charges, nor can we reliably estimate their relative proportions.

4.3. The mass of the Σ^- -hyperon. - In event Y 1, the π^- -meson secondary was emitted in the backward direction in the center of mass system, and, as a result, was slow enough in the laboratory system to come to rest within the emulsion stack, where it produced a characteristic σ -star. For this event, we find that the energy release

$$Q = (123 \pm 2.5) \text{ MeV}$$

and the corresponding hyperon mass

$$\Sigma_{\Sigma^-} = (2\,352 \pm 5) m_e.$$

⁽¹²⁾ L. W. ALVAREZ, H. BRADNER, P. FALK-VAIRANT, J. D. GOW, A. H. ROSENFELD, F. T. SOLMITZ and R. D. TRIPP: *U.C.R.L.* 3583 (1956).

The figure of $\pm 5 m_e$ includes all the statistical sources of uncertainty, arising from range-straggling of the π -meson secondary, uncertainty in original emulsion thickness, normalization of grain density in computing the velocity of the primary particle, and normalization of the range-energy relation for the emulsions used (in which a group of 12 μ -mesons had a mean range of $(592 \pm 7) \mu\text{m}$). Possible systematic sources of error could arise from the range-energy relation used, and from distortion affecting the measured angle of decay. The Barkas range-energy relation was used (BARKAS, private communication) and is considered to be accurate in this region; the distortion in the vicinity of the decay was less than 20 Covans, and no correction for this effect is thus necessary.

The mass of the Σ^+ -hyperon has been well determined by FRY, SCHNEPS, SNOW and SWAMI⁽¹³⁾ to be $M_{\Sigma^+} = (2327 \pm 1) m_e$. The difference between these two values is more than 3 standard deviations, and the high value for the mass of the Σ^- -particle is in agreement with values reported by CHUPP *et al.*⁽¹⁴⁾ and BUDE *et al.*⁽⁷⁾, and BARKAS *et al.*⁽¹⁵⁾.

* * *

We are grateful to Professor C. F. POWELL for his interest in this work, and for the hospitality and facilities of his laboratory. We would also like to thank Mr. P. H. FOWLER and Professor M. F. KAPLON for their advice and discussions. One of us (B.P.E.) would like to thank the D.S.I.R. for a maintenance grant.

⁽¹³⁾ W. F. FRY, J. SCHNEPS, G. A. SNOW and M. S. SWAMI: *Phys. Rev.*, **103**, 226 (1956).

⁽¹⁴⁾ W. CHUPP, G. GOLDBABER, S. GOLDBABER and F. WEBB: *U.C.R.L.* **3044** (1955).

⁽¹⁵⁾ W. H. BARKAS: *U.C.R.L.* **3364** (1956).

RIASSUNTO (*)

Usufruendo di emulsioni fotografiche nucleari si è eseguita una ricerca sistematica sulla produzione di particelle pesanti instabili dovuta a mesoni π^- di 4.5 GeV/c. Nell'esame di 2548 stelle si sono trovati 4 iperoni e 4 mesoni pesanti con velocità inferiori a 0.7c e soddisfacenti a determinati criteri geometrici di selezione. Uno degli iperoni produce un mesone π secondario che si arresta nel pacco di emulsioni. La massa di questo iperone che, per la cattura della sua particella secondaria, risulta carico negativamente, è $(2352 \pm 5) m_e$.

(*) Traduzione a cura della Redazione.

Electromagnetic Properties of Particles with Spin.

V. GLASER and B. JAKŠIĆ

Institute «Rudjer Bošković» and the University of Zagreb - Zagreb, Yugoslavia

(ricevuto il 13 Febbraio 1957)

Summary. — The scattering of a relativistic electron on particles with some electromagnetic structure and spin up to $s = \frac{3}{2}$ is investigated, and the cross-sections, in the first Born approximation for the electromagnetic field, are calculated. A possible estimation of the proton radius is given on the basis of quite general arguments.

The elastic scattering of high-energy electrons offers a powerful means of investigating experimentally the electromagnetic structure of target particles ⁽¹⁾. In this note we will investigate what properties of the bombarded particles can in principle be expected to show up in such an experiment. Besides the relativistic invariance and gauge invariance of our interacting system, we assume only that the electromagnetic interaction of the system target particle-electron can be treated in the first Born approximation—an assumption which is rather feasible for very low values of Z and for energies of the incoming electron higher than a few hundred electron masses. The meson-nucleon interaction will be left unspecified, hence all the relevant physical quantities pertaining to the target particle will be given in terms of a number of relativistically invariant phenomenological form-factors, which for the case of a proton were essentially introduced already by ROSENBLUTH ⁽²⁾. We have pushed our investigation only up to spin $\frac{3}{2}$ for the target particle, since for higher spin values the calculation, although manageable in principle, becomes rather cumbersome and physically not very interesting.

⁽¹⁾ See the review article by R. HOFSTADTER: *Rev. Mod. Phys.*, **28**, 3, (1956).

⁽²⁾ M. N. ROSENBLUTH: *Phys. Rev.*, **79**, 615 (1950).

The electron field $\chi(x)$ and the electromagnetic field $A^\mu(x)$, which transmits the interaction (both should be thought of as renormalized), satisfy the equations:

$$(1) \quad \begin{cases} \mathbf{p}(+m)\chi(x) = -e\mathbf{A}\chi(x); & \square A^\mu(x) = -j^\mu(x) - J^\mu(x), \\ j^\mu(x) = -e\bar{\chi}(x)\gamma^\mu\chi(x), & \partial_\mu j^\mu(x) = \partial_\mu J^\mu(x) = 0, \end{cases}$$

where $J^\mu(x)$ is the current operator of the nucleon and the meson fields. According to the above assumption the explicit form of the equations of the nucleonic and mesonic fields is not needed. Treating the electronic charge ($-e$) as an expansion parameter, we get by standard methods for the relevant S -matrix element in the first Born approximation:

$$(2) \quad \begin{aligned} \langle P'\lambda', p's' | S - 1 | P\lambda, ps \rangle &= i \frac{(2\pi)^4}{q^2} \langle P'\lambda' | J^\mu(0) | P\lambda \rangle \cdot \\ &\cdot \langle p's' | j_\mu(0) | ps \rangle \delta(P' + p' - P - p); \quad q = p' - p = P - P'. \end{aligned}$$

Here p, s and P, λ are the momenta and spins of the incoming electron and the bombarded particle, p', s' and P', λ' their momenta and spins after the elastic scattering; q is the momentum transfer. By defining

$$(3) \quad \begin{aligned} k^{\mu\nu} &= \frac{(2\pi)^6}{2e^2 M^2} \sum_{s,s'} \langle ps | j^\mu(0) | p's' \rangle \langle p's' | j^\nu(0) | ps \rangle = \\ &= \frac{1}{2M^2} \left(p^\mu p'^\nu + p^\nu p'^\mu + g^{\mu\nu} \frac{q^2}{2} \right), \end{aligned}$$

and

$$(4) \quad K^{\mu\nu} = \frac{(2\pi)^6}{e^2 M^2} \frac{1}{2S+1} \sum_{\lambda,\lambda'} \langle P\lambda | J^\mu(0) | P'\lambda' \rangle \langle P'\lambda' | J^\nu(0) | P\lambda \rangle,$$

where M and S are the mass respectively the spin of the target particle, the total cross-section averaged over the initial states of polarization can be written in the form

$$(5) \quad \begin{cases} Q = \alpha^2 \int \frac{K^{\mu\nu} k_{\mu\nu}}{4\eta^2 \sqrt{(p \cdot P)^2 - m^2 M^2}} \delta(P' + p' - P - p) d\sigma(P') d\sigma(p'), \\ \eta = \frac{q^2}{4M^2}, \quad \alpha = \frac{1}{137}. \end{cases}$$

Here the integration goes over the mass hyperboloids $P'^2 + M^2 = 0$, $p'^2 + m^2 = 0$. For very high energies of the electron, $p/m \gg 1$, the differential cross-section in the L.S. for the scattering of an unpolarized electron on an unpolarized

target particle into $d\Omega$ will be

$$(6) \quad \left\{ \begin{aligned} dQ &= \alpha^2 \frac{K^{\mu\nu} k_{\mu\nu}}{4\varepsilon^2 E^2 \sin^4 \vartheta/2} d\Omega; & \varepsilon &= E/M = \sqrt{\mathbf{p}^2 + m^2}/M, \\ E' &= \sqrt{\mathbf{p}'^2 + m^2} = \frac{E}{1 + 2\varepsilon \sin^2 \vartheta/2}, & \eta &= \frac{\varepsilon^2 \sin^2 \vartheta/2}{1 + 2\varepsilon \sin^2 \vartheta/2}. \end{aligned} \right.$$

In order to get the general expression for the cross-section for different spin values S , it is only necessary to find the most general form of the matrix element $\langle P'\lambda' | J^\mu(0) | P\lambda \rangle$ as a function of the four-vectors P , P' and λ , λ' consistent with relativity and the continuity equation. In this way we get the following list:

$$\begin{aligned} S = 0: \quad \langle P'\lambda' | J^\mu(0) | P\lambda \rangle &= \frac{e}{2(2\pi)^3} F_0(\eta)(P + P')^\mu, \\ S = 1/2: \quad \langle P'\lambda' | J^\mu(0) | P\lambda \rangle &= \frac{e}{2(2\pi)^3} \bar{u}(P'\lambda') [F_0(\eta)(P + P')^\mu - 2iG_1(\eta)S^{\mu\nu}q_\nu] u(P\lambda); \\ (P + M)u(P\lambda) &= 0, \quad \bar{u}(P\lambda)u(P\lambda') = \delta_{\lambda\lambda'}, \\ \sum_{\lambda=1,2} u(P\lambda)\bar{u}(P\lambda) &= (M - \underline{P})/2M, \\ S^{\mu\nu} &= \frac{i}{4} (\gamma^\mu \gamma^\nu - \gamma^\nu \gamma^\mu), \\ S = 1: \quad \langle P'\lambda' | J^\mu(0) | P\lambda \rangle &= \frac{e}{2(2\pi)^3} e_\sigma^*(P'\lambda') \left\{ \left[F_0(\eta)g^{\sigma\sigma} + \frac{1}{2M^2} F_2(\eta) \cdot \right. \right. \\ &\quad \cdot \left. \left(q^0 q^\sigma - \frac{q^2}{3} g^{\sigma\sigma} \right) \right] (P + P')^\mu + iG_1(\eta)S^{\mu\nu,\sigma\sigma} q_\nu + \\ &\quad + \frac{i}{M^2} G_2(\eta) \left[q^\mu q^0 q^\sigma - \frac{q^2}{2} (g^{\mu 0} q^\sigma + g^{\mu\sigma} q^0) \right] \Big\} e_\sigma(P\lambda); \\ P^\mu e_\mu(P, \lambda) &= 0, \quad e^{*\mu}(P\lambda)e_\mu(P\lambda') = \delta_{\lambda\lambda'}, \\ \sum_{\lambda=1,2,3} e^\mu(P\lambda)e^{*\nu}(P\lambda) &= g^{\mu\nu} - P^\mu P^\nu / M^2, \\ S^{\mu\nu,\sigma\sigma} &= -i(g^{\mu\sigma}g^{\nu\sigma} - g^{\mu\sigma}g^{\nu\sigma}). \\ S = 3/2: \quad \langle P'\lambda' | J^\mu(0) | P\lambda \rangle &= \frac{e}{2(2\pi)^3} \bar{u}_\sigma(P'\lambda') \left\{ \left[F_0(\eta)g^{\sigma\sigma} + \frac{1}{2M^2} F_2(\eta) \cdot \right. \right. \\ &\quad \cdot \left. \left(q^0 q^\sigma - \frac{q^2}{3} g^{\sigma\sigma} \right) \right] (P + P')^\mu + i\frac{2}{3} G_1(\eta)S^{\mu\nu,\sigma\sigma} q_\nu + \\ &\quad + G_1'(\eta) \cdot \varepsilon^{\mu\nu\sigma\sigma} \gamma_\sigma q_\nu + \frac{i}{M^2} G_2(\eta) \left[q^\mu q^0 q^\sigma - \frac{q^2}{2} (g^{\mu 0} q^\sigma + g^{\mu\sigma} q^0) \right] + \\ &\quad + i\frac{5}{12M^2} G_3(\eta)S^{\mu\nu,\sigma\sigma} q_\nu \left(q^0 q^\sigma - \frac{q^2}{5} g^{\sigma\sigma} \right) \Big\} u_\sigma(P\lambda); \end{aligned}$$

$$\begin{aligned}
 (P + M)u_e(P\lambda) &= 0, & \gamma^e u_e(P\lambda) &= 0, & P^e u_e(P\lambda) &= 0, \\
 \bar{u}_e(P\lambda) u^e(P\lambda') &= \delta_{\lambda\lambda'}, & \sum_{\lambda=1, \dots, 4} u_e(P\lambda) \bar{u}_e(P\lambda) &= \\
 &= \left[g_{e\sigma} + \frac{2}{3} P_e P_\sigma / M^2 + (P_e \gamma_\sigma - P_\sigma \gamma_e) / 3M + \frac{1}{3} \gamma_e \gamma_\sigma \right] (M - \underline{P}) / 2M, \\
 S^{\mu\nu, e\sigma} &= -i(g^{\mu e} g^{\nu \sigma} - g^{\mu \sigma} g^{\nu e}) + \frac{i}{4} (\gamma^\mu \gamma^\nu - \gamma^\nu \gamma^\mu) g^{e\sigma}.
 \end{aligned}$$

From the hermitian character of the current J^μ it follows that the form-factors F and G , as introduced above, are real-valued arbitrary functions of the variable η_j . Physically the form-factors represent the internal electromagnetic structure of the particle, which can be pictured classically by studying the expectation value of the current operator J^μ in x -space. Since it is impossible to localize a relativistic particle better than up to its Compton wavelength, in the authors' opinion the only possibility to interpret classically the various terms in the current is to go to the non-relativistic limit:

$$J_c^\mu(\mathbf{x}) = \langle 0\lambda | J^\mu(\mathbf{x}) | 0\lambda \rangle / \langle 0\lambda | 0\lambda \rangle = \frac{1}{M} \int P' \lambda' J^\mu(0) | P\lambda \rangle_{\text{n.r.}} \exp[i\mathbf{q} \cdot \mathbf{x}] d^3q.$$

Here $|0\lambda\rangle$ is the state vector of the non-relativistic particle localized sharply at the origin, and the current matrix element has to be taken in the non-relativistic limit. By working out the above expressions for different cases one obtains $\varrho_c(\mathbf{x})$ and $\mathbf{J}_c(\mathbf{x})$ as an expansion in terms of electric and magnetic multipole density distributions:

$$(7a) \quad \varrho_c(\mathbf{x}) = Q^{(0)}(r) + \frac{1}{2!} \partial_i \partial_k Q_{ik}^{(2)}(r),$$

$$(7b) \quad \mathbf{J}_c(\mathbf{x}) = \text{rot } \mathbf{M}, \quad M_i = M_i^{(1)}(r) + \frac{1}{2!} \varepsilon_{ijk} \partial_j \partial_l M_{kl}^{(2)}(r) + \frac{1}{3!} \partial_j \partial_k M_{ijk}^{(3)}(r),$$

the radial dependence of which is given by the Fourier transforms of F_0 , F_2 for an electric monopole respectively quadrupole distribution, by G_1 , G_2 , G_3 for a magnetic dipole, quadrupole respectively octupole distribution. The tensors $Q^{(0)}(r)$, $Q_{ik}^{(2)}(r)$, $M_i^{(1)}(r)$, $M_{ik}^{(2)}(r)$ and $M_{ijk}^{(3)}(r)$ are irreducible tensors depending only on $r = |\mathbf{r}|$, their tensor character is due only to polarization vectors. The quantities $F_{0,2}(0)$ and $G_{1,3}(0)$ represent static total multipole moments of the particle: $F_0(0) = Z$, $F_2(0) = Q$ (in units e/M^2), $G_1(0) = \mu_1$ (in units $e/2M$), $G_3(0) = \mu_3$ (in units $e/2M^3$, i.e. $eG_3(0)/2M^3 = \int M_{333}(0) d^3x$ with the spin pointing in the 3-direction). It should be noted, that the distribution due to G_2 is a solenoidal quadrupole density distribution and hence gives rise to no resultant magnetic quadrupole moment of the particle: the corresponding magnetic

field does not reach beyond the boundaries of the particle (*). Besides these non-relativistically interpretable terms there appears in J^μ in the case of spin $\frac{3}{2}$ a term proportional to G'_1 , which has many of the properties of a magnetic dipole distribution, but which vanishes in the non-relativistic limit owing to the presence of γ_5 .

Inserting the expressions of the current into (6) we get

$$(8a) \quad dQ_0 = F_0^2 dq_0, \quad dq_0 = \frac{\alpha^2 \cos^2 \vartheta/2}{4E^2 \sin^4 \vartheta/2} \frac{d\Omega}{1 + 2e \sin^2 \vartheta/2},$$

$$(8b) \quad dQ_{\frac{1}{2}} = [F_0^2 + (F_0 - G_1)^2 \eta + 2G_1^2 \eta \operatorname{tg}^2 \vartheta/2] dq_0,$$

$$(8c) \quad dQ_1 = \left[F_0^2 \left(1 + \frac{4}{3} \eta + \frac{4}{3} \eta^2 \right) + \frac{20}{9} F_0 F_2 \eta^2 \left(1 + \frac{2}{5} \eta \right) + \right. \\ \left. - \frac{8}{9} F_2^2 \eta^2 \left(1 - \frac{2}{3} \eta - \frac{1}{6} \eta^2 \right) - \frac{4}{3} F_0 G_1 \eta (1 + 2\eta) - \frac{16}{9} F_2 G_1 \eta^2 \left(1 + \frac{1}{2} \eta \right) - \right. \\ \left. - \frac{2}{3} G_1^2 \eta (1 - 2\eta) - \frac{8}{3} G_2^2 \eta^3 - \frac{4}{3} \eta (1 + \eta) (G_1^2 + 4G_2^2 \eta^2) \operatorname{tg}^2 \vartheta/2 \right] dq_0.$$

$$(8d) \quad dQ_{\frac{3}{2}} = \left\{ F_0^2 \left(1 - \frac{7}{3} \eta + \frac{20}{9} \eta^2 + \frac{8}{9} \eta^3 \right) - \frac{4}{3} F_0 F_2 \eta^2 \left(1 + \frac{13}{9} \eta + \frac{4}{9} \eta^2 \right) + \right. \\ \left. + \frac{4}{9} F_2^2 \eta^2 \left(1 + \frac{5}{3} \eta + \frac{8}{9} \eta^2 + \frac{2}{9} \eta^3 \right) - \frac{14}{9} F_0 G_1 \eta \left(1 + \frac{40}{21} \eta + \frac{8}{7} \eta^2 \right) - \right. \\ \left. - \frac{16}{27} F_2 G_1 \eta^2 \left(1 + \frac{29}{12} \eta + \eta^2 \right) + \frac{5}{9} G_1^2 \eta \left(1 + \frac{104}{45} \eta + \frac{8}{5} \eta^2 \right) - \right. \\ \left. + \frac{2}{3} F_0 G'_1 \eta \left(1 - \frac{2}{3} \eta \right) - \frac{8}{9} F_2 G'_1 \eta^2 \left(1 + \frac{1}{6} \eta \right) + \frac{8}{27} G_1 G'_1 \eta^2 + \right. \\ \left. - \frac{5}{9} G_1^2 \eta^2 - \frac{4}{3} G_2^2 \eta^3 (1 + \eta) - \left[\frac{10}{9} G_1^2 \eta \left(1 - \frac{28}{15} \eta - \frac{14}{15} \eta^2 \right) - \right. \right. \\ \left. \left. + \frac{4}{9} G_1 G'_1 \eta^2 \left(1 - \frac{2}{3} \eta \right) + \frac{10}{9} G_1^2 \eta^3 + \frac{8}{3} G_2^2 \eta^3 (1 + \eta)^2 \right] \operatorname{tg}^2 \vartheta/2 \right\} dq_0.$$

Here dq_0 is the well-known cross-section for the scattering of a relativistic electron on a spinless point charge. The formula for $dQ_{\frac{1}{2}}$ can be found in ^(1,2). dQ_1 is the most general expression in the first Born approximation (applicable to the case of the deuteron e.g.), while in $dQ_{\frac{3}{2}}$ the contribution of the magnetic

(*) If one assumes invariance under time reversal, this term will not appear, i.e., $G_2 = 0$. However this sort of invariance does not seem absolutely necessary. The authors would like to thank Prof. A. S. WIGHTMAN for illuminating discussions on this point.

octupole form-factor G_3 has been neglected (this formula could be applied to ${}^7\text{Li}$ e.g.). From the above expressions one can conclude, that the dependence of the cross-section on the spin and on the internal structure of the target particle comes into play only for high momentum transfers, i.e. if η is not much smaller than 1 (note that $\eta_{\text{max}} = \varepsilon^2/(1+2\varepsilon)$).

In all this discussion one must bear in mind, that there is no difference between the state vectors describing a composite (stable) particle and an elementary particle: both state vectors form a basis for irreducible representations of the full Lorentz group uniquely specified by a definite mass and spin ⁽³⁾. An elementary particle, however, has a field operator attached to it, say $\psi(x)$. Now, from the causality condition $[\psi(x), A^\mu(x')]_- = 0$ for $(x - x')^2 > 0$, a certain assumption connected with analytic continuation ^(*) and the requirement, that the vacuum polarization should be finite, one may conclude, that the form-factors F_i and G_i should be analytic functions representable in the form:

$$(9) \quad F_i(q^2) = \int_0^\infty \frac{f_i(x^2)}{q^2 + x^2} dx^2, \quad G_i(q^2) = \int_0^\infty \frac{g_i(x^2)}{q^2 + x^2} dx^2,$$

with f_i, g_i some real, but not necessarily positive functions ⁽⁴⁾. For a non-elementary particle such a conclusion could probably not be drawn. It is interesting that in the case of a proton or a neutron one gets as a lower limit in the integrals (9) $(2\mu)^2$ instead of 0, where μ is the mass of the π -meson, if one neglects the electromagnetic self-interaction of the mesonic cloud. Going over to x -space this implies, as it is readily seen, that the upper limit of the radius of the corresponding charge distributions is of the order $1/2\mu \approx 0.7 \cdot 10^{-13}$ cm, which is rather close to the experimental value for a proton ⁽¹⁾.

⁽³⁾ E. WIGNER: *Ann. of Math.*, **40**, 149 (1939) and subsequent papers.

^(*) This problem will be discussed elsewhere.

⁽⁴⁾ Compare: G. KÄLLÉN: *Dan. Mat. Fys. Medd.*, **27**, No. 12 (1953).

RIASSUNTO (*)

Si esamina lo scattering di un elettrone relativistico su particelle con struttura elettromagnetica e spin fino a $s = \frac{3}{2}$ e si calcolano le sezioni d'urto nella prima approssimazione di Born per il campo elettromagnetico. Si dà un possibile valore di stima del raggio protonico sulla base di argomenti del tutto generali.

(*) Traduzione a cura della Redazione

Parent Stars of K^+ -Mesons.

D. F. FALLA and M. W. FRIEDLANDER (*)

H. H. Wills Physical Laboratory - University of Bristol

F. ANDERSON

Physics Department, University College - Dublin

W. D. B. GREENING, S. LIMENTANI and B. SECHI-ZORN (†)

Istituto di Fisica dell'Università - Padova

Istituto Nazionale di Fisica Nucleare - Sezione di Padova

C. CERNIGOI, G. IERNETTI and G. POIANI

Istituto di Fisica dell'Università - Trieste

Istituto Nazionale di Fisica Nucleare - Gruppo di Trieste

(ricevuto il 14 Febbraio 1957)

Summary. — A study has been made of the parent stars of K-mesons produced by the Cosmic Radiation. Emission angle and energy spectra are given for these mesons, together with a distribution of star sizes. An estimate is made of the frequency of occurrence of associated hyperons, other K-mesons and hyperfragments. Three particularly interesting events are described, including one which has enabled the mass of the negative Σ -hyperon to be calculated as $2344 \pm 6 m_p$.

1. — Introduction.

Very little direct evidence has so far been available about the type of star from which K-mesons are emitted. Many individual examples have been published, but no statistically significant analysis has been made of a large

(*) Now at Department of Physics, Washington University, Saint Louis, U.S.A.

(†) Now at Brookhaven National Laboratory, U.S.A.

number of such stars. In the present work the K-mesons which formed the basic material for the G-stack Collaboration (¹) have again been considered, and a search has been made for their origins: these were then analyzed as completely as possible. Specific studies have been made of the following points: the energy and angular distributions of the emitted K-mesons; the distribution of parent star sizes; associated strange particles and hyperfragments; special events. Due to the limited number of cases in which the actual decay mode of the K-meson was known, no sub-division according to type of decay has been attempted. Comparison with other experiments is difficult owing to the virtual absence of published results.

2. — Experimental procedure.

A total of 297 K-mesons which had decayed at rest were available for study at the beginning of this investigation. All had been found by area scanning in the G-stack, a large block of Ilford G5 stripped emulsion, consisting of 250 sheets each 37 cm × 27 cm × 600 μm, which had been exposed to the Cosmic Radiation at a mean altitude of 27 000 metres (90 000 ft) by means of a free balloon. In only one quarter of the cases could the decay mode be identified as γ , τ , etc., while the remainder of the events were classified as K_L (for details of the selection criteria, see the original G-stack paper). Almost all these mesons, whether the decay mode had been identified or not, have been used in the present work.

The track of each K-meson was traced back from the decay point through successive emulsion sheets either to the apparent point of origin within the stack, or to the point at which the particle entered from outside, or entered from a region of the emulsion which had been damaged. The length of the track in each plate was noted, and also any sharp changes of direction. In calculating the range of the meson an original emulsion thickness of 600 μm has been assumed.

All stars have been classified in the accepted manner (BROWN *et al.* (²)) before analysis. Tracks of heavily ionizing particles were followed to their ends in order to detect decays etc.: measurements of ionization and $p\beta$ were made on those shower particles having projected track lengths of at least 3 mm per plate, and such tracks were followed up to 5 cm so as to increase the probability of detecting decays in flight. Where the star consisted

(¹) G-STACK COLLABORATION: *Nuovo Cimento*, **2**, 1063 (1955).

(²) R. H. BROWN, U. CAMERINI, P. H. FOWLER, H. HEITLER, D. T. KING and C. F. POWELL: *Phil. Mag.*, **40**, 862 (1949).

of only a few black or gray prongs and could have been a secondary star produced by the inelastic collision of the heavy meson, an attempt has also been made to follow its apparent primary: by this means 9 tracks were traced back to larger stars.

Tracks were traced through plates held by different laboratories in order to utilize fully the large stack size, and this considerably reduced wastage of events. A considerable fraction of all our K -mesons came from origins external to the stack itself or from damaged regions of the emulsion. All such events, for which the track length represents only a lower limit for the true range, and for which origins have not been found, have been excluded from the analysis and discussion.

For all events in which an origin was found, the co-ordinates of the origin and decay points relative to the edges of the stack were recorded for use in the calculation of the geometrical correction factors (statistical weights) applied to the range and energy distributions.

3. - Results.

3.1 - Angular and energy distributions. - In 224 cases the K -meson could be traced back to a star. Of these, 34 have been classified as K -meson interaction stars, while in a further 9 events the K is seen to interact shortly after emission from the parent star. For such events the measured range can only represent a lower limit for the true range, in which case the statistical weight cannot be calculated (see below). All of these 43 events have therefore been excluded from both the energy and angular distributions, which are based on the remaining 181 events whose ranges are accurately known.

114 K -mesons originated in stars produced by charged primaries: in Fig. 1a the distribution of range and emission angle with respect to the primary is given for these events. As can be seen, there is strong angular anisotropy, with 86 particles being emitted forwards

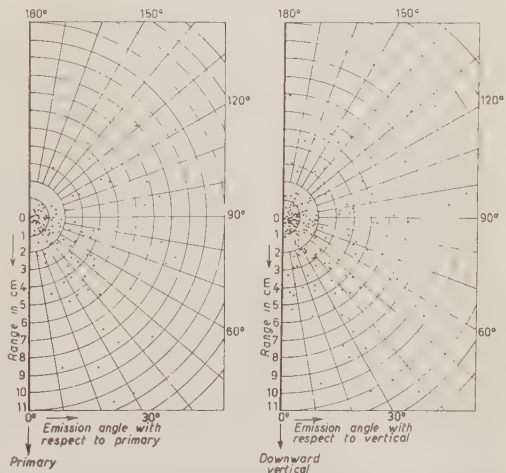


Fig. 1. Distribution of the K -mesons in terms of their ranges and their emission angles with respect to (a) the primary of the star and (b) the vertical.

in the laboratory system and 28 backwards. A division of the events into four equal solid angles shows this effect more clearly:

Angular interval	Number of events
$0^\circ \div 60^\circ$	62
$60^\circ \div 90^\circ$	24
$90^\circ \div 120^\circ$	14
$120^\circ \div 180^\circ$	14

The forward peaking in these distributions is easily explained when one considers the high primary energies involved. A further division according to the number of shower prongs is given in Fig. 2 and shows that the anisotropy does not vary appreciably within the energy range considered (probably from 2 GeV to 20 GeV).

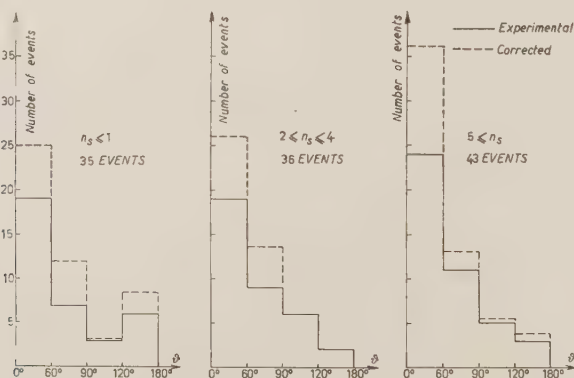


Fig. 2. — Distribution of K-meson emission angles with respect to the primary, for three groups of parent star sizes.

Since 67 of our stars (about one third) were produced by neutral primaries, it has not been possible to include these events in Fig. 1a. In order to make use of them, a second distribution has been prepared based on the angle with respect to the vertical instead of the primary: this is given in Fig. 1b and is for all 181 events. The new distribution must of necessity suffer from considerable smoothing since the primaries of cosmic ray stars may arrive at quite large angles to the vertical. Despite this the general aspect remains the same, though the anisotropy is reduced with respect to Fig. 1a.

The range and energy spectra as measured in the laboratory system are

given in Figs. 3a and 3b respectively. The full lines represent the uncorrected data, while the broken lines are the corresponding distributions after the application of the geometrical correction factor. This factor takes into account the fact that the stack was not infinite, and consequently the probability of

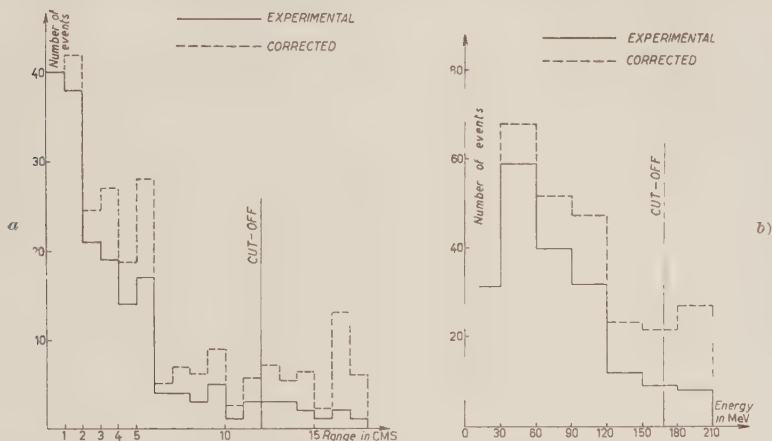


Fig. 3. - Distribution of (a) ranges and (b) energies for 181 K-mesons.

success in finding the parent star was greater for a K of short range than for one with a longer range. It has been calculated as follows: consider a sphere of radius equal to the direct distance between the point of decay and the parent star, centred on the former; the fraction of the surface of the sphere which lies inside the stack then represents the probability that a K of that range, created inside the stack, will decay at that point, and the reciprocal of this fraction then gives the correction factor, or statistical weight. Such a correction is not rigorous, due mainly to the forward peaking (see Fig. 1a), however, for ranges which are small compared with the long side of the stack (which was vertical during the flight) the correction may be considered as approximately valid: we have therefore arbitrarily imposed an upper limit of 12 cm (roughly equal to one third of the long or vertical side of the stack) for our corrected range spectrum, and 170 MeV for the corresponding energy spectrum.

Figs. 3a and 3b show that in the energy range below 120 MeV, the frequency increases towards low energies: this could be due to secondary interactions of the more energetic K-mesons within the parent nucleus leading to a degeneration of their energy. In Fig. 4 a division has been made into groups according to the size of the parent star. For $n_s < 1$ and for $2 < n_s < 4$,

TABLE 1. - Distribution in terms of N_h and n_s of 224 stars from which K-mesons have been seen to come. Those with both $n_s = 0$ and $N_h \leq 5$ have been considered as interaction stars, with the exception of event « J » which consists of a small star ($2 + 0\pi$).

N_h	1	2	3	4	5	6	7	8	9	10	11	12	13	14	15	16	17	18	19	>20	Total	%	Bristol 0.70
n_s																							
0	2	9	10	8	6	3	4	2	2	2	2	1	3	1	1	2	1		1	1	63	28.1	72.4
1	1	1	3	2	5	2	1	2	3		1	1	1	2		3	1		1	2	32	14.3	15.9
2		1	1			3	5	2	1	1		2	1		2	2				2	23	10.3	6.15
3	1		1			2	1		3	3		1	1	1	1	1			1	8	25	11.2	2.04
4					1		1		1	1		2	1	1			1	1		3	13	5.8	1.36
5					3		1		2	1				1	3		2			6	19	8.5	0.87
6				2					1	1		1	1				1		2	2	10	4.5	0.62
7					1			1							1	1				4	9	4.0	0.29
8				1				1	1									1		1	5	2.2	0.25
9														1		1	1		1	3	7	3.1	0.13
10														1	1				1	2	5	2.2	0.11
11																1		1			2	0.9	0.04
12														1						2	3	1.3	0.02
13															1						1	0.45	0.06
14																		1			1	0.45	0.00
>15				1						1									1	3	6	2.7	0.09
Grand Total																					224		

there is an apparent peak at about 50 MeV. The distribution for $5 \leq n_s$ is however quite different: the shape of the distribution is less well defined and the energy spread is much greater. If this difference is significant, a possible explanation may be as follows: in the larger stars the mean energy of the

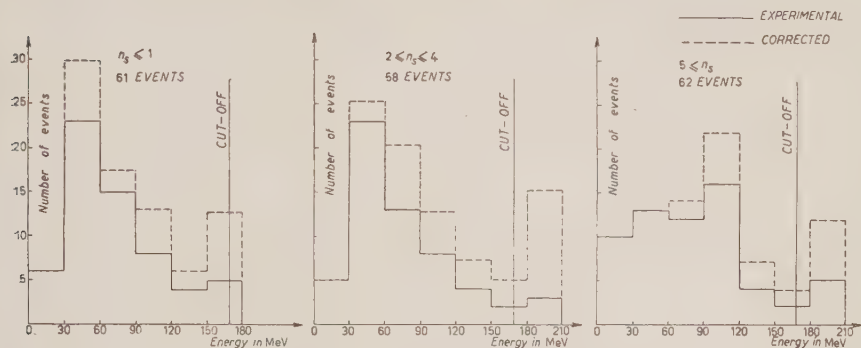


Fig. 4. — Energy distributions of K-mesons, divided according to the size of the parent stars.

K-mesons at production is expected to be greater, and this, coupled with an increase in the number of collisions within the nucleus due to the strongly forward motion and perhaps also to an increase in the collision cross-section, might account for the energy spread for $5 \leq n_s$. There is a further possibility that some of the K-mesons were produced by secondary pions interacting within the parent nucleus. Such pions are produced at energies notable less than that of the primary and therefore could only give rise to relatively low energy K-mesons. In the smaller stars this effect would be comparatively unimportant owing to the low multiplicity, but for $5 \leq n_s$, however, there may be a genuine contribution to the low energy spectrum, especially in view of the fact that the cross-section for production by pions is greater than that for production by nucleons.

3.2. Distributions of star sizes. — Table I gives the distribution of star sizes for 224 stars from which K-mesons were seen to be emitted. In this figure are included those small stars which can be considered as due to inelastic collisions of the K-mesons themselves. Evidence that some of the small stars are in fact interaction stars comes from the 9 cases in which it has proved possible to trace back the primary of a small star to a considerably larger one: unfortunately in none of these cases was the connecting track positively identifiable but it is almost certain that our interpretation is correct. We have therefore arbitrarily assumed that all small stars with $n_s = 0$ and $N_p = 5$,

TABLE II. — Details of 15 associated strange particles. In column 2, « f » signifies that the

K ⁻		STRANGE ASSOCIATED PARTICLES					
Event	K-meson decay mode	PRIMARY					
		Nature of associated particle	Ionization or β	Range	$p\beta c$ in MeV	Mass in m_e	Q in MeV
A		Y^\pm	$\beta = 0.463^{+0.010}_{-0.011}$	f	264 ± 68	2140 ± 550	
		K	$I/I^0 = 1.37$	s	427 ± 94	1090^{+270}_{-250}	
		K	$I/I^0 = 1.25$	s	460 ± 50	1000 ± 100	
B		Σ^-		f		2344 ± 6	
C		Σ^\pm	$\beta = 0.624 \pm 0.024$	f	550 ± 52	2300 ± 200	
D		Σ^+	$\beta = 0.44 \pm 0.01$	f			
E	$K_{\mu 2}$	K	$I/I^0 = 1.19 \pm 0.03$	s	$\tilde{\alpha} = 0.042 \pm 0.04$		
F		Y^\pm or K		f			
G		K	$I/I^0 = 1.36 \pm 0.03$	s	520 ± 75	1220 ± 200	
H		${}^4_\Lambda\text{He}$ or ${}^5_\Lambda\text{He}$		$150 \mu\text{m}$			
J	χ^+	Σ^\pm	$\beta = 0.51 \pm 0.03$	f			11
K		Σ^\pm	$\beta = 0.395 \pm 0.02$	f	195 ± 17.5	2240 ± 200	10
L	τ	Y^\pm or K	$\beta \cong 0.32$	f			
M		$F^* ?$		$4 \mu\text{m}$			
N	χ^+	Σ^\pm	$I/I^0 = 6.55 \pm 0.08$	$217 \mu\text{m}$			1
P	$K_{\mu 2}$	$Y^-(\Sigma^-)$		3.1 mm			
Q	$K_{\mu 2}$	Y^-		0.95 mm		2100 ± 700	

flight, while « s » means that it has been identified amongst the shower prongs of the parent star.

VISIBLE SECONDARY					NOTE
Ionization β	Range	$p\beta c$ in MeV	Mass in m_e	Nature	
≈ 1				π^\pm	See detailed description.
	58.0 mm			π^-	See detailed description.
≈ 1				π^\pm	Primary mass from $p\beta c$ and ionization.
56 ± 0.01		340 ± 30	1760 ± 150	P	
					Decay in flight: not analysable due to strong dip.
	16.64 mm 876 μm		1836 ?	P PDT	Decay at rest into more than three bodies: charge two.
≈ 1		260 ± 30		π^\pm	See detailed description.
≈ 1		227 ± 21		π^\pm	
≈ 1				P (55 MeV)	The secondary interacts with another proton thus permitting a secure identification and energy determination.
782 ± 0.01		135 ± 14	280 ± 50	π^\pm	Decay in flight.
					Captured at rest giving rise to a two-prong star of 7.0 μm and 8.5 μm .
					Captured at rest giving rise to a two-prong star of 7.0 μm and 3.2 μm .

and in which there is no evidence for the presence of a second strange particle, are not genuine production stars but are due to the inelastic interactions in flight of high energy K-mesons (*). There are 43 events which fall into this category, including the 9 already mentioned in which a second star has been found.

We have compared our data with that of CAMERINI *et al.* (³). In the last two columns of Table I are given the percentages of events having various values of n_s both for our data and for Bristol. It will be seen that there is a far larger proportion of big stars amongst our events than amongst the Bristol sample. The frequencies of stars with $n_s = 5, 6$ or 7 are greater in our case by about a factor of ten, and continue high for larger values of n_s . For $n_s = 0$ however, the frequency drops sharply and this effect becomes even more apparent when the small interaction stars are discarded. Two causes may be responsible: one is the difference in the primary energy spectrum for the two experiments (one stack was flown at 68 000 ft over England, while the G-stack was flown at 90 000 ft over Northern Italy) and the other is the fact that more energy is required for the creation of a K-meson than for a pion; this favours the production of pions and reduces the production of K-mesons at relatively low energies. Of the two possible causes, the latter is probably the more important. It would thus appear that the stars from which K-mesons are emitted are generally larger than the normal and more common cosmic ray stars: this in turn implies that production by the more energetic primaries is preferred.

4. - Associated strange particles.

4.1. *Stars with more than one strange particle.* - Of the 224 stars found, 209 were completely analyzed, and of these only 15 yielded a second strange particle (see Table II). It is of interest to see what this implies if we apply the Gell-Mann and Nishijima hypothesis of 100% associated production, a

(*) If this assumption is correct, then these interactions must be due to K-mesons of such high energy that had they not interacted they would normally have succeeded in leaving the stack, in which case they would neither have been seen nor included in our statistics. In addition to those K which interact there is an unknown number of high energy K which escape from the stack without interacting: further there must be many which are created outside the stack and pass right through it unless they happen to interact and so become detectable. For this reason the number of interactions seen and the length of track followed cannot be used for an estimation of the interaction m.f.p.

(³) U. CAMERINI, J. H. DAVIES, P. H. FOWLER, C. FRANZINETTI, H. MUIRHEAD, W. O. LOCK, D. H. PERKINS and G. YEKUTIELI: *Phil. Mag.*, **42**, 1241 (1951).

hypothesis which is almost certainly correct, especially in view of the direct evidence recently obtained at the Brookhaven Cosmotron ⁽⁴⁾.

As has been pointed out above, some of the stars may be due to the inelastic interactions in flight of the K-mesons themselves. None of the 43 events concerned has been considered in this section; on the other hand, all the remaining 166 stars have been assumed to be the genuine origins of the corresponding K-mesons. These stars were made up of 2320 heavy and gray tracks ($1.5 I_{\min} < I$) of which 2064 have been classified, and 708 shower tracks ($I < 1.5 I_{\min}$) of which 115 were suitable for study.

There are several reasons why a second strange particle may escape detection:

(a) Experimental causes:

- (i) failure to recognize some of the decays in flight which follow the scheme

$$\Sigma^+ \rightarrow p + \pi^0$$

since there is only a small mass difference between the Σ^+ and a proton ($\sim 20\%$), and the change in ionization may not be appreciated: the decay is then mis-interpreted as a simple proton scattering;

- (ii) when a Σ^- is captured by a proton it may not produce a visible star

$$\Sigma^- + p \rightarrow n + \Lambda + 82 \text{ MeV};$$

further, the excitation energy is so low that the nucleus may not expel nucleons unless the Λ is also captured and decays within it;

- (iii) inability to identify all the star prongs, owing to technical difficulties.

(b) Intrinsic causes:

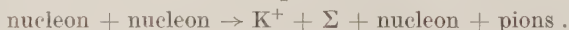
- (iv) the particle was a Σ^0 ,
the particle was a neutral K-meson,
the particle was a Λ .

4.2. *Frequencies of Σ -hyperons.* — 11 associations may be attributed to Σ^\pm : 6 have been definitely identified as such and 5 are very probable cases; they

⁽⁴⁾ S. L. RIDGWAY, D. BERLEY and G. B. COLLINS: *Phys. Rev.*, **104**, 513 (1956).

comprise 9 decays in flight and 2 captures at rest; in 4 cases the sign of charge is known, and these represent the decay in flight of one Σ^+ (proton secondary) and one Σ^- (π^- secondary) and the capture at rest of 2 Σ^- .

At the height at which our stack was flown (~ 27 km) the Cosmic Radiation consists almost exclusively of high energy nucleons. Almost all of our associated Σ were therefore produced in interactions of the type



If there were no pions amongst the secondaries, the charge of the Σ would automatically be defined by the charges of the colliding particles. However, the presence of pions lifts this restriction and there is then no *a priori* reason why one sign of charge should predominate over another, especially since the strangeness is the same for each. If production is the result of the interaction of secondary pions within the parent nucleus, a similar argument can be applied. We have therefore made the simplifying assumption that, under the conditions of our experiment in which pions are almost always produced ($0 < n_s$), the numbers of Σ^+ , Σ^0 and Σ^- at production are equal.

Of our total of 11 Σ^\pm let us assume that 6 are positive and 5 negative. Only one of the 9 hyperons seen to decay gave rise to a proton secondary: thus the 6 Σ^+ consist of 5 which decayed into charged pions and one into a proton. Now recent data from the ALVAREZ group⁽⁵⁾ has confirmed the earlier branching ratio given by FRY⁽⁶⁾, the latest figures being:

$$\frac{\Sigma^+ \rightarrow p + \pi^0}{\Sigma^+ \rightarrow n + \pi^+} = \frac{14}{14} = 1,$$

which implies that we have lost 4 decays which gave rise to protons.

FRY *et al.*⁽⁷⁾ have estimated that 50% of all Σ^- captured at rest give rise to zero-prong stars. We have found two Σ^- captures and each had a two-prong star: we have therefore assumed that we have lost two events of the first type.

The total of charged Σ then becomes 17.

As has already been pointed out, there should be no preference at production for any particular charge state, and we have for this reason estimated the number of neutral Σ as equal to half that of the charged, i.e. 8, giving a total of 25 for all types at emission, assuming that the relative frequencies of the various charge states remain unaltered.

4.3. *Frequencies of K^- and \bar{K}^0 mesons.* — When a second K-meson is produced, the conservation of strangeness requires that it should be a K^- or

(5) F. T. SOLMITZ, L. W. ALVAREZ, H. BRADNER, P. FALK, J. D. GOW, A. H. ROSENFIELD and R. D. TRIPP: *Bull. Am. Phys. Soc.* **1**, 385 (1956), also UCRL-3583.

(6) W. F. FRY: *Proc. Sixth Annual Rochester Conference* (1956), p. v-35.

(7) W. F. FRY, J. SCHNEPS, G. A. SNOW and M. S. SWAMI: *Phys. Rev.*, **100**, 950 (1955).

a K^0 : the actual charge state will depend on the nature of the colliding particles, but as in the case of the Σ , the presence of secondary pions may lift this second restriction, and so we have taken the production frequencies as being equal. Since we have found two charged K (events E and G), we assume that there were also two cases in which \bar{K}^0 were produced: our total of associated K -mesons is then 4.

4.4. *Correction for prongs not analysed.* — Our 166 stars contained a total of 3028 prongs of all degrees of ionization, and of these 2179 have been analyzed, the remainder having been abandoned for technical reasons. In view of the complicated nature of the assumptions which become necessary, no account has been taken of the possibility that having seen one strange particle (i.e. the K^- which led us to the star) amongst the relatively slow prongs, the second might be expected to be fast: the corrected totals then become

$$N(\Sigma^{+}, \pi^{-})_{\text{total}} = 25 \cdot \frac{3028}{2179} = 35 ,$$

$$N(K^{-}, \bar{K}^0)_{\text{total}} = 4 \cdot \frac{3028}{2179} \approx 6 .$$

4.5. *Frequency of hyperfragments.* — One certain example and one probable example have been seen. No correction has been applied as hyperfragments are usually short and are not too difficult to recognize.

4.6. *Frequency of Λ .* — Combining the above estimates, there remain $166 - 35 - 6 - 2 = 123$ events which must be explained by some other mechanism. As a first approximation we may consider all these cases as possible examples of Λ emission: this is quite probably an overestimate, but will serve as a basis for discussion. The ratio at emission then becomes

$$\frac{\text{Number of } \Sigma^{+}, \pi^{-}}{\text{Number of } \Lambda} = \frac{35}{123} = 0.28 .$$

The percentage of cases in which charged hyperons are emitted when K^- -mesons are captured is very different when this takes place in hydrogen or in the heavy nuclei of photoemulsions. The Berkeley group working with a hydrogen bubble chamber ⁽⁷⁾ have seen 83 charged hyperons emitted from 137 K^- captures, while S. GOLDBABER ⁽⁸⁾ has reported seeing 83 hyperons from

(7) S. GOLDBABER: *Proc. Sixth Annual Rochester Conference* (1956), p. vi-8.

617 K^- captures in emulsions. Thus the emission frequency in emulsions is reduced with respect to that in hydrogen by a factor of about 4.5. This may be due to the different charged to neutral ratio arising from the presence of neutrons in the capturing nucleus, and to a strong interaction loss of the charged hyperons before they leave the nucleus. Despite the very different energies involved ($\sim \frac{1}{2}$ GeV for K^- capture, against ten times this figure for the majority of our stars) the fact remains that both in our experiment and in K^- capture in photoemulsions, hyperon production takes place in complex nuclei, and further, the percentage of charged hyperons finally emitted is roughly equal in both cases ($\sim 14\%$). It is thus possible that conversion effects are present in our case, and that the number of Σ^\pm observed is notably inferior to those actually produced (*).

Assuming that associated production always occurs, one may then conclude that: if a positive K-meson is produced in a high energy interaction (~ 5 GeV or more) the probable nature of the associated particle *at emission* from the nucleus is as follows

Nature of particle			Percentage probability
Σ^+	Σ^0	Σ^-	$\sim 21\%$ (7 % each)
K^-	\bar{K}^0		$\sim 3\%$ ($1\frac{1}{2}\%$ each)
Hyperfragments			$\sim 1\frac{1}{2}\%$

while in the remaining cases the particle which is finally emitted is probably a Λ . It is worth noting that the very low ratio of hyperfragments to Λ ($\sim 1/50$)

(*) From the results obtained from K^- capture in bubble chambers (⁶), the production ratio Σ/Λ is found to be about 7. When the corresponding ratio for production in neutrons becomes available, the two ratios may be combined in a suitable way and that for a heavy nucleus may be derived. This in turn may be compared with the K^- results in heavy nuclei in emulsions, and the ratio

$$\frac{\Sigma}{\Lambda} \sim \frac{\Lambda}{\Sigma}$$

may be obtained. Finally this ratio may be applied to our results as a correction factor to obtain the true *production* percentages. Such a correction should not be far from the truth, because on the one hand more heavy nuclei are involved than in the capture of K^- (K^- capture is analogous to the capture of μ and there it is known that there is a preference for the light nuclei: also at our higher energies the cross-section for our primaries would favour interactions with heavy nuclei) thus increasing the conversion $\Sigma \rightarrow \Lambda$. On the other hand, at our primary energies it becomes energetically possible for the reverse conversion to take place, and in addition the cross-section for the forwards conversion may well be reduced as happens in the case of p-nucleon collisions [see also N. DALLAPORTA and F. FERRARI: *Nuovo Cimento*, **5**, 742 (1957)].

may well be due to the relatively high energy at which the Λ have been produced, which leads to a correspondingly low probability of capture.

5. — Special events.

5.1. — Amongst our 15 associated events there are three which deserve special mention. In one of these, three K -mesons and a hyperon were observed to come from the same star ($26+9p$): another represents the decay in flight of a Σ^- hyperon whose π^- secondary interacts at rest, while the third is an example of the elementary interaction

$$\pi^\pm + p \rightarrow \chi^\pm + \Sigma^\pm.$$

The first event demonstrates that at least 4 strange particles can be formed within the same nucleus, though in the present case there is no means of deciding which of several possible mechanisms is responsible. The second provides additional independent evidence that the mass of the negative Σ is 15 or 16 electron masses heavier than its positive counterpart: our figure of $2344 \pm 6 m_e$ is in excellent agreement with the results of other workers⁽⁹⁾. (An event which is almost identical with ours has recently been found at Bristol⁽¹⁰⁾: these workers obtain a mass of $(2352 \pm 5) m_e$). The last event is interesting since it is believed to be the first example of its kind found in nuclear emulsions. Several similar events have been observed in diffusion and bubble chambers (see for example FOWLER *et al.*⁽¹¹⁾) but here the difficulty has been the low probability of seeing both decays and so identifying the decay modes of both strange particles.

5.2. *Event « A ».* — In this event the K -meson was followed back for 1.57 cm when it led to a large star ($26+9p$), a photograph of which is reproduced in Fig. 5. Of the heavy prongs 24 have been identified by following them to their ends, and two of the shower prongs were suitable for ionization and

(9) A. DEBENEDETTI, C. M. GARELLI, L. TALLONE and M. VIGONE: *Nuovo Cimento*, **12**, 952 (1954); W. W. CHUPP, G. GOLDBABER, S. GOLDBABER and F. H. WEBB: *Proc. Pisa Conference, Suppl. Nuovo Cimento* **4**, 382, (1956) also UCRL report 3044; D. M. HASKIN, T. BOWEN and M. SCHEIN: *Phys. Rev.*, **103**, 1512 (1956); R. BUDD, M. CHRETIEN, J. LEITNER, N. P. SAMIOS, M. SCHWARTZ and J. STEINBERGER: *Phys. Rev.*, **103**, 1827 (1956).

(10) B. P. EDWARDS, A. ENGLER, M. W. FRIEDLANDER and A. A. KAMAL: in course of publication.

(11) W. B. FOWLER, R. P. SHUTT, A. M. THORNDIKE and W. L. WITTEMORE: *Phys. Rev.*, **98**, 121 (1955).

scattering measurements. Amongst the former was the decay in flight of a hyperon of mass $(2140 \pm 550) m_e$, while both of the measurable shower prongs were identified as K-mesons (masses $(1090^{+270}_{-240}) m_e$ and $(1000 \pm 100) m_e$ respectively). The secondaries of the star therefore consist of

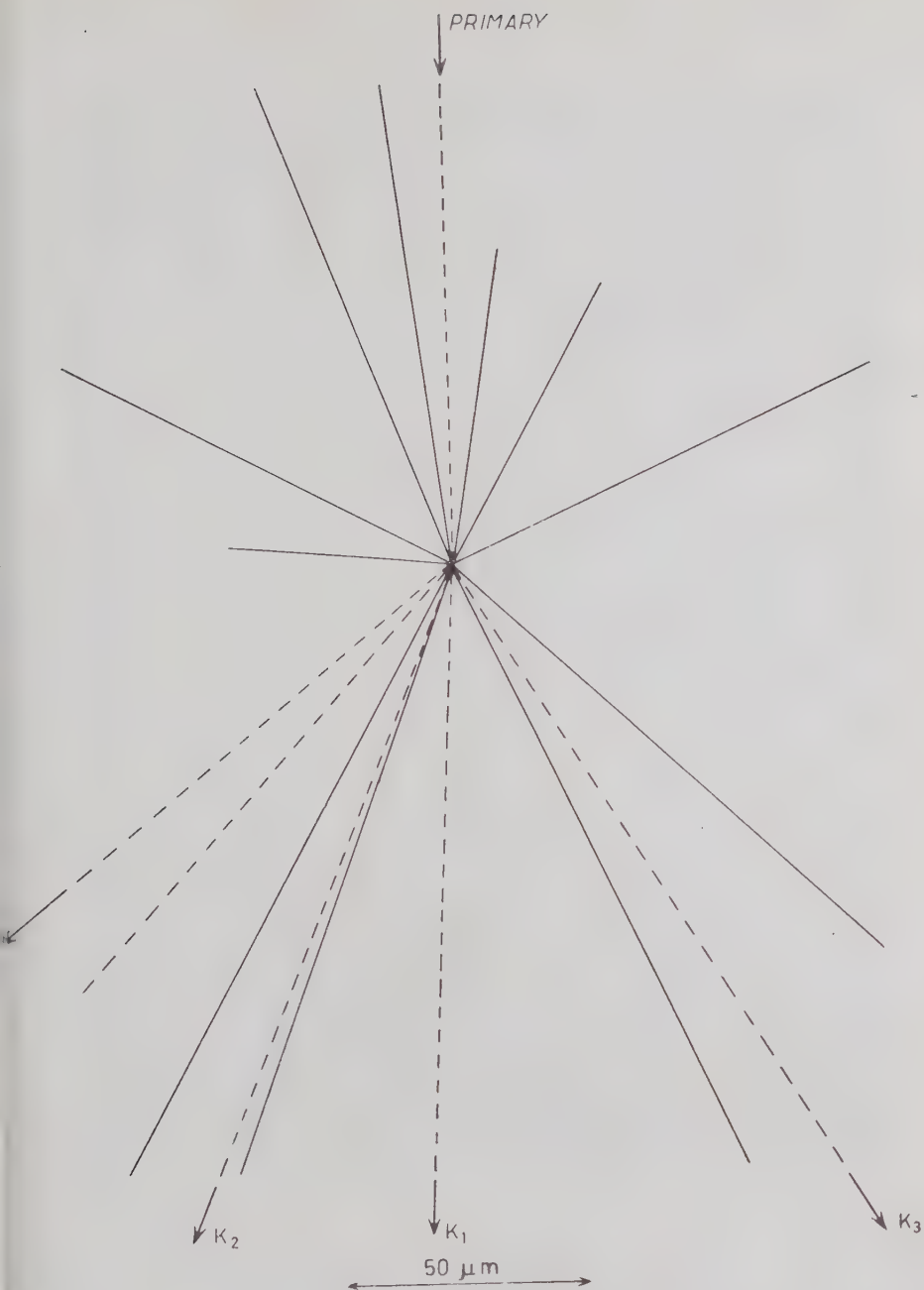
- 22 - protons, deuterons etc.,
- 1 - K^+ -meson decaying at rest,
- 2 - K-mesons amongst the shower prongs,
- 1 - hyperon decaying in flight,
- 2 - unidentified heavily ionizing particles,
- 7 - unidentified shower particles.

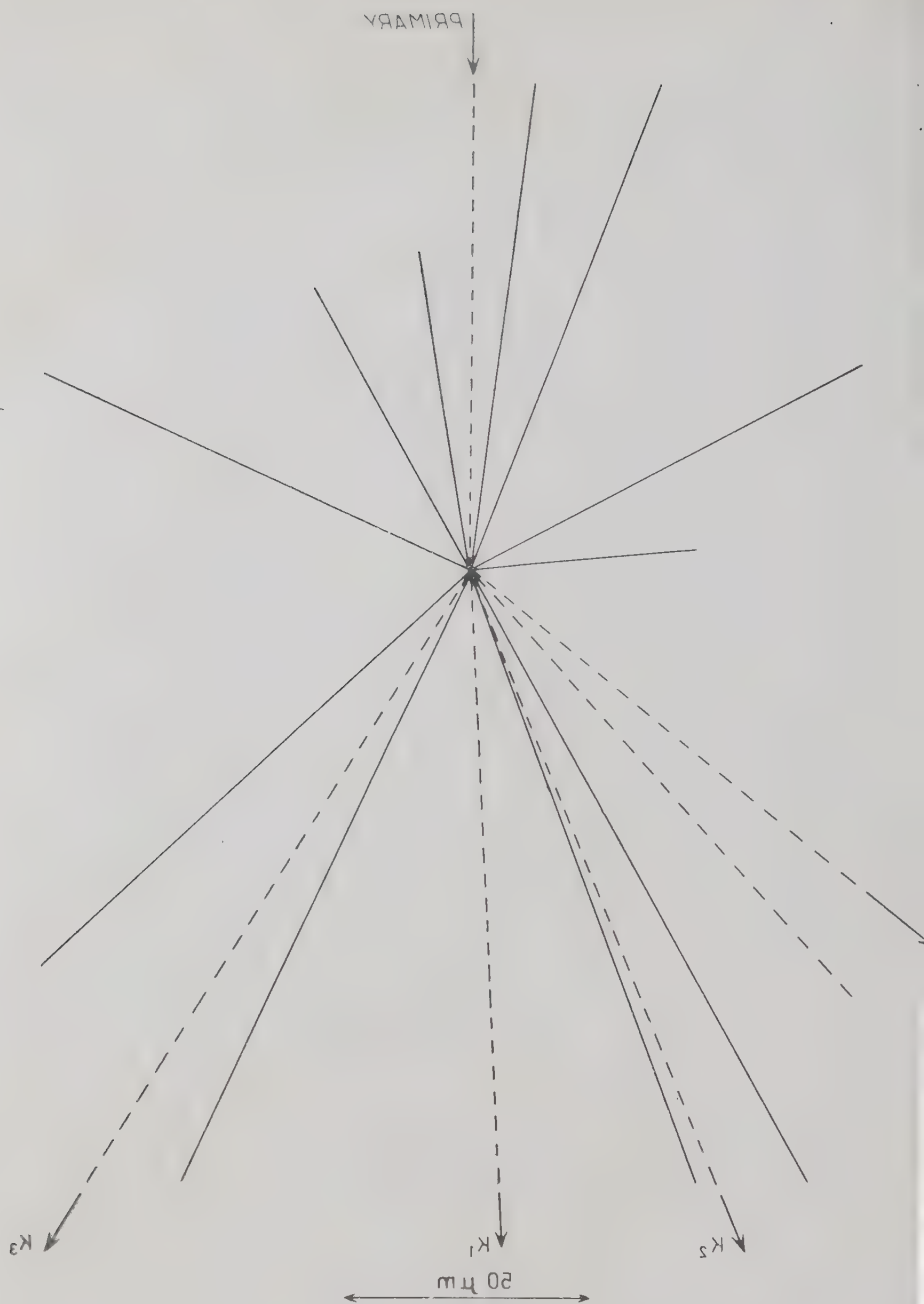
The energy of the star is at least 15 GeV.

The K-meson which led to the discovery of the star decayed at rest and therefore its identification as a K-meson was unambiguous: the other two were identified by ionization and scattering measurements. The star lay in a plate in which an elaborate calibration had already been made for very similar purposes ⁽¹²⁾, however, a check was made by means of two trial protons to confirm that this calibration was also applicable to the actual zone of the plate in which the star lay. Repeated scattering and ionization measurements then led to the identification of the two particles. One left the stack after 4 cm and scattering measurements were carried out over the first two centimeters of its track, yielding a $p\beta$ of (460 ± 50) MeV/c: its specific ionization was $1.25^{+0.04}_{-0.05}$. The mass is then found to be $(1000 \pm 100) m_e$. The other remained flat for 5.8 mm after which its dip increased sharply. Scattering measurements gave its $p\beta$ as (430 ± 95) MeV/c: its specific ionization was 1.37 ± 0.05 : its mass was $(1090^{+270}_{-240}) m_e$.

The hyperon was identified as such by ionization and scattering measurements. Its β was found from a calibration using 5 protons to be $0.463^{+0.010}_{-0.011}$, while its $p\beta$ was (265 ± 70) MeV/c: together these lead to a mass of $(2140 \pm 550) m_e$. The secondary was at minimum ionization and could be followed for only 13 mm after which it was lost in a difficult passage between plates: it was too steep for reasonable scattering measurements. The dynamics are largely compatible with the decay of a Σ into a charged pion and a neutron, but the possibility that it represents the decay of a Ξ^- cannot be excluded.

⁽¹²⁾ M. CECCARELLI, M. GRILLI, M. MERLIN, G. SALANDIN and B. SECHI: *Nuovo Cimento*, **2**, 828 (1955).







I I I I I I

Fig. 5. - Photograph of event «A». The star is of type $(26+9p)$: K.1 decayed at rest: the calculated masses of K.2 and K.3 are (1090^{+270}_{-240}) and $(1\ 000 \pm 100) m_e$ respectively: the mass of the hyperon has been calculated as $(2\ 140 \pm 550) m_e$.

The whole event can be interpreted in a variety of ways:

- it may be due to the individual production of three K -mesons and a hyperon,
- there may have been the production of two pairs of strange particles, such as $(K^+ + K^-)$ and $(K^+ + Y)$.

A rather remote possibility is that the event represents an example of the interaction

$$K^+ + \text{nucleus} \rightarrow K^+ (\text{scattered}) + (K^+ + K^+ + \Xi^-) + \text{nucleons} + \text{pions}.$$

Unfortunately nothing further can be said as no measurements on the primary were possible.

In connection with this event it is interesting to note that there is some evidence that the particles in the core of a jet are not all pions, but that perhaps 25% must be due to other particles including K -mesons and hyperons ⁽¹³⁾.

5.3. *Event «B»*. — An associated Σ^- was emitted from a medium sized star ($15+2p$) and decayed in flight after 850 μm giving rise to a π^- secondary which was captured at rest after 58.0 mm. The space angle between primary and secondary was $100^\circ \pm 1^\circ$: the secondary went backwards both in the laboratory and center of mass systems and produced a three-prong star upon capture. The β of the primary was obtained from a calibration using 8 protons of approximately the same dip ($\sim 32^\circ$) and was found to be $0.402_{-0.016}^{+0.013}$. Taking straggling of the secondary as $3\frac{1}{2}\%$ and the masses of the neutron and the negative pion as being 1838 m_e and 273 m_e respectively, the mass of the decaying Σ^- has been calculated as

$$(2344 \pm 6) m_e$$

where the error is the probable error, the statistical error being $\pm 9 m_e$.

The range energy curves used were those of BARONI *et al.* ⁽¹⁴⁾. A calibration of the stopping power of the emulsion was available from earlier work in the G-stack, and this, together with the ranges and known energies of the secondaries from γ and $K_{\mu 2}$ decays have confirmed the correctness of this part of the curves in this particular stack. An additional check came from the analysis of the decay of a Σ^+ found in the same plates ⁽¹⁵⁾: this decayed at

⁽¹³⁾ F. A. BRISBOUT, C. DAHANAYAKE, A. ENGLER, Y. FUJIMOTO and D. H. PERKINS: *Phil. Mag.*, **1**, 605 (1956).

⁽¹⁴⁾ G. BARONI, G. CASTAGNOLI, G. CORTINI, C. FRANZINETTI and A. MANFREDINI: CERN, Bureau of Standards, Bull. No. 9.

⁽¹⁵⁾ M. CECCARELLI, M. GRILLI, M. MERLIN, G. SALANDIN and B. SECHI: *Suppl. Nuovo Cimento*, **4**, 426 (1956).

rest and gave rise to a π^+ secondary which also decayed at rest. The calculated mass of the primary was found to be in excellent agreement with the established value of $2327 m_e$ (actual value in this case $(2323 \pm 7) m_e$).

5.4. *Event «J»*.— The origin of this K-meson was a small star ($2+0p$), see Fig. 6. The primary was extremely flat and suitable for scattering measurements: it came from outside the

stack, having traversed 12.5 cm of emulsion (6 mm per plate) before producing the star. The other prong was only $455 \mu m$ in length after which the particle decayed into a near minimum secondary which interacted in flight giving rise to a six-prong star at a distance of 4.96 cm from the decay point: this track was also suitable for scattering measurements. The event was coplanar to within the experimental errors (coplanar to within $1\frac{1}{2}^\circ$).

The identification of the primary was clear since both of the other two tracks ended in decays. The coplanarity of the event excluded the presence of neutral secondaries, and this, together with the conservation of charge, required the struck particle to be a proton.

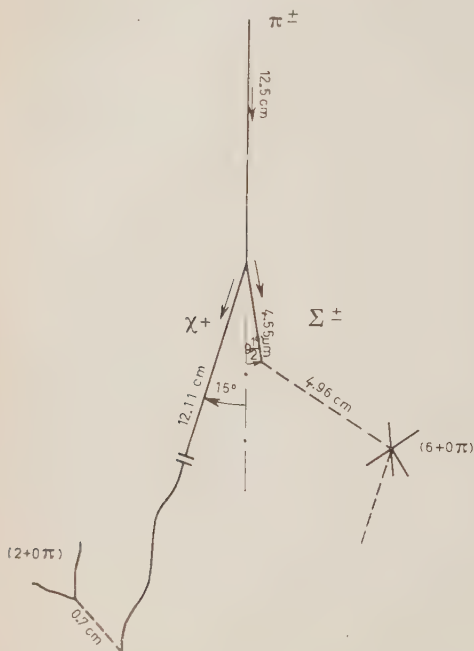


Fig. 6. — Event «J».

From scattering and ionization measurements, the secondary of the K-meson has been identified as an L-meson: the fact that it interacts in flight after 0.7 cm shows that it is a pion: its $p\beta$ has been estimated by the surface angle method as $(130 \pm 60) \text{ MeV}/c$. This in turn identifies the K-meson as a χ , and the fact that the particle decayed at rest shows that its charge was positive.

The particle which decays in flight can be identified partly from the energy of its secondary in the center of mass of the decay, and partly from the conservation of momentum in the event as a whole. From ionization and scattering measurements, the secondary may be shown to be a pion with a $p\beta$ in the laboratory system of $(260 \pm 30) \text{ MeV}/c$. Ionization measurements on the decaying particle yield a β of 0.51 ± 0.03 . Combining this data, the energy of the pion in the center of mass of the decay is then found to be

91^{+21}_{-17} MeV. Combining this data with considerations based on the conservation of momentum in the event as a whole, the decaying particle may be positively identified as a Σ -hyperon. The charge is uncertain since the secondary interacts in flight.

Scattering measurements on the primary yield a $p\beta$ of (990 ± 150) MeV/c, and the specific ionization is 0.93: thus the particle cannot be identified by direct measurements. However, from considerations of energy and momentum conservation it may be shown that the primary must be a pion of 1140^{+125}_{-110} MeV.

The whole interaction may now be written as

$$\pi^\pm + p \rightarrow \chi^\mp + \Sigma^\pm.$$

The kinetic energy of the secondary products in the center of mass may also be calculated: it is (61^{+66}_{-60}) MeV, which is very low. The emission angle in the center of mass is 62° and the Σ goes backwards.

The angle between the normals to the interaction plane and the decay plane of the Σ is $16\frac{1}{2}^\circ$ while the secondary of the χ^+ makes a space angle of 55° with the interaction plane.

6. - Conclusions.

Of the 297 K-mesons available, 224 have been successfully traced back to stars within the emulsion block. Of these, 34 were considered to be due to inelastic interactions in flight of high energy K-mesons: in fact in another 9 cases the primary of a small star was found to originate in a larger star.

The distribution of emission angles in the laboratory system (Figs. 1a, 1b and 2) shows strong forward peaking over the range of star sizes found (probably between 2 GeV and 20 GeV). The energy distribution (Fig. 3b) indicates that in the range below 120 MeV the frequency increases towards low energies, probably due to secondary interactions within the same nucleus, while Fig. 4 shows that there may well be a peak in the energy distribution for small and medium star sizes ($n_s \leq 4$) but that for larger stars the distribution has no clear form.

Our stars seem to be decidedly larger than the average cosmic ray stars studied by CAMERINI *et al.* (see Table I): this appears to indicate that production by the more energetic primaries is preferred.

We have found 15 stars from which a second strange particle or hyperfragment was emitted (see Table II) and have estimated the probable emission rates after allowance has been made for losses in scanning etc. These rates are

Σ^+	Σ^0	Σ^-	$\sim 21 \%$ (7 % each)
K^-	\bar{K}^0		$\sim 3 \%$ ($1\frac{1}{2}\%$ each)
Hyperfragments			$\sim 1\frac{1}{2}\%$.

In the majority of the remaining cases one might assume that the final product is probably a Λ . However the number of Σ -hyperons *at production* may be greater than would appear from the above figures, since there are indications from studies of K^- capture stars that many are converted into Λ -hyperons within the parent nucleus.

Three unusual events have been found. One is a star from which three K -mesons and a charged hyperon are emitted, thus confirming that in certain cases at least 4 strange particles may be produced in the same nucleus. Another is the decay in flight of a Σ^- whose π^- secondary is captured at rest, thereby allowing the mass of the hyperon to be calculated as $(2344 \pm 6) m_e$, which is additional evidence that the mass of the Σ^- is greater by about 15 or 16 electron masses than that of the Σ^+ . The third event is an example of the fundamental interaction

$$\pi^{\pm} + p \rightarrow \gamma + \Sigma^{\pm}.$$

* * *

Our thanks are due to our colleagues who have worked with the G-stack, for the information which they so readily made available to us. One of us (F.A.) has to thank Prof. O'CEALLAIGH, of the Dublin Institute for Advanced Studies, for the loan of plates, while the Groups of Padua and Trieste have to thank the Milan Group for the loan of plates and for having made their events available for further study. Another of us (D.A.F.) has to thank the University of Bristol for a Graduate Scholarship, and both he and M.W.F. wish to thank Prof. C. F. POWELL for the hospitality and facilities of his Laboratory.

Thanks are due to Prof. N. DALLAPORTA and Prof. M. MERLIN for discussions and suggestions, and to the Directors of the respective Laboratories for their help and interest.

RIASSUNTO

È stato compiuto uno studio su stelle madri di mesoni K^+ prodotti dai raggi cosmici. Vengono dati spettri della energia e dell'angolo di emissione per i mesoni K^+ e la distribuzione delle stelle. Viene valutata la frequenza di emissione di iperoni, ulteriori mesoni K^+ e iperframmenti associati. Sono descritti tre eventi particolarmente interessanti, uno dei quali ha permesso di calcolare la massa dell'iperone Σ^- in $(2344 \pm 6) m_e$.

Effects of Proton Correlations on the Scattering of High-Energy Electrons from Nuclei (*).

L. I. SCHIFF (+)

Laboratoire de Physique, École Normale Supérieure, Université de Paris

(ricevuto il 19 Febbraio 1957)

Summary. — This paper investigates the extent to which the correlations between protons in nuclear matter manifest themselves in the scattering of high-energy electrons from nuclei. The infinite-order Born series is summed, so that dispersion effects that arise from excitation of virtual intermediate nuclear states are included to all orders. Use is made of a high-energy approximation developed earlier, and of the static or adiabatic approximation for the nuclear protons, and these are justified for incident electrons; their validity for nucleon scattering is also discussed. Expressions for the large-angle elastic and inelastic differential scattering cross-sections are obtained in this way. It is then shown that correlation effects are difficult to identify so long as the final nuclear state is well-defined. On the other hand, if a sum over final states is carried out, the effects of short-range correlations between protons appear in a characteristic way in the summed differential cross-section. These results are in qualitative agreement with those obtained earlier by others on the basis of the first and second Born approximation.

1. — Introduction.

An interesting question related to the scattering of high-energy electrons from nuclei is the extent to which such experiments bring into evidence the short-range correlations in position between nucleons in nuclear matter. One

(*) Supported in part by the United States Air Force through the European Office, Air Research and Development Command.

(+) Professeur d'échange, and Fellow of the John Simon Guggenheim Memorial Foundation. Permanent address: Stanford University, Stanford, California, U.S.A.

might hope that under suitable conditions, a diffraction pattern characteristic of short-range order would appear in addition to the well-known ⁽¹⁾ diffraction pattern characteristic of the long-range order that arises from the finite size of the nucleus. Several recent calculations ⁽²⁻⁵⁾ of proton-correlation effects have been based on the first or second Born approximation. SMITH ⁽²⁾ and GATTO ⁽³⁾ made use of the first Born approximation, and found that correlation effects do not appear in the differential cross-section for elastic scattering or for inelastic scattering involving excitation of a particular energy level of the nucleus, but that they do appear when the cross-section is summed over all excited nuclear states. These results are in agreement with those for corresponding situations in atomic physics ⁽⁶⁾.

DOWNS ⁽⁴⁾ employed the second Born approximation and calculated only the elastic scattering. He found that there is a correlation contribution, but that it does not have a distinctive or easily recognizable form. The reason for this can be seen most readily from an examination of the paper of LEWIS ⁽⁵⁾, even though he used a different form for the two-proton distribution function. The Fourier transform of the correlation function, $G(\mathbf{K})$ in Lewis' notation, appears directly in the summed inelastic cross-section, his Eq. (19), where $\mathbf{K} = \mathbf{k}_i - \mathbf{k}_f$, and $\hbar\mathbf{k}_i$ and $\hbar\mathbf{k}_f$ are the initial and final momenta of the electron. It is this dependence on the momentum transfer $\hbar\mathbf{K}$, or on the scattering angle θ , since $K \cong 2k_i \sin \frac{1}{2}\theta$, which produces the diffraction pattern most characteristic of short-range order. On the other hand, the correlation function appears in the elastic scattering only in Lewis' Eq. (17c), through integrals involving $G(\mathbf{k}_i - \mathbf{k}')$ and $G(\mathbf{k}' - \mathbf{k}_f)$ over the variable \mathbf{k}' . If we consider for the moment the first of these integrals, we can change the variable of integration from \mathbf{k}' to $\mathbf{k}_i - \mathbf{k}'$, in which case it is apparent that the elastic scattering depends on an integral of G over its argument, and not on $G(\mathbf{K})$. This integration effectively smoothes out the characteristic dependence on \mathbf{K} ,

⁽¹⁾ B. HAHN, D. G. RAVENHALL and R. HOFSTADTER: *Phys. Rev.*, **101**, 1131 (1956) and earlier papers cited there.

⁽²⁾ J. H. SMITH: *Phys. Rev.*, **95**, 271 (1954).

⁽³⁾ R. GATTO: *Nuovo Cimento*, **2**, 669 (1955).

⁽⁴⁾ B. W. DOWNS: *Phys. Rev.*, **101**, 820 (1956). This paper is based on the formalism of an earlier paper by the present author: *Phys. Rev.*, **98**, 765 (1955), in which an estimate of the second-order (dispersion) contribution to the scattering is also made. As pointed out by LEWIS (reference ⁽⁵⁾), this estimate is incorrect; the error lies in the assumption that an integrand that contains a factor $\exp[\frac{1}{2}i\mathbf{q} \cdot \mathbf{s}]$ derives its main contribution from near $\mathbf{s}=0$, whereas actually such a factor does not in itself suffice to give the integrand a well-defined region of stationary phase (compare with reference ⁽⁸⁾). The paper of DOWNS replaces this estimate with a detailed calculation that is based on a specific model.

⁽⁵⁾ R. R. LEWIS: *Phys. Rev.*, **102**, 544 (1956).

⁽⁶⁾ L. VAN HOVE: *Phys. Rev.*, **95**, 249 (1954) and earlier papers cited there.

and yields a correlation contribution to the elastic cross-section that is much more difficult to recognize. The result of this smoothing can be seen in Lewis' Eq. (21), which is for example independent of K and a when K and k large are in comparison with a , that is, in the interesting case for which the wavelength is short in comparison with the correlation distance. In contrast, the correlation part of the summed inelastic cross-section is proportional to $G(K)$, and hence to $(a/K)^4$ in this case (7).

The purpose of the present paper is to determine whether or not this behavior is a property only of the first and second Born approximation. This question can be studied by employing a high-energy approximation method that sums the infinite-order Born series⁽⁸⁾: the application to the present situation is developed in Sect. 2. In order to carry through the calculation, the static or adiabatic approximation^(5,6,9) for the nuclear protons must also be employed. The use of both approximations is justified in Sect. 3 for electrons of more than about 200 MeV energy scattered from medium-weight to heavy nuclei, and their validity for nucleon scattering is also discussed. It is then shown, in Sect. 4, that the behavior described above for the first and second Born approximation is also obtained in the more general case considered here. In order to keep the calculation as simple as possible and still retain its essential features, only Coulomb scattering by the (point) protons is considered. It seems likely that scattering by the magnetic moments of the neutrons and protons, and finite nucleon size effects, will also have to be taken into account in any future comparison with experimental results, but this should not affect the qualitative conclusions obtained here.

2. - Scattered amplitude.

The wave equation for an electron interacting with a nucleus can be written

$$(1) \quad \begin{cases} H\Psi = (E_0 + E)\Psi, \\ H = H_N + i\hbar c\boldsymbol{\alpha} \cdot \boldsymbol{\nabla} - mc^2\beta + V, \\ H_N\psi_a = E_a\psi_a, \\ V(\mathbf{r}, \mathbf{R}_1 \dots \mathbf{R}_Z) = -\sum_{i=1}^Z e^2/|\mathbf{r} - \mathbf{R}_i|. \end{cases}$$

(7) This particular K -dependence is a consequence of the choice of an exponential form for the space correlation function.

(8) L. I. SCHIFF: *Phys. Rev.*, **103**, 443 (1956).

(9) D. M. CHASE: *Phys. Rev.*, **104**, 838 (1956) derives the adiabatic approximation in a different manner and uses it in a different context.

Here H is the entire Hamiltonian; Ψ is the entire wave function, which depends on the co-ordinate \mathbf{r} of the electron, the co-ordinates $\mathbf{R}_1 \dots \mathbf{R}_Z$ of the protons, and the co-ordinates $\mathbf{R}_{Z+1} \dots \mathbf{R}_A$ of the neutrons; H_N is the nuclear Hamiltonian with a complete orthonormal set of eigenfunctions ψ_a , and with eigenvalues E_a of which E_0 is the lowest; E is the total energy of the incident electron; and V is the Coulomb interaction energy between the electron and the nuclear protons. Ψ can be expanded in terms of the nuclear wave functions:

$$\Psi = \sum_a u_a(\mathbf{r}) \psi_a(\mathbf{R}_1 \dots \mathbf{R}_A),$$

and it is easily seen that the u 's satisfy the following set of simultaneous equations:

$$(2) \quad \begin{cases} (-i\hbar c \boldsymbol{\alpha} \cdot \nabla + mc^2 \beta + \hbar c \epsilon_b) u_b(\mathbf{r}) = \sum_a V_{ba}(\mathbf{r}) u_a(\mathbf{r}), \\ V_{ba}(\mathbf{r}) = \int \dots \int \bar{\psi}_b(\mathbf{R}_1 \dots \mathbf{R}_A) V(\mathbf{r}, \mathbf{R}_1 \dots \mathbf{R}_Z) \psi_a(\mathbf{R}_1 \dots \mathbf{R}_A) d\tau_1 \dots d\tau_A, \\ \hbar c \epsilon_b = E - E_b + E_0. \end{cases}$$

We wish solutions of Eqs. (2) that have the asymptotic forms:

$$(3) \quad \begin{cases} u_b(\hat{k}_b r) \xrightarrow{r \rightarrow \infty} \delta_{b0} a_0 \exp[i\mathbf{k}_0 \cdot \mathbf{r}] + r^{-1} \exp[ik_b r] f_b(\mathbf{k}_b, \mathbf{k}_0), \\ \epsilon_0 = E/\hbar c, \quad \mu = mc/\hbar, \quad k_b^2 = \epsilon_b^2 - \mu^2, \end{cases}$$

where a_0 is the incident electron spinor, and \hat{k}_b is a unit vector parallel to \mathbf{k}_b .

In analogy with the procedure adopted in reference (8), solutions with the asymptotic behavior of Eq. (3) can be obtained by rewriting Eq. (2) as an integral equation and iterating it an infinite number of times with the help of the Green's function $G_a(\mathbf{p}) = -(4\pi\epsilon)^{-1} \exp[ik_a \epsilon]$. The result is:

$$(4) \quad \begin{aligned} f_b(\mathbf{k}_b, \mathbf{k}_0) = & (4\pi)^{-1} (\epsilon_b - \boldsymbol{\alpha} \cdot \mathbf{k}_b - \mu\beta) \sum_{n=1}^{\infty} \int \dots \int (\hbar c)^{-n} \exp[-i\mathbf{k}_b \cdot \mathbf{r}_n] \cdot \\ & \cdot \sum_{a_{n-1}} V_{ba_{n-1}}(\mathbf{r}_n) (\epsilon_{a_{n-1}} + i\boldsymbol{\alpha} \cdot \nabla_n - \mu\beta) G_{a_{n-1}}(\mathbf{r}_n - \mathbf{r}_{n-1}) \cdot \\ & \cdot \sum_{a_{n-2}} V_{a_{n-1}a_{n-2}}(\mathbf{r}_{n-1}) (\epsilon_{a_{n-2}} + i\boldsymbol{\alpha} \cdot \nabla_{n-1} - \mu\beta) G_{a_{n-2}}(\mathbf{r}_{n-1} - \mathbf{r}_{n-2}) \dots \\ & \dots \sum_{a_1} V_{a_2a_1}(\mathbf{r}_2) (\epsilon_{a_1} + i\boldsymbol{\alpha} \cdot \nabla_2 - \mu\beta) G_{a_1}(\mathbf{r}_2 - \mathbf{r}_1) V_{a_10}(\mathbf{r}_1) \cdot \\ & \cdot a_0 \exp[i\mathbf{k}_0 \cdot \mathbf{r}_1] d\tau_1 \dots d\tau_n, \end{aligned}$$

Equation (4) is the exact expression for the elastic ($b = 0$) and inelastic ($b \neq 0$) scattering amplitudes.

We now make use of the high-energy approximation developed in reference (8), the applicability of which is justified in Sect. 3. This means that each operator ∇_m can be replaced by $ik_{a_{m-1}} \hat{\rho}_{m-1}$, where we continue to use the notation $\mathbf{p}_{m-1} = \mathbf{r}_m - \mathbf{r}_{m-1}$ ⁽¹⁰⁾. It also means that each term in the summation of Eq. (4) can be thought of as a sequence of very small-angle scatterings during which the electron propagates along a nearly straight line parallel to \mathbf{k}_a , followed by a single large-angle scattering through the angle θ (angle between \mathbf{k}_a and \mathbf{k}_b), and then followed by a sequence of very small-angle scattering during which the electron propagates along a nearly straight line parallel to \mathbf{k}_b . Thus there is one potential matrix element, say $V_{a_n a_{n-1}}(\mathbf{r}_m)$, which gives rise to a large-angle scattering and a large momentum change; all of the other V 's correspond to small momentum changes.

We then make a further approximation, according to which the closure relation may be used to carry out the summations over all the virtual intermediate nuclear states $a_1 \dots a_{n-1}$. As we shall see at the end of this section, this is equivalent to the adiabatic approximation for the nuclear protons. We assume that all of the potential matrix elements that correspond to small momentum changes are negligibly small in magnitude unless the energy difference between the two nuclear states used to calculate each of them is less than a certain small amount ΔE ; the validity of this assumption is established in Sect. 3. This permissible energy interval ΔE is chosen to facilitate the use of the closure relation, and is therefore defined in the following way. Consider a portion of the integrand of Eq. (4) that has the structure:

$$(5) \quad \sum_{a_g} V_{a_{g+1}a_g}(\mathbf{r}_{g+1})(\varepsilon_{a_g} - k_{a_g} \boldsymbol{\alpha} \cdot \hat{\rho}_g - \mu\beta) G_{a_g}(\mathbf{p}_g) V_{a_g a_{g-1}}(\mathbf{r}_g),$$

where we have replaced ∇_{g+1} by $ik_{a_g} \hat{\rho}_g$, as indicated above. We wish to perform the summation over a_g and make use of the closure relation for the nuclear eigenfunctions. In order to do this in the simplest way, we must be able to neglect the dependence of the other factors in (5) on a_g . There are three such factors, all of which depend only on the energy of the state a_g : ε_{a_g} , k_{a_g} , and G_{a_g} ; of these, at high energies, the last-named has the most sensitive dependence since it contains an exponential factor. What is required, then, is that the phase of G_{a_g} should not change appreciably when the energy of the state a_g changes by the amount ΔE . Since ϱ_g is of the order of the nuclear size R , this means that $R\Delta k \ll 1$ when Δk is the change in the k -value of

⁽¹⁰⁾ L. I. SCHIFF: *Phys. Rev.*, **104**, 1481 (1956); see footnote (2) and the discussion below Eq. (6) of this paper.

the electron that corresponds to the energy change ΔE of the electron or of the nucleus (because of Eq. (2), these are the same). Now for small changes in energy, $\Delta E = \hbar v \Delta k$, where v is the speed of the electron, regardless of whether or not the electron is relativistic. We thus require that:

$$(6) \quad R \Delta E / \hbar v \ll 1.$$

When the inequality (6) is satisfied (see Sect. 3), the summation over a_g in (5) is easily carried out with the help of the closure relation, and leads to:

$$\int \dots \int \bar{\psi}_{a_{g+1}}(\mathbf{r}_{g+1}, \mathbf{R}_i) V(\mathbf{r}_g, \mathbf{R}_i) \psi_{a_{g-1}}(\mathbf{r}_g, \mathbf{R}_i) d\tau_1 \dots d\tau_d (\varepsilon_{a_{g-1}} - k_{a_{g-1}} \cdot \hat{\mathbf{Q}}_g - \mu\beta) G_{a_{g-1}}(\mathbf{p}_g).$$

Similar summations can be performed for all of the other virtual intermediate states. It is not necessary that the one matrix element $V_{a_m a_{m-1}}(\mathbf{r}_m)$ that corresponds to large momentum change be small unless its states differ in energy by less than ΔE , since both of its nuclear states a_m and a_{m-1} also appear in neighbouring matrix elements that do satisfy this energy condition and hence can be summed over. Thus in Eq. (4), after all the summations are carried out, we are left with the matrix element of the product of all the potentials V taken between the initial and final nuclear states ψ_0 and ψ_b .

Application of the stationary phase approximation⁽⁸⁾ to the integration of (4) over all of the \mathbf{r} 's except \mathbf{r}_m means that each $\hat{\mathbf{Q}}_g$ can be replaced by $\hat{\mathbf{k}}_0$ if $g < m$, and by $\hat{\mathbf{k}}_b$ if $g > m$. Further, all of the parentheses involving operators ∇_g can be replaced by $(\varepsilon_0 - \boldsymbol{\alpha} \cdot \mathbf{k}_0 - \mu\beta)$ if $g \leq m$, and by $(\varepsilon_b - \boldsymbol{\alpha} \cdot \mathbf{k}_b - \mu\beta)$ if $g > m$. Equation (4) then becomes, for the most interesting case of large scattering angle:

$$(7) \quad f_b(\mathbf{k}_b, \mathbf{k}_0) = -(4\pi\hbar c)^{-1} \sum_{n=1}^{\infty} \sum_{m=1}^n (-i/2k_0\hbar c)^{n-m} (-i/2k_0\hbar c)^{m-1} \cdot \\ \cdot \int d\tau_m \int_0^{\infty} d\varrho_1 \dots \int_0^{\infty} d\varrho_{n-1} \exp[i\mathbf{q} \cdot \mathbf{r}_m] \{ V[\mathbf{r}_m + \hat{\mathbf{k}}_0(\varrho_{n-1} + \dots + \varrho_m)] \dots \\ \dots V[\mathbf{r}_m + \hat{\mathbf{k}}_b\varrho_m] V(\mathbf{r}_m) V(\mathbf{r}_m - \hat{\mathbf{k}}_0\varrho_{m-1}) \dots \\ \dots V[\mathbf{r}_m - \hat{\mathbf{k}}_0(\varrho_{m-1} + \dots + \varrho_1)] \}_{b0} (\varepsilon_b - \boldsymbol{\alpha} \cdot \mathbf{k}_b - \mu\beta)^{n-m+1} (\varepsilon_0 - \boldsymbol{\alpha} \cdot \mathbf{k}_0 - \mu\beta)^{m-1} a_0,$$

where $\mathbf{q} = \mathbf{k}_0 - \mathbf{k}_b$, $\{ \}_{b0}$ signifies the matrix element between initial and final nuclear states, and the proton co-ordinates are not written explicitly as arguments of the V 's. As in reference⁽⁸⁾, we are interested in $\bar{a}_b f_b$, where a_b is a final electron spinor. Then since $(\varepsilon_0 + \boldsymbol{\alpha} \cdot \mathbf{k}_0 + \mu\beta)a_0 = 0$ and $\bar{a}_b(\varepsilon_b + \boldsymbol{\alpha} \cdot \mathbf{k}_b + \mu\beta) = 0$, we have that

$$\bar{a}_b(\varepsilon_b - \boldsymbol{\alpha} \cdot \mathbf{k}_b - \mu\beta)^{n-m+1} (\varepsilon_0 - \boldsymbol{\alpha} \cdot \mathbf{k}_0 - \mu\beta)^{m-1} a_0 = (2\varepsilon_b)^{n-m+1} (2\varepsilon_0)^{m-1} \bar{a}_b a_0.$$

The summation over m and n can now be carried out as in reference (8), with the result that Eq. (7) becomes:

$$(8) \quad \bar{a}_b f_b(\mathbf{k}_b, \mathbf{k}_0) = -(\varepsilon_b/2\pi\hbar c) \int d\tau \left\{ V(\mathbf{r}) \exp \left[i\mathbf{q} \cdot \mathbf{r} - (i/\hbar r_0) \int_0^\infty V(\mathbf{r} - \hat{\mathbf{k}}_0 s) ds - \right. \right. \\ \left. \left. - (i/\hbar v_b) \int_0^\infty V(\mathbf{r} + \hat{\mathbf{k}}_b s) ds \right] \right\} \bar{a}_b a_0,$$

where r_0 and v_b are the initial and final electron speeds, and again the proton co-ordinates are not written explicitly as arguments of the V 's. The large-angle scattering case represented by Eq. (8) is of greatest physical interest since diffraction due to short-range order is expected to be most prominent at large angles. A corresponding formula for small angles could also be obtained without further difficulty.

Equation (8) is in agreement with the well-known corresponding expression derived on the basis of the first Born approximation, except that the phase factors $\int V ds$ are included in the exponent before the matrix element is taken between initial and final nuclear states. This is a partial justification for referring to the present procedure as an adiabatic approximation, since the scattered amplitude is calculated, by means of the formalism of reference (*), as though the protons are at rest (with, however, allowance being made for the difference in speed of the electron before and after the large-angle scattering occurs), and then the matrix element of this amplitude is computed ⁽¹¹⁾.

A separate justification for calling this an adiabatic approximation comes from examination of the inequality (6). If ΔE is the energy spread of those virtual intermediate states of the nucleus that make a significant contribution to the scattering, then $\hbar/\Delta E$ has the order of magnitude of the period of the most important nuclear motions. But since R/r is the transit time of the electron across the nucleus, (6) states that the electron must cross the nucleus in a time short in comparison with the nuclear periods, so that the protons can be regarded as stationary during the scattering process ⁽¹¹⁾.

3. - Validity of the adiabatic and high-energy approximations.

The development of the preceding section is based on the assumption that the adiabatic approximation expressed by the inequality (6) and the high-energy approximation of reference (*) are applicable. Their validity can

⁽¹¹⁾ Similar remarks appear in a different connection in the paper of CHASE (reference (9)).

be gauged by examining the dependence of the Fourier transform of a typical potential matrix element

$$(9) \quad \int V_{ba}(\mathbf{r}) \exp[i\mathbf{x} \cdot \mathbf{r}] d\mathbf{r} = -(4\pi e^2/\kappa^2) \left(\sum_{i=1}^Z \exp[i\mathbf{x} \cdot \mathbf{R}_i] \right)_{ba},$$

on κ and on $\Delta E = E_b - E_a$. It is important to note that both of these approximations involve only the many matrix elements that correspond to very small momentum changes, and not the one matrix element that corresponds to the large momentum change $\hbar\mathbf{q}$. Thus we are concerned primarily with small values of κ .

The diagonal element ($b = a$) of Eq. (9) has $\Delta E = 0$ and is equal to

$$(10) \quad -(4\pi e^2/\kappa^2) Z F_a(\kappa),$$

where $F_a(\kappa)$ is the form factor, or Fourier transform, of the expectation value of the charge density for the state a , normalized so that $F_a(0) = 1$. For all except the lightest nuclei, the general dependence of $F_a(\kappa)$ on κ is much the same for the state a as for the ground state 0, since all or nearly all of the protons occupy the normal nuclear volume. Thus $F_a(\kappa)$ is roughly equal to unity for $\kappa \lesssim 1/R$, and falls off for larger κ .

The off-diagonal elements of (9) can be classified according as the states b and a differ by excitation of a collective mode or differ by excitation of one or more nucleons. The matrix elements for collective excitation are smaller than but comparable in magnitude with the diagonal element (10), and for them $\Delta E \lesssim 1$ MeV for medium-weight to heavy nuclei. We ignore the matrix elements for nucleon excitation for the present, and show in the next paragraph that they can be neglected in comparison with (10). Now for $\Delta E = 1$ MeV and $R = 7 \cdot 10^{-13}$ cm (a very large nucleus), we have that $R \Delta E / \hbar c = 0.036$, so that the inequality (6) is well-satisfied and the use of the adiabatic approximation is justified. Further, in accordance with the discussion following Eq. (13) of reference (8), the high-energy approximation requires that $R/\kappa a^2 \ll 1$ and $VR^2/Ea^2 \ll 1$, where a is the distance over which the potential changes by an appreciable fraction of itself. Because of the slowly-varying character of the Coulomb interaction, $a \sim R$; also, the second condition will be less restrictive than the first for the Coulomb potential. Thus so long as $\kappa R \gg 1$, or $E \gtrsim 40$ MeV for a moderately heavy nucleus, the high-energy approximation can be used.

We shall use the individual-particle model to estimate the matrix elements for nucleon excitation. Then single-proton excitation is most important, and Eq. (9) is of order

$$(11) \quad (4\pi e^2/\kappa^2) F'_{ab}(\kappa),$$

where $F'_{ab}(z)$ is the form factor for the single-particle transition. This form factor is zero for $z = 0$, because of the orthogonality of the initial and final proton wave functions. It is probably a generally increasing function of z until it becomes roughly equal to unity for z so large that direct proton ejection takes place, at which point $\Delta E \sim \hbar^2 z^2 / 2M$. Thus (11) is smaller than (10) by at least a factor $1/Z$ for small values of z . When z has increased to about 10^{13} cm^{-1} , and proton ejection is setting in with $\Delta E \sim 20 \text{ MeV}$, (11) is still very small compared to (10) calculated with $z \lesssim 1/R$, by at least a factor $(10^{-26} \text{ cm}^2)/ZR^2$. The margin by which our estimate shows that the nucleon-excitation matrix elements of Eq. (9) are negligible is so great that a more quantitative discussion does not seem likely to lead to a different conclusion ⁽¹²⁾.

Considerations of this kind can also be applied to the scattering of fast nucleons by nuclei. In this case the interaction potential is much more complicated than the Coulomb interaction, because of its exchange character and isotopic spin dependence. Since for a discussion of validity criteria we are only concerned with small momentum transfers, we shall simplify the situation by assuming that the diagonal and collective off-diagonal matrix elements analogous to Eq. (9) are determined by the optical model potential, and that the nucleon-excitation off-diagonal matrix elements are determined by the nucleon-nucleon interaction. The optical model potential has a strength V_0 extending over the nuclear volume, and the nucleon-nucleon potential has a strength V_N extending over about $1/A$ of the nuclear volume. Thus we expect the first group of matrix elements to be roughly equal to $(4\pi R^3/3)V_0$ for $z \lesssim 1/R$, and to fall off for larger z ; and we expect the second group to be roughly equal to $(4\pi R^3/3A)V_N F'_{ba}(z)$ for $z \lesssim A^{1/3}/R$, and to fall off for larger z . As with electron scattering, $\Delta E \lesssim 1 \text{ MeV}$ for the first group, and for the second group ΔE approaches $\hbar^2 z^2 / 2M$ as z becomes large enough so that direct nucleon ejection takes place. Finally, the v that appears in the inequality (6) is somewhat less than c for incident nucleons; for example, $v = \frac{1}{2}c$ for 140 MeV incident nucleons, for which $k = 2.7 \cdot 10^{13} \text{ cm}^{-1}$.

⁽¹²⁾ LEWIS (reference ⁽⁵⁾) concludes that the adiabatic approximation is no longer valid for 300 MeV electrons. His argument is based on the fact that the matrix elements for direct proton ejection when $z \sim q$, which are of order $4\pi e^2/q^2$, exceed the diagonal matrix elements for the same z , which are of order $(4\pi e^2/q^2)ZF_a(q)$, when E becomes so large that $ZF_a(q)$ is less than unity. He used the second Born approximation, so that one of the two scatterings is through a small angle, as indeed is pointed out elsewhere in his paper. Therefore, he should only have compared the matrix elements for the small-angle scatterings, not for the large-angle scattering for which $z=q$, in order to establish that the closure relation can be employed. Since for small z the diagonal and collective off-diagonal matrix elements dominate, this would have led him to the conclusion expressed in the present paper, according to which the adiabatic approximation is valid for arbitrarily high electron energy.

Since AV_0/V_N is much larger than unity for moderately heavy nuclei, the first group of matrix elements calculated with $\kappa \lesssim 1/R$ is much larger than the second group. Further, the use of v instead of c in (6) will not be important so long as $\Delta E \lesssim 1$ MeV. Thus the adiabatic approximation can also be used for nucleon scattering. As before, the high-energy approximation requires that $R/ka^2 \ll 1$ and $V_0 R^2/E'a^2 \ll 1$, where now E' is the kinetic energy of the incident nucleon, and $a \lesssim R/3$ for the optical model potential. In contrast with electron scattering, the second condition is now more restrictive than the first, so that E' must be large in comparison with $V_0 R^2/a^2$. This makes E' so large that the validity of the underlying equations of motion is open to serious doubt.

It is worth noting that a procedure analogous to that developed in this paper for electron scattering fails for nucleon scattering because of the rapidly-varying character of the optical model potential near the edge of the nucleus, and not because of the excitation of virtual intermediate nuclear states. This suggests that the large-angle elastic and inelastic nuclear scattering of nucleons with more than a hundred MeV energy could perhaps be calculated reasonably well by starting with wave functions computed for the optical model potential. These would take into account the distortion due to the many small-angle scatterings, and one would hope that the one large-angle scattering could be calculated as a single matrix element of an appropriate operator between such wave functions. No justification for such a procedure has been attempted.

4. - Identification of correlation effects.

The differential cross-section for large-angle elastic or inelastic scattering of the electron through the angle between \mathbf{k}_0 and \mathbf{k}_b , in which the nucleus is left in the state b , can be obtained from Eq. (8) in the usual way. For high electron energy the result is

$$(12) \quad \sigma_{b0}(\theta) = (\epsilon_b \cos \frac{1}{2}\theta/2\pi\hbar e)^2 \left| \int d\tau \left\{ V(\mathbf{r}) \exp \left[i\mathbf{q} \cdot \mathbf{r} - (i/\hbar c) \int_0^\infty V(\mathbf{r} - \hat{k}_0 s) ds - \right. \right. \right. \\ \left. \left. \left. - (i/\hbar c) \int_0^\infty V(\mathbf{r} + \hat{k}_b s) ds \right\} \right|_{b0}^2,$$

where $\hbar c \epsilon_b$ is the energy of the outgoing electron, and the proton co-ordinates are not written explicitly as arguments of the V 's. It is not necessary that the initial and final nuclear states be close together in energy. For example, Eq. (12) applies as well to elastic scattering as to electron disintegration of the nucleus.

Exact evaluation of Eq. (12) would require precise knowledge of the initial and final nuclear wave functions ψ_0 and ψ_b . Alternatively, (12) could be expressed in terms of one-proton, two-proton, etc., transition charge densities (^{4,5}); however, an infinite number of these would be required, since the expansion of the exponential function of the V 's brings arbitrarily high powers into the integrand. While this is a natural consequence of an infinite-order calculation such as that of Sect. 2, it makes the interpretation of Eq. (12) impossibly complicated. We therefore adopt an approximation which makes further analysis feasible.

We assume that for all those nucleon configurations for which $\psi_b\psi_0$ is appreciably different from zero, the protons have roughly their normal distribution throughout the nuclear volume. Then $V(\mathbf{r}, \mathbf{R}_1 \dots \mathbf{R}_Z)$ is close to $V_c(\mathbf{r})$, which is the static Coulomb potential of the nucleus in its ground state. We now replace each of the V 's in the exponent by $V_c + (V - V_c)$, expand the exponential functions of $(V - V_c)$, and keep a small number of terms. This should be a good approximation, first because the difference between the Coulomb potentials V and V_c is much less than the difference between the proton distributions that give rise to them, and second because the integration over s further smoothes out the dependence on the co-ordinate \mathbf{r} .

The leading term of this expansion involves the matrix element $V_{i0}(\mathbf{r})$, and hence only the one-proton transition charge density. In order to obtain a proton-correlation effect, it is necessary to keep the second term as well. This yields factors of the general form

$$(13) \quad \int d\tau \left\{ V(\mathbf{r}, \mathbf{R}_1 \dots \mathbf{R}_Z) \int_0^\infty V(\mathbf{r} - \hat{k}_0 s, \mathbf{R}_1 \dots \mathbf{R}_Z) ds \cdot \right. \\ \left. \cdot \exp \left[i\mathbf{q} \cdot \mathbf{r} - (i/\hbar c) \int_0^\infty V_c(\mathbf{r} - \hat{k}_0 s) ds - (i/\hbar c) \int_0^\infty V_c(\mathbf{r} + \hat{k}_0 s) ds \right] \right\}_{b0}.$$

Now (13) clearly involves the two-proton transition charge density, and therefore, at least in principle, it exhibits the effects of correlations between protons. However, these effects are very difficult to identify in the angular distribution of the scattered electrons, that is, in the dependence of (13) on q .

This can be seen by considering a simplified version of (13):

$$(14) \quad \iiint V_1(\mathbf{r} - \mathbf{R}_1) V_2(\mathbf{r} - \mathbf{R}_2) \varrho(\mathbf{R}_1) g(\mathbf{R}_1 - \mathbf{R}_2) \exp[i\mathbf{q} \cdot \mathbf{r}] d\tau d\tau_1 d\tau_2,$$

in which we have dropped the integration over s and over all the nuclear co-ordinates except \mathbf{R}_1 and \mathbf{R}_2 , omitted the slowly-varying factors $\int V_c ds$ in the

exponent, and chosen the simplified form $\varrho(\mathbf{R}_1)g(\mathbf{R}_1 - \mathbf{R}_2)$ for the two-proton transition charge density. Writing V_1 , V_2 , ϱ and g as Fourier integrals, (14) is equal to

$$(15) \quad \iiint \iiint \iiint \varphi_1(\mathbf{k}_1) \varphi_2(\mathbf{k}_2) F(\mathbf{x}) G(\boldsymbol{\gamma}) \exp [i(\mathbf{q} \cdot \mathbf{r} + \mathbf{k}_1 \cdot (\mathbf{r} - \mathbf{R}_1) - \mathbf{k}_2 \cdot (\mathbf{r} - \mathbf{R}_2) + \mathbf{x} \cdot \mathbf{R}_1 + \boldsymbol{\gamma} \cdot (\mathbf{R}_1 - \mathbf{R}_2))] d\tau d\tau_1 d\tau_2 d\mathbf{k}_1 d\mathbf{k}_2 d\mathbf{x} d\boldsymbol{\gamma} = \\ = (2\pi)^9 \iiint \varphi_1(\mathbf{k}_1) \varphi_2(\mathbf{k}_2) F(\mathbf{x}) G(\boldsymbol{\gamma}) \delta(\mathbf{q} + \mathbf{k}_1 + \mathbf{k}_2) \delta(\mathbf{x} + \boldsymbol{\gamma} - \mathbf{k}_1) \cdot \\ \cdot \delta(\boldsymbol{\gamma} + \mathbf{k}_2) d\mathbf{k}_1 d\mathbf{k}_2 d\mathbf{x} d\boldsymbol{\gamma} = (2\pi)^9 F(-\mathbf{q}) \int \varphi_1(\boldsymbol{\gamma} - \mathbf{q}) \varphi_2(-\boldsymbol{\gamma}) G(\boldsymbol{\gamma}) d\boldsymbol{\gamma}.$$

Now in order that we may be able to see correlation effects clearly, (15) should involve a factor $G(\mathbf{q})$: the Fourier component of the correlation function g that corresponds to the momentum transfer $\hbar\mathbf{q}$. Actually, it involves an integral of G over its argument, so that the dependence of (15) on \mathbf{q} is not at all characteristic of g . This is precisely the difficulty pointed out in Sect. 1 in connection with the results of ref. (5) (our \mathbf{q} is the same as Lewis' \mathbf{K}), so that inclusion of all orders of the Born approximation does not change the situation in this respect.

The essential property of (14) from which this result stems is that the only rapidly-varying factor, $\exp[i\mathbf{q} \cdot \mathbf{r}]$, involves only one co-ordinate \mathbf{r} , which is connected with all the proton co-ordinates, in this case \mathbf{R}_1 and \mathbf{R}_2 . It is apparent that not only (13), but also (12), before the assumption of the smallness of $(V - V_c)$ is made, share this property. Thus even if Eq. (12) could be evaluated without further approximation, it would not show the most characteristic correlation effects. What is required to exhibit two-proton correlations clearly is an expression in which the rapidly-varying factor involves two co-ordinates which are connected with the co-ordinates of two different protons, for example $\exp[i\mathbf{q} \cdot (\mathbf{r} - \mathbf{r}')]$, where \mathbf{r} is connected with \mathbf{R}_1 and \mathbf{r}' with \mathbf{R}_2 . A simple form analogous to (14) that has this structure is

$$(16) \quad \iiint \iiint V_1(\mathbf{r} - \mathbf{R}_1) V_2(\mathbf{r}' - \mathbf{R}_2) \varrho(\mathbf{R}_1) g(\mathbf{R}_1 - \mathbf{R}_2) \exp[i\mathbf{q} \cdot (\mathbf{r} - \mathbf{r}')] d\tau d\tau' d\tau_1 d\tau_2.$$

Proceeding as with (14), it is easily seen that (16) is equal to

$$(2\pi)^{12} \varphi_1(-\mathbf{q}) \varphi_2(\mathbf{q}) F(0) G(-\mathbf{q}),$$

which has the required form.

An expression that has a structure like (16) can be obtained from (12) by summation over the final nuclear states b for fixed scattering angle θ . As is

well known^(2,3,5,6), the closure relation for the nuclear states can be employed if the dependence of ε_b and \mathbf{q} on \mathbf{b} is neglected. The result is

$$(17) \quad \sum_b \sigma_{b0}(\theta) \cong (E \cos \frac{1}{2}\theta / 2\pi\hbar^2 c^2)^2 \left\{ \iint d\tau d\tau' V(\mathbf{r}) V(\mathbf{r}') \exp[i\mathbf{q} \cdot (\mathbf{r} - \mathbf{r}')] \cdot \right. \\ \left. \cdot \exp[-(i/\hbar c)] \int_0^\infty [V(\mathbf{r} - \hat{k}_0 s) + V(\mathbf{r} + \hat{k}_0 s) - V(\mathbf{r}' - \hat{k}_0 s) - V(\mathbf{r}' + \hat{k}_0 s)] ds \right\}_{00}.$$

Here E is the incident electron energy, and the proton co-ordinates are not written explicitly as arguments of the V 's; they are of course the same co-ordinates $\mathbf{R}_1 \dots \mathbf{R}_Z$ regardless of whether V depends on \mathbf{r} or on \mathbf{r}' . It should be emphasized that the approximation involved in using the closure relation to obtain (17) is very much poorer than that involved in its use in the work of Sect. 2. This is because for large θ , $\sigma_{b0}(\theta)$ for large electron energy loss may be comparable with or larger than that for small energy loss.

Equation (17) can be simplified in the same way as Eq. (12), by replacing each V in the exponent by $V_c + (V - V_c)$, and expanding the exponential functions of $(V - V_c)$. Two-proton correlation effects now appear in the leading term of this expansion, which is

$$(18) \quad \left\{ \begin{aligned} & (E \cos \frac{1}{2}\theta / 2\pi\hbar^2 c^2)^2 \iint d\tau d\tau' \{ V(\mathbf{r}, \mathbf{R}_1 \dots \mathbf{R}_Z) V(\mathbf{r}', \mathbf{R}_1 \dots \mathbf{R}_Z) \}_{00} \cdot \\ & \cdot u(\mathbf{r}, \mathbf{r}') \exp[i\mathbf{q} \cdot (\mathbf{r} - \mathbf{r}')], \\ & u(\mathbf{r}, \mathbf{r}') = \exp[-(i/\hbar c)] \int_0^\infty [V_c(\mathbf{r} - \hat{k}_0 s) + \\ & + V_c(\mathbf{r} + \hat{k}_0 s) - V_c(\mathbf{r}' - \hat{k}_0 s) - V_c(\mathbf{r}' + \hat{k}_0 s)] ds. \end{aligned} \right.$$

This can be expressed conveniently in terms of the one-proton and two-proton charge densities for the ground state:

$$(19) \quad \left\{ \begin{aligned} & \varrho_{00}^{(1)}(\mathbf{R}) = \int \dots \int \bar{\psi}_0(\mathbf{R}_1 \dots \mathbf{R}_A) \sum_{i=1}^Z \delta(\mathbf{R} - \mathbf{R}_i) \psi_0(\mathbf{R}_1 \dots \mathbf{R}_A) d\tau_1 \dots d\tau_A, \\ & \varrho_{00}^{(2)}(\mathbf{R}, \mathbf{R}') = \int \dots \int \bar{\psi}_0(\mathbf{R}_1 \dots \mathbf{R}_A) \sum_{i=1}^Z \sum_{j \neq i}^Z \delta(\mathbf{R} - \mathbf{R}_i) \cdot \\ & \cdot \delta(\mathbf{R}' - \mathbf{R}_j) \psi_0(\mathbf{R}_1 \dots \mathbf{R}_A) d\tau_1 \dots d\tau_A, \end{aligned} \right.$$

if we take advantage of the slow variation of $u(\mathbf{r}, \mathbf{r}')$ in comparison with the matrix element $\{ \}_{00}$.

We consider a portion of (18), and rewrite it in terms of new variables $\boldsymbol{\rho} = \mathbf{r} - \mathbf{R}_i$ and $\boldsymbol{\rho}' = \mathbf{r}' - \mathbf{R}_j$:

$$\begin{aligned}
 (20) \quad & \iint d\tau d\tau' |\mathbf{r} - \mathbf{R}_i|^{-1} |\mathbf{r}' - \mathbf{R}_j|^{-1} u(\mathbf{r}, \mathbf{r}') \exp[i\mathbf{q} \cdot (\mathbf{r} - \mathbf{r}')] = \\
 & = \exp[i\mathbf{q} \cdot (\mathbf{R}_i - \mathbf{R}_j)] \iint d\tau_\theta d\tau'_\theta (\varrho\varrho')^{-1} u(\mathbf{R}_i + \boldsymbol{\rho}, \mathbf{R}_j + \boldsymbol{\rho}') \exp[i\mathbf{q} \cdot (\boldsymbol{\rho} - \boldsymbol{\rho}')] \cong \\
 & \cong u(\mathbf{R}_i, \mathbf{R}_j) \exp[i\mathbf{q} \cdot (\mathbf{R}_i - \mathbf{R}_j)] \iint d\tau_\theta d\tau'_\theta (\varrho\varrho')^{-1} \exp[i\mathbf{q} \cdot (\boldsymbol{\rho} - \boldsymbol{\rho}')] = \\
 & = (4\pi/q^2)^2 u(\mathbf{R}_i, \mathbf{R}_j) \exp[i\mathbf{q} \cdot (\mathbf{R}_i - \mathbf{R}_j)].
 \end{aligned}$$

We have kept only the leading term of the expansion of u about the point $\mathbf{R}_i, \mathbf{R}_j$ in going from the second to the third line of (20); this is equivalent to neglecting terms of relative order $(uq)^{-1} \nabla_i u \sim V_c/\hbar c q$. For large-angle scattering, this is of order V_c/E , and hence much smaller than unity whenever the high-energy approximation is valid. Substitution of (19) and (20) into (18) gives:

$$\begin{aligned}
 (21) \quad & (E \cos \frac{1}{2}\theta/2\pi\hbar^2 c^2)^2 (4\pi c^2/q^2)^2 \left\{ \sum_{i=1}^Z \sum_{j=1}^Z u(\mathbf{R}_i, \mathbf{R}_j) \exp[i\mathbf{q} \cdot (\mathbf{R}_i - \mathbf{R}_j)] \right\}_{00} = \\
 & = (2c^2 E \cos \frac{1}{2}\theta/\hbar^2 c^2 q^2)^2 \left\{ Z + \iint \varrho_{00}^{(2)}(\mathbf{R}, \mathbf{R}') u(\mathbf{R}, \mathbf{R}') \exp[i\mathbf{q} \cdot (\mathbf{R} - \mathbf{R}')] d\tau_R d\tau_{R'} \right\},
 \end{aligned}$$

where we have made use of the obvious relations

$$u(\mathbf{R}, \mathbf{R}) = 1 \quad \text{and} \quad \int \varrho_{00}^{(0)}(\mathbf{R}) d\tau_R = Z.$$

Equation (21) closely resembles the corresponding expression derived from the first Born approximation^(2,3,5). The first term in the curly brackets is the total scattering from Z independent point protons, and would be modified if the finite size of the proton were to be taken into account. The second term is sensitive to the two-proton correlation function, and differs from the well-known corresponding term based on the first Born approximation only in the inclusion of the slowly-varying phase factor $u(\mathbf{R}, \mathbf{R}')$.

We conclude from this investigation that proton-correlation effects will be very difficult to identify in high-energy electron scattering processes in which the nucleus is left in a well-defined final state, but will be easily recognizable in the total differential scattering cross section, summed over inelastic processes. These conclusions are in qualitative agreement with those

obtained earlier from studies based on the first and second Born approximation. We have now extended them to the infinite-order Born series, so that they are valid for heavy nuclei.

* * *

The author takes pleasure in acknowledging the hospitality extended to him by the Laboratoire de Physique, École Normale Supérieure, during the 1956-57 academic year.

RIASSUNTO (*)

Il presente lavoro studia fino a che punto le correlazioni tra protoni nella materia nucleare si manifestano nello scattering di elettroni di alta energia provocato da nuclei. Si somma la serie di Born di ordine infinito in modo da comprendere in tutti gli ordini gli effetti di dispersione insorgenti dall'eccitazione di stati nucleari virtuali intermedi. Si fa uso di un'approssimazione in alta energia precedentemente sviluppata e dell'approssimazione statica o adiabatica per i protoni nucleari e queste si giustificano per gli elettroni incidenti; si discute anche la loro validità per lo scattering dei nucleoni. Si ottengono in tal modo espressioni per le sezioni d'urto dello scattering differenziale a grandi angoli elastico ed anelastico. Si dimostra poi che è difficile identificare gli effetti di correlazione finchè lo stato nucleare finale è ben definito. D'altra parte se si esegue una somma sugli stati finali, gli effetti delle correlazioni a range breve fra protoni appaiono in modo caratteristico nella sezione d'urto differenziale risultante dalla somma. Questi risultati sono qualitativamente in accordo con quelli ottenuti precedentemente da altri autori sulla base della prima e della seconda approssimazione di Born.

(*) Traduzione a cura della Redazione.

Machine Analysis of Pion Scattering by the Maximum Likelihood Method (*).

H. L. ANDERSON and W. C. DAVIDON (**)

Enrico Fermi Institute for Nuclear Studies, The University of Chicago - Chicago, Ill.

(ricevuto il 22 Febbraio 1957)

Summary. — We report here the method used to carry out a phase shift analysis of the pion-proton scattering events found in photographic emulsions and in the hydrogen diffusion cloud chamber. The method uses an electronic computer to find the best set of phase shifts for a set of scattering events having a given energy, according to a maximum likelihood criterium. This problem was coded for the electronic computer, Avidac, of the Argonne National Laboratory, and used to analyze the events found by various groups of experimenters. Most of the results have already been reported. The analyses were carried out for positive pions scattered by protons and could include *d*-waves as well as *s*- and *p*-waves, together with the effect of the Coulomb interaction.

1. — Maximum likelihood method.

The typical scattering experiment carried out with emulsions, or with an hydrogen diffusion cloud chamber provides a set of angles at which scattering events were found, all at fairly nearly the same energy. The analysis is simplified if the efficiency of observation is independent of the angle of the event. This was the case for most of the work analyzed thus far. A modified code can accommodate different efficiencies in as many as ten different angular ranges. The method of analysis was outlined in the thesis of H. TAFT (1).

(*) Research supported by a joint program of the United States Office of Naval Research, and the United States Atomic Energy Commission.

(**) Now at the Argonne National Laboratory, Lemont, Illinois.

(1) H. D. TAFT: *Phys. Rev.*, **101**, 1116 (1956).

A more complete discussion of the maximum likelihood method applied to the analysis of experiments has been given by SOLMITZ ⁽²⁾.

Let

$$(1) \quad S(x, \alpha) = \frac{d\sigma}{dx},$$

be the differential cross-section, given as a function of $x = 2.7 \cos \theta$ and phase shift angles α , which are capable of describing the scattering. The probability of finding an event within the angular range dx , when there are N scattering centers per cm^2 , is $NS(x, \alpha)dx$. The probability of finding no event in the range dx is $1 - NS(x, \alpha)dx$. The probability of finding a particular distribution of events x_1, x_2, \dots, x_p is the product,

$$(2) \quad P = \prod_{i \neq j} (1 - NS(x_i, \alpha)dx_i) \prod_{j=1}^p NS(x_j, \alpha)dx_j \exp[-t^2/2].$$

The last factor, $\exp[-t^2/2]$, is introduced to take into account the uncertainty in the value of N . It is the probability that the value taken differs from its most probable value N_0 by the amount t , i.e. that $N = N_0 + \mu t$, μ being the standard uncertainty in N_0 . The index i varies over all the angular range looked for in the scanning, so that with dx taken small enough,

$$\begin{aligned} \prod_i (1 - NS(x_i, \alpha)dx_i) &= \prod_i \exp[-NS(x_i, \alpha)dx_i] \\ &= \exp\left[-N \int_{x_{\min}}^{x_{\max}} S(x, \alpha)dx\right], \\ &= \exp[-N\sigma]. \end{aligned}$$

By σ we mean the total cross-section for the angular range covered in the experiment. The index j covers only those values of x at which events were found.

$$(3) \quad \log P = -N\sigma + \sum_{j=1}^p \log [NS(x_j, \alpha)] - t^2/2 + \sum_{j=1}^p \log dx_j.$$

The last term is a constant and is dropped for the purpose of writing the logarithm of the *relative* probability

$$(4) \quad w = -N\sigma + \sum_{j=1}^p \log [NS(x_j, \alpha)] - t^2/2.$$

(2) F. SOLMITZ: *Rev. Mod. Phys.* (in press).

The maximum likelihood method consists in finding those values of the α 's and t which maximize v .

The formula for the differential cross-section which we used was based on one derived by SOLMITZ⁽³⁾, adding terms for d -waves and taking Coulomb phase factors into account up to and including terms of first order in the quantity

$$n = \frac{e^2}{\hbar c} \frac{1}{\beta_\pi},$$

where $\beta_\pi = (1/c)$ times the velocity of the pion in the laboratory.

We used

$$(5) \quad S(x, \alpha) = |f(x, \alpha)|^2 + |g(x, \alpha)|^2,$$

where

$$(6) \quad kf(x) = \frac{1}{2i} \left\{ e_0 + (1 + 2in)(2e_1^+ + e_1^-)x + (1 + 3in)(3e_2^+ + 2e_2^-) \frac{3x^2 - 1}{2} \right\} + \left(-\frac{n}{1-x} + a \right) \left(1 - in \log \frac{1-x}{2} \right),$$

$$(7) \quad kg(x) = -(1-x^2)^{\frac{1}{2}} \left[\frac{1}{2i} \left\{ (1 + 2in)(e_1^+ - e_1^-) + (1 + 3in)(e_2^+ - e_2^-)3x \right\} - \frac{b}{1-x} \right],$$

where k = wave number of the pion in center of mass system

$$a = \frac{n\beta'_p}{1 + \beta'_\pi\beta'_p} \left[\beta'_\pi + \frac{2\mu_p - 1}{2} \beta'_p \right],$$

$$b = \frac{n\beta'_p}{1 + \beta'_\pi\beta'_p} \left[\mu_p\beta'_\pi + \frac{2\mu_p - 1}{2} \beta'_p \right],$$

$\beta'_\pi = (1/c) \times$ velocity of the pion in the center of mass system;

$\beta'_p = (1/c) \times$ velocity of the proton in the center of mass system;

μ_p = magnetic moment of the proton in nuclear magnetons = 2.7896;

$e_i^\pm = \exp[2i\alpha_{3,2l\pm 1}] - 1$;

$\alpha_{3,2l\pm 1}$ is the phase shift of the scattered wave in the isotopic spin $\frac{3}{2}$ state and with total angular momentum $j\hbar = (l \pm \frac{1}{2})\hbar$.

Following Fermi's notation⁽⁴⁾, the s -wave phase shift is written α_3 , the

⁽³⁾ F. SOLMITZ: *Phys. Rev.*, **94**, 1799 (1954).

⁽⁴⁾ H. L. ANDERSON, E. FERMI, R. MARTIN and D. E. NAGLE: *Phys. Rev.*, **91**, 155 (1953).

p -wave phase shifts α_{31} and α_{33} , while to avoid ambiguity, the d -wave phase shifts are written δ_{33} and δ_{35} . These five phase shifts are varied, and in addition, the parameter t , in finding the maximum value for w .

An important feature of the use of an electronic computer in finding the maximum value of w is that not much more work is entailed in carrying out an error analysis for the quantities determined. The general idea is the same as that followed by ANDERSON, DAVIDON, GLICKSMAN and KRUSE⁽⁵⁾. We assume that in the region near its maximum, the quantity w varies quadratically with the deviations of the parameters from their best fit values. Thus, we assume

$$(8) \quad w = w_0 - \frac{1}{2} \sum_{i,j} G_{ij} \varepsilon_i \varepsilon_j,$$

where w_0 is the maximum value of w in this region, ε_i is the deviation of the i^{th} parameter from its best fit value, and G_{ij} is the $(ij)^{\text{th}}$ element of a real symmetric matrix with positive eigenvalues. The matrix elements G_{ij} are determined by varying all the parameters individually and in pairs until w is diminished by $\frac{1}{2}$ in each case. With the notation S_{i+} (S_{i-}) equal to the increase (decrease) in α_i necessary to decrease w from its maximum value by $\frac{1}{2}$, G_{ii} is evaluated from

$$(9) \quad G_{ii} = 4(S_{i+} + S_{i-})^{-2}.$$

For the off-diagonal elements, pairs of parameters were varied. The magnitude of the variation was kept equal for each member of the pair, but all combinations of signs were used. With $S_{i+,j+}$, $S_{i+,j-}$, $S_{i-,j+}$, $S_{i-,j-}$ representing the change in each of the parameters i and j with the signs indicated, to give $w_0 - w = \frac{1}{2}$, G_{ij} is obtained from

$$(10) \quad G_{ij} = (S_{i+,j+} + S_{i-,j-})^{-2} - (S_{i+,j-} + S_{i-,j+})^{-2}.$$

This method for determining G gives an exact result if the surface $w - w_0 = \frac{1}{2}$ is truly an hyper-ellipse centered at the nominal maximum. G is not affected to first order by a small displacement of the hyper-ellipse in any direction.

Since e^w is the relative probability of having obtained the experimental results, given any particular set of parameters, the accuracy with which these parameters have been determined may be expressed by the error matrix G^{-1} with the property

$$(11) \quad \overline{\varepsilon_i \varepsilon_j} = \frac{\int \dots \int \varepsilon_i \varepsilon_j e^w d\varepsilon_1 d\varepsilon_2 \dots d\varepsilon_m}{\int \dots \int e^w d\varepsilon_1 d\varepsilon_2 \dots d\varepsilon_m} = (G^{-1})_{ij}.$$

⁽⁵⁾ H. L. ANDERSON, W. C. DAVIDON, M. GLICKSMAN and U. E. KRUSE: *Phys. Rev.*, **100**, 279 (1955).

The error matrix G^{-1} is obtained by inversion of the matrix G using a standard routine of the Avidac. The square roots of the diagonal elements of G^{-1} give the standard deviations for each of the parameters, while the off-diagonal elements are the products of the correlation coefficients with the two corresponding standard deviations.

2. - Instruction of the computer.

The Avidac is organized to receive words of 10 characters, each character being a sexidecimal number.

Starting with 180° each character is used to indicate the number of events to be included in each degree interval of angle. When the number of events in unit interval exceeded fourteen the letter F instructed the machine to add 15 to the following number. In this scheme the results of most experiments could be stored in somewhat more than 18 words. The events for the various experiments analyzed are so listed in Table XII.

As starting point for the routine we sought the Fermi type solution with the phase angles α_{31} small, α_{33} large and resonant, following the choice of DE HOFFMANN, METROPOLIS, ALEI and BETHE ⁽⁶⁾ and in accordance with our own ⁽⁷⁾, previously expressed view that a solution of this type is most likely the correct one. One of the ways used to determine the starting values was to construct an Ashkin ⁽⁸⁾ diagram, from which a suitable choice could easily be made.

The search for the maximum in w has been much facilitated by the hunting procedure developed by one of us (WCD) and will be described elsewhere. This procedure regards w as a function of a vector x in an n -dimensional space, n being the number of parameters which are varied. The quantity w is maximized by a series of iterations in which successive trials for x are made which increase w . In the neighborhood of the maximum w may be expanded in a Taylor series. The successive trials for x are made assuming that the behavior of w is quadratic near its maximum. When this is the case no more than n additional steps are needed to find the exact maximum.

The machine first calculates the value of w corresponding to the starting values of the parameters. It then calculates the derivatives of w with respect to each of these parameters. With these, an improved value of w is predicted together with an improved set of parameters. These replace the previous set,

⁽⁶⁾ F. DE HOFFMANN, N. METROPOLIS, E. F. ALEI and H. A. BETHE: *Phys. Rev.*, **95**, 1586 (1954).

⁽⁷⁾ H. L. ANDERSON, W. C. DAVIDON and U. E. KRUSE: *Phys. Rev.*, **100**, 339 (1955).

⁽⁸⁾ J. ASHKIN and S. H. VOSKO: *Phys. Rev.*, **91**, 1248 (1953).

and a new value of w is computed. The success is noted by the improvement in the successive values calculated for w . The hunting is stopped when the improvement is less than 2^{-7} . After the best fit is determined, the differential cross-sections as functions of center of mass angle are printed out, using the last set of parameters.

With the best fit parameters, the machine calculates the matrix G according to the method described above. It then inverts this matrix to obtain G^{-1} . As a check it carries out the product $G \times G^{-1}$ to verify that the unit matrix is obtained.

3. - Error matrix.

The error matrix is useful because its diagonal elements give the square of the standard deviation of the derived parameters. Thus, we may judge how well the phase shifts were determined by the experiment. Moreover, the errors to be assigned to any function of the phase shifts may be calculated properly when the full error matrix is available.

Thus, to calculate the error in the quantity $R(\alpha_1, \alpha_2 \dots \alpha_p)$ we write,

$$\Delta R = \sum_{m=1}^p \frac{\partial R}{\partial \alpha_m} \Delta \alpha_m,$$

then,

$$\overline{\Delta R^2} = \sum_{m=1}^p \sum_{n=1}^p \frac{\partial R}{\partial \alpha_m} \frac{\partial R}{\partial \alpha_n} \overline{\Delta \alpha_m \Delta \alpha_n},$$

but

$$\overline{\Delta \alpha_m \Delta \alpha_n} = G_{mn}^{-1}.$$

Hence the mean square error in R is given by,

$$\overline{\Delta R^2} = \sum_{m=1}^p \sum_{n=1}^p G_{mn}^{-1} \frac{\partial R}{\partial \alpha_m} \frac{\partial R}{\partial \alpha_n}.$$

In particular, we will want to calculate the quantity

$$(12) \quad d_+ = \sum_m (j_m + \frac{1}{2}) \sin 2\alpha_m,$$

which is related to the real part of the forward scattering amplitude by

$$(13) \quad D_+(k_b) = \frac{d_+}{2k_b},$$

where k_0 is the wave number of the pion in the center of mass system, and j_m is the total angular momentum in units of \hbar corresponding to the m^{th} phase shift. Then, the root mean square error in the quantity

$$(14) \quad [(\Delta d_+)^2]^{\frac{1}{2}} = 2 \left\{ \sum_{m=1}^p \sum_{n=1}^p (j_m + \frac{1}{2}) \cos 2\alpha_m (j_n + \frac{1}{2}) \cos 2\alpha_n G_{mn}^{-1} \right\}.$$

The total cross-section, in terms of the phase shifts, is given by

$$(15) \quad \sigma_T = \frac{4\pi}{k_b^2} \sum_m (j_m + \frac{1}{2}) \sin 2\alpha_m,$$

and the root mean square error by

$$(16) \quad [\Delta \sigma_T^2]^{\frac{1}{2}} = \frac{4\pi}{k_b^2} \left\{ \sum_{m,n} 2(j_m + \frac{1}{2}) \sin \alpha_m \cos \alpha_m 2(j_n + \frac{1}{2}) \sin \alpha_n \cos \alpha_n (G^{-1})_{nm} \right\}^{\frac{1}{2}}.$$

4. - Coulomb interference.

One object of the experimental work was to determine the sign of the phase shifts from the observation of the interference of the nuclear with the Coulomb scattering. This becomes possible when the observations are extended to angles small enough for the Coulomb effect to become important. Such experiments were carried out with positive pions by OREAR⁽⁹⁾ at 113 MeV, by FERRETTI *et al.*⁽¹⁰⁾ at 120 MeV and by TAFT⁽¹¹⁾ at 217 MeV.

OREAR had already analyzed his own observations by the maximum likelihood method, carrying out the calculation by hand. The same data analyzed by the electronic computer have the results listed in Table I. The solutions given are of the Fermi type with signs chosen first to give destructive interference and then constructive interference. The value of w given allows the comparison between the two possibilities. In the case of Orear's data, the relative probability of destructive over constructive interference is in the ratio

$$\exp[-0.924] \cdot \exp[+4.940] = 55.$$

It is not entirely clear why OREAR obtained the value 4000 for this ratio since his phase shifts are almost identical to the values given here.

(9) J. OREAR: *Phys. Rev.*, **96**, 1417 (1954).

(10) L. FERRETTI, E. MANARES, G. PUPPI, G. QUARENI and A. RANZI: *Nuovo Cimento*, **1**, 1238 (1955).

(11) H. D. TAFT: *Phys. Rev.*, **101**, 1116 (1956).

TABLE I. — *Coulomb Interference in the $\pi^- + p$ scattering. Phase shift angles are given in degrees, t in units of 32/90 of 1 standard deviation. The relative probability w is determined except for an arbitrary constant which is not changed in the different analyses of the same experiment.*

Mean Energy MeV	Number of Events	Coulomb Interference	w	t	α_3	α_{33}	α_{31}	Reference
113	333	destr	-0.924	.07	-10.9	27.1	-2.9	OREAR ⁽⁹⁾
		const	-4.940	0	14.4	-25.7	4.8	
120	871	destr	-0.983	.09	-12.3	31.8	-2.6	FERRETTI <i>et al.</i> ⁽¹⁰⁾
		const	-4.906	-.21	16.9	-30.7	3.5	
217	90	const	-0.040	.01	-22.5	114.0	-11.6	TAFT ⁽¹¹⁾
		destr	-0.439	-.01	24.9	67.4	14.3	

The analysis of the data of FERRETTI *et al.* ⁽¹⁰⁾ including the events found within the energy interval 110 to 130 MeV, gives for the ratio of the relative probability of destructive over constructive interference,

$$\exp[-0.983] \cdot \exp[+4.906] = 51.$$

Taft's data show the preference for constructive interference which was expected from the behavior of the forward scattering amplitude as calculated (?) from the dispersion relations. The number of events observed was not large enough to make the choice decisive, the relative probability favoring constructive interference being 1.5. Taken together the three experiments favor the behavior of the forward scattering amplitude as deduced from the dispersion relations by the factor 4200.

5. — *d*-waves.

An attempt was made to analyze some of the early data of FERRETTI *et al.* ⁽¹⁰⁾ including *d*-waves. There were 295 events obtained by area scanning in the energy interval 120 to 130 MeV, with mean energy 124 MeV. In this case the matrix G turned out to be nearly singular and some of the diagonal elements in G^{-1} were found to be negative. Such improper structure of the matrices indicates that the data were inadequate to determine so many parameters. More reasonable results were obtained when the analysis was restricted to *s*- and *p*-waves (Table II). The analysis of the 114 MeV data of FERRETTI *et al.* ⁽¹⁰⁾ in which 226 events between 110 and 120 MeV were used, also failed

TABLE II. — Analysis of the 124 MeV data of Puppi et al. ⁽¹⁰⁾ (295 events) using *s*- and *p*-waves only. Phase shift angles are given in degrees. Matrix elements of G^{-1} in (degrees)². To obtain the value of t in standard deviations, multiply its value given in degrees by 32/90.

		t	α_3	α_{33}	α_{31}	w
Best Fit		0.072	— 14.42	34.39	— 2.78	— 0.588
G	t	0.208 7	— 0.064 7	0.225 4	— 0.017 3	—
	α_3	—	0.079 0	— 0.145 1	0.022 6	—
	α_{33}	—	—	0.664 5	— 0.047 4	—
	α_{31}	—	—	—	0.127 4	—
G^{-1}	t	7.864	2.614	— 2.110	— 0.182 8	—
	α_3	—	22.55	3.879	— 2.196	—
	α_{33}	—	—	3.080	0.173 3	—
	α_{31}	—	—	—	8.281	—

when *d*-waves were included. In Table III we give the results of the analysis made using only *s*- and *p*-waves. In these tables w is determined except for an arbitrary constant, which is different for the different sets of data, but which is not changed in the different analyses of the same data.

TABLE III. — Analysis of the 114 MeV data of Puppi et al. ⁽¹⁰⁾ (226 events) using *s*- and *p*-waves only. Units are as for Table II.

		t	α_3	α_{33}	α_{31}	w
Best Fit		0.046	— 10.07	29.26	— 2.36	— 0.454
G	t	0.209	— 0.060 3	0.251	— 0.019 0	—
	α_3	—	0.113	— 0.130	0.004 63	—
	α_{33}	—	—	0.799	— 0.052 1	—
	α_{31}	—	—	—	0.168	—
G^{-1}	t	7.93	1.68	— 2.21	0.164	—
	α_3	—	11.19	1.31	0.289	—
	α_{33}	—	—	2.18	0.393	—
	α_{31}	—	—	—	6.10	—

A similar condition developed in the analysis of the 142 MeV data of LORD and WEAVER ⁽¹²⁾. In this case, even when the analysis was restricted to *s*- and *p*-waves, negative diagonal elements appeared in G^{-1} . The data admitted a large change in the direction α_3 less negative, α_{33} more positive, and t more

⁽¹²⁾ J. J. LORD and A. B. WEAVER: private communication.

positive. Since the value of α_3 turned out to be anomalously negative, we also made analyses with α_3 held fixed at less negative values. These results are summarized in Table IV. A change in α_3 by 15.7 degrees gives a fit here which is only 2.2 times less probable than the best fit obtained without d -waves. To some extent this may be due to a peculiarity of the phase shift solutions in this energy region. A similar behavior had been noted at 165 MeV ⁽¹³⁾.

In Table V we give the results of the analyses made with and without d -waves, of the data of Taft ⁽¹¹⁾ at 217 MeV, and of Margulies ⁽¹⁴⁾ at 258, 294, and 395 MeV.

TABLE IV. — Various analyses of the 142 MeV data of Lord and Weaver (1.002 events). Phase shift angles in degrees, t is in units of 32/90 of 1 standard deviation. Quantities underlined were not varied in the calculation. The error analysis was not meaningful in this case.

t	α_3	α_{33}	α_{31}	δ_{35}	δ_{33}	w
0.294	— 27.4	43.1	— 6.1	— 4.4	0.1	+ 0.302
0.717	— 32.6	38.5	2.4	0	0	— 0.186
1.24	— 16.9	41.6	— 2.8	0	0	— 0.971
1.60	— 11.3	41.2	— 3.4	0	0	— 2.59

TABLE V. — Analysis of the data of Taft ⁽¹¹⁾ at 217 MeV, and of Margulies ⁽¹⁴⁾ at 258, 294 and 395 MeV, made with and without d -waves. Quantities underlined were not varied. Phase shift angles are in degrees, t in units of 32/90 of 1 standard deviation. The analysis of the data at 294 MeV was made using as total cross-section 75 ± 5 mb.

Mean Energy MeV	Number of Events	α_3	α_{33}	α_{31}	δ_{35}	δ_{33}	t	w
217	90	— 22.5 \pm 5.8	114.0 \pm 7.4	— 11.6 \pm 9.7	0	0	0.01	— 0.0405
		— 22.5 \pm 7.5	114.0 \pm 9.6	— 11.7 \pm 15.6	0.03 \pm 14.6	0.05 \pm 22.5	0	— 0.0402
258	86	7.1 \pm 7.2	121.3 \pm 6.1	— 3.2 \pm 9.6	0	0	0.07	— 1.36
		3.3	122.3	— 5.2	— 7.2	— 5.1	0.01	— 0.197
294	132	— 13.6 \pm 4.3	128.4 \pm 3.9	— 4.9 \pm 6.2	0	0	0	— 0.32
		— 13.3 \pm 17.6	128.2 \pm 6.4	— 3.7 \pm 9.7	— 0.8 \pm 18.4	— 3.2 \pm 13.0	0.02	— 0.039
395	110	— 22.6 \pm 3.2	148.0 \pm 2.6	— 15.4 \pm 4.5	0	0	0	— 1.56
		— 20.1 \pm 13.3	146.4 \pm 5.9	— 11.4 \pm 9.3	— 3.3 \pm 14.6	— 2.9 \pm 14.1	0.03	— 0.02

⁽¹³⁾ H. L. ANDERSON and M. GLICKSMAN: *Phys. Rev.*, **100**, 268 (1955).

⁽¹⁴⁾ R. S. MARGULIES: *Phys. Rev.* (in press).

The matrix G^{-1} obtained was in all but one of these cases well behaved and so allowed an assignment of error in the phase shift angles. The values of the matrices G^{-1} have already been published in the original reports of these authors (*) and will not be reprinted here. The d -wave phase shifts are seen to be small with an uncertainty several times larger than their best fit values. None of the experiments analyzed here was adequate to determine the presence of d -waves.

6. - Other results.

In subsequent studies of experiments carried out below 200 MeV, we limited the analysis to s - and p -waves alone. Table VI gives the values of the matrices G and G^{-1} for Orear's ⁽⁹⁾ 113 MeV data. Similarly, Tables VII, VIII and IX give the results of the analysis of the data of FERRARI *et al.* ⁽¹⁵⁾ at 80, 100 and 120 MeV. The starting values of the phase shifts used in various of the analyses are collected in Table X. In Table XI all the results are summarized. The best fit phase shifts are given together with their standard

TABLE VI. - Analysis of the data of Orear ⁽⁹⁾ at 113 MeV (333 events) using s - and p -waves only. Phase shifts are in degrees, t is in units $32/90$ of 1 standard deviation.

		t	α_3	α_{33}	α_{31}
Best	Fit	0.07	-10.9	27.1	-2.9
G	t	0.332	-0.123	0.518	-0.0925
	α_3	—	0.190	-0.208	0.0494
	α_{33}	—	—	1.391	-0.213
	α_{31}	—	—	—	0.278
G^{-1}	t	7.96	2.25	-2.59	0.226
	α_3	—	6.97	0.147	-0.378
	α_{33}	—	—	1.776	0.475
	α_{31}	—	—	—	4.116

(*) In MARGULIES 395 MeV analysis correct values are $(G^{-1})_{33, 33} = -72.6$, $(G^{-1})_{35, 33} = -199.0$.

⁽¹⁵⁾ G. FERRARI, L. FERRETTI, R. GESSAROLI, E. MANARESI, G. PUPPI, G. QUARENI, A. RANZI and A. STANGHELLINI: *CERN Symposium*, 2, 230 (1956). This is a preliminary report of the results obtained with somewhat more events than were available to us here.

deviations in all cases where G^{-1} was well behaved. At 142 MeV we give an alternate to the best fit solution in view of the difficulties encountered here as discussed above. We also give the total cross-sections calculated from the phase shifts using Equation (15), together with its standard deviation obtained

TABLE VII. — *Analysis of the data of Ferrari et al. ⁽¹⁵⁾ at 80 MeV (180 events).*

		t	α_3	α_{33}	α_{31}
Best Fit		—	— 10.2	13.7	— 1.4
G	t	0.428	— 0.355	0.801	— 0.070
	α_3	—	0.522	— 0.794	0.060
	α_{33}	—	—	2.23	— 0.187
	α_{31}	—	—	—	0.587
G^{-1}	t	8.31	2.45	— 2.10	0.068
	α_3	—	4.90	0.869	0.067
	α_{33}	—	—	1.52	0.150
	α_{31}	—	—	—	1.75

TABLE VIII. — *Analysis of the data of Puppi et al. ⁽¹⁵⁾ at 100 MeV (450 events).*

		t	α_3	α_{33}	α_{31}
Best	Fit	—	— 10.6	21.7	— 2.5
G	t	0.645	— 0.361	1.15	— 0.107
	α_3	—	0.470	0.608	0.029
	α_{33}	—	—	2.73	— 0.249
	α_{31}	—	—	—	0.592
G^{-1}	t	7.90	2.47	— 2.77	0.146
	α_3	—	3.77	— 1.82	0.186
	α_{33}	—	—	1.51	0.141
	α_{31}	—	—	—	1.76

TABLE IX. — *Analysis of the data of Puppi et al. (10) at 120 MeV (871 events).*

		t	α_3	α_{33}	α_{31}
Best	Fit	0.09	— 12.3	31.8	— 2.6
G	t	0.833	— 0.407	1.212	0.150
	α_3	—	0.323	— 0.577	— 0.115
	α_{33}	—	—	2.178	0.225
	α_{31}	—	—	—	0.446
G^{-1}	t	8.665	4.382	— 3.669	0.058
	α_3	—	8.368	— 0.308	0.833
	α_{33}	—	—	2.427	— 0.066
	α_{31}	—	—	—	2.470

TABLE X. — *Starting values of the phase shifts (degrees).*

Mean Energy	See Table	Analysis	α_3	α_{33}	α_{31}	δ_{35}	δ_{33}
80	VII	s, p	— 11.3	12.5	— 2°	—	—
100	VIII	s, p	— 9.5	22.5	— 3°	—	—
113	VI	s, p	— 11.3	28.7	— 2.8	—	—
120	IX	s, p	— 12.7	31.6	— 2.1	—	—
142	IV	s, p	— 11.3	45.0	5.6	—	—
217	I	s, p	— 22.5	112.5	— 5.6	—	—
—	I	s, p	22.5	— 112.5	5.6	—	—
—	V	s, p, d	— 22.5	113.9	— 11.6	0	0
258	V	s, p	— 12	116	— 11	—	—
294	V	s, p, d	— 17	127	— 4	0	0
395	V	s, p, d	— 22	158	— 22	0	0

using Equation (16). Finally, we give the useful quantity d_- [Equation (12)] together with its standard deviation [Equation (14)] for comparison with the real part of the forward scattering amplitude as obtained from the dispersion relations (?).

TABLE XI. - Summary of phase shift analyses. Phase shifts are in degrees, total cross-section in millibarns calculated from $\sigma_t = 4\pi k^2 \sum_n (i_n + \frac{1}{2}) \sin^2 \alpha_n$; $d_+ = \sum_n (i_n + \frac{1}{2}) \sin 2\alpha_n$. At 142 MeV the phase shifts are not well determined.

Mean Energy MeV	α_0	α_{33}	α_{31}	δ_{35}	δ_{33}	σ_t	d_+	References
80	-10.2 ± 2.2	13.7 ± 1.2	-1.4 ± 1.3	—	—	36.7 ± 5.1	0.52 ± 0.13	PUPPI ⁽¹⁵⁾
100	-10.6 ± 1.9	21.7 ± 1.2	-2.5 ± 1.3	—	—	62.4 ± 8.0	0.93 ± 0.07	PUPPI ⁽¹⁶⁾
113	-10.9 ± 2.7	27.1 ± 1.3	-2.9 ± 2.0	—	—	78.0 ± 6.9	1.15 ± 0.13	OREAR ⁽⁹⁾
114	-10.1 ± 3.5	29.3 ± 1.5	-2.4 ± 2.5	—	—	86.8 ± 7.4	1.28 ± 0.17	PUPPI ⁽¹⁰⁾
120	-12.3 ± 2.9	31.8 ± 1.6	-2.6 ± 1.6	—	—	96.6 ± 8.7	1.46 ± 0.12	PUPPI ⁽¹⁰⁾
124	-14.4 ± 4.8	34.4 ± 1.8	-2.8 ± 2.9	—	—	108.8 ± 8.0	1.29 ± 0.19	PUPPI ⁽¹⁰⁾
142	-16.9	41.6	-2.8	—	—	127	1.33	LORD and WEAVER ⁽¹²⁾
217	-22.5 ± 5.8	114.0 ± 7.4	-11.6 ± 9.7	—	—	151.0 ± 18.2	-2.58 ± 0.47	TAPT ⁽¹¹⁾
217	-22.4 ± 7.5	114.0 ± 9.6	-11.7 ± 15.6	0.0 ± 14.6	0.1 ± 22.5	150.2 ± 18.2	2.59 ± 0.97	—
258	7.1 ± 7.2	121.3 ± 6.1	3.2 ± 9.6	—	—	97.6 ± 12.9	2.13 ± 0.44	MARGULIES ⁽¹⁴⁾
258	3.3	122.3	-5.2	-7.2	-5.1	99.2	-2.97	—
294	-13.6 ± 4.3	128.4 ± 3.9	-4.9 ± 6.2	—	—	72.9 ± 7.9	-2.57 ± 0.25	MARGULIES ⁽¹⁴⁾
294	-13.3 ± 17.6	128.2 ± 6.4	-3.7 ± 9.7	-0.8 ± 18.4	3.2 ± 13.0	73.4 ± 8.8	2.83 ± 0.66	—
395	-22.6 ± 3.2	148.0 ± 2.6	-15.4 ± 4.5	—	—	31.0 ± 3.5	3.03 ± 0.16	MARGULIES ⁽¹⁴⁾
395	20.1 ± 13.3	146.4 ± 5.9	11.4 ± 9.3	3.3 ± 14.6	2.9 ± 14.1	31.1 ± 8.6	3.42 ± 0.54	—

TABLE XII. — *Data of various experiments with events listed by means of the sexidecimal code as described in the text. Here $C_0 = \pi^2 N_0 / q^0 k^2$ and μ is the error in C_0 . In Orear's data the events were specified only to three degree intervals and were analyzed accordingly.*

TABLE XII-a.

Name	PUPPI (¹⁷)
Energy	80 MeV
Efficiencies	Angular Range
1.000	180° — 20.5°
C_0	11.378
μ	1.29
Events	00000 00001
	00122 11130
	24111 42320
	11321 41411
	32212 42172
	02033 32010
	33350 03031
	10014 10112
	01111 42132
	16020 12111
	00210 00011
	20100 10120
	11000 30000
	01010 00101
	10010 10001
	00001 00000

TABLE XII-b.

Name	PUPPI (¹⁵)
Energy	100 MeV
Efficiencies	Angular Range
1.000	180° — 20.5°
C_0	13.165
μ	1.29
Events	00012 01100
	30330 32150
	13373 11456
	99456 28475
	66865 44343
	33724 46254
	14168 265A2
	41017 63755
	30326 12515
	03102 24124
	41443 23132
	14131 32110

TABLE XII-c. — (continued).

Events	22212 15106
	02421 32521
	32020 11141
	00321 20101

TABLE XII-d.

Name	PUPPI (¹⁰)
Energy	114 MeV
Efficiencies	Angular Range
1.000	180° — 15.5°
C_0	4.075
μ214
Events	00001 01003
	01211 11031
	13311 24112
	14501 42211
	34241 01211
	35500 42402
	31143 10112
	32014 10033
	30111 01013
	10113 22111
	01320 14101
	33100 01200
	00203 12411
	03002 11210
	21122 20001
	31110 00120
	02000 00000
	00000 00000

TABLE XII-e.

Name	OREAR (⁹)
Energy	113 MeV
Efficiencies	Angular Range
0	180° — 159°.5
.667	159.5 — 130
1.000	130 — 20
.722	20 — 15
.444	15 — 12.5
C_0	7.827
μ548

TABLE XII-d. - (continued).

Events	00400	40060
	04009	00F00
	0B00A	00600
	0A090	0A007
	00C00	F400D
	00800	A0060
	05003	00800
	800B0	07005
	00300	60070
	03008	00600
	50060	08007
	00800	90030
	09004	00300
	50050	02003
	00200	10000

TABLE XII-e.

Name	PUPPI (¹⁰)
Energy	120 MeV
Efficiencies	Angular Range
.786	180° \div 174° .5
.756	174.5 \div 169.5
.715	169.5 \div 164.5
.671	164.5 \div 159.5
.620	159.5 \div 154.5
.575	154.5 \div 149.5
.534	149.5 \div 144.5
.501	144.5 \div 139.5
.467	139.5 \div 134.5
.175	134.5 \div 14.5

C_0	43.99	
μ	3.55	
Events	01024	7B46A
	997D8	A999F
	DF1F4	9DF1F
	0EF5A	BFF3F
	1AF2F	2F2EB
	F2DAF	89767
	59588	14657
	05355	73313
	27654	44312
	64654	41033
	18512	24354
	31033	32141
	21552	14123
	11107	24355
	31141	13433
	31332	42613
	33333	22311
	21020	01000

TABLE XII-f.

Name	PUPPI (¹⁰)
Energy	124 MeV
Efficiencies	Angular Range
1.000	180° \div 15.5
C_0	3.752
μ176
Events	00000 01100
	21111 40111
	54313 23221
	02221 34222
	54242 46248
	23314 23303
	04430 21215
	33430 21231
	35330 02305
	41111 13320
	02012 00020
	22114 11111
	10521 23120
	11111 32121
	12120 41332
	02212 31001
	00001 00000
	00000 00000

TABLE XII-g.

Name	LORD and WEAVER (¹²)
Energy	142 MeV
Efficiencies	Angular Range
0	180° \div 150.5
.95	150.5 \div 30.5
C_0	8.1037
μ486
Events	00000 00000
	00000 00000
	00000 00000
	8919A A9A7E
	98A68 F3F17
	47DCD B6E77
	7C973 95955
	E381D 92877
	52446 87874
	74656 93444
	66648 65367
	25263 36259
	77551 846D3
	32536 6B224
	B2897 66037
	44000 00000

TABLE XII-*h*.

Name	TART ⁽¹¹⁾	
Energy	217 MeV	
Efficiencies	Angular Range	
1.000	$180^\circ \div 10^\circ$	
C_0465 8	
μ	0.23 3	
Events	00000	00100
	00010	20001
	01101	00000
	11000	00002
	21111	01000
	00000	00120
	01001	00001
	00000	10110
	00001	00010
	10110	02310
	10200	00000
	02100	01010
	10001	12212
	01111	10011
	22030	10311
	00011	01202
	10011	11210
	00000	00000

TABLE XII-*i*.

Name	MARGULIES ⁽¹¹⁾	
Energy	258 MeV	
Efficiencies	Angular Range	
.667	$180^\circ \div 10.5^\circ$	
C_0713	
μ05	
Events	00000	00001
	00010	11001
	00011	20000
	00210	01100
	12011	00110
	10000	01100
	02000	01111
	01011	00000
	01102	10010
	02010	00000
	01101	11000
	00000	20020
	00011	01020
	10010	04210
	20000	01101
	01011	00110
	01203	01022

TABLE XII-*j*.

Name	MARGULIES ⁽¹¹⁾	
Energy	294 MeV	
Efficiencies	Angular Range	
.556	$180^\circ \div 7.5^\circ$	
C_0	1.07	
μ06	
Events	00000	00110
	00010	00001
	01310	10101
	10000	00110
	10411	02200
	11021	01020
	00001	00120
	00201	10000
	11020	10010
	10211	01010
	01010	10000
	02140	02200
	00520	04020
	11110	32002
	13020	50100
	42200	40012
	01200	12011
	10300	00000

TABLE XII-*k*.

Name	MARGULIES ⁽¹¹⁾	
Energy	395 MeV	
Efficiencies	Angular Range	
.667	$180^\circ \div 6.5^\circ$	
C_0	1.639	
μ08	
Events	00000	00000
	00000	00000
	20000	00000
	10110	10011
	00001	00101
	00001	00101
	00000	00000
	00000	00100
	01000	00010
	01111	00000
	00001	11010
	22110	11100
	01010	02203
	72002	10020
	25200	20130
	53102	20110
	22021	03320
	34010	00000

* * *

We thank Dr. M. FLANDERS and Miss J. HALL of the Argonne National Laboratory for the use of the electronic computer Avidac. Also, we thank Doctors J. OREAR, J. J. LORD, A. B. WEAVER, H. TAFT, R. S. MARGULIES and Professors G. PUPPI and G. QUARENI for making their data available to us for analysis. One of us (HLA) is grateful to the Guggenheim Foundation for a Fellowship, and to the Istituto di Fisica « Guglielmo Marconi » in Rome for the hospitality which helped make possible the present work.

RIASSUNTO (*)

Esponiamo il metodo da noi usato per eseguire un'analisi in sfasamenti degli eventi di scattering pione-protone trovati in emulsioni nucleari e nella camera a diffusione a idrogeno. Il metodo impiega una calcolatrice elettronica per trovare la serie di sfasamenti che, seguendo un criterio di massima verosimiglianza, meglio si adatti ad una determinata serie di eventi di scattering aventi una data energia. Il problema fu impostato sulla calcolatrice elettronica Avidac dell'Argonne National Laboratory e l'impostazione servì ad analizzare gli eventi scoperti da vari gruppi di sperimentatori. La maggior parte dei risultati è già stata resa nota. Le analisi furono eseguite per lo scattering di pioni positivi su protoni e potevano includere tanto onde d quanto onde s e p assieme all'effetto dell'interazione coulombiana.

(*) Traduzione a cura della Redazione.

Charge Dependent Corrections to Dispersion Relations. I.

A. AGODI and M. CINI

Istituto di Fisica dell'Università - Catania
Centro Siciliano di Fisica Nucleare - Catania

(ricevuto il 25 Febbraio 1957)

Summary. — The corrections to the forward dispersion relations for pion-nucleon scattering due to the mass difference between charged and neutral π -mesons are evaluated. Since the dispersion relations obtained from a relativistic theory have essentially the same form as those derived from a fixed source Hamiltonian with s and p waves, our calculation has been performed by introducing in the latter Hamiltonian the observed meson masses. The correction term to the dispersion relations is different for positive and negative mesons but turns out to be small. For mesons of momentum q of the order of the meson mass this gives a difference between the two cases which amounts to about 1% of f^2 .

1. — Introduction.

The dispersion relations discovered by GOLDBERGER ⁽¹⁾ for meson nucleon scattering have been shown to be well satisfied by experimental data ⁽²⁾. The evaluation of the coupling constant f^2 from experiment by means of these relations yields $f^2 = 0.08$ ⁽³⁾, in fair agreement with the coupling constant derived independently from photoproduction data ⁽⁴⁾ and with the value obtained by means of the Low equation for the fixed source meson theory ⁽⁵⁾.

⁽¹⁾ M. L. GOLDBERGER: *Phys. Rev.*, **97**, 508 (1955); see also for the latest developments A. SALAM: *CERN Symposium*, **2**, 176 (1956).

⁽²⁾ H. L. ANDERSON, W. C. DAVIDON and U. E. KRUSE: *Phys. Rev.*, **100**, 339 (1955).

⁽³⁾ U. HABER-SCHAIM: *Phys. Rev.*, **104**, 1113 (1956); W. C. DAVIDON and M. L. GOLDBERGER: *Phys. Rev.*, **104**, 1119 (1956).

⁽⁴⁾ M. BENEVENTANO, G. STOPPINI, L. TAU and G. BERNARDINI: *CERN Symposium*, **2**, 259 (1956).

⁽⁵⁾ M. CINI, S. FUBINI and A. STANGHELLINI: *Nuovo Cimento*, **3**, 1380 (1956).

Recently, however, a more refined analysis of the available data has been made (*), and some indications have been found that the scattering amplitudes for negative mesons fail to satisfy the dispersion relations with the value of f^2 determined from the positive mesons scattering data.

Since dispersion relations have been derived from a charge independent meson theory some corrections are expected to be necessary when charge dependent effects are taken into account. It is worthwhile to examine if the known charge dependent interactions are sufficient to eliminate the above mentioned discrepancy between theory and experiment, also in view of the suggestion that the presence of heavy mesons and hyperons might produce deviations from the theoretical predictions of magnitude as yet unknown (†) (*).

The electromagnetic interaction gives rise to competition between π^- elastic scattering and π^- radiative capture from the proton, and is also probably responsible for the mass difference between charged and neutral mesons as well as between proton and neutron. A large effect due to the meson mass difference has been found in an approximate calculation of nuclear forces (‡). A phenomenological calculation of the correction to the s -wave phase shifts due to these factors has been performed by NOYES (⁹) by means of a potential model of the scattering, and found to be important. It is not sufficient, however, to consider the corrections to the diagonal elements of the scattering matrix (phaseshifts) because when isotopic spin is not a good quantum number also off-diagonal elements contribute to the scattering amplitudes.

The purpose of this note is to compute the mass corrections. The radiative capture effect will be the object of a further research.

It has been shown recently (¹⁰) that a fixed source Hamiltonian with s - and p -waves gives dispersion relations which have essentially the same form as those derived from a relativistic theory. This fact indicates that the neutron-proton mass difference can be expected not to affect significantly the latter ones and justifies the use of the fixed source relations to compute the corrections due to the mass difference between neutral and charged mesons, by introducing explicitly the observed meson masses in the Hamiltonian. By using this approach it turns out that these corrections are quite negligible. Furthermore it can be shown in this way that the form of the dispersion relations does not depend on the strength of the neutral mesons coupling with the source.

(⁵) G. PUPPI and A. STANGHELLINI: *Progr. Report*. N. 4 (Bologna, 1956).

(⁷) B. VITALE: *Nuovo Cimento*, **5**, 732 (1957).

(*) *Note added in proof*. - Actually it turns out that no modifications to the pion-nucleon dispersion relations arise from pion-hyperon interactions.

(⁸) RIAZZUDIN: *Nucl. Phys.*, **2**, 188 (1956).

(⁹) H. P. NOYES: *Phys. Rev.*, **101**, 320 (1956).

(¹⁰) A. KLEIN: *Phys. Rev.*, **104**, 1131, 1136 (1956).

2. Derivation of the dispersion relations for the scattering amplitudes.

We start from the interaction Hamiltonian ⁽¹⁰⁾

$$(1) \quad H' = (4\pi)^{\frac{1}{2}} f^{(0)} \sum_{\alpha} \int d^3 \mathbf{x} s(\mathbf{x}) \boldsymbol{\sigma} \cdot \nabla \varphi_{\alpha}(\mathbf{x}) \tau_{\alpha} \frac{1}{\mu_{\alpha}} + \lambda_0^{(0)} \sum_{\alpha} \left[\int d^3 \mathbf{x} s(\mathbf{x}) q_{\alpha}(\mathbf{x}) \right]^2 \\ + \lambda_0^{(0)} \sum_{\alpha \alpha' \alpha''} \varepsilon_{\alpha \alpha' \alpha''} \tau_{\alpha} \int d^3 \mathbf{x} s(\mathbf{x}) \varphi_{\alpha'}(\mathbf{x}) \int d^3 \mathbf{x}' s(\mathbf{x}') \tau_{\alpha''}(\mathbf{x}')$$

μ_{α} being the charged meson's mass for $\alpha = 1, 2$ and the neutral meson's one for $\alpha = 3$; $s(\mathbf{x})$, the fixed source extension, is chosen to be spherically symmetric, thus restricting the theory to s and p waves only

$$s(\mathbf{x}) = \left(\frac{1}{2\pi} \right)^3 \int d^3 \mathbf{q} \exp[i\mathbf{q}\mathbf{x}] v(q); \quad q = |\mathbf{q}|.$$

The free Hamiltonian is now

$$(2) \quad H_0 = \sum_q \omega_q a_q^+ a_q.$$

Let us consider the transition matrix $T_m(\omega)$ for forward scattering of mesons of charge m on nucleons (*) as a function of the meson energy ω and as an operator with respect to nucleon spin and isotopic spin. Its matrix elements still satisfy, as in the conventional theory, the Low equations

$$(3) \quad \langle rt | T_m(\omega) | r't' \rangle = \langle \Psi_{rt}, [a_{qm}, V_{qm}] \Psi_{r't'} \rangle + \\ - \sum_r \left\{ \frac{(\Psi_{rt}, V_{qm} \Psi_n^{(-)}) (\Psi_n^{(-)}, V_{qm} \Psi_{r't'})}{\omega + i\varepsilon - E_n} + \frac{(\Psi_{rt}, V_{qm} \Psi_n^{(-)}) (\Psi_n^{(-)}, V_{qm} \Psi_{r't'})}{-\omega - E_n + i\varepsilon} \right\}^*$$

where

$$(4) \quad V_{qm} = [H', a_{qm}^+]; \quad q = \sqrt{\omega^2 + \mu_c^2}$$

and

$$(5) \quad a_{qm}^+ = - \sum_{\alpha} \frac{m}{\sqrt{2}} (\delta_{\alpha 1} + im \delta_{\alpha 2}) a_{q\alpha}^+; \quad (m = \pm 1),$$

is a creation operator of a meson of charge m .

(*) Since we are interested only in charged mesons m will take only the values ± 1 .

The bare nucleon states $|rt\rangle$ as well as the physical nucleon states Ψ_{rt} are labelled with the spin index r and isotopic spin index t ($t = \pm$ corresponding to the proton and $t = 0$ corresponding to the neutron). $\Psi_n^{(-)}$ are the incoming eigenstates of the total Hamiltonian.

By explicitly evaluating the commutator (4) it is easy to verify (*), by means of eq. (3), that

$$(6) \quad T_m^+(\omega) = -T_m^-(\omega).$$

As a function of the complex variable z , the matrix $zT_m(z)$ has a simple pole at $z = 0$ and branch points, on the real axis, at $z = \mu_0$ and at $z = -\mu_0$. This because the smallest value of E_n different from zero is μ_0 , corresponding to a state with one nucleon and one neutral meson at rest. The transition amplitude at a given physical energy ω is defined, as usually, by means of

$$(7) \quad T_m(\omega) = \lim_{\text{Im } z \rightarrow 0+} T_m(z). \quad (\text{Re } z = \omega):$$

Then the function of complex variable

$$(8) \quad Q_m(z) = \frac{zT_m(z)}{u^2(z)(z - \mu_c)(z^2 - \omega^2)}; \quad \lim_{\text{Im } z \rightarrow 0+} u(z) = v(q), \quad (\text{Re } z = \omega),$$

is analytic in the upper imaginary half plane, has simple poles on the real axis at $z = 0, z = \mu_c, z = \pm \omega$, and $zQ_m(z) \rightarrow 0$ uniformly for $|z| \rightarrow \infty, 0 \leq \arg z \leq \pi$. We can therefore apply the Cauchy theorem, following Klein's procedure ⁽¹⁰⁾:

$$(9) \quad \int_{-\infty}^{+\infty} Q_m(\omega') d\omega' = \pi i \sum_j R_j$$

where R_j are the residues of $Q_m(z)$ at its poles on the real axis. A discussion of the residue at $z = 0$ is worthwhile. From eq. (3) one finds

$$(10) \quad \lim_{z \rightarrow 0} \frac{z^2}{u^2(z)} \langle rt | T_m(z) | r't' \rangle = 4\pi f^{(0)2} \sum_{r''t''} [- (\Psi_{rt}, \tau_{-m}\sigma_3\Psi_{r''t''})(\Psi_{r''t''}, \tau_m\sigma_3\Psi_{r't'}) + (\Psi_{rt}, \tau_m\sigma_3\Psi_{r''t''})(\Psi_{r''t''}, \tau_{-m}\sigma_3\Psi_{r't'})] -$$

We use now the property

$$(11) \quad \begin{cases} (\Psi_{r+}, \tau_m\sigma_3\Psi_{r'+}) = 0 \\ (\Psi_{r+}, \tau_m\sigma_3\Psi_{r'0}) = q\langle r+ | \tau_m\sigma_3 | r'0 \rangle, \end{cases}$$

(*) See Appendix.

to obtain

$$(12) \quad \lim_{z \rightarrow 0} \frac{z^2}{u^2(z)} \langle rt | T_m(z) | r't' \rangle = 4\pi f^2 m \delta_{rr'}; \quad f^2 = \rho^2 f^{(0)2}.$$

The forward scattering amplitude is defined in terms of $T_m(\omega)$ as follows:

$$(13) \quad f_m(\omega) = -\frac{\omega}{2\pi} \langle r + | T_m(\omega) | r + \rangle.$$

The imaginary part of eq. (9) gives, after straightforward manipulations:

$$(14) \quad \frac{1}{u^2(\omega)} \operatorname{Re} f_m(\omega) - \frac{1}{2} \left(1 + \frac{\omega}{\mu_c} \right) \operatorname{Re} f_m(\mu_c) - \frac{1}{2} \left(1 - \frac{\omega}{\mu_c} \right) \operatorname{Re} f_{-m}(\mu_c) = \\ = \frac{q^2}{\pi} \int_0^\infty \frac{d\omega'}{u^2(\omega') q'^2} \left[\frac{\operatorname{Im} f_m(\omega')}{\omega' - \omega} + \frac{\operatorname{Im} f_{-m}(\omega')}{\omega' + \omega} \right] + \frac{2mq^2}{\mu_c^2 \omega} f^2.$$

We stress that this result follows only from the requirement of charge symmetry implied by eq. (11), and holds even if the coupling constant of the neutral mesons to the source differs from the coupling constant of the charged ones (*).

3. - Behaviour of the imaginary part of the scattering amplitude.

We notice that

$$(15a) \quad \operatorname{Im} f_m(\omega) = 0, \quad \omega < \mu_0,$$

$$(15b) \quad \operatorname{Im} f_m(\omega) = \frac{q}{4\pi} \sigma_m(\omega), \quad \omega > \mu_c,$$

where $\sigma_m(\omega)$ is the total cross section for mesons of charge m against protons.

Clearly, in the range $\mu_0 < \omega < \mu_c$ there is no physical scattering. However, while $\operatorname{Im} f_+(\omega)$ is also zero, $\operatorname{Im} f_-(\omega)$ is different from zero and is given by

$$(16) \quad \operatorname{Im} f_-(\omega) = \operatorname{Im} f_-^{\text{ex}}(\omega) = \frac{\omega}{2} \sum_{\text{neutral}} \delta(\omega - E_n) (\Psi_{r+}, V_{a-}^+ \Psi_n^{(-)}) (\Psi_n^{(-)}, V_{a-} \Psi_{r+}), \\ (\mu_0 < \omega < \mu_c),$$

(*) This indeed is the case in our theory because of the factor $f^{(0)}/\mu_x$ in the p -wave interaction hamiltonian.

were the sum is carried only on states with one meson of charge zero, and the notation $\text{Im } f_-^{\text{ex}}$ stresses that only charge exchange processes appear in the intermediate states.

The ω -dependence of $\text{Im } f_-(\omega)$ appears explicitly from the expressions (A.1) (see Appendix): it is easily seen that $\text{Im } f_-(\omega)/u^2(\omega)$ is analytic at $\omega = \mu_c$ and its value in the unphysical range can be obtained by analytic continuation from its value immediately above threshold ($\omega \gtrsim \mu_c$). In this region the total cross section $\sigma_-(\omega)$ can be splitted into charge exchange $\sigma_{\text{ex}}^-(\omega)$ and elastic $\sigma_{\text{el}}^-(\omega)$ cross sections. Of these ⁽¹¹⁾

$$(17) \quad \sigma_-^{\text{ex}}(\omega) = \frac{4\pi}{q_c} \text{Im } f_-^{\text{ex}}(\omega) = \frac{8\pi}{9} \frac{q_0}{q_c} \Delta^2,$$

where

$$(18) \quad \Delta = \frac{\alpha_3 - \alpha_1}{q_c} \approx 0.27 \mu_c,$$

is constant at threshold and we have introduced explicitly the notation $q_0 = \sqrt{\omega^2 - \mu_0^2}$, $q_c = \sqrt{\omega^2 - \mu_c^2}$ to distinguish neutral mesons momenta from charged mesons momenta corresponding to the same energy.

Therefore we infer easily

$$(19) \quad \text{Im } f_-(\omega) = \frac{2}{9} q_0 \Delta^2.$$

We are ready now to write explicitly our dispersion relations (14) as follows (*):

$$(20) \quad \text{Re } f_m(\omega) - \frac{1}{2} \left(1 + \frac{\omega}{\mu_c} \right) \text{Re } f_m(\mu_c) - \frac{1}{2} \left(1 - \frac{\omega}{\mu_c} \right) \text{Re } f_{-m}(\mu_c) = \\ - \frac{2}{9\pi} q_c^2 \Delta^2 \int_{\mu_0}^{\mu_c} \frac{d\omega'}{q_c'^2} q_0' \frac{1}{\omega' + m\omega} + \frac{2mq_c^2}{\mu_c^2 \omega} f^2 + \frac{q_c^2}{4\pi^2} \int_{\mu_c}^{\infty} \frac{d\omega'}{u^2(\omega')} \frac{1}{q_c'} \left[\frac{\sigma_m(\omega')}{\omega' - \omega} + \frac{\sigma_{-m}(\omega')}{\omega' + \omega} \right].$$

At first sight one might consider the first term of the r.h.s. of eq. (20) as the correction to the dispersion relations we are looking for, since all the other expressions appearing in this equation are identical to the ones of the conventional dispersion relations. However this term is not finite, because the

⁽¹¹⁾ H. A. BETHE and F. DE HOFFMANN: *Mesons and Fields* (New York), vol. 2.

(*) We assume $u^2(\omega) = 1$ for the energy values of interest.

integrand diverges logarithmically at the upper limit. A closer examination of the integral on the cross sections gives immediately the answer to this puzzle. In fact the total cross sections introduced in the conventional dispersion relations coincide with the experimental ones except at very low energies, because the divergence at threshold of the exchange cross section (17) is not taken into account. In other words the conventional evaluation of the integrals on the total cross sections is performed by extrapolating to zero energy the experimental total cross sections at, say, 30 MeV, with the assumption that mesons have all the same mass. In formulae, while the experimental total cross section is given by

$$(21) \quad \sigma_-(\omega) = \sigma_-^{\text{ex}}(\omega) + \sigma_-^{\text{el}}(\omega),$$

the usual procedure amounts practically to assume for the cross section the expression

$$(22) \quad \sigma'_-(\omega) = \sigma_-^{\text{ex}'}(\omega) + \sigma_-^{\text{el}}(\omega),$$

where

$$(23) \quad \sigma_-^{\text{ex}'}(\omega) = \frac{q_c}{q_0} \sigma_-^{\text{ex}}(\omega).$$

In conclusion we write the corrected dispersion relations as

$$(24) \quad \text{Re } f_{\pm}(\omega) - \frac{1}{2} \left(1 + \frac{\omega}{\mu_c} \right) \text{Re } f_{\pm}(\mu_c) - \frac{1}{2} \left(1 - \frac{\omega}{\mu_c} \right) \text{Re } f_{\mp}(\mu_c) = \\ = \pm \frac{2q_c^2}{\mu_c^2 \omega} f^2 + \frac{q^2}{4\pi^2} \int_{\mu_c}^{\infty} \frac{d\omega'}{u^2(\omega')q'_c} \left[\frac{\sigma'_{\pm}(\omega')}{\omega' - \omega} + \frac{\sigma'_{\mp}(\omega')}{\omega' + \omega} \right] + C_{\pm}(\omega),$$

where the correction is given by:

$$(25) \quad C_{\pm}(\omega) = \frac{2q_c^2}{9\pi} A^2 \int_{\mu_0}^{\mu_c} \frac{d\omega'}{\omega'^2 - \mu_c^2} \frac{q'_0}{\omega' \pm \omega} - \frac{q_c^2}{4\pi^2} \int_{\mu_c}^{\infty} \frac{d\omega'}{u^2(\omega')q'_c} \frac{\sigma_-^{\text{ex}}(\omega')}{\omega' \pm \omega} \left(\frac{q'_c - q'_0}{q'_0} \right).$$

Since $\sigma_-^{\text{ex}}(\omega)$ at threshold is given by eq. (17) it is easy to see that $C_{\pm}(\omega)$ has to be calculated as a principal value integral with the singularity $1/(\omega'^2 - \mu_c^2)$ and is therefore finite.

4. - Numerical results.

We write C_{\pm} as follows:

$$(26) \quad C_{\pm} = C_{\pm}^I + C_{\pm}^{II} + C_{\pm}^{III},$$

where

$$(27a) \quad C_{\pm}^I = \frac{2q_c^2}{9\pi} \Delta^2 \int_{\mu_c(1-\varepsilon)}^{\mu_c(1+\varepsilon)} d\omega' \frac{1}{\omega'^2 - \mu_c^2} \frac{q'_0}{\omega' \pm \omega},$$

$$(27b) \quad C_{\pm}^{II} = \frac{2q_c^2}{9\pi} \Delta^2 \int_{\mu_c(1-\varepsilon)}^{\mu_c(1+\varepsilon)} d\omega' \frac{1}{q'_c} \frac{1}{\omega' \pm \omega},$$

$$(27c) \quad C_{\pm}^{III} = \frac{q_c^2}{4\pi^2} \int_{\mu_c(1-\varepsilon)}^{\infty} d\omega' \frac{\sigma_{-}^{ex'}(\omega')}{u^2(\omega') q_c'^2} \frac{q'_0 - q'_c}{\omega' \pm \omega},$$

with ε defined by $\mu_0 = \mu_c(1 - \varepsilon)$.

The evaluation of C_{\pm}^I is made by considering $\omega' \pm \omega$ a constant in the range of integration and taking as independent variable q'_0 :

$$(28) \quad C_{\pm}^I \approx \frac{2}{9\pi} q_c^2 \Delta^2 \frac{1}{\mu \pm \omega} \int_0^{2\sqrt{\varepsilon}} \frac{x^2 dx}{x^2 - 2\varepsilon} = \frac{2}{9\pi} q_c^2 \Delta^2 \sqrt{\varepsilon} \frac{0.75}{\mu \pm \omega}.$$

Since this evaluation introduces errors of order ε relatively to C_{\pm}^I , μ indicates either of the values μ_0 or μ_c .

Similarly C_{\pm}^{II} is easily evaluated as

$$(29) \quad C_{\pm}^{II} = -\frac{2}{9\pi} q_c^2 \Delta^2 \sqrt{\varepsilon} \frac{1.41}{\mu \pm \omega}.$$

A little more care is required to evaluate C_{\pm}^{III} . First of all the upper limit can be replaced by $\mu_c(1 + \alpha)$ where α is something of the order of 0.3 (corresponding to an energy $\omega' - \mu_c \approx 40$ MeV) since at this energy $q'_c - q'_0$ is already negligible.

Secondly we still replace $\omega' \pm \omega$ with $\mu \pm \omega$. This is a good approximation for the interesting values of ω ($\omega - \mu \approx 120$ MeV).

Thirdly we again replace $\sigma_{-}^{ex'}$ by its constant value at threshold. Since the

cross section varies at most of 30% in the whole range of integration, the error introduced will not exceed this value. Taking the value at threshold gives an upper limit for the total correction C_{\pm} . Thus we write

$$(30) \quad C_{\pm}^{\text{III}} \cong \frac{2}{9\pi} q_c^2 A^2 \frac{1}{\mu \pm \omega} \int_{\sqrt{2\varepsilon}}^{\sqrt{2\alpha + \alpha^2}} \frac{dx}{x} [\sqrt{x^2 + 2\varepsilon} - x] = \frac{2}{9\pi} q_c^2 A^2 \frac{\sqrt{\varepsilon}}{\mu \pm \omega} 0.44.$$

Collecting the results (28), (29), (30) we obtain

$$(31) \quad C_{\pm} \approx \frac{2}{9\pi} q_c^2 A^2 \frac{\sqrt{\varepsilon}}{\mu \pm \omega} 0.22.$$

In the energy range of interest the correction C_- to the dispersion relation for negative mesons is several times larger than the correction C_+ for positive ones. However the difference is by far too small to account for the results of the Bologna group. For instance, at $q_c = \mu$ Eq. (31) gives for this difference about 1% of f^2 .

* * *

We are grateful to prof. G. PUPPI and dr. A. STANGHELLINI for communication of their results and for helpful discussions.

APPENDIX

By performing the commutator indicated in eq. (4) it is easy to obtain the following expression ($m = \pm 1$).

$$(A.1) \quad V_{qm} = \frac{v(q)}{(2\omega_{qm})^{\frac{1}{2}}} \left\{ i(4\pi)^{\frac{1}{2}} f^{(0)} \boldsymbol{\sigma} \cdot \mathbf{q} \tau_m \frac{1}{\mu_c} - \right. \\ \left. - \sqrt{\frac{m}{2}} \sum_{\alpha'} (\delta_{\alpha'1} + im\delta_{\alpha'2}) \int d^3\mathbf{x} s(\mathbf{x}) [2\lambda_0^{(0)} \varphi_{\alpha'}(\mathbf{x}) + \lambda^{(0)} \sum_{\alpha\alpha''} \varepsilon_{\alpha\alpha'\alpha''} \tau_{\alpha} (\pi_{\alpha''}(\mathbf{x}) + i\omega_{qm} \varphi_{\alpha''}(\mathbf{x}))] \right\}.$$

Similarly one has ($m = \pm 1$)

$$(A.2) \quad [a_{qm}, V_{qm}] = \frac{v^2(q)}{\omega_{qm}} (1 \cdot \lambda_0^{(0)} + m\omega_{qm} \tau_3 \lambda^{(0)}).$$

RIASSUNTO

Si calcolano le correzioni alle relazioni di dispersione per scattering in avanti pione-nucleone dovute alla differenza di massa tra mesoni π carichi e neutri. Poichè le relazioni di dispersione ottenute da una teoria relativistica hanno essenzialmente la stessa forma di quelle derivate da una hamiltoniana di sorgente fissa con onde s e p , il calcolo è stato effettuato introducendo in tale hamiltoniana le masse mesoniche osservate. Il termine di correzione alle relazioni di dispersione è differente per mesoni positivi e negativi, ma risulta piccolo. Per mesoni d'impulso q dell'ordine della massa mesonica esso introduce una differenza tra i due casi che ammonta a circa l'uno per cento di f^2 .

On the Problem of the Static Helium Film.

III. - The Profile of the Film and its Dependence on Temperature.

S. FRANCHETTI

Istituto di Fisica dell'Università - Firenze

(ricevuto il 28 Febbraio 1957)

Summary. — The profile of the film and its dependence on temperature, both below and above the λ -point, are studied on the basis of the results reached in papers I and II of the present series. The conclusions appear to be in fair agreement with experiment. The thermodynamic condition for film formation under the action of Van der Waals forces, is also discussed and found to be fulfilled.

1. - Introduction.

If t is the thickness of the film at a height z above the free surface of the bulk liquid, the profile of the film will be given by a function $t = t(z, T)$ which is the unknown of the problem. To determine it an equation (eq. (2)) has been given in the first paper of this series ⁽¹⁾, namely

$$(1) \quad \frac{\partial}{\partial t} \Delta F(z, t) = 0,$$

with

$$(2) \quad \Delta F = F_{\text{film}} - F_{\text{bulk}},$$

where F_{film} is the free energy per cm^2 of the film at a given height z , while

⁽¹⁾ S. FRANCHETTI: *Nuovo Cimento*, **4**, 1504 (1956) and **5**, 183 (1957) (henceforth referred to as I and II).

F_{bulk} is the free energy of the same amount of helium belonging to the bulk of the liquid ⁽²⁾.

ΔF can be written as a sum of four contributions (eq. (3) I)

$$(3) \quad \Delta F = \Delta F_w + \Delta W_g + \Delta E_0 + (\Delta F)_{\text{exc}}.$$

We shall now review these contributions.

2. The Van der Waals and gravity contributions ΔF_w and ΔW_g

These have already been given explicitly in eqs. (10) and (3'') of I and are simply recalled here for convenience. They may be written

$$(4) \quad \Delta F_w = \text{const} + \frac{\rho_0}{2m} (A_f - 2A_{\text{He}}) t^{-2},$$

$$(5) \quad \Delta W_g = \rho_0 g z t.$$

(The reader is referred to the «key» in Appendix B of the present paper for the meaning of these and subsequent symbols). In rewriting the expression for ΔF_w the last term in eq. (10) I, being very small, has been omitted and the first two have been replaced by «const.»; indeed, being independent of t they do not contribute to eq. (1).

3. - The «zero point energy» and the «exciton» contributions ΔE_0 and $(\Delta F)_{\text{exc}}$

These involve the effects due to the smallness of the film thickness t , treated in paper II. Eqs. (10') and (12'') II give on two different assumptions the change of zero point energy per atom. Taking 0.86 as an average of the two numerical coefficients, we have only to multiply by the number of atoms per cm^2 of the film, namely $(\rho_0/m)t$, to get E_0 ⁽³⁾

$$(6) \quad \Delta E_0 = 0.86 \cdot 10^{-31} \frac{\rho_0}{m} t^{-1} = 1.87 \cdot 10^{-9} t^{-1}$$

As regards $(\Delta F)_{\text{exc}}$, there are two contributions to it arising from excitons,

⁽²⁾ Use of free energy is due to the assumption of negligible external pressure (See I, Sect. 2). About condition (1) see also Appendix A of this paper.

⁽³⁾ The effect of the non rigorous uniformity of the density is entirely negligible in this connection.

that we shall call type *A* and type *B*, whose energy is respectively a *linear* and a *quadratic* function of momentum. It will be convenient to consider the respective contributions to the free energy per gram of the liquid, which we denote by f .

In the linear case, we have from eq. (28) II, putting v for the average specific volume of the liquid

in the *film*

$$(7) \quad f = f_{\infty} + \frac{3.774}{h^2 C^2} v (kT)^3 t^{-1}; \quad (A \text{ excitons}),$$

in the *bulk liquid* (characterized by the subscript 0)

$$(7') \quad f_0 = f_{0\infty}. \quad (A \text{ excitons}).$$

Subtracting and recalling (28a) II gives

$$(8) \quad (\Delta f)_A = f - f_0 = -\frac{27.20}{h^3} (kT)^4 \Delta \left(\frac{v}{C^3} \right) + \frac{3.774}{h^2} (kT)^3 \frac{v}{C^2} t^{-1}.$$

For type *B* excitons, the equation needed is (22) II which gives in the *film*

$$(9) \quad f = f_{\infty} + \frac{5.165}{h^2} (kT)^2 v \mu t^{-1}; \quad (B \text{ excitons}),$$

in the *bulk liquid*

$$(9') \quad f = f_{0\infty}. \quad (B \text{ excitons}).$$

Subtracting and recalling eq. (22a) II gives

$$(10) \quad (\Delta F)_B = -\frac{1.341(2\pi)^{\frac{3}{2}}}{h^3} (kT)^{\frac{3}{2}} \Delta(v\mu^{\frac{3}{2}}) + \frac{5.165}{h^2} (kT)^2 v \mu t^{-1}.$$

To get the phonon contribution to eq. (1) one has only to multiply expression (8) by qt and take the derivative with respect to t . Since we have (I, eq. (18'))

$$(11) \quad \frac{\partial}{\partial t} = v_0 \frac{\Delta_1 t}{(t + \Delta_1 t)^2} \frac{\partial}{\partial v},$$

the procedure requires the knowledge of $\partial C/\partial v$ and $\partial^2 C/\partial v^2$. For these quan-

tities the values

$$(12) \quad \left(\frac{\partial C}{\partial v}\right)_{p=0} = -7.61 \cdot 10^3, \quad \left(\frac{\partial^2 C}{\partial v^2}\right)_{p=0} = 1.04 \cdot 10^4 \quad (\text{abs. un.})$$

have been derived from the data of ATKINS and STASIOR⁽⁴⁾.

The final result, dropping smaller terms, is

$$(13) \quad \frac{\partial}{\partial t}(\Delta F)_A = 1.79 \cdot 10^3 T^3 \Delta_i t \cdot t^{-2}.$$

The procedure is therefore a straightforward one in this case. Type *B* excitons, on the contrary, require a careful discussion concerning: *a*) the temperature dependence of the terms in eq. (10), and, *b*) the volume dependence of the effective mass μ .

The trouble with the *temperature dependence* arises because expression (10) was derived by treating type *B* excitons as a saturated Bose-Einstein perfect gas with an energy spectrum $(1/2\mu)\mathbf{p}^2$. It is well known, however, that such a simple treatment does not lead to quantitatively satisfactory results. In particular the number N_n of particles (other than phonons) constituting the normal fluid, that is belonging to excited states, would have to vary as $T^{1.5}$, whereas experiments give a much more rapidly varying function. This suggests to introduce an empirical factor in the expression of N_n writing it as

$$(14) \quad N_n = \eta(T) N_n^0,$$

where N_n^0 is the number given by condensation theory. Since experiments give for N_n a dependence approaching $T^{5.5}$ towards the λ -point, we shall assume in the region between, say, 1.4 °K and T_λ

$$(14') \quad \eta(T) \approx \eta_0 T^4. \quad (1.4 < T < T_\lambda).$$

At lower temperatures this correction is undoubtedly insufficient; however, in that region the temperature dependent terms in the equation for the film thickness are negligible anyway, so we need not worry about them. The region beyond T_λ is also excluded. It will be considered in Sect. 5.

It is an obvious incompleteness of the theory that the number of «excited particles» has to be corrected empirically. However, we prefer to take this course until the origin of type *B* excitons has been further elucidated⁽⁵⁾.

(4) K. R. ATKINS and R. A. STASIOR: *Canad. Journ. of Phys.*, **31**, 1156 (1953).

(5) In Landau's treatment as well, there is an empirically adjusted element in the expression for roton concentration. The difference is that here we are trying to remain within the frame of a London type theory.

The constant η_0 in (14') can be determined through the equation characteristic of the λ -point, namely $N_n = N$, which will become

$$(15) \quad N = \eta_0 T_\lambda^4 N_n^0(T_\lambda).$$

Since we have

$$(16) \quad N_n^0(T) = \frac{2.612}{h^3} V (2\pi\mu kT)^{1.5},$$

introducing the value $12.5 \cdot 10^{-24}$ g for μ (already employed in Sect. 2 of II) one gets

$$(14'') \quad \eta_0 = 0.0291 \text{ } (^{\circ}\text{K})^{-4}.$$

Experimental data about specific heats support—at least approximately—the assumption that type *B* excitons, except for their number, behave as the non-condensed part of a Bose-Einstein perfect gas. (The energy per particle is more or less that expected in this hypothesis). The simplest course to take (although by no means rigorous) is therefore to introduce the same $\eta(T)$ factor in the expression for $(\Delta F)_B$ ⁽⁶⁾. We thus get

$$(10') \quad \Delta f_B = -4.74 \cdot 10^{38} T^{6.5} \Delta(v\mu^{\frac{3}{2}}) + 6.52 \cdot 10^{19} T^6 v\mu t^{-1} \quad (T < T_\lambda).$$

It should be noted that the use of the *same* $\eta(T)$ factor for both the bulk liquid and the liquid in the film, involves in particular the simplifying assumption that the total number of *B*-excitons per gram undergoes no significant change in going from the bulk liquid to the film. Put in another form, this means the neglect of any *direct* perturbation from the Van der Waals field of the wall on *B* excitons (and as a consequence on the corresponding occupation numbers).

To get the contribution to eq. (1) there remains (as for *A* excitons) to apply the operator

$$\frac{\partial}{\partial t} \cdot q t = v_0 \frac{\Delta_f t}{(1 + \Delta_f t)^2} \frac{\partial}{\partial v} \cdot q t.$$

Here comes in the problem of the volume dependence of the effective mass μ

⁽⁶⁾ This procedure is less unjustified for the second term (« limitation effect ») which is rather independent of the condensation mechanism (II, App. A). This term is likely to be the leading one. (See Sect. 4).

(1-st and 2-nd derivatives). Since there is no hope of deriving these quantities from the semi-empirical method employed in determining μ ⁽⁷⁾, the only thing to do is to write

$$(17) \quad \mu(v) = \mu_0 \left[1 - \alpha \frac{v - v_0}{v_0} + \beta \left(\frac{v - v_0}{v_0} \right)^2 \right],$$

where α and β are dimensionless constants to be determined experimentally. Clearly, we should expect them—especially α —to be of the order of some units at most (See Sec. 5).

Taking $\mu_0 = 12.5 \cdot 10^{-24}$ g (see II, Appendix B) the final result is, dropping smaller terms

$$\frac{\partial}{\partial t} (\Delta F)_B = -3.14 \cdot 10^4 \left(\alpha - \beta - \frac{\alpha^2}{4} \right) T^{6.5} \frac{\Delta_i t}{t^2} - 0.815 \cdot 10^{-3} \alpha T^6 \frac{\Delta_i t}{t^2} \quad (T < T_\lambda).$$

Combining with (13) one gets

$$(18) \quad \frac{\partial}{\partial t} (\Delta F)_{\text{exc}} = -R(T) \cdot 10^{-9} t^{-2},$$

with

$$(18') \quad R(T) = \left[3.14 \left(\alpha - \beta - \frac{\alpha^2}{4} \right) T^{3.5} 10^7 \Delta_i t + 0.815 \alpha T^3 - 1.79 \right] \cdot 10^6 T^3 \Delta_i t. \quad (T < T_\lambda)$$

(We recall that $\Delta_i t$ is a function of T and of the nature of the wall, given graphically and numerically in two instances in Fig. 2 and Table III of paper I). The first term in the above expression comes from the first one in (10') (« ordinary » density effect). The last two are due to « limitation » effects (B and A excitons respectively) ⁽⁸⁾.

4. - The equilibrium equation.

Eqs. (4), (5), (6) and (18), (18') give what is needed for setting up the final equation $(\partial/\partial t)(\Delta F) = 0$.

⁽⁷⁾ S. FRANCHETTI: *Nuovo Cimento*, **12**, 749 (1954) and II, App. B.

⁽⁸⁾ Strictly, one should introduce in the term $0.815 \alpha T^3$ the correction contained in eqs. (22'), (22'') of II. It amounts to about a 5% increase at T_λ .

It reads ⁽⁹⁾

$$(19) \quad 2.18 \cdot 10^{22} (A_f - 2A_{\text{He}}) t^{-3} + [1.87 + R(T)] \cdot 10^{-9} t^{-2} = 142z$$

or else, by putting

$$(19') \quad \tau = \tau(z, T) = 10^6 t$$

(so that τ is the film thickness in units of 10^{-6} cm)

$$(20) \quad \mathcal{A} + [1.87 + R(T)]\tau = 142z\tau^3,$$

with

$$(20') \quad \mathcal{A} = 2.18 \cdot 10^{37} (A_f - 2A_{\text{He}}).$$

Some values for the A coefficients—of whom A_f is specific of the nature of the wall—have been given in paper I (eqs. (6'), (15), (A.1')). In the experiments of JACKSON and co-workers ⁽¹⁰⁾, a metal wall was coated with a thin layer of Ba-stearate. In this case, the values of Δt (appearing in $R(T)$) appropriate for *stearate* must be used, but A_f has to be that of the *metal* of the wall. The reason is that the very thin coating (about 24 Å thick) affects the liquid only in its vicinity—the region important in determining Δt , but not at larger distances. A common value $\mathcal{A} = 10.8$ was adopted both for a typical metal (such as copper) and for a stearate coated metal wall.

At this point an experimental datum has to be inserted to get a condition for the two constants α, β appearing in $R(T)$ ⁽¹¹⁾. For this purpose we have chosen the relative increase (6.5%) of the film thickness at 1 cm height between 1.32 °K and 2.05 °K, which results from HAM and JACKSON's measurements (ref. ⁽¹⁰⁾). In other words we have imposed

$$(21) \quad \frac{\tau(1, 2.05)}{\tau(1, 1.32)} = 1.065.$$

⁽⁹⁾ In writing down eq. (19), the surface energy has been assumed to be thickness-independent. Indeed, C. G. KUPER [*Physica*, **22**, 1291 (1956)] has recently suggested that surface waves might be affected by the Van der Waals field of the wall. This would bring about a t -dependent term, concerning mainly the zero point energy of these waves. An exact treatment of such an effect would be rather difficult. However, a rough evaluation of orders of magnitude leads to a contribution to eq. (19) which is *negligible* in comparison of the Van der Waals term even for a thickness of 10^{-6} cm (corresponding to more than 1 dm height).

⁽¹⁰⁾ In particular, A. C. HAM and L. C. JACKSON: *Phil. Mag.*, **45**, 1084 (1954).

⁽¹¹⁾ Of course these should not depend on the nature of the wall.

Table I gives the pairs of values for α and β fulfilling the imposed requirement ⁽¹²⁾.

TABLE I.

α	1.0	1.5	2.0	2.25	2.5	2.6	3.0	4.0
β	-4.12	-2.03	0.063	0.87	1.78	2.13	3.50	6.55
$r(2)$	1.28	0.52	0.14	0.0	-0.085	-0.124	-0.24	-0.43

It is worth noting that, as regards the behaviour up to the λ -point, it practically does not matter which pair is chosen. The same, however, is not true above the λ -point. The values $\alpha = 2.6$ and $\beta = 2.13$ have been adopted to suit the results in this region. (See following section).

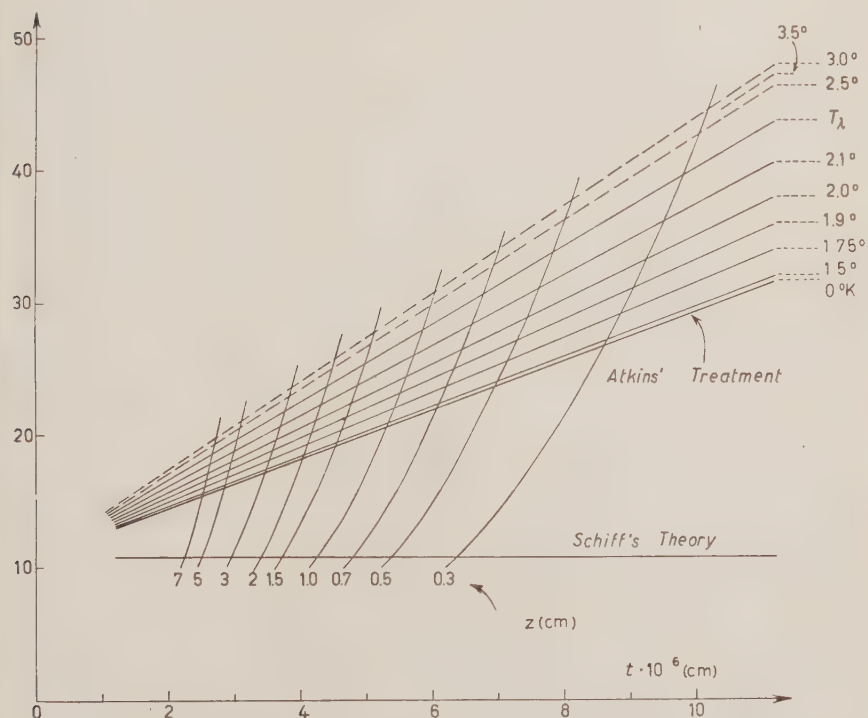


Fig. 1. - Graph for the thickness of the static helium film on a vertical stearate coated metal surface, as a function of temperature (T) and height (z) above the free surface of the liquid. The thickness is given by the abscissa of the interception of the straight line labeled according to T and the parabolic curve labeled according to z .

⁽¹²⁾ The 3^d row gives the ratio r of the first term to the second one in expression (18') at $T = 2^\circ\text{K}$. (See footnote 6).

The values of $\tau(z, T)$ can be obtained graphically by plotting the two sides of eq. (20) as functions of τ at various temperatures and looking for the abscissae of the interceptions. Fig. 1 and 2 show two such graphs, while in Fig. 3 the relative increase of thickness at 1 cm height is plotted as a function of T .

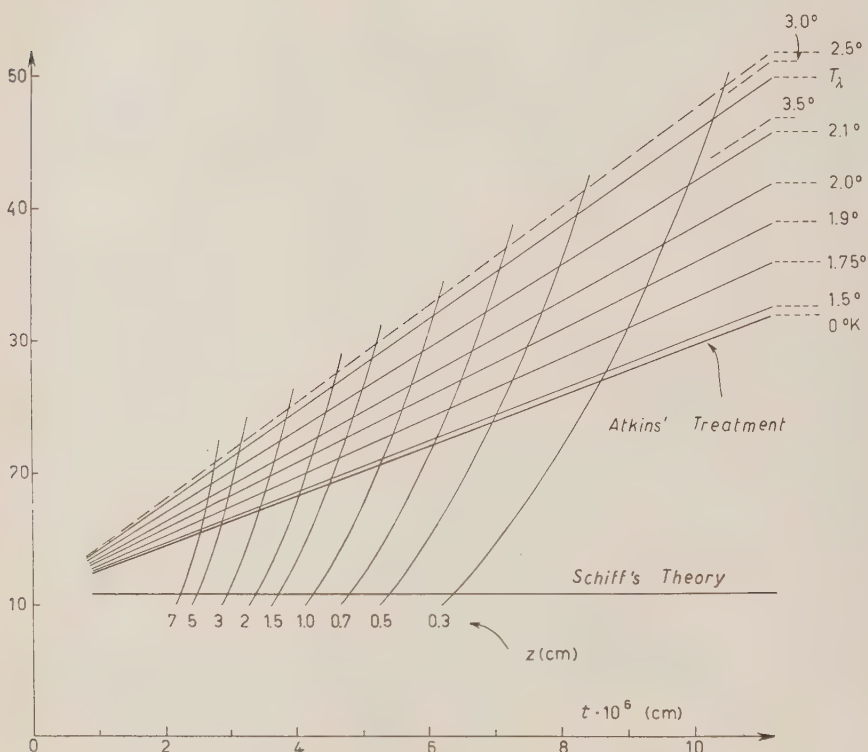


Fig. 2. — Same graph as in Fig. 1, for a copper surface.

It can be seen that the values of the thickness at $z = 1$ cm are somewhat larger than those of HAM and JACKSON (ref. (10)) or ATKINS (13) but definitely lower than those of BOWERS (14) or DAUNT and MENDELSSOHN (15).

Very often experimental results are expressed by a formula of the type

$$(22) \quad \tau = \tau_1 z^{-1/2}.$$

(13) K. R. ATKINS: *Proc. Roy. Soc.*, **203**, 119 (1950).

(14) R. BOWERS: *Phil. Mag.*, **44**, 1309 (1953).

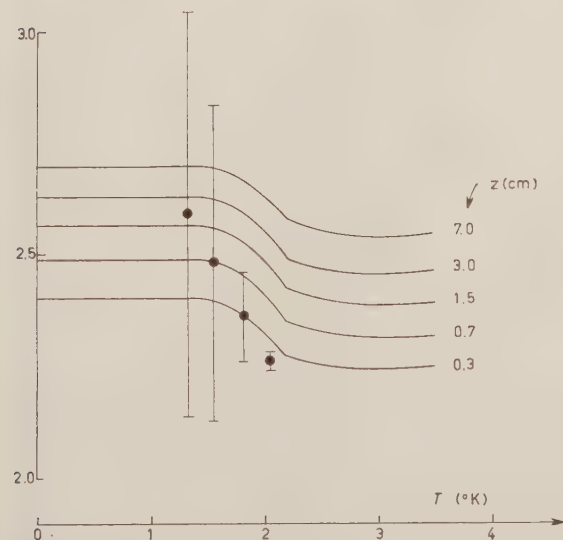
(15) J. G. DAUNT and K. MENDELSSOHN: *Proc. Roy. Soc.*, **170**, 439 (1939).

In the present theory q is not a constant but a function of z and T (or τ and T). Identifying q with $-\text{d}(\log z)/\text{d}(\log \tau)$ one finds easily from eq. (10) the formula

$$(23) \quad q = \frac{3\mathcal{A} + 2[1.87 + R(T)]\tau}{\mathcal{A} + [1.87 + R(T)]\tau} :$$

(giving values between 2 and 3) by means of which q can be computed.

Fig. 4 shows—for a stearate coated wall—some $q(T)$ curves for various values of the height z . On the same graph are plotted for comparison some experimental data obtained by HAM⁽¹⁶⁾ for a height z of about 1 cm. Although all but one of these data are rather uncertain,



5. - The film at temperatures beyond the λ -point.

Some uncertainties are encountered in trying to extend the theory beyond

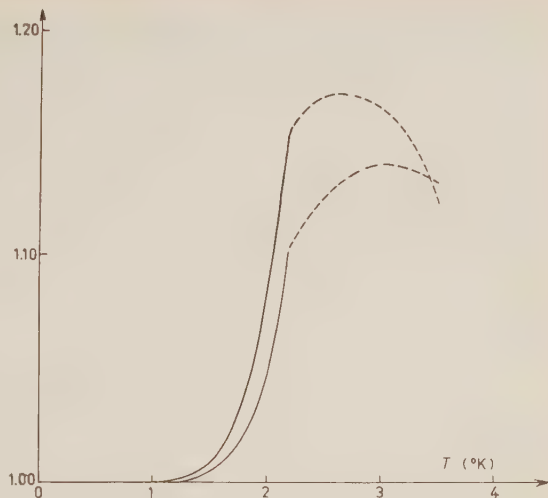


Fig. 3. - The relative increase of the film thickness at 1 cm height. Upper curve: copper surface. Lower curve: stearate coated surface.

Fig. 4. - Curves for the parameter $q(T, z)$ appearing in eq. (22).

⁽¹⁶⁾ A. C. HAM: *Thesis* (Bristol, 1954).

⁽¹⁷⁾ Same observation as for (18') [footnote (8)] concerning the term $60.4 \propto T^{0.5}$.

the λ -point. In the first place, the exciton free energy change $(\Delta F)_{\text{exc}}$ has been worked out on assumptions applying only up to the λ -point. For the purpose of what may be not better than a simple estimate, we may try to correct the contribution to $(\Delta F)_{\text{exc}}$ from type *B* exciton—which alone undergo Bose-Einstein condensation—so as to take into account (at least) the fact that their number no longer increases above the λ -point. Roughly this can be done by putting $T_{\lambda}^{5.5} T^{n-5.5}$ in place of T^n in the first two terms of the expression for $R(T)$, eq. (18'), getting (17)

$$(18'') \quad R(T) = \left[2.32 \left(\alpha - \beta - \frac{\alpha^2}{4} \right) T \cdot 10^9 \Delta_i t + \right. \\ \left. + 60.4 \alpha T^{0.5} - 1.79 T^3 \right] 10^6 \Delta_i t. \quad (T > T_{\lambda}).$$

A further difficulty arises because the choice among the pairs of Table I is no longer irrelevant for $T > T_{\lambda}$. This means the need for more experimental information. According to the work of HAM and JACKSON (ref. (10)) there is no significant change in the thickness of the film at $z = 1$ cm between T_{λ} and 3.8 °K. If we take this as an indication that $\tau(1, T)$ must be stationary at some point T_0 between T_{λ} and 3.8 °K, we may add to (21) the further condition

$$(21') \quad \frac{d}{dT} \tau(1, T) = 0, \quad (T = T_0),$$

which in turn requires

$$(21'') \quad \frac{d}{dT} R(T) = 0. \quad (T = T_0).$$

Taking $T_0 = 3.0$ °K one finds from (21) and (21')

$$\alpha = 2.6, \quad \beta = 2.13.$$

(The values adopted in drawing the graphs in Fig. 1 and 2). Taking instead $T_0 = 3.5$ °K the values would be $\alpha = 2.35$ and $\beta = 1.24$, which means that β is very uncertain but α should be in the neighbourhood of 2.5.

Needless to say, it would have been preferable not to have introduced any adjusted constants like α and β . It is however satisfactory that the experimental temperature dependence of the film can at least be explained by giving quite reasonable values to these unknown parameters. This may be taken as a hint that the theory is essentially right, although an argument of

this kind cannot, of course, exclude the neglect in the equilibrium equation of terms having the same importance and a similar temperature dependence than those taken into consideration. Indeed their absence might not alter the order of magnitude of α and β .

It may also be noted that the values of the constants lie in the field where the ratio r of the «ordinary» term to the «limitation term in the expression for $R(T)$ is small (see Table I). This shows the importance of the latter effect for the temperature dependence of the film.

6. - Conclusions.

Summarizing, the main results of the theory are as follows.

1) The form of the film is determined by a delicate balance between several small effects, among which there are «limitation» effects, that is effects on the thermodynamic functions due to the smallness of the thickness.

2) The temperature dependent properties of the static film are essentially due to «limitation» effects on *excitons*, the main contribution coming from «quadratic» ones

3) The thickness of the static film at a given height above the surface of the bulk liquid increases with temperature for temperatures below the λ -point. This effect should be somewhat greater for a metal wall than for a stearate coated one. (See graphs in Fig. 3). Above T_λ the situation is more uncertain but, presumably, the thickness of the film should reach a maximum and then decay by increasing temperature, although it is very likely that the critical temperature is reached before the film has faded away. (See also Appendix A).

4) Representing the thickness of the static film as $t = t_1 z^{-1/2}$ the value of q is between 2 and 3. It increases with height and decreases slightly with increasing temperature (Fig. 4).

5) The value of q (by given height and temperature) depends on the nature of the wall. Walls exerting stronger Van der Waals attraction should give q values nearer to 3. (Qualitatively $q_{\text{metal}} > q_{\text{glass}} > q_{\text{paraffin}}$).

* * *

In concluding, it is a pleasure for the Author to thank Dr. A. C. HAM and Prof. L. C. JACKSON for kind intercourse and valuable informations about experimental details as well for the permission to quote the experimental data plotted in Fig. 3.

APPENDIX A

« Affinity » for film formation.

The equilibrium condition for the film, recalled at the beginning of Sect. 1, namely

$$\frac{\partial}{\partial t}(F_{\text{film}} - F_{\text{bulk}}) = 0,$$

is of course only a *necessary*, not a sufficient one. It should be supplemented by an existence condition, namely

$$\Delta F = F_{\text{film}} - F_{\text{bulk}} < 0,$$

meaning a positive « affinity » for film formation.

It is not difficult to set up an expression for ΔF , the starting points being eqs. (3), (5), (6), (8), (10') (the latter with the appropriate corrections dealt with for $T < T_\lambda$ in Sect. 3 and for $T > T_\lambda$ in Sect. 5), together with eq. (10) of paper I⁽¹⁸⁾.

We shall however not enter into details which would bring about nothing essentially new. The most important *negative* contribution to ΔF (practically, both T and t independent) turns out to come from the third term in eq. (10) I, expressing the Van der Waals energy wall-film. With $x_0 = 3 \cdot 10^{-8}$ cm this term gives about -6 erg cm⁻² for a copper wall and about -1.7 erg cm⁻² for a stearate coated one. The other terms, mostly positive, are much smaller (for current values of t) at least until T is not substantially greater than T_λ . This ensures the necessary *negative* sign for ΔF . (And at the same time makes the calculation less critical).

Above T_λ the situation is more uncertain. The most important *positive* term in this region is one in T^4 due to phonons and, at about 13 °K for a copper wall or about 10 °K for a stearate coated one, it would balance the negative Van der Waals term. However, we should expect the phonon term to rise less rapidly than T^4 for various reasons (finiteness of Debye temperature, change in the character of the thermal motion). Thus, compensation should take place at even higher temperatures. Imperfect as it may be, this analysis renders nevertheless very unlikely that any change of sign for ΔF will occur below the critical temperature. This is the ground for the statement made on the subject at point 3) of Sect. 6. At the same time the existence of a stationary point in the thickness versus temperature curves somewhere above T_λ is made understandable by these considerations⁽¹⁹⁾.

⁽¹⁸⁾ Note that the expression for ΔF obtained in this way is valid only for a *liquid* layer. The considerations that follow would therefore not apply to any *gaseous* film.

⁽¹⁹⁾ This result does not depend on the parameters α , β introduced into eq. (17), in which enter only terms of higher order than those important for ΔF .

It may be mentioned that among the «small terms» referred to above, there is a term E_{sol} which is the change in free energy associated with the solidification of the inner layers of the film. In evaluating it one should not confuse it with the work spent in compressing that portion of the film. Rather, it is of the order of $T\Delta S = (\text{melting heat per gram}) \times (\text{mass of solid layer per cm}^2)$. At 2.5 °K this gives about 0.44 erg/cm² for a copper wall and 0.30 erg/cm² for stearate. Smaller values obtain at lower temperatures.

APPENDIX B

List of the main symbols employed.

(Greek letters are listed together with the corresponding Latin ones. In references the first number indicates the paper, the second the section).

A	constant in the espression Ax^{-3} for $V(x)$ (see). I, 1.
\mathcal{A}	III, eq. (20').
α, β	constants in the expression of μ as a function of v . III, eq. (17).
e	constant in the expression $-cr^{-6}$ for the mutual Van der Waals potential energy between two atoms.
C	velocity of ordinary sound in liquid ⁴ He.
ΔE_0	difference in zero point energy between an amount of helium in the film and the same amount in the bulk liquid. Usually referred to the amount present in a cm ² of the film (at a given height z).
ΔF	difference in free energy, in the same conditions as for ΔE_0 .
$(\Delta F)_{\text{exc}}$	contribution to ΔF due to the exciton gases present in liquid He.
Δt	difference of thickness between the film and a layer of the same mass per cm ² having density ϱ_0 (see).
$\Delta t'$	I, 2 eq. (8).
$\Delta_t t$	like Δt , but referring to the <i>liquid</i> portion of the film.
$\Delta_s t$	increase of thickness of the film due to expansion of the surface layers (with respect to the bulk liquid). I, 3 eq. (17).
ΔW_g	gravitational energy per cm ² of the film ($= \varrho_0 g z t$).
E^0, E_0	zero point energy (the first symbol for a system of Debye waves).
\mathcal{E}_0	zero point energy per atom.
F	Helmholtz free energy $U - TS$ for the system under consideration.
\mathcal{F}	Helmholtz free energy per atom.
F	«ordinary» free energy (i.e. for a <i>macroscopic</i> sample). II, 3·1.
$q(r)$	local eigenfunction describing the motion of a helium atom in its cell. II, 2·2.
g	gravity acceleration.
K_D	Debye cutoff wave number.

L	see II, Fig. 1.
λ	the length $hC(2kT)^{-1}$. II, 3·2.
λ_D	Debye cutoff wavelength.
Λ	the length $h(8\pi\mu kT)^{-\frac{1}{2}}$. II, 3·1.
m	mass of helium atom.
μ	effective mass of quadratic exciton. II, 2·2, Appendix B.
N	number of atoms in the sample.
ν_D	Debye cutoff frequency.
p	pressure (hydrostatic).
q	parameter in the expression $t = t_1 z^{-1/q}$.
ρ	density.
ρ_0	density of liquid ^4He under zero pressure. Practically constant between 0° and T_λ . Value adopted 0.1445 g/cm^{-3} .
$R(T)$	function of the temperature (and of the nature of the wall). See III, eq. (18') and (18'').
S	entropy.
t	thickness of the film (in cm).
t_s	thickness of the solidified layer.
τ	the same as t , but in units of 10^{-6} cm .
τ_1	as above, for $z = 1 \text{ cm}$.
U	internal energy.
v	specific volume ($\text{cm}^3 \text{ g}^{-1}$).
v_0	reciprocal of ρ_0 (see).
V	volume of the sample.
$V(x)$	potential energy of an atom at a distance x from a (plane) wall (*).
x	distance from a (plane) wall (*).
x_0	minimal distance of a He atom from the wall.
x_l	parameter of the order of 3 \AA units. I, 3 (end).
z	height above the free surface of the bulk liquid.

(*) Does not apply to II, App. B.

RIASSUNTO

Sulla base dei risultati raggiunti nelle note I e II della stessa serie, si studia il profilo del film e la sua dipendenza dalla temperatura tanto al disotto che al disopra del punto λ . Le conclusioni sembrano essere in discreto accordo con l'esperienza. Viene anche discussa la condizione termodinamica per il formarsi del film sotto l'azione delle forze di Van der Waals e si verifica che essa è effettivamente soddisfatta.

The Mass of the Neutrino and the Non-Conservation of Parity.

B. F. TOUSCHEK

Scuola di Perfezionamento in Fisica Nucleare dell'Università - Roma
Istituto Nazionale di Fisica Nucleare - Sezione di Roma

(ricevuto il 5 Marzo 1957)

Summary. — A special form of the theory of LEE and YANG ⁽¹⁾ is obtained by imposing an invariance principle, which insures that the mass as well as the magnetic moment ⁽²⁾ of the neutrino is identically zero. This invariance property leads to the conservation of a quantum number n . The non-conservation of parity is discussed for the chain of decays $\pi \rightarrow \mu + \nu$, $\mu \rightarrow e + \bar{\nu} + \nu$. It is shown that the present theory contains as a special case the «screwon» theory recently proposed by LEE and YANG ⁽³⁾ and a similar theory proposed by Salam ⁽⁴⁾.

In a recent letter ⁽⁵⁾ it has been proposed to connect the observed non-conservation of parity in processes involving the emission and absorption of neutrinos to an invariance principle which insures that the mass (and also the magnetic moment) of the neutrino is identically zero. The invariance principle may be stated in the following form:

All observable quantities of field theory are invariant under the transformation

$$(1) \quad \nu' = \exp[i\gamma_5 \alpha] \nu, \quad \bar{\nu}' = \bar{\nu} \exp[i\gamma_5 \alpha],$$

(1) T. D. LEE and C. N. YANG: *Phys. Rev.*, **104**, 256 (1956).

(2) This has been pointed out to the author by Prof. L. RADICATI, see also ref. ⁽⁴⁾.

(3) T. D. LEE and C. N. YANG: *Parity Non-Conservation and a Two Component Theory of the Neutrino*. Submitted for publication in the *Phys. Rev.*

(4) A. SALAM: *Nuovo Cimento*, **5**, 299 (1957).

(5) B. F. TOUSCHEK: *Nuovo Cimento*, **5**, 754 (1957).

of the neutrino field and the simultaneous transformation

$$(2) \quad \psi'_i = \exp[in_i \alpha] \psi_i,$$

of all the other fields. Here ψ_i is the fieldoperator of the i -th field and n_i is a number characteristic of this field. α in (1) and (2) is an arbitrary real parameter.

It follows immediately from (1) that the mass of the neutrino must be zero. For the Lagrangian of the free neutrino field

$$(3) \quad \mathcal{L}_0 = -\bar{\psi} \left(\gamma_\mu \frac{\partial}{\partial x_\mu} + m \right) \psi,$$

is only invariant under (1) if $m = 0$. If the neutrino would have a magnetic moment this would give rise to an interaction energy

$$(4) \quad H' = i\mu F_{\mu\nu} (\bar{\psi} \gamma_{[\mu\nu]} \psi),$$

with the electromagnetic field $F_{\mu\nu}$; μ is the magnetic moment of the neutrino. It is clear that, since γ_5 commutes with all the $\gamma_{[\mu\nu]}$, that (4) cannot be invariant under the transformation (1) and that therefore the magnetic moment of the neutrino must be zero.

The conservation law corresponding to (1) and (2) is immediately obtained by considering α infinitesimal. With

$$(5) \quad J_\mu = -i \left(\sum_i \frac{\partial \mathcal{L}}{\partial (\partial_\mu \psi_i)} n_i \psi_i - \bar{\psi} \gamma_\mu \gamma_5 \psi \right),$$

it immediately follows that

$$(6) \quad \partial_\mu J_\mu = 0.$$

The first term in (5) refers to all particles but the neutrino. As long as no neutrinos can be produced or destroyed we have the conservation law

$$(7) \quad \sum_i \int d^3x J_0^i = \text{const}, \quad J_0 = -iJ_4,$$

where

$$(8) \quad J_0^i = \sum_k n_i (n(k, i) - \bar{n}(k, i))$$

and $n(k, i)$ is the number of particles of species i , $\bar{n}(k, i)$ the number of anti-particles.

The physical significance of the neutrino term in (5) becomes obvious if one remembers that

$$(9) \quad \gamma_5 = -(\underline{a}\underline{e})(\underline{\sigma}\underline{e}),$$

where \underline{a} are the usual Dirac matrices and \underline{e} is an arbitrary unit vector, $\underline{\sigma}$ is the spin operator. It then follows that

$$(10) \quad -J_0^v = n_v - n_a + \bar{n}_p - \bar{n}_a$$

where n_a is the number of neutrinos with spin directed antiparallel to the momentum and n_p the number of neutrinos with spin parallel. The bar () indicates antineutrinos. In processes in which neutrinos are produced or destroyed one therefore has the general conservation law

$$(11) \quad \sum_i J_0^i + J_0^v = \text{const.}$$

In the following we shall not make any specific assumptions about the attribution of the numbers n to the various kinds of known particles. It is sufficient to note that charge conjugate particles must have opposite values of n and that particles described by observable fields must have $n = 0$. In fact the latter assumption has been used in showing that the magnetic moment of the neutrino must be zero. A possible choice of n has been discussed in reference (5): all Bosons have $n = 0$, Fermions $n = 1$ and Antifermions $n = -1$.

We now want to show that the invariance property (1) (2) is in general not compatible with the conservation of parity in processes in which one neutrino is emitted or absorbed. For non derivative couplings the Lagrangian which gives rise to the emission or absorption of neutrinos will be of the form

$$(12) \quad \mathcal{L}' = \bar{S}\nu + \bar{\nu}S, \quad \bar{S} = S^+\gamma_4,$$

S is the source density of the neutrino field and will transform like a spinor under Lorentz transformations. We shall not insist on the invariance of (12) under the full Lorentz group but content ourselves with the invariance under proper Lorentz transformations. In this case S can be assumed to be of the form

$$(13) \quad S = (\varepsilon + \eta\gamma_5)T,$$

where T is an operator which transforms like ν under the full Lorentz group. That (13) is the most general expression which renders (12) invariant under proper Lorentz transformations follows from the fact that the factor of T

in (13) must commute with all the generators $\gamma_{[\mu\nu]}$ of the transformations of the proper Lorentz group. ε and η will in general be complex numbers. Since (12) is supposed to describe the production of only one neutrino it is clear that N —and with it T —are independent of the neutrino amplitudes. To describe the β -decay of the neutron in a scalar theory one would choose

$$T = \psi_e(\bar{\psi}_p\psi_n)g,$$

where the indices e, p and n refer respectively to positrons, protons and neutrons and g is the Fermi constant. In terms of T we may now write for (12)

$$(14) \quad \mathcal{L}' = \bar{T}(\varepsilon^* - \eta^*\gamma_5)\nu + \bar{\nu}(\varepsilon + \eta\gamma_5)T.$$

Apart from a common factor the parameters ε and η can easily be determined from the invariance requirement (1), (2). For under the transformation (1), (2) T will transform as

$$(15) \quad T' = \exp i[\alpha\Delta n]T,$$

where Δn is the difference between the numbers n ; of the particles destroyed and those created together with the creation of a neutrino. By means of the identity

$$(16) \quad \exp[i\alpha\gamma_5] = \cos\alpha + i\gamma_5\sin\alpha,$$

we now find that (1) and (2) require that

$$(17) \quad \varepsilon + \Delta n\eta = 0 \quad \Delta n\varepsilon + \eta = 0.$$

These homogeneous equations in ε and η immediately give the selection rule

$$(18) \quad \Delta n^2 = 1, \quad \Delta n = \pm 1,$$

so that apart from a common factor which we may consider as absorbed in the Fermi constant we have instead of (14)

$$(19) \quad \mathcal{L}' = \bar{T}(1 \pm \gamma_5)\nu + \bar{\nu}(1 \mp \gamma_5)T.$$

Here the upper sign corresponds to the selection rule $\Delta n = +1$ the lower sign to the selection rule $\Delta n = -1$. From a comparison with equations (10) and (11) it is now easily seen that $\Delta n = +1$ corresponds to the production of a neutrino with its spin antiparallel to its momentum and that $\Delta n = -1$

corresponds to the production of a neutrino with its spin parallel to its momentum.

It is also obvious that a Lagrangian of the form (19) will in general not conserve parity. For under space reflections one has

$$(20) \quad Rv(x, t)R^{-1} = \gamma_4 v(-x, t), \quad RT(x, t)R^{-1} = \gamma_4 T(-x, t),$$

so that the sign of γ_5 will change in equation (19). This is also quite plausible from a physical point of view. For under space reflections a « parallel » neutrino is converted into an antiparallel neutrino. But since the conservation law (11) imposes the orientation of the spin of the neutrino relative to its momentum a transformation which reverses this orientation cannot leave the Lagrangian invariant.

It has been shown by PAULI ⁽⁶⁾ that in a theory of this type it is in general not possible to conserve the invariance under charge conjugation or weak time reflection. It depends on the choice of the coupling in (19) whether or not the theory is invariant under charge conjugation. If it is invariant it cannot be reversible. The Lagrangian (19) gives a « maximum » of observable non-conservation of parity: the effects of the γ_5 -coupling always appear in the form of interference terms with the parity conserving parts and this interference is maximum if parity conserving and non-conserving parts have equal intensity. The general effects of parity non-conserving terms in the theory of β -decay have recently been discussed by OEHME, LEE and YANG ⁽⁷⁾.

At present it is not yet known whether recent experiments by WU ⁽⁸⁾ can be in quantitative agreement with the strong non-conservation of parity prescribed by the Lagrangian (19).

As an application of the general argument we now want to discuss the reaction

$$(21) \quad \pi \rightarrow \mu + \nu.$$

In a series of brilliant experiments GARWIN, LEDERMAN and WEINRICH ⁽⁹⁾ have recently shown that parity cannot be conserved in this process and that the

⁽⁶⁾ W. PAULI: *Niels Bohr and the Development of Physics* (London, 1955). See also G. LUEDEERS: *Dan. Mat. Fys. Medl.*, **28** (1954).

⁽⁷⁾ R. OEHME, T. D. LEE and C. N. YANG: *Remarks on Non-Invariance under Time-reversal and Charge Conjugation*. Submitted for publication in the *Phys. Rev.*

⁽⁸⁾ C. S. WU, E. AMBLER, R. W. HAYWARD, D. D. HOPPE and R. P. HUDSON: *An Experimental Test of Parity Conservation in Beta Decay*. Preprint.

⁽⁹⁾ R. L. GARWIN, L. M. LEDERMAN and M. WEINRICH: *Observations of the Failure of Parity and Charge Conjugation in Meson Decays: The Magnetic Moment of the Free Muon*. Preprint.

μ -meson must leave the reaction (21) strongly polarized in the direction of motion. We shall show that in the present theory the μ -meson is completely polarized (whether parallel or antiparallel depends on the assignment of n -values) and that the polarization of the μ^- -meson is opposite to that of the μ^+ -meson. In keeping with the restriction to non-derivative couplings we shall assume that the Lagrangian giving rise to the reaction (21) is of the form:

$$(22) \quad \mathcal{L}' = f\Pi(\bar{\mu}(\Delta n - \gamma_5)v) + f^*\Pi^+(\bar{v}(\Delta n + \gamma_5)\mu).$$

Here f is a coupling constant, Π is the operator which destroys a positive π -meson and creates a negative π -meson, μ is the operator which destroys a positive and creates a negative μ -meson and

$$(23) \quad \Delta n = n_{\pi^+} - n_{\mu^+} \quad \Delta n^2 = 1.$$

The second term in (22) ensures that this Lagrangian is Hermitian. It is easily verified that the expression (22) is invariant under the substitution

$$(24) \quad (\Pi, \mu, v, \Delta n, f) \rightleftharpoons (\Pi^+, \mu^\dagger, v^\dagger, -\Delta n, \mp f^*).$$

The upper sign with f^* holds if it is assumed that the operators of the μ -mesons and neutrinos anticommute, the positive sign holds if they commute. Majorana-gauge ($\gamma_i^* = \gamma_i$, $\gamma_4^* = -\gamma_4$, $\gamma_5^* = -\gamma_5$) has been used throughout. The polarization of the μ^+ -meson can now be determined by the usual method of evaluating the trace of the modulus square of the first term in (22). Using the projection operator

$$(25) \quad P = \frac{1}{2} \left(1 + \frac{s}{k} (\sigma k) \right), \quad s = \pm 1,$$

in which k represents the momentum of the emitted μ^+ -meson we find immediately that the meson-intensity is proportional to

$$\frac{1}{2} (1 - s \Delta n).$$

This means of course that the μ^+ -meson is emitted with

$$(26) \quad s = -\Delta n, \quad \text{for } \mu^+,$$

i.e. that its polarization is complete in the direction of emission and that the sign of the polarization depends on the assignment of n -values to π^+ and μ^+ -meson. Since the intensity is proportional to $|f|^2$ and because of the in-

variance property under the transformation (24) it follows immediately that for the μ^- we must have

$$(26') \quad s = +\Delta n, \quad \text{for } \mu^-.$$

The result (26), (26') can also be expressed by saying that (if the μ -meson has no anomalous magnetic moment) the magnetic moment of the μ -meson produced in π -decay is oriented in the same manner for positive and negative μ 's.

There exists at least one process in nature in which two neutrinos are produced in a decay phenomenon. GARWIN, LEDERMAN and WEINRICH observed a strong correlation between the direction of emission of the electron in μ -decay and the direction of emission of the μ -meson in π -decay. As has already been observed such a correlation can only be explained by assuming that in both π - and μ -decay parity is not conserved. To describe the decay of the μ -meson we have to investigate the implications of the principle (1), (2) applied to Lagrangian densities which describe the production of two neutrinos. These Lagrangians will be of the form

$$(27) \quad \mathcal{L}'' = F(\bar{\nu}\Gamma'\nu) + \text{H.C.}$$

if the two neutrinos produced are of different type (i.e. one a neutrino, the other an antineutrino) and it will be of the form

$$(28) \quad \mathcal{L}'' = F(\bar{\nu}\Gamma'\nu^+) + \text{H.C.}$$

if both neutrinos emitted are of the same type (neutrinos). H.C. signifies the hermitian conjugate. We shall assume that F transforms with integral spin under Lorentz transformations and in particular (that is in the absence of derivative couplings) in any one of the ways usually denoted by S , P , V , A , T . It is assumed that Γ' transforms in the same way as F under proper Lorentz transformations and that we must therefore have that

$$(29) \quad \Gamma' = F(\varepsilon + \eta\gamma_5),$$

where ε and η are c -numbers and Γ' transforms like F under the full Lorentz-group. It should be noted that (28) is an invariant only in the Majorana-gauge in which ν^+ transforms in the same manner as ν . Under the transformation (1), (2) F will transform like

$$(30) \quad F' = F \exp[i\alpha\Delta n],$$

where Δn is the change of n associated with a particular process described

by (27) or (28). If the term represented explicitly in equations (27) or (28) is supposed to describe the decay of the $\mu\tau$ -meson we have, that in this case

$$(31) \quad \Delta n = n_{\mu^+} - n_{e^+}.$$

The selection rules which one obtains for Δn depend on the transformation character of F under proper Lorentz transformations and are because of $\gamma_5^* = -\gamma_5$ independent of the alternative (27), (28). The results are summarized in the following table:

		S, P	V, A	T
(32)	(27)	± 2	0	± 2
		no	yes	no

The columns refer to the way in which F transforms under proper Lorentz transformations. The figures in the table give the selection rules for the quantity n and « yes » and « no » answers the question: « is parity conservation possible? » It is immediately seen, that the selection rule $\Delta n = 0$ does not force us to introduce terms which do not conserve parity. The selection rule $\Delta n = \pm 2$ on the other hand seems to be in contrast with experiment. The reason for this is the following: the possibility of β -decay together with the observed reaction

$$\gamma + p \rightarrow n + \pi^+,$$

lead to the relation

$$(33) \quad n_{\pi^+} = n_{e^+} \pm 1.$$

Equation (33) together with

$$n_{\mu^+} - n_{e^+} = \pm 2$$

can only be satisfied if $n_{\pi^+} - n_{\mu^+}$ and $n_{\mu^+} - n_{e^+}$ have a different sign. For if they have the same sign it follows immediately that $n_{\pi^+} = n_{e^+} \pm 3$. But if $n_{\pi^+} - n_{\mu^+}$ and $n_{\mu^+} - n_{e^+}$ have different sign it can immediately be seen that at maximum energy of the electron the backward intensity must be zero. To see this assume that

$$(34) \quad n_{\pi^+} - n_{\mu^+} = 1, \quad n_{\mu^+} - n_{e^+} = -2.$$

Then according to (10) the neutrino of π -decay must have its spin oriented antiparallel to its direction of flight, i.e. parallel to the direction of the μ -meson. (The μ -meson spin is antiparallel, compare equation (26).) Now, if in μ -decay the electrons are emitted in the backward direction, both neutrino and anti-neutrino must be emitted in the forward direction. Since because of (34) and (10) their spins are oriented in the direction of motion, also these two particles have their spin pointing in the direction of flight of the μ -meson. The neutrinos have therefore carried away a spin — in the direction of motion of the μ -meson. The μ -meson having been first created and then destroyed does not enter the balance and the electron cannot compensate a spin $\frac{3}{2}$. It is therefore impossible to emit an electron of maximum energy in the backward direction. It follows that for $|\Delta n| = 2$ the angular distribution of the fastest electrons emitted in μ -decay should be

$$(35) \quad (1 + \cos \theta)$$

and this at the time seems to be strongly in contradiction with Lederman's experiment.

This result is borne out by a more detailed calculation. Using an (S, P, T)—mixture—which because of (32) is compatible with the hypothesis (27) and $\Delta n = \pm 2$ one obtains for the spectral distribution

$$(36) \quad S(p) = p^2 \{ [(6 + 3\tau) - (2 + 3\tau)p] - \eta s [(2 + 3\beta) + (2 - 3\beta)] \cos \theta \}.$$

Here p is the momentum of the electron (half the rest-mass of the μ -meson as a unit) and the parameters τ, β, η and s are real. τ and β are defined in terms of the coupling constants g_1, g_2, g_3 of the S, P and T -interactions:

$$(37) \quad \tau = \frac{|g_1|^2 + |g_2|^2}{|g_3|^2}, \quad \beta = \frac{g_1 g_2^* + g_2 g_1^*}{|g_3|^2},$$

and one obviously has

$$(38) \quad \varrho = \frac{6}{6 + \tau}, \quad 0 < \tau < \infty, \quad -\tau < \beta < +\tau.$$

For positive μ -mesons s is defined by equation (26) and η is given by

$$(39) \quad \eta = -(n_{\mu} - n_{\bar{\mu}})_{\frac{1}{2}}.$$

From the possibility of β -decay it follows that one must have $\eta s = -1$ and this bears out the complete cancellation of the backward intensity at maximum energy already foreseen by the qualitative consideration based on the con-

servation law (11). It seems highly improbable that (36) could be brought into quantitative agreement with experiment. For it is fairly certain that Michel's q -value is > 0.5 and that therefore $\tau < 6$. To describe the proper sign of the integrated asymmetry the most favourable choice would be $\tau = 6$ and $\beta = -6$. In this case the spectrum becomes proportional to

$$(40) \quad p^2[(6 - 5p) - \cos \theta (4 - 5p)]$$

and the integrated asymmetry is only slightly more than -11% , as compared with Lederman's 33% . Also the energy dependence does not seem to be of the form indicated in Lederman's experiment.

The spectrum (36) is the most general spectrum compatible with the hypothesis $|\Delta n| = 2$: it is easily seen that in the case (28) a tensor calculation is not compatible with the Pauli principle and that therefore $\rho = 0$.

The experiments therefore indicate that μ -decay is governed by the selection rule $\Delta n = 0$. In this case the predictions of the present theory are identical with those of LEE and YANG: either alternative (27), (28) gives $q = 0.75$. The same authors also give the spectral distribution and angular dependence of electron emission as:

$$(41) \quad S(p) = p^2((3 - 2p) + \beta \cos \theta(1 - 2p)),$$

where β is given by

$$(42) \quad \beta = \frac{g_3 g_4^* + g_4 g_3^*}{|g_3|^2 + |g_4|^2}.$$

The anisotropy of the direction of emission of the electron is not predictable in the case of theories with $|\Delta n| = 0$. As one sees from (41) and (42) it enters the description of the process in the form of a parameter and there is no theoretical necessity for assuming that this parameter is $\neq 0$.

It is seen from these considerations that the invariance principle presented here leaves one a wider choice of theories to represent experimental data. The theory of Lee and Yang enters as a special case. The equivalence holds in particular in the absence of reactions which change the spin of the neutrino. Such a reaction would be possible in all the theories of the type (27) in which two neutrino emission is described by the selection rule $|\Delta n| = 2$.

An unsatisfactory feature of both the present theory and the theory of Lee and Yang is that in the case $\Delta n = 0$ no reason can be given for the non-conservation of parity. This non-conservation has obviously nothing to do with the structure of the neutrino since either theory allows one to construct bilinear forms from the neutrino operators which do conserve parity. In this type of theory therefore parity non-conservation in two neutrino decays enters

as a special hypothesis. If one is prepared to introduce this hypothesis then there is of course no reason for not introducing it also to «explain» the decay of strange particles, about which present theories tell us nothing. The question remains of how the neutrino can be made responsible for the non-conservation of parity in the decays of the K-meson in which no neutrinos are actually produced. It is tempting to assume that this non-conservation of parity is due to the virtual emission and absorption of neutrinos. Processes of this type however are generally assumed to be described by matrix elements proportional to the square of the Fermi-constant. If perturbation theory has any meaning in the case of Fermi type couplings they should therefore be very slow. The only way to overcome this difficulty seems to us to consist in assuming that in a future theory the divergences of Fermi type processes will be treated in such a way that wherever the emission and reabsorption of a virtual Fermion has to be considered the ordering of matrix element in powers of g loses its meaning, that is that what hitherto has been referred to as a second order matrix element would go with g and not with g^* .

Note added in proof.

The theory which we have here presented is compatible with a reality condition, which in the Majorana gauge may be written as:

$$P = P^*$$

and which has been proposed by M. FIERZ (W. PAULI, private communication). This reality condition excludes tensor and polar vector terms of the form $v\gamma_4\gamma_{[\mu\nu]}v$, $v\gamma_4\gamma_\nu v$ resp. As a result the transitions in μ -decay with $\Delta n = 2$ have necessarily $Q = 0$ and the theory becomes completely equivalent to that of Lee and Yang. The author is extremely grateful to Prof. W. PAULI for a stimulating exchange of correspondence.

RIASSUNTO

Si discute una proprietà di invarianza che garantisce che la massa ed il momento magnetico del neutrino sono identicamente zero. L'invarianza conduce ad una legge di conservazione che sostituisce la conservazione di parità. Si discute la teoria della catena di decadimenti π - μ - e mostrando che la teoria a due componenti, recentemente proposta da LEE and YANG, risulta come caso particolare.

Scattering of Fast Electrons by Polarized Nuclei.

M. BERNARDINI, P. BROVETTO and S. FERRONI

Istituto di Fisica dell'Università - Torino

Istituto Nazionale di Fisica Nucleare - Sezione di Torino

(ricevuto l'8 Marzo 1957)

Summary. — In the present work are given detailed calculations of the cross section for fast electrons on polarized nuclei. The results are applied to the case of $^{181}_{73}\text{Ta}$; the predicted azimuthal anisotropy in the cross-section varies from 130% to 50% according to the shape chosen for the distribution of nuclear charge.

1. — Introduction.

Methods have been recently developed by which high degrees of nuclear polarization can be obtained on paramagnetic substances ⁽¹⁾. In the present work calculations are made in Born's approximation for the elastic scattering cross-section of high energy electrons against polarized nuclei. A first approach to this problem can be found in a paper by FERRONI and FUBINI ⁽²⁾. In the present work attention is paid to the effect on the scattering of the quadrupole moment of the polarized nucleus, and the azimuthal anisotropy in the cross-section is derived as a function of the nuclear charge distribution. We shall assume in the following that the target nuclei are in a time constant impure spin state.

⁽¹⁾ A. W. OVERHAUSER: *Phys. Rev.*, **8**, 689 (1953); **92**, 411 (1953) P. BROVETTO and G. CINI: *Nuovo Cimento*, **11**, 618 (1954); P. BROVETTO and S. FERRONI: *Nuovo Cimento*, **12**, 90 (1954); M. E. ROSE: *Phys. Rev.*, **75**, 213 (1949); C. J. GORTER: *Physica*, **14**, 504 (1948); A. SIMON, M. E. ROSE and J. M. JAUCH: *Phys. Rev.*, **84**, 1155 (1951).

⁽²⁾ S. FERRONI and S. FUBINI: *Nuovo Cimento*, **1**, 263 (1955).

2. - Theory.

An ensemble of nuclei in an impure spin state is described by a density matrix ϱ of the type ⁽³⁾:

$$(1) \quad \varrho_{m,m'} = \exp\left(-\frac{m}{I}\mu\right)\delta_{m,m'},$$

where m is the component of the nuclear spin moment I along the quantization axis. Polarization P is related to the parameter μ by:

$$(2) \quad P = \frac{\text{Tr}(m\varrho)}{I \text{Tr}(\varrho)}.$$

The differential cross-section is related to the scattering matrix M by:

$$(3) \quad \sigma d\Omega = \frac{\text{Tr}(\varrho M^* M)}{\text{Tr}(\varrho)} d\Omega.$$

2'1. *Calculation of the scattering matrix M .* - The elastic scattering matrix M is:

$$(4) \quad M_{m,m'} = \frac{E}{2\pi\hbar^2 c^2} \left\langle \Psi_m(\mathbf{r}_P) \chi_f(\mathbf{r}_e) \left| \frac{Ze^2}{|\mathbf{r}_e - \mathbf{r}_P|} \right| \Psi_{m'}(\mathbf{r}_P) \chi_i(\mathbf{r}_e) \right\rangle,$$

where E is the energy of the scattered electron, $\Psi_m(\mathbf{r}_P)$ is the normalized wave function of a proton in the nucleus, $\chi_i(\mathbf{r}_e)$, $\chi_f(\mathbf{r}_e)$ are the wave functions of the electron initial and final state respectively. One has:

$$(5) \quad \begin{cases} \chi_i(\bar{\mathbf{r}}_e) = a_i \exp[i\mathbf{p}_i \cdot \mathbf{r}_e/\hbar], \\ \chi_f(\bar{\mathbf{r}}_e) = a_f \exp[i\mathbf{p}_f \cdot \mathbf{r}_e/\hbar], \end{cases}$$

where a_i , a_f are Dirac's amplitude matrices. By use of equation (5), equation (4) becomes:

$$(6) \quad M_{m,m'} = \frac{Ze^2 E}{2\pi\hbar^2 c^2} \langle a_f | a_i \rangle \int_{\tau_P} d\tau_P \Psi_m^* \Psi_m \int_{\tau_e} d\tau_e \frac{\exp[i\mathbf{q} \cdot \mathbf{r}_e]}{|\mathbf{r}_e - \mathbf{r}_P|},$$

where $\hbar\mathbf{q} = \mathbf{p}_i - \mathbf{p}_f$ is the momentum transfer related to the scattering

⁽³⁾ J. VON NEUMAN: *Die mathematischen Grundlagen der Quantenmechanik* (Leipzig, 1932), p. 173.

angle ϑ by:

$$(7) \quad \hbar q = 2p \sin \frac{\vartheta}{2}.$$

Integrating over \mathbf{r}_e (see Appendix I) equation (6) becomes:

$$(8) \quad M_{m,m'} = \frac{Ze^2E}{2\pi\hbar^2c^2} \langle a_f | a_i \rangle \left[\frac{4\pi}{q^2} \int_{\tau_P} \Psi_m^* \Psi_{m'} j_0(qr_P) d\tau_P - \right. \\ \left. - \frac{4\pi}{q^2} \frac{5}{6} \sum_{i,j} Q_{ij} \int_{\tau_P} \Psi_m^* \Psi_{m'} \frac{3x_i x_j - \delta_{ij} r_P^2}{r_P^2} j_2(qr_P) d\tau_P \right].$$

In this equation j_0 , j_2 are the spherical Bessel functions, x_i , x_j are the components of \mathbf{r}_P and Q_{ij} is the tensor related to the components q_i , q_j of \mathbf{q} by the equation:

$$(9) \quad Q_{ij} = \frac{3q_i q_j - q^2 \delta_{ij}}{q^2}.$$

As the function $j_0(qr_P)$ is a zero-order tensor the first integral in equation (8) is invariant for rotation of the axes, and can therefore be written as:

$$(10) \quad \int_{\tau_P} \Psi_m^* \Psi_{m'} j_0(qr_P) d\tau_P = F(q) \delta_{m,m'},$$

where

$$(11) \quad F(q) = \int_{\tau_P} |\Psi_I|^2 j_0(qr_P) d\tau_P.$$

The symmetric second-order tensor in the second integral of equation (8) can be transformed by means of the relation (4):

$$(12) \quad (3x_i x_j - \delta_{ij} r_P^2) \frac{j_2(qr_P)}{r_P^2} = C T_{ij},$$

where

$$(13) \quad T_{ij} = \frac{3}{2} (I_i I_j + I_j I_i) - \delta_{ij} I^2.$$

In this equation, I , and I_j are the components of the angular momentum oper-

(4) H. WEYL: *The Classical Groups* (Princeton, 1939), p. 149.

ator I . The constant C can be determined by considering the matrix element between states m , $m' = I$ of the component $i, j = 3$ of the tensor on both sides of equation (12). The result is:

$$(14) \quad \int |\Psi_I|^2 \frac{3a_3^2 - r_P^2}{r_P^2} j_2(qr_P) d\tau_P = C \langle I, I | T_{33} | I, I \rangle,$$

from which

$$(15) \quad C = \frac{2G(q)}{I(2I-1)},$$

where

$$(16) \quad G(q) = \int_{\tau_P} |\Psi_I|^2 P_2(\cos \alpha) j_2(qr_P) d\tau_P.$$

In this equation, α is the angle between \mathbf{r}_P and the nuclear axis. We can now calculate the matrix M^*M . We shall consider diagonal elements only, since the density matrix ϱ is diagonal. Taking into account equations (8), (10), (12), (15) and averaging over the electron initial and final spin states, one has:

$$(17) \quad (M^*M)_{m,m'} = \left(\frac{2Ze^2E}{\hbar^2 c^2 q^2} \right)^2 \langle a_f | a_i^2 | a_v \rangle \cdot \left\{ [F(q)]^2 - 2F(q)G(q) \frac{2}{I(2I-1)} \frac{5}{6} \sum_{i,j}^3 Q_{ij} \langle I, m | T_{ij} | m, I \rangle + \left[\frac{5}{6} \frac{2G(q)}{I(2I-1)} \right]^2 \sum_{m''} \left| \sum_{i,j}^3 Q_{ij} \langle I, m | T_{ij} | m', I \rangle \right|^2 \right\}.$$

The average over spin states of the incident and scattered waves can be easily performed and yields (5):

$$(18) \quad a_f | a_v^2 | a_v \rangle = \left(\frac{m_0 c^2}{E} \right)^2 - \left(\frac{cp}{E} \right)^2 \cos^2 \frac{\theta}{2}.$$

In the following calculations the rest energy $m_0 c^2$ of the electron will be neglected.

2.2. Formulae for the differential cross section. — By means of equations (7), (17) and (18) and averaging over nuclear spin states, equation (3) can be

shown to become:

$$(19) \quad \sigma = \frac{Z^2 e^4 \cos^2(\vartheta/2)}{4E^2 \sin^4(\vartheta/2)} \left\{ [F(q)]^2 - 5F(q)G(q) \frac{3q_3^2 - q^2}{q^2} K(I, \mu) + \right. \\ \left. + [5G(q)]^2 \left[\left(\frac{3q_3^2 - q^2}{2q^2} \right)^2 U(I, \mu) + \frac{9}{2} \left(\frac{q_3}{q} \right)^2 \frac{q^2 - q_3^2}{q^2} V(I, \mu) + \right. \right. \\ \left. \left. + \frac{9}{8} \left(\frac{q^2 - q_3^2}{q^2} \right)^2 W(I, \mu) \right] \right\}.$$

The trivial but rather tedious calculations are summarized in Appendix II. In this equation one has:

$$(20) \quad K(I, \mu) = \frac{1}{I(2I-1)} \left[2I(I+1) - 3IB_I \left(\frac{\mu}{2I} \right) \coth \frac{\mu}{2I} \right], \\ U(I, \mu) = \frac{1}{I^2(2I-1)^2} \left\{ I(I+1)[4I(I+1) - 9] - 6IB_I \left(\frac{\mu}{2I} \right) \coth \frac{\mu}{2I} \cdot \right. \\ \left. \cdot \left[2I(I+1) - 3 + \frac{9}{2} \coth^2 \frac{\mu}{2I} \right] + 18 \coth^3 \frac{\mu}{2I} \cdot I(I+1) \right\}, \\ V(I, \mu) = \frac{1}{I^2(2I-1)^2} \left\{ IB_I \left(\frac{\mu}{2I} \right) \coth \frac{\mu}{2I} \left[4I(I+1) - 3 + 12 \coth^2 \frac{\mu}{2I} \right] \right. \\ \left. - 8I(I+1) \coth^2 \frac{\mu}{2I} \right\}, \\ W(I, \mu) = \frac{1}{I^2(2I-1)^2} \left\{ 2I(I+1) - 3IB_I \left(\frac{\mu}{2I} \right) \coth \frac{\mu}{2I} \left(\coth^2 \frac{\mu}{2I} + 1 \right) + \right. \\ \left. + 2I(I+1) \coth^2 \frac{\mu}{2I} \right\},$$

where $B_I(\mu/2I)$ is Brillouin's function.

Where μ goes to infinity, i.e. polarization P takes its maximum value 1, the function defined in equation (20) can be easily shown to become:

$$(21) \quad \begin{cases} K(I, \mu)_{\mu=\infty} = 1; & U(I, \mu)_{\mu=\infty} = 1, \\ V(I, \mu)_{\mu=\infty} = \frac{1}{I}; & W(I, \mu)_{\mu=\infty} = \frac{2}{I(2I-1)}. \end{cases}$$

When no magnetic field is applied, μ is zero, and, for equations (1), (2), polarization P is also zero, the quantization axis is parallel to the momentum transfer \mathbf{q} , i.e. $q_3 = q$.

In this case with simple calculations one gets:

$$(22) \quad K(I, 0) = 0; \quad U(I, 0) = \frac{1}{5} \frac{I+1}{I} \frac{4I(I+1)-3}{(2I-1)^2},$$

and the differential cross-section is simply:

$$(23) \quad \sigma = \frac{Z^2 e^4 \cos^2(\vartheta/2)}{4E^2 \sin^4(\vartheta/2)} \left\{ [F(q)]^2 + 5[G(q)]^2 \frac{I+1}{I} \frac{4I(I+1)-3}{(2I-1)^2} \right\}.$$

Equation (23) is the quantum mechanical correct expression of a relation already obtained by SCHIFF for the cross-section on non polarized nuclei and the two expressions become identical for $I = \infty$ ⁽⁶⁾.

2.3. Some nuclear models. — Let us now consider the function $|\Psi_I|^2$ representing the nuclear charge distribution, and expand it into spherical functions, neglecting the terms corresponding to multipoles of order higher than four. One has:

$$(24) \quad |\Psi_I|^2 = \varrho_0(r_P) + \varrho_2(r_P) P_2(\cos \alpha).$$

The nuclear radius R and the quadrupole moment Q are defined by the the following expressions:

$$(25) \quad R^2 = \int_{\tau_P} |\Psi_I|^2 r_P^2 d\tau_P,$$

$$(26) \quad Q = 2Z \int_{\tau_P} |\Psi_I|^2 P_2(\cos \alpha) r_P^2 d\tau_P.$$

We shall now require from the function $\varrho_2(r_P)$ some conditions, so that equation (24) represents in a plausible way the nuclear charge distribution. We shall therefore consider the quantities r_0^2 and r_2^2 defined by the equations:

$$(27) \quad R^2 = \overline{r_0^2} \int_{\tau_P} |\Psi_I|^2 d\tau_P,$$

$$(28) \quad Q = \overline{r_2^2} 2Z \int_{\tau_P} |\Psi_I|^2 P_2(\cos \alpha) d\tau_P.$$

⁽⁶⁾ L. I. SCHIFF: *Phys. Rev.*, **92**, 988 (1953), eq. (21). See this work also for the discussion about the applicability of the Born approximation in this case.

We shall assume that:

$$(29) \quad r_0^2 = r_2^2.$$

With this condition, the anisotropic term of the charge distribution has the same range as the spherically symmetric one. Moreover, it is plausible to assume that the charge density is approximately constant inside the nucleus, and that the quadrupole moment mainly derives from the elongated shape of the nucleus. This consideration implies a further restriction on the function $\varrho_2(r_p)$. In fact, let us consider a distribution $\varrho_0(r_p)$ practically constant inside the nucleus. The function $\varrho_2(r_p)P_2(\cos \alpha)$ decreases the charge density for $\alpha = \pi/2$ and increases it for $\alpha = 0$. In order that the effect of the term $\varrho_2(r_p)P_2(\cos \alpha)$ should be that of altering the spherical shape of the nucleus leaving the charge density constant inside it, the function $\varrho_2(r_p)$ must satisfy the condition:

$$(30) \quad \frac{\varrho_2(r_p)}{\varrho_2(0)} \gg 1 \quad \text{for} \quad r_p \simeq R.$$

A first rough model introduced by SCHIFF⁽⁶⁾ is given by the following expressions for the functions $\varrho_0(r_p)$ and $\varrho_2(r_p)$:

$$(31) \quad \begin{aligned} \varrho_0(r_p) &= \begin{cases} \varrho_0 & \text{for } r_p < R \\ 0 & \text{for } r_p > R \end{cases} \\ \varrho_2(r_p) &= B \delta(r_p - R). \end{aligned}$$

The parameters appearing in eq. (31) are found by taking into account the normalization of Ψ_I , and eq. (26). One has:

$$(32) \quad \begin{cases} \frac{4\pi}{3} \varrho_0 R^3 = 1, \\ \frac{8\pi}{5} Z R^2 B = Q. \end{cases}$$

For this model the conditions required for $\varrho_2(r_p)$ are automatically satisfied.

Eq. (11) and (16) allow us to find the expressions for $F(q)$ and $G(q)$, that are given by:

$$(33) \quad \begin{cases} F(q) = \frac{3}{qR} j_1(qR), \\ G(q) = \frac{Q}{2ZR^2} j_2(qR). \end{cases}$$

Another more satisfactory model is defined by the equations:

$$(34) \quad \begin{cases} \varrho_0(r_P) = \varrho_0 \exp \left[-\frac{r_P}{a} \right], \\ \varrho_2(r_P) = \varrho_0 k \left(\frac{r_P}{a} \right)^n \exp \left[-\lambda \frac{r_P}{a} \right]. \end{cases}$$

For the conditions of normalization and taking into account eq. (25) and (26), one has:

$$(35) \quad 8\pi\varrho_0 a^3 = 1; \quad R^2 = 12 a^2; \quad k = \frac{5\lambda^{n+3}}{(n+2)!Z} \frac{Q}{R^2},$$

the parameter λ is determined through eq. (27) and (28) and condition (29):

$$(36) \quad \lambda = \left(1 - \frac{n}{4} \right) \left(1 - \frac{n}{3} \right).$$

In this case, eq. (11) and (16) become (7):

$$(37) \quad \begin{cases} F(q) = \frac{1}{(1 + a^2 q^2)^2}, \\ G(q) = \frac{\sqrt{\pi}}{80} \frac{\Gamma(n+5)}{\Gamma(7/2)} k \frac{q^2 a^2}{(\lambda^2 + a^2 q^2)^{(n+5)/2}} {}_2F_1 \left(\frac{n+5}{2}, \frac{1-n}{2}; \frac{7}{2}; \frac{a^2 q^2}{\lambda^2 + a^2 q^2} \right). \end{cases}$$

In these equations, ${}_2F_1$ represents, with Barnes' notation, a generalized hypergeometric function.

In the particular cases $n = 1$ or $n = 2$, the second of eq. (37) becomes:

$$(38) \quad \begin{cases} G(q) = \frac{4}{5} k \frac{q^2 a^2}{(\lambda^2 + a^2 q^2)^3}, & \text{for } n = 1, \\ G(q) = \frac{24}{5} k \lambda \frac{q^2 a^2}{(\lambda^2 + a^2 q^2)^4}, & \text{for } n = 2. \end{cases}$$

3. - Numerical results and discussion.

In the following discussion, we shall take the quantization axis z orthogonal to \mathbf{p}_i and we shall indicate with q the angle between the projection of \mathbf{p}_i on the plane orthogonal to \mathbf{p} , and the z -axis. It is clear, from eq. (19) that

(7) G. N. WATSON: *Theory of Bessel Function* (Cambridge, 1952), p. 385.

in these conditions the cross-section shows the maximum anisotropy with respect to φ . With this choice of the z -axis one has:

$$(39) \quad \frac{q_3}{q} = -\cos \frac{\vartheta}{2} \cos \varphi.$$

We shall apply the previous results to the case of $^{181}_{73}\text{Ta}$ for which $Q = 6 \cdot 10^{-24} \text{ cm}^2$, one of the largest values known, and $I = \frac{7}{2}$.

The neutral Ta atom, and the ion Ta^{++} contain an odd number of electrons, and are therefore paramagnetic and can be polarized ⁽¹⁾. In the following numerical calculations, we shall assume $P = 0.8$, i.e. $\mu = 3.062$. Eq. (20) gives:

$$K = 0.531; \quad U = 0.642; \quad V = 0.326; \quad W = 0.174.$$

Let us consider the sharp-edge charge distribution described by eq. (30): the nuclear radius, calculated with the rule $R = 1.4 \cdot 10^{-13} A^{\frac{1}{3}} \text{ cm}$ results

$$R = 7.9 \cdot 10^{-13} \text{ cm.}$$

Fig. 1 shows, for $E = 125 \text{ MeV}$, the values of the anisotropy $\sigma(\vartheta, \varphi)/\sigma(\vartheta, 0)$. It is interesting to notice that, increasing ϑ from 45° to 60° , the anisotropy goes from values larger than one, to values smaller than one. This is due to the fact that in such an interval for ϑ , the function $F(q)$ (see. eq. (33)) shows an inversion of sign.

The smooth charge distribution model given by eq. (34),

according to Hofstadter's measurements ⁽²⁾ on non polarized nuclei, best represents the experimental-data, if $a = 2.80 \cdot 10^{-13} \text{ cm}$ is assumed for Ta. For this value of a , from the second of eq. (35) we have $R = 9.7 \cdot 10^{-13} \text{ cm}$. For $n = 1, 2$ the function $g_2(r_p)$ (eq. (34)) satisfies condition (30); in this way we obtain a more satisfactory description of the nuclear charge distribution than for $n = 0$.

The third of eq. (35) and eq. (36) yield:

$$\begin{array}{lll} k = 0.202 & \lambda = 1.291 & \text{for } n = 1, \\ k = 0.180 & \lambda = 1.581 & \text{for } n = 2. \end{array}$$

⁽²⁾ R. HOFSTADTER, H. R. FECHTER and J. A. MCINTYRE: *Phys. Rev.*, **92**, 978 (1953).

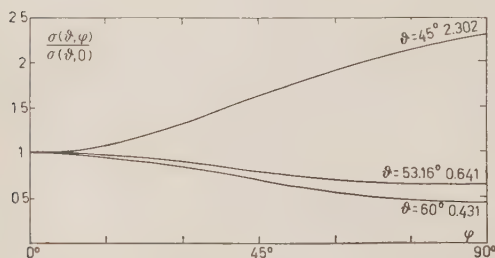


Fig. 1. — Azimuthal anisotropy $\sigma(\vartheta, \varphi)/\sigma(\vartheta, 0)$ as a function of φ for $\vartheta = 45^\circ, 60^\circ, 90^\circ$, in the case of the sharp-edge charge distribution model eq. (31). Bombarding energy 125 MeV.

Using these values, the graphs of Fig. 2 and 3 are obtained in which anisotropy is plotted against the azimuthal angle φ , for $E = 125$ MeV and $\vartheta = 45^\circ, 60^\circ, 90^\circ$.

It is clear that the function $\sigma(\vartheta, \pi/2)/\sigma(\vartheta, 0)$ has a maximum for $45^\circ < \vartheta < 90^\circ$. Anisotropies of the order of 50% are predicted.

It can be stated in general that anisotropy decreases with increasing n .

When the nucleus we consider is bound in a paramagnetic compound, where the other atoms have a much lower Z , as it is the case for Ta in the compound TaCl_3 , the contribution of these other nuclei to the scattering of the electrons is small, and does not smooth out appreciably the anisotropy, since the cross-section varies practically as Z^2 .

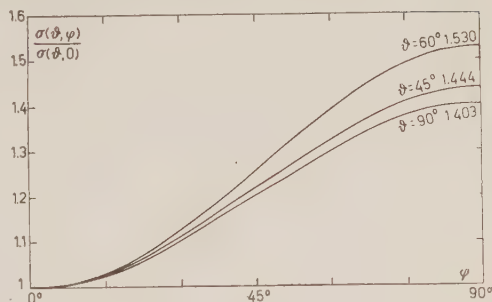


Fig. 2. - Azimuthal anisotropy $\sigma(\vartheta, \varphi)/\sigma(\vartheta, 0)$ as a function of φ for $\vartheta = 45^\circ, 60^\circ, 90^\circ$, in the case of the smooth charge distribution model eq. (34) with the choice $n = 1$. Bombarding energy 125 MeV.

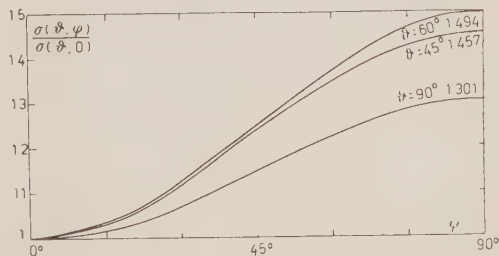


Fig. 3. - Azimuthal anisotropy $\sigma(\vartheta, \varphi)/\sigma(\vartheta, 0)$ as a function of φ for $\vartheta = 45^\circ, 60^\circ, 90^\circ$, in the case of the smooth charge distribution model eq. (34) with the choice $n = 2$. Bombarding energy 125 MeV.

* * *

We are grateful to Prof. M. VERDE for very useful discussions and criticism.

APPENDIX I

The integral appearing in eq. (6) of the text by using the Fourier transformation:

$$(40) \quad \int \frac{\exp[i\mathbf{q} \cdot \boldsymbol{\xi}]}{|\boldsymbol{\xi}|} d^3\xi = \frac{4\pi}{q^2},$$

becomes:

$$(41) \quad \frac{4\pi}{q^2} \int_{\tau_P} \Psi_m^* \Psi_{m'} \exp[i\mathbf{q} \cdot \mathbf{r}_P] d\tau_P.$$

Taking into account the expansion ⁽⁹⁾:

$$(42) \quad \exp[i\mathbf{q} \cdot \mathbf{r}_P] = \sum_l i^l (2l+1) j_l(qr_P) P_l(\cos \gamma),$$

where γ is the angle between the vectors \mathbf{q} , \mathbf{r}_P , the eq. (41) can be written:

$$(43) \quad \frac{4\pi}{q^2} \left[\int_{\tau_P} \Psi_m^* \Psi_{m'} j_0(qr_P) d\tau_P - 5 \int_{\tau_P} \Psi_m^* \Psi_{m'} j_2(qr_P) P_2(\cos \gamma) d\tau_P \right].$$

In eq. (43) for parity considerations only even order Legendre polynomials appear; also polynomials of order higher than two will be neglected. In fact they are responsible for terms corresponding to multipoles of order higher than four, whose contribution is by all means negligible.

Let us indicate with x_i the components of \mathbf{r}_P , and with q_i the components of \mathbf{q} ; the following identity can be easily proved:

$$(44) \quad P_2(\cos \gamma) = \frac{1}{6r_P^2 q^2} \sum_{i,j}^3 (3x_i x_j - \delta_{ij} r_P^2)(3q_i q_j - \delta_{ij} q^2).$$

By means of eq. (43), (44) eq. (8) of the text is immediately derived.

APPENDIX II

The summations over i, j appearing in eq. (17) can be easily evaluated remembering eq. (9) and using the expressions for the matrix elements of operator T_{ij} ⁽¹⁰⁾. One has:

$$(45) \quad \left\{ \begin{aligned} \sum_{i,j}^3 Q_{ij} \langle I, m | T_{ij} | m, I \rangle &= \frac{3}{2} \frac{3q_3^2 - q^2}{q^2} [3m^2 - I(I+1)], \\ \sum_{i,j}^3 Q_{ij} \langle I, m | T_{ij} | m \pm 1, I \rangle &= \frac{9}{2} \frac{q_3}{q} \frac{q_1 + iq_2}{q} (2m \pm 1) \sqrt{(I \mp m)(I \pm m + 1)}, \\ \sum_{i,j}^3 Q_{ij} \langle I, m | T_{ij} | m \pm 2, I \rangle &= \\ &= \frac{9}{4} \left(\frac{q_1^2 - q_2^2}{q^2} + 2i \frac{q_1 q_2}{q^2} \right) \sqrt{(I \mp m)(I \mp m - 1)(I \pm m + 1)(I \pm m + 2)}. \end{aligned} \right.$$

⁽⁹⁾ G. N. WATSON: *Theory of Bessel Function* (Cambridge, 1952), p. 128.

⁽¹⁰⁾ N. F. RAMSEY: *Nuclear Moments* (New York, 1953), p. 22.

Elementary calculations yield the following equations:

$$(46) \quad \left\{ \begin{aligned} & \frac{\sum_{-I}^I m^2 \exp\left(-\frac{\mu}{I} m\right)}{\sum_{-I}^I \exp\left(-\frac{\mu}{I} m\right)} = I(I+1) - IB_I\left(\frac{\mu}{2I}\right) \cotgh \frac{\mu}{2I}, \\ & \frac{\sum_{-I}^I m^4 \exp\left(-\frac{\mu}{I} m\right)}{\sum_{-I}^I \exp\left(-\frac{\mu}{I} m\right)} = \frac{1}{2} \left\{ \frac{2}{3} [I(I+1) - 1] + \cotgh^2 \frac{\mu}{2I} \right\}, \\ & \left\{ 4I(I+1) - 6IB_I\left(\frac{\mu}{2I}\right) \cotgh \frac{\mu}{2I} \right\} - \frac{1}{3} I(I+1)[I(I+1) - 1], \end{aligned} \right.$$

where $B_I(\mu/2I)$ is the Brillouin's function.

Applying eq. (45), (46) the following equations are found:

$$(47) \quad \left\{ \begin{aligned} & \frac{\text{Tr} \left\{ \varrho_m \sum_{i,j}^3 Q_{ij} \langle I, m | T_{ij} | m, I \rangle \right\}}{\text{Tr } \varrho_m} = \frac{3}{2} \frac{3q_3^2 - q^2}{q^2} \left[2I(I+1) - 3IB_I\left(\frac{\mu}{2I}\right) \cotgh \frac{\mu}{2I} \right], \\ & \frac{\text{Tr} \left\{ \varrho_m \left| \sum_{i,j}^3 Q_{ij} \langle I, m | T_{ij} | m, I \rangle \right|^2 \right\}}{\text{Tr } \varrho_m} = \\ & \quad - \left(\frac{3}{2} \frac{3q_3^2 - q^2}{q^2} \right) \left\{ I(I+1)[I(I+1) - 9] - 6IB_I\left(\frac{\mu}{2I}\right) \cotgh \frac{\mu}{2I} \right. \\ & \quad \left. \cdot \left[2I(I+1) - 3 + \frac{9}{2} \cotgh^2 \frac{\mu}{2I} \right] + 18I(I-1) \cotgh^2 \frac{\mu}{2I} \right\}, \\ & \frac{\text{Tr } \varrho_m \left\{ \left| \sum_{i,j}^3 Q_{ij} \langle I, m | T_{ij} | m+1, I-1 \rangle + \sum_{i,j}^3 Q_{ij} \langle I, m | T_{ij} | m-1, I+1 \rangle \right|^2 \right\}}{\text{Tr } \varrho_m} = \\ & \quad - \frac{81}{8} \left(\frac{q_3}{q} \right)^2 \frac{q^2 - q_3^2}{q^2} \left\{ IB_I\left(\frac{\mu}{2I}\right) \cotgh \frac{\mu}{2I} \left[4I(I+1) - 3 + 12 \cotgh^2 \frac{\mu}{2I} \right] - \right. \\ & \quad \left. - 8I(I+1) \cotgh^2 \frac{\mu}{2I} \right\}, \\ & \frac{\text{Tr } \varrho_m \left\{ \left| \sum_{i,j}^3 Q_{ij} \langle I, m | T_{ij} | m+2, I \rangle + \sum_{i,j}^3 Q_{ij} \langle I, m | T_{ij} | m-2, I \rangle \right|^2 \right\}}{\text{Tr } \varrho_m} = \\ & \quad = \frac{81}{8} \left(\frac{q_3}{q} \right)^2 \frac{q^2 - q_3^2}{q^2} \left\{ 2I(I+1) - 3IB_I\left(\frac{\mu}{2I}\right) \cotgh \frac{\mu}{2I} \left(\cotgh^2 \frac{\mu}{2I} + 1 \right) + \right. \\ & \quad \left. + 2I(I+1) \cotgh^2 \frac{\mu}{2I} \right\}. \end{aligned} \right.$$

RIASSUNTO

In questo lavoro si sviluppano in dettaglio, mediante l'approssimazione di Born, i calcoli riguardanti la sezione d'urto di elettroni veloci da parte di nuclei polarizzati. I risultati ottenuti vengono applicati al caso del $^{181}_{73}\text{Ta}$; si prevede un'anisotropia azimutale della sezione d'urto variabile dal 130% al 50% a seconda della forma della distribuzione di carica nucleare scelta.

Determination of the Pion-Nucleon Interaction Coupling Constant from Scattering Experiments Using Dispersion Relations.

G. PUPPI and A. STANGHELLINI

Istituto di Fisica dell'Università - Bologna

(ricevuto l'11 Marzo 1957)

Summary. — We have calculated the renormalized coupling constant of the pion-nucleon interaction by fitting the experimental data of the scattering with the dispersion relations. For the $\pi^+ + p \rightarrow \pi^+ + p$, we have found: $f^2 = 0.095 \pm 0.005$ and the experimental data and the theory well consistent. For the $\pi^- + p \rightarrow \pi^- + p$, we have found a coupling constant appreciably smaller. The fact is not understandable in the frame of the usual theory of the pion-nucleon interaction.

Introduction.

Two types of methods have been used for the calculation of the renormalized coupling constant f^2 from pion-nucleon scattering experiments.

1. — Fixed source theory.

The first method consists in adopting the results of the fixed source theory obtained by CHEW and Low ⁽¹⁾. This method for the nature of the theory in itself supplies information only on the P waves and may be used in various approximations, i. e.:

1.1. Effective range. — The lower the energy of the experimental data from which one extrapolates to zero total energy, the better the reliability of the effective range for the determination of the coupling constant.

(¹) G. F. CHEW and F. E. LOW: *Phys. Rev.*, **101**, 1570 (1956).

At this moment only the $\alpha_{33}P$ wave phase shift could be analyzed in this sense and the calculation of f^2 is made by the relation:

$$(1) \quad \frac{4\eta^3}{3\omega^*} \cot \alpha_{33} - \frac{1}{f^2} \left(1 - \frac{\omega^*}{\omega_0} \right).$$

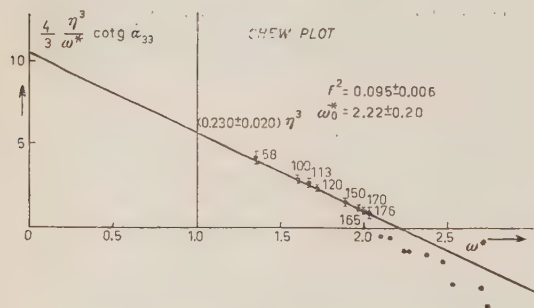


Fig. 1.

In Fig. 1 ⁽²⁾ an analysis based on the most reliable experiments of π^+ -meson scattering on protons in the energy interval below resonance has been reported and the result is

$$f^2 = 0.095 \pm 0.006,$$

$$\omega_0 = 2.22 \pm 0.20.$$

The so calculated value of f^2 has recently been confirmed by J. OREAR ⁽³⁾ and agrees with our former calculation ⁽⁴⁾.

This value is slightly higher than the ones obtained in other previous calculations ⁽⁵⁾ owing to the fact that high energy data were employed which now do not seem to be easily fitted with the straight line drawn through the lower energy data.

In Fig. 2 ⁽²⁾ the result of an effective range analysis is reported, in which we have taken into account the Serber term i.e.

$$(2) \quad \frac{4}{3} \left(\frac{\eta^3}{\omega^*} \cot \alpha_{33} - \frac{1}{\omega^*} \right) = \frac{1}{f^2} \left(1 - \frac{\omega^*}{\omega_0} \right),$$

from which

$$f^2 = 0.107 \pm 0.007,$$

$$= 2.08 \pm 0.20.$$

Without discussing the suitable expansion to be used as effective range formula, it is evident that the coupling constant obtained from this approximation points towards a value of about 0.1 with a 10 % error.

⁽²⁾ G. PUPPI and A. STANGHELLINI: *CERN Symposium* (1956).

⁽³⁾ J. OREAR: *Nuovo Cimento*, **4**, 856 (1956).

⁽⁴⁾ G. PUPPI and A. STANGHELLINI: *Nuovo Cimento*, **3**, 491 (1956).

⁽⁵⁾ S. J. LINDENBAUM and L. C. L. YUAN: *Phys. Rev.*, **101**, 307 (1955).

1.2. — Still considering the fixed source theory as a base of analysis it is possible to determine the coupling constant using directly the one-meson equations deduced by CHEW and LOW ⁽¹⁾ without having recourse to an effective range approximation.

In this sense the calculation of f^2 has been made by CINI *et al.* ⁽⁶⁾ making use of the sum rules in the α_{33} phase shift which appears as main factor and they obtained

$$f^2 = 0.107 \pm 0.010.$$

This calculation may be considered as a better approximation of the f^2 value in the limits of a well defined meson theory.

On the other hand, one of us ⁽⁷⁾ has shown that the sum-rule for the α_{31} phase shift is satisfied by introducing experimental data and a coupling constant f^2 not very different from the one obtained by CINI *et al.*

We note that in the forementioned calculations, owing to the fact that one takes into account only the α_{33} phase shift, the f^2 is substantially obtained from the $\pi^+ + p$ charge state scattering. This happens especially when one uses the graphical method for phase shift analysis of experimental data. When one analyzes the experimental data with an electronic computer the data of $\pi^+ + p$ charge state and that of $\pi^- + p$ scattering are used at the same time. Therefore the phase shifts of $T = \frac{3}{2}$ isotopic spin state are a sort of mean value of that which one obtains if the analyses were made separately.

It would be interesting to follow up this last point of view and make comparisons. The present situation suggests that there are no substantial differences for the α_{33} phase shift.

2. — Dispersion relations.

The second method consists in deducing the value of the coupling constant through the dispersion relations for the charged pions scattered by protons as obtained by GOLDBERGER ⁽⁸⁾.

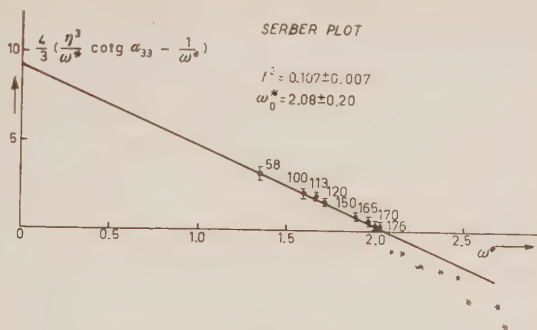


Fig. 2.

(1) M. CINI, S. FUBINI and A. STANGHELLINI: *Nuovo Cimento*, **3**, 1380 (1956).

(7) A. STANGHELLINI: *Nuovo Cimento*, **4**, 168 (1956).

(8) M. L. GOLDBERGER: *Phys. Rev.*, **99**, 508 (1955); M. L. GOLDBERGER, H. MIZAYAWA and R. OEHME: *Phys. Rev.*, **99**, 986 (1955).

These relations connect the real and the imaginary parts of the forward scattering amplitude.

Making use of the optical theorem and of λ_3 theory, the integrals are changed into integrals on the total cross sections with the addition of a term in which appears the coupling constant f^2 .

ANDERSON *et al.* ⁽⁹⁾ have used these relations in order to show the coherence of the real part of the forward scattering amplitude calculated from the phase shifts with that obtained by means of the integrals on the total cross sections and assuming the f^2 equal to 0.08 according to CHEW.

The first attempt to determine the coupling constant has been carried out by HABER-SCHAIM ⁽¹⁰⁾, who handles the dispersion relations so as to obtain the f^2 with a linear extrapolation. The value obtained by HABER-SCHAIM is

$$f^2 = 0.082 \pm 0.015.$$

In a recent attempt DAVIDON and GOLDBERGER ⁽¹¹⁾ use the dispersion relations for the derivative of the spin flip scattering amplitude obtained by OEHME ⁽¹²⁾. Introducing the α_{33} and α_{31} phase shifts of the Anderson analysis ⁽¹³⁾, they find

$$f^2 = 0.1.$$

We have reexamined the problem of the calculation of the coupling constant making use of the dispersion relations relative to the $\pi^+ + p$ and $\pi^- + p$ charge state scattering.

These relations are:

$$(2) \quad \frac{k}{k^2} D_{\pm}^b(k) = \frac{1}{2} \left(1 + \frac{\omega}{\mu} \right) D_{\pm}(0) + \frac{1}{2} \left(1 - \frac{\omega}{\mu} \right) D_{\mp}(0) + \\ + \frac{k^2}{4\pi^2} \int_{\mu}^{\infty} d\omega' \left[\frac{\tau \pm (\omega')}{\omega' - \omega} + \frac{\sigma \mp (\omega')}{\omega' + \omega} \right] + \pm \frac{2f^2}{\mu^2} \frac{k^2}{\omega \mp (\mu^2/2M)},$$

Later we shall describe the calculation method of the various terms from the experimental data of the processes:

$$(4) \quad \left\{ \begin{array}{l} a) \quad \pi^- + p \rightarrow \pi^- + p, \\ b) \quad \pi^- + p \rightarrow \pi^- + p, \\ c) \quad \pi^- + p \rightarrow \pi^0 + n. \end{array} \right.$$

⁽⁹⁾ H. L. ANDERSON, W. C. DAVIDON and U. E. KRUSE: *Phys. Rev.*, **104**, 339 (1955).

⁽¹⁰⁾ U. HABER-SCHAIM: *Phys. Rev.*, **104**, 1113 (1956).

⁽¹¹⁾ W. C. DAVIDON and M. L. GOLDBERGER: *Phys. Rev.*, **104**, 1119 (1956).

⁽¹²⁾ R. OEHME: *Phys. Rev.*, **100**, 1503 (1955); **102**, 1174 (1956).

⁽¹³⁾ H. L. ANDERSON: *VI Rochester Conference* (1956) and private communication.

Now we want to discuss our results in comparison with the previous calculations.

In Figs. 3 and 4 the experimental D_+^b and D_-^b ($r_0 = \hbar/\mu_\pi c$ units) in c.m.s. system are drawn with their errors. The continuous curves represent the second term of (2) and (3) calculated with various values of f^2 .

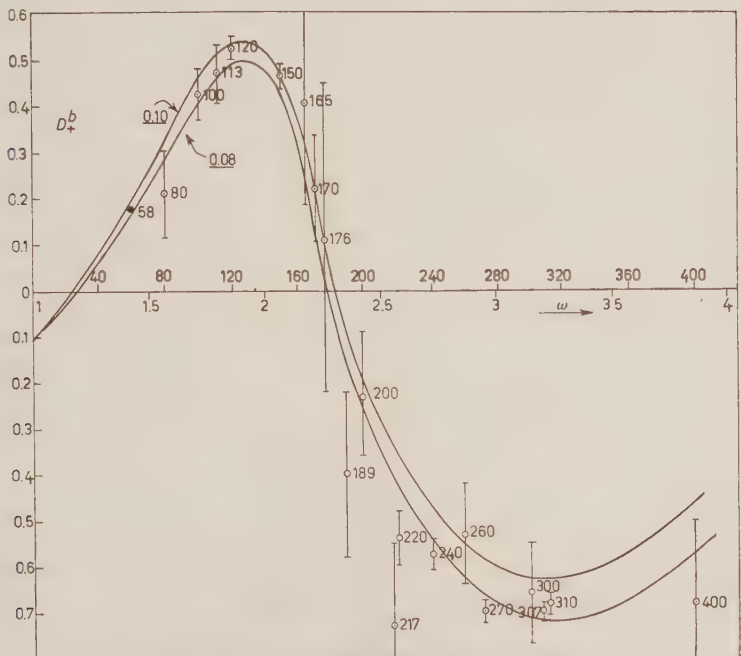


Fig. 3.

If one considers Fig. 3 relative to the process (1a) it becomes evident that the good agreement of the experimental data with the continuous curves, allows for a calculation of f^2 , which results to be

$$f^2 = 0.095 \pm 0.005.$$

This result is in agreement with the values obtained in the calculations in which the process (4a) is predominant.

It seems however evident that as far as the $\pi^+ + p$ charge state is concerned the method of approximation employed for the calculation of f^2 is not very important. Therefore one may give the value of f^2 that allows to

arrange all the $\pi^+ + p \rightarrow \pi^+ + p$ scattering experiments in a sufficiently wide range of energy (from 0 up to 400 MeV).

On the contrary the Fig. 4 relative to the process (4b) shows a particular situation, that is to say a lower value of f^2 of about 0.04 in the energy interval below resonance. The experimental situation is not so good as for the process (4a) but the agreement of the various points below resonance is suggestive enough.

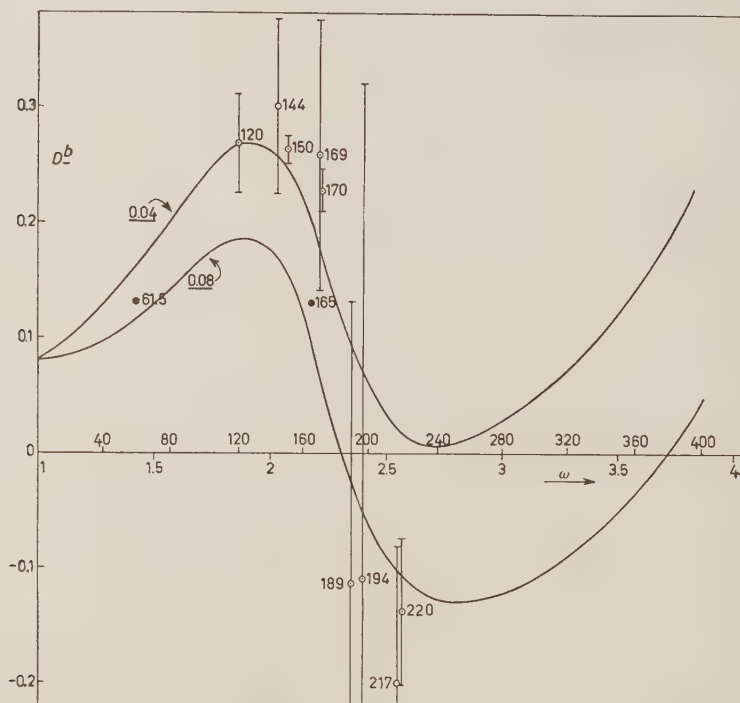


Fig. 4.

There may arise the doubt that the error lies in the continuous curves, but an analysis of the various terms making up the continuous curves shows a maximum error of about 20% while the deviation is more consistent.

There are few experiments above resonance. They seem to be in disagreement with the previous consideration, but we note that in the energy interval the relative error due to the integrals on the total cross sections are very big.

If we consider only the information below resonance, it becomes evident

that there is an inconsistency in the calculation of f^2 . This disagreement cannot be made clear by any of the previous calculations, because some of them use the $T = \frac{3}{2}$ phase shifts which, as we have noted before derive from the process (4a).

In the calculation of Haber-Schaim this disagreement is disguised because he used the combination:

$$(5) \quad D^{(2)} = \frac{D_- - D_+}{2},$$

and makes a particular choice of the phase shifts.

If we compute the means suggested by (5), we find a value for f^2 not far from 0.08 as shown in Fig. 5.

In assuming this state of fact to be real, and awaiting new experiments for (4b) and (4c) processes which may clarify the situation, we put some questions.

We have noted that the dispersion relations relative to the process (4a), calculated with the same f^2 which one can derive from the fixed source

theory, is in good agreement with the experimental data. This may suggest that the experimental phase shifts for $T = \frac{3}{2}$ isotopic spin state and α_1 with its behaviour towards 0, are consistent with the dispersion relations.

From this fact, we could say that the impossibility of deducing the same coupling constant for the process (4b) depends on the phase shifts of $T = \frac{1}{2}$ isotopic spin state, i.e. α_1 with its behaviour at high energy and α_{13} , α_{11} phase shifts.

These two latter phase shifts also do not seem to agree with the last predictions of the fixed source theory as one can see from the last data of ASHKIN⁽¹⁴⁾ and from the analysis of ANDERSON. But this disagreement does

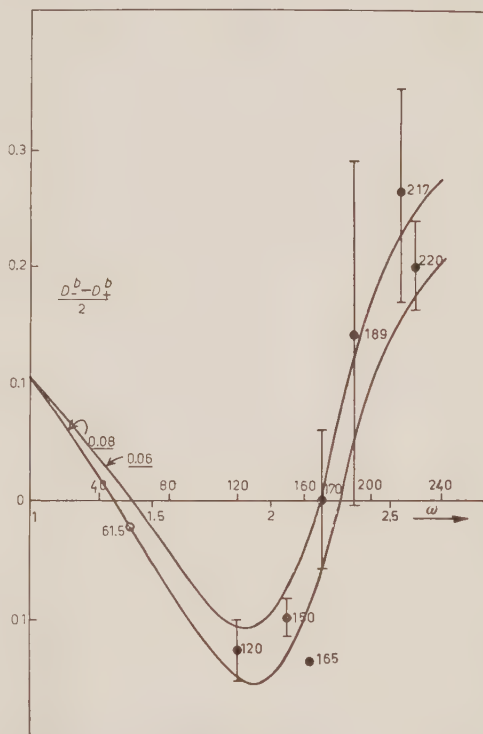


Fig. 5.

⁽¹⁴⁾ D. BODANSKY, A. M. SACHS and J. STEINBERGER: *Phys. Rev.*, **93**, 1367 (1954); G. PUPPI: *VI Rochester Conference* (1956) and *CERN Symposium* (1956); J. ASHKIN,

not surprise considering that this theory is based on particular hypotheses. What surprises on the contrary is that there is a disagreement in the dispersion relations which are deduced from general physical hypotheses.

At first time we were inclined to believe that the inconsistency depends on the failure of the isotopic spin conservation, owing to the electromagnetic effects and the mass differences between the charged and neutral pions.

However a preliminary calculation performed by CINI *et al.* shows that this is not the case, because the corrections are very small and essentially of kinematical character.

In conclusion, in the frame of the standard meson theory, which only considers pions and nucleons, it seems difficult to find out an explanation of the observed effect.

* * *

We should like to acknowledge, with thanks, the assistance given us by Proff. H. L. ANDERSON, G. BERNARDINI, M. CINI and J. OREAR, with their interesting discussions, and we should like to thank also our colleagues L. BERTOCCHI and A. MINGUZZI, who took great interest in this work.

APPENDIX

Numerical calculations.

Now we analyse the method used in the calculation of the various terms of dispersion relations from the experimental data. We write the dispersion relations in this way:

$$(6) \quad \frac{D_{\pm}^b}{r_0}(k) = \eta\eta_0 \left(\frac{\pm 2f^2}{\omega \mp (\mu^2/2M)} + \frac{S_{\pm}}{4\pi^2\eta_0^2} + \frac{T_{\pm}}{\eta^2} \right).$$

D_{\pm}^b is the real part of the forward scattering amplitude in c.m.s. for the (1a)

J. P. BLASER, F. FEINER and M. O. STERN: *Phys. Rev.*, **101**, 1149 (1956) and *CERN Symposium* (1956), p. 225; A. J. MUKHIN, E. B. OZEROV, B. M. PONTECORVO and E. L. GRIGORYEV: *CERN Symposium* (1956), p. 204; R. S. MARGULIES: *Bull. of Amer. Phys. Soc.*, **7** (1955); H. L. ANDERSON, E. FERMI, R. MARTIN and D. E. NAGLE: *Phys. Rev.*, **91**, 155 (1953); H. L. ANDERSON and M. GLICKSMAN: *Phys. Rev.*, **100**, 268 (1955); H. L. ANDERSON, W. C. DAVIDON, M. GLICKSMAN and U. E. KRUSE: *Phys. Rev.*, **100**, 279 (1955); J. OREAR: *Phys. Rev.*, **96**, 1417 (1956); O. TAFT: *Phys. Rev.*, **101**, 1116 (1956); M. GLICKSMAN: *Phys. Rev.*, **94**, 1335 (1954).

and (4b) processes

$$S_{\pm} = \int_1^{\infty} \frac{d\omega'}{\eta'} \left[\frac{\sigma \pm (\omega')}{\omega' - \omega} + \frac{\sigma \mp (\omega')}{\omega' + \omega} \right],$$

$$T_{\pm} = \frac{1}{2r_0} [(D_-(0) + D_+(0)) \pm \omega(D_-(0) - D_+(0))],$$

where energy, momenta and masses are measured in $\mu_{\pi}c^2 = 140$ MeV units. It is possible to calculate D_{\pm} without making up a phase shift analysis directly from the coefficients of the angular distribution ⁽¹⁴⁾. These coefficients have been corrected taking into account the Coulomb interference effects, that can be well calculated by an approximate knowledge of the phase shifts.

We remember that in the case that only S and P waves enter in the considered processes, the differential cross sections can be written:

$$\frac{d\sigma(\vartheta)_{\pm}}{d\Omega} = |F(\vartheta)|^2 = a_{\pm} + b_{\pm} \cos \vartheta + c_{\pm} \cos^2 \vartheta,$$

$$F(\vartheta) = D(\vartheta) - iA(\vartheta);$$

for $\vartheta = 0$

$$|F(0)|^2 = a_{\pm} + b_{\pm} + c_{\pm}$$

$$|D_{\pm}| = \sqrt{k_{\pm}^2 - A_{\pm}^2}.$$

On the other hand making use of the optical theorem, we obtain:

$$A_{\pm} = \frac{\eta_0}{r_0} \left(a_{\pm} + \frac{c_{\pm}}{3} \right),$$

$$A_{\pm} = \frac{\eta_0}{r_0} \left(a_{\pm} - a_0 - \frac{c_{\pm} - c_0}{3} \right).$$

The absolute values of D_{\pm} are in this way calculated and the sign can be determined from the general behaviour of the right hand member of (6).

This method has the advantage of separating the experimental data of the $\pi^+ + p$ and $\pi^- + p$ charge state in the calculation of D_{\pm} . If more than two waves are important, the generalization is evident.

As far as T_{\pm} is concerned, the calculation is performed using the S waves behaviours given by J. OREAR ⁽¹⁵⁾, which are

$$a_3 = (0.105 \pm 0.010)\eta_0,$$

$$a_1 = (0.165 \pm 0.012)\eta_0,$$

⁽¹⁵⁾ J. OREAR: *Phys. Rev.*, **96**, 176 (1954).

and the result is

$$T_{\pm} = -0.016 \pm 0.104\omega.$$

The integrals on total cross sections ⁽¹⁶⁾ have to be extended to ∞ , whereas the total cross sections are known up to 1.9 GeV. We have supposed that σ^{-} and σ^{+} are constant in the energy interval above 1.9 GeV, and equal to $\sigma_{+} = \sigma^{-} = 30$ mb as the value obtained by BANDTEL *et al.* seems to confirm. Calling:

$$C = \sigma_{\pm} \int_{14}^{\infty} \frac{d\omega'}{\eta'} \left(\frac{1}{\omega' - \omega} - \frac{1}{\omega' + \omega} \right),$$

we have

$$C = 4.4 \text{ mb}.$$

One may check this hypothesis with the experimental data at low energy by calculating the quantity:

$$2f^2 \pm C \left(\omega \mp \frac{\mu^2}{2M} \right).$$

In this way one could obtain the coupling constant and the contribution of high energy on the integrals. We have made this calculation and have found that there are no indication that C is different from 0 outside the errors, which is in agreement with the small value of C calculated from the integrals. The integrals are computed numerically after having subtracted the singularity, i.e.

$$\int \frac{f(\omega')}{\omega' - \omega} d\omega' = \int \frac{f(\omega') - f(\omega)}{\omega' - \omega} d\omega' + f(\omega) \int \frac{d\omega'}{\omega' - \omega},$$

in the kinetic energy interval from 0 to 400 MeV.

A comparison of our integrals with those of ANDERSON ⁽⁹⁾ shows a close agreement with deviations not greater than 10%.

⁽¹⁶⁾ H. L. ANDERSON, E. FERMI, E. A. LONG and D. E. NAGLE: *Phys. Rev.*, **85**, 936 (1952); S. J. LEONARD and D. H. STORK: *Phys. Rev.*, **93**, 568 (1954); J. ASHKIN, J. P. BLASER, F. FEINER, J. G. GORMAN and M. O. STERN: *Phys. Rev.*, **96**, 1104 (1954); A. E. IGNATENKO, A. I. MUKHIN, E. B. OZEROV and B. M. PONTECORVO: *Sov. Phys. JETP*, **3**, 10 (1956); S. J. LINDENBAUM and L. C. L. YUAN: *Phys. Rev.*, **100**, 306 (1955); R. COOL, O. PICCIONI and D. CLARK: *Phys. Rev.*, **103**, 1083 (1956).

RIASSUNTO

Abbiamo calcolato la costante d'accoppiamento rinormalizzata dell'interazione pione-nucleone, adattando i dati sperimentali dello scattering alle relazioni di dispersione. Per lo scattering $\pi^+ + p \rightarrow \pi^+ + p$ abbiamo trovato: $f^2 = 0.095 \pm 0.005$ e una buona consistenza tra i dati sperimentali e la teoria. Per lo scattering $\pi^- + p \rightarrow \pi^- + p$ abbiamo trovato una costante d'accoppiamento sensibilmente minore. Il fatto non è spiegabile nell'ambito dell'usuale teoria dell'interazione pione-nucleone.

Effetti isotopici nell'adsorbimento di gas su solidi (*).

P. CALDIROLA e G. ROSSI (+)

Istituto di Scienze Fisiche dell'Università - Milano
Istituto Nazionale di Fisica Nucleare - Sezione di Milano

(ricevuto il 29 Marzo 1957)

Riassunto. — Gli effetti isotopici, che si manifestano nel processo di adsorbimento di un miscuglio gassoso da parte della superficie di un solido, sono stati studiati in base alla teoria di Lennard-Jones sulla interazione di atomi e molecole con superficie solide. Di questa teoria sono state riportate le linee generali, adattate al problema in esame. Le formule dedotte per un miscuglio di due generiche specie isotopiche sono state applicate al caso particolare dell'adsorbimento di elio ($^3\text{He}_2$ ed $^4\text{He}_2$) su fluoruro di litio. Si è trovato che sulla superficie adsorbente l'arricchimento isotopico δ_{ads} in condizioni stazionarie è sempre inferiore a quello δ_k di Knudsen caratteristico del fenomeno di diffusione, avvicinandosi ad esso al crescere della temperatura.

È nota l'importanza dei fenomeni superficiali nei processi di diffusione di gas attraverso sistemi porosi solidi. In questo lavoro ci siamo proposti di studiare gli eventuali effetti isotopici che si accompagnano all'adsorbimento di gas su solidi.

Precisamente abbiamo preso in esame il processo di adsorbimento di gas su un solido a reticolo cristallino perfetto, nell'ipotesi che detto adsorbimento si manifesti in uno strato unimolecolare.

Per un siffatto processo è stata sviluppata da LENNARD-JONES e collaboratori (1) in una serie di lavori dal 1935 al 1937 una teoria « fondamentale »

(*) Lavoro eseguito nel quadro di una collaborazione con i laboratori CISE.

(+) Attualmente all'Ufficio Studi dell'Agip Nucleare - Milano.

(1) Serie di articoli di J. E. LENNARD-JONES e collaboratori in *Proc. Roy. Soc. A*, 150, 442, 456 (1935); 156, 6, 29, 37 (1936); 158, 253, 591 (1937); 163, 101, 123, 132 (1937).

basata sullo studio, secondo la meccanica quantistica, della interazione fra gli atomi della fase adsorbita e quelli del reticolo del solido.

Partendo da questa teoria, che riproduciamo in forma schematica nelle prime tre sezioni adattandola al nostro problema, abbiamo dedotto in modo esplicito le formule, relative agli effetti isotopici associati all'adsorbimento.

Infine abbiamo applicato, eseguendo i relativi calcoli numerici, i risultati ottenuti al caso dell'adsorbimento di un miscuglio di ^3He e ^4He su fluoruro di litio.

1. - Richiami alla teoria di Lennard-Jones per l'adsorbimento.

In questa teoria il solido viene schematizzato come un cristallo cubico contenente G^3 atomi di massa M . Un atomo del gas di massa m interagisce con un atomo della superficie del reticolo, il quale ha subito uno spostamento dalla propria posizione di equilibrio dovuto all'agitazione termica; la proiezione di tale spostamento nella direzione perpendicolare alla superficie è indicata con Z .

Il moto dell'atomo del gas viene considerato unidimensionale (coordinata z) e l'interazione viene rappresentata con una funzione potenziale del tipo di Morse, caratterizzata dai consueti parametri:

D : profondità del minimo,

κ : inverso del « range »,

b : distanza tra il minimo e l'atomo del cristallo.

L'equazione d'onda del sistema totale (reticolo + atomo del gas) è pertanto:

$$\left\{ \sum'_{fgh} \sum'_1 \left[\frac{\hbar^2}{2M_0} \left(\frac{\partial^2}{\partial a_{fghj}^2} + \frac{\partial^2}{\partial b_{fghj}^2} \right) - 2\pi^2 v_{fghj}^2 M_0 (a_{fghj}^2 + b_{fghj}^2) \right] + \right. \\ \left. + \frac{\hbar^2}{2m} \frac{\partial^2}{\partial z^2} - (D \exp[-2\kappa(z-b-Z)] - 2D \exp[-\kappa(z-b-Z)] - \frac{\hbar}{i} \frac{\partial}{\partial t}) \right\} \Psi = 0,$$

dove sono state usate le notazioni di Wilson per la parte che riguarda le vibrazioni del reticolo, e cioè:

$$M_0 = \frac{1}{2} MG^3; \quad a_{fghj}, b_{fghj}, v_{fghj} \quad \text{coordinate e frequenze normali del reticolo}$$

(f, g, h , prendono i valori interi da $-G/2$ a $G/2$, cosicchè ogni terna f, g, h , caratterizza un atomo del reticolo); \sum' sta a indicare che la sommatoria va estesa ad una metà del « cubo delle fasi », per avere il corretto numero totale di vibrazioni normali.

Se l'agitazione termica del cristallo non è troppo intensa, la quantità κZ risulta piccola e ciò permette di scrivere il potenziale $V(z)$ atomo del gas-atomo del reticolo come somma di due termini:

$$V_I + V_{II} = D(\exp[-2\kappa(z-b)] - 2\exp[-\kappa(z-b)]) + \\ + 2\kappa Z D(\exp[-2\kappa(z-b)] - \exp[-\kappa(z-b)]).$$

V_{II} è il termine di accoppiamento e può essere trattato come una perturbazione.

L'ordinario formalismo della teoria delle perturbazioni dipendenti dal tempo porta a considerare lo sviluppo

$$\Psi = \sum_{mn} a_{mn}(t) \psi_m \Phi_n \exp \left[-i \frac{W_m + E_n}{\hbar} t \right],$$

dove ψ_m , W_m sono l'autofunzione e il relativo autovalore della equazione di Schrödinger degli stati stazionari del reticolo, Φ_n , E_n l'autofunzione e il relativo autovalore dell'equazione di Schrödinger degli stati stazionari di un atomo di massa m nel campo di potenziale rappresentato dal termine V_I .

I coefficienti $a_{mn}(t)$ sono soluzioni dell'equazione

$$\dot{a}_{rs}(t) = -\frac{i}{\hbar} \sum_{mn} a_{mn}(t) (rs | V_{II} | mn) \exp \left[i \frac{W_r + E_s - W_m - E_n}{\hbar} t \right].$$

In prima approssimazione si assumono i coefficienti a_{mn} tutti nulli tranne uno, ad esempio a_{pi} , cui si attribuisce il valore 1 per $t = 0$. Si ottiene in tal modo la probabilità di transizione $p, l \rightarrow r, s$ all'istante t :

$$\Gamma_{p,rs}(t) = 2 |(rs | V_{II} | pl)|^2 \frac{1 - \cos(W_r + E_s - W_p - E_l)t/\hbar}{(W_r + E_s - W_p - E_l)^2}.$$

2. Valutazione della probabilità di transizione per un processo di attivazione o deattivazione.

L'elemento di matrice che compare nell'espressione della probabilità di transizione ha la forma

$$(rs | V_{II} | pl) = 2\kappa D \int \prod \chi_r(a_{fghj}) \chi_r(b_{fghj}) Z \prod \chi_p(a_{fghj}) \chi_p(b_{fghj}) \cdot \prod da_{fghj} \prod db_{fghj} \cdot \\ \cdot \int_{-\infty}^{+\infty} \Phi_s^*(\exp[-2\kappa(z-b)] - \exp[-\kappa(z-b)]) \Phi_l dz,$$

dove $\chi(u_{fghj})$ è l'autofunzione normalizzata dell'oscillatore armonico corrispondente alla coordinata normale a_{fghj} , ecc.

La parte dell'elemento di matrice che contiene le coordinate normali del reticolo si valuta tenendo presente l'espressione dello « spostamento » Z in funzione delle stesse coordinate, che è

$$Z = \sum_{fgh} \sum_1^3 \left[a_{fghj} \cos \frac{2\pi}{G} (f\xi + g\eta + h\zeta) + b_{fghj} \sin \frac{2\pi}{G} (f\xi + g\eta + h\zeta) \right] (u_{fghj})_z,$$

dove: ξ, η, ζ caratterizzano l'atomo del reticolo cui ci si vuole riferire (i risultati si rivelano indipendenti dalla particolare scelta di ξ, η, ζ); $(u_{fghj})_z$ è la z -componente di un vettore (unitario) avente la direzione specificata dalla terna fgh per $j=1$, e direzione perpendicolare a questa per $j=2, 3$.

Applicando risultati validi nel caso limite di onde elastiche propagantisi in un mezzo continuo, si ha che, fissato uno stato iniziale p , sono possibili transizioni a stati r , durante le quali l'oscillatore corrispondente ad a_{fghj} , b_{fghj} emette o assorbe un quanto $2\pi\hbar\nu_{fghj}$, dove

$$\nu_{fghj} = \frac{c_j}{Ga} \sqrt{j^2 + g^2 + h^2},$$

(c_j = velocità del suono per la vibrazione j ; c_1 velocità delle onde longitudinali, c_2 - c_3 velocità delle onde trasversali, tutte si suppongono costanti; a = costante del reticolo).

Gli elementi di matrice $\neq 0$ sono:

$$\sqrt{\frac{\hbar(\sigma+1)}{4\pi M_0 \nu_{fghj}}} \cdot \begin{cases} \cos \frac{2\pi}{G} (f\xi + g\eta + h\zeta) \cdot (u_{fghj})_z \\ \sin \frac{2\pi}{G} (f\xi + g\eta + h\zeta) \cdot (u_{fghj})_z \end{cases},$$

per assorbimento da parte degli oscillatori a_{fghj} , b_{fghj} rispettivamente;

$$\sqrt{\frac{\hbar\sigma}{4\pi M_0 \nu_{fghj}}} \cdot \begin{cases} \cos \frac{2\pi}{G} (f\xi + g\eta + h\zeta) \cdot (u_{fghj})_z \\ \sin \frac{2\pi}{G} (f\xi + g\eta + h\zeta) \cdot (u_{fghj})_z \end{cases},$$

per emissione da parte degli stessi oscillatori.

L'intero σ , numero quantico che caratterizza lo stato iniziale dell'oscilla-

tore, viene sostituito con il valore medio

$$\bar{\sigma} = \frac{1}{\exp[2\pi\hbar\nu/kT] - 1}$$

del numero di oscillatori di energia $\hbar\nu$ alla temperatura T .

Per le transizioni durante le quali il cristallo assorbe energia, il quadrato del modulo del fattore di $\langle rs | V_{II} | pl \rangle$ contenente le coordinate normali del reticolo assume così la forma:

$$\frac{\hbar G a}{4\pi c_j M_0 (f^2 + g^2 + \hbar^2)^{\frac{1}{2}}} \cdot \frac{1}{1 - \exp[-2\pi\hbar\nu_{fghj}/kT]} \cdot \left\{ \frac{\cos^2}{\sin^2} \frac{2\pi}{G} (f\xi + g\eta + \hbar\zeta) \cdot (u_{fghj})_z \right\}$$

con

$$(u_{fgh1})_z^2 = \frac{\hbar^2}{f^2 + g^2 + \hbar^2}; \quad (u_{fgh1})_z^2 = \frac{f^2 + g^2}{f^2 + g^2 + \hbar^2}.$$

La parte dell'elemento di matrice $\langle rs | V_{II} | pl \rangle$ che contiene la coordinata z dell'atomo adsorbito si valuta tenendo presenti i risultati relativi allo spettro energetico discreto della funzione potenziale di Morse

$$\Phi_n(u) = \frac{1}{N_n} \exp[-de^{-\kappa u}] (2de^{-\kappa u})^{(2d-2n-1/2)} L_{2d-n-1}^{2d-2n-1}(2de^{-\kappa u})$$

$$u = z - b, \quad d = \frac{\sqrt{2mD}}{\kappa\hbar},$$

$$N_n^2 = \frac{[I(2d-n)]^3}{\kappa(2d-2n-1)n!},$$

$$E_n = -\frac{\kappa^2 \hbar^2 b_n^2}{8m}, \quad b_n = 2d - 1 - 2n.$$

Si ottiene

$$\int_{-\infty}^{\infty} \Phi_s^*(u) (\exp[-2\kappa n] - \exp[-\kappa u]) \Phi(u) du \equiv g_{ss} =$$

$$= \frac{(-1)^{l+s}}{4d^2} \left[\frac{\Gamma(d-l) \cdot l!}{\Gamma(2d-s) \cdot s!} \right]^{\frac{1}{2}} [(2d-2l-1)(2d-2s-1)]^{\frac{1}{2}} \cdot (l-s) \cdot (2d-l-s-1)$$

quando sia $l > s$.

È noto che il contributo prevalente alla probabilità di transizione totale, per una data transizione $l > s$ dell'atomo del gas, proviene dai processi in cui l'energia è conservata, e questi riguardano gli atomi del cristallo caratte-

rizzati da valori f, g, h che soddisfano approssimativamente alla relazione

$$(1) \quad \frac{2\pi\hbar c_j(f^2 + g^2 + h^2)^{\frac{1}{2}}}{Ga} = \frac{\kappa^2\hbar^2}{2m} (l-s)(2d-1-l-s).$$

La sommatoria \sum'_{fgh} potrà sostituirsi con un integrale in uno spazio delle « fasi » di coordinate f, g, h ; ammettendo di attribuire ad ogni terna di valori f, g, h lo stesso peso unitario, basterà introdurre l'elemento di volume dello spazio f, g, h

$$df dg dh = \frac{G^3 a^3}{e_j^3} v^2 dv d\Omega$$

(poichè $v_{fgh}^2 = c_j^2(f^2 + g^2 + h^2)/G^2 a^2$).

La (1) è l'equazione di una superficie sferica nello spazio f, g, h il cui raggio risulta fissato dalla particolare transizione $l \rightarrow s$ dell'atomo del gas che si considera:

$$v_s = \frac{E - E_s}{2\pi\hbar}.$$

La sommatoria \sum'_{fgh} diventa così una integrazione su uno strato sferico di spessore Δv_l , ed anzi — tenendo conto della prescrizione per la somma \sum' data in Sez. 1 — una integrazione su uno strato *semisferico* di quello spessore.

Come risultato di questa integrazione si ottiene la probabilità di transizione $l \rightarrow s$ per un atomo del gas al tempo t .

$$F_{ls}t = \frac{4\kappa^2 D^2 g_{ls}^2 a^3}{3} \left(\frac{1}{e_1^3} + \frac{2}{e_2^3} \right) \frac{(\sigma_r - 1) v_{ls}}{M\hbar} t = \frac{\kappa^2 a^3 \hbar^4}{64\pi m^3 M} \left(\frac{1}{3e_1^3} + \frac{2}{3e_2^3} \right) \cdot \frac{(l-s)^3 (2d-1-s-l)^3 (2d-2l-1)(2d-2s-1)}{1 - \exp[-\hbar v_l/kT]} \cdot \frac{l!}{s!} \frac{\Gamma(2d-l)}{\Gamma(2d-s)} t.$$

Per un processo di « attivazione » dell'atomo adsorbito (transizione $l \rightarrow s$ con $l < s$) la probabilità di transizione per unità di tempo G_{ls} si ricava dalla formula precedente scambiando l con s , e sostituendo il fattore di temperatura

$$\bar{\sigma}_v + 1 = \frac{1}{1 - \exp[-\hbar v_{ls}/kT]}$$

relativo all'assorbimento di energia da parte del solido, con il fattore

$$\sigma_v = \frac{1}{\exp[\hbar v_{ls}/kT] - 1}$$

relativo all'emissione.

3. - Probabilità di transizione per un processo di condensazione e di evaporazione di un atomo del gas.

I processi di condensazione ed evaporazione di un atomo del gas corrispondono — nello schema generale delineato nelle Sez. 1-2 — a transizioni dell'atomo del gas da livelli di energia > 0 a livelli di energia < 0 , e viceversa.

I livelli di energia $E > 0$ dell'equazione di Schrödinger per un atomo di massa m in un campo di potenziale del tipo di Morse formano uno spettro continuo. Le relative *autofunzioni* sono $\psi = \Phi \exp[-iEt/\hbar]$ ($E \geq 0$) con Φ soluzione dell'equazione

$$\frac{d^2\Phi}{dz^2} + \frac{2m}{\hbar^2} (E - D \exp[-2\kappa(z-b)] + 2D \exp[-\kappa(z-b)]) \Phi = 0,$$

la quale, grazie alle trasformazioni

$$2d \exp[-\kappa u] = \eta \quad (u = z - b)$$

$$\Phi = \eta^{-\frac{1}{2}} g$$

assume la forma

$$\frac{d^2 g}{d\eta^2} + \left\{ -\frac{1}{4} + \frac{d}{\eta} + \frac{\frac{1}{4} - (i\mu)^2}{\eta^2} \right\} g = 0, \quad \left(d = \frac{\sqrt{2mD}}{\kappa\hbar}; \mu = \frac{\sqrt{2mE}}{\kappa\hbar} \right).$$

Questa equazione è del tipo ipergeometrico confluyente, ed ammette come integrali linearmente indipendenti le funzioni $W_{a,i\mu}(\eta)$, $W_{-a,i\mu}(-\eta)$ definite in WHITTAKER e WATSON, cap. XVI, delle quali solo la prima è limitata per $\eta \rightarrow \infty$.

Pertanto possiamo assumere come autofunzioni non normalizzate dello spettro continuo

$$\Phi(E, u) = (2d \exp[-\kappa u])^{-\frac{1}{2}} W_{a,i\mu}(2d \exp[-\kappa u]).$$

La *normalizzazione* si effettua nel modo consueto per le autofunzioni degli spettri continui, ossia in termini di autodifferenziali.

Posto $\Delta_n F = \int_{A_n E} N(E) \Phi(E, u) dE$, si deve determinare $N(E)$ in modo che sia

$$\int_{-\infty}^{+\infty} \Delta_n F \Delta_m F^* du = \Delta_{mn} E,$$

dove $\Delta_{mn} E$ è la parte comune a $\Delta_m E$, $\Delta_n E$.

La relazione che determina il fattore di normalizzazione $N(E)$ si può ridurre alla seguente:

$$4\pi\hbar \sqrt{\frac{E}{2m}} Q Q^* N(E) N^*(E) = 1,$$

dove

$$Q = (2d)^{i\mu} \frac{\Gamma(-2i\mu)}{\Gamma(\frac{1}{2} - i\mu - d)}.$$

La probabilità di transizione contiene pertanto ora un fattore della forma

$$\begin{aligned} & \left| \int \Delta F^*(\exp[-2\kappa u] - \exp[-\kappa u]) \Phi_l du \right|^2 = \\ &= N(E) N^*(E) \left| \int_{-\infty}^{+\infty} \Phi^*(E, u) (\exp[-2\kappa u] - \exp[-\kappa u]) \Phi_l(u) du \right|^2 = \\ &= \frac{m}{2\pi\hbar^2\kappa\mu} \frac{|\Gamma(\frac{1}{2} - d + i\mu)|^2}{|\Gamma(2i\mu)|^2} \left\{ \frac{\Gamma(2d-l)^2}{l! N_l} \right\} \frac{|I|^2}{(4d^2\kappa)^2}, \end{aligned}$$

dove

$$\begin{aligned} I &= \int_0^{+\infty} W_{d-i\mu}(\eta)(\eta^d - 2d\eta^{d-1}) \cdot \\ &\cdot [1 - l(2d-l-1)\eta^{-1} + O(\eta^{-2})] \exp\left[-\frac{\eta}{2}\right] d\eta \quad (\eta = 2d \exp[-\kappa u]). \end{aligned}$$

Usando per la funzione $W_{d-i\mu}$ la rappresentazione integrale di Barnes, si può mostrare che $I = |\Gamma(d + \frac{1}{2} + i\mu)|^2 \{ (d-l-\frac{1}{2})^2 + \mu^2 \}$.

Pertanto il fattore che contiene le autofunzioni del potenziale di Morse nella probabilità di transizione del sistema totale (solido + atomo del gas) avrà la forma

$$\begin{aligned} g(l, E) &= \frac{m}{4\hbar^2 d^3 \kappa^2} \cdot \frac{\sinh 2\mu\pi \cdot |\Gamma(d + \frac{1}{2} + i\mu)|^2}{(\cos 1/2\mu\pi\sigma - \cos 2\mu_0\pi)} \cdot \frac{\mu_l(\mu^2 + \mu_l^2)^2}{l! \Gamma(2d-l)} \\ &\left[\mu = \frac{\sqrt{2mE}}{\kappa\hbar}; \mu_l = d - l - \frac{1}{2} = \frac{\sqrt{-2mE_l}}{\kappa\hbar} \right]. \end{aligned}$$

La probabilità di transizione per unità di tempo dal livello E_l all'intervallo $(E, E + dE)$ del continuo si otterrà sostituendo nella espressione di $G_{l,}$

data in Sez. 2 il fattore g_{ls} con quello $g(l, E)$ ora ottenuto. Sarà così:

$$\begin{aligned}
 G_{l,E} dE &= \frac{2\kappa^2 D^2 a^3}{3\pi M \hbar^2} \left(\frac{1}{c_1^3} + \frac{2}{c_2^3} \right) \frac{(E - E_l) g(l, E) dE}{\exp[(E - E_l)/kT] - 1} = \\
 &= \frac{\kappa' D^2 a^3}{12\pi m M d^4} \left(\frac{1}{c_1^3} + \frac{2}{c_2^3} \right) \cdot \frac{1}{\exp[(\kappa^2 \hbar^2 (\mu^2 + \mu_l^2))/2mkT] - 1} \cdot \frac{\mu_l}{l! I(2d - l)} \cdot \\
 &\quad \frac{(\mu^2 + \mu_l^2)^3 |I(d + \frac{1}{2} + i\mu)|^2 \mu \sinh 2\mu\pi d\mu}{\cosh 2\mu\pi - \cos 2\mu_0\pi}.
 \end{aligned}$$

La probabilità di transizione per unità di tempo relativa al processo di adsorbimento $\Gamma_{E,l} dE$ dall'intervallo $(E, E + dE)$ del continuo al livello E_l si ottiene da $G_{l,E}$ con la semplice sostituzione del fattore di temperatura $(1 - \exp[-\kappa^2 \hbar^2 (\mu^2 + \mu_l^2)/2mkT])^{-1}$ a quello che compare in $G_{l,E}$ (cfr. Sez. 2 alla fine), ossia

$$\Gamma_{E,l} = G_{l,E} \exp \left[\frac{\kappa^2 \hbar^2 (\mu^2 + \mu_l^2)}{2mkT} \right].$$

4. - Flusso di adsorbimento e flusso di evaporazione per una superficie solida.

Siamo ora in grado di calcolare il flusso di adsorbimento e il flusso di evaporazione relativi alla superficie S di un solido, su cui si abbiano n_s « posti » per l'adsorbimento per unità di superficie, e ad una massa gassosa di densità ν (numero di atomi per unità di volume).

Il flusso di adsorbimento Φ_{ads} è dato dal numero di atomi del gas che vengono adsorbiti per unità di tempo dalla superficie S , ossia che incidendo sulla superficie S con una energia cinetica qualsiasi compiono la transizione ad uno qualsiasi dei livelli energetici discreti del potenziale di Morse. Si ha:

$$(2) \quad \Phi_{ads} = S(1 - \theta) \nu \int_0^{\hbar \nu_M} q(E) \sum_s \bar{I}_{E,s} dE,$$

dove:

θ rappresenta la frazione di « posti » occupata da atomi del gas: si assume infatti che l'adsorbimento possa avvenire solo in « posti » liberi;

$q(E) dE$ rappresenta il contributo al flusso incidente dovuto ad atomi con energia (associata alla componente del moto normale alla superficie) tra E ed $E + dE$, riferito all'unità di superficie e a densità unitaria della fase gassosa: considerazioni elementari danno $q(E) = \exp[-E/kT]/\sqrt{2k\pi mT}$;

$\bar{I}_{E,s}$ è la probabilità di transizione per unità di tempo, riferita ad un flusso incidente unitario, da un livello E del continuo al livello E_s .

La valutazione di $\bar{I}_{E,s}$ si fa tenendo presente che le autofunzioni dello spettro continuo del potenziale di Morse

$$\Phi(E, u) = (2d \exp[-\kappa u])^{\frac{1}{2}} W_{d, i\mu}(2d \exp[-\kappa u])$$

si possono considerare come la somma di due onde, incidente e riflessa rispetto alla superficie del solido:

$$\Phi = \Phi_i + \Phi_r.$$

Il flusso corrispondente all'onda incidente

$$f_\mu = \frac{\hbar}{2im} \left(\Phi_i \frac{\partial \Phi_i^*}{\partial z} - \Phi_i^* \frac{\partial \Phi_i}{\partial z} \right)$$

risulta dato da

$$f_\mu = \frac{\hbar \kappa \mu}{m} \frac{|I(2i\mu)|^2}{|I(\frac{1}{2} + i\mu - d)|^2}$$

e normalizzando l'autofunzione si ha $f_\mu = 1/\hbar$.

Ne deriva che se $I_{E,s}$ rappresenta la probabilità di transizione $s \rightarrow s'$ di un atomo del gas dall'intervallo $(E, E+dE)$ al livello E_s , questa riferita ad un flusso unitario è

$$\bar{I}_{E,s} = \hbar I_{E,s}.$$

L'intervallo di integrazione $0 \rightarrow \hbar \nu_M$ ha come limite superiore la quantità massima di energia che in un singolo processo può essere emessa o assorbita dal cristallo: nel presente schema gli scambi di energia riguardano infatti un singolo quanto per ogni processo.

La sommatoria che compare nell'espressione di Φ_{ads} si estende ad un numero di termini che varia procedendo da un estremo all'altro dell'intervallo di integrazione.

Precisamente, questo va suddiviso in tanti intervalli parziali in ciascuno dei quali il numero degli addendi della sommatoria è costante. Il numero massimo dei livelli interessati al processo di adsorbimento è dato dai livelli compresi tra $-\hbar \nu_M$ e 0. Siano essi, in ordine di energia crescente:

$$E_0, E_1, E_2, \dots, E_n;$$

nell'intervallo $0 \rightarrow \hbar \nu_M - |E_0|$ la sommatoria va estesa a tutti questi livelli, nel successivo intervallo $\hbar \nu_M - |E_0| \rightarrow \hbar \nu_M - |E_1|$ essa va estesa ai livelli E_1, \dots, E_n ; e così via.

Il flusso di evaporazione Φ_{ev} è dato dal numero di atomi del gas, adsorbiti sulla superficie S , che lasciano la superficie per evaporazione nell'unità di tempo, ossia che essendo adsorbiti in un livello discreto E_s qualsiasi del potenziale di Morse compiono la transizione ad un livello E qualsiasi della distribuzione continua di livelli ad energia positiva dello stesso potenziale:

$$\Phi_{ev} = S\theta n_s \sum_s \int_0^{\hbar\nu_M - |E_s|} \pi(E_s) G_{s,E} dE,$$

dove n_s rappresenta il numero di « posti » per l'adsorbimento per unità di superficie del solido (nel presente schema questo corrisponderebbe al numero di ioni del reticolo cristallino che generano un campo di potenziale di Morse come quello sopra descritto, nell'ipotesi che i processi che interessano ciascuno di tali ioni avvengano in modo del tutto indipendente l'uno dall'altro); $\pi(E_s)$ è la probabilità che un atomo adsorbito occupi il livello E_s ; assumendo una distribuzione di Boltzmann si ha $\pi(E_s) = (\exp[-E_s/kT]) / (\sum_s \exp[-E_s/kT])$; $G_{s,E} dE$ è la probabilità di transizione per unità di tempo dal livello E_s a un intervallo $(E, E + dE)$ del continuo.

La sommatoria è estesa a tutti i livelli discreti del potenziale di Morse, e il limite superiore dell'intervallo di integrazione risulta ancora determinato dall'ipotesi che la massima quantità di energia che il cristallo può cedere a un atomo del gas è $\hbar\nu_M$.

In Sez. 3 sono state date le formule esplicite per le probabilità di transizione $\Gamma_{E,s}$ e $G_{s,E}$ e pertanto — noti i valori delle costanti che caratterizzano il campo reticolo-gas — il calcolo di Φ_{ads} , Φ_{ev} è ricondotto alle quadrature.

5. — Effetto isotopico nel fenomeno di adsorbimento.

Posta una massa gassosa di densità ν in presenza di una superficie solida S , si ha equilibrio quando il numero di atomi che nell'unità di tempo vengono adsorbiti dalla superficie è eguale al numero di atomi adsorbiti che nell'unità di tempo « evaporano » dalla superficie. Ossia la condizione di equilibrio è espressa dalla relazione $\Phi_{ads} = \Phi_{ev}$.

La condizione di equilibrio fornisce una equazione che ci permette di calcolare la frazione di superficie « coperta » da atomi adsorbiti all'equilibrio. Ricordando le espressioni date in Sez. 4 per Φ_{ads} e Φ_{ev} si ha:

$$S(1-\theta)\nu \int_0^{\hbar\nu_M} \sum_s \frac{\exp[-E/kT] \hbar \Gamma_{E,s}}{(2\pi m_e T)^{\frac{1}{2}}} dE = S\theta n_s \sum_s \int_0^{\hbar\nu_M - |E_s|} \frac{\exp[-E_s/kT]}{\sum_s \exp[-E_s/kT]} G_{s,E} dE$$

e per la relazione tra $G_{s,E}$ e $\Gamma_{E,s}$

$$(1 - \theta)\nu \int_0^{\hbar\nu_M} \sum_s \frac{\exp[-E/kT] \hbar \Gamma_{E,s}}{(2\pi m k T)^{\frac{1}{2}}} dE = \theta n_s \sum_s \int_0^{\hbar\nu_M - |E_s|} \frac{\exp[-E/kT] \Gamma_{E,s}}{\sum_s \exp[-E_s/kT]} dE.$$

Tenendo presenti le prescrizioni indicate in Sez. 4 per l'integrazione che compare nel primo membro, si riconosce facilmente che detto integrale può scriversi in modo seguente:

$$\sum_s \int_0^{\hbar\nu_M - |E_s|} \dots dE,$$

ossia in modo formalmente identico alla doppia somma del secondo membro. Ne consegue che la condizione di equilibrio può essere espressa dall'equazione

$$(3) \quad \frac{(1 - \theta)\nu \hbar}{(2\pi m k T)^{\frac{1}{2}}} = \sum_s \frac{\theta n_s}{\exp[-E_s/kT]}.$$

Questa equazione si poteva ottenere direttamente, ammettendo l'esistenza di un bilancio dettagliato tra un livello di adsorbimento E , e l'intervallo $(E, E + dE)$ del continuo.

Se la massa gassosa a contatto con la superficie S contiene due specie isotopiche di massa m_1 ed m_2 , per ciascuna di esse si potrà scrivere una condizione di equilibrio analoga alla (3).

Precisamente, dette θ_1 , θ_2 le frazioni di superficie coperte da atomi delle due specie e ν_1 , ν_2 le rispettiva densità, si avranno le equazioni:

$$(4) \quad \begin{cases} \frac{(1 - \theta_1 - \theta_2)\nu_1 \hbar}{(2\pi m_1 k T)^{\frac{1}{2}}} = \sum_s \frac{\theta_1 n_s}{\exp[-E_s^{(1)}/kT]} \\ \frac{(1 - \theta_2 - \theta_1)\nu_2 \hbar}{(2\pi m_2 k T)^{\frac{1}{2}}} = \sum_s \frac{\theta_2 n_s}{\exp[-E_s^{(2)}/kT]} \end{cases},$$

dove $1 - \theta_1 - \theta_2$ è la frazione di superficie libera da atomi dell'una o dell'altra specie.

Definiamo ora l'arricchimento isotopico δ sulla superficie S

$$\delta = \frac{\theta_1/\theta_2}{\nu_1/\nu_2}$$

(l'indice 1 contrassegna l'isotopo di massa minore).

Dalle equazioni (4) si ha immediatamente

$$(5) \quad \delta = \sqrt{\frac{m_2}{m_1}} \frac{\sum_s \exp[-E_s^{(1)}/kT]}{\sum_s \exp[-E_s^{(2)}/kT]}.$$

Noti i livelli energetici $E_s^{(i)}$ per le due specie isotopiche ($i=1,2$) l'andamento di δ in funzione della temperatura T risulta determinato. Se i livelli energetici $E_s^{(i)}$ vengono classificati in ordine di profondità decrescente, ossia di valore relativo crescente

$$E_0^{(i)} < E_1^{(i)} < \dots < E_{\max}^{(i)}$$

e se i livelli relativi alla specie isotopica (1) sono più alti (meno profondi) di quelli dello stesso ordine relativi alla specie isotopica (2), l'andamento della funzione $\delta = \delta(T)$ è del tipo di quello indicato nel grafico di Fig. 1, calcolato per il caso particolare di adsorbimento di elio (^3He e ^4He) su fluoruro di litio.

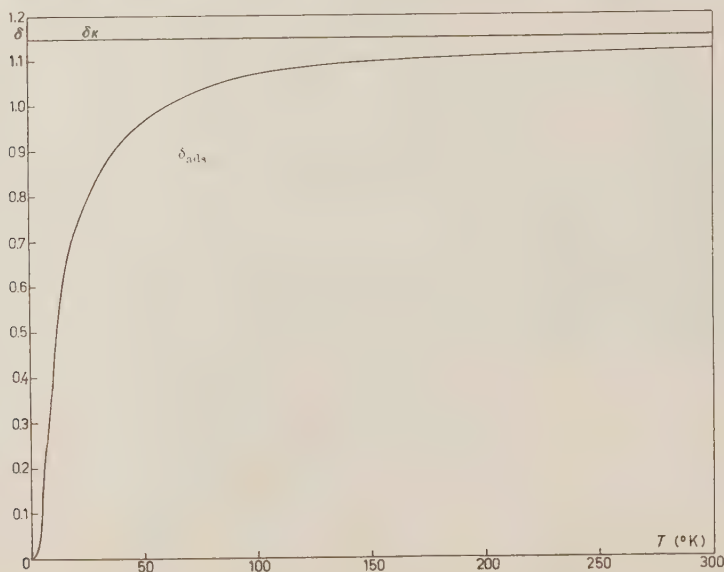


Fig. 1. — Dipendenza dalla temperatura dell'arricchimento isotopico della fase adsorbita (miscuglio ^3He e ^4He).

Benchè a temperatura elevata lo schema da noi adottato non sia il più adatto ad una descrizione corretta dei fenomeni (già a temperatura ambiente il tempo medio trascorso da un atomo del gas sul livello fondamentale prima di essere eccitato è dell'ordine del periodo di vibrazione dell'atomo in quel livello) è possibile interpretare le principali caratteristiche della curva $\delta = \delta(T)$.

Si tenga presente l'andamento di θ in funzione della temperatura T per una singola specie isotopica: dalla equazione (3) si ha facilmente

$$\lim_{T \rightarrow 0} \theta = 1,$$

$$\lim_{T \rightarrow \infty} \theta = 0.$$

Alle alte temperature un atomo trascorre un tempo estremamente piccolo in uno stato di adsorbimento e l'arricchimento isotopico è determinato essenzialmente dalle velocità di incidenza degli atomi del gas, ossia si riduce all'arricchimento isotopico nel puro fenomeno di diffusione.

A temperature vicine allo zero, sia l'una che l'altra specie isotopica tenderebbero separatamente a ricoprire completamente la superficie del cristallo, ma la specie isotopica più pesante tende a farlo più rapidamente al diminuire della temperatura: infatti le quantità $1 - \theta$ sono infinitesimi per $T \rightarrow 0$ di ordine superiore per la specie isotopica che ha i livelli di adsorbimento più profondi.

6. - Applicazioni numeriche.

Abbiamo applicato la teoria svolta al caso di adsorbimento di un miscuglio di isotopi ^3He e ^4He su fluoruro di litio.

In questo caso infatti sono disponibili dati numerici abbastanza precisi per le costanti che caratterizzano il potenziale ione del reticolo-atomo del gas. Da esperienze di diffrazione di atomi di He da parte di un cristallo di LiF si è potuto ricavare la « profondità » di due livelli energetici di detto potenziale, e da questi risalire ai valori delle costanti D , α ⁽²⁾. Si è assunto che tali valori siano gli stessi per l'uno e per l'altro degli isotopi in questione:

$$D = 175 \text{ cal (grammoatomo)}^{-1},$$

$$\alpha = 1.10 \cdot 10^8 \text{ cm}^{-1}.$$

Ne derivano i seguenti valori di $d = \sqrt{2mD}/\alpha\hbar$

$$d^{(1)} \sim 3 \quad ({}^3\text{He}),$$

$$d^{(2)} \sim 3.5 \quad ({}^4\text{He}).$$

I livelli energetici di adsorbimento risultano in conseguenza tre per l'una e

(2) J. E. LENNARD-JONES e A. F. DEVONSHIRE: *Proc. Roy. Soc.*, A **156**, 242 (1936).

per l'altra specie isotopica:

$$E_0^{(1)} \sim -73.32 \cdot 10^{-16} \text{ erg} \quad E_0^{(2)} \sim -88.8 \cdot 10^{-16} \text{ erg}$$

$$E_1^{(1)} \sim -30.19 \cdot 10^{-16} \text{ erg} \quad E_1^{(2)} \sim -39.5 \cdot 10^{-16} \text{ erg}$$

$$E_2^{(1)} \sim -3.26 \cdot 10^{-16} \text{ erg} \quad E_2^{(2)} \sim -9.9 \cdot 10^{-16} \text{ erg}$$

Con questi valori abbiamo calcolato la curva $\delta_{\text{ads}}(T)$ data dalla (5), che dà l'arricchimento isotopico in funzione della temperatura T , riportata in Fig. 1. Come si vede lo scostamento dal valore $\delta_{\text{max}} = \sqrt{m_2/m_1}$ è sensibile solo a temperature molto basse.

Un dato che per il fluoruro di litio è alquanto incerto è ν_M , ossia la frequenza massima di vibrazione del reticolo nella teoria di Debye: fortunatamente fin tanto che interessa il puro arricchimento isotopico esso non compare nei calcoli.

Esso interviene nel calcolo dei flussi totali di adsorbimento e di evaporazione relativi ad una superficie S (si veda la formula (2)): noi abbiamo calcolato le curve $\Phi_{\text{ads}}(T)$, $\Phi_{\text{ev}}(T)$ per le due specie isotopiche assumendo un valore di ν_M quale si deduce da $h\nu_M = k\Theta$ con $\Theta = 717^\circ\text{K}$ per il fluoruro di litio.

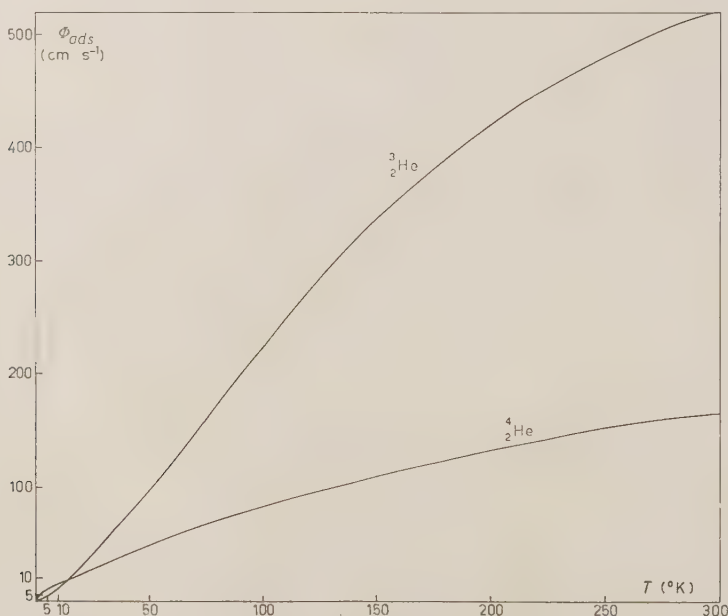


Fig. 2. — Variazione con la temperatura del flusso adsorbico per i due isotopi dell'elio.

Per quanto riguarda le velocità di propagazione c_1 , c_2 del suono nel reticolo ci siamo valse della relazione che le lega a v_M nella teoria di Debye:

$$\frac{4\pi a^3}{9} \left(\frac{1}{c_1^3} + \frac{2}{c_2^3} \right) = \frac{1}{v_M^3}.$$

Le integrazioni sono state effettuate numericamente, le quantità $I'(d \pm \frac{1}{2} \cdot i\mu)^2$ essendo di facile dominio nel nostro caso particolare, che comporta valori approssimativamente interi o semiinteri di d .

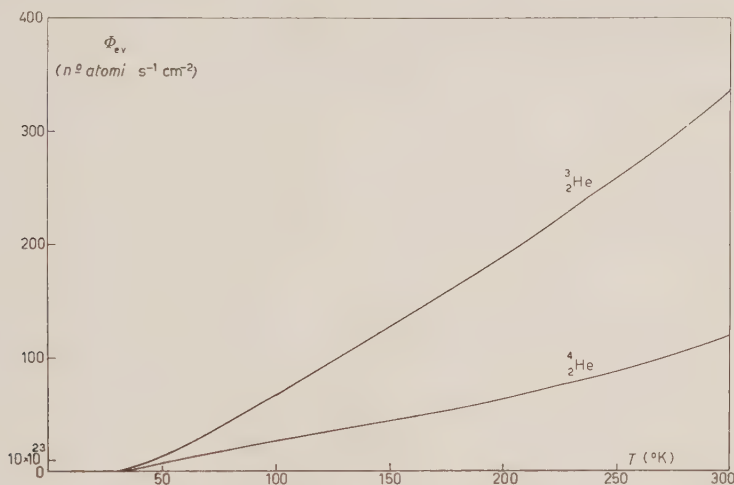


Fig. 3. — Variazione con la temperatura del flusso di evaporazione per i due isotopi dell'elio.

Il flusso di adsorbimento è riferito ad una superficie unitaria, a densità unitaria della massa gassosa sovrastante e ad una condizione in cui la superficie sia completamente libera da atomi adsorbiti ($\theta = 0$); il flusso di evaporazione è riferito ad una superficie unitaria e ad una condizione in cui la superficie sia completamente ricoperta da atomi del gas ($\theta = 1$).

Le curve ottenute sono riportate in Fig. 2 e in Fig. 3: come si vede Φ_{ads} e Φ_{ev} crescono ambedue al crescere della temperatura, ma l'influenza della temperatura è assai più marcata su Φ_{ev} che su Φ_{ads} .

7. — Conclusioni.

Dati sperimentali che permettano una verifica diretta dell'effetto isotopico calcolato non si trovano nella letteratura. Effetti isotopici sono stati consta-

tati nella formazione di strati di ossido di metallo nell'adsorbimento di ossigeno su tungsteno ⁽³⁾ o anche nell'adsorbimento di ³He e ⁴He su carbone di legna ⁽⁴⁾.

Il meccanismo con cui questi fenomeni di adsorbimento si verificano non è però quello dell'adsorbimento fisico unimolecolare da noi considerato (e che è descritto dalla teoria di Lennard-Jones) e pertanto non è possibile utilizzare i dati sperimentali relativi per un confronto con la teoria sviluppata in questo lavoro.

I risultati da noi stabiliti possono essere utilizzati per l'interpretazione dei dati sperimentali relativi alla separazione isotopica nei sistemi porosi.

Una verifica diretta dei nostri risultati teorici potrebbe però presentare un certo interesse.

* * *

Ringraziamo il dott. CODURI per la sua collaborazione nell'eseguire i calcoli numerici.

⁽³⁾ A. MALCOLM DALE and G. A. LANE: *Journ. Chem. Phys.*, **22**, 949 (1954).

⁽⁴⁾ C. I. HOFFMANN, F. I. EDESKUTY e C. H. HAMMEL: *Journ. Chem. Phys.*, **24**, 124 (1956).

SUMMARY (*)

The isotopic effects which appear in the adsorption process of a gaseous mixture on a solid surface are studied basing on the theory of Lennard-Jones on the interaction of atoms and molecules with solid surfaces. We report the general features of this theory adapting them to the examined problem. The formulae deduced for a mixture of two generic isotopic species have been applied to the special case of the adsorption of helium (³He₂ and ⁴He₂) on lithium fluoride. We have found that on the adsorbent surface the isotopic enrichment δ_{ads} in stationary conditions is always inferior to the enrichment δ_k of Knudsen, which is characteristic of the diffusion phenomenon, approaching it with rising temperature.

(*) Editor's translation.

LETTERE ALLA REDAZIONE

(La responsabilità scientifica degli scritti inseriti in questa rubrica è completamente lasciata dalla Direzione del periodico ai singoli autori)

Application of the Klausen Micrometer to the Measurements of Multiple Scattering of Elementary Particles in Nuclear Emulsions.

G. ALVIAL and S. STANTIC

*Centro de Investigación de Física Nuclear y Radiación Cósmica
Universidad de Chile - Santiago*

(ricevuto il 10 Settembre 1956) (*)

1. -- The application of the Klausen micrometer to the measurements in nuclear emulsions was first suggested and carried out by BONETTI, DILWORTH, LADU and OCCHIALINI⁽¹⁾. Later on it was used in ionization measurements^(2,3).

In order to know the possible advantages supplied by the use of the Klausen micrometer over the filar micrometer in the measurements of multiple scattering of the elementary particles in nuclear emulsions, the authors of the present work performed a series of measurements the results of which are here reported.

For this purpose π -mesons of the same plate were taken and measured at the end of their range, both with a

Klausen micrometer and a filar micrometer of Koristka manufacture fitting the microscope MS2 of the same factory.

2. -- First, the final part of a track of a π -meson (this segment was about 500 μ m in length) was repeatedly measured 40 times, being always set parallel to the X axis displacement in the same fixed position. The set of variable cells of the microscope MS2 was used, which on being corrected by a small factor turned out to be very close to the cell scheme for π -mesons presented by FAY, GOTTSTEIN and HAIN⁽⁴⁾.

The determination of the « y » coordinates of the track was always performed by placing the index of the corresponding micrometer on the centre of gravity of a number of grains.

The mean value of the second differences for the 40 measurements is as follows:

Klausen Micrometer: $(0.446 \pm 0.004) \mu\text{m}$.

Filar Micrometer: $(0.443 \pm 0.004) \mu\text{m}$.

(*) La pubblicazione di questa lettera avviene con ritardo per alcuni scambi di vedute intercorsi nel frattempo fra gli Autori e la Redazione del Giornale (N.d.D.).

(¹) A. BONETTI, C. DILWORTH, M. LADU and G. OCCHIALINI: *Rend. Acc. Naz. Lincei*, s. VIII, **12**, fasc. 6, Dicembre 1954.

(²) G. ALVIAL, A. BONETTI, C. DILWORTH, M. LADU, J. MORGAN and G. OCCHIALINI: *Suppl. Nuovo Cimento* **4**, 244 (1955).

(³) M. LADU, R. LEVI SETTI, L. SCARSI and G. TOMASINI: *Suppl. Nuovo Cimento*, **4**, 621 (1956).

(⁴) H. FAY, K. GOTTSTEIN and K. HAIN: *Suppl. Nuovo Cimento*, **11**, 234 (1954).

The above results show that there is no differences between the measurements performed either with one or other type of micrometer upon a common track segment always set in a fixed position.

Subsequently, another π -meson track was successively measured ten times at the end of its range with each micrometer. But now the track was not in a fixed position: it was turned 6 times on each measurement so as to orientate it properly. The measurements were carried on the last 263 μm of the track.

The results obtained for the mean value of the sagitta of scattering are these:

Klausen Micrometer: $(0.425 \pm 0.004) \mu\text{m}$.

Filar Micrometer: $(0.432 \pm 0.005) \mu\text{m}$.

Between these figures no significant difference can be observed again.

Finally, we have measured with the Klausen micrometer 15 tracks of different π -mesons belonging to the same plate, strictly considering the scheme of variable cells above mentioned (-). The characteristics of this micrometer which permits to measure the « y » coordinates and at the same time to adjust to the displacements corresponding to the lengths of the variable cells were used for this purpose. The selected tracks presented a dip smaller than 10° and the segments on which the measurements were performed varied from 1244 to 10337 μm . The mean range length was of 3435 μm .

The fine adjustment was performed within an interval of 5 μm due to the fact that the microscope grants minimum controlled displacements of 10 μm in the X -axis direction.

The result obtained is:

$$\overline{D_{sc}} = 0.429 \pm 0.015 \mu\text{m}.$$

The sagitta of scattering has been calculated by using the method of Bristol for eliminating the noise.

Taking the expression c/\sqrt{N} as the

statistical error, the value of c experimentally determined is 1.26.

According to the preceding facts we may conclude:

a) the precision of the Klausen micrometer is the same as that of the filar micrometer in multiple scattering measurements:

b) the Klausen micrometer allows to perform the measurements quicker than the filar micrometer, as long as the sets of variable or fixed cells of the microscope are used: we have obtained the value 1.7 for the ratio of the time necessary to perform a given measurement with a conventional micrometer the corresponding one to and make the same measurement with the Klausen micrometer;

c) in case that it is not possible to adjust the microscope to the corresponding scheme of cells it is possible to adjust to them the Klausen micrometer itself, in an interval limited by the optical curvature of the field, and

d) working with a lamina of right thickness it is possible to exclude automatically those measurements yielding, for the ratios between the first differences and their corresponding lengths of cells, superior values to a preestablished limit, as recommended by DILWORTH, GOLDSACK and HIRSCHBERG^(*). This limit is $\delta_1/t \leq 1/5$, where δ_1 is the first difference and t is the cell length.

* * *

Our thanks to the Rector de la Universidad de Chile, Profesor JUAN GOMEZ MILLAS, for his interest and financial support to our work; finally we give thanks to Mr. T. JARUFE for his valuable contribution in measurements and calculations of this work.

(*) C. DILWORTH, S. J. GOLDSACK and L. HIRSCHBERG: *Nuovo Cimento*, **11**, 113 (1954).

On the Phase-Shift Analysis of High-Energy p-p Scattering.

R. J. N. PHILLIPS

Atomic Energy Research Establishment - Harwell, Berks, England.

(ricevuto il 9 Gennaio 1957)

In the region of 140 MeV, where p-p polarization (^{1,2}) reveals large F -wave effects, it is hoped that S , P , D and F waves will be sufficient to describe the scattering. However, single- and double-scattering experiments do not yield enough information for a full analysis in terms of all eight phase shifts, together with the 3P_2 - 3F_2 coupling parameter. With present experimental errors, the polarization data can be fitted by a curve.

$$(1) \quad P(\theta)\sigma(\theta) = \sin \theta \cos \theta (a + b \cos^2 \theta),$$

and thus provide two independent pieces of information. The unpolarized cross-section (^{2,5}) yields essentially four more, (which may be taken as its values at 90° and at 40° c.m., with the position and height of the minimum at small angles). To extract three more parameters from these two quantities, one would

need experimental errors impossibly small with present techniques. An appeal to charge-independence and the use of n-p scattering data prove to be of little help; although seven (or, optimistically, eight) more independent pieces of information (*) are provided, a further seven unknown quantities enter the analysis.

With these inadequate data, the most natural step is to consider only the 3F_2 wave, which one might expect to be favoured through a tensor coupling to 3P_2 , but to ignore the coupling parameter itself. (This has been done by FELDMAN and OHNUMA (⁶) at the nominal energy 150 MeV). Only six unknowns remain, and the problem is determinate.

However, certain features of the phase-shift analyses at 310 MeV (^{7,8}) (where triple-scattering experiments have been carried out) cast doubt on this procedure, though they are not conclu-

(¹) J. M. DICKSON and D. C. SALTER: *Nature*, **173**, 946 (1954).

(²) A. E. TAYLOR: *Report at 6th Rochester Conference on High-Energy Nuclear Physics*, 1956.

(³) J. M. CASSELS, T. G. PICKAVANCE and G. H. STAFFORD: *Proc. Roy. Soc., A* **214**, 262 (1952). These results are taken normalized to 3.7 mb/sr at 90° c.m. See refs. (^{4,5}).

(⁴) J. M. CASSELS: *Proc. Phys. Soc., A* **69**, 495 (1956).

(⁵) A. E. TAYLOR and E. WOOD: *Proc. Phys. Soc., A* **69**, 645 (1956).

(*) The present n-p data near 140 MeV are worth less than this, but could be improved.

(⁶) S. OHNUMA and D. FELDMAN: *Phys. Rev.*, **102**, 1641 (1956).

(⁷) H. P. STAPP: California thesis UCRL 3098 (1955).

(⁸) T. YPSILANTIS: *Report at 6th Rochester Conference*, 1956. (Later amended. There were numerical errors in the original report).

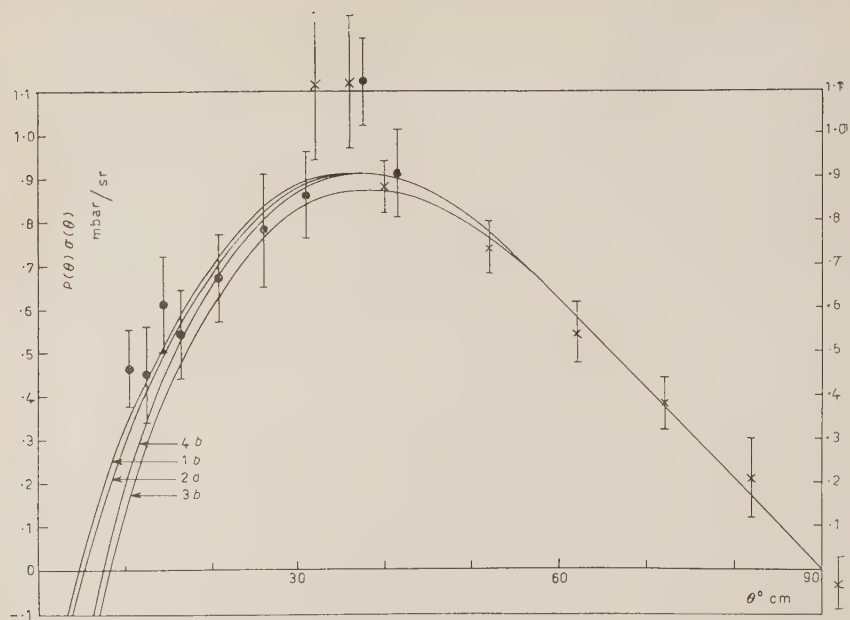


Fig. 1.

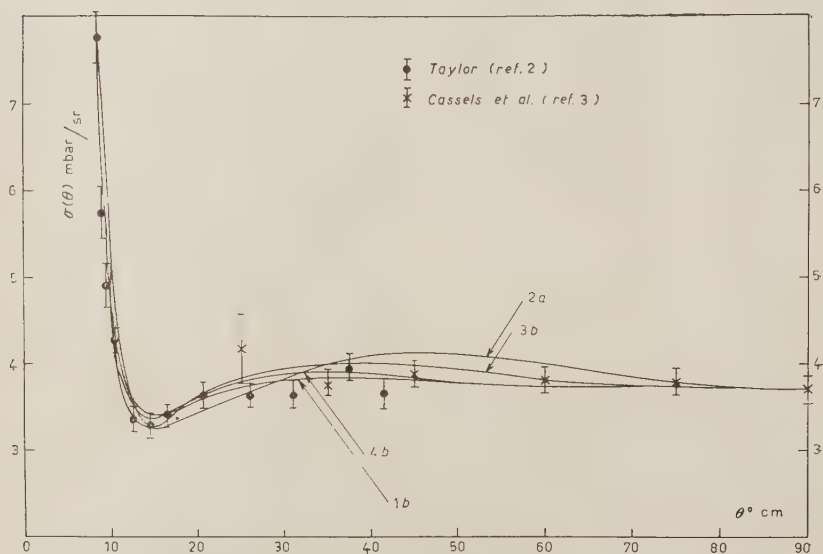


Fig. 2.

sive objections. It is found that 3P_2 - 3F_2 coupling is small, leaving small reason to prefer 3F_2 . Again, 3F_2 is not the dominant F -wave in any of the «best fits». Lastly, the F -phase shifts are smaller than in typical fits of Feldman and Ohnuma.

« G » solution; (his other solutions in this range, « E » and « F », give the wrong shape for $\sigma(\theta)$ at small angles). Using 3F_4 , however, three different fits were found. Fit 1 corresponds most nearly to Fit 4, but with significant differences such as the inversion of the

TABLE I.

Fit no.	Phase-shifts in degrees						
	δ_0	δ_2	δ_1^0	δ_1^1	δ_1^2	δ_3^2	δ_3^4
1a	-21	3	-31	12	8	—	1.0
1b	-28	2	-26	8	10	—	1.5
2a	32	3	-28	-8	8	—	1.2
2b	29	2	-38	0	6	—	0.9
3a	20	-4	-29	15	8	—	1.0
3b	18	-2	-36	14	6	—	0.8
4a	-25	6	-20	14	8	-5.2	—
4b	-19	8	-18	16	7	-6	—

The notation used is δ_L^I for triplet, δ_L for singlet phase-shifts.

There remains the hope that the particular form of F -wave interaction assumed, to explain specifically F -wave effects, may make little difference to the other partial waves. This hope can be exploded by considering the examples below.

A phase-shift analysis has been made of the latest 140 MeV p-p scattering data (*) using either the 3F_2 wave without coupling, or the 3F_4 wave. Small discrete regions of fit were found, typified by the sets of phase shifts in Table I. Unlike that of Feldman and Ohnuma, this analysis did not cover all possible values of the phase shifts, but only those consistent with $6^\circ \leq \delta_1^2 \leq 12^\circ$, and $\delta_1^0 < 0$. Only one 3F_2 solution was found (Fit 4), corresponding to Feldman's 3P levels. Fit 3 is similar to Feldman's « E » and « F » cases. Fit 2, however, is unlike any solution that can be obtained using 3F_2 alone.

The analysis was carried out with a desk computer. The fits to data are all roughly the same: examples are shown in the diagrams. The curves shown include relativistic and magnetic moment corrections of the types given by GARREN⁽⁹⁾ and justified by BREIT⁽¹⁰⁾. The differences between the fits to $\sigma(\theta)$ are partly due to giving the phase shifts in round numbers. The fits to $P(\theta)\sigma(\theta)$ differ more widely at small angles than is strictly necessary, through being made identical at large angles.

These phase shift fits are offered to show the large effect of particular assumptions about the form of the 3F interaction on the form of solution that can be found. There is clearly a need for triple-scattering and/or correlation experiments to be performed in this energy region, in spite of experimental difficulties, so that a reliable analysis of the nucleon-nucleon interaction may be made.

(*) Not available at the time of Feldman and Ohnuma's work.

(9) A. GARREN: USAEC report NYO-7102 (1955) and *Phys. Rev.*, **101**, 419 (1956).

(10) G. BREIT: *Phys. Rev.*, **99**, 1581 (1955).

Angular Distribution of Photoprotons from Oxygen.

C. MILONE and R. RICAMO

Istituto di Fisica dell'Università - Catania
Centro Siciliano di Fisica Nucleare - Catania

(ricevuto il 6 Febbraio 1957)

The angular distribution of photoprotons from oxygen observed by SPICER (1), with a bremsstrahlung spectrum of maximum energy 18.7 MeV, was of the form $(a+b \cos^2 \theta)$ indicating that the reaction proceeded mainly through $E2$ or $M1$ photon absorption. This distribution refers to the little resonance peaked around $E_\gamma=15$ MeV. To prove that the $0(\gamma, p)$ reaction in the region of the giant resonance ($E_\gamma=25$ MeV) is due to $E1$ photon absorption (2) we measured the angular distribution of photoprotons with the bremsstrahlung beam of 30 MeV maximum energy of the Brown Boveri betatron of the University of Turin.

Normal Ilford C2 nuclear plates as well as water loaded plates have been exposed parallelly to the γ -rays; the dose of irradiation was 5 roentgens at the plate position. The water content was 1 ± 0.1 g for nuclear plate of 1 in. \times 3 in. \times 200 μ m. The distance of the plates from the betatron target was 2 m. After processing, the shrinkage factor was 8 ± 1 in water loaded plates and 2.5 in dry plates.

The results refer to proton tracks beginning and finishing in emulsion and having a dip angle $\beta < 30^\circ$ in the unprocessed plates (as well dry as loaded).

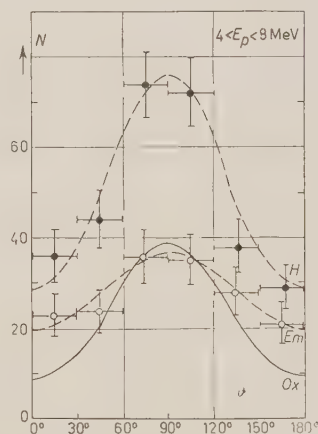


Fig. 1. - Angular distribution of photoprotons in water loaded emulsion = H , dry emulsion = Em and Oxygen $Ox = H - Em$. N = number of observed photoprotons in the energy interval 4 to 8 MeV, for constant solid angle.

As most of photoprotons with energy $E_p > 8$ MeV escaped from the emulsion, only protons with $E_p < 8$ MeV have

(1) B. M. SPICER: *Phys. Rev.*, **99**, 33 (1955).(2) C. MILONE, R. RICAMO and R. RINZIVILLO: *Nuovo Cimento*, **5**, 532 (1957).

been included. In addition, protons with $E_p < 4$ MeV have been disregarded in order to select protons due mainly to the giant resonance in $O(\gamma, p)$ process. The proton energy in water loaded emulsions has been calculated from the range, taking account of the results of WÄFFLER and YOUNIS ⁽³⁾ and of HUGHES and SINCLAIR ⁽⁴⁾.

The angular distribution of photoprotons with energy $4 \text{ MeV} < E_p \leq 8 \text{ MeV}$ found in 0.6 cm^2 of water loaded emulsion (H) and dry emulsion (Em) is shown in Fig. 1. N is the number of photoprotons for a constant solid angle; ϑ is

the angle between the γ -rays and the projection of proton track in the plane of the plate. Experimental points can be fitted with curves $(a+b \sin^2 \vartheta)$. The $Ox=H-Em$ curve is the contribution of the oxygen. A maximum around 90° is evident.

As this work was in progress we learned of the results of COHEN and cow. ⁽⁵⁾. The angular distribution of the photoprotons, obtained by them, by irradiation of an oxygen gas target with 25 MeV bremsstrahlung exhibits in the interval 30° to 150° a maximum around 90° for protons with $E_p > 6 \text{ MeV}$ in good agreement with our results.

⁽³⁾ H. WÄFFLER and S. YOUNIS: *Helv. Phys. Acta*, **24**, 483 (1951).

⁽⁴⁾ I. S. HUGHES and D. SINCLAIR: *Proc. Phys. Soc.*, **A 69**, 125 (1956).

⁽⁵⁾ L. COHEN, A. K. MANN, B. J. POTTAN., K. REEBEL, W. E. STEPHENS and E. J. WINHOLD: *Phys. Rev.*, **104**, 108 (1956).

Associated Production of Strange Particles (*).

J. J. SAKURAI

Laboratory of Nuclear Studies, Cornell University - Ithaca, New York

(ricevuto il 19 Febbraio 1957)

Experiments by BUDDE, CHRETIEN, LEITNER, SAMIOS, SCHWARTZ, and STEINBERGER, have revealed the following points about the associated production of strange particles by π -mesons on protons ⁽¹⁾.

(1) For the $K^0\Lambda^0$ (or $K^0\Sigma^0$) production the angular distribution of the K^0 is peaked so strongly forward that it is not possible to analyze the data under the assumption that only s - and p -waves are involved in this process.

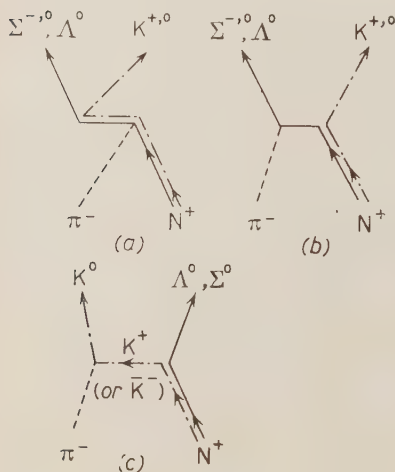


Fig. 1. — Lowest-order diagrams for associated production. We indicate the «direction» of the isospin as well as that of the baryon.

(2) For the $K^+\Sigma^-$ production the angular distribution of the K^+ is preferentially backward. Similar results have been obtained by BROWN, GLASER and PERL ⁽²⁾.

The purpose of this note is to give a simple field-theoretical explanation of the above results, under the assumptions that perturbation calculations are valid and that the spins of the K and the Λ (Σ) are 0 and $\frac{1}{2}$ respectively.

It was pointed out by several authors that the above difference in angular distributions may arise if the K -meson can emit or absorb pions ⁽³⁾. Thus, in addition to the usual diagrams such as 1(a) and 1(b), we must consider 1(c). Clearly the latter kind of diagram is absent for the $K^+\Sigma^-$ production.

In perturbation calculation it is im-

(*) Supported by the joint program of the Office of Naval Research and the Atomic Energy Commission.

⁽¹⁾ R. BUDDE, M. CHRETIEN, J. LEITNER, N. P. SAMIOS, M. SCHWARTZ and J. STEINBERGER: *Phys. Rev.*, **103**, 1827 (1956).

⁽²⁾ J. L. BROWN, D. A. GLASER and M. L. PERL: *Annual Meeting of the American Physical Society* (1957).

⁽³⁾ M. GOLDBABER: *Phys. Rev.*, **101**, 433 (1956); S. BARSHAT: *Phys. Rev.*, **104**, 853 (1956); J. SCHWINGER: *Phys. Rev.*, **104**, 1164 (1956).

portant to note that the angular distribution is sensitive to the type of coupling we assume. For instance, if the K- Λ -N interaction involves γ_5 , the forward amplitude for 1(c) will be greatly diminished. We have reached good agreement with the observed angular distribution under the assumption that the Λ^0 -K 0 production takes place predominantly through 1(c) and that the interactions at the two vertices are given respectively by

$$\varphi^{\dagger(K)} C_P \varphi^{(K)} \varphi^{(\pi)} \quad \text{and} \quad \varphi^{\dagger(K)} \bar{\psi}^{(\Lambda)} \psi^{(N)},$$

where C_P is the parity conjugation operator of Lee and Yang (⁴). The angular dependence can be easily computed by the Feynman-Dyson technique. In addition to the virtual dissociation of N $^-$ into K $^-$ and Λ^0 considered by SCHWINGER we take into account the effect of the virtual pair production of K 0 and K $^-$ by π^- . In terms of Feynman graphs K $^{+,0}$ mesons propagating backward in time are to be regarded as K $^{-,0}$ -mesons propagating forward in time

$$\left(\frac{d\sigma}{d\Omega} \right)_{\text{C.M.}} \propto \left\{ 1 + \frac{(E_N(\mathbf{p})E_\Lambda(\mathbf{p}') - pp' \cos \theta)}{M_N M_\Lambda} \right\} \{ 2\omega_K(\mathbf{p})\omega_\pi(\mathbf{p}') - \mu_\pi^2 - 2pp' \cos \theta \}^{-2}$$

where \mathbf{p} and \mathbf{p}' stand respectively for the momenta of the incoming mesons and of the outgoing K-mesons in the center of mass system. (Other energy dependences which do not depend on θ are omitted.) We have plotted this angular distribution in Fig. 2 for $p=0.714$ GeV/c. The experimental angular distribution by STEINBERGER *et al.* and SHUTT *et al.* (⁵) at this energy is shown for comparison. The main feature of the curve will not be altered if we consider Σ^0 instead of Λ^0 as the outgoing hyperon.

We have also examined the angular distribution for the K $^+$ - Σ production under various assumptions. The desired backward distribution can be obtained if we assume that the predominant process is 1(b) rather than 1(a) where the π - Σ - Λ or π - Σ - Σ coupling may or may not involve γ_5 .

In this note we have tacitly assumed the validity of perturbation theory. The fact that the perturbation calculations are not in contradiction with various

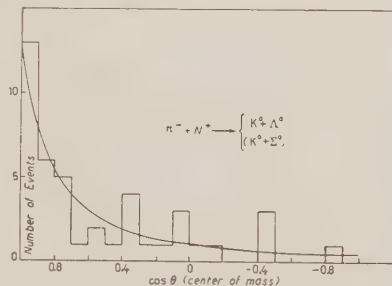


Fig. 2. — The solid curve represents the theoretical angular distribution computed from 1(c) at $p=0.714$ GeV/c (in cm) under the assumption that the K- Λ -N interaction is direct and does not involve γ_5 . Experimental histograms based on 43 events observed by STEINBERGER *et al.* and SHUTT *et al.* are shown for comparison.

(⁴) T. D. LEE and C. N. YANG: *Phys. Rev.*, **102**, 290 (1956).

(⁵) R. BUDDE *et al.*: loc. cit.; W. B. FOWLER, R. P. SHUTT, A. M. THORNDIKE and M. L. WHITTEMORE: *Phys. Rev.*, **98**, 121 (1954).

experimental phenomena may indicate that the excited isobaric states which play such an important role in the pion-nucleon interaction are relatively unimportant in those strange-particle interactions ⁽⁶⁾.

* * *

The author wishes to acknowledge his indebtedness to Professor S. HAYAKAWA, Dr. T. KINOSHITA, and Dr. A. Sirlin for helpful discussions.

⁽⁶⁾ As first pointed out by K. BRUECKNER and A. PAIS, the largeness of the K-N cross section in comparison with the \bar{K} -N cross section can also be explained from perturbation theory, if one simply considers energy denominators consistent with the conservation of strangeness. See footnote ⁽⁴⁾ of FOURNET and WIDGOTT: *Phys. Rev.*, **102**, 929 (1956).

D Wave Effects in Positive Pion-Proton Scattering.

E. CLEMENTEL and C. VILLI (*)

Istituti di Fisica dell'Università di Padova e di Trieste ()**Istituto Nazionale di Fisica Nucleare - Sezione di Padova**(*) Istituto Nazionale di Fisica Nucleare - Gruppo di Trieste*

(ricevuto il 22 Febbraio 1957)

The data of A. I. MUKHIN *et al.* (1) have been used to investigate the interactions of positive pions with protons at 270 and 307 MeV. The results of this analysis are somewhat different from those of the Russian Authors, because among the four causal solutions, existing when D waves are considered, there are two, and not only one, which involve the Fermi set of P phase shifts. Furthermore, the linearity of α_3 versus the relative momentum η has not been found consistent with the best fit of the 307 MeV data.

These results have been obtained using the analytical approach outlined in a previous paper (2). The difference $\Delta\beta = \beta_{33} - \beta_{35}$ between the two D phase shifts is assumed as independent variable. From Eqs. (I-33) and (I-29) we determine the following parameters

$$(1a) \quad u'(\Delta\beta) = 2[3 - A_0 - (A_2/3) - (A_4/9) - \cos 2\Delta\beta],$$

$$(1b) \quad v'(\Delta\beta) = V_{\pm}[13 + 12 \cos 2\Delta\beta - (U - u')^2]^{\frac{1}{2}},$$

where the A_n 's are the least squares coefficients of the angular distribution expanded according to Eq. (I-25), and U , V are given by Eqs. (I-28a, b) respectively (3). The kinematical meaning of u' and v' (coordinates of the auxiliary track in the (U, V) -plane) is clearly exhibited by the fact that when $\beta_{33} = \beta_{35} = 0$, Eqs. (1a, b) identify with Eqs. (I-9a, b) ($u' = U - 5 = u_3$; $v' = V = v_3$). The difference $\Delta\alpha = \alpha_{31} - \alpha_{33}$, following from the definition of u' and v' in terms of phase shifts (I - Sect. 4), is

(1) A. I. MUKHIN, E. B. OZEROV, B. M. PONTECORVO, E. L. GRIGORIEV and N. A. MITIN: *Proceedings of CERN Symposium* (Geneva, 1956), vol. II, p. 204.

(2) E. CLEMENTEL and C. VILLI: *Suppl. Nuovo Cimento*, **3**, 474 (1956). This paper will be quoted as I.

(3) Since we are dealing with the scattering of positive pions only, we drop the suffix + in the notation adopted in Eq. (I-28a, b; 29; 33). In the term on the right of Eq. (I-28b) a factor 2 is missing.

given by

$$(2) \quad \cos 2\Delta\alpha = \frac{1}{4}[(u' - \cos 2\alpha_3)^2 + (v' - \sin 2\alpha_3)^2 - 5].$$

Then, from Eqs. (2) and (1.34) the S wave phase shift is determined as a function of $|\Delta\beta|$ only, i.e.

$$(3a) \quad \cos(2\alpha_3 - \Phi_0) = \frac{u'^2 + v'^2 - 4(3 - 2A_0 + 2A_4/15)}{2[(3 + 2u' - U)^2 + (2v' - V)^2]^{\frac{1}{2}}},$$

$$(3b) \quad \tan \Phi_0 = (2v' - V)/(3 + 2u' - U).$$

When both D waves are zero, Eqs. (3a, b) reduce to Eqs. (I-12a, b), valid in the S and P wave approximation ⁽⁴⁾.

Since the even angular distribution coefficients [Eqs. (I-26a, c, e)] can be expressed as functions of u' , v' and α_3 only, it follows that they are reproduced by all values of $|\Delta\beta|$, compatible with the conditions that v' be real and $|\cos(2\alpha_3 - \Phi_0)| \leq 1$, and by whatever combination of the Fermi and Yang set of P phase shifts with each one of the two possible sets of D phase shifts, satisfying the ambiguity relation (I-32b). This is not any more true for the odd coefficients A_1 and A_3 [Eqs. (I-26b, d)], because the quantity

$$(4) \quad \text{Re}(\mathbf{b}_1^* \mathbf{b}_2) = 4 \sin \Delta\alpha \sin \Delta\beta \cos [(\alpha_{31} + \alpha_{33}) - (\beta_{33} + \beta_{35})],$$

does indeed depend on the combination of the two P and D sets of phase shifts. Therefore, the fit of $\text{Re}(\mathbf{b}_1^* \mathbf{b}_2)$, derived from any one of the two odd coefficients, is essential in order to find out the possible solutions of Eqs. (I-26) at a given scattering energy.

We shall indicate with $\alpha_{31}^{(-)}$, $\alpha_{33}^{(-)}$ ($\Delta\alpha < 0$) and with $\alpha_{31}^{(+)}$, $\alpha_{33}^{(+)}$ ($\Delta\alpha > 0$) the Fermi respectively the Yang set of P phase shifts. Similarly, we shall indicate with $\beta_{33}^{(-)}$, $\beta_{35}^{(-)}$ ($\Delta\beta < 0$) one of the two sets of D phase shifts and with $\beta_{33}^{(+)}$, $\beta_{35}^{(+)}$ ($\Delta\beta > 0$) the set associated to the former according to Eq. (I-32b). The symbol $[\alpha^{(\pm)}|\beta^{(\pm)}] \equiv [\alpha_3, \alpha_{31}^{(\pm)}, \alpha_{33}^{(\pm)}|\beta_{33}^{(\pm)}, \beta_{35}^{(\pm)}]$ will be used to denote briefly the complete set of five phase shifts.

The phase shifts $\alpha_{3,2j}^l$ for the $(l, j = l \pm \frac{1}{2})$ states ($\alpha_{3,2j}^1 \equiv \alpha_{3,2j}$, $\alpha_{3,2j}^0 \equiv \beta_{3,2j}$) satisfy the following equations ⁽²⁾ ($l = 1, 2$)

$$(5a) \quad (l+1) \cos 2\alpha_{3,2l+1}^l + l \cos 2\alpha_{3,2l-1}^l = C_l,$$

$$(5b) \quad (l+1) \sin 2\alpha_{3,2l+1}^l + l \sin 2\alpha_{3,2l-1}^l = S_l,$$

where

$$(6a) \quad C_l(\Delta\beta) = (l-1)U + (l-2) \cos 2\alpha_3 + (-1)^{l+1}u',$$

$$(6b) \quad S_l(\Delta\beta) = (l-1)V + (l-2) \sin 2\alpha_3 + (-1)^{l+1}v'.$$

⁽⁴⁾ Eq. (I-12a) contains two misprints: the alternative on the sign of the right hand side should be dropped and the sign in front of $4(1 + w_2)$ should be negative.

From Eqs. (5a, b) one has

$$(7a, b) \quad \cos(2\alpha_{3,2l+1}^l - \Phi_l) = \frac{C_l^2 + S_l^2 + 2l + 1}{2(l+1)(C_l^2 + S_l^2)^{\frac{1}{2}}}; \quad \operatorname{tg} \Phi_l = \frac{S_l}{C_l}.$$

From Eqs. (7a, b) we derive $2(\alpha_{3,2l+1}^l)^{(\pm)} = \Phi \pm |2\alpha_{3,2l+1}^l - \Phi|$, and consequently $(\alpha_{3,2l+1}^l)^{(\pm)} = (\alpha_{3,2l+1}^l)^{(\pm)} \pm |\Delta\alpha|$. For $l = 1$, one should add π to $2\alpha_{33}$ in order to preserve the monotonic increase of α_{33} above the resonance energy. The stability of all the sets of phase shifts thus determined can be investigated using an obvious extension of the method suggested in a previous paper (5).

The values of the causal phase shift solutions at 270 and 307 MeV, corresponding to the central values of the least squares coefficients, listed in Table I, are given in Table II.

TABLE I. - Angular distribution coefficients in the expansion

$$k^3\sigma(\theta) = \sum_{n=0}^1 A_n \cos^n \theta \text{ at 270 and 307 MeV } (1).$$

Energy	270 MeV		307 MeV	
Waves	<i>S-P</i>	<i>S-P-D</i>	<i>S-P</i>	<i>S-P-D</i>
A_0	0.594	0.554	0.553	0.460
A_1	0.954	0.835	1.199	1.075
A_2	2.135	2.441	2.167	3.292
A_3	—	0.293	—	0.245
A_4	—	-0.234	—	-1.372
M_0	5.2	3.54	10.56	1.48

The negative value of A_4 fixes a lower limit $\Delta\beta_0$ for the difference $\Delta\beta$; solutions of Eqs. (I-26) exist only for $|\Delta\beta| \geq |\Delta\beta_0|$. At 270 and 307 MeV it is found $|\Delta\beta_0| = 9.3^\circ$ and 11.9° respectively. Because of the sign ambiguity appearing in Eq. (1b) two cases must be considered: (a) $|v'| < |V|$ and (b) $|v'| > |V|$. The solutions $[\alpha^{(-)}|\beta^{(+)}]$, $[\alpha^{(+)}|\beta^{(+)}]$ and $[\alpha^{(+)}|\beta^{(-)}]$ belong to the case (a) at 270 MeV and to the case (b) at 307 MeV; the reverse is true for the solution $[\alpha^{(-)}|\beta^{(-)}]$. The solutions $[\alpha^{(+)}|\beta^{(-)}]$ and $[\alpha^{(+)}|\beta^{(+)}]$ at 270 MeV correspond to the same value $|\Delta\beta| = 9.4^\circ$, whereas at 307 MeV the solutions $[\alpha^{(-)}|\beta^{(-)}]$ and $[\alpha^{(+)}|\beta^{(+)}]$ are both found for $|\Delta\beta| = 25.1^\circ$. The solution $[\alpha^{(-)}|\beta^{(+)}]$ ($\Delta\beta = 10.9^\circ$) at 270 MeV has been found also by A. I. MUKHIN *et al.* (1), using an electronic computer. At 270 MeV α_3 satisfies surprisingly well Orear's linear relation (6) $\alpha_3 = -0.11\eta$, but at 307 MeV the Russian data do not give any evidence that the *S* wave phaseshift is still a linear function of the relative momentum. The value of the quantity $M = \sum_{\theta} [\Delta(\theta)/\epsilon(\theta)]^2$, where $\epsilon(\theta)$ is the experimental error and $\Delta(\theta)$ is the deviation of the calculated from the observed cross-section, evaluated at 307 MeV using the solution $[\alpha^{(-)}|\beta^{(+)}]$ ($\Delta\beta = 24.8^\circ$) co-

(5) I. GABRIELLI, G. IERNETTI, E. CLEMENTEL and C. VILLI: *Suppl. Nuovo Cimento*, **3**, 498 (1956).

(6) J. OREAR: *Phys. Rev.*, **100**, 288 (1956).

incides with the least squares value M_0 (Table I), whereas using the Russian solution it is found $M = 3.84$.

TABLE II. — Causal solutions (in degrees) for positive pion-proton scattering at 270 and 307 MeV.

270 MeV						
Waves	S-P		S-P-D			
Solutions	$[\alpha^{(-)}]$	$[\alpha^{(+)}]$	$[\alpha^{(-)} \beta^{(+)}]$	$[\alpha^{(+)} \beta^{(+)}]$	$[\alpha^{(+)} \beta^{(-)}]$	$[\alpha^{(-)} \beta^{(-)}]$
α_3	- 19.5	- 19.5	- 13.2	- 18.7	- 18.7	- 22.5
α_{31}	- 6.3	291.9	- 4.0	292.6	292.6	- 9.1
α_{33}	128.8	154.9	128.9	155.9	155.9	131.7
β_{33}	—	—	4.3	5.0	- 6.5	- 5.2
β_{35}	—	—	- 6.6	- 4.5	2.9	4.2
307 MeV						
Waves	S-P		S-P-D			
Solutions	$[\alpha^{(-)}]$	$[\alpha^{(+)}]$	$[\alpha^{(-)} \beta^{(+)}]$	$[\alpha^{(+)} \beta^{(+)}]$	$[\alpha^{(+)} \beta^{(-)}]$	$[\alpha^{(-)} \beta^{(-)}]$
α_3	- 23.6	- 23.6	- 9.8	- 31.8	- 21.2	- 31.8
α_{31}	- 8.5	297.3	- 3.6	317.0	303.7	- 15.9
α_{33}	132.3	156.2	134.4	157.1	159.0	144.0
β_{33}	—	—	12.5	18.1	- 14.0	- 12.3
β_{35}	—	—	- 12.3	- 7.0	9.8	12.8

If the solutions $[\alpha^{(+)}|\beta^{(+)}]$ and $[\alpha^{(+)}|\beta^{(-)}]$, which involve the Yang set of P phase shifts, are rejected (^{7,8}), there still remains the problem of the correct choice between the solutions $[\alpha^{(-)}|\beta^{(+)}]$ and $[\alpha^{(-)}|\beta^{(-)}]$, fitting the data equally well. As it is seen from Table II, these two solutions are substantially different. The set $[\alpha^{(-)}|\beta^{(+)}]$ implies a repulsive $D_{\frac{3}{2}}$ state and the linearity of α_3 according to Orear's relation at least up to 270 MeV. The phase shift $|\alpha_{31}|$ appears to be a slowly decreasing function of the energy and therefore, in order to preserve the continuity, this solution suggests that $|\alpha_{31}|$ should have a maximum at lower energies if one accepts the conventional values of this phase shift in the energy region where the interactions in the D state are practically absent. On the contrary, the set $[\alpha^{(-)}|\beta^{(-)}]$ is characterized by an attractive $D_{\frac{3}{2}}$ state and by the two phase shifts α_3 and α_{31} increasing with the energy, but the behavior of the former is not linear versus the relative momentum (⁹).

(⁷) A. SALAM: *Proceedings of CERN Symposium* (Geneva, 1956); vol. II, p. 176; W. GILBERT and G. R. SCREATON: *Phys. Rev.*, **104**, 1758 (1956).

(⁸) W. C. DAVIDON and M. L. GOLDBERGER: *Phys. Rev.*, **104**, 1119 (1956).

(⁹) This behavior of α_3 and α_{31} is in agreement with the analysis performed by G. PUPPI and A. STANGHELLINI: *Nuovo Cimento*, **3**, 491 (1956) and by A. STANGHELLINI: *Nuovo Cimento*, **4**, 168 (1956).

Although in principle this new kind of ambiguity, brought about by the D waves, could be eliminated on the basis of dispersion theory (⁷), a clear-cut argument would be provided by the measurement of the polarization $P(\theta)$ of the recoiling proton. The quantity $\sigma(\theta)P(\theta)$ is defined as

$$(8) \quad \sigma(\theta)P(\theta) = \text{Tr} [f^*(\theta)\boldsymbol{\sigma}f(\theta)] = k^{-2} \sin \theta \sum_n B_n P_n(\cos \theta),$$

where the elastic pion-proton scattering amplitude, written as a matrix in spin space, reads

$$(9) \quad kf(\theta) = [a(\theta) + \boldsymbol{\sigma} \cdot \mathbf{n} b(\theta)]\chi_p,$$

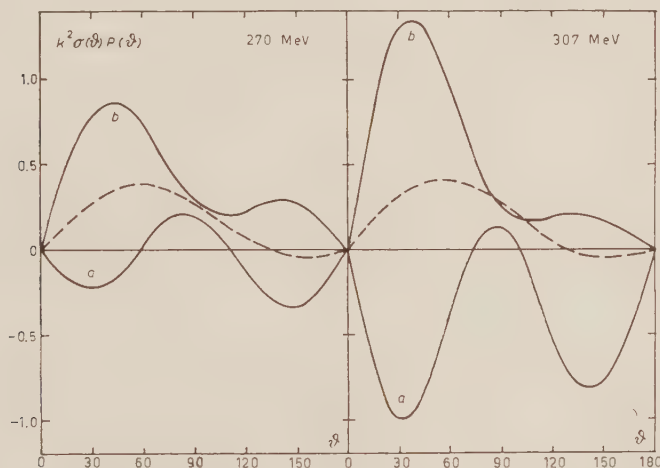


Fig. 1. — Polarization of the recoiling proton in positive pion-proton scattering at 270 and 307 MeV. The curves (a), (b) have been calculated using in Eq. (8) the solutions $[\alpha^{(-)}|\beta^{(+)}]$ respectively $[\alpha^{(-)}|\beta^{(-)}]$. The dotted curves correspond to the solutions $[\alpha^{(-)}]$.

being χ_p the spin function of the proton and \mathbf{n} the unit vector normal to the plane of scattering. Using the notation of Sect. 4 of ref. (²), the functions $a(\theta)$ and $b(\theta)$ are given by

$$(9b) \quad a(\theta) = \sum_l (\mathbf{a}_l/2i)P_l(\cos \theta), \quad b(\theta) = i \sum_l (\mathbf{b}_l/2i)P_l^1(\cos \theta).$$

Including all the waves up to $l_{\max} = 2$, the expansion coefficients B_n are expressed in terms of phase shifts by the following relations ($n_{\max} = 2l_{\max} - 1$)

$$(10) \quad \begin{cases} B_0 = 2[(\alpha_3|\alpha_{33}) - (\alpha_3|\alpha_{31}) - (\alpha_{31}|\beta_{33}) + (\alpha_{31}|\beta_{35}) + 2(\alpha_{33}|\beta_{35}) - 2(\alpha_{33}|\beta_{33})], \\ B_1 = 6[(\alpha_3|\beta_{35}) - (\alpha_3|\beta_{33}) + (\alpha_{31}|\alpha_{33}) + 2(\beta_{33}|\beta_{35})], \\ B_2 = 2[(\alpha_{33}|\beta_{35}) + 5(\alpha_{31}|\beta_{35}) - 6(\alpha_{33}|\beta_{33})], \\ B_3 = 18(\beta_{33}|\beta_{35}), \end{cases}$$

where $(\alpha|\beta) = \sin \alpha \sin \beta \sin(\alpha - \beta)$.

The behavior of the quantity $k^2\sigma(\vartheta)P(\vartheta)$ at the two energies of 270 and 307 MeV for those sets of Table II having $\Delta\alpha < 0$ is shown in Fig. 1. It is clear that a polarization experiment at about $\vartheta = 30^\circ$ or $\vartheta = 150^\circ$ could simply from the sign of the polarization decide between the $[\alpha^{(-)}|\beta^{(+)}]$ and $[\alpha^{(-)}|\beta^{(-)}]$ solutions.

The scattering data ⁽¹⁾ at 240 MeV are not accurate enough for this kind of analysis on *D* wave effects.

* * *

We thank Dr. L. BERETTA and Miss A. CAPONIO for computational assistance.

On the Theory of Leptons.

K. NISHIJIMA (*)

Max-Planck-Institut für Physik - Göttingen

(ricevuto il 23 Febbraio 1957)

In the last few years the theory of hyperons and heavy mesons made a great progress and it became clear that the invariance of the theory against rotations in isotopic space plays an important rôle. In this paper we would like to discuss a new invariance principle upon which many properties of leptons can be explained.

According to the well-known classification of interactions, all interactions are divided into three classes: (a) charge independent interactions, (b) electromagnetic interactions, and (c) weak interactions. Since leptons have no interactions of the type (a), let us first study if there is any invariance property in the electromagnetic interaction of leptons. We start with stating the following theorem:

Theorem I. The following two sets of field equations (1) and (2) lead to the same S matrix:

$$(1) \quad \begin{cases} [\gamma_\mu(\partial_\mu - ieA_\mu) + m]\psi = 0, \\ \square A_\mu = -ie\bar{\psi}\gamma_\mu\psi, \end{cases}$$

$$(2) \quad \begin{cases} [\gamma_\mu(\partial_\mu - ieA_\mu) + m \exp [2i\alpha\gamma_5]]\psi = 0, \\ \square A_\mu = -ie\bar{\psi}\gamma_\mu\psi. \\ (\alpha: \text{real constant}). \end{cases}$$

(Proof.) It is clear that the set (1) is transformed into (2) under the transformation

$$(3) \quad \psi \rightarrow \exp [i\alpha\gamma_5]\psi, \quad \bar{\psi} \rightarrow \bar{\psi} \exp [i\alpha\gamma_5],$$

(*) On leave of absence from Osaka City University, Osaka, Japan.

which leaves the canonical commutation relations invariant. Let us distinguish the operators appearing in eq. (1) from those in (2) by a subscript 0, then one can write

$$(4) \quad \psi_0 = \exp[i\alpha\gamma_5]\psi, \quad \bar{\psi}_0 = \bar{\psi} \exp[i\alpha\gamma_5].$$

In deriving eq. (2) from eq. (1) through the transformation (4), we must notice the following relation:

$$(5) \quad \exp[i\alpha\gamma_5]\gamma_\mu \exp[i\alpha\gamma_5] = \gamma_\mu,$$

or more generally

$$(6) \quad \exp[i\alpha\gamma_5] O \exp[i\alpha\gamma_5] = \begin{cases} O, & \text{for } O = \gamma_\mu, \gamma_5\gamma_\mu, (V, A), \\ O \exp[2i\alpha\gamma_5], & \text{for } O = 1, \gamma_5, \sigma_{\mu\nu}, (S, P, T). \end{cases}$$

The Dirac four spinors of free particles corresponding to eqs. (1) and (2) are related to one another through

$$(7) \quad \begin{cases} u(p, \sigma) = \exp[-i\alpha\gamma_5]u_0(p, \sigma), \\ \bar{u}(p, \sigma) = \bar{u}_0(p, \sigma) \exp[-i\alpha\gamma_5]. \end{cases}$$

Thereby it must be noticed that both u and u_0 belong to the same eigenvalue of the spin operator, since the spin operator $\sigma_{\mu\nu}$ is commutative with γ_5 .

The transformation of the propagation function is given by

$$(8) \quad \begin{cases} S_F(x-y) = \langle \Omega, T[\psi(x), \bar{\psi}(y)]\Omega \rangle \\ = \exp[-i\alpha\gamma_5] \langle \Omega, T[\psi_0(x), \bar{\psi}_0(y)]\Omega \rangle \exp[-i\alpha\gamma_5] \\ = \exp[-i\alpha\gamma_5] S_{F_0}(x-y) \exp[-i\alpha\gamma_5], \end{cases}$$

where T is Wick's chronological symbol and Ω the vacuum state. Now let us prove that the S matrix is independent of the choice of α .

The contributions of the spinor field to the S matrix consist of two kinds of Feynman diagrams, closed loops and open polygons. The contributions from the closed loops are generally of the form

$$(9) \quad \text{Tr} [\gamma_\lambda S_F(p_1) \gamma_\mu S_F(p_2) \dots \gamma_r S_F(p_n)].$$

If we insert eq. (8) into the above expression, we get

$$= \text{Tr} [(\exp[-i\alpha\gamma_5] \gamma_\lambda \exp[-i\alpha\gamma_5]) S_{F_0}(p_1) (\exp[-i\alpha\gamma_5] \gamma_\mu \exp[-i\alpha\gamma_5]) S_{F_0}(p_2) \dots].$$

according to eq. (5), the above expression is again reduced to

$$(10) \quad = \text{Tr} [\gamma_\lambda S_{F_0}(p_1) \gamma_\mu S_{F_0}(p_2) \dots \gamma_r S_{F_0}(p_n)].$$

The result means that the contributions of the closed loops to the S matrix are invariant against the transformation (3). The contributions from the open polygons are generally given by

$$\bar{u}(p_f, \sigma_f) \gamma_\lambda S_F(p_1) \gamma_\mu S_F(p_2) \dots S_F(p_n) \gamma_\nu u(p_i, \sigma_i) .$$

Again inserting eqs. (7) and (8) into this expression, one arrives at

$$= \bar{u}_0(p_f, \sigma_f) \gamma_\lambda S_{F_0}(p_1) \gamma_\mu S_{F_0}(p_2) \dots S_{F_0}(p_n) \gamma_\nu u_0(p_i, \sigma_i) .$$

Thus we have completed the proof of the statement that the S matrix is invariant against the transformation (3). Even if we take account of the renormalization procedures and of the existence of bound states, Theorem I still holds.

As one can readily see in eq. (10), the Dirac matrix γ_μ plays the essential rôle to absorb the transformation factor $\exp[-i\alpha\gamma_5]$. One can adopt an equation of the form (2) to nucleons only at the cost of abandoning the parity conservation in strong interactions, since the pseudoscalar coupling between nucleon and pion fields destroys this invariance property. Thus we can apply the transformation (3) only upon leptons whose strongest interactions are electromagnetic. The only possibility to distinguish between eqs. (1) and (2) is therefore to examine the weak interactions. Instead of examining this possibility, however, one can require that the S matrix be strictly invariant against such a transformation so that in principle one cannot distinguish between eqs. (1) and (2), at least for leptons.

Before entering into the discussion of weak interactions, let us make a short remark. Since quantum electrodynamics is clearly invariant against the transformation

$$(11) \quad \psi \rightarrow \exp[i\beta]\psi, \quad \bar{\psi} \rightarrow \bar{\psi} \exp[-i\beta] \quad (\beta: \text{real constant})$$

we can generalize the transformation (3) as

$$(12) \quad \psi \rightarrow \exp[i\alpha\gamma_5 + i\beta]\psi, \quad \bar{\psi} \rightarrow \bar{\psi} \exp[i\alpha\gamma_5 - i\beta],$$

which leaves the S matrix in quantum electrodynamics again invariant.

Although quantum electrodynamics is invariant against a wide class of transformations of the form (12), it is no more the case in weak interactions as we shall see later. This situation has a strong resemblance to the charge independence in the sense that the strongest interactions of the class (a) are invariant against all rotations in isotopic space but the electromagnetic interactions (b) are invariant only against the rotations around the third axis in isotopic space.

Recently LEE and YANG⁽¹⁾ and also independently SALAM⁽²⁾ have proposed the so-called screwon theory of the neutrino to guarantee the vanishing rest mass of the neutrino. This theory is invariant against the following transformation of the neutrino field:

$$(13) \quad \psi \rightarrow \mp \gamma_5 \psi, \quad \bar{\psi} \rightarrow \pm \bar{\psi} \gamma_5 .$$

(1) T. D. LEE and C. N. YANG: *Phys. Rev.*, to be published.

(2) A. SALAM: *Nuovo Cimento*, **5**, 299 (1957).

Without loss of generality, we shall choose the upper sign and assume this invariance from now on.

Let us now investigate what kind of restrictions should be imposed upon the choice of the parameters α and β in order that the weak interactions be invariant against the transformation of the form (12) (See Note (1)).

To see this invariance requirement more closely, we shall discuss a simple example, the π - μ decay. According to the screwon theory, the decay interaction is given by

$$(14) \quad H_{\text{decay}} = g_s \bar{\psi}_\mu (1 - \gamma_5) \psi_\nu \cdot \varphi + g_v \bar{\psi}_\mu \gamma_\lambda (1 - \gamma_5) \psi_\nu \cdot \frac{\partial \varphi}{\partial x_\lambda} + \text{herm. conj.}$$

Through the transformation (12), H_{decay} is transformed as

$$(15) \quad \left\{ \begin{aligned} H_{\text{decay}} &\rightarrow H'_{\text{decay}} = g_s \bar{\psi}_\mu \exp [i\alpha\gamma_5 - i\beta] (1 - \gamma_5) \psi_\nu \cdot \varphi + \\ &\quad + g_v \bar{\psi}_\mu \exp [i\alpha\gamma_5 - i\beta] \gamma_\lambda (1 - \gamma_5) \psi_\nu \cdot \frac{\partial \varphi}{\partial x_\lambda} + \text{herm. conj.} \\ &= \exp [-i(\alpha + \beta)] g_s \bar{\psi}_\mu (1 - \gamma_5) \psi_\nu \cdot \varphi \\ &\quad + \exp [i(\alpha - \beta)] g_v \bar{\psi}_\mu \gamma_\lambda (1 - \gamma_5) \psi_\nu \cdot \frac{\partial \varphi}{\partial x_\lambda} + \text{herm. conj.} \end{aligned} \right.$$

From this result one can conclude that if $g_v = 0$ or $g_s = 0$ the theory is invariant against the transformations of the form

$$(16) \quad \bar{\psi}_\mu \rightarrow \bar{\psi}_\mu \exp [i\alpha(\gamma_5 + 1)] \quad \text{or} \quad \bar{\psi}_\mu \rightarrow \bar{\psi}_\mu \exp [i\alpha(\gamma_5 - 1)],$$

and the invariance of the theory requires $g_s g_v = 0$.

In the above discussion one can see that the invariance of the theory is attained only when H_{decay} is accompanied by the matrix $(1 - \gamma_5)$. Contrary to the case of quantum electrodynamics the Dirac matrix $(1 - \gamma_5)$ accompanied by the neutrino field plays the rôle of the absorber of the transformation factor $\exp [i\alpha\gamma_5 - i\beta]$. If we assume furthermore that the neutrino operators appear always only in the combination $(1 - \gamma_5) \psi_\nu$ or $\bar{\psi}_\nu (1 + \gamma_5)$ and that this is the only source of the parity non-conservation in lepton interactions, then it is not hard to prove the following theorem:

Theorem II. Weak interactions involving only a μ -meson-electron pair cannot be invariant against transformations of the form (12).

Hence the invariance requirement forbids the following unwanted processes:

$$K \rightarrow \mu + e, \quad \text{or} \quad \pi + \mu + e,$$

$$\mu \rightarrow e + \gamma, \quad \text{or} \quad \mu \rightarrow e + e + e,$$

$$\mu + N \rightarrow N + e, \quad \text{etc.}$$

It must be noticed that the emission of an electron pair or a μ -meson pair is not forbidden by this theorem. But the process

$$(\text{spin } 0) \rightarrow \nu + \bar{\nu}$$

is strictly forbidden in the screwon theory.

If we apply the above argument to the β -decay, we get the following theorem:

Theorem III. The β -decay interaction must be either of the *STP* combination or of the *AV* combination.

To prove this theorem one has only to remember eq. (6).

If we now choose according to experiment the *STP* combination, the theory is invariant against the transformation of the electron operators

$$(17) \quad \psi_e \rightarrow \exp[i\alpha(\gamma_5 - 1)]\psi_e, \quad \bar{\psi}_e \rightarrow \bar{\psi}_e \exp[i\alpha(\gamma_5 + 1)].$$

By similar arguments we can prove through the process (*)

$$\mu \rightarrow e + \nu + \bar{\nu} \quad \text{or} \quad e + \nu + \nu \quad \text{or} \quad e + \bar{\nu} + \bar{\nu},$$

that the theory is invariant against the transformation of the μ -meson operators

$$(18) \quad \psi_\mu \rightarrow \exp[i\alpha'(\gamma_5 - 1)]\psi_\mu, \quad \bar{\psi}_\mu \rightarrow \bar{\psi}_\mu \exp[i\alpha'(\gamma_5 + 1)],$$

and that in all interactions the operators $\bar{\psi}_\mu O \psi_\nu$, $\bar{\psi}_e O \psi_\nu$ and their hermitian conjugates appear only in *STP* combinations. On the contrary, the transformation of the neutrino field which leaves the theory invariant is given by

$$(19) \quad \psi_\nu \rightarrow \exp[i\alpha''(\gamma_5 + 1)]\psi_\nu, \quad \bar{\psi}_\nu \rightarrow \bar{\psi}_\nu \exp[i\alpha''(\gamma_5 - 1)].$$

Thus we have clarified the universality of *STP* combination in weak interactions.

The present theory does not contradict the results of the analysis of the decay processes ⁽³⁾

$$K_{\mu 3} \rightarrow \mu + \pi + \nu,$$

$$K_{e 3} \rightarrow e + \pi + \nu,$$

that the *STP* combination is likely in both interactions.

Finally it must be remarked that according to the present theory the decay interactions for

$$\pi \rightarrow \mu + \nu, \quad K_{\mu 2} \rightarrow \mu + \nu$$

(*) In any case we assume the conservation of the lepton number for a suitable particle-anti-particle assignment to electron, μ -meson, and neutrino.

(³) S. FURUICHI, Y. SUGAHARA, A. WAKASA and M. YONEZAWA: *Nuovo Cimento*, **5**, 285 (1957). Their analysis is based on Crussard's talk in the 6th Rochester Conference.

are not of the AV type as believed so far to account for the small rates of $(\pi \rightarrow e + \nu)/(\pi \rightarrow \mu + \nu)$ and of $(K \rightarrow e + \nu)/(K \rightarrow \mu + \nu)$. These small rates must be attributed to another source.

Once the present theory were justified, we would be free to substitute an equation of the form $(\gamma\partial + m \exp [2i\alpha\gamma_5])\psi = 0$ for the ordinary Dirac equations of leptons.

Note added in proof.

For the sake of clarity it must be mentioned that by invariance we mean in this paper the invariance of the interaction Hamiltonian which is enough to guarantee that the S matrix is independent of the choice of the parameter α appearing in the modified Dirac equation as seen in the discussion of quantum electrodynamics.

If the neutrino-antineutrino mode is granted for the μ -decay, the interaction is given uniquely by

$$H_{\text{decay}} = f \bar{\psi}_\mu \gamma_\lambda (1 + \gamma_5) \psi_e \cdot \bar{\psi}_\nu \gamma_\lambda (1 - \gamma_5) \psi_\nu + \text{herm. conj.}$$

* * *

The author would like to express his sincere thanks to Prof. W. HEISENBERG for the hospitality extended to him in the Max-Planck-Institut für Physik. Thanks are also due Prof. W. HEISENBERG for suggesting this problem and for his interest and encouragement, and to Dr. R. HAAG for his helpful discussions.

Thallium Activated CsI for Scintillation Spectroscopy.

W. BEUSCH, H. KNOEPFEL, E. LOEPFE, D. MAEDER and P. STOLL

Swiss Federal Institute of Technology - Zürich

(ricevuto il 26 Febbraio 1957)

In a recent paper ⁽¹⁾ we have demonstrated that thallium activated CsI crystals are very suitable for α and proton spectroscopy, because CsI is non-hygroscopic. By using the Po- α -line (5.3 MeV) we have obtained a line width of 3.5 per cent. The scintillation efficiency ^(2,3) with α excitation is comparable with that of NaI. The emission spectrum ^(1,2) is very broad and the strongest part is situated in the red. The scintillation decay time is 0.55 μ s. The crystals are easy to grow to appreciable dimensions. As the effective Z -value is slightly higher than that of NaI, we can expect a higher response probability. Especially for angular correlation experiments this fact may be very important. It appeared of interest to examine the suitability of a thallium activated CsI crystal for γ -spectroscopy. (Size of the crystal: $d = 2.5$ cm, $l = 2.5$ cm) (*).

(1) H. KNOEPFEL, E. LOEPFE and P. STOLL: *Helv. Phys. Acta*, **29**, 241 (1956).

(2) H. KNOEPFEL, E. LOEPFE and P. STOLL: *Zeits. f. Naturwiss.* (to be published).

(3) B. HAHN and J. ROSSEL: *Helv. Phys. Acta*, **26**, 271 (1953).

(*) Our grateful thanks are due to Dr. G. WEISSENBERG and to Dr. NITSCHMANN of Ernst Leitz GmbH (Wetzlar, Germany) for their kindness in giving us a CsI-crystal.

In handling the crystals the following points must be observed: the crystal should be conserved in total darkness to avoid an excitation of a long lived fluorescence emission. By warming up the crystal to 150 °C this background will disappear. On the other hand, by very intense γ -irradiation ($> 100r$) red centres are formed, as shown by a reddish colour. By thermal treatment these colour centres disappear.

In Table I the calculated linear absorption coefficients μ of the scintillator and the photo coefficients μ_P are compared for CsI and NaI using the results of MAEDER *et al.* ⁽⁴⁾. The linear absorption coefficients μ and the photo coefficients μ_P of the CsI are at all energies at least 20 per cent higher than those of NaI. Especially in the energy range 1-2 MeV the ratio of the photo-fraction to Compton fraction is more favorable, i.e. the effective photo fraction is higher. In Table II experimental values for the photo fraction of a CsI crystal (size: $d = 2.5$ cm, $l = 2.5$ cm) are tabulated. The corresponding data for NaI are taken from the paper ⁽⁴⁾.

The light efficiency of the thallium-

(4) D. MAEDER, R. MÜLLER and V. WINTERSTEIGER: *Helv. Phys. Acta*, **27**, 3 (1954).

TABLE I.

γ - energy MeV	μ linear ab- sorption coef- ficient in cm^{-1}		μ_p/μ (*)		Response probability					
					$l = 1 \text{ cm}$		$l = 2.5 \text{ cm}$		$l = 10 \text{ cm}$	
	NaI	CsI	NaI	CsI	NaI	CsI	NaI	CsI	NaI	CsI
0.25	0.77	1.12	0.52	0.60	0.54	0.67	0.85	0.94	1	1
0.5	0.33	0.43	0.17	0.21	0.28	0.35	0.56	0.66	0.96	0.98
1	0.21	0.25	0.049	0.068	0.19	0.22	0.40	0.46	0.87	0.92
2	0.147	0.180	0.016	0.025	0.136	0.165	0.31	0.36	0.77	0.83
3	0.125	0.155	0.008	0.009	0.117	0.143	0.27	0.32	0.71	0.78

(*) μ_p : linear photo-absorption coefficient in cm^{-1} .

TABLE II.

Source	Energy keV	Effective photo fraction for cylindrical crystal $d = 2.5 \text{ cm}$, $l = 2.5 \text{ cm}$		Photons in the photo fraction number of incident photons	
		CsI	NaI	CsI	NaI
^{203}Hg	279	82%	75%	73%	60%
^{137}Cs	661	39%	30%	22%	14%

activated CsI crystal is comparable with that of NaI. We measured efficiencies that lay between those of two different specimens of NaI crystals. The NaI

crystals vary in the light efficiency depending on the manufacturer and the size. (Other factors are: degree of activation, purity of crystal and qua-

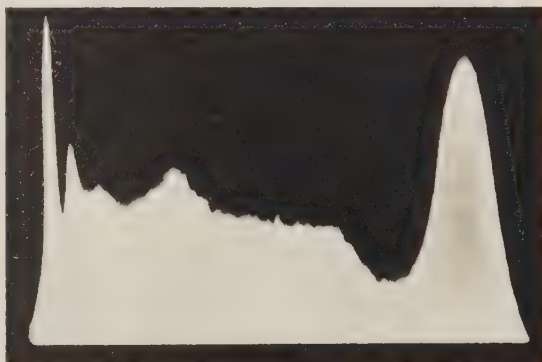


Fig. 1. - Pulse spectrum produced by the 661 keV ^{137}Cs -line in a thallium activated CsI crystal ($d = 2.5 \text{ cm}$, $l = 2.5 \text{ cm}$).

lity of the surrounding light reflector). Our crystal is not optimal, because the percentage of thallium activation is too high (1 per cent). Fig. 1 shows the pulse spectrum of the 661 keV ^{137}Cs -line. The pulses originating in the Du Mont 6292 phototube were amplified and fed to a photographic gray wedge pulse spectrograph. The experimental half width of the photopeak is 14 per cent for the thallium activated CsI-crystal with

a size of 2.5 cm diameter, 2.5 cm length and a γ -energy of 661 keV.

Thus CsI crystals are shown to be very suitable also for γ -spectroscopy, especially if high efficiency is needed.

* * *

We would like to express our hearty thanks to Prof. P. SCHERRER for the support of this work.

Angular Correlation of Radiations with Parallel Angular Momenta.

U. FANO (*)

*Istituto di Fisica dell'Università - Roma**Istituto Nazionale di Fisica Nucleare - Sezione di Roma*

(ricevuto il 7 Marzo 1957)

The discovery ⁽¹⁾ of parity non-conservation in the disintegration of ⁶⁰Co has attracted attention to the chain of emission processes which starts from ⁶⁰Co with spin $j_a=5$ and yields: ⁶Ni with $j_f=0$, an electron with $j_e=\frac{1}{2}$, a neutrino with $j_v=\frac{1}{2}$, and two γ -rays with $j_\gamma=2$, so that $j_a=j_f+j_e+j_v+2j_\gamma$. Such a chain of emission processes, with « parallel angular momenta », is by no means unusual because radiation emission with least angular momentum is generally favored by selection rules. In this special but interesting case, the theory of angular correlation and distribution of radiation simplifies considerably, as noticed by Cox and TOLHOEK ⁽²⁾.

The simplification may be expressed as a theorem which is almost obvious when stated in terms of the vector model. Consider the angular correlation between two radiations emitted with angular momenta \mathbf{j}_1 and \mathbf{j}_2 anywhere along a chain of emission processes. The quantum number J corresponding to the resultant $\mathbf{J}=\mathbf{j}_1+\mathbf{j}_2$ has a single possible value, namely $J=j_1+j_2$, if \mathbf{j}_1 and \mathbf{j}_2 are « parallel ». Under this condition, the angular correlation depends on the quantum numbers j_1 , j_2 , and J , and on *no other* angular momentum. One may then calculate the correlations as though there were only an unoriented particle with spin J which disintegrates into two radiations and leaves no residue. The correlation between the orientation of the initial nuclear spin \mathbf{j}_a and any successive radiation with angular momentum \mathbf{j}_1 depends similarly on j_a , j_1 and on $J=|j_a \pm j_1|$, as though the radiation were emitted directly by the nucleus in its initial state, leaving it with a residual spin $\mathbf{J}=\mathbf{j}_a-\mathbf{j}_1$. The actual order of emissions is immaterial, provided only that the parallelism of angular momenta fixes the value of the quantum number J unambiguously.

These statements are proved, when the theory is formulated in terms of Racah

(*) On leave from the U. S. National Bureau of Standards under a Rockefeller Public Service Award.

⁽¹⁾ C. S. Wu, E. AMBLER, R. W. HAYWARD, D. D. HOPFES and R. P. HUDSON: *Phys. Rev.*, in press.

⁽²⁾ J. A. M. Cox and H. A. TOLHOEK: *Physica*, **19**, 671 (1953), Eq. (15).

coefficients ⁽³⁾, by a recoupling transformation of these coefficients. The angular correlation of two radiations is usually expanded as a sum of Legendre polynomials

$$(1) \quad W(\theta) = \sum_k a_k P_k(\cos \theta).$$

When two radiations are emitted with angular momenta \mathbf{j}_1 and \mathbf{j}_2 in transitions between with spins \mathbf{j}_a , \mathbf{j}_b and \mathbf{j}_c , as shown in the figure, each coefficient a_k levels of (1) contains the factor ⁽⁴⁾

$$(2) \quad (-1)^{j_1+j_2+j_a+2j_b+j_c} (2j_b+1) \overline{W} \begin{pmatrix} j_1 & j_1 & k \\ j_b & j_b & j_a \end{pmatrix} \overline{W} \begin{pmatrix} j_2 & j_2 & k \\ j_b & j_b & j_c \end{pmatrix}.$$

Each \overline{W} in this formula corresponds to one of the triangles in the vector diagram (in a cascade of n radiations the vector diagram contains n triangles and (2) contains n factors \overline{W}). We wish to express (2) as a function of the quantum number J , corresponding to the total angular momentum $\mathbf{J} = \mathbf{j}_1 + \mathbf{j}_2$ of the two radiations. According to the Biedenharn identity ⁽⁵⁾, (2) is equal to

$$(3) \quad \sum_J (-1)^{j_1+j_2+J+k} (2j_b+1) (2J+1) \left[\overline{W} \begin{pmatrix} j_1 & j_2 & J \\ j_c & j_a & j_b \end{pmatrix} \right]^2 \overline{W} \begin{pmatrix} j_1 & j_1 & k \\ j_2 & j_2 & J \end{pmatrix}.$$

Notice that only the last factor of (3) depends on k , whereas the other factors are common to all terms of the expansion (1). The replacement of (2) with (3) becomes decidedly convenient for parallel angular momenta, because there is then a single value of J consistent with the triangular conditions $\mathbf{J} = \mathbf{j}_1 + \mathbf{j}_2$ and $\mathbf{J} = \mathbf{j}_a - \mathbf{j}_c$. In this case the summation in (3) reduces to a single term and the factor $(2j_b+1)(2J+1) \cdot [\overline{W}(j_1 j_2 J / j_c j_a j_b)]^2$ reduces to one, because of the normalization of \overline{W} ⁽⁶⁾. Thereby (3) becomes

$$(4) \quad (-1)^{2J+k} \overline{W} \begin{pmatrix} j_1 & j_1 & k \\ j_2 & j_2 & J \end{pmatrix},$$

which is independent of j_a , j_b and j_c , as we wanted to show. When several radiations are emitted, the proof may require repeated application of the Biedenharn identity and elimination of factors that reduce to one.

⁽³⁾ See, e.g., G. RACAH: *Phys. Rev.*, **84**, 910 (1951); also: L. C. BIEDENHARN and M. E. ROSE: *Rev. Mod. Phys.*, **25**, 729 (1953); K. SIEGBAHN, ed.: *Beta and Gamma Spectroscopy* (Amsterdam, 1955), Chap. 19, or U. FANO and G. RACAH: *Irreducible Tensorial Sets* (New York, 1957), Sect. 19.

⁽⁴⁾ The Racah coefficients are normalized here with $\overline{W} \begin{pmatrix} a & b & e \\ d & c & f \end{pmatrix} = (-1)^{a+b+c+d} W(a b c d; e f)$; see FANO and RACAH: l. c., note ⁽³⁾, Sect. 11.

⁽⁵⁾ L. C. BIEDENHARN: *Journ. Math. Phys. (M.I.T.)*, **31**, 287 (1953).

⁽⁶⁾ The general normalization condition is $\sum_J (2j_b+1)(2J+1) [W(j_1 j_2 J / j_c j_a j_b)]^2 = 1$; in our case the summation reduces to a single term which is itself equal to one. In the general case where J takes more than one value, the expression (3) may be called $\langle (-1)^{j_1+j_2+J+k} \overline{W}(j_1 j_2 J / j_c j_a j_b) \rangle$.

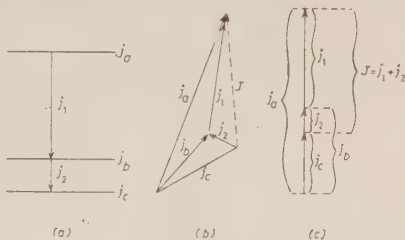


Fig. 1.

As an application we outline the calculation of a β - γ correlation. In this process, each coefficient a_k of the correlation formula (1) will contain a factor of the type (4) with quantum numbers $j_1=j_e$ and $j_2=j_\gamma$. If the β emission is allowed, j_e is $\frac{1}{2}$, \overline{W} vanishes in (4) for $k > 1$, and the correlation function reduces to the form

$$(5) \quad 1 + \frac{a_1}{a_0} \cos \theta = 1 + \alpha_\beta \alpha_G \alpha_\gamma \cos \theta.$$

The single coefficient is factored here into three components, which depend respectively on the β emission, on (4), and on the γ emission.

We have

$$(6) \quad \alpha_G = - \frac{\overline{W} \begin{pmatrix} \frac{1}{2} & \frac{1}{2} & 1 \\ j_\gamma & j_\gamma & \frac{1}{2} + j_\gamma \end{pmatrix}}{\overline{W} \begin{pmatrix} \frac{1}{2} & \frac{1}{2} & 0 \\ j_\gamma & j_\gamma & \frac{1}{2} + j_\gamma \end{pmatrix}} = - \sqrt{\frac{j_\gamma}{3(j_\gamma + 1)}}.$$

The coefficients α_β would vanish if the state of the emitted electron, with $j_e = \frac{1}{2}$, had either of the spectroscopic classifications $s_{\frac{1}{2}}$ or $p_{\frac{1}{2}}$. Non-conservation of parity yields a superposition of $s_{\frac{1}{2}}$ and $p_{\frac{1}{2}}$ and thereby a value of $\alpha_\beta \neq 0$, which coincides with the parameter β_{LY} of Lee and Yang (⁷). The coefficient α_γ is proportional to the efficiency ε_c of the γ -ray detector as an analyzer of circular polarization, defined in terms of its responses I_l and I_d to left- and right-circular polarization. One finds

$$(7) \quad \alpha_\gamma = \sqrt{\frac{3}{j_\gamma(j_\gamma + 1)}} \varepsilon_c = \sqrt{\frac{3}{j_\gamma(j_\gamma + 1)}} \frac{I_l - I_d}{I_l + I_d}.$$

In conclusion Eq. (6), with

$$(8) \quad \alpha_\beta \alpha_G \alpha_\gamma = - \frac{\beta_{LY} \varepsilon_c}{j_\gamma + 1},$$

gives the β - γ correlation for any γ -ray linked with an allowed β process in a chain with parallel angular momenta, i.e. with $J=j_\gamma + \frac{1}{2}$.

(⁷) T. D. LEE and C. N. YANG: *Phys. Rev.*, **104**, 254 (1957), Eq. (A.6).

On the Nucleons Magnetic Moments Contribution to the Radiative Pion-Nucleon Scattering.

B. Bosco (*)

CERN - Geneva

(ricevuto l'11 Marzo 1957)

With the aim to get more and more information on the pion-nucleon interaction many efforts have been devoted until now, both experimentally and theoretically, to investigate phenomena involving pion-nucleon scattering with and without the presence of an electromagnetic field.

It is well known that the most successful theory in explaining such a type of phenomena is the so-called cut-off form of the Yukawa theory, first proposed by CHEW ⁽¹⁾.

Recently the results of this theory have been very much improved by using the CHEW, Low ⁽²⁾ and WICK ⁽³⁾ techniques.

It seems then interesting to apply this theory to the radiative pion-nucleon scattering.

Of course the experimentally observed γ -rays-spectrum is composed of both nuclear and bremsstrahlung spectra.

We wish in this letter only to outline the treatment of the nuclear current while the complete results including the bremsstrahlung spectrum will appear in the near future.

Following the Chew-Low idea of the photoproduction theory ⁽⁴⁾ we can write down the matrix element

$$\mathcal{H}_k^2(q, q'),$$

due to the current j for the radiative scattering from a meson q' in a meson q

(*) On leave from Istituto di Fisica dell'Università, Torino (Italy).

⁽¹⁾ G. CHEW: *Phys. Rev.*, **89**, 591 (1953) and **95**, 1669 (1954).

⁽²⁾ G. CHEW and F. LOW: *Phys. Rev.*, **101**, 1570 (1956) and *Phys. Rev.*, **101**, 1579 (1956); this paper will be denoted in the following as C.L.

⁽³⁾ G. C. WICK: *Rev. Mod. Phys.*, **27**, 339 (1955).

⁽⁴⁾ See foot-note ⁽²⁾.

with emission of a photon k in the form:

$$(1) \quad \mathcal{H}_k^j(q, q') = \left(\psi_q^{(-)}, \int d\nu (-\mathbf{j} \cdot \mathbf{A}_k) \psi_q^{(+)} \right).$$

Here the indexes q, k, q' stand for all the variable of the particles to which they refer; $\mathbf{A}_k = (1/\sqrt{2k})\boldsymbol{\epsilon} \exp[-i\mathbf{k} \cdot \mathbf{r}]$ is the electromagnetic vector potential associated with the emission of photon k and $\psi_q^{(-)}(\psi_q^{(+)})$ is the exact eigenvector of the Schrödinger equation for the meson-nucleon system which asymptotically contains no incoming (no outgoing) particles.

If then we assume \mathbf{j}' as nucleonic density current operator and make the Chew-Low decomposition $\mathbf{j}' = \mathbf{j}_v + \mathbf{j}_s$ we can write immediately

$$(2) \quad \mathcal{H}_k^{j_v}(q, q') = \frac{1}{(4\pi)^{\frac{1}{2}}(f/\mu)} \frac{g_P - g_N}{2} \frac{e}{2M} F(k) \left(\frac{\omega_P}{k} \right)^{\frac{1}{2}} \frac{1}{r(\rho)} (\psi_q^{(-)}, V_P^0 \psi_q^{(+)}).$$

Where all the symbols all the same as in C-L Work.

The analogous term for \mathbf{j}_s can be neglected for the same reason for which it is omitted in Cl, i.e. for the smallness of the ratio $(g_P + g_N)/(g_P - g_N)$.

Unfortunately here, also working only with eq. (2), there does not exist a simple connection between the matrix element

$$(\psi_q^{(-)}, V_P^0 \psi_q^{(+)}),$$

and the scattering matrix.

However, this expression can be cast into a form consisting in a sum of terms of the type

$$\left(\psi_0 V \frac{1}{H + \dots} V \frac{1}{H + \dots} V \psi_0 \right),$$

and then evaluated first introducing the one-meson approximation and then retaining only the terms which can be expressed by means of the scattering matrix.

This calculation is not difficult but rather cumbersome and we will give details in the more complete paper; the results for the reaction

$$\pi^+ + p \rightarrow \pi^+ + p + \gamma.$$

read:

$$(3) \quad (\psi_q^{(-)}, V_P^0 \psi_q^{(+)}) = \text{Born term} + \langle \alpha | [h_1(q, q') \boldsymbol{\sigma} \cdot \mathbf{p} \mathbf{q} \cdot \mathbf{q}' + h_2(q, q', p) \boldsymbol{\sigma} \cdot \mathbf{q} \mathbf{p} \cdot \mathbf{q}' + \\ + h_3(q, q', p) \boldsymbol{\sigma} \cdot \mathbf{q}' \mathbf{p} \cdot \mathbf{q} + h_4(q, q', p) \mathbf{p} \wedge \mathbf{q} \times \mathbf{q}'] | \alpha' \rangle,$$

where h_i are quite complicate functions of the phase-shifts and

$$|\alpha'\rangle \quad (|\alpha\rangle),$$

are the spin function of the proton in the initial (final) state and the Born term is:

$$(4) \quad \text{Born term} = 4i(4\pi)^{\frac{3}{2}} \left(\frac{f}{\mu}\right)^{\frac{3}{2}} \frac{v(q)v(p)v(q')}{\sqrt{2\omega_q}\sqrt{2\omega_p}\sqrt{2\omega_{q'}}} \cdot \left\langle \chi \left| \left[\frac{1}{\omega_q k} \boldsymbol{\sigma} \cdot \mathbf{q}' \mathbf{p} \cdot \mathbf{q} - \frac{1}{\omega_q k} \boldsymbol{\sigma} \cdot \mathbf{q} \mathbf{p} \cdot \mathbf{q}' \right] \chi' \right. \right\rangle.$$

Since all the h_i are such that they vanish if all the phase-shifts are put equal to zero the approximation expressed by (3) means that we have decomposed the process in Born approximation plus scattering corrections.

We give here the cross-section in Born approximation: by substitution of (4) in (2) and using the usual formula for the cross-section one finds:

$$(5) \quad \frac{d\sigma}{d\Omega_k}(k, q') = \frac{1}{12\pi^2} \left(\frac{f}{\mu}\right)^4 (g_P - g_N)^2 \frac{e^2}{M^2} \frac{v^2(q')v^2\{[(\omega_{q'} - k)^2 - \mu^2]^{\frac{1}{2}}\}}{(\omega_{q'} - k)^3 \omega_{q'}^2} \cdot \lambda_q^2 q_{11}^2 (\omega_{q'} - k)^2 - \mu^2 \} \{ 2(\omega_{q'} - k)^2 + [3\omega_{q'}^2 - 2\omega_{q'}(\omega_{q'} - k)] \cos \Theta \} k dk,$$

where Θ is the angle between \mathbf{q}' and $\mathbf{p} = \mathbf{k} \wedge \boldsymbol{\epsilon}$. $\cos \Theta$ can be expressed in terms of the angle θ between \mathbf{k} and \mathbf{q} and the angle α between $\boldsymbol{\epsilon}$ and the (\mathbf{q}, \mathbf{k}) plane by the relation:

$$\cos \Theta = \sin \theta \sin \alpha.$$

If we are not interested in the polarization of the emitted radiation we have to preform the sum over the polarizations; then we get:

$$(6) \quad \frac{d\sigma}{d\Omega_k}(q', k) = \frac{1}{12\pi^2} \left(\frac{f}{\mu}\right)^4 (g_P - g_N)^2 \frac{e^2}{M^2} \frac{v^2(q')v^2\{[(\omega_{q'} - k)^2 - \mu^2]^{\frac{1}{2}}\}}{(\omega_{q'} - k)^3 \omega_{q'}^2} \cdot \lambda_q^2 [(\omega_{q'} - k)^2 - \mu^2]^{\frac{1}{2}} \{ 4(\omega_{q'} - k)^2 + [3\omega_{q'}^2 - 2\omega_{q'}(\omega_{q'} - k)] \sin^2 \theta \} k dk.$$

In Fig. 1 we give the graphical representation of (6) for incident 220 MeV energy of π^+ in the laboratory system and for $\theta = 45^\circ$ and 90° .

Since this cross-section is very small if the scattering corrections will not turn out to change very much the order of magnitude of the Born approximation, we can conclude that the contribution of the nucleons magnetic moment to the radiative scattering is very small and that significant contributions to the complete spectrum only can derive from interference terms.

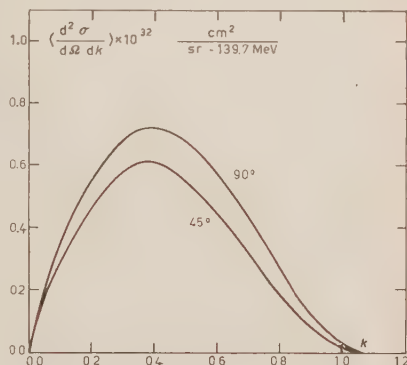


Fig. 1.

I am greatly indebted to Prof. B. FERRETTI for very useful discussions and kind interest in this work. I also wish to thank the Istituto di Fisica dell'Università di Torino for my leave.

The Parity Non-Conservation and the Strength of the Interaction of Elementary Particles.

S. TANAKA

Department of Physics, Rikkyo University - Tokyo

(ricevuto il 12 Marzo 1957)

Recently, LEE and YANG ⁽¹⁾ proposed an important question of the parity conservation in the weak interaction. Being motivated by their proposal, Wu and her collaborators have made experiments of decay processes and showed definitely the right- and left-asymmetry by which Lee and Yang's anticipation, the violation of the parity conservation and that of the invariance with respect to the particle conjugation, has been confirmed.

Now, this negative result against the conventional view-point seems to have a possibility to give a clue to discover a future theory. In order to turn this passive consequence into a positive direction, we should try to discover the law of the violation of invariances. We believe the violation of the parity conservation is closely related to the fundamental aspect of the structure of elementary particles.

As a result of the discovery of many new particles, we became aware of the distinction of interactions of the elementary particles, for instance, about the strength of the coupling. However, there seems to exist a slightly profound aspect concerning the property of the strong and the weak coupling themselves. For example, in the hypothesis of the composite theory of new particles proposed by SAKATA ⁽²⁾, interactions of such type as

$$(1) \quad \bar{N}N\bar{N}N, \quad \bar{\Lambda}\Lambda\bar{\Lambda}\Lambda, \quad \bar{N}N\bar{\Lambda}\Lambda,$$

are conceived to be strong, and

$$(2) \quad \bar{N}N\bar{\Lambda}N, \quad \bar{N}N \begin{Bmatrix} \bar{\mu} \\ \bar{e} \end{Bmatrix} \nu, \quad \bar{\Lambda}N \begin{Bmatrix} \bar{\mu} \\ \bar{e} \end{Bmatrix} \nu, \quad \text{etc.},$$

to be weak ⁽³⁾. Here, it is noteworthy that, qualitatively speaking, in the strong interactions the same kinds of particles occur necessarily associated in pairs, but in

⁽¹⁾ T. D. LEE and C. N. YANG: *Phys. Rev.*, **104**, 254 (1956).

⁽²⁾ S. SAKATA: *Prog. Theor. Phys.*, **16**, 686 (1956).

⁽³⁾ S. TANAKA: *Prog. Theor. Phys.*, **16**, 631 (1956).

the weak interactions particles take place in a somewhat irregular way. Hence, one may conceive that each elementary particle possesses some internal structure concerning the mass, which affects the strength of the coupling and the mixing of parity in the weak interaction.

In the present letter, we shall try to get a theoretical inner relation which may exist among the kinds of particles, the strength of couplings and the violation of the parity conservation, etc., introducing the internal degrees of freedom.

According to the above considerations, we propose a six-dimensional basic equation for the elementary particles,

$$(3) \quad \left(\gamma_\mu \frac{\partial}{\partial x_\mu} + \gamma_5 \frac{\partial}{\partial u_1} + \gamma_6 \frac{\partial}{\partial u_2} \right) \Phi(x_\mu, u_a) = 0,$$

where $\gamma_5 = \gamma_1 \gamma_2 \gamma_3 \gamma_4$, $\gamma_6 = i$ and u_a 's ($a = 1, 2$) represent the internal variables. Now, let us postulate the fundamental principle of our theory:

The theory should be invariant under both the proper Lorentz transformation (R s) and the proper rotation in the (u_1, u_2) space (Rm), while it need not be invariant with respect to inversions such as the space reflection, the time reversal, or the particle conjugation.

From (3), one sees

$$(4) \quad \left(\frac{\partial^2}{\partial x_\mu^2} + \frac{\partial^2}{\partial u_1^2} + \frac{\partial^2}{\partial u_2^2} \right) \Phi(x_\mu, u_a) = 0.$$

By comparing this equation with the Klein-Gordon equation, one finds that the internal freedom relates to the mass of elementary particles and $(-\partial^2/\partial u_1^2 - \partial^2/\partial u_2^2)^{1/2}$ can be interpreted as a mass operator and that $\Phi(x_\mu, u_a)$ may be considered to be a unified field similar to the non-local field. In order to make possible the unified field to involve both a real and a complex field, we assume the reality condition

$$(5) \quad \Phi(x_\mu, u_a) = \Phi^c(x_\mu, u_a) \equiv C \bar{\Phi}(x_\mu, -u_a).$$

Then, by using the usual Dirac spinor $\psi(x_\mu, \kappa)$ with the mass κ , the solution of (3) can be written as follows,

$$(6) \quad \Phi(x_\mu, u_a) = \psi(x_\mu, u_a) + \psi^c(x_\mu, u_a),$$

where

$$(7) \quad \psi(x_\mu, u_a) = \sum_{l,m} \psi_{lm}(x_\mu, u_a),$$

$$(8) \quad \begin{aligned} \psi_{lm}(x_\mu, u_a) &= \frac{1}{2\pi} \int_0^{2\pi} d\theta \exp[-i(l + \frac{1}{2})\theta] \exp[\gamma_5 \gamma_6 \theta/2] \psi(x_\mu, \kappa_{lm}) \cdot \\ &\cdot \exp[-i\kappa_{lm}(u_1 \sin \theta + u_2 \cos \theta)] = \frac{1}{2} (-1)^{l+1} \exp[i(l + \frac{1}{2})\varphi - \gamma_5 \gamma_6 \varphi/2] \cdot \\ &\cdot \{J_{l+1}(\kappa_{lm} r) - J_l(\kappa_{lm} r) - \gamma_5 J_{l+1}(\kappa_{lm} r) - \gamma_5 J_l(\kappa_{lm} r)\} \psi(x_\mu, \kappa_{lm}), \end{aligned}$$

and (r, φ) denotes a polar coordinate of (u_1, u_2) . In the above equations, the mass spectrum κ_{lm} may be obtained by a suitable boundary condition for $\Phi(x_\mu, u_a)$ in

the internal space. Henceforth, we regard $\psi_{lm}(x_\mu, u_a)$ as a new representation of an elementary particle. Further, we find that

$$(9) \quad \left(\frac{\partial^2}{\partial u_1^2} + \frac{\partial^2}{\partial u_2^2} + \kappa_{lm}^2 \right) \psi_{lm}(x_\mu, u_a) = 0,$$

$$(10) \quad \left\{ \begin{array}{l} \left(-i \frac{\partial}{\partial \varphi} - i\gamma_5 \gamma_6 / 2 \right) \psi_{lm}(x_\mu, u_a) = (l + \frac{1}{2}) \psi_{lm}(x_\mu, u_a), \\ \left(-i \frac{\partial}{\partial \varphi} - i\gamma_5 \gamma_6 / 2 \right) \psi_{lm}^c(x_\mu, u_a) = -(l + \frac{1}{2}) \psi_{lm}^c(x_\mu, u_a), \end{array} \right.$$

and that the rotation Rm can be represented by a unitary operator, as

$$U_\alpha \Phi(x_\mu, u'_a) U_\alpha^{-1} = \exp[-\gamma_5 \gamma_6 \alpha / 2] \Phi(x_\mu, u_a).$$

Such a unitary operator can be determined by

$$(11) \quad U_\alpha \psi(x_\mu, \kappa_{lm}) U_\alpha^{-1} = \exp[-i(l + \frac{1}{2})\alpha] \psi(x_\mu, \kappa_{lm}).$$

Now, for instance, let us take a Fermi-type interaction for $\psi(x_\mu, u_a)$, which should be invariant under both R_s and Rm due to our fundamental postulate and constituted from irreducible quantities given by Table I. For example, we investigate the following interaction in detail,

$$H^i = g_1 \int dx_\mu du_a \sum_{a=5,6} \bar{\psi} \gamma_a \psi \bar{\psi} \gamma_a \psi.$$

TABLE I.

	Type	R_s	Rm
I	$\bar{\psi} \gamma_a \psi$	scalar	vector
II	$\bar{\psi} \gamma'_\mu \psi$ $i \bar{\psi} \gamma_5 \gamma'_\mu \psi$	vector	scalar
III	$\bar{\psi} \gamma'_{[\mu} \gamma'_\nu \gamma'_a \psi$	tensor	vector
IV	$\bar{\psi} \gamma_a \partial_a \psi$	scalar	scalar
II'	$\bar{\psi} \gamma_\mu \partial_a \psi$ $i \bar{\psi} \gamma_5 \gamma'_\mu \partial_a \psi$	vector	vector
V	$\bar{\psi} \gamma'_{[\mu} \gamma'_\nu \gamma'_a \partial_a \psi$	tensor	scalar

$:\gamma_a \partial_a \equiv \gamma_5 \frac{\partial}{\partial u_1} + \gamma_6 \frac{\partial}{\partial u_2}, \quad \gamma_a = \gamma_5, \gamma_6.$

Substituting for ψ from (7) and (8), one obtains many interaction terms among elementary particles. The general term consisting of four particles with quantum numbers l_i, m_i ($i = 1, 2, 3, 4$) and masses $\kappa_i \equiv \kappa_{l_i m_i}$ can be expressed by

$$(12) \quad \delta_{l_1+l_3, l_2+l_4} \int d\mathbf{x}_\mu [\bar{g}_1 (-\bar{\psi}_1 \psi_2 \bar{\psi}_3 \psi_4 + \bar{\psi}_1' \psi_2' \bar{\psi}_3' \psi_4) + \bar{g}_1' (\bar{\psi}_1 \psi_2 \bar{\psi}_3' \psi_4 - \bar{\psi}_1' \psi_2' \bar{\psi}_3 \psi_4)],$$

where ψ_i denotes $\psi(x_\mu, \kappa_i)$ and

$$(13) \quad \left\{ \frac{\bar{g}_1}{\bar{g}_1'} \right\} = g_1 \pi \int_0^\infty r d\gamma [J_{l_1+1}(\kappa_1 r) J_{l_2}(\kappa_2 r) J_{l_3}(\kappa_3 r) J_{l_4+1}(\kappa_4 r) \cdot \\ \cdot \{\pm\} J_{l_1}(\kappa_1 r) J_{l_2+1}(\kappa_2 r) J_{l_3+1}(\kappa_3 r) J_{l_4}(\kappa_4 r)].$$

The other type of interactions $H^{II}, H^{IV}, H^{VI}, H^V$, which correspond to the respective row in Table I, can be also treated in the same way. Now referring to the special case given by (12), we shall tentatively summarize the main results:

i) A universally conserving quantity ($l + \frac{1}{2}$) is obtained, which takes the place of the usual ones derived from invariances of several inversions. ii) With the exceptions discussed in iii), the even coupling and the odd coupling coexist, in general, that is, the violation of the parity conservation occurs in a definite rate, which can be predicted theoretically. The coupling constants of both interactions are always real, that is, as a result the theory is invariant under the time reversal of Wigner type. iii) For the cases as $NNNN, \bar{\Lambda}\bar{\Lambda}\bar{\Lambda}\bar{\Lambda}$ in (I) (which are characterized as a strong interaction), where four fields belong to the same kind, the odd couplings in H^I , and H^{II}, H^{IV} (if $g_2 = g_3, g_2' = g_3'$) completely vanish, but this is not the case in H^{IV} and H^V . iv) As seen in (13), the strength of the effective coupling is determined by the internal structure of the elementary particle, which acts as a form factor. It is expected that, for the cases of coupling as (2), where several kinds of particles take part in some irregular way, the strength of coupling becomes weak due to the unfavoured overlapping of the internal wave functions.

By considering the above qualitative results, the present approach may be able to explain the distinction of the strength of the actual interactions of elementary particles and to give the law of the violation of the parity conservation or the particle conjugation. Then, of course, the well-known puzzle of θ - and τ -events may be solved qualitatively at the same time. The detailed discussion will be presented in a forthcoming paper.

* * *

The author wishes to thank Dr. K. AIZU and Dr. S. MACHIDA for their helpful discussions.

On the Solutions of the Fluctuation Problem in Cascade Showers.

J. W. GARDNER

English Electric Co. Ltd., Whetstone - Leicester, England

(ricevuto il 14 Marzo 1957)

In a recent paper with the above title ⁽¹⁾ Professor MESSEL describes a practical method of obtaining numerical results in special cases for the longitudinal number distribution function in shower theory. The essence of the method is to use the following expansion of the distribution function Φ in terms of its factorial moments T_n (the notation of ⁽¹⁾ is retained throughout).

$$\Phi\left(\varepsilon > \frac{1}{n+J}, n, z\right) = - \sum_{k=0}^{J-1} \frac{(-1)^k}{k! n!} T_{n+k} \left(\varepsilon > \frac{1}{n+J}, z\right).$$

For very restricted, albeit experimentally interesting, values of n and z , this series converges rapidly enough to be terminated after the first few terms without practical error. In such cases, then, if one knows the first few moments, the calculation of Φ is trivial. MESSEL was able to use numerical values of the moments T_1, T_2, T_3 obtained from his earlier work in collaboration with H. GELLMAN and the present author ⁽²⁾

for computing the distribution functions tabulated in ⁽¹⁾.

Since MESSEL describes the work reported in ⁽²⁾ as «long and tedious» it is perhaps worth pointing out that this length and tedium (which are undeniable and probably ineluctable) stem primarily from the computation of the moments T_1, T_2, T_3 , and only secondarily from the construction of Φ by the polynomial method ⁽³⁾ using a Polya weight function. The problem of obtaining accurate numerical values of T_1, T_2, T_3 and, if possible, T_4 over an adequate range in ε and z , and for more realistic cascades than the simple model used in ⁽²⁾, is not circumvented by the method of ⁽¹⁾ and remains in truth a fascinating challenge to modern automatic computing. Given these numerical values the procedure of ⁽¹⁾ does indeed offer a quick practical method for calculating Φ for a few restricted values of the parameters. The work reported in ⁽²⁾ aimed at fitting a distribution to a much wider range of parametric values, particularly in n , and was not claimed to be necessarily the best method if one were interested only in $n \leq 2$.

⁽¹⁾ H. MESSEL: *Nuovo Cimento*, **4**, 1339 (1956).

⁽²⁾ J. W. GARDNER, H. GELLMAN, and H. MESSEL: *Nuovo Cimento*, **2**, 58 (1955).

⁽³⁾ H. S. GREEN and H. MESSEL: *Quarterly of Applied Maths.*, **11**, 403 (1954).

Law of Molecular Interaction for Krypton (*).

M. P. MADAN

*Research Laboratory of Electronics, Massachusetts Institute of Technology
Cambridge, Massachusetts*

(ricevuto il 16 Marzo 1957)

A study of laws of molecular interaction using coefficient of thermal diffusion in conjunction with an exponential: a six potential energy function ⁽¹⁾ is much more useful and preferable than any other method ^(1,2). Using thermal diffusion, we report here the evaluation of force parameters for krypton.

Different methods are used to reduce the values of the thermal separation ratio R_T to a particular temperature ^(3,5). The relation $R_T = A - B/T$ as assumed by BROWN ⁽¹⁾ is never truly valid over any extended region, nevertheless it can be

used to reduce the data with different sets of constants for different regions of temperatures. Following a method by SRIVASTAVA and MADAN ⁽³⁾, the thermal diffusion data ⁽⁶⁾ were examined to give R_T at different temperatures with the help of equations of the type

$$(1) \quad R_T^* = A + B(1/T_2 - 1/T_1)(\ln T_2/T_1)^{-1},$$

where R_T^* is the experimentally determined value of R_T . The values of R_T thus obtained are plotted against \bar{T} (\bar{K}) and a smooth curve is drawn. This smoothing of the data to a certain extent, removes the uncertainty in the precision of the experimental measurements. The experimental curve R_T versus T used in conjunction with the theoretical curve R_T versus kT/ϵ for the exp: six-potential following a method reported in a previous paper ⁽²⁾ yielded the value of the parameter ϵ . The value of α is taken to be $\alpha=12$ as suggested by viscosity data

(*) This work has been supported in part by the U.S. Army (Signal Corps), the U.S. Air Force (Office of Scientific Research, Air Research and Development Command), and the U.S. Navy (Office of Naval Research).

$$^{(1)} E(r) = \frac{\epsilon}{1-(6/\alpha)} \left[\left(\frac{6}{\alpha} \right) \exp[\alpha(1-r/r_m)] - \left(\frac{r_m}{r} \right) \right];$$

for explanation of symbols, see reference ⁽¹⁾ or ⁽²⁾.

⁽¹⁾ E. A. MASON and W. E. RICE: *Journ. Chem. Phys.*, **22**, 843 (1954).

⁽²⁾ M. P. MADAN: *Journ. Chem. Phys.*, **23**, 763 (1955).

⁽³⁾ B. N. SRIVASTAVA and M. P. MADAN: *Journ. Chem. Phys.*, **21**, 807 (1953).

⁽⁴⁾ H. BROWN: *Phys. Rev.*, **58**, 661 (1940).

⁽⁵⁾ E. M. HOLLERAN: *Journ. Chem. Phys.*, **21**, 1901 (1953).

⁽⁶⁾ J. W. CORBETT and W. W. WATSON: *Journ. Chem. Phys.*, **25**, 385 (1956).

⁽⁷⁾ W. G. KANNULAIK and E. H. CARMAN: *Proc. Phys. Soc. (London)*, **B 65**, 701 (1952).

⁽⁸⁾ F. G. KEYES: *Trans. Amer. Soc. Mech. Engrs.*, **77**, 1395 (1955).

following a procedure described by MASON and RICE ⁽¹⁾. The values of ϵ calculated above from thermal diffusion can now be used to compute r_m from thermal conductivity data ^(7,8). The results show a slight dependence of ϵ and r_m on temperature, similar to one found for the case of argon ^(2,3), however, we may select a mean value for the limited range 130 to 400 °K. The values of parameters thus found are $\epsilon=224.0$ °K and $r_m=3.972$ Å. These can be compared with the values $\epsilon=158.3$ °K and $r_o=4.056$ Å with $\alpha=12.3$ found by MASON and RICE ⁽¹⁾ using viscosity, crystal and virial properties and the values $\epsilon=135.5$ °K and $r_m=4.341$ Å with $\alpha=13.1$ found by SRIVASTAVA ⁽⁹⁾, using thermal conductivity.

To test the suitability of the parameters ϵ and r_m , obtained above, only the self-diffusion and viscosity coefficients ^(10,11) were used to compare the φ theoretical results with experiment thereby restricting the problem to non-equilibrium states.

⁽⁹⁾ B. N. SRIVASTAVA: Private communication.

⁽¹⁰⁾ W. GROTH and P. HARTECK: *Zeits. Electrochem.*, **47**, 167 (1941).

The calculated value of the self-diffusion coefficient is 0.0936 at a temperature of 293 °K against the experimental value of 0.093 ± 0.0045 , (D_{11} in $\text{cm}^2 \text{s}^{-1}$).

The comparison for calculated and observed viscosities is shown in Table I.

TABLE I. — Comparison of observed and calculated viscosity data for krypton.
 $\eta \cdot 10^5 \text{ g} \cdot \text{cm}^{-1} \text{ s}^{-1}$

Temp. °K	Calculated	Observed
288.4	2.422	2.436
289.2	2.428	2.441
372.6	3.092	3.062
283.8	2.379	2.405
289.5	2.427	2.459
373.2	3.106	3.063

The agreement is seen to be good. If the experimental errors in the measurement of thermal diffusion are kept in mind, this agreement is very satisfactory.

Details are being published elsewhere.

⁽¹¹⁾ A. O. RANKINE: *Proc. Roy. Soc. (London)*, **A 83**, 516 (1910); **A 84**, 181 (1910); A. G. NASINI and C. ROSSI: *Gazz. Chim. Ital.*, **58**, 433 (1928).

Some Remarks about a Paper by Fukutome and Nogami.

M. CINI

Istituto di Fisica dell'Università - Catania
Centro Siciliano di Fisica Nucleare - Catania

S. FUBINI

Fermi Institute for Nuclear Studies - University of Chicago ()*

(ricevuto il 22 Marzo 1957)

In a recent paper FUKUTOME and NOGAMI ⁽¹⁾ have discussed the results of an investigation of ours in which, after having deduced three sum-rules for the exact scattering amplitudes of the fixed source meson theory we made use of them with the purpose of testing the existing approximations to the unknown exact solution, and of investigating the properties of the latter ⁽²⁾.

It was certainly very kind of these authors to summarize in their paper the results of our investigation. We discovered, however, that, due probably to our poor english, it happened that our conclusion: «It is shown that agreement between theory and experiment at low energy requires the high energy

(above the cut-off) contribution to the sum rules to be dominant» ⁽³⁾ has been reported as follows: «The possibility that the contribution (to the sum-rules) from the energy region above the cut-off is large is ruled out» ⁽⁴⁾.

Since most people will be inclined to agree with us that the interpreters have slightly altered the meaning of our words, we hope that a brief summary of our statements will not be considered completely useless.

1. - Test of the existing approximations.

In I we find that if a square cut-off is adopted, the one-meson approximation is not a good approximation to the exact solution in the high energy region because the sum-rules are violated by a large amount. No definite statement is made if the cut-off goes to zero sufficiently slowly as $p \rightarrow \infty$. In II also this possibility is ruled out and we conclude that,

(*) On leave from Istituto di Fisica dell'Università di Torino.

⁽¹⁾ H. FUKUTOME and Y. NOGAMI: *Nuovo Cimento*, **5**, 347 (1957), referred to in the following as FN.

⁽²⁾ M. CINI and S. FUBINI: *Nuovo Cimento*, **3**, 1380 (1956), referred to as I; *Phys. Rev.*, **102**, 1687 (1956), referred to as II; *Proceedings of CERN Symposium 1956*, **2**, 171, referred to as III.

⁽³⁾ I, abstract.

⁽⁴⁾ FN, p. 348.

since « agreement between theory and experiment in the low energy region can only be obtained if high energy contributions are dominant », then many meson states must contribute appreciably at higher energies. In this case a square cut-off is admissible. In III we again summarize this conclusion with the words: « This failure (to satisfy the sum-rules) can be shown to be due to the neglect of states with two or more mesons which give strong contributions to the scattering amplitudes in the energy region above the cut-off ». We may add that the sum-rules have been used also to show ⁽⁵⁾ that the intermediate coupling approximation fails to describe the experimental low energy scattering, and gives inadmissible values for the quantities ϱ_1 and ϱ_2 .

2. - Discussion of the exact solution.

Since the exact solution is not known one cannot infer from the sum-rules strict mathematical consequences, but two alternatives are left open. In I the situation was presented as follows: « We conclude that *if* the common viewpoint is adopted according to which the cut-off factor of the fixed source theory *should* make all high energy contributions negligible, the exact solutions of this theory cannot agree with experiment even at low energies. » This clearly means that *if* the exact solution does agree with experiment in the low energy region, then the cut-off does not eliminate all the high energy contributions, i.e. *large contributions arise from the region above the cut-off*. This was explicitly stated in the abstract with the words quoted above ⁽³⁾. In II we further stressed this point by finding, as stated before, that many meson states must contribute appreciably at high energies, and in III the situation was summarized as follows: « These re-

sults lead us to formulate the following two alternatives concerning the behaviour of the exact scattering amplitudes: (a) The exact solution agrees with experiment in the low energy region, thus coinciding practically with the one-meson approximation, but must radically differ from it *in the region above the cut-off*, showing complicated unphysical resonances due to many meson states; (b) The exact solution is completely different in the low energy region from the one-meson approximation. » It may be added that it is plausible that alternative (b) does not hold, but it cannot be proved. For further discussion on this point see a forthcoming paper by W. THIRRING and one of us (S.F.).

A few further remarks about some other comments by F.N. are in order. About the possibility of determining an upper limit to the cut-off k_{\max} , we have stated in II that in the integral

$$(1) \quad \int_{\mu}^{\infty} \frac{d\omega}{v^2(p)p} \frac{\sigma^+(p) - \sigma^-(p)}{(\omega_p + \omega_k)^2},$$

the contribution from the range above the cut-off is negligible.

This statement is *not* based on any assumption on the behaviour (or to use the words of F.N. on an « improper treatment ») of $\sigma(p)/v^2(p)$ but derives simply from the fact (clearly pointed out in II) that we have *proved* that in the integrals

$$(2) \quad \int_{\mu}^{\infty} \frac{d\omega}{v^2(p)p} \frac{\sigma^+(p) + \sigma^-(p)}{(\omega_x \pm \omega_k)},$$

the contribution above the cut-off must be negligible if agreement with experiment at low energies is required ⁽⁶⁾⁽⁷⁾.

⁽⁵⁾ M. CINI, S. FUBINI and A. STANGHELINI: *Nuovo Cimento*, **3**, 1380 (1956).

⁽⁷⁾ In the quoted forthcoming paper by THIRRING and one of us (S.F.) it is further shown that also a lower limit for k_{\max} can be obtained. The two limits are very close to each other.

⁽⁶⁾ R. STROFFOLINI: *Phys. Rev.*, **104**, 1146 (1956).

Of course if one manipulates (as done by F.N.) the integral (I) in order to reduce the powers of p in the denominator which insure the convergence, then one does obtain expressions about which no definite statements can be made because the contribution above the cut-off becomes important. It seems therefore somewhat «improper» to deduce anything from expressions as F.N. (4.3) which strongly depend on the unknown behaviour of $\sigma(p)/v^2(p)$ in the region above the cut-off. In this connection we may add that we have *never* assumed (as stated by the authors in question) that the total cross-section $\sigma(p)$ is proportional to $v(p)$, and in fact we have stated in footnote (11) of I exactly what they assert, namely that the inelastic part of $\text{Im } g(p)$ is proportional to $v^2(p)$.

That these authors probably paid little attention to our footnotes is further shown by the fact that two of the conditions rediscovered by them ($\alpha < -\frac{1}{3}$

and $1+2\alpha-3\beta > 0$ eqs. FN(2.4) and (2.5)) are contained in the «Note added in proof» of I and in eq. (10) and footnote (5) of II. No mention to THIRRING, to whom—as stated in our papers—these relations are due, is found in F.N. It may be added that also the other two relations of FN(2.4) had been found by THIRRING and communicated to the 1956 Rochester Conference (8). A sketch of their proof is even quoted in footnote (9) of another paper by one of us (9).

As a conclusion we should like to emphasize that we are glad to see that the result of FN, even if the authors seem to be convinced of the contrary, confirms what we have repeatedly stated about the behaviour of the exact solution of the fixed source meson theory.

(8) *Proc. 6-th Rochester Conference* (1956), 3, 18 (New York).

(9) S. FUBINI: *Nuovo Cimento*, 3, 1425 (1956), footnote (4).

Influenza dell'adsorbimento e della migrazione superficiale sulla separazione isotopica nella diffusione di un gas attraverso una parete porosa (*).

P. CALDIROLA e G. ROSSI (+)

Istituto di Scienze Fisiche dell'Università - Milano

Istituto Nazionale di Fisica Nucleare - Sezione di Milano

(ricevuto il 29 Marzo 1957)

Nello studio della separazione di isotopi col procedimento della diffusione gassosa attraverso una parete porosa, possono avere importanza, in determinate condizioni, i fenomeni di adsorbimento e di migrazione superficiale del gas.

Si è fatta una valutazione dell'influenza di questi processi allo scopo soprattutto di stabilire la loro dipendenza dei vari parametri e in particolare dalla temperatura.

Nella parete porosa, che supporremo costituita da granuli compressi (sinterizzati) a contatto col gas possono aver luogo, come illustrato in Fig. 1, i seguenti processi:

- a) adsorbimento di atomi del gas sulla superficie dei granuli;
- b) evaporazione di atomi adsorbiti dalla superficie dei granuli;
- c) migrazione di atomi adsorbiti

lungo la superficie dei capillari risultanti dalla sinterizzazione dei granuli e entro i quali si manifesta il flusso di Knudsen.

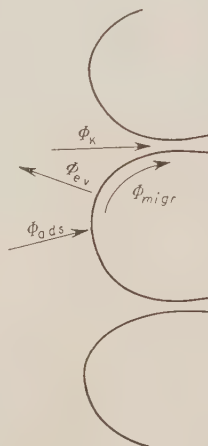


Fig. 1. - Schematizzazione del processo di migrazione superficiale sui grani di una parete porosa.

(*) Lavoro eseguito nel quadro di una collaborazione con i Laboratori CISE.

(+) Attualmente all'Ufficio Studi dell'Agip Nucleare, Milano.

In condizioni stazionarie sarà valida la conservazione dei flussi per entrambi

gli isotopi considerati:

$$(1) \quad \Phi_{ads}^{(i)} = \Phi_{ev}^{(i)} + \Phi_{migr}^{(i)} \quad (i = 1, 2).$$

L'arricchimento isotopico nella fase che attraversa la parete porosa in seguito ai processi di adsorbimento e di migrazione superficiale sarà dato da:

$$(2) \quad \delta_{migr} = \frac{\Phi_{migr}^{(1)} / \Phi_{migr}^{(2)}}{\nu_1 / \nu_2},$$

essendo ν_1/ν_2 il rapporto fra le densità dei due isotopi nel gas prima dell'attraversamento.

Esplicitando la (1) si ha allora:

$$\begin{aligned} S(1 - \theta - \theta) \nu \int_0^{h\nu_M} dE \varphi(E) \sum_s h\Gamma_{cs}^{(i)} = \\ = S\theta_i n_s \sum_s \int_0^{h\nu_M - |E_c|} \pi(E) \cdot G_{s,E}^{(i)} dE + f\theta n_L L \frac{1}{\tau_0}, \end{aligned}$$

ove i simboli dei primi due flussi hanno lo stesso significato che in (I), mentre quelli che compaiono nel flusso di migra-

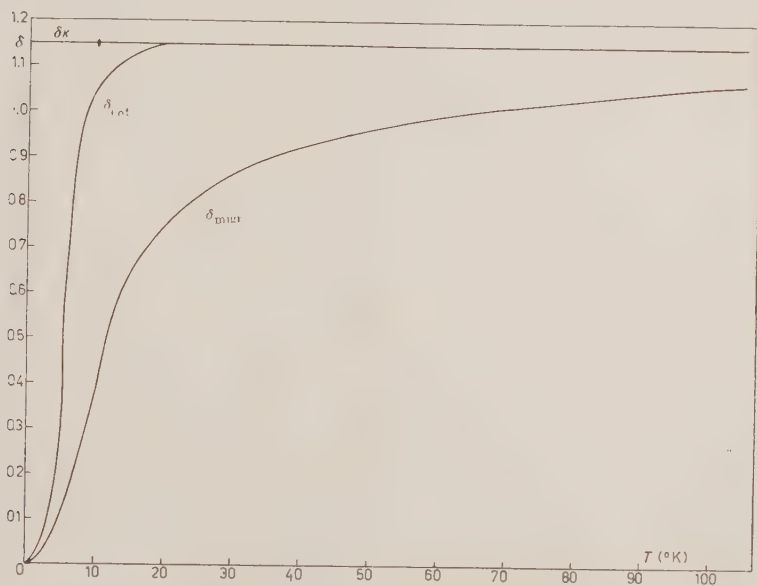


Fig. 2 - Dipendenza dalla temperatura dell'arricchimento isotopico della fase adsorbita che migra superficialmente (curva δ_{migr}) e dell'arricchimento isotopico totale (curva δ_{tot}).

Supponendo che l'adsorbimento abbia luogo in uno strato unimolecolare, un calcolo da noi sviluppato ⁽¹⁾ partendo dalla teoria di Lennard Jones e collaboratori, permette di valutare i flussi di adsorbimento e di evaporazione.

⁽¹⁾ P. CALDIROLA e G. ROSSI: *Nuovo Cimento*, **5**, 1316 (1957) [indicato con (I)].

zione denotano rispettivamente: f un parametro connesso con la possibilità di libero movimento di un atomo adsorbito nella direzione di attraversamento della parete, n_L il numero di posti a disposizione per l'adsorbimento, per unità di lunghezza sul perimetro L dell'imboccatura (« fronte » di migrazione) di un singolo capillare lungo le pareti del quale

ha luogo la migrazione e infine τ_0 è il valore medio dell'intervallo di tempo che separa l'adsorbimento di due atomi in un posto determinato del «fronte» di migrazione.

Il calcolo di f e di τ_0 è piuttosto complicato; si può però rendersi conto abbastanza facilmente che per i casi di interesse pratico è in generale $\Phi_{\text{migr}} \ll \Phi_{\text{ev}}$ per cui il rapporto θ_1/θ_2 è praticamente eguale a quello calcolato in (I) nel caso del puro processo di adsorbimento. In queste condizioni si ha pure: $\delta_{\text{migr}} \approx \delta_{\text{ads}}$.

Abbiamo eseguito un'applicazione numerica al caso di un gas formato da un miscuglio dei due isotopi ^3He ed ^4He che attraversi una parete di polvere compressa di LiF, assumendo gli stessi valori dei vari parametri usati in (I).

I risultati sono riportati in Fig. 2. La curva δ_{migr} dà la dipendenza dalla temperatura dell'arricchimento isotopico per il flusso di migrazione. È interessante osservare che dai nostri risultati deriva che quando il flusso di migrazione superficiale si sovrappone al consueto flusso di Knudsen, l'arricchimento isotopico risultante δ_{tot} viene ad essere diminuito rispetto a quello δ_k che si ha per il solo flusso di Knudsen. Precisamente la diminuzione è tanto più forte quanto più la temperatura è bassa e ciò anche perchè, diminuendo T , diminuisce pure il rapporto $(^2)$ $\Phi_k/\Phi_{\text{migr}}$.

Concludendo vogliamo osservare che i risultati dei nostri calcoli si accordano,

almeno qualitativamente, con i risultati sperimentali ottenuti a Oak Ridge da TRAWICK e BERMAN ⁽³⁾, sperimentando sulla separazione isotopica dell'ossigeno, azoto e argon per mezzo della diffusione attraverso polveri compresse di silice. Detti autori, come è noto, non hanno confermato i risultati precedenti di HAUL ⁽⁴⁾, che probabilmente non sono interpretabili come effetto dell'adsorbimento e della migrazione superficiale ma, come è stato già osservato, come fenomeni transitori.

Naturalmente una diminuzione dell'arricchimento isotopico rispetto a $\delta_k = \sqrt{m_2/m_1}$ si può avere, oltre che per effetto dell'adsorbimento, anche per altre ragioni. Fra queste possono avere particolare importanza il fatto che il diametro dei pori della parete non è trascurabile rispetto al libero cammino medio delle molecole nel gas ⁽⁵⁾ e il fatto che quando il gas scorre tangenzialmente alla parete (come si ha di regola negli impianti) si produce la formazione di uno strato limite nel quale non si ha l'immediato rimescolamento ⁽⁶⁾.

⁽³⁾ W. G. TRAWICK and A. S. BERMAN: *Report A.E.C. K-1236* (1956).

⁽⁴⁾ R. A. W. HAUL: *Naturwiss.*, **41**, 255 (1954).

⁽⁵⁾ W. G. POLLARD and R. D. PRESENT: *Phys. Rev.*, **73**, 762 (1948); W. G. POLLARD and A. J. DE BÉTHUNE: *Phys. Rev.*, **75**, 1050 (1949); v. anche: P. CALDIROLA e L. SELMI: *Rapporto CISE* n. 41 (1954).

⁽⁶⁾ P. CALDIROLA: *Rapporto CISE* n. 34 (1953). L'esistenza di questo effetto è stata provata da G. PERONA con esperienze eseguite presso i laboratori del CISE [cfr. G. PERONA: *International Symposium on Isotope Separation* (Amsterdam, 1957)].

⁽²⁾ Questo rapporto è stato valutato in base a considerazioni teoriche. In pratica è più conveniente ricavare sperimentalmente la sua dipendenza dalla temperatura.

LIBRI RICEVUTI E RECENSIONI

Progress in Nuclear Energy, serie II. *Reactors*, vol. I - Editors: R. A. CHARPIE; D. J. LITTLER; D. J. HUGHES; M. TROCHERIS. Pergamon Press, London e New York, 1956, pag. 492, prezzo 100 s.

Questo volume fa parte di una collezione recentemente iniziata sui diversi aspetti e problemi della produzione e dell'uso dell'energia nucleare; esso contiene articoli monografici ciascuno dei quali descrive uno o più reattori nucleari destinati a scopo di ricerca o a produzione di energia; la raccolta è notevole per la sua completezza e per i dettagli costruttivi che vi sono esposti.

Sono qui riunite per la prima volta informazioni da tutti i principali paesi che hanno impostato e risolto problemi di costruzione di reattori nucleari, e gli articoli sono scritti dagli stessi specialisti che lavorano negli impianti o che collaborano ai progetti: la possibilità di una simile rassegna internazionale deriva evidentemente dallo scambio di vedute che si è avuta l'anno scorso alla conferenza di Ginevra.

I primi cinque capitoli sono dedicati ai reattori costruiti a scopo di ricerca: nel Canada, negli Stati Uniti, in Russia, in Inghilterra ed in Europa.

Segue la descrizione di cinque tipi diversi di reattori per la produzione di energia, sia già costruiti che in progetto: l'impianto di Shippingport ad acqua sotto pressione, un prototipo di reattore ad acqua bollente realizzato all'Argonne Nat. Lab., possibilità di impianto e pro-

spettive economiche di reattori omogenei col « combustibile » in soluzione acquosa, reattori a grafite col raffreddamento a gas del tipo già in esercizio nel Regno Unito; e finalmente pile col raffreddamento a sodio liquido.

L'ultimo capitolo è una rassegna sui reattori rapidi di potenza ad opera di W. H. Zinn.

Il volume si chiude con un catalogo di reattori nucleari aggiornato al 15 Aprile 1956, comprendente i reattori esistenti, quelli oggi demoliti e quelli in progetto.

In questa linea sono inclusi numerosi riferimenti bibliografici.

L'interesse del volume è evidente, non solo come rassegna generale, ma anche per le geniali soluzioni di tanti piccoli e grandi problemi, che possono essere di prezioso aiuto ad ogni futuro progettista, e per la ricchezza di dati numerici, e costruttivi, che fino ad oggi non era facile trovare riuniti.

F. A. LEVI

Z. KOPAL - *Astronomical Optics and Related Subjects*. North-Holland Publishing Company, Amsterdam 1956; 428 pagg., 17 tavole fuori testo; prezzo non indicato.

La storia delle Scienze ci offre numerosi esempi di una stretta collaborazione fra discipline affini ma il caso dell'Ottica e dell'Astronomia è veramente particolare. Ambedue queste discipline si può dire che nascono e si sviluppano in stretta

unione ed i progressi dell'una si ripercuotono in nuove conquiste per l'altra; gli astronomi sono anche ottici e se qualche sperimentatore incomincia a lavorare come ottico ben presto diviene astronomo. Le vicende di Galileo, Keplero, Newton ed altri per arrivare fino al nostro G. B. Amici sono troppo note per insistervi.

Nei tempi più recenti la necessaria specializzazione fa sì che le due discipline tendono a divergere anziché marciare unite come prima per cui, salvo casi piuttosto rari come il Lyot in Francia, il Colacevich in Italia ed il Baker negli S.U., gli ottici vengono a costituire una schiera di ricercatori ben differenziata dagli astronomi. Ma i punti di contatto, i problemi comuni non mancano e ad acuire il reciproco interesse e a provvedere al necessario scambio di informazioni pensano i congressi specializzati o Simposii come il recente Simposio di Ottica Astronomica tenutosi per iniziativa di Zdenek Kopal nel 1955 a Manchester.

Il volume in esame rappresenta la raccolta delle note presentate a tale Simposio; esso consta di 428 pagine ed è suddiviso in sette sezioni nelle quali gli argomenti trattati sono strettamente affini. La divisione adottata per i 46 contributi originali rende superfluo un indice per materie che infatti l'Editore ha ommesso.

Voler riferire dettagliatamente su tutte le note è praticamente impossibile, ci limiteremo a dire che il volume dà un panorama fedele dello stato attuale dell'ottica in relazione all'Astronomia, ed a riferire per sommi capi gli argomenti principali qui nel seguito.

Particolarmente interessanti per la novità degli argomenti sono le prime due sezioni che sono dedicate alla teoria delle informazioni in ottica ed allo studio delle immagini ottiche. Vi si espongono i problemi connessi con il miglioramento della risoluzione e gli sforzi che si fanno per superare il limite teorico fino ad ora accettato.

Più classica la sezione seguente dove si tratta di interferometria e dei problemi di coerenza; si passa poi alle applicazioni dell'elettronica all'ottica astronomica ed in particolare si parla dei successi ottenuti applicando le tecniche televisive all'osservazione del cielo, della luna e dei fenomeni solari. Ricco di promesse il dispositivo per immagazzinare gli impulsi luminosi che nelle speranze degli ideatori dovrebbe decuplicare la potenza degli attuali telescopi.

Nella quinta sezione il massimo contributo al problema del potere risolutivo in relazione alle proprietà delle immagini ottiche viene dato dalla scuola di Arcetri; gli altri contributi riguardano invece la scintillazione atmosferica, l'analisi degli effetti, la sua natura e le possibilità future di compensare con dispositivi terrestri le irregolarità prodotte dalla nostra atmosfera.

Il trasporto della luce lungo fibre di materiale trasparente viene abordato e discusso insieme ai precedenti problemi, anzi si prevede già un'importante applicazione tendente ad utilizzare tutta la luce dell'immagine stellare nella spettroscopia astronomica.

Più tecniche le ultime due sezioni nelle quali sono trattati i problemi riguardanti le superfici asferiche, i sistemi grandangolari ed i filtri di luce per la fotografia. Particolarmente interessanti fra questi ultimi i filtri interferenziali a strati multipli che oggi hanno raggiunto un'altissima perfezione. Ne fanno fede le belle fotografie di oggetti celesti ottenute dagli ottici inglesi sfruttando le prestazioni del telescopio di Asiago e di quello minore di Lojano (Bologna). Ancora agli inizi ma ben promettente il filtro ad alto ordine di interferenza capace di dare una banda passante di meno di due angström.

Il volume, che inizia con una ben dosata messa a punto dei problemi di ottica astronomica da parte del Kopal, è dedicato al più giovane partecipante P. Y. Mills che a distanza di pochi mesi dalla fine del Simposio doveva perdere

la vita al Jungfrauoch mentre proseguiva le esperienze di fotografia astronomica sulle quali aveva riferito durante il simposio stesso.

Veste tipografica eccellente, caratteri nitidi, accurato indice per autori ed elegante rilegatura.

G. RIGHINI

Quantum Theory of Fields, fascicolo della «Series of Selected Papers in Physics», pubblicata a cura della Società Giapponese di Fisica (Physical Society of Japan, 1956).

In questo fascicolo sono riprodotti alcuni dei più importanti articoli apparsi recentemente che riguardano la teoria dei campi. I recenti sviluppi in questa branca della Fisica teorica, spostando l'interesse della ricerca dalla elaborazione di metodi di approssimazione per la valutazione della matrice di scattering allo studio delle sue proprietà analitiche generali fondato essenzialmente sull'uso della rappresentazione di Heisenberg, si sono svolti secondo due filoni principali. Il primo ha condotto alle note regole di dispersione di Goldberger stabilite dapprima in via approssimata per il campo elettromagnetico, quindi in modo più generale per lo scattering pione-nucleone, e attualmente estese ad altri fenomeni come fotoproduzione.

Questi risultati hanno condotto sul piano applicativo pratico ad una prima sistemazione, sia pure non ancora definitiva, dei fenomeni mesonici sui quali fino a un paio di anni fa regnava ancora un buio quasi completo. Non altrettanto definitivi i risultati della seconda direzione di ricerca, mirante a stabilire dal punto di vista matematico l'esistenza stessa di soluzioni alle equazioni fondamentali della teoria dei campi, anche se le ricerche di Källén, Lehmann, Nambu e di Landau e collaboratori rappresentano un notevole passo avanti in questa direzione.

In questo fascicolo il primo gruppo di lavori non è, purtroppo, molto esaurientemente rappresentato, anche perchè l'argomento è ancora tema di ricerca attivissima e ogni giorno, si può dire, appare qualcosa di nuovo. Soltanto i primi lavori di GELL-MANN, GOLDBERGER e THIRRING (*Phys. Rev.*, **95**) e di GOLDBERGER (*Phys. Rev.*, **97** e **99**) oltre a quello di KARPLUS e RUDERMAN (*Phys. Rev.*, **98**) sono riportati. Più numerosi sono invece i lavori sul secondo argomento, che comprendono il lavoro di KÄLLÉN sugli Atti danesi, tre lavori di LEHMANN e collaboratori, due di NAMBU, uno di GELL-MANN e GOLDBERGER, il lavoro di LEE che ha dato origine alla nota caccia ai «ghosts», quattro di LANDAU e collaboratori (in russo), uno di MATTHEWS e SALAM.

La raccolta è, anche se incompleta, molto utile per i ricercatori che si occupano di questi argomenti. Svantaggio notevole è che non sia in commercio.

M. CINI

A. DUSCHEK - *Vorlesungen über höhere Mathematik*, I Bd, II Auflage; Wien, Springer-Verlag, 1956; pagg. XII+440; figg. 169; DM. 48.

Questa seconda edizione del 1° Volume del noto trattato di Analisi Matematica del DUSCHEK, si presenta notevolmente arricchita, soprattutto per un maggior approfondimento dei singoli argomenti. Caratteristica generale dell'opera, che conterà di quattro volumi, è di offrire ai fisici e ai tecnici un vasto panorama dei rami dell'Analisi Matematica che più interessano le applicazioni e che normalmente — per mancanza di tempo — non possono essere svolte nei corsi universitari, sia di Ingegneria che di Fisica. Oltre al Calcolo differenziale e integrale, i volumi successivi tratteranno il Calcolo delle probabilità, il Calcolo tensoriale e il Calcolo delle variazioni; inoltre la

teoria delle equazioni differenziali, ordinarie e a derivate parziali avrà un assai ampio sviluppo insieme con le equazioni integrali e le trasformazioni funzionali (in particolare la trasformazione di Laplace).

Questo primo volume è come l'introduzione all'opera e ne rivela già le caratteristiche essenziali: grande semplicità di esposizione, senza rinunciare con ciò al rigore; messa in luce opportuna dei risultati fondamentali di ogni teoria, illustrandoli spesso con esempi assai significativi. Il capitolo di Calcolo delle probabilità, che nella prima edizione era inserito nel primo volume, è stato sostituito con un capitolo sulle serie, che rende così più omogeneo il carattere propedeutico del primo volume. Il calcolo delle probabilità e le sue applicazioni passeranno a far parte, nella seconda edizione, del secondo volume, di cui è annunciata prossima l'apparizione.

Il primo volume è diviso in 7 capitoli. Il I cap. contiene gli elementi della teoria degli insiemi e il concetto di limite per le successioni di numeri reali. Nel II cap. viene esposto il concetto di funzione e quello di limite per le funzioni, con particolare riguardo alle proprietà delle funzioni continue. Il III cap. tratta dell'integrale e della derivata. Seguendo un ordine poco consueto, ma forse ritenuto più adatto a chi la matematica intende solo applicarla, viene prima esposto il

concetto di integrale definito e le sue principali proprietà; vien poi dato quello di derivata di una funzione, ricollegando poi questo al primo mediante la nozione di un integrale indefinito.

Dopo una parentesi (IV cap.) dedicata allo studio delle trascendenti elementari (logaritmo, esponenziale, funzioni circolari e iperboliche e loro inverse), nel V cap. vengono insieme completati il calcolo differenziale e l'integrale per le funzioni di una variabile, con particolare riguardo alle applicazioni, sia alla geometria che alla meccanica. Il VI cap. è dedicato allo studio delle funzioni ed equazioni algebriche, con particolare rilievo ai metodi di calcolo numerico delle soluzioni. L'ultimo capitolo tratta delle serie: serie numeriche, serie di potenze e serie di Fourier. L'esposizione è assai rapida, pur contenendo i risultati di effettivo interesse generale per le applicazioni.

Un'appendice dà la risoluzione dei problemi proposti in tutto il volume.

Per la chiarezza e la semplicità dell'esposizione ritengo che quest'opera risponda pienamente allo scopo cui è destinata: offrire ai fisici e ai tecnici un quadro vasto e sufficientemente approfondito dei metodi e dei risultati che l'Analisi Matematica ha approntato per la Fisica e le Scienze applicate.

S. FAEDO

PROPRIETÀ LETTERARIA RISERVATA

Direttore responsabile: G. POLVANI

Tipografia Compositori - Bologna

Questo fascicolo è stato licenziato dai torchi il 29-IV-1957